CATALYSIS BY METAL COMPLEXES 37

Series Editors C. Bianchini · D.J. Cole-Hamilton
P.W.N.M. van Leeuwen
Volume Editors M. Peruzzini · L. Gonsalvi

Phosphorus Compounds

Advanced Tools in Catalysis and Material Sciences

Springer

Catalysis by Metal Complexes

Volume 37

For further volumes:
http://www.springer.com/series/5763

Catalysis by Metal Complexes

This book series covers topics of interest to a wide range of academic and industrial chemists, and biochemists. Catalysis by metal complexes plays a prominent role in many processes. Developments in analytical and synthetic techniques and instrumentation, particularly over the last 30 years, have resulted in an increasingly sophisticated understanding of catalytic processes.

Industrial applications include the production of petrochemicals, fine chemicals and pharmaceuticals (particularly through asymmetric catalysis), hydrometallurgy, and waste-treatment processes. Many life processes are based on metallo-enzyme systems that catalyse redox and acid–base reactions.

Catalysis by metal complexes is an exciting, fast developing and challenging interdisciplinary topic which spans and embraces the three areas of catalysis: heterogeneous, homogeneous, and metallo-enzyme.

Catalysis by Metal Complexes deals with all aspects of catalysis which involve metal complexes and seeks to publish authoritative, state-of-the-art volumes which serve to document the progress being made in this interdisciplinary area of science.

Series Editors

Prof. Claudio Bianchini
Institute of Chemistry of Organometallic
Compounds of the Italian National
Research Council (ICCOM-CNR)
Via Madonna del Piano 10
50019 Sesto Fiorentino
Italy

Prof. D. J. Cole-Hamilton
School of Chemistry
University of St Andrews
North Haugh
St Andrews KY16 9ST
UK

Prof. Piet W. N. M. van Leeuwen
Institute of Chemical Research
of Catalonia
Av. Paisos Catalans 16
43007 Tarragona
Spain

VOLUME 37:
PHOSPHORUS COMPOUNDS: ADVANCED TOOLS IN CATALYSIS AND MATERIAL SCIENCES

Volume Editors

Dr. Maurizio Peruzzini and Dr. Luca Gonsalvi
ICCOM CNR, Via Madonna del Piano, 10
50019 Sesto Fiorentino
Italy

Maurizio Peruzzini · Luca Gonsalvi
Editors

Phosphorus Compounds

Advanced Tools in Catalysis and Material Sciences

Springer

Editors
Dr. Maurizio Peruzzini
Institute of Chemistry of Organometallic Compounds of the Italian National Research Council (ICCOM-CNR)
Via Madonna del Piano 10
50019 Sesto Fiorentino
Italy
e-mail: maurizio.peruzzini@iccom.cnr.it

Dr. Luca Gonsalvi
Institute of Chemistry of Organometallic Compounds of the Italian National Research Council (ICCOM-CNR)
Via Madonna del Piano 10
50019 Sesto Fiorentino
Italy
e-mail: l.gonsalvi@iccom.cnr.it

ISSN 0920-4652

ISBN 978-90-481-3816-6 e-ISBN 978-90-481-3817-3

DOI 10.1007/978-90-481-3817-3

Springer Dordrecht Heidelberg London New York

© Springer Science+Business Media B.V. 2011

No part of this work may be reproduced, stored in a retrieval system, or transmitted in any form or by any means, electronic, mechanical, photocopying, microfilming, recording or otherwise, without written permission from the Publisher, with the exception of any material supplied specifically for the purpose of being entered and executed on a computer system, for exclusive use by the purchaser of the work.

Cover design: eStudio Calamar, Berlin/Figueres

Printed on acid-free paper

Springer is part of Springer Science+Business Media (www.springer.com)

Preface

More than any other element in the periodic table, phosphorus represents a bridge between the living and non-living worlds. It takes part in the DNA–RNA biological cycle, but is also of importance in several inorganic cycles i.e. when used in fertilizers. This unique role makes phosphorus chemistry also valuable for applications in innovative areas at the forefront of molecular sciences, such as materials and polymer sciences, nanotechnology, catalysis, and life sciences, including medicinal applications. The linear relationship of phosphorus with its neighbouring elements (nitrogen, arsenic, silicon, and sulphur) and diagonal relationship with carbon (e.g., P is isolobal with C–H), endows an incredible, but still undervalued potential in many contemporary topics of basic and applied research.

This book aims at collecting state-of-the-art research highlights from world renowned experts in various fields of application of phosphorus, either in the form of review or own research account style articles. The topics covered by the authors fit well with the general objectives of this Book Series, and catalytic applications of phosphorus based compounds are thoroughly described in their multifaceted aspects.

Phosphorus is a key element in catalysis, and the last two Nobel prizes in molecular chemistry were awarded to Noyori, Sharpless and Knowles (2001) for their work on enantioselective catalysis and to Grubbs, Schrock and Chauvin (2005) for their work on the chemistry of transition metal carbene complexes and their applications in metathesis. In both cases the development of highly efficient, specifically tailored phosphorus based ligands are of paramount importance The book opens with an account of the recent studies on a new family of air-stable chiral primary phosphines based on the binaphthyl backbone and their applications in asymmetric hydrosilylations (Chap. 1). The concept of applying phosphorus ligands to enantioselective catalysis is also the main subject of Chaps. 5 and 10, dealing with P-based planar chiral ferrocenes and chiral phosphorus ligands for enantioselective enyne cycloisomerizations, respectively.

Selected classes of compounds which have found interesting use as ligands for catalytic applications are represented by phosphinines (Chap. 6) and the water soluble 7-phospha-1,3,5-triazaadamantane ligand PTA and its derivatives (Chap. 7). The effect of phosphorus-based ligands in catalysis has also been reviewed for cross-coupling reactions under the mechanistic point of view in Chap. 3.

Some of the chapters of this book are more focused on the synthetic developments in phosphorus containing materials. This is the case of Chap. 2, which reviews the aspects concerning phosphine acetylenic macrocycles and cages, and Chap. 12, which deals with the important field of P-based cryptands, cyclophanes, and corands. Chapter 4 addresses the potential applications of metal complexes containing anionic phosphorus chains for the synthesis of metal phosphides, whereas the synthesis of P-compounds via the metal catalysed addition of P–H bonds to unsaturated organic molecules is thoroughly reviewed in Chap. 8.

The design of advanced phosphorus-containing materials through supramolecular assembly of phosphole-based conjugated ligands is another important field of application which is reviewed in Chap. 12.

Nanotechnology is a multidisciplinary field of applied science and technology covering a broad range of topics from materials science, colloidal science, applied physics, supramolecular chemistry, and even mechanical and electrical engineering. Chapter 9 describes the synthesis and applications of phosphorus-containing dendrimers in catalysis, materials science, and the biological fields.

Phosphorus is also a key element in all known forms of life from bacteria to humans. Phosphate, PO_4^{3-}, plays a major role in key biological molecules, such as DNA and RNA, phospholipids or as calcium phosphate which is central in the metabolism of teeth and bone tissues. Emerging research areas are the application of organophosphorus and bioorganometallic compounds in medicine for the understanding of specific biological functions and processes, diagnosis and treatment of a number of different diseases, with applications ranging from antitumour agents, to treatment of malaria, AIDS, tuberculosis, Parkinson's disease, bone tissue diseases and dismetabolism, etc. Some of these aspects are covered in the final Chap. 13.

The scientists who agreed to join their knowledge and expertise in this Book are not only part of the international community working in the field of phosphorus chemistry, but also members of the *European Phosphorus Sciences Network* (**PhoSciNet**), part of the European cooperation in science and technology (COST) action (www.phoscinet.org), teaming-up to advance phosphorus based sciences by an integrated and targeted research approach in high-impact fields by organising interactions (workshops), by exchange of young researchers, and by fostering the participation of industrial partners.

We are grateful to COST and to all authors to have accepted with enthusiasm the invitation to write this book. We are certain it will be of interest to scientists skilled-in-the-art, by providing a generous and up-to-date source of inspiration, and for those academics and advanced level students who want to enter the

multifaceted field of phosphorus chemistry. It should also enable industry-based researchers to engage with state-of-the-art science at the top level.

Finally, we want to thank the team at Springer London and our coworkers at ICCOM (Drs. M. Caporali, B. Di Credico, L. Zani and Mr. V. Mirabello) for their help in editing this book.

Maurizio Peruzzini and Luca Gonsalvi
Consiglio Nazionale delle Ricerche (CNR)
Istituto di Chimica dei Composti Organo Metallici (ICCOM)
Via Madonna del Piano 10, 50019 Sesto Fiorentino (Firenze), Italy
e-mail: maurizio.peruzzini@iccom.cnr.it, l.gonsalvi@iccom.cnr.it

Contents

1 **The Primary Phosphine Renaissance** 1
Lee J. Higham

2 **Phosphine Acetylenic Macrocycles and Cages: Synthesis and Reactivity** 21
Wannes Weymiens, J. Chris Slootweg and Koop Lammertsma

3 **Theoretical Evaluation of Phosphine Effects in Cross-Coupling Reactions** 57
Max García-Melchor, Gregori Ujaque, Feliu Maseras and Agustí Lledós

4 **Metal Complexes with Anionic Polyphosphorus Chains as Potential Precursors for the Synthesis of Metal Phosphides** . . . 85
Santiago Gómez-Ruiz and Evamarie Hey-Hawkins

5 **Phosphine-Containing Planar Chiral Ferrocenes: Synthesis, Coordination Chemistry and Applications to Asymmetric Catalysis** 121
Eric Manoury and Rinaldo Poli

6 **Phosphinine-Based Ligands in Homogeneous Catalysis: State of the Art and Future Perspectives** 151
Christian Müller and Dieter Vogt

7 **Aqueous Phase Reactions Catalysed by Transition Metal Complexes of 7-Phospha-1,3,5-triazaadamantane (PTA) and Derivatives** 183
Luca Gonsalvi and Maurizio Peruzzini

8 Synthesis of Phosphorus Compounds via Metal-Catalyzed Addition of P–H Bond to Unsaturated Organic Molecules 213
Irina P. Beletskaya, Valentine P. Ananikov and Levon L. Khemchyan

9 Phosphorus-Containing Dendrimers: Uses as Catalysts, for Materials, and in Biology 265
Anne-Marie Caminade and Jean-Pierre Majoral

10 Chiral Phosphorus Ligands for Enantioselective Enyne Cycloisomerizations 305
Angela Marinetti and Delphine Brissy

11 Coordination-Driven Supramolecular Assembly of Phosphole-Based π-Conjugated Ligands 343
J. Crassous, C. Lescop and R. Réau

12 Phosphorus Based Macrocyclic Ligands: Synthesis and Applications. 375
Andrey A. Karasik and Oleg G. Sinyashin

13 Metal Phosphorus Complexes as Antitumor Agents 445
Alexey A. Nazarov and Paul J. Dyson

Index 463

Contributors

Valentine P. Ananikov
Russian Academy of Sciences, Zelinsky Institute of Organic Chemistry, Leninsky Prospect 47, 119991 Moscow, Russia

Irina P. Beletskaya
Chemistry Department, Lomonosov Moscow State University, Vorob'evy gory, 119899 Moscow, Russia

Delphine Brissy
CNRS UPR 2302, Institut de Chimie des Substances Naturelles, Av. de la Terrasse, 91198 Gif-sur-Yvette Cedex, France

Anne-Marie Caminade
CNRS LCC (Laboratoire de Chimie de Coordination), Université de Toulouse UPS, INPT; LCC, 205 route de Narbonne, 31077 Toulouse, France

Jeanne Crassous
CNRS- Université de Rennes 1, Sciences Chimiques de Rennes, UMR 6226, Campus de Beaulieu, 35042 Rennes Cedex, France

Paul J. Dyson
Ecole Polytechnique Fédérale de Lausanne (EPFL), Institut des Sciences et Ingénierie Chimiques, CH-1015 Lausanne, Switzerland

Santiago Gómez-Ruiz
Departamento de Química Inorgánica y Analítica, E.S.C.E.T. Universidad Rey Juan Carlos, Calle Tulipán sn, 28933 Móstoles, Spain

Luca Gonsalvi
Consiglio Nazionale delle Ricerche (CNR), Istituto di Chimica dei Composti Organometallici (ICCOM), Via Madonna del Piano 10, 50019 Sesto Fiorentino (Firenze), Italy

Evamarie Hey-Hawkins
Universität Leipzig, Institut für Anorganische Chemie der Universität Leipzig, Johannisallee 29, 4103 Leipzig, Germany

Lee J. Higham
School of Chemistry, Newcastle University, Bedson Building, NE1 7RU Newcastle, United Kingdom

Andrey A. Karasik
Kazan Scientific Centre of Russian Academy of Sciences, A. E. Arbuzov Institute of Organic and Physical Chemistry, Arbuzov street 8, 420088 Kazan, Russia

Levon L. Khemchyan
Russian Academy of Sciences, Zelinsky Institute of Organic Chemistry, Leninsky Prospect 47, 119991 Moscow, Russia

Koop Lammertsma
Department of Chemistry and Pharmaceutical Sciences, Faculty of Sciences, VU University Amsterdam, De Boelelaan 1085, 1081 HV Amsterdam, The Netherlands

Agustí Lledós
Departament de Química, Universitat Autònoma de Barcelona, Edifici Cn, 08193 Bellaterra, Catalonia, Spain

Jean-Pierre Majoral
CNRS LCC (Laboratoire de Chimie de Coordination), France and Université de Toulouse UPS, INPT; LCC, 205 route de Narbonne, 31077 Toulouse, France

Eric Manoury
CNRS LCC (Laboratoire de Chimie de Coordination), France and Université de Toulouse, UPS, INPT; LCC, 205 route de Narbonne, 31077 Toulouse, France

Angela Marinetti
Institut de Chimie des Substances Naturelles, CNRS UPR 2301, Av. de la Terrasse, 91198 Gif-sur-Yvette Cedex, France

Feliu Maseras
Institute of Chemical Research of Catalonia (ICIQ), Av. Països Catalans 16, 43007 Tarragona, Catalonia, Spain
Departament de Química, Universitat Autònoma de Barcelona, Edifici Cn, 08193 Bellaterra, Catalonia, Spain

Max García Melchor
Departament de Química, Universitat Autònoma de Barcelona, Edifici Cn, 08193 Bellaterra, Catalonia, Spain

Christian Müller
Department of Chemical Engineering and Chemistry, Homogeneous Catalysis and Coordination Chemistry, Eindhoven University of Technology, Den Dolech 2, 5600 MB Eindhoven, The Netherlands

Alexey A. Nazarov
Ecole Polytechnique Fédérale de Lausanne (EPFL), Institut des Sciences et Ingénierie Chimiques, CH-1015 Lausanne, Switzerland

Maurizio Peruzzini
Consiglio Nazionale delle Ricerche (CNR), Istituto di Chimica dei Composti Organometallici (ICCOM), Via Madonna del Piano 10, 50019 Sesto Fiorentino (Firenze), Italy

Rinaldo Poli
CNRS LCC (Laboratoire de Chimie de Coordination), Université de Toulouse UPS, INPT; LCC, 205 route de Narbonne, 31077 Toulouse, France
CNRS LCC (Laboratoire de Chimie de Coordination), Institut Universitaire de France, 103, bd Saint-Michel, 75005 Paris, France

Régis Réau
Sciences Chimiques de Rennes, CNRS- Université de Rennes 1, UMR 6226, Campus de Beaulieu, 35042 Rennes Cedex, France

Oleg G. Sinyashin
Kazan Scientific Center of Russian Academy of Sciences, A. E. Arbuzov Institute of Organic and Physical Chemistry, Arbuzov str. 8, 420088 Kazan, Russia

J. Chris Slootweg
Department of Chemistry and Pharmaceutical Sciences, Faculty of Sciences, VU University Amsterdam, De Boelelaan 1084, 1081 HV Amsterdam, The Netherlands

Gregori Ujaque
Departament de Química, Universitat Autònoma de Barcelona, Edifici Cn, 08193 Bellaterra, Catalonia, Spain

Dieter Vogt
Department of Chemical Engineering and Chemistry, Homogeneous Catalysis and Coordination Chemistry, Eindhoven University of Technology, Den Dolech 3, 5600 MB Eindhoven, The Netherlands

Wannes Weymiens
Department of Chemistry and Pharmaceutical Sciences, Faculty of Sciences, VU University Amsterdam, De Boelelaan 1083, 1081 HV Amsterdam, The Netherlands

Abbreviations

1-Ad	1-Adamantyl
Acac	Acetylacetone
AFM	Atomic force microscopy
AIBN	Azobisisobutyronitrile
B3LYP	Becke's three-parameter, Lee–Yang–Parr exchange-correlation functional
B3PW91	Becke's three parameter, Perdew–Wang 91 exchange-correlation functional
BET	Brunauer, Emmett and Teller
BICP	2,2′-Bis(diphenylphosphino)-1,1′-dicyclopentane
BINAP	2,2′-Bis(diphenylphosphino)-1,1′-binaphthyl
Binepine	4,5-Dihydro-3H-dinaphtho[2,1-c;1′,2′-e]phosphepine
BINOL	1,1′-Binaphthalene-2,2′-diol
BIPHEP	2,2′-Bis(diphenylphosphino)-1,1′-biphenyl
BSE	Bovine spongiform encephalopathy
C3-Tunaphos	1,13-Bis(diphenylphosphino)-7,8-dihydro-6H-dibenzo[f,h][1,5]dioxonin
Cod	1,5-Bis(cyclooctadiene)-1,4-cyclooctadiene
CP MAS	Cross polarization magic angle spinning
CTAB	Cetyltrimethylammonium bromide
Cy	Cyclohexyl
Cya	Cyanine
Cyp	Cyclopentyl
DBA	Dibenzylideneacetone
DDQ	2,3-Dichloro-5,6-dicyanobenzoquinone
DFT	Density Functional Theory
DIOP	4,5-Bis(diphenylphosphinomethyl)-2,2-dimethyl-1,3-dioxolane
DMA	*N*,*N*-Dimethylacetamide

DME	1,2-Dimethoxyethane
DMF	Dimethylformamide
Dmpe	1,2-Bis(dimethylphosphino)ethane
DMSO	Dimethyl sulfoxide
DNA	Deoxyribonucleic acid
Dppb	1,4-Bis(diphenylphosphino)butane
Dppben	1,2-Bis(diphenylphosphino)benzene
Dppe	Bis(diphenylphosphino)ethane
Dppf	1,1′-Bis(diphenylphosphino)ferrocene
EDTA	Ethylenediaminetetraacetic acid
EGFP	Enhanced green fluorescent protein
FAB-MS	Fast atom bombardment mass spectrometry
FITC	Fluorescein isothiocyanate
FRET	Förster resonance energy transfer
H8-BINAP	2,2′-Bis(diphenylphosphino)-5,5′,6,6′,7,7′,8,8′-octahydro-1,1′-binaphthalene
HAS	Human serum albumin
HeLa	Human epithelioid cervical carcinoma
HEK 293	Human transformed primary embryonal kidney
HIV	Human immunodeficiency virus
HMPA	Hexamethylphosphoramide
HUVEC	Human umbilical vein endothelial cell
LAH	Lithium aluminium hydride
LBL or LbL	Layer-by-layer
LDA	Lithium diisopropylamide
LP	Lone pair
LSPR	Localized surface plasmon resonance
MCM	Mobil composition of matter
Me-DUPHOS	1,2-Bis(2,5-dimethylphospholano)benzene
MeO-BIPHEP	2,2′-Bis(diphenylphosphino)-6,6′-dimethoxy-1,1′-biphenyl
Mes	mesityl (2,4,6-$Me_3C_6H_2$)
MONOPHOS	(3,5-Dioxa-4-phosphacyclohepta[2,1-a;3,4-a′]dinaphthalen-4-yl)dimethylamine
Nbd	2,5-Norbornadiene
NHC	*N*-Heterocyclic carbene
NK	Natural killer
NMR	Nuclear magnetic resonance
NPs	Nanoparticles
OLEDs	Organic light emitting diodes
PAH	Poly(allylamine hydrochloride)
PAMAM	Poly(AMidoAMine)
PBEPBE	Perdew–Burke–Ernzerhof exchange-correlation functional

PBMCs	Peripheral blood mononuclear cells
PEI	Poly(ethyleneimine)
PL	Photoluminescence
PMDETA	*N*,*N*,*N*′,*N*″,*N*″-Pentamethyldiethylenetriamine ($Me_2NCH_2CH_2NMeCH_2CH_2NMe_2$)
PrP^{Sc}	Scrapie isoform of the prion protein
PSS	Poly(styrenesulfonate)
PTA	1,3,5-Triaza-7-phosphaadamantane
PVK	Poly(vinylcarbazole)
QDs	Quantum dots
QM	Quantum Mechanics
QM/MM	Quantum Mechanics/Molecular Mechanics
ROMP	Ring-Opening Metathesis Polymerization
SDP	7,7′-Bis(diphenylphosphino)-2,2′,3,3′-tetrahydro-1,1′-spirobiindane
SegPHOS	5,5′-Bis(diphenylphosphino)-4,4′-bi-1,3-benzodioxole
Skewphos	2,4-Bis(diphenylphosphino)pentane
SN2	Bimolecular nucleophilic substitution
Sphos	2-(2′,6′-Dimethoxybiphenyl)-dicyclohexylphosphine
SPR	Surface plasmon resonance
TEOS	Tetraethoxysilane
TGA	Thermogravimetrical analysis
THF	Tetrahydrofuran
TMEDA	*N*,*N*,*N*′,*N*′-Tetramethylethylenediamine ($Me_2NCH_2CH_2NMe_2$)
TPA	Two-photon absorption
TPEF	Two-photon excited fluorescence
TTF	Tetrathiafulvalene
UV	Ultra-violet
Xantphos	4,5-Bis(diphenylphosphino)-9,9-dimethylxanthene

Chapter 1
The Primary Phosphine Renaissance

Lee J. Higham

Abstract Primary phosphines are renowned for being toxic, volatile, pyrophoric compounds which have to be handled under an inert atmosphere due to their ease of air-oxidation. Thus despite numerous potential applications, they remain underutilized precursors in synthetic chemistry. Only a small number of air-stable primary phosphines are known, and their stability is either attributable to high steric hindrance about the phosphino group or the underlying factors are as yet undetermined. This work is an account of the recent studies carried out by our research group and presents a new family of air-stable *chiral* primary phosphines (*R*)-**5** and (*S*)-**6** based on the binaphthyl backbone. The stabilization is a result of π-conjugation and is discussed with reference to naphthyl- and phenyl-based analogues. Computational studies based on the DFT B3LYP/6-31G* level of theory suggests significant π-conjugation or sufficient heteroatom presence dislocates the phosphorus away from the HOMO of the ground state and raises the energy of the HOMO in the associated radical cation, with a threshold of stability emerging. Novel phosphonites, phospholanes and bis(hydroxymethyl)phosphines were synthesized from (*R*)-**5** and (*S*)-**6** and tested in the catalytic asymmetric hydrosilylation of styrene.

1.1 Stability of the Air-Stable Primary Phosphines

Primary phosphines [1–23] have a notorious reputation for being difficult compounds to work with as a result of their commonly perceived undesirable properties of high volatility, toxicity, stench and spontaneous inflammability.

L. J. Higham (✉)
School of Chemistry, Bedson Building, Newcastle University,
Newcastle upon Tyne, NE1 7RU, UK
e-mail: Lee.higham@ncl.ac.uk

M. Peruzzini and L. Gonsalvi (eds.), *Phosphorus Compounds*,
Catalysis by Metal Complexes, 37, DOI: 10.1007/978-90-481-3817-3_1,
© Springer Science+Business Media B.V. 2011

The compounds shown in Fig. 1.1 are hazardous to work with and require special procedures for their handling; phosphine **1** is used in an industrial safety demonstration[1] and the heterocyclic derivatives **2** and **3** [24] 'are extremely malodorous and sensitive to oxygen, igniting on the tip of a syringe' whilst **4** is explosive [25]. For this reason, despite the fact that they are readily functionalized as a result of the two reactive P–H bonds, and have applications in fields as diverse as medicinal chemistry [3], polymer science [26, 27], carbohydrate modification [28] and macrocyclic research [29], they remain underused and poorly understood as a compound class.

Accordingly, chiral primary phosphines have seldom been employed as synthons [30–36], which is a pity because their use would permit the synthesis of otherwise inaccessible and highly novel asymmetric ligands.

As part of our research into P-stereogenic MOP derivatives [37], we wished to synthesize the chiral primary phosphine precursors (*R*)-2-phosphino-2′-methoxy-1,1′-binaphthyl (*R*)-**5** and the H-MOPH$_2$ analogue (*S*)-2-phosphino-1,1′-binaphthyl (*S*)-**6**. Both were prepared by following the methodology shown in Fig. 1.2.

Both phosphines were isolated in high yield as white powders, with ^{31}P NMR and IR data as expected for this compound class: ((*R*)-**5** δ_P −126.3 ppm, average $^1J_{P-H}$ = 202.6 Hz, ν(P–H) = 2,291 cm^{-1}; (*S*)-**6** δ_P −126.7 ppm, $^1J_{P-H}$ = 203.8 Hz, ν(P–H) = 2,297 cm^{-1}). An acetonitrile solution of (*R*)-**5** yielded crystals which were suitable for study by X-ray crystallography and the resulting structure (Fig. 1.3) represents the first such characterization of an optically-pure primary phosphine [38, 39]. The P–C bond length of 1.811(6) Å correlates with the few other crystal structures reported of uncoordinated primary phosphines [1, 6–11, 40]. The solid-state nature of (*R*)-**5** prompted us to investigate its sensitivity to aerobic oxygen; after 7 days left standing on the bench in air, no oxidation was evident by ^{31}P NMR spectroscopy. The solid-state molecular structure does not appear to indicate a crowded environment about the P-atom, nor does there appear to be any interaction between it and the oxygen of the methoxy substituent, apparently ruling both out as contributors to the compound's air-stability.

Under the same experimental conditions (*S*)-**6** also demonstrates the same level of resistance to air-oxidation as (*R*)-**5**, supporting the earlier hypothesis that the methoxy group plays no role in stabilizing the latter phosphine. A small number of achiral, air-stable primary phosphines have been reported (Fig. 1.4) but these are stabilized on account of high steric hindrance such as supermesityl phosphine **7** [4, 5], triptycylphosphine **8** [6] and various related compounds [1], or their stability is not understood. Examples of the latter class are the air-stable ferrocene derivative **9** [7], and the heteroatom-containing diprimary phosphines

[1] Rhodia created a safety video for internal use showing the spontaneous combustion of this primary phosphine in air to illustrate its pyrophoricity.

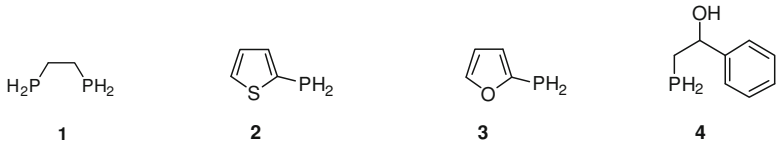


Fig. 1.1 A variety of structurally diverse, highly air-sensitive primary phosphines

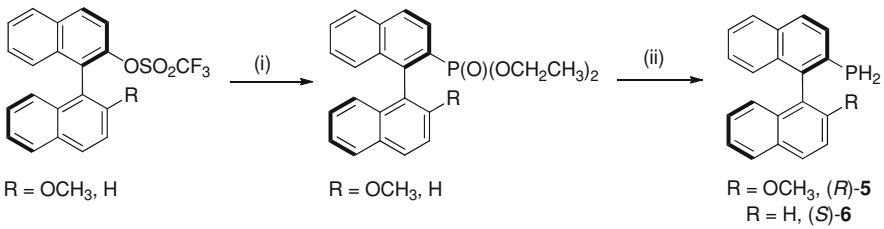


Fig. 1.2 The synthetic route to the chiral primary phosphines (*R*)-**5** and (*S*)-**6**; note that the CIP rules determine the (*R*) and (*S*) stereochemistry of **5** and **6** respectively, despite their possession of identical axial configurations

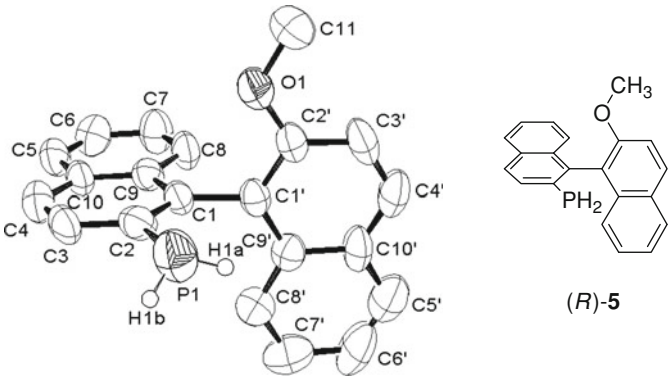


Fig. 1.3 The X-ray crystal structure of (*R*)-**5**. Hydrogen atoms attached to carbon are omitted for clarity

10 [9] and **11** [1, 2]. For **9**, the authors suggest the oxidative resistance may be due to an alkyl spacer group effect, whilst for the latter compounds the presence of the remote heteroatoms are postulated to possibly confer stability via negative hyperconjugation [9, 13, 14]. For (*S*)-**6**, none of these factors can be responsible for its stability to air.

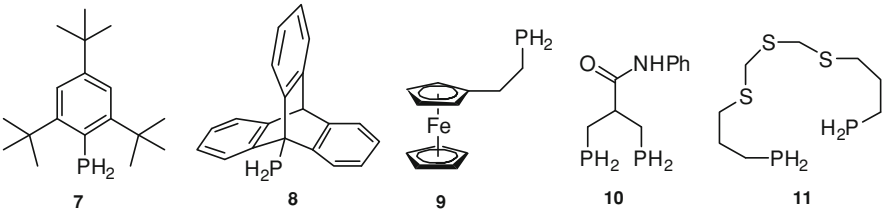
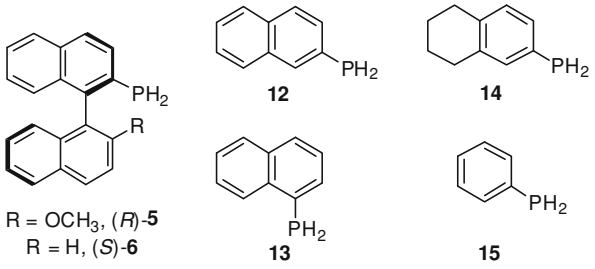


Fig. 1.4 Phosphines **7**-**11** all possess a high degree of air-stability

Fig. 1.5 The π-conjugated primary phosphines which were synthesized in order to study their air-sensitivity, consisting of binaphthyl-, naphthyl- and phenyl-based backbones



To establish that the oxidative stability of (*R*)-**5** and (*S*)-**6** was indeed due to the extra π-conjugation present as a result of the binaphthyl backbone, we undertook a comparative study of the sensitivity of the related phenyl-, naphthyl- and binaphthyl-substituted phosphines shown in Fig. 1.5.

2-naphthylphosphine (2-NAPH$_2$) **12** is a white solid which exhibited good air-stability; after 7 days 88% phosphine remains. For comparison, the regioisomer 1-naphthylphosphine **13** was also synthesized and showed significantly more oxidation (only 17% of **13** remains), but we attribute this to the fact that it is an *oil* under ambient conditions. We then prepared the related compound 5,6,7,8-tetrahydro-2-naphthylphosphine **14** (2-THNPH$_2$), where the ring without the phosphorus substituent is hydrogenated and the conjugation is thereby reduced. This compound is also an oil, and had low air-stability commensurate with that of phenylphosphine **15** (Fig. 1.6).

Often when workers refer to the air-stability of primary phosphines they are describing only the behavior of neat samples, but we were concerned that the nature of the compound (crystalline solid or oil) would influence the rate of oxidation. Therefore (in experiments rarely attempted by others [7, 8]) we exposed solutions of our primary phosphines in bench *d*-chloroform to air, over 7 days in uncapped NMR tubes. Under these conditions, we found that remarkably (*R*)-**5** and (*S*)-**6** exhibited no signs of oxidation (Fig. 1.6).

Thus their air-stability is not simply a result of the slower rate of solid-state reactions; even when solutions of (*S*)-**6** were enriched with dioxygen there was still no oxidation over 24 h. The solution behavior indicates a trend towards resistance to air-oxidation with increasing π-conjugation. In solution, the naphthylphosphines **12** and **13** show similar levels of oxidation, with notable quantities of both

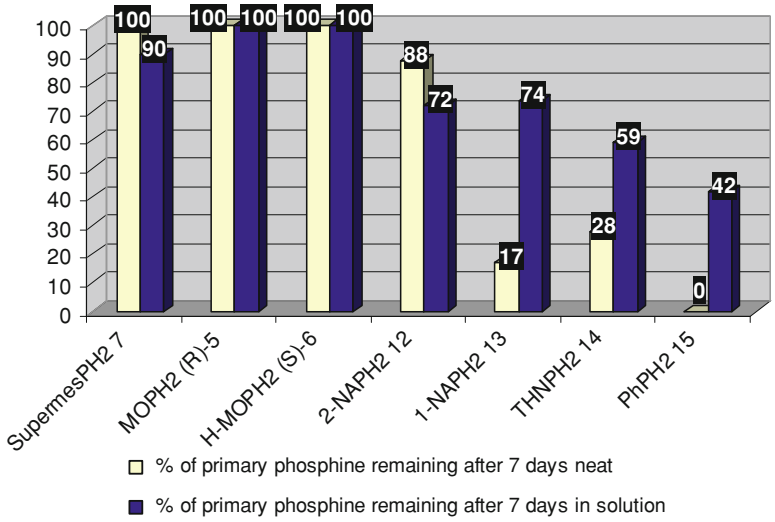


Fig. 1.6 The 7 day neat (*left bar*) and *d*-chloroform solution (*right bar*) oxidation profiles of selected primary phosphines; increasing π-conjugation stabilizes the -PH_2 group to air-oxidation

the oxides and corresponding H-phosphinic acids being produced. This indicates that the sensitivity of neat **13** relates to it being an oil at ambient temperature. The mono-arenes 2-THNPH_2 **14** and PhPH_2 **15** had oxidized to a larger extent by the end of the seven days, but were still more stable than in their neat state as oils.

To probe this electronic stabilization further we needed more information on the character of the phosphorus lone pair. Unfortunately, both low basicities ((*S*)-**6** was not protonated with 6 M HCl) and solubility difficulties precluded their pK_a measurement. Henderson and Alley [12] reacted two equivalents of $FcCH_2PH_2$ with *cis*-$[Mo(C_5H_{11}N)_2(CO)_4]$ to give *cis*-$[Mo(FcCH_2PH_2)_2(CO)_4]$; we then adopted the same protocol to gain an insight into the net electron donor nature of the above primary phosphines. An inspection of entries 4 and 8 in Table 1.1 show that both the air-stable (*S*)-**6** and the reactive phenylphosphine **15** gave the same $\nu_{(CO)}$ (A_1) stretching frequency. Therefore this routine method to assess phosphine basicity cannot be extrapolated to predict their air-stability.

The electrochemical behavior of the phosphines was then examined by voltammetry using a Pt disk electrode. As a result of the irreversibility of phosphine oxidation under these experimental conditions, we have used the potential of maximum slope, $E_{s,max}$ [38, 39, 41, 42], to quantify the position of the waves on the potential axis. The values so obtained (Table 1.1) do suggest a general trend in accord with the observed oxidative stability.

The lowest potentials are found for the most readily oxidized compounds **14** and **15**. Intermediate in value and very similar in magnitude, are the naphthylphosphines **12** and **13**—again emphasizing that the difference observed in the oxidation of the *neat samples* is directed by kinetic factors (a solid versus an oil), but also confirming that the position of substitution has little effect in solution.

Table 1.1 The oxidation potentials of the phosphines studied in this series, and their $\nu_{(CO)}$ (A_1) vibrations in *cis*-[Mo(RPH_2)$_2$(CO)$_4$], including the value for FerrocenylCH_2PH_2

	RPH_2	$E_{s,max}$ mV[a]	v(CO) cm^{-1}
1	FerrocenylCH_2PH_2	_	2,020[7]
2	SupermesPH_2 **7**	960	_[c]
3	MOPH_2 (*R*)-**5**	1,005[b]	2,023
4	H-MOPH_2 (*S*)-**6**	1,170	2,025
5	2-NAPH_2 **12**	850	2,027
6	1-NAPH_2 **13**	845	2,027
7	THNPH_2 **14**	770[d]	2,025
8	PhPH_2 **15**	795	2,025

[a] Tetrabutylammonium tetrafluoroborate (0.1 M) as the supporting electrolyte, scan rate 100 mV s^{-1}, 20 °C; potential in mV, measured with a Pt disk working electrode in degassed dichloromethane solution. The values are referenced to the ferrocene/ferrocinium couple

[b] This value is attributable to the ether group as (*R*)-2,2′-dimethoxy-1,1′-binaphthylene gave a value of 1,030 mV

[c] The *cis* compound was not formed

[d] Partially masked by wave of oxidation product at 1,160 mV

Finally the oxidation resistant (*S*)-**6** shows a relatively high $E_{s,max}$ value. The oxidation of phosphines by elemental oxygen has been postulated to go via a radical mechanism [43, 44] with the possibility of radical cation involvement. These results suggest a correlation between the ease of electrochemical oxidation and air-stability and more sophisticated experiments are now underway.[2] One other possibility for the stability of (*S*)-**6** relative to **15** is that the latter may be ordinarily contaminated by some species which promotes oxidation; however when (*S*)-**6** was purposefully contaminated with **15**, no oxidation was evident even after 25 days.

Evidently the simple addition of a benzene ring to phenylphosphine imparts stability towards air-oxidation. The source of this stabilization therefore is attributable to a conjugative effect, confirmed by the fact that when the additional ring is saturated, there is only a small improvement in air-stability (compare **14** with **12** and **15**). In principle this effect could be between the phosphorus lone pair and the aromatic system, or simply within the aromatic system itself, or both. In considering this, we take into account the following: (1) conjugation of the phosphino group and aromatic rings has been a most contentious issue in the literature [15, 46–49]; (2) both 1-naphthyl and 2-naphthyl substitution lead to a similar stabilization, whereas a conjugative effect to the lone pair might be expected to show a difference; (3) there appears to be no simple relationship between the basicity of the phosphine (as defined in terms of its effect on transition metal-bound carbonyls) and its air-stability, which would again imply that the phosphorus 'lone pair' is not involved in the factors imparting the air-stability; (4) a higher oxidation potential of the phosphine seems to correlate with greater air-stability; (5) PES studies [46–48] have

[2] We emphasize here that both (*R*)-**5** and (*S*)-**6** will oxidize rapidly in the presence of peroxides, but that this process occurs via a different mechanism (see Ref. [45]).

established that the HOMO of phenylphosphine is a perturbed π-orbital of the benzene ring. The greater conjugation in (*R*)-**5** and (*S*)-**6** could either raise the energy required to form a $[RPH_2]^{+\cdot}$ type radical cation, or, conversely, stabilize it, rendering it less reactive in the next stage of the oxidation.

To understand this issue in more detail we have undertaken molecular modeling studies of many relevant primary phosphines [50]. The geometry optimizations of each of the phosphines were performed in the gas phase at the DFT level of theory using the B3LYP functional with a 6-31G* basis set, as employed in the *Spartan '06 Essential* edition from Wavefunction, Inc. In each case the calculations were considered to be complete and converged to a minimum on the potential energy surface after vibrational frequency analysis did not report any negative frequencies. The results of the calculations for (*R*)-**5**, **12** and **14** indicate a trend; increasing π-conjugation results in progressively less phosphorus character in the HOMO of the ground state, culminating in there being no appreciable phosphorus participation in the HOMO of (*R*)-**5** (Fig. 1.7). We also modeled the corresponding radical cation for each phosphine, and found the HOMO distribution in all cases incorporates significant phosphorus character. The calculated HOMO energies of the radical cations are again indicative of a trend—when the value falls below −10 eV the phosphine is found to be air-sensitive (Table 1.2).

Phosphines **9**, **10** and **11** (Fig. 1.4) possess air-stability that has not been fully accounted for, and these compounds were also modeled using the same methodology as that described above. The model suggests the phosphorus atom does not participate in the HOMO of the ground state structures for these air-stable compounds, as was also the case for (*R*)-**5**, and importantly, the HOMO energies of the radical cations are again all above −10 eV (Fig. 1.8, Table 1.2).

The calculations suggest that extensive delocalization and/or sufficient heteroatom presence raises both the energy of the ground state HOMO and that of its associated radical cation; it is plausible that this destabilization of the radical cation precludes it from participating in the subsequent oxidative step with O_2 and results in air-stability. An accompanying effect which may or may not be intrinsically

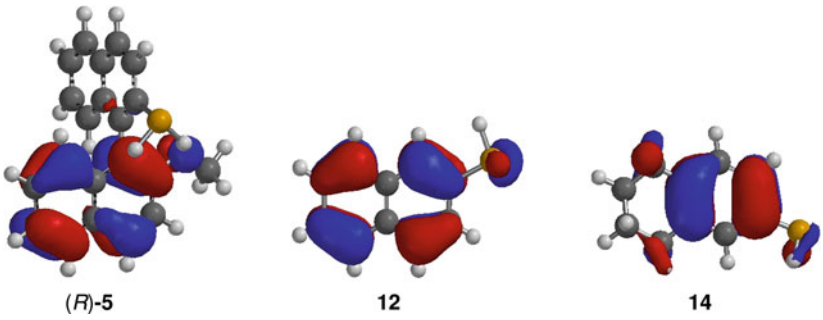


Fig. 1.7 DFT calculations indicating the ground state HOMO distribution for (*R*)-**5**, **12** and **14**. Increasing conjugation reduces then eliminates phosphorus incorporation in the HOMO

Table 1.2 The calculated radical cation (RC) HOMO energies of the phosphines depicted in Figs. 1.7 and 1.8. A threshold value of −10 eV correlates well with air-sensitivity/stability

	RPH_2	RC HOMO/eV
1	$MOPH_2$ (*R*)-**5**	−9.14
2	**9**	−9.58
3	**10**	−9.97
4	**11**	−9.74
5	2-$NAPH_2$ **12**	−10.64
6	$THNPH_2$ **14**	−10.90

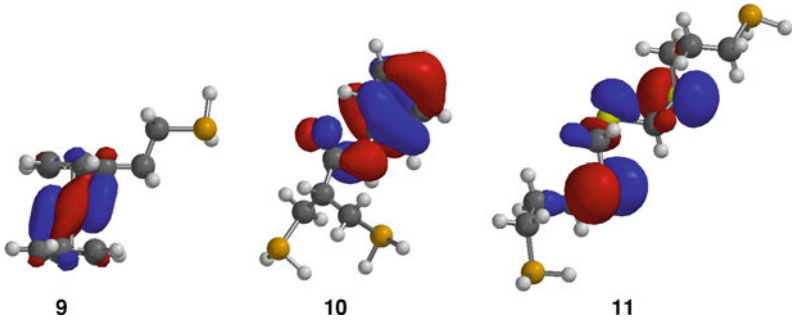


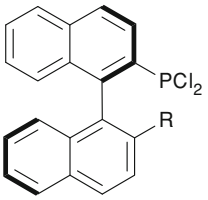
Fig. 1.8 Our DFT calculations for the ground state HOMO distribution of the air-stable primary phosphines **9**, **10** and **11**. Extensive conjugation and/or heteroatom presence reduces phosphorus incorporation from the HOMO and destabilizes the energy of the HOMO radical cation

linked is the increasing isolation of the phosphorus from the HOMO distribution. Work is ongoing in our laboratory to better understand this phenomenon.

In conclusion to this section, we have found the first air-stable chiral primary phosphines (*R*)-**5** and (*S*)-**6**, and attributed that stability to conjugation in their aryl backbones. The molecular model we have now developed suggests that despite the varied structures shown in Fig. 1.8, we may be able to rationalize and predict the sensitivity of known and unknown primary phosphines; we hope that this will prompt a renaissance in the use of primary phosphines as synthetic precursors. In the following section we show that (*R*)-**5** and (*S*)-**6** are convenient chiral starting materials.

1.2 Reactivity of the Air-Stable Primary Phosphines

Whereas stabilizing reactive functionality by using high steric hindrance can inhibit the reactivity profile of that group toward other reagents, the startling air-stability of (*R*)-**5** and (*S*)-**6** does not impede on the reactivity of the phosphino group toward substitution. It appears that in practice we have only 'turned-off' their sensitivity towards aerobic oxygen. Thus we sought to prepare previously inaccessible ligands via functionalization of the phosphorus hydrogen bonds.



R = OCH_3, (*R*)-**16**
R = H, (*S*)-**17**

Fig. 1.9 The dichlorophosphines (*R*)-**16** and (*S*)-**17** prepared from PCl_5

Hayashi's MOP family have been utilized in a number of catalytic asymmetric transformations[3] [51] and are typically somewhat restricted in type by their formulation from the secondary phosphine or secondary phosphine oxide precursors [52, 53]. In a number of catalytic transformations, the available MOP ligands do not provide optimum levels of conversion or enantioselectivity, whilst (*R*)-MOP itself is also rather expensive [54–56]. Thus we were keen to test the reactivity of our primary phosphines and also develop chemistry that would allow us to supply new MOP ligand families to those working in this field [57].

1.2.1 Chiral Phosphonites

We first sought to convert the primary phosphines into dichlorophosphines (Fig. 1.9); these are typically reactive electrophilic reagents and enantiopure examples would be especially valuable for synthetic operations [36]. A library of phosphonites [58–60] could then be prepared by reaction of these dichlorophosphines with the appropriate alcohols and phenols in the presence of a tertiary amine base, and our exemplar targets were phosphonites based on enantiopure binol as shown in Fig. 1.10. Treatment of (*R*)-**5** and (*S*)-**6** with phosphorus pentachloride [61] in toluene yielded (*R*)-**16** and (*S*)-**17** in almost quantitative conversion.

The dichlorophosphine (*R*)-**16** was then used to generate the binol-derived MOP phosphonite diastereomers (R,R_{ax})-**18a** and (S,R_{ax})-**18b** with (*R*)- and (*S*)-binol respectively, using excess triethylamine as base in tetrahydrofuran; similarly (*S*)-**17** was used to prepare (R,S_{ax})-**19a** and (S,S_{ax})-**19b** (Fig. 1.10).

1.2.2 Chiral Phospholanes

Next we sought to examine the acidity of the phosphorus hydrogen bond. Thus the second reaction of interest was the classic deprotonation of a primary phosphine

[3] The parent (*R*)-MOP is (*R*)-5 with phenyls in place of the hydrogens on the phosphorus.

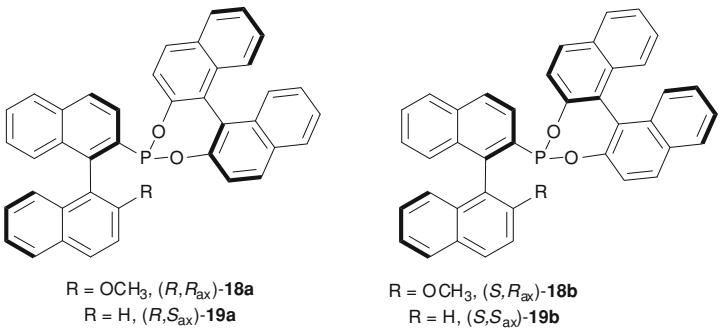


Fig. 1.10 The binol-derived MOP phosphonites prepared from (*R*)-**5** and (*S*)-**6**

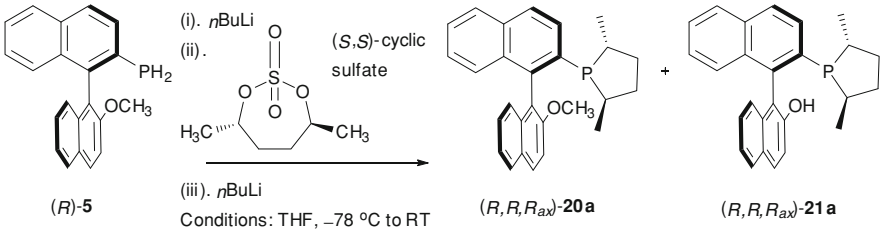


Fig. 1.11 Preparation of phospholanes (*R*,*R*,R_{ax})-**20a** and (*R*,*R*,R_{ax})-**21a**; use of the (*R*,*R*)-cyclic sulfate gave phospholanes (*S*,*S*,R_{ax})-**20b** and (*S*,*S*,R_{ax})-**21b**

with a strong base such as *n*-butyllithium, which generates a phosphorus nucleophile that can subsequently be reacted with a wide variety of electrophiles. Burk synthesized [62, 63] the highly useful phospholane ligand class with the phosphorus incorporated into a five-membered ring [30–33, 64, 65], by reaction of a doubly deprotonated primary phosphine with electrophilic, chiral cyclic sulfates. Following this methodology, our targets were the MOP and H-MOP phospholane 'hybrids'. The reaction of (*R*)-**5** with the (*S*,*S*)-cyclic sulfate in our hands presented a complication; a ^{31}P NMR spectrum of the crude reaction mixture before the aqueous quench showed two peaks at δ −3.0 and −33.2 ppm, neither of which split in the ^{31}P–^{1}H coupled spectrum. The peak at δ −33.2 ppm did not disappear but it did diminish when water was added. After an aqueous-organic work-up, a crude orange/yellow solid resulted which gave two peaks by ^{31}P NMR spectroscopy at δ −2.1 ppm for (*R*,*R*,R_{ax})-**20a** and at −2.8 ppm for (*R*,*R*,R_{ax})-**21a** (Fig. 1.11).

In the ^{1}H NMR spectrum only one methoxy group signal was observed at δ 3.46 ppm, assignable to (*R*,*R*,R_{ax})-**20a**, with a smaller, broader singlet at δ 4.71 ppm. We speculate that the peak at δ −33.2 ppm in the ^{31}P NMR spectrum (before the quench) is the phenoxide generated by cleavage of the ether group. This phenoxide is then protonated during the work-up to give the phenolic MOP phospholane (*R*,*R*,R_{ax})-**21a** at δ −2.8 ppm, and thereby accounts for the phenolic proton peak observed at δ 4.71 ppm by ^{1}H NMR spectroscopy (in *d*-chloroform).

The borane adducts of (R,R,R_{ax})-**20a** and (R,R,R_{ax})-**21a** were prepared from the crude products to allow for purification by column chromatography. Borane (R,R,R_{ax})-**20a**.BH_3 was isolated in 24% overall yield (based on the amount of (R)-**5** used), and was characterized by a broad peak at δ 43.4 ppm in the ^{31}P NMR spectrum, with the methoxy signal evident at δ 3.78 in the ^{1}H NMR spectrum. Borane (R,R,R_{ax})-**21a**.BH_3 was obtained in 23% overall yield and was characterized by a broad peak at δ 45.6 ppm in the ^{31}P NMR spectrum, with the phenolic proton appearing at δ 4.63 ppm in the ^{1}H NMR spectrum. These phospholanoboranes were deprotected by heating to 50 °C overnight in excess diethylamine, but the products were contaminated by quantities of the aminoborane by-product. In the case of (R,R,R_{ax})-**20a**, attempted purification with a methanol wash was impeded by the solubility of the phosphine itself in that solvent. For (R,R,R_{ax})-**21a** an aqueous acidic work-up was carried out, but this necessitated treatment with diethylamine (to convert the phosphonium salt that evidently formed back to the phosphine) followed by column chromatography in order to purify the compound.

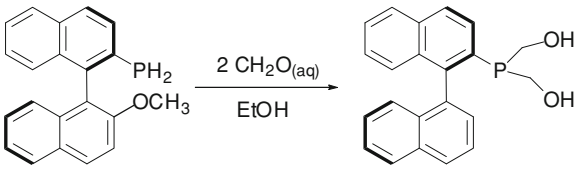
In the case of the (S,S,R_{ax})-MOP phospholanes, the corresponding methoxy and phenolic compounds were also obtained, and were converted as above to their borane adducts yielding a yellow solid (39% combined mass), which was poorly soluble in most common solvents. After column chromatography, the methoxy compound (S,S,R_{ax})-**20b**.BH_3 was obtained in an impure form and in such a small quantity as to render further purification impractical. A small amount (10%) of the phenolic compound (S,S,R_{ax})-**21b**.BH_3 was isolated by column chromatography.

Whilst we were synthesizing (R,R,R_{ax})-**20a** and (S,S,R_{ax})-**20b**, RajanBabu and Saha reported their use in the catalytic hydrovinylation of styrene derivatives [66]. However, their 16% yield of the preceding primary phosphine can be improved to quantitative levels [38, 39] by using lithium aluminum hydride in conjunction with chlorotrimethylsilane, and their 5% yield of the phospholanes can now be rationalized at least in part by our isolation of the phenolic compounds (R,R,R_{ax})-**21a** and (S,S,R_{ax})-**21b**. These phenolic phospholanes should prove to be interesting 'L–X' ligands in their own right; the parent 2-diphenylphosphino derivative has already been shown to be an effective chiral base in the asymmetric aza-Baylis–Hillman transformations of *N*-sulfonated imines, by virtue of its phenolic residue [67].

Preparation of H-MOP phospholane (R,R,S_{ax})-**22a** employed the same methodology starting from (S)-**6** and it was isolated as a white solid in 69% yield. For comparative purposes we also synthesized 2-naphthylphospholane (R,R)-**23**. For (S,S,S_{ax})-**22b** it was necessary to purify the compound via the borane adduct (S,S,S_{ax})-**22b**.BH_3 which again impacted on the final yield.

1.2.3 Hydrophosphination

The third reaction type which we wished to study was the hydrophosphination of unsaturated substrates, specifically where a P–H bond adds across a double bond to yield dialkylarylphosphines. For our purposes we chose to study the reaction of



(*R*)-**5** (*R*)-**24**

Fig. 1.12 Hydrophosphination of (*R*)-**5** with formaldehyde to yield (*R*)-**24**

(*R*)-**5** with formaldehyde (Fig. 1.12); phosphines with the resulting substituents have found numerous applications in catalysis and medicinal chemistry [3, 13, 14, 68–75].

The reaction of (*R*)-**5** and aqueous formaldehyde (Fig. 1.12) produced the chiral bis(hydroxymethyl)phosphine (*R*)-**24** in 88% yield. Attempts to prepare a pure sample of the corresponding diol from (*S*)-**6** were thwarted due to the difficulties in removing the minor quantity of phosphine oxide generated, a notorious problem with this ligand class [68].

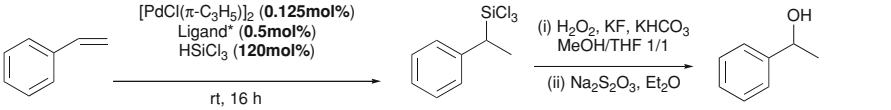
1.3 Asymmetric Catalysis: Hydrosilylation

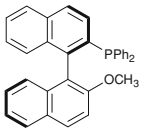
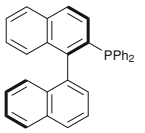
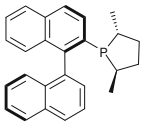
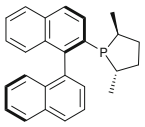
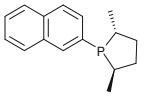
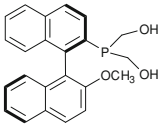
Having demonstrated that the stability of the primary phosphines to air-oxidation does not appear to inhibit their conversion to tertiary phosphines, we were keen to compare and contrast the new ligands in benchmark MOP-based catalysis. In the first instance, we have investigated the palladium-catalyzed synthesis of phenylethanol via the hydrosilylation of styrene by trichlorosilane[4] (Table 1.3) [76, 77]. The parent (*R*)-MOP reportedly demonstrates poor enantioselectivity for this reaction, with (*R*)-1-phenylethanol being obtained in 100% conversion but only 14% ee over 24 h (although carrying out the reaction in benzene gave an ee of 71%). In our hands (*R*)-MOP consistently gave an ee of 48% (Table 1.3, entry 1) when the experiments were performed at room temperature (not at 0 °C), according to the procedure adopted by Johannsen et al. [78] With (*S*)-H-MOP the enantioselectivity was found to be high; (*R*)-1-phenylethanol was obtained in 100% yield and 93% ee over 12 h (Table 1.3, entry 2) [79, 80].

Phospholanes (*R*,*R*,R_{ax})-**20a** and (*S*,*S*,R_{ax})-**20b** gave low yields and poor enantioselectivities. However, consistent with Hayashi et al. findings that H-MOP is much more effective than MOP in this transformation, we found the H-MOP phospholanes (Table 1.3, entries 3 for **22a** and 4 for **22b**) also gave good conversions and respectable ees. Both (*R*,*R*,S_{ax})-**22a** and (*S*,*S*,S_{ax})-**22b** display similar asymmetric induction profiles and it would appear therefore that this reaction is dominated by the binaphthyl backbone rather than the chirality of the phospholane

[4] (*S*)-MOPs had previously proven very effective for the hydrosilylation of 1-alkenes.

Table 1.3 The Pd-catalyzed asymmetric hydrosilylation of styrene to give 1-phenylethanol



Entry	Ligand		Con. (%)[b]	ee (%)[c]
1	(*R*)-MOP		100	48(*R*)
2	(*S*)-H-MOP[a]		100	93(*R*)
3	(R,R,S_{ax})-**22a**		70	71(*R*)
4[d]	(S,S,S_{ax})-**22b**		100	73(*R*)
5	(*R,R*)-**23**		<1	–
6	(*R*)-**24**		72	54(*S*)

The procedure of Johannsen et al. was followed [78]

[a] Literature values [79, 80]

[b] Percentage conversion was determined by ^{1}H NMR of the crude reaction mixture, except for entry 2 where it refers to the distilled silane

[c] Percentage ee of the alcohol product was determined by chiral GC

[d] This reaction was carried out for 20 h

ring (although other factors could be at work). Addition of [Pd(η^3-allyl)Cl]$_2$ to (R,R,S_{ax})-**22a** in a 1:2 ratio of palladium to phospholane (the ratio used in the asymmetric hydrosilylation reaction) gave two significant peaks at δ 52.8 and δ 47.7 ppm in *d*-chloroform in the ^{31}P NMR spectrum, with the former of the highest intensity. These may represent either variable bonding modes in equilibrium, or simply unrelated species; [Pd(η^3-allyl)(R,R,S_{ax})-**22a**]$^+$ was identified by mass

spectrometry. The 2-naphthylphospholane (*R,R*)-**23** showed almost no activity in this reaction (Table 1.3, entry 5). The result is a significant finding because the ligand is similar to **22a** but lacking the lower naphthyl ring. It has been shown in the literature [81] that Pd can bind in an η^2 fashion between C1′ and C2′′ in the parent H-MOP, and by comparing entries 3, 4 and 5 we can see how critical the presence of the second naphthyl group is to conversion. Perhaps the active complex in palladium-catalyzed asymmetric hydrosilylations with H-MOP ligands is one with this bonding mode between the palladium atom and ligand; since more simple monophosphines such as 2-naphthylphospholane (*R,R*)-**23** cannot offer this type of coordination, the consequence may be low activity in this reaction; mass spectrometry indicates two phosphines bind per palladium in the case of (*R,R*)-**23**.

The MOP-diol ligand (*R*)-**24** gave very interesting results (Table 1.3, entry 6); the yield is good and there is a moderate ee of 54% despite the presence of the bis(hydroxymethyl) groups, which could be considered too flexible to influence the stereoselectivity. Also the sense of enantioselection is the opposite of that observed with the H-MOP phospholane ligands. We are currently investigating the molecular entities and bonding modes present in both this and the phospholane systems.

In conclusion, the air-stable chiral primary phosphines (*R*)-**5** and (*S*)-**6** have been shown to demonstrate chemistry typical of this functional group despite their air-stability, and are highly useful ligand precursors for asymmetric catalytic transformations. A number of libraries of chiral ligands should now be accessible as demonstrated by our representative syntheses using hydrophosphination reactions and both phospholane and phosphonite preparations. The binaphthyl H-MOP phospholanes (R,R,S_{ax})-**22a** and (S,S,S_{ax})-**22b** show promising conversions and reasonable enantioselectivities for the hydrosilylation of styrene (70 and 100% conversion; 71 and 73% ee respectively) and the MOP diol (*R*)-**24** interestingly gave the opposite sense of product stereoselectivity in 54% ee; note that none of these reactions have yet been optimized. The synthesis of improved, second-generation ligand libraries is now underway using these easy-to-handle primary phosphine precursors. Finally we note the recent work [82] on introducing bis(trifluoromethyl) substituents onto related primary phosphines, which should also be applicable to our systems.

Acknowledgments The author wishes to thank the EPSRC for the award of a Career Acceleration Fellowship. He also thanks Prof. D. G. Gilheany, Prof. A. Harriman, Dr. Rachel M. Hiney, Dr. Helge Müller-Bunz, Dr. Beverly Stewart and Arne Ficks for their significant and valued contributions to the work in this chapter.

References

1. Brynda M (2005) Towards "user-friendly" heavier primary pnictanes: recent developments in the chemistry of primary phosphines, arsines and stibines. Coord Chem Rev 249:2013–2034
2. Katti KV, Pillarsetty N, Raghuraman K (2003) New vistas in chemistry and applications of primary phosphines. In: Marjoral J-P (ed) Topics in current chemistry, vol 229. Springer, Berlin, pp 121–141 and references cited therein

3. Katti KV, Gali H, Smith CJ, Berning DE (1999) Design and development of functionalized water-soluble phosphines: catalytic and biomedical implications. Acc Chem Res 32:9–17 and references cited therein
4. Yoshifuji M, Shibayama K, Inamoto N (1983) Isolation of some sterically protected unsymmetrical diphosphenes: nature of the phosphorus-phosphorus double bond. J Am Chem Soc 105:2495–2497
5. Yoshifuji M, Shibayama K, Toyota K, Inamoto N (1983) Preparation and characterization of sterically protected primary phosphine sulfide and oxide. Tetrahedron Lett 24:4227–4228
6. Ramakrishnan G, Jouaiti A, Geoffroy M, Bernardinelli G (1996) 9-Substituted triptycene as a probe for the study of internal rotation around a C–PH bond in the solid state: a single crystal EPR study at variable temperature. J Phys Chem 100:10861–10868
7. Goodwin NJ, Henderson W, Nicholson BK, Fawcett J, Russell DR (1999) (Ferrocenylmethyl) phosphine, an air-stable primary phosphine. J Chem Soc Dalton Trans 1785–1793
8. Brauer DJ, Fischer J, Kucken S, Langhans KP, Stelzer O, Weferling N (1994) Water-soluble phosphines. III. Water-soluble primary phosphines with ammonium groups NR2R′ in the side chain–donor functionalized amphiphiles. Z Naturforsch B 49:1511–1524
9. Pillarsetty N, Raghuraman K, Barnes CL, Katti KV (2005) Design, synthesis, and chemistry of sterically nondemanding primary bisphosphines. J Am Chem Soc 127:331–336
10. Pet MA, Cain MF, Hughes RP, Glueck DS, Golen JA, Rheingold AL (2009) Synthesis and structure of ferrocenylmethylphosphines, their borane adducts, and some related derivatives. J Organomet Chem 694:2279–2289
11. Reiter SA, Assmann B, Nogai SD, Mitzel NW, Schmidbaur H (2002) (Benzene-1,3,5-triyl) tris[phosphine] ($C_6H_3(PH_2)_3$) and (Benzene-1,3,5-triyl)tris[phosphonic acid] ($C_6H_3[P(O)(OH)_2]_3$). Absence of hydrogen bonding in solid primary phosphines. Helvetica Chimica Acta 85:1140–1150
12. Henderson W, Alley SR (2002) 'User-friendly' primary phosphines and an arsine: synthesis and characterization of new air-stable ligands incorporating the ferrocenyl group. J Organomet Chem 656:120–128
13. Gali H, Karra SR, Reddy VS, Katti KV (1999) Design and development of the first peptide-chelating bisphosphane bioconjugate from a novel functionalized phosphorus(III) hydride synthon. Angew Chem Int Ed 38:2020–2023
14. Gali H, Karra SR, Reddy VS, Katti KV (1999) Design and development of the first peptide-chelating bisphosphane bioconjugate from a novel functionalized phosphorus(III) hydride synthon. Angew Chem 111:2152–2155
15. Noble-Eddy R, Masters SL, Rankin DWH, Wann DA, Robertson HE, Khater B, Guillemin J-C (2009) Primary phosphines studied by gas-phase electron diffraction and quantum chemical calculations. Are they different from amines? Inorg Chem 48:8603–8612
16. Voituriez A, Panossian A, Fleury-Brégeot N, Retailleau P, Marinetti A (2009) Synthesis of chiral 2-phospha[3]ferrocenophanes and their behaviour as organocatalysts in [3 + 2] cyclization reactions. Adv Synth Catal 351:1968–1976
17. Anderson BJ, Guino-o MA, Glueck DS, Golen JA, DiPasquale AG, Liable-Sands LM, Rheingold AL (2008) Platinum-catalyzed enantioselective tandem alkylation/arylation of primary phosphines. Asymmetric synthesis of P-stereogenic 1-phosphaacenaphthenes. Org Lett 10:4425–4428
18. Scheer M, Kuntz C, Stubenhofer M, Zabel M, Timoshkin AY (2010) Stepwise expansion of a Cp* ring at pentelidene complexes and stereoselective formation of triphosphines. Angew Chem Int Ed 49:188–192
19. Scheer M, Kuntz C, Stubenhofer M, Zabel M, Timoshkin AY (2010) Stepwise expansion of a Cp* ring at pentelidene complexes and stereoselective formation of triphosphines. Angew Chem 122:192–196
20. Xie J, Huang J-S, Zhu N, Zhou Z-Y, Che C-M (2005) Primary and secondary phosphane complexes of metalloporphyrins: isolation, spectroscopy, and X-ray crystal structures of ruthenium and osmium porphyrins binding phenyl- or diphenylphosphane. Chem Eur J 11:2405–2416

21. Bender M, Niecke E, Nieger M, Pietschnig R (2006) Bis(stannyl)phosphanyl-substituted dichlorosilanes/germanes—potential precursors for a novel strategy toward P-Si/Ge multiple bonds? Eur J Inorg Chem 380–384
22. Dell'Anna MM, Mastrorilli P, Nobile CF, Calmuschi-Cula B, Englert U, Peruzzini M (2008) Reactivity of mononuclear Pd(II) and Pt(II) complexes containing the primary phosphane (ferrocenylmethyl)phosphane towards metal chlorides and PPh_3. Dalton Trans 6005–6013
23. Quin LD (2000) A guide to organophosphorus chemistry. Wiley-Interscience, Weinheim, pp 101, 180–183
24. Reiter SA, Nogai SD, Schmidbaur H (2005) Synthesis and auration of primary and di-primary heteroaryl-phosphines. Dalton Trans 247–255
25. Arbuzova SN, Brandsma L, Gusarova NK, van der Kerk AHTM, van Hooijdonk MCJM, Trofimov BA (2000) A convenient synthesis of primary 2-hydroxyorganophosphines from red phosphorus and oxiranes. Synthesis 1:65–66
26. Dorn H, Singh RA, Massey JA, Lough AJ, Manners I (1999) Rhodium-catalyzed formation of phosphorus–boron bonds: synthesis of the first high molecular weight poly(phosphinoborane). Angew Chem Int Ed 38:3321–3323
27. Dorn H, Singh RA, Massey JA, Lough AJ, Manners I (1999) Rhodium-catalyzed formation of phosphorus–boron bonds: synthesis of the first high molecular weight poly(phosphinoborane). Angew Chem 111:3540–3543
28. Hanaya T, Yamamoto H (1989) Synthesis and structural analysis of 4-deoxy-4-(hydroxyphosphinyl and phenylphosphinyl)-D-ribofuranoses. Bull Chem Soc Jpn 62:2320–2327
29. Kyba EP, Liu S-T (1985) Synthesis of unusual phosphine ligands. Use of the 1-naphthylmethyl moiety as a P–H protecting group in the synthesis of a phosphino macrocycle that contains a secondary-phosphino ligating site. Inorg Chem 24:1613–1616
30. Clarke TP, Landis CR (2004) Recent developments in chiral phospholane chemistry. Tetrahedron Asymmetry 15:2123–2137
31. Hoge G, Samas B (2004) Application of *P*-chirogenic bisphospholane ligands to rhodium catalyzed asymmetric hydrogenation of α- and β-acetamido dehydroamino acid derivatives. Tetrahedron Asymmetry 15:2155–2157
32. Schmid R, Broger EA, Cereghetti M, Crameri Y, Foricher J, Lalonde M, Müller RK, Scalone M, Schoettel G, Zutter U (1996) New developments in enantioselective hydrogenation. Pure Appl Chem 68:131–138
33. Brauer DJ, Kottsieper KW, Roβenbach S, Stelzer O (2003) Novel P,N ligands derived from (*R*)- and (*S*)-1-phenylethylamine with (2*R*,5*R*)-2,5-dimethylphospholanyl groups (DuPHAMIN) for asymmetric catalysis. Eur J Inorg Chem 1748–1755
34. Herrbach A, Marinetti A, Baudoin O, Guénard D, Guéritte F (2003) Asymmetric synthesis of an axially chiral antimitotic biaryl via an atropo-enantioselective Suzuki cross-coupling. J Org Chem 68:4897–4905 and references therein
35. Chatterjee S, George MD, Salem G, Willis AC (2001) Optically active asymmetric di(tertiary phosphines). Crystal and molecular structure of [*SP*-4-3-(S_P,*S*)]-{1-[(2-chlorophenyl)-methylphosphino]-2-(dimethylphosphino)benzene-*P*,*P*′}{1-[1-(dimethylamino)ethyl]naphthyl-C^2,*N*} palladium(II) hexafluorophosphate. J Chem Soc Dalton Trans 1890–1896
36. Dahlenburg L, Kaunert A (1998) (1*S*,2*S*)-cyclopentane-1,2-diyl-bis(phosphonous dichloride) (1*S*,2*S*)-$C_5H_8(PCl_2)_2$—a versatile optically active reagent. Eur J Inorg Chem 885–887
37. Higham LJ, Clarke EF, Müller-Bunz H, Gilheany DG (2005) P-chirogenic phosphines MOP/DiPAMP hybrids, their oxide crystal structures, reduction studies and alternative syntheses. J Organomet Chem 690:211–219
38. Hiney RM, Higham LJ, Müller-Bunz H, Gilheany DG (2006) Taming a functional group: creating air-stable, chiral primary phosphanes. Angew Chem Int Ed 45:7248–7251
39. Hiney RM, Higham LJ, Müller-Bunz H, Gilheany DG (1999) Taming a functional group: creating air-stable, chiral primary phosphanes. Angew Chem 118:7406–7409
40. Bartlett RA, Olmstead MM, Power PP, Sigel GA (1987) Synthesis and spectroscopic and X-ray structural studies of the mesitylphosphines PH_2Mes and $PHMes_2$ (Mes = 2,4,6-$Me_3C_6H_2$) and their lithium salts [$Li(THF)_3PHMes$] and [{$Li(OEt_2)PMes_2$}$_2$]. Inorg Chem 26:1941–1946

41. Oldham KB (1985) The steepness of voltammetric waves. J Electroanal Chem 184:257–267
42. Lyne PD, O'Neill RD (1990) Stearate-modified carbon paste electrodes for detecting dopamine in vivo: decrease in selectivity caused by lipids and other surface-active agents. Anal Chem 62:2347–2351
43. Buckler SA (1962) Autoxidation of trialkylphosphines. J Am Chem Soc 84:3093–3097
44. Bartlett PD, Cox EF, Davis RE (1961) Reactions of elemental sulfur. IV. Catalytic effects in the reaction of sulfur with triphenylphosphine. J Am Chem Soc 83:103–109
45. Hudson HR (1990) Nucleophilic reactions of phosphines. In: Hartley FR (ed) The chemistry of organophosphorus compounds, vol 1. Wiley, New York, pp 438–439 and references therein
46. Miqueu K, Sotiropoulos J-M, Pfister-Guillouzo G, Rudzevich V, Romanenko V, Bertrand G (2004) Role of the 2,6-Bis(trifluoromethyl)phenyl group on the acidity of the corresponding phosphane. Eur J Inorg Chem 381–387
47. Nyulászi L, Szieberth D, Csonka GI, Réffy J, Heinicke J, Veszprémi T (1995) The photoelectron spectrum and conformation of phenylphosphine and phenylarsine. Struct Chem 6:1–7
48. Cabelli DE, Cowley AH, Dewar MJS (1981) UPE studies of conjugation involving group 5A elements. 1. Phenylphosphines. J Am Chem Soc 103:3286–3289
49. Debies TP, Rabalais JW (1974) Photoelectron spectra of substituted benzenes. III. Bonding with Group V substituents. Inorg Chem 13:308–312
50. Stewart B, Harriman A, Higham LJ (2010) Predicting the air-stability of phosphines. Submitted to organometallics om-2011-00070a
51. Hayashi T (2000) Chiral monodentate phosphine ligand MOP for transition-metal-catalyzed asymmetric reactions. Acc Chem Res 33:354–362 and references therein
52. Cai D, Payack JF, Bender DR, Hughes DL, Verhoeven TR, Reider PJ (1994) Synthesis of chiral 2,2′-Bis(diphenylphosphino)-1,1′-binaphthyl (BINAP) via a novel nickel-catalyzed phosphine insertion. J Org Chem 59:7180–7181
53. Kurz L, Lee G, Morgans D Jr, Waldyke MJ, Ward T (1990) Stereospecific functionalization of (R)-(−)-1,1′-Bi-2-naphthol triflate. Tetrahedron Lett 31:6321–6324
54. The use of MOPs in catalysis which resulted in low/moderate enantioselectivities: Sakai M, Ueda M, Miyaura N (1998) Rhodium-catalyzed addition of organoboronic acids to aldehydes. Angew Chem Int Ed 37: 3279–3281
55. The use of MOPs in catalysis which resulted in low/moderate enantioselectivities: Sakai M, Ueda M, Miyaura N (1998) Rhodium-catalyzed addition of organoboronic acids to aldehydes. Angew Chem 110:3475–3477
56. The use of MOPs in catalysis which resulted in low/moderate enantioselectivities: Park H, RajanBabu TV (2002) Tunable ligands for asymmetric catalysis: readily available carbohydrate-derived diarylphosphinites induce high selectivity in the hydrovinylation of styrene derivatives. J Am Chem Soc 124:734–735
57. Hiney RM, Ficks A, Gilheany DG, Higham LJ (2011) Diverse MOP ligands from air-stable chiral primary phosphines. Manuscript in preparation
58. Bruneau C, Renaud J-L (2008) Monophosphinites, -aminophosphinites, -phosphonites, -phosphites and -phosphoramidites. In: Börner A (ed) Phosphorus ligands in asymmetric catalysis: synthesis and applications. Wiley-VCH, Weinheim, pp 36–69
59. Göthlich APV, Tensfeldt M, Rothfuss H, Tauchert ME, Haap D, Rominger F, Hofmann P (2008) Novel chelating phosphonite ligands: syntheses, structures, and nickel-catalyzed hydrocyanation of olefins. Organometallics 27:2189–2200
60. Zhao B, Peng X, Wang Z, Xia C, Ding K (2008) Modular chiral bidentate phosphonites: design, synthesis, and application in catalytic asymmetric hydroformylation reactions. Chem Eur J 14:7847–7857
61. Weferling NZ (1987) New methods for the chlorination of organophosphorus compounds with P–H functions. Z Anorg Allg Chem 548:55–62
62. Burk MJ (1991) C_2-symmetric bis(phospholanes) and their use in highly enantioselective hydrogenation reactions. J Am Chem Soc 113:8518–8519

63. Burk MJ (2000) Modular phospholane ligands in asymmetric catalysis. Acc Chem Res 33:363–372
64. Shang G, Zhang X (2008) Phospholes, phospholenes, phospholanes and phosphinanes. In: Börner A (ed) Phosphorus ligands in asymmetric catalysis: synthesis and applications. Wiley-VCH, Weinheim, pp 135–177
65. Kadyrov R, Monsees A (2008) Practical routes to chiral phospholanes. In: Börner A (ed) Phosphorus ligands in asymmetric catalysis: synthesis and applications. Wiley-VCH, Weinheim, pp 1234–1243
66. Saha B, RajanBabu TV (2007) Syntheses and applications of 2-phosphino-2′-alkoxy-1,1′-binaphthyl ligands. Development of a working model for asymmetric induction in hydrovinylation reactions. J Org Chem 72:2357–2363
67. Shi M, Chen L-H (2003) Chiral phosphine Lewis base catalyzed asymmetric aza-Baylis-Hillman reaction of *N*-sulfonated imines with methyl vinyl ketone and phenyl acrylate. Chem Commun 1310–1311
68. Higham LJ, Whittlesey MK, Wood PT (2004) Water-soluble hydroxyalkylated phosphines: examples of their differing behaviour toward ruthenium and rhodium. Dalton Trans 4202–4208
69. Pinault N, Bruce DW (2003) Homogeneous catalysts based on water-soluble phosphines. Coord Chem Rev 241:1–25
70. Smith CJ, Sieckman GL, Owen NK, Hayes DL, Mazuru DG, Kannan R, Volkert WA, Hoffman TJ (2003) Radiochemical investigations of gastrin-releasing peptide receptor-specific [^{99m}Tc(X)(CO)$_3$-Dpr-Ser-Ser-Ser-Gln-Trp-Ala-Val-Gly-His-Leu-Met-(NH$_2$)] in PC-3, tumor-bearing, rodent models: syntheses, radiolabeling, and in vitrolin vivo studies where Dpr = 2,3-diaminopropionic acid and X = H_2O or $P(CH_2OH)_3$. Cancer Res 63:4082–4088
71. Schibli R, Katti KV, Volkert WA, Barnes CL (2001) Development of novel water-soluble, organometallic compounds for potential use in nuclear medicine: synthesis, characterization, and ^{1}H and ^{31}P NMR investigations of the complexes *fac*-[ReBr(CO)$_3$L] (L = bis(bis(hydroxymethyl)phosphino)ethane, bis(bis(hydroxymethyl)phosphino)benzene). Inorg Chem 40:2358–2362
72. Börner A (2004) Other concepts: hydroxyphosphines as ligands. In: Cornils B, Herrmann WA (eds) Aqueous-phase organometallic catalysis, 2nd edn. Wiley-VCH, Weinheim, pp 187–193
73. Joó F, Kathó A (1997) Recent developments in aqueous organometallic chemistry and catalysis. J Mol Catal A Chem 116:3
74. Henderson W, Alley SR (2002) Ferrocenyl hydroxymethylphosphines (η^5–C_5H_5)Fe[η^5–$C_5H_4P(CH_2OH)_2$] and 1,1′-[Fe{η^5–$C_5H_4P(CH_2OH)_2$}$_2$] and their chalcogenide derivatives. J Organomet Chem 658:181–190
75. Gonschorowsky M, Merz K, Driess M (2006) Cyclohexylbis(hydroxymethyl)phosphane: a hydrophilic phosphane capable of forming novel hydrogen-bonding networks. Eur J Inorg Chem 455–463
76. Uozumi Y, Kitayama K, Hayashi T (1993) Regio- and enantioselective hydrosilylation of 1-arylalkenes by use of palladium-MOP catalyst. Tetrahedron Asymmetry 4:2419–2422
77. Uozumi Y, Hayashi T (1991) Catalytic asymmetric synthesis of optically active 2-alkanols via hydrosilylation of 1-alkenes with a chiral monophosphine-palladium catalyst. J Am Chem Soc 113:9887–9888
78. Jensen JF, Svendsen BY, la Cour TV, Pedersen HL, Johannsen M (2002) Highly enantioselective hydrosilylation of aromatic alkenes. J Am Chem Soc 124:4558–4559
79. Kitayama K, Uozumi Y, Hayashi T (1995) Palladium-catalysed asymmetric hydrosilylation of styrenes with a new chiral monodentate phosphine ligand. J Chem Soc Chem Commun 1533–1534
80. Hayashi T, Hirate S, Kitayama K, Tsuji H, Torii A, Uozumi Y (2001) Asymmetric hydrosilylation of styrenes catalyzed by palladium-MOP complexes: ligand modification and mechanistic studies. J Org Chem 66:1441–1449

81. Kumar PGA, Dotta P, Hermatschweiler R, Pregosin PS (2005) Bonding in palladium(II) and platinum(II) allyl MeO- and H-MOP complexes. Subtle differences via ^{13}C NMR. Organometallics 24:1306–1314 and references cited therein
82. Armanino N, Koller R, Togni A (2010) Electrophilic trifluoromethylation of primary phosphines: synthesis of a *P*-bis(trifluoromethyl) derivative of BINAP. Organometallics 29:1771–1777

Chapter 2
Phosphine Acetylenic Macrocycles and Cages: Synthesis and Reactivity

Wannes Weymiens, J. Chris Slootweg and Koop Lammertsma

Abstract The syntheses, structural properties, and reactivities are reviewed for phosphine-acetylenic macrocycles and cages. These compounds are of current interest for their phosphorus-containing π-conjugated molecular frameworks. A distinction is made between organic compounds, in which the building blocks are assembled by consecutive transformations, and organometallic structures, in which the coordinative ability of phosphorus is employed to assemble the monomeric building blocks.

2.1 Introduction

Phosphorus-containing π-conjugated materials have potential in (opto)-electronic devices because of their conjugative properties [1–4]. Incorporating phosphorus atoms into carbon molecular frames adds a new dimension, enabling communication between carbon-based units over phosphorus-based connectors. In this chapter we focus on phosphine-acetylenic units of the type $R_2P–(C{\equiv}C)_n–R$ as building blocks from which such macrocyclic systems can be assembled either by consecutive transformations or by means of organometallic structures that make use of the coordinative ability of phosphorus. Molecular assemblies of phosphorus-bridged acetylenic units are termed phosphapericyclines and those with larger spacers, such as diacetylenes, 'exploded' pericyclines.

Besides the covalent main group molecular frameworks, also organometallic macrocycles and cages are known in which the transition metal centers are

W. Weymiens · J. C. Slootweg · K. Lammertsma (✉)
Department of Chemistry and Pharmaceutical Sciences, Faculty of Sciences, VU University Amsterdam, De Boelelaan 1083, 1081 HV, Amsterdam, The Netherlands
e-mail: k.lammertsma@vu.nl

M. Peruzzini and L. Gonsalvi (eds.), *Phosphorus Compounds*, Catalysis by Metal Complexes, 37, DOI: 10.1007/978-90-481-3817-3_2,
© Springer Science+Business Media B.V. 2011

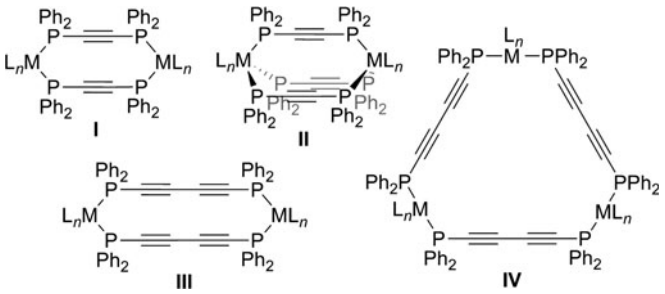


Fig. 2.1 Phosphine acetylenic macrocycles assembled through metal coordination

connected by two or three bis(diphenylphosphino)acetylene (dppa) ligands, as in dimeric $[(ML_n)_2(\mu\text{-dppa})_2]$ (**I**), $[(ML_n)_2(\mu\text{-dppa})_3]$ (**II**) and 'exploded' $[(ML_n)_2(\mu\text{-dppda})_2]$ (**III**), but trimeric systems like **IV** are also known and even tetrameric macrocycles have been reported (Fig. 2.1).

Before embarking on their building block potential, we note that phosphine-acetylenes are also gaining ground as acceptor ligands with small cone angles [5] as in Au-catalyzed alkyne cyclizations [6] and Rh-catalyzed hydrosilylation of ketones [7]. Their synthetic potential is larger than the here presented scope as indicated by the rhodium-catalyzed assembly of bulky arylphosphines (**1**) [8] and triazole-based phosphascorpionate ligands (**2**) [9], generated by a triple 'click'-reaction of $OP(C{\equiv}CH)_3$ with phenyl azide (Fig. 2.2).

Conjugated P/C rings and cages without acetylenic units will not be discussed, except for the few that are prepared from low-valent P-fragments and acetylenic units (Fig. 2.3). Exemplary amongst the extensively reviewed three-membered ring structures [10, 11] are the thiophene-substituted (**4**) [12] and extended (**5**,**6**) [13] phosphirenes that are obtainable by [1 + 2]-cycloaddition of electrophilic phosphinidene complexes to triple bonds [14, 15]. Very diverse simple P/C-cages can be prepared by cyclooligomerization of phosphaalkynes (P≡CR), a topic that has been well reviewed [16–22]. Illustrative examples are cubane **8** [23], prismane **10** [24, 25], and pentaprismane **13** (Fig. 2.4) [26, 27].

2.2 Organic Phosphine Acetylenic Macrocycles and Cages

Pericyclines are macrocyclic structures, in which saturated corner atoms are connected by ethynyl linkages [28–30]. Examples where this acetylenic scaffolding [31–35] is extended in three-dimensional space are the 'exploded' cubane **14** [36] and cyclophane 15 [37–39] (Fig. 2.5). Few silapericyclines [40–49] are known and those with other heteroatoms are even rarer [50]. Attempts to synthesize the parent 3D analogues of the phosphapericyclines [51], tetrahedron **16**, and cubes **17** and **18** (Fig. 2.6) were unsuccessful [52, 53]. DFT calculations indicated the cubes to exhibit cyclic delocalization, as suggested by the elongated

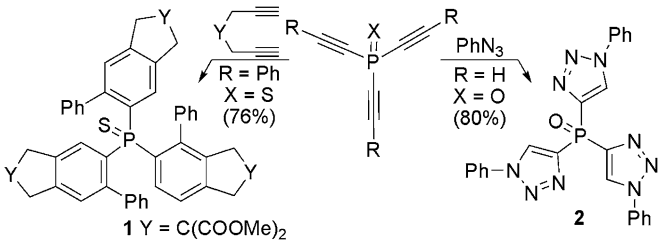


Fig. 2.2 Application of phosphine acetylenes in the construction of bulky arylphosphines (**1**) and phosphascorpionates (**2**)

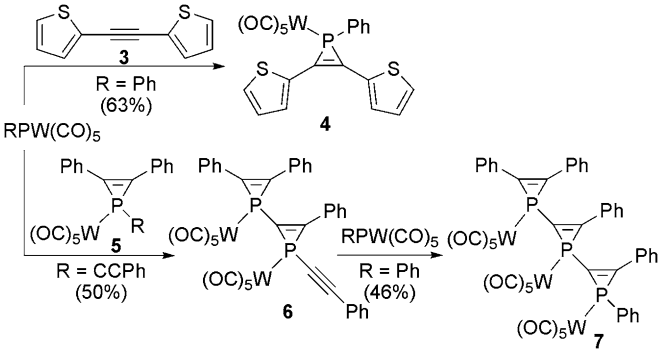


Fig. 2.3 P/C rings (**4**, **6**, **7**) obtained from phosphinidene addition to CC triple bonds

C≡C and shortened P–C bonds. We describe in this section reported approaches toward differently sized P/C rings and cages using phosphorus containing building blocks [53].

2.2.1 Pericycline-Based Macrocycles

The first phosphapericyclines were reported in 1990 by Scott and Unno [52]. By condensing *t*-BuPCl$_2$ with doubly deprotonated **19** and **20**, both formed from *t*-BuPCl$_2$ and HC≡CMgBr, they were able to generate small quantities of tetraphospha[4]pericycline **21** (11%) and triphospha[3]pericycline **22** (16%), respectively (Fig. 2.7). Four isomers were observed in the product mixture of **21** and one for **22**. The most abundant *cis*,*cis*,*trans*-**21** isomer shows three resonances in the ^{31}P NMR spectrum, while each of the others show a single one. X-ray crystal structures were reported for all-*trans*-**21** and *cis*,*trans*-**22**. Both compounds display a broad UV-absorption around 225 nm, which is indicative of (cyclic) electronic delocalization, either over the phosphorus centers or by means of through-space interaction of the in-plane acetylenic π-bonds [52].

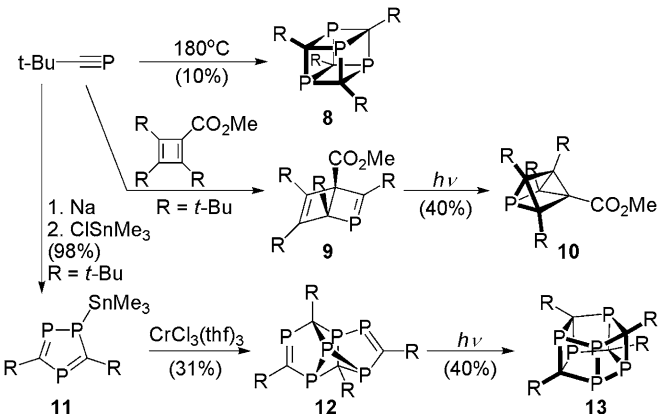


Fig. 2.4 P/C cages obtained by cyclooligomerization of phosphaalkynes (**11–13**)

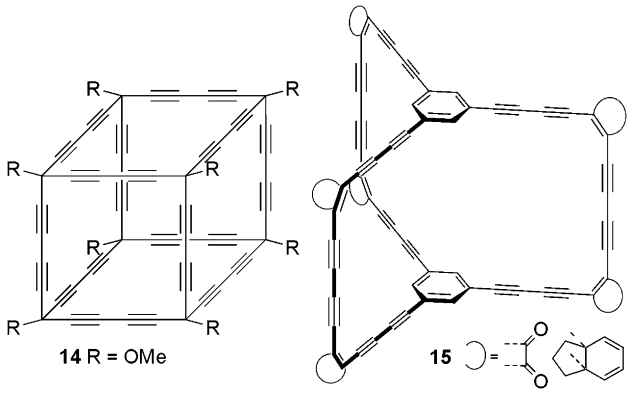


Fig. 2.5 Acetylenic carbon scaffolds

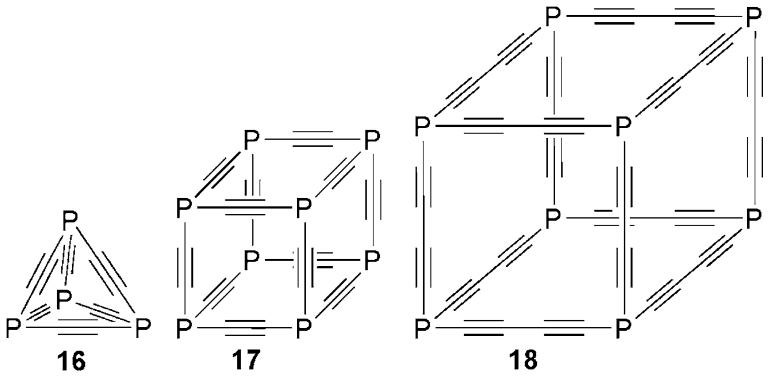


Fig. 2.6 Phosphine acetylenic scaffolding in 3-D

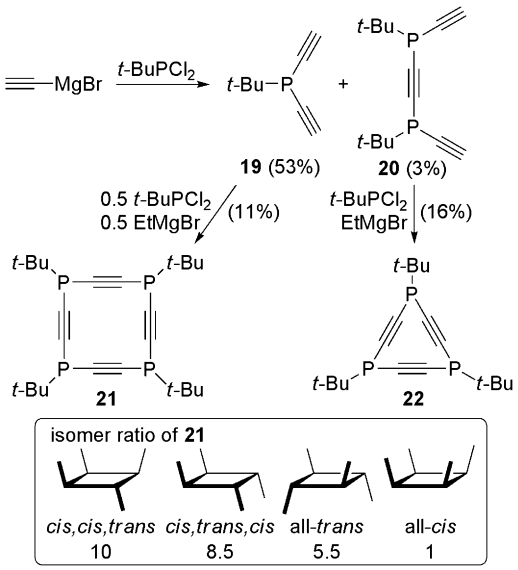


Fig. 2.7 Synthesis of tetraphospha[4]pericycline **21** and triphospha[3]pericycline **22**

Tetraphospha[4]pericycline **25**, bearing $(i\text{-Pr})_2N$ substituents, was obtained likewise as a mixture of four isomers directly from the reaction of **23** with $(i\text{-Pr})_2NPCl_2$ (9%) or via intermediate **24** (Fig. 2.8) [53]. However, due to its instability, purification of **24** was not possible and the product ratio and yield of **25** did not improve.

The amino substituents of these systems can be exchanged for others, as shown for **26**, where an additional acetylene moiety is introduced to give tris(acetylene)phosphines **27** (Fig. 2.9), a process that only works for λ^3-phosphines [53]. The introduction of this differently protected acetylene moiety could make **27** a building block for the synthesis of three-dimensional frameworks, e.g., **16–18**, but such chemistry remains to be explored.

12-Membered square **28** with alternating silicon and phosphorus atoms at its corners has been synthesized in very low yield (2.3–6.4%) by treating $(R^1)_2Si(C{\equiv}CH)_2$ (R^1 = Ph, *i*-Pr) with EtMgBr and R^2PCl_2 (R^2 = Ph, *t*-Bu) (Fig. 2.10) [54]. X-ray crystal structures were reported for the *trans*-isomers. Macrocycle **28b** has a center of symmetry and a flat 12-membered ring, while the molecular structures of **28a** and **28c** deviate slightly from planarity, having dihedral angles between the P–Si–P planes of 177.6° and 176.4°, respectively. The *cis*-isomer was observed in an equimolar amount for **28a**, present as a trace for **28b**, and absent for **28c**.

Square 1,7-diphospha[4]pericycline (**30**) and hexagon 1,7,13-triphospha[6]pericycline (**31**) with alternating carbon- and phosphorus-based corners result from the subsequent treatment of 3,3-dimethyl-1,4-pentadiyne (**29**) with *n*-BuLi and *t*-$BuPCl_2$ (Fig. 2.11) [28–30, 55]. *Cis*-**30** (2.2%), *trans*-**30** (1.3%), and *cis*,*trans*-**31** (1.0%) could be isolated, but all-*cis*-**31** not. 3,3,6,6,9,9-Hexamethyl-1,4,7,10-undecatetrayne (**32**) gives similarly monophospha[4]pericycline **33** (1.3%) and

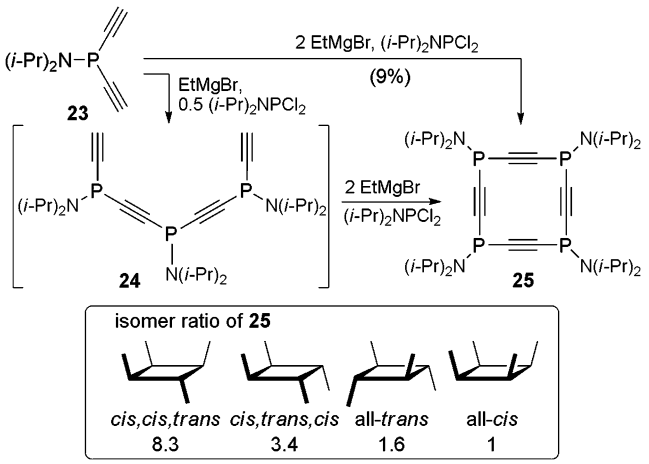


Fig. 2.8 One-step and stepwise synthesis of tetraphospha[4]pericycline **25**

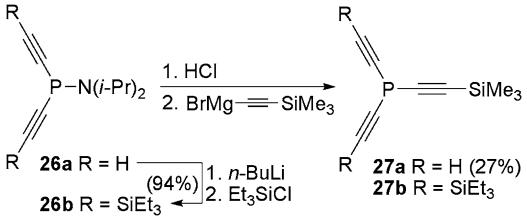


Fig. 2.9 The construction of nonsymmetrically protected tris(acetylene)phosphines **27**

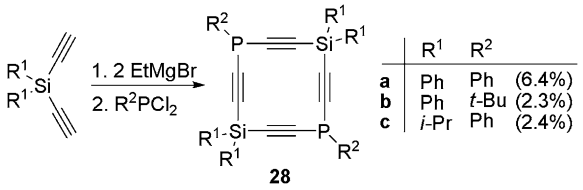


Fig. 2.10 Synthesis of diphosphadisila[4] pericyclines **28**

1,13-diphospha[8]pericycline **34** (2.5%). It was speculated that the low yields may be due to rapid oxidation of the products in air. Mixed heterocyclic 1-phospha-7-thio[4]pericyclines **36**, which does not oxidize in air, has been prepared from bis(3,3-dimethyl-1,4-pentadiynyl)-sulfane (**35**) in 5.6% yield (Fig. 2.12) [28–30, 55].

2.2.2 Exploded Pericycline-Based Macrocycles

Exploded phospha[*n*]pericyclines (**38**, $n = 3$–6) with butadiyne linkages have been prepared by Märkl et al., both by a one-pot approach and by stepwise

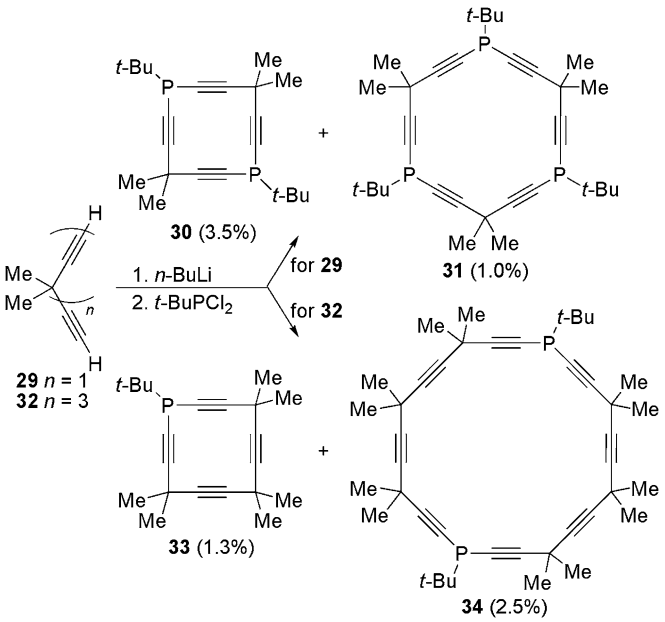


Fig. 2.11 Mono-, di- and triphosphapericyclines

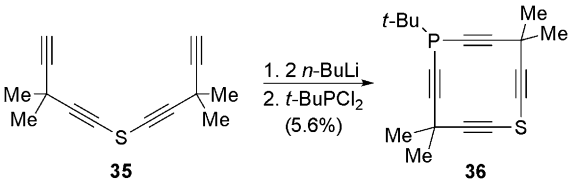


Fig. 2.12 Phosphathio[4]pericycline **36**

coupling of open-chain precursors (Fig. 2.13) [60]. One-pot oxidative Eglinton coupling of building block Mes*P(C≡CH)$_2$ (**37**, Mes* = 2,4,6-tri-*tert*-butylphenyl) using Cu(OAc)$_2$ was reported to give a mixture of four macrocycles (**38a–d**), of which triangular **38a** and pentagonal **38c** could be isolated in very small amounts; square **38b** and hexagonal **38d** were inseparable. The stepwise (de)protection approach performed better. Eglinton coupling of **39a** gave mainly dimer **38b** (86%) with some trimer and tetramer. This product mixture was not separated, since all products could be obtained in pure form by different approaches. In this respect, coupling of **39b** yielded mainly triangle **38a** (70%) with only some dimer (hexagonal **38d**) and also the coupling of **39c** gave mainly the monomer (**38b**). Eglinton coupling of **39f** afforded ring-closed octagonal product **38e** (9%), which was not obtained in the one-pot procedure, while pentagonal species **38c** was obtained only via this procedure [56].

Triangular 15-membered **38a** is present in solution as a mixture of *cis*,*trans* and all-*cis* isomers in 1.3:1 ratio as determined by ^{31}P NMR. The barrier for phosphorus

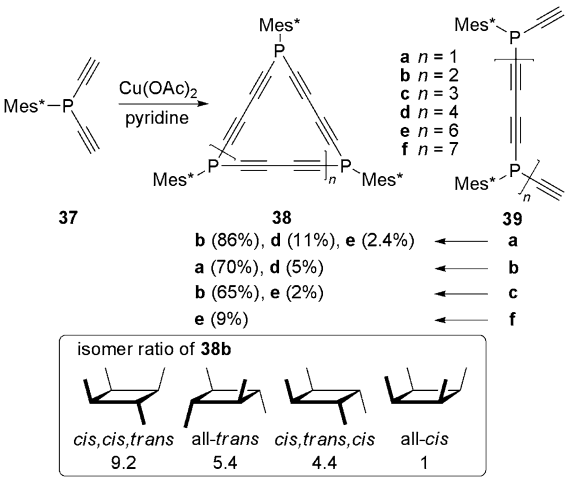


Fig. 2.13 Exploded phospha[*n*]pericyclines **38** via a one-pot approach from **37** and from linear precursors **39**

inversion of 18 kcal/mol, deduced from the ^{31}P NMR coalescence temperature of 83.8 °C, is much less than the typical 30–34 kcal/mol for phosphines [57, 58] and was attributed to the stabilized planar 18e aromatic transition in which the phosphorus lone pairs overlap with the out-of-plane acetylene π-bonds. Surprisingly, linear **39a** may have an even lower inversion barrier, as its ^{31}P NMR resonances coalesce already at 3 °C. The four isomers of 20-membered **38b** are distinguishable at −20 °C by ^{31}P NMR spectroscopy, while only one single sharp signal was observed at 140 °C. At room temperature one broad ^{31}P NMR resonance was observed for the 30-membered hexagonal **38d** and a sharp one for the 40-membered octagonal **38e** [56]. This behavior may indicate either a further lowering of the phosphorus inversion barrier or dynamic behavior of the macrocycle.

Square and hexagonal phospha[*n*]pericyclines **41** and **42** have been obtained by oxidative Hay coupling of building block **40** (Fig. 2.14), which was synthesized from $(i\text{-Pr})_2$NP(O)(C≡CH)$_2$ by oxidative coupling [59]. Macrocycle **41** consists of several isomers, cf. **38b**, as suggested by the observed four ^{31}P NMR resonances, whereas 30-membered ring structure **42** shows one sharp signal, due to the all-*cis* or all-*trans* isomer, and a broad signal for the other isomers. The whisker-like 'crystals' of **42** suggest the formation of nanotubes from one-dimensional stacking of the macrocycle in the solid phase [59].

2.2.3 Miscellaneous Macrocycles

Coupling of $(i\text{-Pr})_2$NP(O)Br$_2$ with dilithiated 1,2-bisethynylbenzene reportedly gives ring structure **43** in a 2:3 *cis*:*trans* ratio (Fig. 2.15) [59]. The X-ray crystal structure for the *trans*-isomer revealed a puckered macrocycle due to the pyramidal nature of the phosphorus centers.

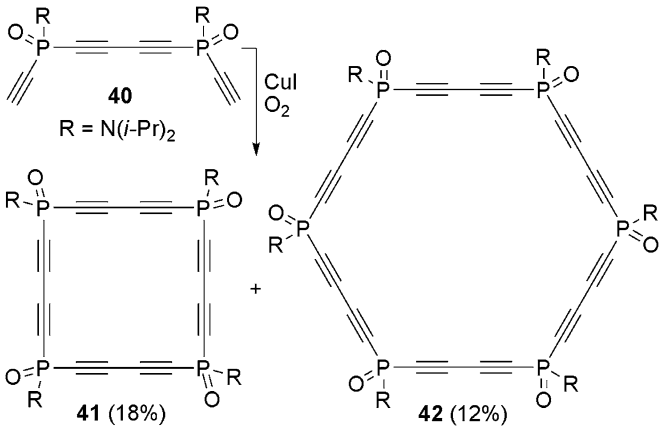


Fig. 2.14 Exploded phospha[*n*]pericyclines **41** ($n = 4$) and **42** ($n = 6$)

The only known phosphole-based acetylenic macrocycle, 10-membered **47**, was synthesized by Mathey et al. [60], who coupled C_2Cl_4 with diphosphole dianion **46** (Fig. 2.16). The dianion was generated by sodium cleavage of cyclotetraphosphole **45** that was obtained from monomer **44** by condensations reactions involving a series of [1–4, 8] sigmatropic shifts and dehydrogenations. The X-ray crystal structure of **47** shows bending of the P–C≡C units (170–174°), implying a strained system.

2.2.4 Phosphine Acetylenic Cages

The synthesis of three-dimensional structures, in which phosphapericycline units are extended in the third dimension, was pursued by Scott and co-workers [28–30, 55]. In pursuit of phosphapericycline-based cage **48**, they treated precursor triethynylphosphine **49**, prepared from *t*-BuP(C≡CH)$_2$ (**19**) and PCl_3, with EtMgBr followed by $POCl_3$ trapping. Instead of **48**, they obtained the remarkable phosphine acetylenic cage **51**, likely formed by dimerization of intermediate **50** (Fig. 2.17). Molecular cage **51**, of which an X-ray structure was reported [28–30, 55], is so far the only known compound with a 3D phosphine-acetylenic architecture without the presence of transition metal complexes.

Characteristic to phosphine based P/C molecular frames described in this chapter is the difficulty in preparing and isolating them. Most reactions give low yields of inseparable mixtures of isomers, which are further complicated by their sensitivity to oxidation. Assembling macrocycles and cages based on the phosphine acetylene moiety can be helped by making use of the ability of the phosphorus atom to coordinate to transition metal complexes. The next section describes these P/C ring structures with transition metals.

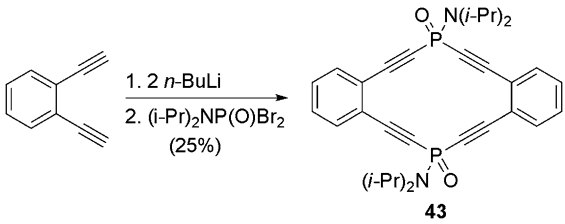


Fig. 2.15 Formation of 14-membered macrocycle **43**

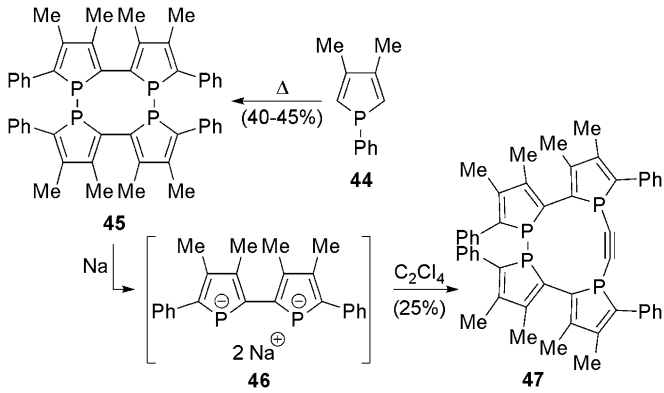


Fig. 2.16 Synthesis of phosphole-based acetylenic macrocycle **47**

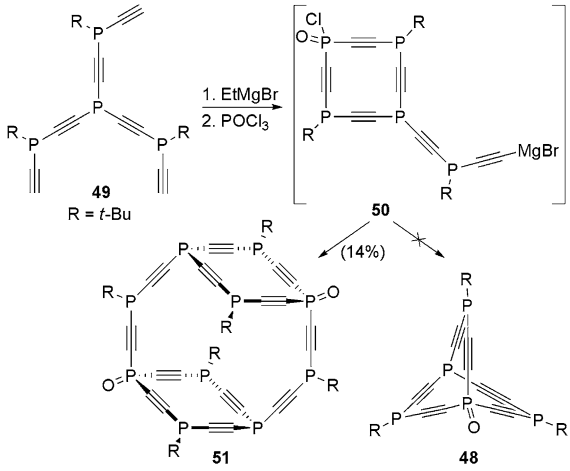


Fig. 2.17 Construction of phosphine-acetylenic Cage **51**

2.3 Organometallic Phosphine Acetylenic Macrocycles and Cages

We start by addressing first the chelating diphosphaacetylenic unit that forms the rigid rod in the transition metal embedded P/C macrocycles and cages **I–IV** (Fig. 2.1). The potential of bis(diphenylphosphino)acetylene (dppa) and its 'exploded' variant bis(diphenylphosphino)diacetylene (dppda) as bi- and tridentate binuclear diphosphine bridging ligands was recognized in the late 1960s. Due to its rigidity, dppa cannot chelate a single metal center and only twice has dppa been reported to bridge a metal–metal bond [61, 62]. Coordination occurs preferentially through the phosphorus atoms, leaving the acetylenic moiety unperturbed. With a few exceptions [63–66], carbon–carbon triple bond coordination occurs only when both phosphorus lone pairs are blocked by metal centers [67, 68]. It is of note that when coordination of the alkyne moiety occurs, the linear dppa fragment bends, thereby enabling it to bridge a metal–metal bond and even chelate a single metal center [69–71].

The extent of metal-P coordination is reflected in the Raman C≡C stretch frequency [72]. Uncoordinated dppa has a lower ν(C≡C) of 2,097 cm^{-1} than most disubstituted acetylenes (ν = 2,190–2,260 cm^{-1}) as the conjugated phosphorus lone pair causes π-electron depletion from the triple bond (Fig. 2.18). Transition metal complexation suppresses this effect. The magnitude of $\Delta\nu$(C≡C), i.e., ν(complexed dppa) − ν(free dppa), then reflects the degree of P → M σ-bonding. Electron depletion of the triple bond has been inadvertently attributed to the contribution of P(d,π) orbitals, as well as M → P π-bonding to the increase in $\Delta\nu$(C≡C) [72].

2.3.1 Dppa- and Dppda-Based Pt and Pd Containing Macrocycles

Carty and coworkers conducted the first coordination studies on dppa. They prepared $[(MX_2)_2(\mu\text{-dppa})_2]$ (M = Pt, **52**; Pd, **53**) by mixing the ligand and the corresponding tetrahalometallate ($NaMX_4$; X = Cl, Br, I). $NaMCl_4$ with additional KSCN afforded the corresponding thiocyanates **52**, **53d** (Fig. 2.19) [73, 74].

X-ray crystal structures show a planar arrangement for binuclear $PdCl_2$ macrocycle **53a**, with both square planar coordination spheres in the same plane, while the macrocyles of the $PtCl_2$ (**52a**) and PtI_2 (**52c**) complexes are highly puckered with angles θ between the Pt-coordination planes of 32.8 and 42.5°, respectively (Fig. 2.20) [68, 75]. This difference was attributed to the dominant ring π-bonding in the palladacycle, while the platinacycles favor an orthogonal orientation of the

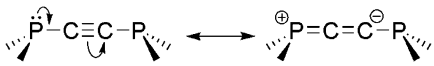


Fig. 2.18 Resonance structures of dppa

P–Pt bonds from the same bridge, to align each of them with one of the C≡C π-orbitals.

Ligand exchange of the monodentate phosphine ligands of $[(MCl(PMe_2Ph))_2(\mu\text{-}Cl)_2]$ (**54**, M = Pt, Pd) for dppa also led to **52a** and **53a** (Fig. 2.21). Formation of heterobimetallic macrocycle **55** via a similar ligand exchange from mixed complex **54c** was not conclusive as co-crystallization of **52a** and **53a** could not be excluded as in solution, the three metallocycles (**52a**, **53a** and **55**) equilibrate by exchange of $PtCl_2$ and $PdCl_2$ [76].

By the addition of one or two equivalents of $PdCl_2$ to **52a** or **53a**, the alkyne-coordinated tri- and tetrametallic species **56** and respectively **57** could be obtained (Fig. 2.22) [68]. On the other hand, adding $PtCl_2$ to platinacycle **52a** gave no reaction, while with palladacycle **53a** only metal exchange occurred, resulting in an equilibrium between Pt_2 complex **52a**, Pd_2 complex **53a**, and heterobimetallic **54** [76]. The terminal Cl ligands of **52a** or **53a** can be exchanged by iodide ligands, forming **52c** or **53c**, or by one or four nitro ligands, giving mononitro platinacycle **52e** or tetranitro palladacycle **53e**. Exchange of two chlorines of **52a** with 2,2′-bipyridine (bipy) affords **58**, but this complex is too sterically congested for a second bipy ligand to add. Furthermore, the platinum center of **52a** can be oxidized with chlorine to *cis*-$[(PtCl_4)_2(\mu\text{-dppa})_2]$ (**52f**; Fig. 2.22) [68].

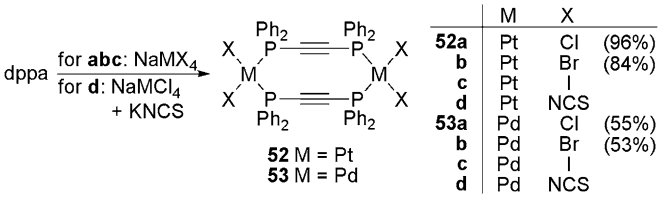


Fig. 2.19 First dppa-based macrocycles

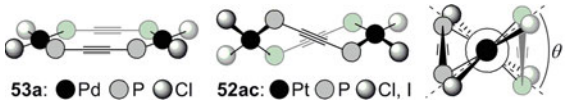
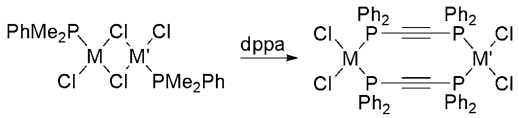


Fig. 2.20 Schematic representations of the solid state structures of palladacycle **53a** and platinacycles **52ac**. θ is the angle between both Pt-coordination planes

Fig. 2.21 Formation of **52a**, **53a** and mixed metal species **55**



Terminal methyl and CF_3-ligated analogues of **52a** were obtained by dppa ligand exchange from the corresponding [Pt(COD)] complexes, affording $[(Pt(R_2)_2(\mu\text{-dppa})_2]$ (**59a** R = CH_3; **59b** R = CF_3) [77]. Lowering in $\Delta\nu$(C≡C) from 39 cm^{-1} for Cl-ligated **52a** to 34 cm^{-1} for CF_3-ligated **59b** and 27 cm^{-1} for CH_3-ligated **59a** implies a decrease in acceptor power of the platinum centre [77]. Similar exchange with the extended dppda gave besides exploded **60a** also some trimer **61a** (Fig. 2.23) [78]. The dimer has a twisted structure with orthogonal planar Pt-centers ($\theta = 86°$; cf. **52a** (Fig. 2.20)). In the trimer, these centers are nearly orthogonal ($\sim 74°$) to the plane of the three Pt atoms, giving rise to a helical structure. The analogous approach toward chloro derivatives **60b** and **61b** gave instead the formal [4 + 4]-cycloadduct **62** and [4 + 4 + 4]-cycloadduct **63**, both having planar central rings with alternating double and triple bonds (Fig. 2.23). Exchange of the methyl ligands for chlorides, using HCl for **60a** and CuCl for **61a**, results in immediate rearrangement; the intermediate chloro-macrocyles **60b** and **61b** only stable below −20 °C [78].

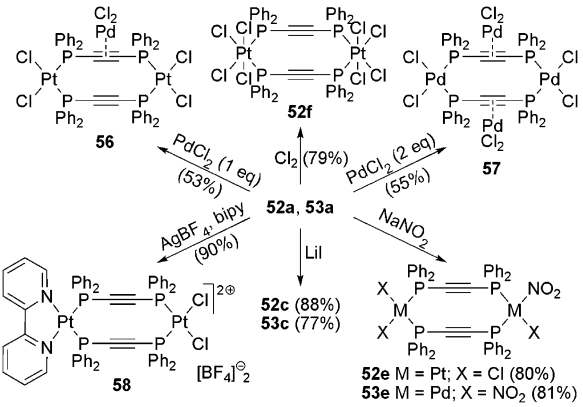


Fig. 2.22 Modifications of platinacycle **52a** and palladacycle **53a**

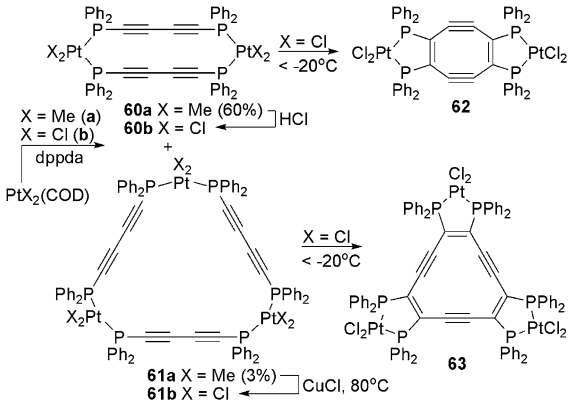


Fig. 2.23 Exploded platinacyles **60** and **61** and their rearranged products

Pt- and Pd-macrocycles with pendant phosphines are also known. Low yields were reported for $[(M(PPh_3)_2)_2(\mu\text{-dppa})_2]$ (**64** M = Pt; **65** M = Pd) on mixing $[M(PPh_3)_4]$ with dppa (21% for **64** and 14% for **65**) [79], but high yields of $[(M(dppm))_2(\mu\text{-dppa})_2][(OTf)_4]$ (**66** M = Pt; **67** M = Pd; dppm = bis(diphenylphosphino)methane) were obtained by mixing $[(dppm)M(OTf)_2]$ and dppa (Fig. 2.24). X-ray analysis of platinacycle **66** revealed a planar ring structure as the dppm bite-angle (70°) enlarges the ring P–Pt–P angle [80]. The corresponding Pt(0) system with bis(diphenylphosphino)ethane (dppe), $[(Pt(dppe))_2(\mu\text{-dppa})_2]$ (**68**) was obtained by reductive Cl-exchange from **52a**, but those with still larger chelating ligands proved inaccessible [81]. Reaction of $[(dppm)Pt(OTf)_2]$ with excess dppa gives **69** with pendant dppa ligands, that reacts with added $[(dppm)Pd(OTf)_2]$ to the mixed bimetallic macrocycle **70** (Fig. 2.24); the addition of the metallic complexes can also be reversed [80].

Bimetallic **66**, **67**, and **70** are photoluminescent [80]. Excitation at $\lambda = 450$ nm causes Pt species **66** to emit at $\lambda_{em} = 512$–518 nm ($\Phi_F = 2.3$–4.0×10^{-2}) and the Pd analogue **67** at $\lambda_{em} = 530$–532 nm ($\Phi_F = 3.4$–5.9×10^{-3}); the absorption maxima of the Pd species are significantly red-shifted ($\lambda_{abs} = 345$–350 nm) with respect to the Pt one ($\lambda_{abs} = 272$–273 nm). Heterobimetallic complex **70** exhibits absorptions attributable to both the Pt and Pd centers, but emission occurs only from the Pd center ($\lambda_{em} = 530$ nm, $\Phi_F = 9.0 \times 10^{-3}$), which was suggested to be caused by energy transfer between the metal centers. Guest inclusion in the cavity of **66**, as monitored by Φ_F, revealed the smaller anisole to bind more tightly than dimethoxybenzene, while a small change in the ^{31}P NMR chemical shift of ~0.2 ppm for the dppa phosphorus atom of **67** was taken to indicate guest inclusion [80].

Alkyne ligated macrocycle **71**, obtained from dppa and $[(COD)Pt(C{\equiv}CR)_2]$ (R = Ph, *t*-Bu), reacts with *cis*-$[Pt(C_6F_5)_2(tht)_2]$ (**72**) to form the trinuclear (**73**) and tetranuclear platinum complexes (**74**) without additional coordination to the bridging alkyne units (Fig. 2.25) [82]. This kind of complexation also does not occur for the analogous $[(Pt(C_6F_5)_2)_2(\mu\text{-dppa})_2]$ (**75**), synthesized from *cis*-$[Pt(C_6F_5)_2(tht)_2]$ (**72**) and dppa in 41% yield [82]. The structure of **75** has square planar platinum centers with dppa bridges in a puckered arrangement.

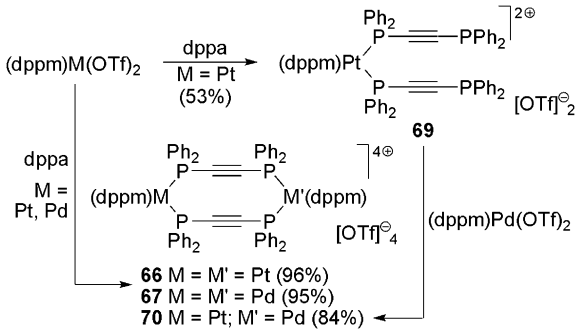


Fig. 2.24 Synthesis of dppm-ligated macrocycles **66**, **67** and **70**

Thiolated complexes **76a–d** are formed by exchange of the Cl ligands of **52a** by the corresponding thiolates [75], or by assembly from $Pt(acac)_2$, dppa and benzene-1,2-dithiol as reported for **76e** (Fig. 2.26). Similarly, reaction with catechol or oxalic acid results in oxo complexes **77** [83], while seleno analogue **78** results from transmetallation between **52a** and $[TiCp_2(Se_2C_2(CO_2Me)_2]$ (Fig. 2.26) [84]. Alternatively, **76d** is also prepared in a stepwise fashion via intermediate $[(Pt(OTf)_2)_2(\mu\text{-dppa})_2]$ (**79**), formed from **52a** and AgOTf, which then reacts with potassium thiolate, giving **76d** in slightly better overall yield (75%) [85]. X-ray crystallography of **76d** showed the presence of two stereoisomers, a left-handed and a right-handed distorted macrocycle. This complex shows photoluminescence at $\lambda_{em} = 469$ nm ($\tau = 78$ ns) [85]. The C≡C vibration observed in the IR spectra of **70**, has been attributed to an asymmetric environment for the acetylenic units caused by disordering of the functional groups [75].

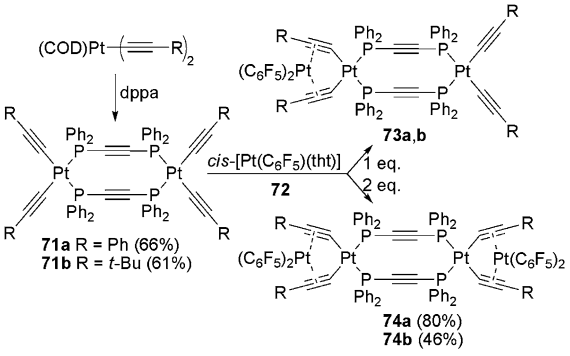


Fig. 2.25 Formation of trimetallic and tetrametallic platinacycles

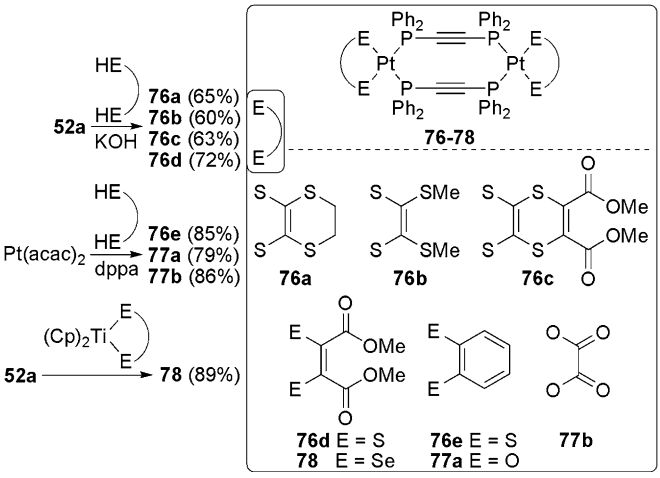


Fig. 2.26 Dichalcogenate complexes of $[Pt_2(\mu\text{-dppa})_2]$ (**76–78**)

2.3.2 Dppa- and Dppda-Based Macrocycles with Other Transition Metals

Numerous transition metals other than platinum and palladium have been used to construct doubly bridged dppa macrocycles, silver being among the first. An early report suggested that treating $[Ag(NO_3)(\mu\text{-dppa})]_n$ (**80**) with dppa and KX ($X = PF_6$, BF_4) gives polymeric $[Ag(\mu\text{-dppa})_2]_n[X]_n$ (**81**; Fig. 2.27), based on the absence of anion coordination to the silver centers and the fact that the polymer gives a conducting colloidal solution in nitrobenzene [86]. A similar reaction with KY (Y = Br, I, NCS) resulted in insoluble polymer material $[AgY(\mu\text{-dppa})]_n$, suggested to have structure **82**, bearing non-cyclic units. Insolubility in nitrobenzene excludes a structure analogous to **81**, with $[AgY_2]$ counter-ions. Similar linear polymers were obtained with mercury, while complexation to cadmium or zinc failed completely [86].

By using cage compound $[Ag_2(\mu\text{-dppa})_3][OTf]_2$ (see Sect. 2.3.4), James and coworkers observed the slow formation of a similar coordination polymer (**83**; Fig. 2.28), for which an X-ray structure analysis showed a distorted tetrahedral geometry for the silver atoms. Polymer formation occurs more rapidly with bulkier bridging ligands [87, 88]. Treatment of $AgSbF_6$ with one equivalent of dppa gives a mixture of mono, di-, and tri-bridged $[Ag_2(\mu\text{-dppa})_n][SbF_6]_2$ in a 1:2:1 ratio; the fully characterized tri-bridged $[Ag_2(\mu\text{-dppa})_3][SbF_6]_2$ can also be prepared exclusively from a 2:3 molar ratio of $AgSbF_6$: dppa (see Sect. 2.3.4) [89].

Reacting one equivalent of dppa with $[Ni(CO)_4]$ results in the formation of $[(Ni(CO)_2)_2(\mu\text{-dppa})_2]$ (**84**) [90] and with *cis*-$[Mo(CO)_4(piperidine)_2]$ in the corresponding *cis*-$[(Mo(CO)_4)_2(\mu\text{-dppa})_2]$ (**85**; Fig. 2.29) [91]. The X-ray crystal structure of **85** revealed a puckered conformation of both dppa bridges analogous to **52a**. Looking down the Mo–Mo axis (Fig. 2.29) one dppa unit is in a staggered conformation and virtually unstrained (∠ Mo–P–C = 108.5°, 110.5°), while the other adopts an eclipsed-type conformation (∠Mo–P–C = 122.7°, 113.3°).

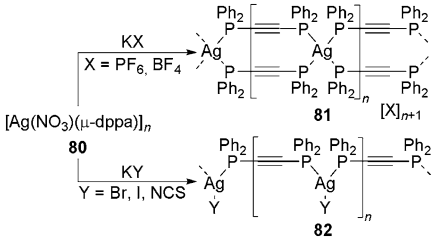


Fig. 2.27 Ag-dppa-based polymers **81** and **82**

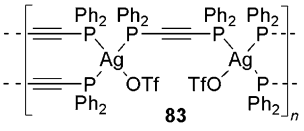


Fig. 2.28 A chain of polymeric mono-bridged silvercycles

However, the appearance of only a single resonance in the ^{31}P NMR spectrum suggests rapid interconversion of the dppa bridges in solution.

The seven-coordinated transition metal complexes $[MI_2(CO)_3(NCMe)_2]$ (M = Mo, W) react with one equivalent of dppa to form the corresponding macrocycles $[(MI_2(CO)_3)_2(\mu\text{-dppa})_2]$ (**86** M = Mo; **87** M = W; Fig. 2.30), but monomeric derivatives with two pendant dppa ligands are formed on using two equivalents of dppa [92]. Both the ^{13}C NMR and IR spectra indicate that the macrocycles do not support a capped octahedral geometry that is characteristic for the monomers.

Dimeric hexametallic complex **88** with a rhodium dppa macrocyclic core has been prepared by COD displacement from $[W((\mu\text{-}S)_2Rh(COD))_2]$ by dppa (Fig. 2.31) [93]. In contrast, reaction of $[Rh(CO)_2(Cl)_2]$ with an equimolar amount of dppa gave exclusively the linear polymeric compound $[Rh(CO)Cl(\mu\text{-dppa})]_n$ [94].

Rhodium macrocycles $[((Rh(acac))_2(\mu\text{-}L)_2]$ (**89** L = dppa; **90** L = dppda) have been prepared from $[Rh(acac)(cyclooctene)_2]$ and L (Fig. 2.32) [95]. These compounds proved to be effective catalysts for the hydroboration of unhindered vinyl arenes, giving selectivities up to 98%.

Treating $[Fe(NO)_2(CO)_2]$ with 0.5 equivalent of dppa results in CO displacement to give monobridged $[(Fe(NO)_2(CO))_2(\mu\text{-dppa})]$. Subsequent addition of dppa gives $[(Fe(NO)_2)_2(\mu\text{-dppa})_2]$ (**91**; Fig. 2.33), of which the X-ray crystal

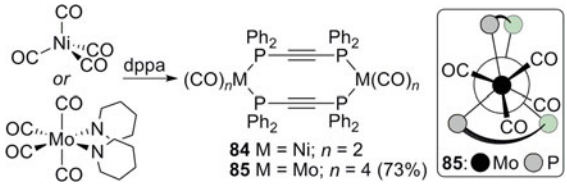


Fig. 2.29 Formation of $Ni(CO)_2$ and $Mo(CO)_4$ macrocycles **84** and **85**. Inset: Representation of **85**, viewed along the Mo–Mo vector. Phosphorus atoms of the same dppa bridge are connected

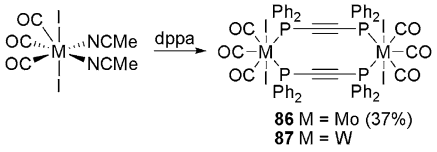


Fig. 2.30 Synthesis of seven-coordinate Mo and W macrocycles **86** and **87**

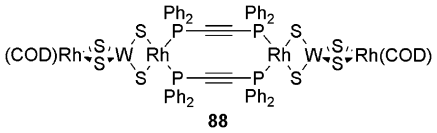


Fig. 2.31 Hexametallic rhodium-dppa macrocycle **88**

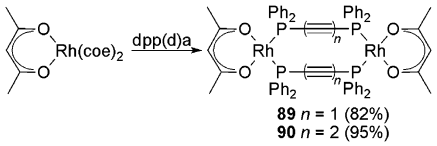


Fig. 2.32 10-membered and 14-membered Rh-dppa macrocycles

structure shows two puckered dppa bridges, one in a staggered conformation and the other in an eclipsed one (cf. **85**; Fig. 2.29) [96]. Mono-bridged complexes are formed in the reaction of dppa with Fe-thiolene ligands, except for $[Fe(S_2C_4F_6)_2]$ that gives double bridged macrocycle **92** (Fig. 2.33) [97].

Irradiation (Hg-source) of a mixture of $CpV(CO)_4$ and dppa reportedly gives, besides other products, $[(CpV(CO)_2)_2(dppa)_2]$ (**93**), that was characterized by elemental analysis and IR spectroscopy [98]. In line with these analyses, a macrocycle with *trans*-dispositioned dppa moieties around the vanadium center was suggested (Fig. 2.34a), but not only would this conformation be severely strained, it would also contrast all other binuclear doubly dppa-bridged macrocycles. Instead, the insolubility in virtually all solvents would suggest a polymeric structure with vanadium centers singly-bridged by *trans*-positioned dppa ligands (Fig. 2.34b).

Reaction of $[Re(CO)_5Cl]$ with an equimolar amount of dppa gave a mixture of the 10- and 20-membered macrocycles **94** and **95** (Fig. 2.35) [99]. The crystal structure of **94** reveals a chair-like conformation having two parallel *cis*-coordinated dppa bridges with octahedral rhenium centers above and below the plane of the bridges; the chlorines are *cis* to both phosphorus atoms and the CO groups are in a facial arrangement. The molecules of **94** stack in the crystal to form a microchannel [99]. Likewise, reaction of $[Re(CO)_5Cl]$ with dppda gave dimeric $[(ReCl(CO)_3)_2(\mu\text{-dppda})_2]$ (**96**) and tetrameric $[(ReCl(CO)_3)_4(\mu\text{-dppda})_4]$ (**97**; Fig. 2.35); ^{31}P NMR showed a single singlet, indicating that all phosphorus atoms are equivalent in solution on the NMR time-scale [99]. The analogous mixed-metal macrocycle **99** has been prepared by reaction of $[Re(CO)_5Cl]$ with $[Os(bipy)_2(dppa)_2][PF_6]_2$ (**85**), which was obtained by treating $[Os(bipy)_2(CO_3)]$ with dppa and NH_4PF_6 (Fig. 2.35) [99]. Attempts to synthesize the corresponding dppda-based rhenium–osmium mixed-metal macrocycle resulted only in the 14-membered $[(Os(bipy)_2)_2(\mu\text{-dppda})_2][PF_6]_4$ (**100**) with two osmium centers.

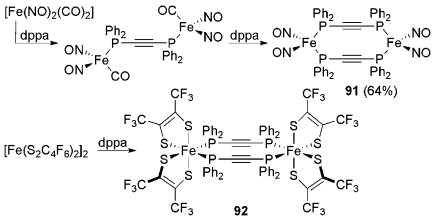


Fig. 2.33 Iron-dppa macrocycles **91** and **92**

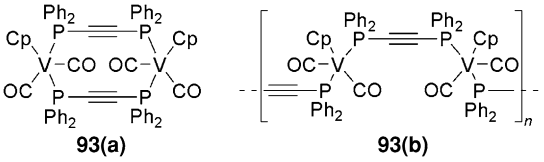


Fig. 2.34 $[(CpV(CO)_2)_2(dppa)_2]$ (**93**); reported macrocyclic structure (**a**) and more probable polymeric structure (**b**)

The emission of the rhenium macrocycles **94** and **95** at $\lambda_{em} = 525$ nm shows short life times ($\tau = 3.4$–3.8 ns) and low quantum yields ($\Phi_F = 3.8$–6.8×10^{-4}). The incorporated osmium(II) center in mixed-metal species **99**, however, makes it more emissive ($\lambda_{em} = 600$ nm; $\tau = 650$ ns; $\Phi_F = 0.17$). From its decrease in emission upon inclusion of a guest in the cavity of **99**, binding constants were determined that indicated a better fit for smaller guests ($K_b = 775$ M^{-1} (anisole), 1,580 M^{-1} (1,4-dimethoxy-benzene), 1,680 M^{-1} (1,3,5-trimethoxybenzene)) [99].

14-Membered macrocyclic dimer $[(RuCl(tpy))_2(\mu\text{-dppda})_2][PF_6]_2$ (**101**; tpy = 2,2′:6′,2″-terpyridine) and 21-membered trimer $[(RuCl(tpy))_3(\mu\text{-dppda})_3][PF_6]_3$ (**102**), prepared from $[RuCl_3(tpy)]$, dppda and KPF_6 (Fig. 2.36) [100], emit light at respectively $\lambda_{em} = 565$ nm and 550 nm upon excitation at $\lambda = 470$ nm. In these cases enhanced luminescence was observed with increasing the concentration of the guest molecule. Macrocycle **101** gave rather small binding constants of 220–250 M^{-1} for anisole and dimethoxybenzene, but for **102** with its larger cavity much larger values were found of 2,370 and 1,390 M^{-1}, respectively.

Smaller ruthenium-based macrocycle $[(Ru(acac)_2)_2(\mu\text{-dppa})_2]$ (**104**) with dppa bridges was prepared recently by heating coordination polymer **103**, which was obtained from $Ru(acac)_2(coe)_2$ by ligand exchange (Fig. 2.37) [101]. The crystal

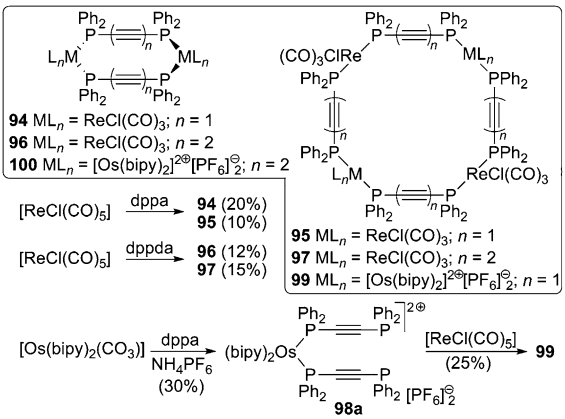


Fig. 2.35 Re and mixed Re/Os macrocycles

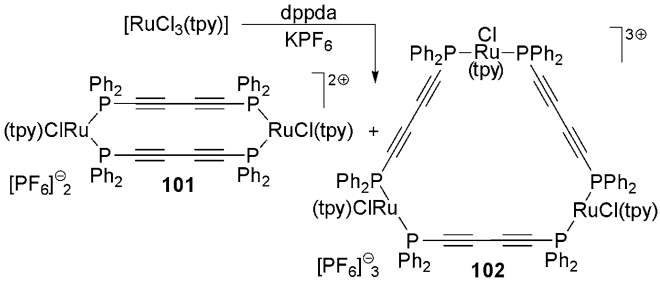


Fig. 2.36 Formation of Ru-dppda macrocycles **101** and **102**

structure of **104** reveals a puckered 10-membered ring. UV–Vis spectroscopy and CV analysis indicated the absence of electronic conjugation through the macrocycle.

The di-copper macrocyclic $[Cu_2(\mu\text{-dppa})_2(dpyk)_2][BF_4]_2$ (**105**; dpyk = di-2-pyridyl ketone) has been prepared in 97% yield by treating cage compound $[Cu_2(\mu\text{-dppa})_3(MeCN)_2][BF_4]_2$ (**127a**; see Fig. 2.51) with dpyk (Fig. 2.38) [102]. The formation of this bright yellow product results from the elimination of one dppa bridge, probably induced by the chelating effect of dpyk. The crystal structure shows a chair-like conformation with parallel dppa bridges and distorted tetrahedral copper centers above and below the plane formed by these bridges. The two pyridine rings of the chelating dpyk ligands are non-equivalent and oriented *endo* and *exo* with respect to the macrocycle, but the ^{1}H NMR spectrum at −60 °C showed only one set of pyridyl protons, suggesting that fast ring flipping between the chair-like conformers occurs in solution (Fig. 2.38).

The tetra-gold 26-membered macrocycle **106** was obtained by the reaction of $[(AuCl)_2(\mu\text{-dppa})]$ with *ortho*-dilithiated 2,6-diphenylpyridine (dppy; Fig. 2.39) [103]. Its molecular structure in the solid state reveals parallel dppa ligands bridging the two $[Au_2(dppy)]$ moieties that each show a weak aurophilic attraction (Au–Au = 3.18 Å). In this *meso*(*P,M*)-isomer, the dppy ligands are positioned above and below the plane of the dppa bridges, giving the macrocycle two helical twists [103]. In solution, an equilibrium exists between the *P,M* and the *M,P* conformations (Fig. 2.39) that can be frozen at low temperatures (−53 °C), where also an intermediate [**106**]* is detected by ^{31}P NMR spectroscopy. In this

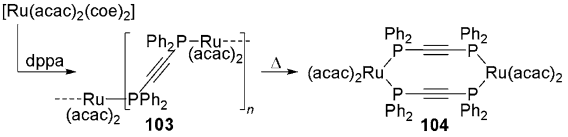


Fig. 2.37 Ru-dppa macrocyle **104** by heating of polymer **103**

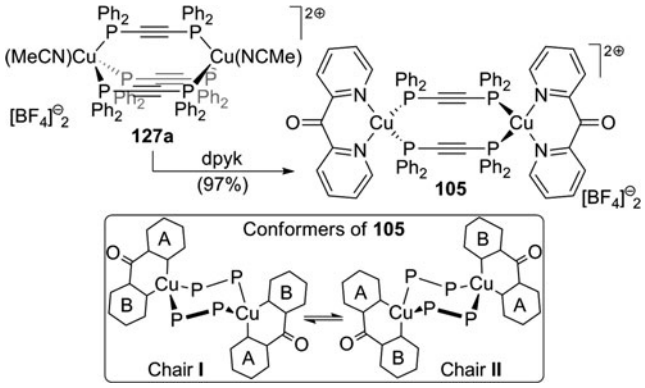


Fig. 2.38 Structure and conformation of Cu-dppa macrocycle **105**

species, both dppy ligands are in a halfway position with the nitrogen atoms in the plane of both dppa bridges (Fig. 2.39). Neither the *M*,*M* nor the *P*,*P* conformer is observed, which would suggest these conformers with both dppy ligands on the same side of the dppa plane may be too sterically congested [103].

To complete this section, we focus briefly on dppa as a stabilizing or bridging ligand between transition metal clusters. Typically two metal clusters are bridged by a single dppa ligand [104–112] or a large inorganic cluster is stabilized by dppa ligands at its surface [113–115], but a few examples are known in which dppa connects small metal clusters to form macrocyclic species.

Exemplary is the reaction of osmium cluster $[Os_3(CO)_{10}(MeCN)_2]$ with dppa, that gives over a period of 6 h a mixture of dimeric $[(Os_3(CO)_{10})_2(\mu\text{-dppa})_2]$ (**107**), trimeric $[(Os_3(CO)_{10})_3(\mu\text{-dppa})_3]$ (**108**) and tetrameric $[(Os_3(CO)_{10})_4(\mu\text{-dppa})_4]$ (**109**; Fig. 2.40) [116]. **108** and **109** were the only products after a reaction time of 12 h [117]. A crystal structure was obtained for dimer **107**.

Mixed osmium–gold macrocycle **110** is formed when the cationic osmium cluster $[Os_4H_3(CO)_{12}][N(PPh_3)_2]$ is treated with $[(AuCl)_2(\mu\text{-dppa})]$ in the presence of excess NEt_3 and $TlPF_6$ (Fig. 2.41) [117]. Surprisingly, only two instead of four gold atoms were inserted between the osmium clusters and the dppa ligands, which was confirmed by a crystal structure determination. ^{31}P NMR spectroscopy also revealed the non-equivalence of the phosphorus atoms ($\delta = -149.0$ and

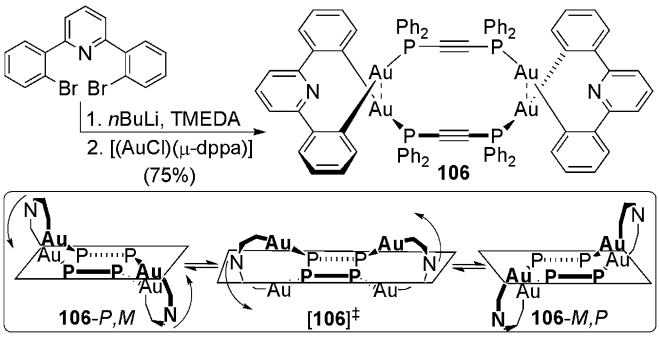


Fig. 2.39 Structure and conformations of **106**. The movement of the dppy ligands is indicated with arrows

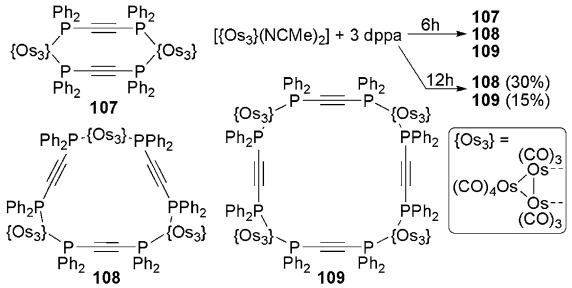


Fig. 2.40 Formation of triosmium-dppa macrocycles **107**–**109**

−84.6 ppm) and ^{1}H NMR revealed the characteristic hydride at $\delta = -20.51$ ppm that was not apparent from the crystal structure [117, 118].

Gold atoms are introduced at all four position between the ruthenium–rhodium clusters and the dppa bridges by reacting $[RhRu_3H(Cp^*)(CO)_9BH][N(PPh_3)_2]$ with $[(AuCl)_2(\mu\text{-dppa})]$ [119]. One hydride per cluster is lost on coordinating dppa, while both AuCl units of the fragmented $[(AuCl)_2(\mu\text{-dppa})]$ coordinate to one of the Ru-clusters to give **111** (Fig. 2.42). ^{31}P NMR spectroscopy reveals that the phosphorus–gold units are asymmetrically attached to the transition metal cluster [119].

Reaction of **112**, generated from $[Co_2(CO)_8]$ and $Me_3SiC{\equiv}CH$, with dppa afforded macrocycle **113** (Fig. 2.43) [120]. The crystal structure showed the acetylenic carbons of the Co_2C_2 cluster located inside the cavity of the macrocycle with the two CH moieties directed toward each other. The bridging dppa ligands of **113** are unperturbed but subsequent reaction with $[Co_2(CO)_8]$ resulted in alkyne coordination, thereby bending the dppa bridges, causing contraction and leading to the formation of two molecules of **114** (Fig. 2.43) [120].

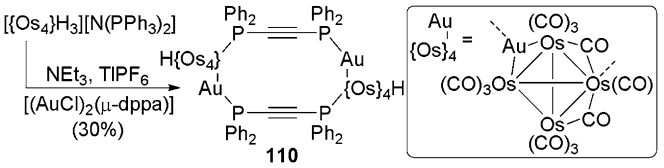


Fig. 2.41 Two Os_4Au clusters (**110**) doubly bridged by dppa

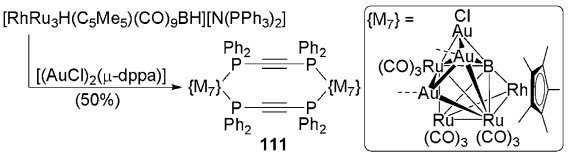


Fig. 2.42 Heptametallic clusters bridged by dppa (**111**)

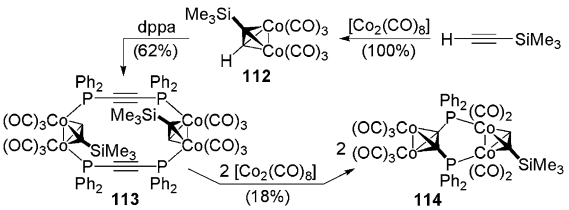


Fig. 2.43 Formation of tetracobalt-dppa macrocycle **113** and subsequent alkyne coordination by $[Co_2(CO)_8]$

2.3.3 Miscellaneous Macrocycles

The conjugated diphosphine bridges can be elongated by formally inserting unsaturated groups between the acetylenic moieties of dppda. Exemplary is the *cis*-1,5-hexadiyne-3-ene moiety (also referred to as enediyne), with an additional C=C double bond, which was used in a computational study of the diligated Pt_2 model complex **115** (Fig. 2.44) [121]. However, virtually all synthesized macrocycles are derived from complexes containing the *ortho*-bis(diphenyl-phosphinoethynyl)benzene (*o*-dppeb) ligand (see for example Fig. 2.46).

Enediynes can condense to 1,4-benzene biradicals, known as the Bergmann cyclization, and abstract hydrogens from, e.g., the sugar backbone of DNA to form benzene (Fig. 2.45), and are thus often used in antibiotic studies [122, 123]. The cyclization rate strongly depends on the distance between the acetylene termini (*d*), which can be decreased by metal complexation [124].

Metal complexation of *o*-dppeb readily affords the 9-membered macrocycles [MCl_2(*o*-dppeb)] (**116a** M = Pd; **116b** M = Pt; **116c** M = Hg) that have shortened distances between the alkyne termini (Fig. 2.46) [125]. Whereas a distance of 3.34 Å is taken as the threshold for the Bergmann cyclization to occur, compounds with $d < 3.2$ Å cyclize spontaneously [123, 126]. The Pd and Pt-complexes of *o*-dppeb have an intermediate *d* of ca. 3.3 Å and therefore cyclize at moderate temperatures (Table 2.1) to form naphtyl biradicals **117**, which are trapped by

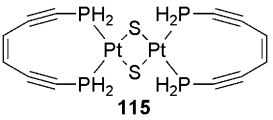


Fig. 2.44 Pt($(PH_2)_2C_6H_2$) double macrocycle **115**

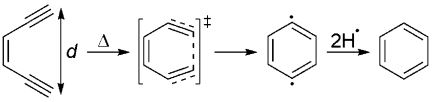


Fig. 2.45 Bergmann cyclization and hydrogen abstraction

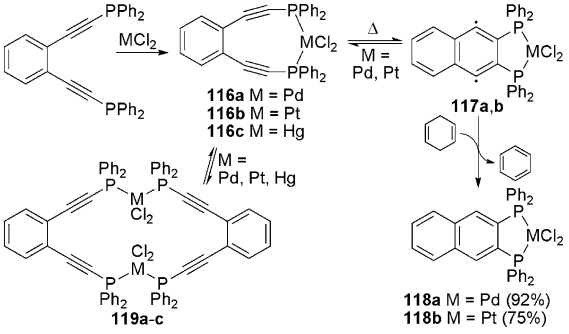


Fig. 2.46 Formation of monomeric (**116a–c**) and dimeric (**119a–c**) [MCl_2(*o*-dppeb)] macrocycles and subsequent Bergmann cyclization

Table 2.1 Bergmann cyclization temperatures (T_B) for *o*-dppeb and complexes thereof

Compound	T_B (°C)	*d* (Å)
o-dppeb	243	4.1[a]
[$PdCl_2$(*o*-dppeb)] (**116a**)	61	3.3[a]
[$PtCl_2$(*o*-dppeb)] (**116b**)	81	3.3[a]
[$HgCl_2$(*o*-dppeb)] (**116c**)	>450	3.4[a]
[Pd(*o*-dppeb)$_2$] (**120**)	222	3.47[b]
[Cu(*o*-dppeb)$_2$][PF_6] (**121a**)	227	3.44[b]
[Ag(*o*-dppeb)$_2$][PF_6] (**121b**)	266	3.62[b]

[a]Determined by MM2 calculations
[b]Determined by X-ray crystallography

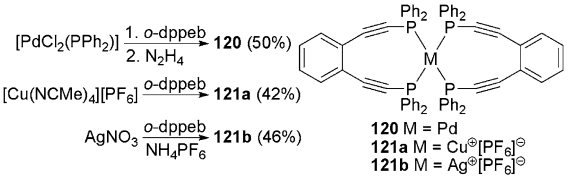


Fig. 2.47 d^{10} Metal centers chelated by two *o*-dppeb moieties (**120**–**121**)

cyclohexadiene to form benzene and **118** (Fig. 2.46). Pd-complexation accelerates the rate of ring closure of *o*-dppeb ($d = 4.1$ Å) by over 3×10^4, while the Hg-complex ($d = 3.4$ Å) does not react at temperatures up to 450 °C. Based on a kinetic study on the Pd-complex in solution, it was suggested that **116** is in equilibrium with the dimeric 18-membered macrocycle **119** (Fig. 2.46) [125].

The square planar conformation of the transition metal in **116** can be distorted toward a tetrahedral coordination, thereby increasing the value of *d*, by using two *o*-dppeb ligands around a d^{10} metal center. The [Pd(*o*-dppeb)$_2$] complex (**120**) has been synthesized from *o*-dppeb, [$PdCl_2(PPh_3)_2$] and hydrazine [127], whereas metallo-enediynes [M(*o*-dppeb)$_2$][PF_6] (**121a** M = Cu; **121b** M = Ag) were created starting with [$Cu(MeCN)_4$][PF_6] or $AgNO_3$ respectively (Fig. 2.47) [128]. All these metallo-enediynes were characterized by crystal structure determinations and shown to undergo the Bergmann cyclization in the solid state; Table 2.1 list the temperatures at which this occurs. For **121b** the cyclization temperature is much higher than for the other two, which is in accordance with its higher value of *d*. Interestingly, the *d* values for **121** and **121** are above the noted threshold for cyclization.

Besides *ortho*- also *para*-bis(diphenyl-phosphino-ethynyl)benzene (*p*-dppeb) has been explored as ligand for organometallic complexes, which have, of course, a different structure. Thus, *p*-dppeb reacts with [K_2PtCl_4] to afford quantitatively the trimeric 33-membered macrocycle **122a**, in which the *cis*-configured platinum square planes are perpendicular to the mean plane of the macrocycle (Fig. 2.48) [129]. Halogen exchange to iodide derivative **122b** proceeded in high yield, but the product slowly underwent a double [2 + 2 + 2] ring fusion to **123** [129].

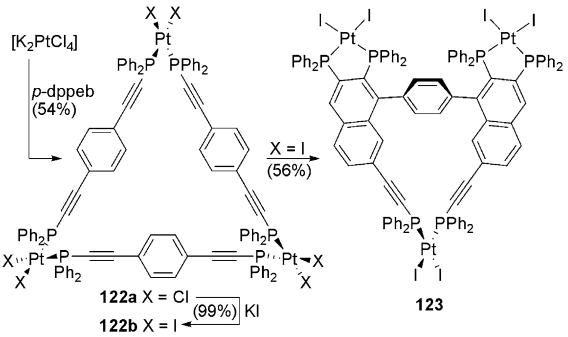
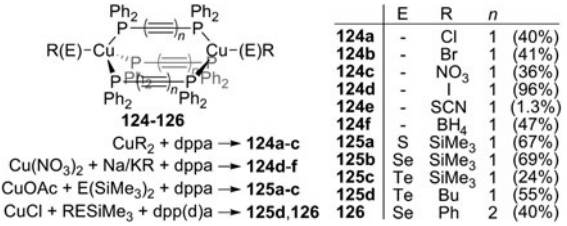


Fig. 2.48 Trimeric PtX_2(*p*-dppeb) macrocycles **122** and rearrangement to ring-fused **123**



	E	R	*n*	
124a	-	Cl	1	(40%)
124b	-	Br	1	(41%)
124c	-	NO_3	1	(36%)
124d	-	I	1	(96%)
124e	-	SCN	1	(1.3%)
124f	-	BH_4	1	(47%)
125a	S	$SiMe_3$	1	(67%)
125b	Se	$SiMe_3$	1	(69%)
125c	Te	$SiMe_3$	1	(24%)
125d	Te	Bu	1	(55%)
126	Se	Ph	2	(40%)

Fig. 2.49 Synthesis of Cu-dpp(d)a cages **124–126**

2.3.4 Dppa- and Dppda-Based Cages

Bridging two metal centers with three or more dppa ligands results in cages with the phosphine acetylenic units at the edges of general structure **II** (Fig. 2.1). Most of the research in this area has been performed on binuclear copper and gold complexes bearing three dppa bridges.

A series of Cu-containing cages, such as [$(CuX)_2$(μ-dppa)$_3$] (**124a** X = Cl; **124b** X = Br; **124c** X = NO_3; **124d** X = I; **124e** X = SCN; **124f** X = BH_4; Fig. 2.49), have been synthesized from Cu(II)X_2 and dppa [130]. The strong Raman resonance at ca. 2120 cm^{-1} for the symmetric C≡C stretch of these complexes suggests σ-donation from the phosphorus atom to the metal [130]. Similar cages with terminal chalcogenolate ligands (**125**) have been prepared as well from a 2:3 mixture of CuOAc or CuCl and dppa, with an excess of the corresponding trimethylsilyl-chalcogen (Fig. 2.49) [114, 132, 133]. Extended cage compound [$(Cu_2(SePh)_2$(μ-dppda)$_3$] (**126**) with dppda bridges has been synthesized in a similar fashion (Fig. 2.49) [114].

The crystal structures reveal that the cages **125** and **126** possess helical character, which is evident by looking down the Cu–Cu vector as shown in the projection in Fig. 2.50. The three bridges are in a partially eclipsed configuration causing a helical twist (θ = 20–29° (**125**); 5.5° (**126**)). The substituents of the chalcogens are staggered with respect to the dppa or dppda bridges. Due to the eclipsed conformation of the $SiMe_3$ groups of **125**, the phosphorus atoms are not equivalent, but the single ^{31}P NMR resonance suggests rapid bond rotations [114, 132].

Cage compounds $[Cu_2(\mu\text{-dppa})_3(MeCN)_2][BF_4]_2$ (**127a**; Fig. 2.51) and $[Cu_2(\mu\text{-dppa})_3(OTf)_2]$ (**127b**) are formed by mixing dppa in a 3:2 ratio with the BF_4^- and OTf^- salts of $[Cu(MeCN)_4]^+$ respectively [131]. Whereas BF_4^- is a non-coordinating anion, leaving one acetonitrile molecule attached to each copper centre, the triflate anion does coordinate via an oxygen atom, avoiding the need for additional donor ligands. Cage **127a** has a helical twist θ of 18.6° with a Cu–Cu distance of 6.25 Å, and cage **127b** has similar dimensions. For both cages, the labile ligands (MeCN or OTf) are replaceable, such as with di-2-pyridyl ketone (dpyk), as reported earlier, that gives **105** (see Fig. 2.38) or with bis(diphenylphosphino)ferrocene (dppf) that affords the singly bridged binuclear **128** (Fig. 2.51) [102]. Steric factors determine this difference in reactivity.

Di-gold cage compounds $[(AuX)_2(\mu\text{-dppa})_3]$ (**129a** X = Cl; **129b** X = I; **129c** X = NCS) have been synthesized from the mono-bridged $[(AuCl)_2(\mu\text{-dppa})]$ (Fig. 2.52) [131, 134]. The crystal structure of **129a** revealed a Au–Au distance of 5.77 Å and a helical twist around the Au–Au vector of 26.2° (cf. Fig. 2.50) [134].

Exceptional di-gold complexes $[Au_2(\mu\text{-dppa})_4][X]$ (**130a** X = BF_4; **130b** X = PF_6), bearing four bridging dppa ligands, were reported to be the likely product of the reaction of $[(AuCl)_2(\mu\text{-dppa})]$ with excess dppa and addition of $NaBF_4$ or KPF_6 (Fig. 2.52). Both MS and solubility studies supported the quadruply bridged geometry of **130** [131].

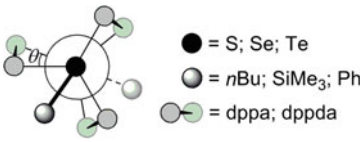


Fig. 2.50 Representation of **124** and **125**, viewed along the Cu–Cu vector. Helical twist θ is the P–Cu–Cu–P dihedral angle, in which both phosphorus atoms belong to the same dpp(d)a bridge

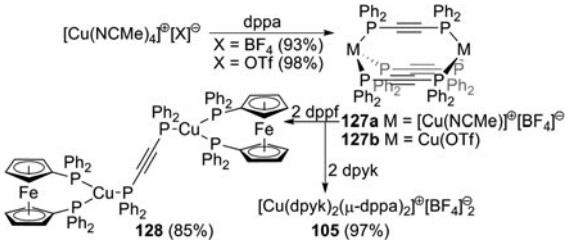


Fig. 2.51 Formation of Cu-cage compounds **127** and ring opening reactions

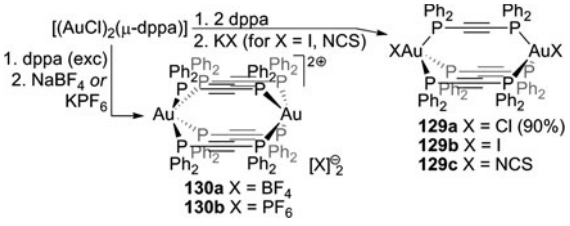


Fig. 2.52 Formation of gold-dppa cages **129** and **130**

The Raman shift in alkyne frequency $\Delta\nu$(C≡C) of the gold and copper binuclear cages with three bridging dppa ligands (**124–127**, **129**) are similar (19–28 cm^{-1}), suggesting that copper and gold have similar σ-bonding abilities; $\Delta\nu$(C≡C) of quadruply bridged **130** is somewhat lower (16–20 cm^{-1}), indicating less donation of electron density to the metal per dppa bridge.

The di-silver cages $[Ag_2(\mu\text{-dppa})_3](X)_2$ (**131a** X = SbF_6; **131b** X = BF_4; **131c** X = OTf; **131d** X = NO_3) could be synthesized as tight ion pairs by reaction of AgX with dppa in a 2:3 ratio (Fig. 2.53) [88, 89]. The crystal structures of **131a–d**, which have a helical twist θ of 27–35°, show that the anion can stretch the cage. A tighter bound anion like NO_3^- increases the pyramidal nature of the silver center, thereby lengthening and narrowing the cage (Table 2.2) [89]. Increasing the coordinative power of the anion ($SbF_6 < BF_4 < OTf < NO_3$) increases the Ag–Ag distance (*l*), decreases the distance of the C≡C bond centroid of the dppa bridges to the molecular centroid (*w*) and rehybridizes the Ag centers from trigonal planar toward tetrahedral (indicated by an increasing distance *p* between Ag and the P_3-plane). The stability of these cages is accounted for by the numerous π- and t-stacking interactions between the many phenyl rings [88, 89].

Reaction of $[Ag(NO_3)(\mu\text{-dppa})]_n$ (**80**) with KCl and excess dppa was reported to give the di-silver cage $[(AgCl)_2(\mu\text{-dppa})_3]$ **131e** (Fig. 2.53) in seeming contrast to the reactions with KBr and KI that result in polymer **82** (Sect. 2.3.2; Fig. 2.27), but the evidence is solely based on elemental analyses, which are identical for the cage and polymeric structure and their resemblance with copper cages **124** [86].

Reaction of macrocylic $[(M(CO)_n)_2(\mu\text{-dppa})_2]$ (**84** M = Ni; *n* = 2; **85** M = Mo; *n* = 4) with dppa affords cage $[(Ni(CO))_2(\mu\text{-dppa})_3]$ **132** [90] or *fac*,*fac*-$[(Mo(CO)_3)_2(\mu\text{-dppa})_3]$ **133** [91] (Fig. 2.54). Di-nickel cage **132** could also be obtained by reaction of dppa with $[Ni(CO)_4]$ or $[CpNi(CO)]_2$. The ν(C≡C) of 2120 cm^{-1} is indicative of reasonable σ-bonding from the d^{10} metal center to the phosphorus atoms [90]. Alternatively, ligand distribution of molybdenum cycle **85** through thermolysis gave cage **133**, together with mono-bridged $[(Mo(CO)_5)_2(\mu\text{-dppa})]$. The crystal structure of **133** showed a facial arrangement of the phosphorus ligands around the molybdenum centers and nearly parallel dppa bridges, which contrasts the puckered geometry of macrocycle **85** (see Sect. 2.3.2, Fig. 2.29). The bridges lock the molybdenum tricarbonyl fragments in eclipsed conformations [91].

Di-tungsten cage $[(W(CO)_3)_2(\mu\text{-dppa})_3]$ **135** is prepared by reaction of $[W(CO)_3(Me_3tach)]$ **134** (Me_3tach = 1,3,5-trimethyl-1,3,5-triazacyclohexane)

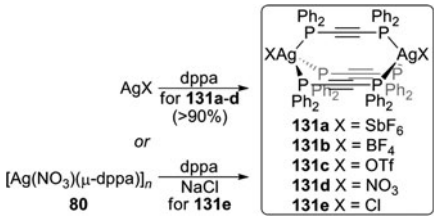


Fig. 2.53 Silver-dppa cage compounds **131**

Table 2.2 Structural parameters for complexes **131**

Compd	Anion X	Ag–X (Å)[a]	*l* (Å)[b]	*w* (Å)[c]	*p* (Å)[d]	θ (deg)[e]	π–π[f]
131a	SbF_6	2.5–2.8	5.46	2.57	0.48	33.0	18–22
131b	BF_4	2.66–2.75	5.66	2.48	0.55	27	16
131c	OTf	2.43–2.56	5.88	2.50	0.62	35.3	[g]
131d	NO_3	2.39–2.40	6.21	2.39	0.83	28.6	[g]

[a]The distance between the silver atom and the closest atom of the anion; cf., the sum of the Ag and F van der Waals radii is 3.19 Å and that of Ag and O is 3.18 Å
[b]Length of the cage, expressed by the Ag–Ag distance
[c]Width of the cage, expressed by the average distance of the C≡C bond centroid to the molecular centroid
[d]Distance of Ag to the P_3 plane
[e]Helical twist as defined in Fig. 2.50
[f]Number of arene–arene interactions (π-stacking and t-stacking) between 3.5 and 3.8 Å
[g]Not mentioned

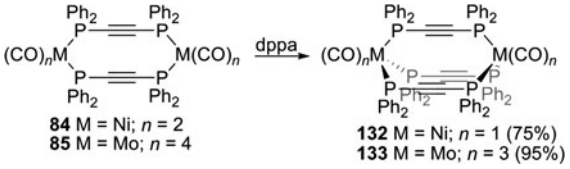


Fig. 2.54 Formation of Ni-cage **132** and Mo-cage **133**

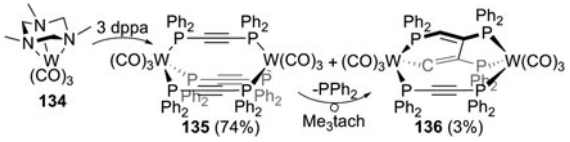


Fig. 2.55 Formation and rearrangement of W-cage **135**

with dppa in a 1:3 ratio, together with some rearranged cage product **136** (Fig. 2.55). Apparently, the liberated Me_3tach acts as a base that induces C–C coupling, C–P bond-cleavage, and hydrogen abstraction [135].

Cage **135** crystallizes as a racemic mixture of Δ and Λ helical cages, with a W–W length of 7.39 Å, an average helical twist θ of 21° and both $W(CO)_3$ fragments in an eclipsed conformation. The crystal structure of the unique cage **136** showed a W=C bond length of 1.95 Å, as expected for a tungsten carbene complex, with a rather bend W=C=C unit (158.6°). ^{31}P NMR spectroscopy revealed all PPh_2 moieties to be inequivalent.

2.4 Concluding Remarks

Assembling phosphine acetylenic building blocks in macrocycles and cages is greatly assisted by metal complexation, as the syntheses of the organic compounds described in Sect. 2.2 suffer from low yields and difficult work-up procedures. Linear diphosphines such as dppa and dppda tend to bridge two metal centers

twice or three times, provided that they are mixed in the proper stoichiometry, and provide relatively easy access to macrocyclic and cage structures. It is then no surprise that since the introduction in the late 1960s of the coordination chemistry of dppa by Carty and coworkers, the number of reported organometallic derivatives has grown tremendously and far exceeds that of the all-organic systems.

Whereas a plethora of compounds has been generated, there has been little focus on possible applications, despite the (opto)electronic properties these compounds are anticipated to have. Electronic communication in phosphine acetylenic systems is hardly regarded, which is surprising considering the growing interest in phosphorus containing π-conjugated materials. We feel that the full potential of the macrocycles and cages described in this review has by no means been reached and are convinced that the phosphine acetylenic building block may be of value for the preparation of compounds suitable for the fabrication of electronic devices.

References

1. Baumgartner T, Réau R (2006) Organophosphorus π-conjugated materials. Chem Rev 106:4681–4727
2. Hissler M, Dyer PW et al (2005) The rise of organophosphorus derivatives in π-conjugated materials chemistry. Top Curr Chem 250:127–163
3. Hissler M, Lescop C et al (2005) Organophosphorus π-conjugated materials: the rise of a new field. J Organomet Chem 690:2482–2487
4. Hissler M, Dyer PW et al (2003) Linear organic π-conjugated systems featuring the heavy group 14 and 15 elements. Coord Chem Rev 244:1–44
5. Hightower SE, Corcoran RC et al (2005) Unusual, bifurcated photoreactivity of a rhenium(I) carbonyl complex of triethynylphosphine. Inorg Chem 44:9601–9603
6. Ochida A, Ito H et al (2006) Using triethynylphosphine ligands bearing bulky end caps to create a holey catalytic environment: application to gold(I)-catalyzed alkyne cyclizations. J Am Chem Soc 128:16486–16487
7. Ochida A, Sawamura M (2007) Phosphorus ligands with a large cavity: synthesis of triethynylphosphines with bulky end caps and application to the rhodium-catalyzed hydrosilylation of ketones. Chem Asian J 2:609–618
8. Kondoh A, Yorimitsu H et al (2007) Synthesis of bulky phosphines by rhodium-catalyzed formal [2 + 2 + 2] cycloaddition reactions of tethered diynes with 1-alkynylphosphine sulfides. J Am Chem Soc 129:6996–6997
9. Van Assema SGA, Tazelaar CGJ et al (2008) Phospha-scorpionate complexes by click chemistry using phenyl azide and ethynylphosphine oxides. Organometallics 27: 3210–3215
10. Lammertsma K (2003) Phosphinidenes. Top Curr Chem 229:95–119
11. Mathey F (1988) The organic chemistry of phospholes. Chem Rev 88:429–453
12. Huy NHT, Perrier E et al (2006) The use of phosphirenes as conjugating spacers in polythiophene chains. Organometallics 25:5176–5179
13. Huy NHT, Ricard L et al (2001) Stepwise building of polyphosphirene chains. Angew Chem Int Ed 40:1253–1255
14. Marinetti A, Mathey F et al (1982) Generation and trapping of terminal phosphinidene complexes. Synthesis and X-ray crystal structure of stable phosphirene complexes. J Am Chem Soc 104:4484–4485

15. Borst MLG, Bulo RE et al (2005) 3*H*-Benzophosphepine complexes: versatile phosphinidene precursors. J Am Chem Soc 127:16985–16999
16. Regitz M, Hoffman A et al (1995) Phosphaalkynes—starting point for the synthesis of phosphorus-carbon cage compounds. In: Stang PJ, Diederich F (eds) Modern acetylene chemistry, 1st edn. VCH, Weinheim
17. Regitz M (1990) Phosphaalkynes: new building blocks in synthetic chemistry. Chem Rev 90:191–213
18. Regitz M (1994) Organophosphorus compounds. 75. Phosphaalkynes—new building blocks in heterocyclic chemistry. J Heterocyc Chem 31:663–677
19. Nixon JF (1995) Phospha-alkynes, RC≡P: new building blocks in inorganic and organometallic chemistry. Chem Soc Rev 24:319–328
20. Bergsträsser U (2004) Product class 6: phosphaalkynes (alkylidynephosphines). Sci Synth 19:427–444
21. Lynam JM (2007) Recent advances in the chemistry of phosphaalkynes: building blocks for novel organophosphorus compounds. Organomet Chem 33:170–178
22. Mathey F (2003) Phospha-organic chemistry: panorama and perspectives. Angew Chem Int Ed 42:1578–1604
23. Wettling T, Schneider J et al (1989) Tetra-*tert*-butyltetraphosphacubane: the first thermal cyclooligomerization of a phosphaalkyne. Angew Chem Int Ed Engl 28:1013–1014
24. Fink J, Rösch W et al (1986) 2-Dewar phosphinines—a new class of compounds containing two-coordinate phosphorus. Angew Chem Int Ed Engl 25:280–282
25. Blatter K, Rösch W et al (1987) Isomerization reactions in the system dewar-phosphinine/phosphaprismane/phosphabenzvalene/phosphinine. Angew Chem Int Ed Engl 26:85–86
26. Elvers A, Heinemann FW et al (1999) 1-Triorganylstannyl-1,2,4-triphosphole: a versatile starting material for phosphorus-rich cage compounds and π-complexes. Chem Eur J 5:3143–3153
27. Al-Ktaifani MM, Bauer W et al (2002) Hexaphosphapentaprismane: a new gateway to organophosphorus cage compound chemistry. Chem Eur J 8:2622–2633
28. Scott LT, DeCicco GJ et al (1983) Decamethyl[5]pericyclyne. A novel homoconjugated cyclic polyacetylene. J Am Chem Soc 105:7760–7761
29. Scott LT, DeCicco GJ et al (1985) Pericyclynes of order [5], [6], [7], and [8]. Simple convergent syntheses and chemical reactions of the first homoconjugated cyclic polyacetylenes. J Am Chem Soc 107:6546–6555
30. Scott LT, Cooney MJM (1995) Macrocyclic homoconjugated polyacetylenes. In: Stang PJ, Diederich F (eds) Modern acetylene chemistry, 1st edn. VCH, Weinheim
31. Diederich F (2001) Carbon-rich acetylenic scaffolding: rods, rings and switches. Chem Commun 219–227
32. Nielsen MB, Diederich F (2002) The art of acetylenic scaffolding: rings, rods, and switches. Chem Rec 2:189–198
33. Kivala M, Mitzel F et al (2006) Two-dimensional acetylenic scaffolding: extended donor-substituted perethynylated dehydroannulenes. Chem Asian J 1:479–489
34. Nielsen MB, Diederich F (2005) Conjugated oligoenynes based on the diethynylethene unit. Chem Rev 105:1837–1867
35. Maraval V, Chauvin R (2006) From macrocyclic oligo-acetylenes to aromatic ring *carbo*-mers. Chem Rev 106:5317–5343
36. Manini P, Amrein W et al (2002) Expanded cubane: synthesis of a cage compound with a C_{56} core by acetylenic scaffolding and gas-phase transformations into fullerenes. Angew Chem Int Ed 41:4339–4343
37. Rubin Y, Parker TC et al (1998) Acetylenic cyclophanes as fullerene precursors: formation of $C_{60}H_6$ and C_{60} by laser desorption mass spectrometry of $C_{60}H_6(CO)_{12}$. Angew Chem Int Ed 37:1226–1229
38. Tobe Y, Nakagawa N et al (1998) [16.16.16](1,3,5)Cyclophane-tetracosayne ($C_{60}H_6$): a precursor to C_{60} fullerene. J Am Chem Soc 120:4544–4545

39. Tobe Y, Nakagawa N et al (2001) Polyyne cyclization to form carbon cages: [16.16.16](1,3,5)Cyclophane-tetracosayne derivatives $C_{60}H_6$ and $C_{60}C_{16}$ as precursor to C_{60} fullerene. Tetrahedron 57:3629–3636
40. Yarosh OG, Zhilitskaya LV et al (2005) Novel highly unsaturated macrocyclic and macrobicyclic silahydrocarbons containing Si_3H bonds and exocyclic vinyl groups. Russ J Gen Chem 75:1094–1097
41. Yarosh OG, Zhilitskaya LV et al (2004) Novel acyclic and macrocyclic highly unsaturated silahydrocarbons. Russ J Gen Chem 74:1496–1500
42. Kwon E, Sakamoto K et al (2004) Synthesis and structures of sila-macrobicyclic compounds: *syn* and *anti* isomers of hexasilabicyclo[12.8.8]triacontane. Silicon Chem 1:391–395
43. Unno M, Saito T et al (2001) Synthesis and crystal structures of silapericyclynes. Bull Chem Soc Jpn 74:2407–2413
44. Unno M, Negeshi K et al (2001) Extended silapericyclynes. Chem Lett 30:340–341
45. Unno M, Saito T (1999) Silapericyclyne, $(Ph_2SiC{\equiv}C)_6$: spontaneous conformational resolution of boat- and chair-'exploded' cyclohexane. Chem Lett 28:1235–1236
46. Voronkov MG, Yarosh OG et al (1990) Highly unsaturated macrocyclic silicohydrocarbons. J Organomet Chem 389:1–22
47. Bortolin R, Brown SSD et al (1989) Peficyclynosilanes: single crystal X-ray structure of dodecamethyl(6)pericyclynosilane, $(Me_2SiC{\equiv}C)_6$. Inorg Chim Acta 158:137–139
48. Hengge E, Baumegger A (1989) Synthese und eigenschaften einiger ethinylsilane. J Organomet Chem 369:C39–C42
49. Gleiter R, Schäfer W et al (1985) Evidence for a strong σ/π interaction in 3,4,7,8-tetrasilacycloocta-1,5-diyne and 3,4,7,9,11,12-hexasilacyclododecal-1,5,9-triyne. J Am Chem Soc 107:3046–3050
50. Voronkov MG, Yarosh NO (2003) Cyclogermasilethynes. Russ J Gen Chem 73:1555–1556, for some thiapericyclenes, see ref [18]
51. Dillon KD, Mathey F et al (1998) Phosphorus, the carbon copy. Wiley, Chichester
52. Scott LT, Unno M (1990) Novel heterocycles comprising alternating phosphorus atoms and alkyne units. J Am Chem Soc 112:7823–7825
53. Van Assema SGA, Kraikivskii PB et al (2007) Building blocks for phospha[*n*]pericyclynes. J Organomet Chem 692:2314–2323
54. Shiozowa R, Sakamoto K (2003) Synthesis and structures of cyclic ethynylphosphine ligands. Chem Lett 32:1024–1025
55. Cooney MJM (1993) PhD Dissertation, University of Nevada, Reno
56. Märkl G, Zollitsch T et al (2000) Polyphospha[*m*]cyclo[*n*]carbons ($m + n = 15$, 20, 25, 30, 40). Chem Eur J 6:3806–3820
57. Baechler RD, Mislow K (1970) The effect of structure on the rate of pyramidal inversion of acyclic phosphines. J Am Chem Soc 92:3090–3093
58. Rauk A, Allen LC et al (1970) Pyramidal inversion. Angew Chem Int Ed Engl 9:400–414
59. Van Assema SGA, De Jong GB et al (2007) Acetylene-substituted phosphane oxides: building blocks for macrocycles. Eur J Org Chem 2405–2412
60. Laporte F, Mercier F et al (1994) Tetraphosphorus macrocycles from phosphole tetramers. J Am Chem Soc 116:3306–3311
61. Adams CJ, Bruce ML et al (1993) Cluster chemistry LXXXVII. Some homo- and heteronuclear complexes derived from $C_2(PPh_2)_2$: crystal structures of $Re_3(\mu\text{-H})_3(\mu\text{-dppa})(CO)_{10}$ {dppa = $C_2(PPh_2)_2$}, $Re_3(\mu\text{-H})_3(CO)_{11}\{PPh_2[\mu\text{-}C_2Ru_2(\mu\text{-}PPh_2)(CO)_6]\}$ and $Os_3Ru_2(\mu_5\text{–}C_2PPh_2)(\mu\text{-}PPh_2)(CO)_{13}$. J Organomet Chem 447:91–101
62. Lee J, Humphrey MG (1993) Mixed-metal cluster chemistry. Site-selective reactions of $CpWIr_3(CO)_{11}$ with PPh_3 and bidentate phosphines: X-ray crystal structures of $CpWIr_3(\mu\text{-dppe})(\mu\text{-CO})_3(CO)_6$, $CpWIr_3(\mu\text{-dppm})(\mu\text{-CO})_3(CO)_6$, and $CpWIr_3(\mu\text{-dppa})(\mu\text{-CO})_3(CO)_6$. Organometallics 12:3468–3473

63. Hong FE, Huang YL et al (1999) Preparation of a new cobalt-containing diphosphine ligand and its reaction towards dicobalt octacarbonyl; X-ray crystal structure of $[Co_2(CO)_4(\mu\text{-}CO)_2\{\mu\text{-P, P-}(\mu\text{-}PPh_2C{\equiv}CPPh_2)Co_2(CO)_6\}]$. Inorg Chem Commun 2:450–452
64. Rodewald D, Schulzke C et al (1995) Alkyne-niobium(I) complexes with functionalized alkynes: synthesis, structure and reactivity. J Organomet Chem 498:29–35
65. Ward BC, Templeton JL (1980) Nuclear magnetic resonance studies of alkynes as four-electron donor ligands in monomeric tungsten(II) complexes. J Am Chem Soc 102:1532–1538
66. Melník M, Sundberg M et al (1983) Study of copper(II) propionate adducts with diphenylphosphinoacetylene and bis(diphenylphosphino)acetylene. Acta Chim Scan A 37:659–662
67. Went MJ (1995) Multidentate ligands bound via alkyne and group 15 or 16 donor sites. Polyhedron 4:465–481
68. Oberhauser W, Bachman C et al (1997) Binuclear palladium(II), platinum(II) and platinum(IV) complexes containing 1,2-bis(diphenylphosphino)acetylene: different orientations of the diphosphine-bridges due to metal-phosphorus $d\pi$–$d\pi$ back bonding. Inorg Chim Acta 256:223–234
69. Powell AK, Went MJ (1992) Phosphorus donor chemistry of $[W(CO)(Ph_2PC{\equiv}CPPh_2)(S_2CNEt_2)_2]$. J Chem Soc Dalton Trans 439–445
70. Nickel TM, Yau SYW et al (1989) A new chelating ligand: co-ordination chemistry of $[W(CO)(Ph_2PC{\equiv}CPPh_2)(S_2CNEt_2)_2]$. J Chem Soc Chem Commun 775–776
71. Hong FE, Chang YL et al (2004) Preparation and NMR studies of cobalt-containing diphosphine ligand chelated W, Ru, Au and Pd complexes: Suzuki cross-coupling reactions and carbonylation catalyzed by the Pd complex. Dalton Trans 157–165
72. Carty AJ, Efraty A (1968) Evidence for metal–phosphorus d_π–d_π bonding from ν(C≡C) Raman shifts in complexes of bis(diphenylphosphino)acetylene. Chem Commun 1559–1561
73. Carty AJ, Efraty A (1968) A new class of palladium and platinum complexes: diphosphine bridged $M_2X_4L_2$ species. (L = bis diphenylphosphinoacetylene). Inorg Nucl Chem Lett 4:427–431
74. Carty AJ, Efraty A (1969) Coordination complexes of acetylene diphosphines. II. Diphosphine bridged palladium(II) and platinum(II) derivatives. Can J Chem 47:2573–2578
75. Shin KS, Noh DY (2004) Binuclear platinum(II) building-blocks for the metal-coordinated self-assembly: (dithiolate)Pt$(\mu\text{-dppa})_2$Pt(dithiolate) where dppa = bis(diphenylphosphino) acetylene. Bull Korean Chem Soc 25:130–132
76. Clark HC, Fergusson G et al (1985) Synthesis of heterobimetallic bis(dipheny1phosphino) acetylene-bridged palladium–platinum complexes. Crystal and molecular structure of $[PdPtCl_4(Ph_2PC{\equiv}CPPh_2)_2]{\cdot}2CHCl_3$. Inorg Chem 24:3924–3928
77. Clark HC, Manzer LE (1973) Reactions of (π-1,5-cuclooctadiene)organo-platinum(II) compounds and the synthesis of perfluoroalkylplatinum complexes. J Organomet Chem 59:411–428
78. Martin-Redondo MP, Scoles L et al (2005) Metal-templated diyne cyclodimerization and cyclotrimerization. J Am Chem Soc 127:5038–5039
79. Weelock KS, Nelson JH et al (1970) Zerovalent and divalent palladium and platinum complexes with phosphinoacetylenes. Inorg Chim Acta 4:399–403
80. Xu D, Murfee HJ et al (2000) Photoluminescent macrocyclic Pd(II) and Pt(II) dimeric complexes with Ph_2P–C≡C–PPh_2 spacer. J Organomet Chem 596:53–63
81. Clark HC, Kapoor PN et al (1984) Mixed ligand complexes of platinum(0) containing diphosphines. J Organomet Chem 265:107–115
82. Falvello LR, Fornies J et al (2001) Some platinum(II) complexes containing bis (diphenylphosphino)acetylene $PPh_2C{\equiv}CPPh_2$: synthesis, characterisation and crystal structures. J Chem Soc Dalton Trans 2132–2140
83. Praingam N, Anderson GK et al (2007) Base-promoted synthesis of monometallic and bimetallic platinum complexes containing chelating O,O- or S,S-donor ligands. Inorg Chim Acta 360:1767–1770

84. Bolinger CM, Rauchfuss TB (1982) Template syntheses of 1,2-alkene dichalcogenide chelates via the addition of activated acetylenes to dicyclopentadienyltitanium pentachalcogenides. Inorg Chem 21:3947–3954
85. Noh DY, Shin KS et al (2007) Synthesis, X-ray crystal structure and luminescence properties of binuclear platinum(II) complex with PtP_2S_2 core and acetylenic bridge. Bull Korean Chem Soc 28:343–346
86. Anderson WA, Carty AJ et al (1969) Coordination complexes of acetylene diphosphines. Part III. Silver(I) and mercury(II) complexes. Can J Chem 47:3361–3366
87. James SL, Xu X et al (2003) Phosphine-based coordination cages and nanoporous coordination polymers. Macromol Symp 196:187–199
88. Lozano E, Nieuwenhuyzen M et al (2001) Ring-opening polymerisation of silver-diphosphine $[M_2L_3]$ coordination cages to give $[M_2L_3]_\infty$ coordination polymers. Chem Eur J 7:2644–2651
89. James SL, Lozano E et al (2000) Triply-bridged diphos disilver helical complexes $[Ag_2(\mu_2\text{-dppa-}P,P')_3(\text{anion})_2]$ [dppa = bis(diphenylphosphino)acety-lene]. Chem Commun 617–618
90. Carty AJ, Efraty A et al (1969) Some new diphosphine-bridged nickel carbonyl and cyclopentadienyl compounds. Can J Chem 47:1429–1431
91. Hogarth G, Norman T (1996) Linking metal centres with bis(diphenylphosphino)acetylene (dppa): syntheses and molecular structures of $[\{Mo(CO)_4(\mu\text{-dppa})\}_2]$ and $[\{Mo(CO)_3\}_2(\mu\text{-dppa})_2]$. Polyhedron 15:2859–2867
92. Baker PK, Armstrong EM (1990) Mono- and dinuclear phosphine coordinated 1,4-bis (diphenylphosphino)ethyne seven-coordinate complexes of molybdenum(II) and tungsten(II). Polyhedron 9:801–804
93. Howard KE, Rauchfuss TB (1986) Organometallic derivatives of the tetrathiometallates: syntheses, structures, and reactions of $MS_4[Rh(COD)]_2$ and $MS_4[(C_5H_5)Ru(PPh_3)]_2$ (M = Mo, W). J Am Chem Soc 108:297–299
94. Peli G, Rizzato S et al (2005) Carbonyl complexes of Rh(I) and Ir(I) and P-donor ligands as useful "building blocks" for the self-assembly of new organometallic polymers. Cryst Eng Commun 7:575–577
95. Vogels CM, Decken A et al (2006) Rhodium(I) acetylacetonato complexes containing phosphinoalkynes as catalysts for the hydroboration of vinylarenes. Can J Chem 84:146–153
96. Li L, Reginato N et al (2003) The synthesis and structural characterization of linear and macrocyclic bis(dinitrosyliron) complexes supported by bis(phosphine) bridging ligands. J Can Chem 81:468–475
97. Eaton GR, Holm RH (1971) Bridged binuclear bis-dithiolene complexes of iron and cobalt. Inorg Chem 10:805–811
98. Bechtold HC, Rehder D (1979) The coordinative properties of *cis/trans*-1,4-diphosphabutene and 1,4-diphosphabutyne in carbonylvanadium compounds. J Organomet Chem 172:331–339
99. Xu D, Khin KT et al (2001) Metallocyclic receptors with Re^{I}/Os^{II}-based moieties: molecular photophysics and selective molecular sensing. Chem Eur J 7:2425–2434
100. Xu D, Hong B (2000) Investigation of electronic communication and guest inclusion using photoluminescent macrocyclic receptors with Ru^{II} centers and $Ph_2P–C{\equiv}C–C{\equiv}C–PPh_2$ spacers. Angew Chem Int Ed 39:1826–1829
101. Bennett MA, Byrnes MJ et al (2007) Bis(acetylacetonato)ruthenium(II) complexes containing alkynyldiphenylphosphines. Formation and redox behaviour of $[Ru(acac)_2(Ph_2PC{\equiv}CR)_2]$ (R = H, Me, Ph) complexes and the binuclear complex *cis*-$[\{Ru(acac)_2\}_2(\mu\text{-}Ph_2PC{\equiv}CPPh_2)\}_2]$. J Chem Soc Dalton Trans 1677–1686
102. Liu YC, Li CI et al (2006) Syntheses and structural characterization of dicopper(I) bis(diphenylphosphino)acetylene complexes containing tricyclic, cyclic and linear frameworks. Inorg Chim Acta 359:2361–2368
103. Kui SCF, Kuang JS et al (2006) Self-assembly of a highly stable, topologically interesting metallamacrocycle by bridging gold(I) ions with pyridyl-2,6-diphenyl^{2-} and diphosphanes. Angew Chem Int Ed 45:4663–4666

104. Viau L, Willis AC et al (2007) Ruthenium cluster chemistry: monodentate bis(diphenylphosphino)acetylene-ligated cluster modules in chain and dendrimer formation. J Organomet Chem 692:2086–2091
105. Johnson BFG, Sanderson KM et al (2000) Electron-beam induced formation of nanoparticle chains and wires from a ruthenium cluster polymer. Chem Commun 1317–1318
106. Chen JL, Zhang LY et al (2003) Syntheses, structures, and redox properties of dimeric triruthenium clusters bridged by bis(diphenylphosphino)acetylene and -ethylene. Inorg Chem 43:1481–1490
107. Housecroft CE, Rheingold AL et al (1998) Towards linked clusters: reactions of $[Ru_6(CO)_{17}B]$-with dppm and [ClAu(L–L)AuCl] (L–L=bis(diphenylphosphino)-alkanes, -ethene and -ethyne, and the crystal structure of $[HRu_6(CO)_{15}(P, P'$-dppm)B] (dppm=bis (diphenylphosphino)methane). J Organomet Chem 565:105–114
108. Adams CJ, Bruce MI et al (1998) Carbonyl substitution reactions of ruthenium cluster complexes containing dicarbon (C2) ligands: X-ray structures of $Ru_5(\mu_5\text{–}C_2)(\mu\text{-SMe})_2(\mu\text{-PPh}_2)_2(CO)_{10}(L)$ [L=CNBut, $P(OMe)_3$]. J Organomet Chem 561:97–107
109. Bruce MI, Humphrey PA et al (1997) Acetylenic phosphines bridging two cluster units: molecular structure of $\{Ru_3(\mu\text{-H})(\mu_3\text{–}C_2Bu^t)(CO)_8\}_2(\mu\text{-dppa})$ [dppa $= C_2(PPh_2)_2$]. Austr J Chem 50:535–538
110. Louattani E, Suades J et al (1996) Synthesis of a zwitterionic P-coordinated complex with bis(diphenylphosphino)acetylene. Organometallics 15:468–471
111. Osella D, Hanzlík J (1993) Electronic interactions in multicluster arrays. An electrochemical approach. Part III. Inorg Chim Acta 213:311–317
112. Sappa E (1988) Bis(diphenylphosphino)acetylene as a bridging ligand between homo- and hetero-metallic clusters. J Organomet Chem 352:327–336
113. Bettenhausen M, Eichhöfer A et al (1999) Synthese und strukturen neuer selenido- und selenolatoverbrückter kupfercluster: $[Cu_{38}Se_{13}(SePh)_{12}(dppb)_6]$ (1), $[Cu(dppp)_2][Cu_{25}Se_4(SePh)_{18}(dppp)_2]$ (2), $[Cu_{36}Se_5(SePh)_{26}(dppa)_4]$ (3), $[Cu_{58}Se_{16}(SePh)_{24}(dppa)_6]$ (4) und $[Cu_3(SeMes)_3(dppm)]$ (5). Z Anorg Allg Chem 625:593–601
114. Semmelmann M, Fenske D et al (1998) Copper-chalcogenide clusters stabilised with linear bidentate phosphine ligands. J Chem Soc Dalton Trans 2541–2545
115. Sevillano P, Fuhr O et al (2007) Synthese und struktur von $[Au_{10}Se_5(dppa)_4\{Co_2(CO)_5\}_4]$. Z Anorg Allg Chem 633:1783–1786
116. Amoroso AJ, Johnson BFG et al (1992) The use of bis(diphenylphosphinoacetylene) and its digold derivative as linking groups in osmium cluster chemistry. Crystal structures of $[\{Os_3(CO)_{11}\}_2(dppa)]$, $[Os_3(CO)_{10}(dppa)]_2$ and $[Os_4H(CO)_{12}Au(dppa)]_2$ (dppa $= Ph_2PC{\equiv}CPPh_2$). J Organomet Chem 440:219–231
117. Johnson BFG, Lewis J et al (1990) Synthesis and characterisation of linked triosmium clusters using the bis(diphenylphosphino)acetylene ligand. J Organomet Chem 397:C28–C30
118. Amoroso AJ, Lewis J et al (1993) Mixed-metal clusters containing osmium and gold. In: Welch AJ, Chapman SK (eds) The chemistry of the copper and zinc triads, 1st edn. Royal Society of Chemistry, Cambridge
119. Galsworthy JR, Housecroft CE et al (1995) Unexpected gold-containing boride clusters formed from the reactions of $[RhRu_3H(\eta^5\text{-}C_5Me_5)(CO)_9BH]^-$ with gold(I) phosphine derivatives: crystal structures of $[RhRu_3H(\eta^5\text{-}C_5Me_5)(CO)_9B\{Au(PPh_3)\}_2(AuCl)]\cdot CH_2Cl_2$ and $[RhRu_3H(\eta^5\text{-}C_5Me_5)(CO)_9B\{Au_2(dppf)\}(AuCl)]\cdot CH_2Cl_2$ [dppf $= 1,1'$-bis (diphenylphosphino)ferrocene]. J Chem Soc Dalton Trans 2639–2647
120. Hong FE, Chang H et al (2001) Preparation and characterization of a cyclic compound consisting of bis(diphenylphosphino)acetylene joined alkyne-bridged dicobalt fragments. Chem Lett 30:1130–1131
121. Aullón G, Hamidi M et al (2004) Chalcogen-chalcogen bonds in edge-sharing Square-planar d^8 complexes. Are they possible? Inorg Chem 43:3702–3714
122. Nicolaou KC, Smith AL (1995) The enediyne antibiotics. In: Stang PJ, Diederich F (eds) Modern acetylene chemistry, 1st edn. VCH, Weinheim

123. Nicolaou KC, Zuccarello G et al (1988) Cyclic conjugated enediynes related to calicheamicins and esperamicins: calculations, synthesis, and properties. J Am Chem Soc 110:4866–4868
124. Basak A, Mandal S et al (2003) Chelation-controlled Bergman cyclization: synthesis and reactivity of enediynyl ligands. Chem Rev 103:4077–4094
125. Warner BP, Millar SP et al (1995) Controlled acceleration and inhibition of Bergman cyclization by metal chlorides. Science 269:814–816
126. Nicolaou KC, Dai WM (1991) Chemistry and biology of the enediyne anticancer antibiotics. Angew Chem Int Ed Engl 30:1387–1416
127. Coalter NL, Concolino TE et al (2000) Structure and thermal reactivity of a novel Pd(0) metalloenediyne. J Am Chem Soc 122:3112–3117
128. Schmitt EW, Huffmann JC et al (2001) Thermal reactivities of isostructural d^{10} metalloenediynes: metal-dependent Bergman cyclization. Chem Commun 167–168
129. Baumgartner T, Huynh K et al (2002) Metallochain cluster complexes and metallomacrocyclic triangles based on coordination bonds between palladium or platinum and diphosphinoacetylene ligands. Chem Eur J 8:4622–4632
130. Carty AJ, Efraty A (1968) Binuclear copper(I) complexes with bridging bis (diphenylphosphino)acetylene groups. Can J Chem 46:1598–1599
131. Carty AJ, Efraty A (1969) Coordination complexes of acetylene diphosphines. I. diphosphine-bridged binuclear copper(I) and gold(I) complexes of bis(diphenylphosphino)acetylene. Inorg Chem 8:543–550
132. Wallbank AI, Corrigan JF (2002) Triply bridged dicopper-bis(trimethylsilylchalcogenolates): synthesis and characterization of the series of helical complexes $[(Me_3SiE\text{-}Cu)_2(\mu\text{-}Ph_2PC{\equiv}CPPh_2\text{-}\kappa^2P)_3]$ (E = S, Se, Te). Can J Chem 80:1592–1599
133. DeGroot MW, Corrigan JF (2006) Metal-chalcogenolate complexes with silyl functionalities: synthesis and reaction chemistry. Z Anorg Allg Chem 632:19–29
134. Bardaji M, De la Cruz MT et al (2005) Luminescent dinuclear gold complexes of bis(diphenylphosphano)acetylene. Inorg Chim Acta 358:1365–1372
135. Yeh WY, Peng SM et al (2003) Synthesis and reactivity of ditungsten helical complex $W_2(CO)_6(\mu\text{-}Ph_2PC{\equiv}CPPh_2)_3$. J Organomet Chem 671:145–149

Chapter 3
Theoretical Evaluation of Phosphine Effects in Cross-Coupling Reactions

Max García-Melchor, Gregori Ujaque, Feliu Maseras and Agustí Lledós

Abstract Cross-coupling reactions are one of the most useful reactions in organic synthesis. Among all the transition metal complexes developed as catalysts for this reaction those based on Pd are by far the most utilized ones. The most common stoichiometry of this family of catalyst is PdL_2 with L = phosphine ligands. The effects of the phosphine ligands on the reaction mechanism evaluated by means of theoretical calculations are reviewed in these lines. How the nature of the phosphine ligand affects each of the elementary processes involved in a cross-coupling reaction, namely oxidative addition, transmetalation and reductive elimination will be exposed separately. The transmetalation process has its own particular mechanistic details depending on the cross-coupling reaction; those for the Suzuki–Miyaura and Stille reactions will be described here. The dichotomy between the monophosphine and bisphosphine reaction pathways will be also discussed.

3.1 Introduction

During the last decades the design of new and more efficient transition metal catalysts has become of major importance in organometallic chemistry and homogenous catalysis [1, 2]. In this research field, the change of the ligands coordinated to

M. García-Melchor · G. Ujaque · F. Maseras · A. Lledós (✉)
Departament de Química, Edifici Cn, Universitat Autònoma de Barcelona, 08193 Bellaterra, Catalonia, Spain
e-mail: agusti@klingon.uab.es

F. Maseras
Institute of Chemical Research of Catalonia (ICIQ), Av. Països Catalans, 16, 43007 Tarragona, Catalonia, Spain

M. Peruzzini and L. Gonsalvi (eds.), *Phosphorus Compounds*, Catalysis by Metal Complexes, 37, DOI: 10.1007/978-90-481-3817-3_3,
© Springer Science+Business Media B.V. 2011

the metal center modifying their properties has emerged as an elegant and useful alternative for that purpose [3–10]. Particularly, phosphorus compounds with the general structure PA_3 (A = R, X, NR_2, OR) or asymmetric substitution patterns PA_2A', $PAA'A''$ are a milestone, since the steric and electronic properties of the catalyst can be modified or fine-tuned by introducing different substituents on the phosphorus donor atom. These changes in the catalyst properties may modify its reactivity and therefore, the catalytic activity of that transition metal complex. For this reason, it is not surprising that steric and electronic parameters of an immense variety of phosphorus compounds have been analyzed in the literature [5–10].

In the last years, due to the growth in the development of new technologies and more powerful computers, theoretical calculations started to become more relevant in the design of new transition metal catalysts. In particular, the contributions from computational methods have enabled not only the better understanding of catalytic reactions, but in some cases the possibility to predict and suggest new transition metal complexes as more efficient catalysts [11, 12]. Thus, theoretical methods provide a big support to experimental techniques, besides being less expensive and more sustainable, which nowadays is a concern within the Chemist community.

Due to the limitations in computational resources, most of the initial computational studies of catalytic reactions were performed by quantum mechanic (QM) calculations, modeling the substituents on the phosphorus atom. Among all the models, PH_3 was the earliest and most widely used, and was shown to give acceptable results in many cases [13, 14]. However, with the appearance of more powerful computers the calculation of catalytic systems with the real phosphine ligands has been achieved, initially with hybrid methods like quantum mechanics/molecular mechanics (QM/MM) [15–19], and afterwards with full QM calculations [20, 21]. Thus, at present, the computation of catalytic systems with simplified phosphines is particularly useful when exploring multiple reaction pathways (qualitative studies), but care is needed when quantitative information for a particular system is required.

In this current chapter, we will focus on how transition metal catalysts containing phosphine ligands have been computationally treated and which is the effect of these ligands on their catalytic activity. Particularly, computational studies concerning one of the most important transformations in organometallic chemistry will be reviewed: The palladium-catalyzed C–C Cross-Coupling reactions.

3.2 Overview of C–C Cross-Coupling Reactions

The catalyzed C–C cross-coupling reactions have become increasingly important in modern organic synthesis and in organometallic chemistry during the last decades. A huge variety of complex compounds can be synthesized from readily accessible reactants [22–25]. These reactions consist in the carbon–carbon bond formation between an organic electrophile R-X and an organometallic nucleophile R-m in the presence of a catalyst [M] (Fig. 3.1). The catalysts most broadly used are the transition metal complexes from groups 8–10, especially Ni [26] and Pd [27, 28].

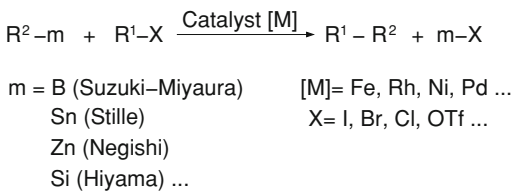


Fig. 3.1 General scheme for C–C cross-coupling reactions

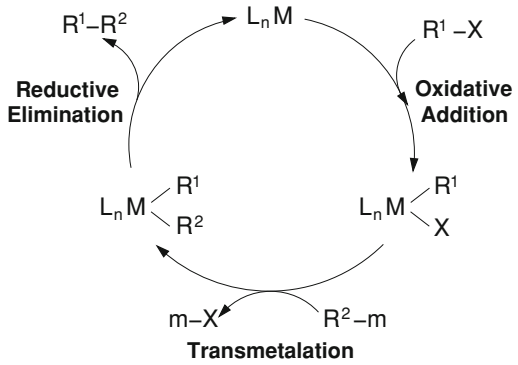


Fig. 3.2 General catalytic cycle for C–C cross-coupling reactions

Cross-coupling reactions can be classified depending on the metal or semimetal present in the nucleophile. For instance, Stille reaction [29, 30] is tin-mediated, Suzuki–Miyaura [31, 32] boron-mediated, Negishi [33, 34] zinc-mediated, etc. In general, these reactions follow a general accepted reaction pathway that consists of three steps (Fig. 3.2) [35]: (1) *oxidative addition* or insertion of the low valent transition metal into the electrophilic carbon-heteroatom bond, (2) *transmetalation* or displacement of a heteroatom leaving group by the nucleophile, and finally, (3) *Reductive elimination* to form the new C–C bond with the concomitant regeneration of the catalyst. The former and the latter steps are common to all cross-coupling reactions and have been studied in some depth both by experimental [36–39] and computational [40–42] methods. Hence, the mechanisms for these two steps are quite well understood. In contrast, the various cross-coupling reactions differ in the nucleophile used for transmetalation and, consequently, in the transmetalation step. In addition, experimental evidence for this process is particularly difficult to obtain due to the complexity that involves the isolation and characterization of key intermediates. Thus, it is not surprising that the mechanistic studies concerning this step are scarce [43–45] or even for some cross-coupling reactions it still remains unknown.

Initially, cross-coupling reactions had the important limitation that only aryl bromides and iodides could be employed as substrates. However, as aryl chlorides are more profusely available and in general are less expensive than their bromide and iodide analogs, many efforts to find a solution on that issue have been made since then [46]. In this way, important advances for the past few years are mainly

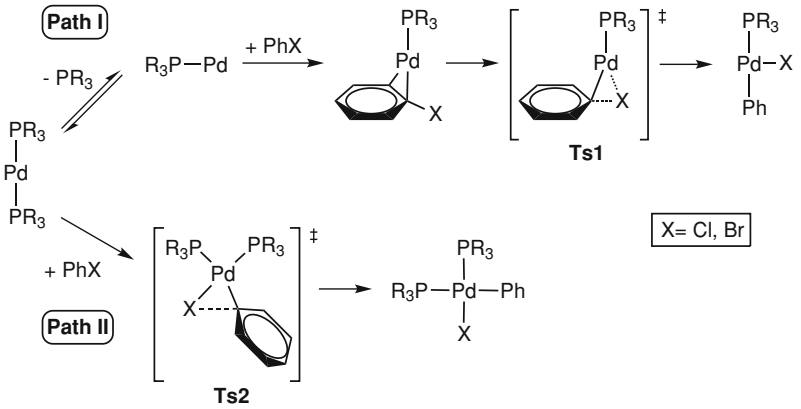


Fig. 3.3 Reaction mechanisms for the oxidative addition of PhX to $[Pd(PR_3)_2]$ [53]

due to the development of new transition metal complexes containing electron rich and bulky ligands (mostly phosphines [47–49], but also carbenes [50, 51]).

In the following sections, we will review some of the most relevant computational mechanistic studies on the three steps of some Pd-catalyzed C–C cross-coupling reactions and how the phosphine ligands coordinated to the transition metal center affect the catalyst reactivity within these steps. Most of the results reported have been obtained using the Density Functional Theory (DFT) with the hybrid functional B3LYP, although other functionals as B3PW91 have been also employed.

3.3 Phosphine Effects in Oxidative Addition

Oxidative addition constitutes the first step in cross-coupling reactions and it has drawn enough attention since it has been suggested to be rate-limiting step in some reactions, particularly when X = Cl. Even though this process has been investigated in some depth during the last years [37, 40–42] there are still some aspects that are not completely fully understood, such as the enhanced reactivity of transition metal complexes containing electron-rich and bulky ligands. This enhanced reactivity has been attributed to the formation of monoligated [ML] species which can undergo oxidative addition more rapidly than the corresponding bis-ligated ones $[ML_2]$ [52]. In order to shed light on this issue, Liu et al. recently reported a computational study in which the oxidative addition of aryl halides PhX to $Pd(PR_3)_2$ (R = Me, Et, *i*-Pr, *t*-Bu, Ph) was investigated at the Density Functional Theory (DFT) level [53]. In particular, the mechanisms for the oxidative addition reaction through both palladium complexes with one and two coordinated phosphine ligands were evaluated (Fig. 3.3). Geometry optimizations were performed by means of the B3PW91 functional and subsequently, single-point calculations were carried out at the PBEPBE level.

Path I involves dissociation of one phosphine ligand from the initial complex [Pd(PR_3)$_2$] followed by the coordination of PhX to form the complex [Pd(η^2-PhX)PR_3]. Afterwards, this last complex undergoes oxidative addition through **Ts1** resulting in the tricoordinated complex [Pd(PR_3)(Ph)X]. In contrast, Path II involves the direct oxidative addition to the initial Pd complex via the bisphosphine transition state **Ts2** to form *cis*-[Pd(PR_3)$_2$(Ph)X].

According to the results obtained by Liu et al. for the oxidative addition of PhCl to [Pd(PR_3)$_2$], a preference for the monophosphine pathway (Path I) was showed for all the analyzed PR_3 ligands (R = Me, Et, *i*-Pr, *t*-Bu, Ph) with energy differences ranging from 2.0 (R = Me) to 14.1 kcal/mol (R = *i*-Pr). Besides, the oxidative addition through Path II was found to be higher in energy, and even in the case of R = *t*-Bu, no transition state **Ts2** could be located. In the latter case, all the attempts to find the corresponding transition state always led to the substitution of one phosphine ligand by PhCl. The transition state for this substitution was located, but it resulted to be higher in energy compared to dissociation of one phosphine ligand via Path I (ca. 24 kcal/mol higher). The computational study reported by Liu was also extended to bromines for some PR_3 compounds.

Interestingly, among the different PR_3 ligands analyzed by Liu et al., no significant differences were found in the computed free-energy barriers for the oxidative addition of PhCl to the monophosphine species [Pd(PR_3)] (i.e. less than 2 kcal/mol); this indicates that this reaction is nearly independent of the organic group R. Conversely, a significant difference was found for the dissociation energy of one phosphine ligand from the initial Pd complex. Specifically, the computed dissociation energies for the different PR_3 ligands followed the order: R = Me > Et > PPh_3 > *i*-Pr > *t*-Bu with energy values ranging from 26.0 (R = Me) to 19.4 kcal/mol (R = *t*-Bu). This energy difference to generate the monophosphine Pd species was proposed by the authors to govern the different reactivity of the distinct PR_3 ligands in the oxidative addition process. In particular, the authors attributed the unique capability of P(*t*-Bu)$_3$ of accomplishing cross-coupling of inactivated aryl chlorides to that energy difference. Similar conclusions have been also reported by Ariafard and Yates in a very recent computational study with palladium catalysts containing the ligands L = P(*t*-Bu)$_3$, PPh_3 and PMe_3 [54].

More recently, Hartwig et al. reported an exhaustive kinetic study [55] parallel to that previously reported by Liu et al. Therein, the oxidative addition of aryl halides PhX (X = I, Br, Cl) to the complexes PdL_2 (L = P(*t*-Bu)$_3$, 1-AdP(*t*-Bu)$_2$ (1-Ad = 1-adamantyl), CyP(*t*-Bu)$_2$, and PCy_3) was examined. The aim of their work was to analyze the steric effects of the ligands on the coordination number of the species that undergo oxidative addition, and to determine whether the halide present in the PhX plays a role or not, in this step. For this investigation, three potential mechanisms for the oxidative addition reaction were considered (Fig. 3.4). The pathways A and C correspond to the same reaction pathways that Liu et al. previously examined in their work (Path II and Path I, respectively) [53] while pathway B assumes an oxidative addition from a monophosphine species generated via associative displacement of the ligand by the haloarene.

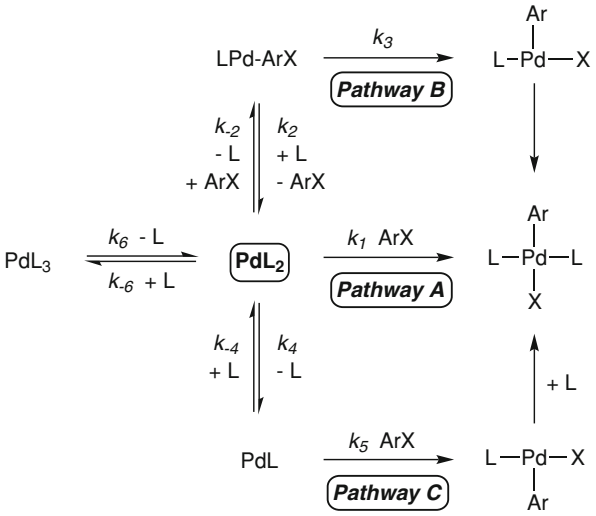


Fig. 3.4 Scheme of the three proposed mechanisms for the oxidative addition of ArX to $[PdL_2]$ [55]

The kinetic results obtained by Hartwig et al. revealed that the rate constants for the oxidative addition reaction depend more on the identity of the halide than on the steric bulk of the ligand. All the reactions with iodoarenes were found to occur by rate-determining reaction involving a bisphosphine complex, whereas all the reactions with chloroarenes occur by rate-determining reaction with a monophosphine complex. Particularly, the reactions with iodoarenes follow the pathway B,[1] whereas the reactions with chloroarenes follow the dissociative pathway C. Further, the authors proposed that iodoarenes react with the bisphosphine complexes via an irreversible process because they are softer and more reactive than the other haloarenes. In contrast, in the case of chloroarenes they suggested that the generation of the more reactive monophosphine species is required because they are poorer ligands and necessitate a more reactive intermediate to cleave the less reactive C–Cl bond. These conclusions are in agreement with the recently reported low energy barriers for oxidative addition of chloroarenes to monophosphine Pd(0) species and high energy barriers for oxidative addition of chloroarenes to bisphosphine Pd(0) [42, 56].

As far as the bromoarenes are concerned, the oxidative addition to Pd complexes containing the ligands L = 1-AdP(*t*-Bu)$_2$ and L = CyP(*t*-Bu)$_2$ appeared to occur by two competitive paths involving rate-determining reactions of bisphosphine complexes to give rise to monophosphine intermediates (i.e. pathway B and pathway C). Besides, the oxidative addition to Pd complexes with the ligand

[1] For Pd complexes containing the ligand L = PCy_3, Hartwig et al. concluded that the reaction would take place from $Pd(PCy_3)_3$ (the major species under reaction conditions) via reversible dissociation of one phosphine ligand to generate the $Pd(PCy_3)_2$ species. Then, this species would react irreversibly with PhI. However, the mechanism for this reaction could not be confirmed whether it would occur through either the pathway A or the pathway B.

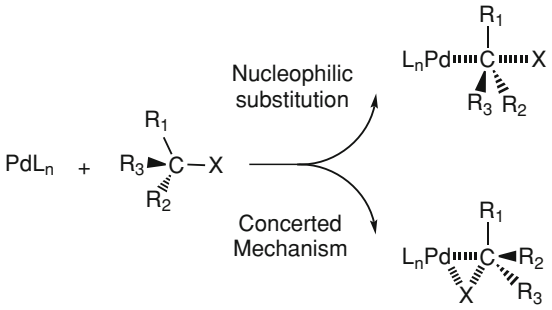


Fig. 3.5 Mechanisms proposed for the oxidative addition reaction

L = PCy_3 was consistent with both the pathway A and B, and so, no distinction between this two paths could be done.

More recently, the effect of the phosphine ligands L = PMe_3, $P(CF_3)_3$, PPh_3 and $P(t\text{-}Bu)_3$ within the full catalytic cycle of Suzuki cross-coupling reaction was computationally analyzed by Harvey et al. [57] by using steric and electronic descriptors [58–60] in multiple linear regression models. In particular, the oxidative addition step was found to be mainly dominated by ligand electronics which agrees with the fact that better σ-donor ligands lead to lower oxidative addition barriers [61]. The computed energy barrier heights for the oxidative addition with the electron poorer $P(CF_3)_3$ was found to be higher than that for the electron-rich ligands $P(t\text{-}Bu)_3$, PMe_3 and PPh_3.

The oxidative addition process commented so far are used to be described as a concerted process. Nevertheless, "nucleophilic attack" to the carbon center of the metal species [Pd(0)L_n] has been also proposed for the oxidative addition process (Fig. 3.5). Initial proposals for this process were done by Stille studying experimentally the oxidative addition of benzyl halides to Pd(0); the authors postulated a S_N2-type process with inversion of configuration at the benzylic center [62]. Such a substitution mechanism is commonly proposed in organic reactions mechanisms. The nucleophilic attack mechanism has been also postulated by means of theoretical studies on several oxidative addition processes [40, 41, 63, 64]. In the particular case of the oxidative addition of sp^3 carbons in α-sulfoxide systems the reaction was found to be fast and stereoselective, presenting an inversion of configuration [65]. The reaction mechanism for this process was investigated by DFT calculations for both the monophosphine and bisphosphine systems leading to qualitatively similar results. In all cases the nucleophilic substitution transition states showed lower barrier than their corresponding concerted pathways [66].

3.4 Phosphine Effects in Transmetalation

As we stated before, the mechanism for the transmetalation process is expected to show differences depending on the cross-coupling reaction since they differ in the nucleophile used. Thus, perhaps not surprisingly, the mechanism for this step has

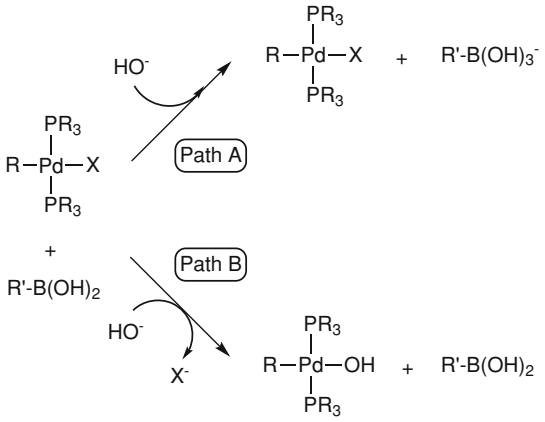


Fig. 3.6 Two main proposed reaction pathways for the role of the base in Suzuki–Miyaura reaction

been studied in less depth compared to the other ones, and the number of computational and experimental studies dealing with transmetalation is still lower. Among them, the Suzuki and Stille cross-coupling reactions are probably the most studied. Therefore, herein we present an overview of the reported studies on the transmetalation process within these two cross-coupling reactions, with special focus on the effects of phosphine ligands.

3.4.1 The Transmetalation Step in the Suzuki–Miyaura Reaction

Since the publication of the seminal paper of Miyaura et al. [31, 32] in 1979, some issues concerning the mechanistic details of the transmetalation step in the Suzuki–Miyaura reaction have appeared. For example, the role of the base was not clear and several proposals were made [67]. In order to cast light on this issue, many experimental studies were carried out [31, 32, 68, 69]. Particularly, two main pathways consisting on the base attacking first either the palladium complex or the organoboronic acid were proposed to account for the effect of the base in this step (Fig. 3.6).

The role of the base was unraveled through DFT-B3LYP studies by Maseras, Ujaque and co-workers [70] concluding that the role of the base was to react with the organoboronic acid to generate the anionic species $[RB(OH)_3]^-$; this is the reactive species taking part in the transmetalation process by substituting the halide and the subsequent transmetalation step.

With the role of the base established, another issue in the Suzuki–Miyaura reaction was to elucidate whether the mechanism for the transmetalation step involved either one or two phosphine ligands in the Pd catalytic species. On this issue, Maseras et al. reported a thorough computational study at DFT-B3LYP level of the full catalytic cycle for the coupling of vinyl bromide and vinylboronic acid $H_2C{=}CHB(OH)_2$ catalyzed by both $[Pd(PH_3)_2]$ and $[Pd(PH_3)]$ [71]. Moreover, alternative mechanisms for the transmetalation step depending on the *cis* or *trans*

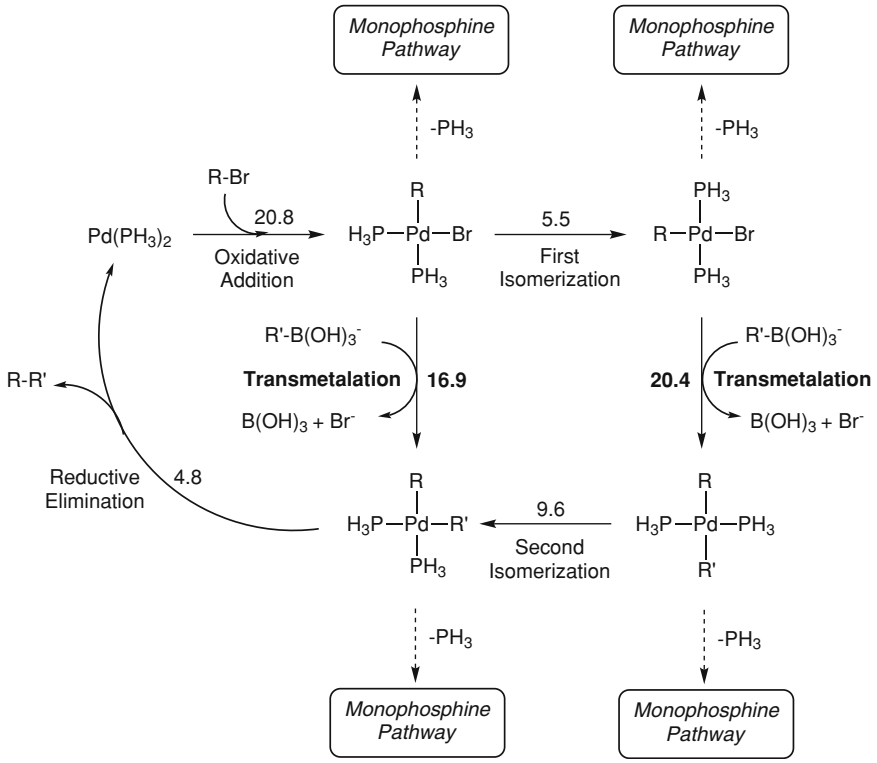


Fig. 3.7 Full reaction mechanism for the Suzuki reaction through bisphosphine Pd complexes theoretically analyzed by Maseras et al. [71] (Energies in kcal/mol)

isomery were also considered. According to their results, the transmetalation through both the bisphosphine pathways (Fig. 3.7) and the monophosphine pathways (Fig. 3.8) have reasonably low energy barriers, though lower energy barriers were found for the monophosphine reaction pathways.

However, special cautiousness should be taken when considering these mechanisms since it was generally assumed that the initial palladium complex (the one generated after the oxidative addition process) is a bisphosphine Pd complex when using regular phosphines. Thus, an additional energy for the dissociation of one of the phosphine ligands to generate the monophosphine species is required. A precise calculation of ligand dissociation processes in solution by means of static QM methods is not an obvious issue.

This study was later extended to aryls by the same authors obtaining qualitatively the same overall mechanism and suggesting that results of general validity can be obtained with the less computationally demanding vinyl systems [72]. Besides, this study also supported that the role of the base is to react with the boronate species regardless of which the electrophilic organic substrate is.

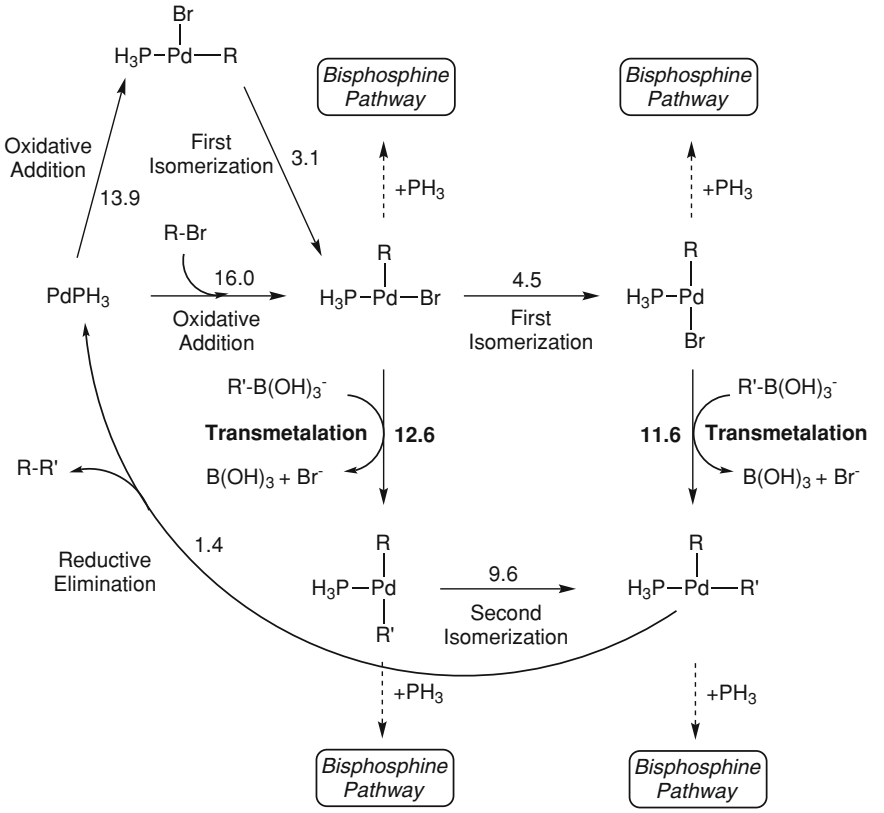


Fig. 3.8 Full reaction mechanism for the Suzuki reaction through monophosphine Pd complexes theoretically analyzed by Maseras et al. [71] (Energies in kcal/mol)

A related theoretical study on palladium-catalyzed borylation of iodobenzene with diboron was reported by Sakaki et al. [73]. Specifically, the mechanism for the transmetalation step between the Pd complexes $Pd(X)(Ph)(PH_3)_2$ (X = OH, F) and diboron $B_2(eg)_2$ (eg = $–OCH_2CH_2O–$) was investigated. Other theoretical studies, but now within the context of organic acids as electrophiles, were reported by Goo*ß*en et al. [74, 75]. The palladium catalyzed Suzuki reaction of carboxylic anhydrides with arylboronic acids was analyzed, showing that in those cases monophosphine complexes were also involved in the transmetalation process.

With the aim of designing new and more efficient catalysts for Suzuki reaction, the bulky and electron-rich dialkylbiaryl phosphine ligands (Fig. 3.9) were found to dramatically improve the efficiency and selectivity of this type of reactions [76]. In particular, Buchwald's group reported that the use of 2-(2′,6′-dimethoxybiphenyl)-dicyclohexylphosphine, SPhos (Fig. 3.9) in the palladium-catalyzed Suzuki reaction exhibited unprecedented scope, reaction rate, and stability [77]. More specifically, the use of this ligand conferred to the catalyst a unique activity allowing the coupling of boronic acids with aryl bromides and chlorides with low

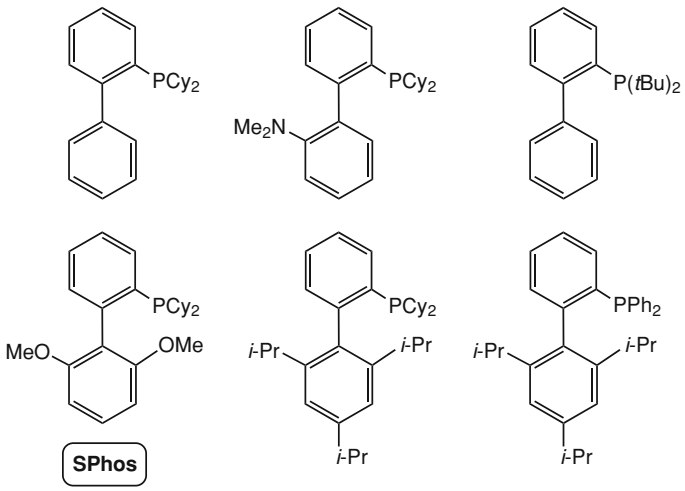


Fig. 3.9 Some examples of dialkylbiarylphosphines [76]

catalyst loadings. This enhanced reactivity was, in general, attributed by the authors to a combination of electronic and steric properties of this kind of ligands that favor the stabilization of the mono-ligated [PdL] intermediates, which are believed to be key species within the catalytic cycle [78]. So, this enhanced reactivity was not directly attributed to one step in particular, but to the full catalytic cycle in general.

The effect of different phosphine ligands over the Suzuki–Miyaura reaction was also experimentally and theoretically reported by Baillie et al. [79] and Hong et al. [80] respectively. In the first one, the effect of the size of phosphine ligands of type $P(biphenyl)_nPh_{3-n}$ in the palladium-catalyzed Suzuki reaction with aryl bromides and chlorides was investigated. Among the analyzed ligands, the highest conversions and turnovers were obtained using $P(biphenyl)Ph_2$, which the authors attributed to the contribution of both steric and electronic effects. On the other hand, in the study from Hong et al. [80], the effect of phosphorus and nitrogen chelating ligands (diphosphine, diimines, diamines) was computationally evaluated at DFT-B3LYP level for the palladium-catalyzed Suzuki reaction of phenyl chloride and phenylboronic acid. This type of ligands are particularly interesting within cross-coupling reactions because they provide kinetic and thermodynamic stability for the active species and further, forcing the entering ligands to be in a *cis* disposition with respect to each other; this allows to skip the *trans* to *cis* isomerization previous to the reductive elimination step. The results reported by Hong et al. with these chelating ligands revealed that the catalytic reaction employing diimine as the chelating ligand provide the most energetically feasible pathway. On the other hand, surprisingly high energies barriers in gas phase were found for the transmetalation processes with the different chelating ligands.

More recently, Hong et al. [81] reported a combined experimental and DFT-B3LYP computational study on bulky chelated ligands in which the application to

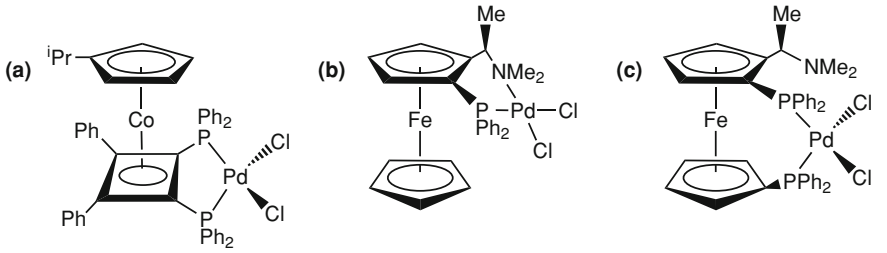


Fig. 3.10 Examples of Pd catalysts reported by Hong et al. [81]: **a** Pd complex synthesized by Hong et al. and applied to the Suzuki–Miyaura reaction. **b** and **c** Examples of other palladium complexes evaluated in their conformational study

the Suzuki reaction of a palladium-complex containing a cobalt sandwich diphosphine ligand [(η^5-$C_5H_4^i$Pr)Co(η^4-$C_4(PPh_2)_2Ph_2$)] was investigated (Fig. 3.10). The results reported therein showed that this ligand can be successfully applied in the synthesis of ferrocenylarenes. Furthermore, the computational analysis on various Pd complexes with different chelating ligands (Fig. 3.10) revealed that the most favorable conformation of these ligands in their corresponding Pd complexes is the one with a bite angle close to 90°.

Up until now, in most of the experimental and computational studies that were reviewed in this section, the effect of phosphine ligands such as electron-rich and bulky phosphine ligands in the Suzuki–Miyaura reaction has been analyzed as a global effect over the reaction rather than their isolated effect over the different steps within it. Harvey and co-workers very recently reported a DFT-B3LYP computational study on the effect of phosphine ligands over the different steps of the Suzuki–Miyaura reaction [57]. Therein, the effect of the phosphine ligands PMe_3, $P(CF_3)_3$, PPh_3 and P(*t*-Bu)$_3$ along the different steps in the full catalytic cycle was investigated by using steric and electronic descriptors in conjunction with DFT methods. Concerning the transmetalation step, the effects of those phosphine ligands were analyzed considering a mechanism in which the Pd complex had only one coordinated phosphine ligand. The transmetalation from a tetracoordinated square planar complex due to the chelating nature of boronate takes place through a four member ring transition state, resulting in a palladium complex with the two organic groups in a *cis* arrangement (Fig. 3.11). The results derived from this study revealed that both steric and electronic effects are important within this step. In particular, the computation of the steric descriptors showed that the bulkier ligands may produce higher energy barriers for this process probably due to the possible interactions with the rest of the substituents on the palladium complex in the rearrangement previous to the transition state. The conjuction of these steric and electronic effects resulted in the following order in the computed energy barriers with the different ligands: $P(CF_3)_3 < PPh_3 < PMe_3 <$ P(*t*-Bu)$_3$. Besides, the computation of the electronic descriptors pointed out that better π-acceptor phosphines may contribute to lowering the energy barrier for the transmetalation process. The authors rationalize this fact by the ability of these ligands to better stabilize the developing additional electron

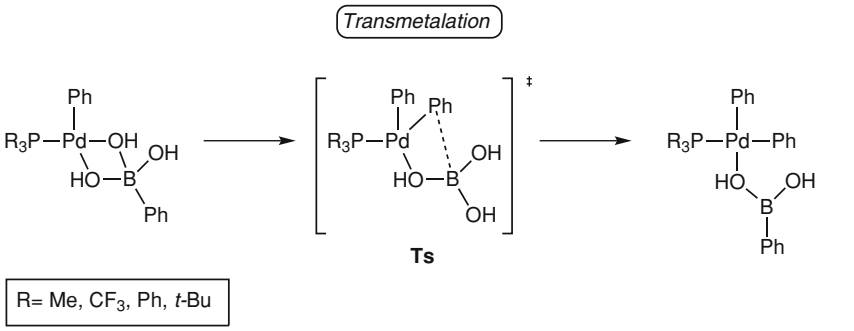


Fig. 3.11 Transmetalation process analyzed by Harvey et al. with different phosphine ligands

density on the metal as a result of the nucleophilic attack of the boronate phenyl group to the Pd atom.

3.4.2 The Transmetalation Step in the Stille Reaction

As stated in the beginning of the section, the Stille reaction along with the Suzuki–Miyaura reaction are the most broadly studied C–C cross-coupling reactions [82]. For the transmetalation process involved in the Stille reaction two main mechanisms dubbed as *cyclic mechanism* and *open mechanism* have been proposed in order to account for the reported experimental evidences (Fig. 3.12). In particular, the cyclic mechanism was proposed to account for the evidences of Stille processes in which the products exhibit retention of configuration at the transmetalated carbon [83], whereas the open mechanism was proposed for processes in which inversion of configuration was observed [84].

As far as concerns the cyclic mechanism (Fig. 3.12), it consists in a two step reaction process in which the first one corresponds to the substitution of a ligand L by the stannane. Afterwards, the transmetalation reaction between the stannane and palladium occurs via a cyclic four-coordinated transition state resulting in a square planar complex where the two organic groups are in a *cis* arrangement. Then, in order to afford the coupled product and regenerate the catalyst, the reductive elimination reaction is required.

In the cyclic mechanism the initial substitution of the ligand L by the stannane is, in general, believed to occur through a ligand exchange pathway [43, 85, 86] although other alternatives such as a dissociative mechanism [87] or a mechanism in which the catalytic species is the one generated after the substitution of a ligand L by a solvent molecule [88] have been also proposed. The latter, consisting in a solvent assisted process, was recently investigated through DFT-B3LYP calculations by Alvarez et al. [89] for the transmetalation reaction with vinylstannane. In particular, the results employing DMF as solvent showed lower energy barriers for the DMF-for-stannane substitution compared to the

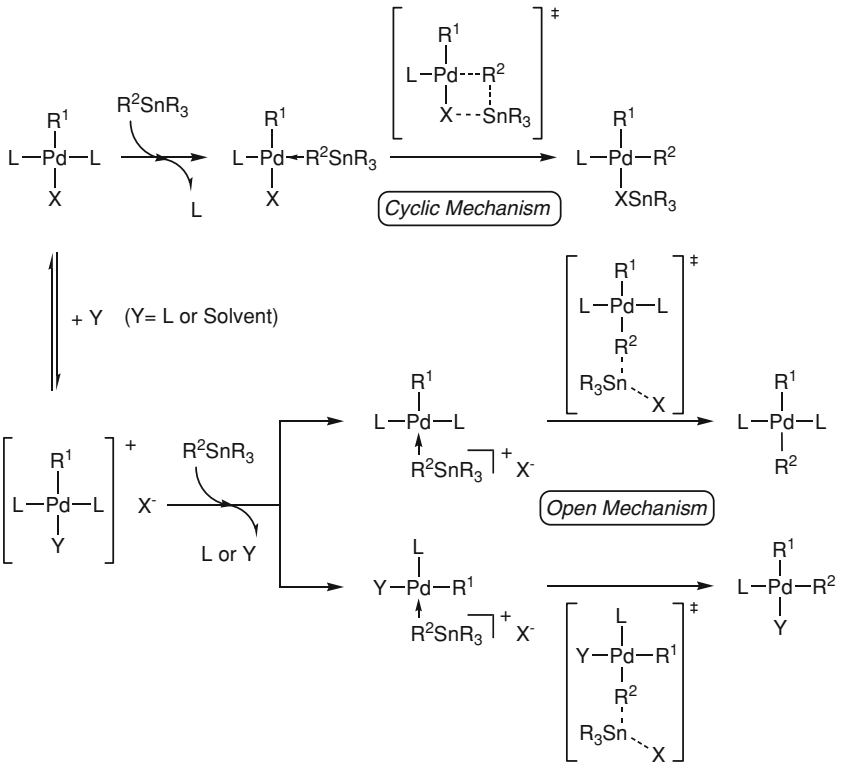


Fig. 3.12 The two mechanisms proposed for the transmetalation step in the Stille reaction

direct L-for-stannane substitution from the initial complex [PdR^1XL_2]. Similarly, the DFT-B3LYP results reported by Nova et al. [90] with THF as solvent showed lower energy barriers for the solvent assisted process. However, after considering the solvent-for-L exchange energy, the authors concluded that both processes may have competitive rates and one or the other might predominate depending on the solvent, the ligand L, and the concentration of this latter. The effect of model ligands (L = PH_3 and AsH_3) as well as the effect of the solvent (S = THF and PhCl) was computationally evaluated by the same authors [90]. According to their results, both the ligand-for-stannane substitution and the transmetalation process with L = PH_3 were found to be thermodynamically and kinetically less favored than those with L = AsH_3, which was consistent with the higher reaction rates experimentally observed for $AsPh_3$ as compared to PPh_3 [87, 88]. This enhanced reactivity is, in general, attributed to the easier dissociation of $AsPh_3$. On the other hand, the introduction of the solvent effects (THF and PhCl) in the transmetalation process with both ligands by means of a continuum model was found to increase the energies for both overall mechanisms, and thus, the authors suggested that the choice of solvents with small dielectric constants might favor this mechanism.

Lin and co-workers reported a DFT-B3LYP computational study on the effect of the leaving group X and the effect of the phosphine ligand for the transmetalation reaction of trimethyl vinyl tin with $L_nPd(Ar)(X)$ ($L = PH_3$, PMe_3; $X = Cl$, Br, I) [91]. Concerning the effect of the leaving group, their results revealed that the overall activation barrier for the transmetalation process (i.e. substitution of L by the stannane followed by the transmetalation reaction properly speaking) increases in the order: $Cl < Br < I$. However, although the transmetalation step with aryl chlorides was found to be faster than with the bromide and iodide analogues, the authors wisely emphasized that one should take into consideration that the oxidative addition step with aryl chlorides may be rate-determining, and therefore, the Stille reaction become more challenging. On the other hand, the evaluation of the effect of the ligands $L = PMe_3$ and $L = PH_3$ showed that the more electron-donating phosphine ligands increase the overall transmetalation barriers, which agreed with the Farina's et al. experimental observation that phosphine ligands of high donicity prevent transmetalation [87]. In particular, this enhancement of the reaction rates with less electron-donating phosphines was attributed by these authors to the less strong Pd–P bond, which facilitates the substitution of the phosphine by the stannane, and to the weaker *trans* influence on the Pd–vinyl bond, which stabilizes the transmetalation product.

As far as the open mechanism is concerned (Fig. 3.12), this mechanism consists of three steps. First, the substitution of the heteroatom X by a neutral ligand Y (Y = L or Solvent) occurs resulting in a cationic species $[PdYL_2R^1]^+$, which is supposed to be more reactive due to its higher electrophilic character. Afterwards, the coordination of the stannane to the palladium complex takes place via substitution of either the neutral ligand Y or a ligand L followed by the proper transmetalation step giving rise to the *trans* and *cis* transmetalated complexes, respectively.

The theoretical evaluation of this mechanism was also carried out by Nova et al. [90] revealing that this mechanism might be favored with catalysts containing good leaving groups (i.e. triflate) and with solvents with high dielectric constant because they facilitate and stabilize the formation of the cationic species. Conversely to the cyclic mechanism, the highest energy barrier within this mechanism was found to be the second step (i.e. the stannane-for-L substitution) and further, the energy barriers for phosphine resulted slightly lower than for the arsine ligand. On the other hand, the analysis of the *cis* and *trans* reaction pathways were found to be energetically comparable, thus confirming the experimental observations.

The Stille reaction mechanism was also evaluated by Alvarez et al. at DFT-B3LYP level obtaining similar conclusions: the open mechanism is favored when anionic ligands (i.e. triflate) are used, whereas the cyclic mechanism is favored for X = halides [92]. These authors also investigated the role of the additive LiCl in the Stille reactions of vinylbromide and vinyl triflate with trimethyl vinyl tin catalyzed by $Pd(PMe_3)_2$. According to their results, the added chloride anion drives the expected transmetalation step from the open one with triflates to the cyclic mechanism in the presence of the additive.

Table 3.1 Gibbs energy barriers calculated by Ariafard and Yates for the transmetalation reaction with different ligands L [54]

Ligand (L)	ΔG_{solv} (kcal/mol)
P(*t*-Bu)$_3$	34.9
PPh_3	23.9
PPh_2Me	28.3
$PPhMe_2$	34.4
PMe_3	35.8

More recently, the reported accelerating effect of CsF [93] as well as the effect of different phosphine ligands on palladium(II) catalysts was analyzed at DFT-B3LYP level by Ariafard and Yates for the model Stille reaction of (vinyl)$SnMe_3$ with $L_nPd(Ph)(Cl)$ (L = P(*t*-Bu)$_3$, PPh_3, PPh_2Me, $PPhMe_2$ and PMe_3) [54]. In particular, the effect of the additive CsF was analyzed for the transmetalation reaction with L = P(*t*-Bu)$_3$ confirming that the addition of the anion F^- increases the reactivity of stannane reagents toward the transmetalation. Furthermore, to account for this enhanced reactivity with the additive, the transmetalation reaction with (vinyl)$SnMe_3$ was proposed to proceed with a lower energy barrier from the fluoro complex [(P(*t*-Bu)$_3$)Pd(F)(Ph)] which is generated from the initial complex (P(*t*-Bu)$_3$)Pd(Cl)(Ph) by interaction of the F^- and following dissociation of the chloride. The evaluation of the effect of the different phosphine ligands for the same model reaction revealed that these ligands play a very important role in the transmetalation step (Table 3.1). For example, the use of very bulky ligands such as P(*t*-Bu)$_3$ was shown to increase considerably the energy barrier for the transmetalation step because it makes the coordination of the stannane to the palladium complex more difficult.

In the case of the non bulky ligand PMe_3, it leads to a special case in which there is an over stabilization of the previously formed complex *trans*-[Pd(L)$_2$(Cl)(Ph)] that increases the total energy barrier for the transmetalation process. This additional stabilization of the tetracoordinated complex was attributed by the authors to the less sterically demanding PMe_3 that binds stronger to Pd than the other L ligands. Furthermore, according to results from a previous study [94], the authors suggested that the strength of the Pd–L bond is positively correlated to the σ-donor ability of L; this is consistent with the conclusions previously reported by Lin et al. [91] that the stronger σ-donor ligand, the higher energy barrier for the transmetalation reaction. Alternatively, the moderate bulky ligand L = PPh_3 provided the lowest energy barrier for this process which can be rationalized to the right steric balance that this ligand confers. On the other hand the corresponding fine-tuned ligands L = PPh_2Me and L = $PPhMe_2$ provided higher energy barriers for the transmetalation step than the ligand L = PPh_3, which is in agreement with the experimental findings of Farina et al. [87] concerning the higher reactivity of Pd(II)/PPh_3 compared to Pd(II)/PPh_2Me. On the basis of all the results, the authors concluded that in theoretical studies on the transmetalation step where the steric effects are very important, the use of PMe_3 to model PPh_3 is not good enough to provide accurate results.

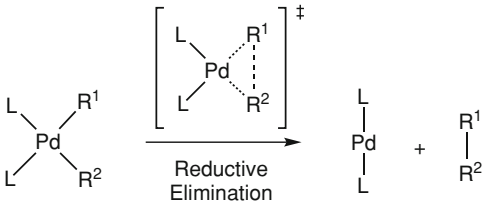


Fig. 3.13 Generally accepted mechanism for the reductive elimination step

3.5 Phosphine Effects in Reductive Elimination

To complete the full catalytic cycle a reductive elimination step is needed after the transmetalation process. This last step, in contrast with the other ones, which are frequently reversible [95], is irreversible. Thus, it is often taken for granted to be critical for the success of the whole reaction because it must pull the catalytic cycle forward. Even though the reductive elimination from a Pd(II) complex, in general, proceeds very readily and it is not rate-limiting, many efforts have been done to improve the efficiency of this step.

The generally accepted mechanism for this process is concerted, starting from the complex formed in the transmetalation step, having the two organic groups in *cis* position (Fig. 3.13). Otherwise, a *trans* to *cis* isomerization reaction previous to the reductive elimination is required. The transition state for this last step corresponds to a cyclic three-coordinated transition state which leads to the final C–C coupling and the regeneration of the catalytic species PdL_2.

Since the early theoretical works of Tatsumi, Hoffmann, Yamamoto and Stille [96] and Low and Goddard [97, 98], the reductive elimination step had received scant attention, but recently, extensive studies on the C–C reductive elimination have been carried out. In particular, in 2002 Ananikov, Musaev, and Morokuma reported a DFT-B3LYP study on the effects of different X ligands in the reductive elimination from bis-σ-vinyl complexes $[Pd(CH{=}CH_2)_2X_n]$ (X = Cl, Br, I, NH_3, PH_3). The results reported therein showed that activation barriers for the C–C bond formation reaction decreases in the following order: Cl > Br, NH_3 > I > PH_3 [99]. Lately, the same authors investigated theoretically most of the common types of coupling partners in the square-planar *cis*-$[PdRR'(PH_3)_2]$ complexes (R or R′ = Me, vinyl, Ph, ethynyl) [100]. The authors concluded that the energy barrier for the carbon–carbon coupling from the symmetrical complex $R_2Pd(PH_3)_2$ increases in the order: R = Vinyl < Ph < Ethynyl < Me. The activation free energies in gas phase for these reactions were found to range from 6.0 (R = vinyl) to 23.6 kcal/mol (R = Me), respectively. Besides, the energy barriers and the exothermicities for the asymmetrical coupling R–R′ from $RR'Pd(PH_3)_2$ resulted to be very close to the averages of the corresponding values with the symmetrical R–R and R′–R′ coupling reactions in $R_2Pd(PH_3)_2$ and $R'_2Pd(PH_3)_2$, respectively.

On the other hand, the nature of the ancillary L ligands is believed to have an important effect on the rate of the reductive elimination reaction. For example, the

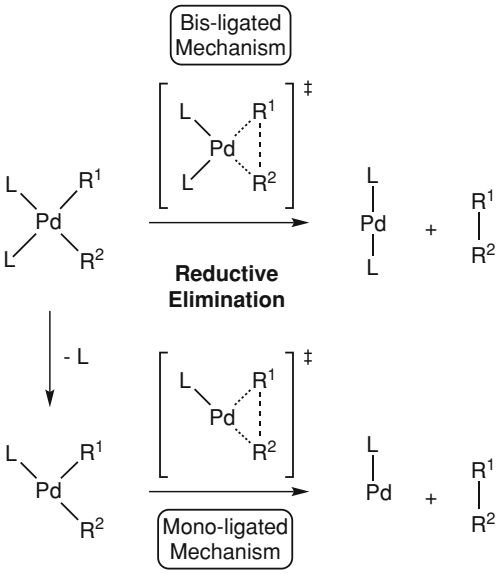


Fig. 3.14 Proposed mechanisms for the reductive elimination reaction from PdR_2L_2

steric effects provided by bulky phosphine ligands have been proposed to promote an accelerating effect on this reaction [101]. This effect can be rationalized as the repulsive interaction between the ancillary ligands and the two organic groups in the initial complex R_2PdL_2 that forces the two species to be very close from each other facilitating, thus, reductive elimination. Moreover, a reaction mechanism through the three-coordinated species formed by dissociation of one phosphine ligand from the initial complex has been also proposed to account for this enhanced reactivity, since the dissociation energy of bulky ligands is very low (Fig. 3.14) [102–105]. The use of phosphine ligands with low electron-donating character produces a clear enhancement in the rate of reductive elimination [106]. A possible explanation for this trend is that Pd(II) complexes which are more electrophilic than Pd(0) complexes, become more stable with phosphine ligands with high donicity [107]. Hence, these ligands stabilize the complex R_2PdL_2 compared to the corresponding transition state increasing the energy barrier for this process. In contrast, the influence of the bite angle in chelating diphosphine ligands showed that wide bite angle ligands destabilize the reactant and stabilize the transition state and therefore, accelerate the reaction [107].

In order to shed light on the influence of the steric and electronic properties of phosphine ligands in reductive elimination, several theoretical studies have been carried out very recently. Ananikov, Musaev and Morokuma reported a computational study by means of the ONIOM approach in which the Me–Me coupling from the complexes $[PdR_2L_n]$ ($L = PPh_3$, PCy_3, PMe_3, and PH_3; $n = 1, 2$) was investigated [108]. According to their results, the steric effects were found to mainly influence the energy of the initial complex, whereas the electronic effects have the largest impact on the energy of the transition state. Furthermore, the

Table 3.2 Relative energies (in kcal/mol) for the reductive elimination reaction from $PdMe_2L_n$ ($n = 1, 2$)

Ligand L	Bis ligated mechanism		Mono ligated mechanism	
	PdR_2L_2	Ts	$PdR_2L + L$	Ts
PMe_3	0.0	28.3	18.8 (0.0)	31.4 (12.6)
PH_3	0.0	23.3	14.2 (0.0)	26.1 (11.9)
PCl_3	0.0	13.2	10.3 (0.0)	20.7 (10.4)

Values in *parenthesis* are relative to $PdR_2L + L$

results revealed that different L ligands may involve different mechanisms of the reductive elimination (Fig. 3.14). In particular, the PCy_3 was proposed to facilitate the mono-ligated reaction pathway and to increase the reactivity, while the PMe_3 ligand stabilizes the four-coordinated complexes and decreases the reactivity toward reductive elimination. Alternatively, the PPh_3 ligand resulted to be a more universal choice, since it showed good reactivity for both mechanisms.

More recently, Ariafard and Yates investigated the steric and electronic effects of the model phosphine ligands L = PMe_3, PH_3, PCl_3 and the experimentally reported ligands L = PPh_3, PPh_2Me, $PPhMe_2$ on the Me–Me reductive elimination from the complexes [PdR_2L_2] and [PdR_2L] [109]. The computed energy barriers at DFT-B3LYP level with the model ligands from the four-coordinated and the three-coordinated complexes are listed in Table 3.2. These results are consistent with the experimental observations that reductive elimination is accelerated by the presence of ligands with low-electron donating properties. Interestingly, this feature has a significant effect on the energy of the transition state for the reductive elimination for the four-coordinated complex (bis-ligated mechanism), while its effect is much lower on the energy of the corresponding transition state for the three-coordinated species (mono-ligated mechanism). In the former case the greater the electron-donation of L, the higher the energy barrier for this process. In the latter case, it is the dissociation of the phosphine ligand that leads to the different overall energy barrier. This dissociation energy is also controlled by the basicity of L because the stronger electron donation leads to a stronger Pd–L bond, and thus a higher overall barrier.

According to the results shown in Table 3.2 the relative energy barriers for the mono-ligated pathways are higher than that through the bis-ligated ones. However, one should take into account that the introduction of the entropic effects may change these results, since a large positive entropy change is expected for the dissociation of one phosphine ligand from the initial Pd complex. The calculation of this process is not an easy task [71]. An estimation of the corresponding Gibbs free energies (which includes entropic contributions) can be roughly obtained by deducting 8–10 kcal/mol [110] from all the electronic energies in the mono-ligated pathway. With this correction, the mechanism via three-coordinated species is favored toward the bis-ligated mechanism, which is in agreement with the experimental observations.

On the other hand, the results obtained for the reductive elimination with the ligands L = PPh_3, PPh_2Me, $PPhMe_2$ (Table 3.3) showed an increase in the energy

Table 3.3 Relative energies (in kcal/mol) for the reductive elimination reaction from $PdMe_2L_n$ ($n = 1, 2$)

Ligand L	Bis ligated mechanism		Mono ligated mechanism	
	PdR_2L_2	Ts	$PdR_2L + L$	Ts
PPh_3	0.0	20.4	11.2 (0.0)	24.0 (12.8)
PPh_2Me	0.0	24.7	16.8 (0.0)	29.4 (12.6)
$PPhMe_2$	0.0	27.9	18.9 (0.0)	31.5 (12.6)

Values in *parenthesis* are relative to $PdR_2L + L$

barrier in the order $PPh_3 < PPh_2Me < PPhMe_2$. This trend was observed regardless of the mechanism, which agrees with the experimental observations [106]. Similarly to the reaction with the model ligands (Table 3.2), the energy barriers for the mono-ligated reaction pathways were found to be lower than those with the bis-ligated ones. Moreover, for all the L ligands the reductive elimination from PdR_2L was found to be almost independent of the bulk of the L ligand. This fact was supported by very small steric repulsions between the L and Me ligands calculated in the mono-phosphine species. Furthermore, the energy-decomposition analyses of the reaction barriers revealed that the electronic effects are very similar to each other and that the steric effects destabilize the initial complex PdR_2L_2 but not the transitions states; this involves a decrease in the barriers to reductive elimination compared to the smaller phosphine ligands.

The C–C coupling on the complex $[PdMe_2(PMe_3)_2]$ as well as on complexes $[PdMe_2(PMe_3)L]$ generated by the addition of coupling promoters (L = acetonitrile, ethylene, maleic anhydride (ma)), and on the tricoordinated intermediate $PdR_2(PMe_3)$ (represented as L = empty) was investigated by Alvarez, Maseras, Espinet and co-workers [111]. The computed activation energies at DFT-B3LYP level were found to increase in the order: ma < "empty" < ethylene < $PMe_3 \approx$ MeCN which confirmed that the energy barrier decreases with the π-acceptor ability of L. Consistently, ma produces a lower coupling barrier because it is a better π-acceptor than ethylene which in turn is better than PMe_3. Furthermore, the barrier with L = ma resulted to be lower to the point that the coupling is easier for the four-coordinated complex with ma than for the three-coordinated species ($\Delta G^{\ddagger}$ is 13.2 kcal/mol for L = empty and 8.6 kcal/mol for L = ma). Moreover, the effect of added olefins revealed that olefins with electron-withdrawing substituents facilitate the coupling through $[PdMe_2(PMe_3)(olefin)]$ intermediates with much lower activation energies than the starting complex or a three-coordinated intermediate.

3.6 Concluding Remarks

Cross-coupling reactions are one of the most common and useful organic tools in the laboratory. Several metal catalysts have been developed for this reaction but those based on Pd are the most developed ones. The stoichiometry of the Pd-based

catalyst uses to be PdL_2; as in many other transition metal catalysts phosphines are the most common ligands.

The reaction mechanism for the Pd-catalyzed cross-coupling reaction is commonly accepted that takes place in three main reaction steps: (1) oxidative addition, (2) transmetalation and (3) reductive elimination. The first and the third processes are common in many other catalytic reactions. The transmetalation, however, is quite particular of the cross-coupling reactions. The effect of the phosphine on each of these reaction steps studied by means of theoretical methods has been reviewed in this chapter.

As far as the oxidative addition is concerned, two different mechanisms are proposed for this step: a concerted mechanism and a nucleophilic attack mechanism. Calculations on the concerted mechanism show that the size of the phosphine does not significantly affect this process for monophosphine catalytic systems. In fact, it is experimentally shown that the rate constants for the oxidative addition depend more on the identity of the halide of the ArX electrophilic reactant than of the steric bulk of the phosphine ligands. The nature of the phosphine ligand may affect this process not because of the oxidative addition elementary step itself (where the effect is rather small), but due to its own intrinsic capability of generating mono- or bisphosphine catalysts. The oxidative addition process in monophosphine systems are more favorable than in their bisphosphine counterparts. In fact, the most active phosphine ligands known are the bulky and electron-rich dialkylbiaryl phosphines developed by Buchwald's group.

On the other hand, in the nucleophilic attack mechanism an inversion of configuration on the organic reaction was observed. For the particular case of sp^3 carbon atoms in α-sulfoxide systems the mechanism was proposed to be rather similar for both the mono- or bisphosphine catalysts.

The transmetalation process has been described for the Suzuki–Miyaura and the Stille cross-coupling reactions. For the first reaction, the computational analysis of the transmetalation process using a model PH_3 phosphine ligand showed that this step presents a relatively low energy barrier for both mono- and bisphosphine catalytic species, though mono-phosphine system was favored. Taking the monophosphine as the catalytic species the theoretical studies revealed that for this particular process the steric effects are more important than the electronic effects. Hence, the computation of steric descriptors showed that bulkier ligands may produce higher energy barriers whereas electronic descriptors revealed that better π-acceptor phosphines may contribute to lowering the energy barrier for this process.

In the case of the Stille reaction two different alternative mechanisms have been proposed: cyclic and open. The cyclic pathway is proposed for those cases where retention of configuration is observed, whereas the open pathway is proposed to take place when an inversion of configuration is obtained in the product. The cyclic pathway requires a ligand (phosphine) substitution process to coordinate the stannane species. Thus, the nature of the phosphine may significantly affect this process; phosphine ligands with high donor capacity should prevent transmetalation. As far as the open pathway is concerned, the theoretical study revealed that this pathway is favored for catalysts containing easily removal ligands (i.e. triflate) and

using solvents of high dielectric constants because they favor the formation of cationic intermediates. Regarding the phosphine effects, the theoretical evaluation points out that the use of bulky ligands increases considerably the energy barrier for the transmetalation step because prevents the coordination of the stannane to the metal center; good σ-donor phosphines also increases the barrier for the transmetalation due to the stabilization of the phosphine coordinated intermediates.

The reductive elimination can be considered the reverse pathway of the oxidative addition. Nevertheless, there is an important difference; the reductive elimination is an irreversible pathway within the catalytic cycle. The transition step for this process is calculated to be concerted leading to the final C–C coupling and regeneration of the Pd catalyst. Theoretical evaluation of the steric and electronic effects on this process showed that whereas the steric effects mainly influence the relative energy of the initial intermediate, electronic effects have the largest impact on the energy of the transition state. Thus, the use of low electron-donating phosphines diminishes the energy of the transition state therefore producing an enhancement of the reductive elimination rate. For chelating bisphosphine ligands theoretical studies showed that ligands with wide bite angle destabilize the initial intermediate and stabilize the transition state for the reductive elimination. The presence of coupling promoters acting as a second ligand along with the phosphine was also computationally evaluated. Theoretical analysis showed that the energy barrier for the coupling process decreases with the π-acceptor ability of the coupling promoter.

Overall a proper balance between steric and electronic effects is needed in the phosphine ligands in order to optimize the efficiency in cross-coupling reactions. Once again theoretical methods are shown as a valuable tool for analyzing reaction mechanisms, particularly the effect of the phosphine ligands in cross-coupling reactions. In spite of the great advances performed on the understanding of these processes, much work is still needed in order to have a more general picture of the cross-coupling reactions beside the Suzuki–Miyaura and Stille reactions.

Acknowledgments We thank the Ph.D. students and postdocs who have contributed to developing this research topic in our groups. Fruitful collaborations with experimental groups (Pablo Espinet, Gregorio Asensio, Rosana Alvarez and Angel Rodríguez de Lera) are also acknowledged. The Spanish MICINN is gratefully acknowledged for funding this research through projects CTQ2008-06866-C02-01, CTQ2008-06866-C02-02 and Consolider-Ingenio 2010 (CSD2007-00006 and CSD2006-0003).

References

1. Cornils B, Herrmann WA (2002) Applied homogeneous catalysis with organometallic compounds. Wiley-VCH, Weinheim
2. Hagen J (2006) Industrial catalysis: a practical approach, 2nd edn. Wiley-VCH, Weinheim
3. Miura M (2004) Rational ligand design in constructing efficient catalyst systems for Suzuki–Miyaura coupling. Angew Chem Int Ed 43:2201–2203
4. Chen W, Li R, Han B, Li B-J, Chen Y-C, Wu Y, Ding L-S, Yang D (2006) The design and synthesis of bis(thiourea) ligands and their application in Pd-catalyzed Heck and Suzuki reactions under aerobic conditions. Eur J Org Chem 1177–1184

5. Tolman CA (1977) Steric effects of phosphorus ligands in organometallic chemistry and homogeneous catalysis. Chem Rev 77:313–348
6. Brown TL, Lee KJ (1993) Ligand steric properties. Coord Chem Rev 128:89–116
7. Dias PB, de Piedade MEM, Martinho Simões JA (1994) Bonding and energetics of phosphorus (III) ligands in transition metal complexes. Coord Chem Rev 135(136):737–807
8. Bunten KA, Chen L, Fernandez AL, Poë AJ (2002) Cone angles: Tolman's and Plato's. Coord Chem Rev 233(234):41–51
9. Kühl O (2005) Predicting the net donating ability of phosphines- do we need sophisticated theoretical methods? Coord Chem Rev 249:693–704
10. Kamer PCJ, van Leeuwen PWNM, Reek JNH (2001) Wide bite angle diphosphines: Xantphos ligands in transition metal complexes and catalysis. Acc Chem Res 34:895–904
11. Wang Y, Wang J, Su J, Huang F, Jiao L, Liang Y, Yang D, Zhang S, Wender PA, Yu Z-X (2007) A computational designed Rh(I)-catalyzed two-component [5 + 2 + 1] cycloaddition of ene-vinylcyclopropanes and CO for the synthesis of cyclooctenones. J Am Chem Soc 129:10060–10061
12. Houk KN, Cheong PH-Y (2008) Computational prediction of small-molecule catalysts. Nature 455(7211):309–313
13. Ananikov VP, Orlov NV, Kabeshov MA, Beletskaya IP, Starikova ZA (2008) Stereodefined synthesis of a new type of 1,3-dienes by ligand-controlled carbon-carbon and carbon-heteroatom bond formation in nickel-catalyzed reaction of diaryldichalcogenides with alkynes. Organometallics 27:4056–4061
14. Abe Y, Kuramoto K, Ehara M, Nakatsuji H, Suginome M, Murakami M, Ito Y (2008) A mechanism for the palladium-catalyzed regioselective silaboration of allene: a theoretical study. Organometallics 27:1736–1742
15. Maseras F, Morokuma K (1995) IMOMM: A new integrated ab initio + molecular mechanics geometry optimization scheme of equilibrium structures and transition states. J Comput Chem 16:1055–1179
16. Ujaque G, Maseras F (2004) Applications of hybrid DFT/molecular mechanics to homogeneous catalysis. Struct Bond 112:117–149
17. Bo C, Maseras F (2008) QM/MM methods in inorganic chemistry. Dalton Trans 2911–2919
18. Carbo JJ, Maseras F, Bo C, van Leeuwen WNM (2001) Unraveling the origin of regioselectivity in rhodium diphosphine catalyze hydroformylation. A DFT QM/MM study. J Am Chem Soc 123:7630–7637
19. Garcia-Cuadrado D, de Mendoza P, Braga AAC, Maseras F, Echavarren AM (2007) Proton-abstraction mechanism in the palladium-catalyzed intramolecular arylation: substituents effects. J Am Chem Soc 129:6880–6886
20. Liu S, Saidi O, Berry N, Ruan J, Pettman A, Thomson N, Xiao J (2009) Electron-deficient phosphines accelerate the Heck reaction of electron-rich olefins in ionic liquids. Lett Org Chem 6:60–64
21. Moncho S, Ujaque G, Lledos A, Espinet P (2008) When are tricoordinated PdII species accessible? Stability trends and mechanistic consequences. Chem Eur J 14:8986–8994
22. de Meijere A, Diederich F (2004) Metal-catalyzed cross-coupling reactions. Wiley-VCH, Weinheim
23. Cross-Coupling reactions: A practical guide (2001) No 219. In: Miyaura N (ed) Topics in current chemistry. Springer, Berlin
24. Buchwald SL (ed) (2008) Cross-coupling. Acc Chem Res 41(special issue):1439–1564
25. Tamao K, Hiyama T, Negishi E (eds) (2002) 30 years of cross-coupling reaction. J Organomet Chem 653(special issue):1–303
26. Phapale VB, Cardenas DJ (2009) Nickel-catalyzed Negishi cross-coupling reactions: scope and mechanisms. Chem Soc Rev 38:1598–1607
27. Nicolaou KC, Bulger PG, Sarlah D (2005) Palladium-catalyzed cross-coupling reactions in total synthesis. Angew Chem Int Ed 44:4442–4489
28. Xue L, Lin Z (2010) Theoretical aspects of palladium-catalyzed carbon-carbon cross-coupling reactions. Chem Soc Rev 39:1692

29. Kosugi M, Sasazawa K, Shimizu Y, Migita T (1977) Reactions of allyltin compounds. 3. Allylation of aromatic halides with allyltributyltin in presence of tetrakis(triphenylphosphine) palladium(0). Chem Lett 3:301–302
30. Stille JK (1986) The palladium-catalyzed cross-coupling reactions of organotin reagents with organic electrophiles. Angew Chem Int Ed 25:508–524
31. Miyaura N, Yamada K, Suzuki A (1979) New stereospecific cross-coupling by the palladium-catalyzed reaction of 1-alkenylboranes with 1-alkenyl or 1-alkynyl halides. Tetrahedron Lett 36:3437–3440
32. Miyaura N, Suzuki A (1995) Palladium-catalyzed cross-coupling reactions of organoboron compounds. Chem Rev 95:2457–2483
33. Negishi E, King AO, Okukado N (1977) Selective carbon-carbon bond formation via transition-metal catalysis. 3. Highly selective synthesis of unsymmetrical biaryls and diarylmethanes by nickel-catalyzed or palladium-catalyzed reaction of aryl derivatives and benzylzinc derivatives with aryl halides. J Org Chem 42:1821–1823
34. Fuentes B, García-Melchor M, Lledos A, Maseras F, Casares JA, Ujaque G, Espinet P (2010) Palladium round trip in the Negishi coupling of trans-[PdMeCl($PMePh_2$)$_2$] with ZnMeCl: An experimental and DFT study of the transmetalation step. Chem Eur J 16:8596–8599
35. Braga AAC, Ujaque G, Maseras F (2008) Mechanism of palladium-catalyzed cross-coupling reactions. In: Morokuma K, Musaev DG (eds) Computational modeling for homogeneous and enzymatic catalysis. Wiley-VCH, Weinheim
36. Amatore C, Jutand A (2000) Anionic Pd(0) and Pd(II) intermediates in palladium-catalyzed Heck and cross-coupling reactions. Acc Chem Res 33:314–321
37. Galardon E, Ramdeehul S, Brown JM, Cowley A, Hii KK, Jutand A (2002) Profund steric control of reactivity in aryl halide addition to bisphosphane palladium(0) complexes. Angew Chem Int Ed 41:1760–1763
38. Hartwig JF (2007) Electronic effects on reductive elimination to form carbon-carbon and carbon-heteroatom bonds from palladium(II) complexes. Inorg Chem 46:1936–1947
39. Yandulov DV, Tran NT (2007) Aryl-Fluoride reductive elimination from Pd(II): Feasibility assessment from theory and experiment. J Am Chem Soc 129:1342–1358
40. Senn HM, Ziegler T (2004) Oxidative addition of aryl halides to palladium(0) complexes: A density-functional study including solvation. Organometallics 23:2980–2988
41. Gossen LJ, Koley D, Hermann HL, Thiel W (2005) Mechanistic pathways for oxidative addition of aryl halides to palladium(0) complexes: A DFT study. Organometallics 24: 2398–2410
42. Lam KC, Marder TB, Lin Z (2007) DFT studies on the effect of the nature of the aryl halide Y-C6H4-X on the mechanism of its oxidative addition to Pd0L versus Pd0L2. Organometallics 26:758–760
43. Casado AL, Espinet P (1998) Mechanism of the Stille reaction. 1. The transmetalation step. Coupling of R_1I and R_2SnBu_3 catalyzed by trans-[PdR_1IL_2] ($R_1 = C_6C_{12}F_3$; R_2 = vinyl, 4-methoxyphenyl; L = $AsPh_3$). J Am Chem Soc 120:8978–8985
44. Sicre C, Braga AAC, Maseras F, Cid MM (2008) Mechanistic insights into the transmetalation step of a Suzuki-Miyaura reaction of 2(4)-bromopyridines: Characterization of an intermediate. Tetrahedron 64:7437–7443
45. Liu Q, Lan Y, Liu J, Li G, Wu Y-D, Lei A (2009) Revealing a second transmetalation step in the Negishi coupling and its competition with reductive elimination: Improvement in the interpretation of the mechanism of biaryl synthesis. J Am Chem Soc 131:10201–10210
46. Littke AF, Fu GC (2002) Palladium-catalyzed coupling reactions of aryl chlorides. Angew Chem Int Ed 41:4176–4211
47. Wolfe JP, Singer RA, Yang BH, Buchwald SL (1999) Highly active palladium catalysts for Suzuki coupling reactions. J Am Chem Soc 121:9550–9561
48. Zapf A, Ehrentraut A, Beller M (2000) A new highly efficient catalyst system for the coupling of nonactivated and deactivated aryl chlorides with arylboronic acids. Angew Chem Int Ed 39:4153–4155

49. Fleckenstein CA, Plenio H (2010) Sterically demanding trialkylphosphines for palladium-catalyzed cross-coupling reactions- alternatives to Pt-Bu_3. Chem Soc Rev 39:694–711
50. Kantchev EAB, O'Brien CJ, Organ MG (2007) Palladium complexes of N-Heterocyclic carbenes as catalysts for cross-coupling reactions. A synthetic chemist's perspective. Angew Chem Int Ed 46:2768–2813
51. Marion N, Nolan SP (2008) Well-defined *N*-Heterocyclic carbenes-palladium(II) precatalysts for cross-coupling reactions. Acc Chem Res 41:1440–1449
52. Ahlquist M, Fristrup P, Tanner D, Norrby P-O (2006) Theoretical evidence for low-ligated palladium(0): [Pd–L] as the active species in oxidative addition. Organometallics 25:2066–2073
53. Li Z, Fu Y, Guo Q-X, Liu L (2008) Theoretical study on monoligated Pd-catalyzed cross-coupling reactions of aryl chlorides and bromides. Organometallics 27:4043–4049
54. Ariafard A, Yates BF (2009) Subtle balance of ligand steric effects in Stille transmetalation. J Am Chem Soc 131:13981–13991
55. Barrios-Landeros F, Carrow BP, Hartwig JF (2009) Effect of ligand steric properties and halide identity on the mechanism for oxidative addition of haloarenes to trialkylphosphine Pd(0) complexes. J Am Chem Soc 131:8141–8154
56. Ahlquist M, Norrby P-O (2007) Oxidative addition of aryl chlorides to monoligated palladium(0): A DFT-SCRF study. Organometallics 26:550–553
57. Jover J, Fey N, Purdie M, Lloyd-Jones GC, Harvey JN (2010) A computational study of phosphine ligand effects in Suzuki-Miyaura coupling. J Mol Catal A 324:39–47
58. Fey N, Tsipis AC, Harris SE, Harvey JN, Orpen AG, Mansson RA (2006) Development of a ligand knowledge base, Part 1: Computational descriptors for phosphorus donor ligands. Chem Eur J 12:291–302
59. Fey N, Orpen GA, Harvey JN (2009) Building ligand knowledge bases for organometallic chemistry: Computational description of phosphorus(III)-donor ligands and the metal-phosphorus bond. Coord Chem Rev 253:704–722
60. Fey N (2010) The contribution of computational studies to organometallic catalysis: descriptors, mechanisms and models. Dalton Trans 39:296–310
61. Corbet J-P, Mignani G (2006) Selected patented cross-coupling reaction technologies. Chem Rev 106:2651–2710
62. Stille JK, Lau KS (1977) Mechanisms of oxidative addition of organic halides to group-8 transition metal complexes. Acc Chem Res 10:434–442
63. Feliz M, Freixa Z, van Leeuwen PWNM, Bo C (2005) Revisiting the methyl iodide oxidative addition to rhodium complexes: A DFT study of the activation parameters. Organometallics 24:5718–5723
64. Diefenbach A, de Jong GT, Bickelhaupt FM (2005) Activation of H–H, C–H, C–C and C–Cl bonds by Pd and PdCl. Understanding anion assistance in C–X bond activation. J Chem Theory Comput 1:286–298
65. Rodriguez N, Ramirez de Arellano C, Asensio G, Medio-Simon M (2007) Palladium-catalyzed Suzuki-Miyaura reaction involving a secondary sp3 carbon: Studies of stereochemistry and scope of the reaction. Chem Eur J 13:4223–4229
66. Gourlaouen C, Ujaque G, Lledos A, Medio-Simon M, Asensio G, Maseras F (2009) Why is the Suzuki–Miyaura cross-coupling of sp3 carbons in α-Bromo sulfoxide systems fast and stereoselective? A DFT study on the mechanism. J Org Chem 74:4049–4054
67. Miyaura N (2002) Cross-coupling reaction of organoboron compounds via base-assisted transmetalation to palladium(II) complexes. J Organomet Chem 653:54–57
68. Smith GB, Dezeny GC, Hughes DL, King AO, Verhoeven TR (1994) Mechanistic studies of the Suzuki cross-coupling reaction. J Org Chem 59:8151–8156
69. Matos K, Soderquist JA (1998) Alkylboranes in the Suzuki–Miyaura coupling: stereochemical and mechanistic studies. J Org Chem 63:461–470
70. Braga AAC, Morgon NH, Ujaque G, Maseras F (2005) Computational characterization of the role of the base in the Suzuki–Miyaura cross-coupling reaction. J Am Chem Soc 127:9298–9307

71. Braga AAC, Ujaque G, Maseras F (2006) A DFT study of the full catalytic cycle of the Suzuki-Miyaura cross-coupling on a model system. Organometallics 25:3647–3658
72. Braga AAC, Morgon NH, Ujaque G, Lledos A, Maseras F (2006) Computational study of the transmetalation process in the Suzuki-Miyaura cross-coupling of aryls. J Organomet Chem 691:4459–4466
73. Sumimoto M, Iwane N, Takahama T, Sakaki S (2004) Theoretical study of trans-metalation process in palladium-catalyzed borylation of iodobenzene with diboron. J Am Chem Soc 126:10457–10471
74. Goo*β*en LJ, Koley D, Hermann HL, Thiel W (2005) The palladium-catalyzed cross-coupling reaction of carboxylic anhydrides with arylboronic acids: a DFT study. J Am Chem Soc 127:11102–11114
75. Goo*β*en LJ, Koley D, Hermann HL, Thiel W (2006) Palladium monophosphine intermediates in catalytic cross-coupling reactions: a DFT study. Organometallics 25:54–67
76. Martin R, Buchwald SL (2008) Palladium-catalyzed Suzuki-Miyaura cross-coupling reactions employing dialkylbiaryl phosphine ligands. Acc Chem Res 41:1461–1473 (references therein)
77. Barder TE, Walker SD, Martinelli JR, Buchwald SL (2005) Catalysts for Suzuki-Miyaura coupling processes: scope and studies of the effect of the ligand structure. J Am Chem Soc 127:4685–4696
78. Christmann U, Vilar R (2005) Monoligated palladium species as catalyst in cross-coupling reactions. Angew Chem Int Ed 44:366–374
79. Joshaghani M, Faramarzi E, Rafiee E, Daryanavard M, Xiao J, Baillie C (2006) Efficient Suzuki cross-coupling reactions using bulky phosphines. J Mol Catal A 259:35–40
80. Huang Y-L, Weng C-M, Hong F-E (2008) Density functional studies on palladium-catalyzed Suzuki-Miyaura cross-coupling reactions assisted by N- or P-chelating ligands. Chem Eur J 14:4426–4434
81. Chang C-P, Weng C-M, Hong F-E (2010) Preparation of cobalt sandwich diphosphine ligand [(η^5–$C_5H_4{}^{i}Pr$)Co(η^4–$C_4(PPh_2)_2Ph_2$)] and its chelated palladium complex: application of diphosphine ligand in the preparation of mono-substituted ferrocenylarenes. Inorg Chim Acta 363:412–417
82. Espinet P, Echavarren AM (2004) The mechanisms of the Stille reaction. Angew Chem Int Ed 43:4704–4734
83. Ye J, Bhatt RK, Falck JR (1994) Stereospecific palladium/copper cocatalyzed cross-coupling of α-alkoxy- and α-aminostannanes with acyl chlorides. J Am Chem Soc 116:1–5
84. Labadie JW, Stille JK (1983) Mechanisms of the palladium-catalyzed couplings of acid chlorides with organotin reagents. J Am Chem Soc 105:6129–6137
85. Casares JA, Espinet P, Salas G (2002) 14-electron T-shape [PdRXL] complexes: evidence or illusion? Mechanistic consequences for the Stille reaction and related processes. Chem Eur J 8:4843–4853
86. Napolitano E, Farina V, Persico M (2003) The Stille reaction: a density functional analysis of the transmetalation and the importance of coordination expansion at Tin. Organometallics 22:4030–4037
87. Farina V, Krishnan B (1991) Large rate accelerations in the Stille reaction with tri-2-furylphosphine and triphenylarsine as palladium ligands: mechanistic and synthetic implications. J Am Chem Soc 113:9585–9595
88. Amatore C, Bahsoun AA, Jutand A, Meyer G, Ntepe AN, Ricard L (2003) Mechanism of the Stille reaction catalyzed by palladium ligated to arsine ligand: $PhPdI(AsPh_3)(DMF)$ is the species reacting with vinylstannane in DMF. J Am Chem Soc 125:4212–4222
89. Alvarez R, Faza ON, Lopez CS, de Lera AR (2006) Computational characterization of a complete palladium-catalyzed cross-coupling process: The associative transmetalation in the Stille reaction. Org Lett 8:35–38
90. Nova A, Ujaque G, Maseras F, Lledos A, Espinet P (2006) A critical analysis of the cyclic and open alternatives of the transmetalation step in the Stille cross-coupling reaction. J Am Chem Soc 128:14571–14578

91. Ariafard A, Lin Z, Fairlamb IJS (2006) Effect of the leaving ligand X on transmetalation of organostannanes (vinylSnR_3) with $L_nPd(Ar)(X)$ in Stille cross-coupling reactions. A density functional theory study. Organometallics 25:5788–5794
92. Alvarez R, Perez M, Faza ON, de Lera AR (2008) Associative transmetalation in the Stille cross-coupling reaction to form dienes: Theoretical insights into the open pathway. Organometallics 27:3378–3389
93. Littke AF, Schwarz L, Fu GC (2002) Pd/P(t-Bu)$_3$: a mild and general catalyst for Stille reactions of aryl chlorides and aryl bromides. J Am Chem Soc 124:6343–6348
94. Fazaeli R, Ariafard A, Jamshidi S, Tabatabaie ES, Pishro KA (2007) Theoretical studies of the oxidative addition of PhBr to $Pd(PX_3)_2$ and $Pd(X_2PCH_2CH_2PX_2)$ (X = Me, H, Cl). J Organomet Chem 692:3984–3993
95. Perez-Temprano MH, Nova A, Casares JA, Espinet P (2008) Observation of a hidden intermediate in the Stille reaction. Study of the reversal of the transmetalation step. J Am Chem Soc 130:10518–10520
96. Tatsumi K, Hoffmann R, Yamamoto A, Stille JK (1981) Reductive elimination of d^8-organotransition metal complexes. Bull Chem Soc Jpn 54:1857–1867
97. Low JJ, Goddard WA (1986) Theoretical studies of oxidative addition and reductive elimination. 2. Reductive coupling of H–H, H–C, and C–C bonds from palladium and platinum complexes. Organometallics 5:609–622
98. Low JJ, Goddard WA (1986) Theoretical studies of oxidative addition and reductive elimination. 3. C–H and C–C reductive coupling from palladium and platinum bis(phosphine) complexes. J Am Chem Soc 108:6115–6128
99. Ananikov VP, Musaev DG, Morokuma K (2002) Vinyl-vinyl coupling on late transition metals through C–C reductive elimination mechanism. A computational study. J Am Chem Soc 124:2839–2852
100. Ananikov VP, Musaev DG, Morokuma K (2005) Theoretical insight into the C–C coupling reactions of the vinyl, phenyl, ethynyl, and methyl complexes of palladium and platinum. Organometallics 24:715–723
101. Choueiry D, Negishi E-I (2002) Pd(0) and Pd(II) complexes containing phosphorus and other group 15 atom ligands. In: Negishi E (ed) Handbook of organopalladium chemistry for organic synthesis. Wiley, New York
102. Ozawa F, Ito T, Nakamura Y, Yamamoto A (1981) Mechanisms of thermal decomposition of trans- and cis-Dialkylbis(tertiary phosphine)palladium(II). Reductive elimination and trans to cis isomerization. Bull Chem Soc Jpn 54:1868–1880
103. Ozawa F, Kurihara K, Yamamoto T, Yamamoto A (1985) Alteration of reaction course in thermolysis of cis-diethylbis(tertiary phosphine)palladium(II) from reductive elimination to β-elimination process induced by addition of tertiary phosphine ligand. Bull Chem Soc Jpn 58:399–400
104. Brown JM, Cooley NA (1988) Carbon-carbon bond formation through organometallic elimination reactions. Chem Rev 88:1031–1046
105. Macgregor SA, Neave GW, Smith C (2003) Theoretical studies on C-heteroatom bond formation via reductive elimination from group 10 $M(PH_3)_2(CH_3)(X)$ species (X = CH_3, NH_2, OH, SH) and the determination of metal-X bond strengths using density functional theory. Faraday Discuss 124:111–127
106. Negishi E, Takahashi T, Akiyoshi K (1987) Palladium-catalyzed -or promoted reductive carbon–carbon coupling. Effects of phosphines and carbon ligands. J Organomet Chem 334: 181–194
107. Zuidema E, van Leeuwen PWNM, Bo C (2005) Reductive elimination of organic molecules from palladium-diphosphine complexes. Organometallics 24:3703–3710
108. Ananikov VP, Musaev DG, Morokuma K (2007) Critical effect of phosphane ligands on the mechanism of carbon-carbon bond formation involving palladium(II) complexes: a theoretical investigation of reductive elimination from square-planar and T-shape species. Eur J Inorg Chem 5390–5399

109. Ariafard A, Yates BF (2009) In-depth insight into the electronic and steric effects of phosphine ligands on the mechanism of the R–R reductive elimination from $(PR_3)_2PdR_2$. J Organomet Chem 694:2075–2084
110. Watson L, Eisenstein O (2002) Entropy explained: the origin of some simple trends. J Chem Educ 79:1269–1277
111. Perez-Rodriguez M, Braga AAC, Garcia-Melchor M, Perez-Temprano M, Casares JA, Ujaque G, de Lera AR, Alvarez R, Maseras F, Espinet P (2009) C–C reductive elimination in palladium complexes, and the role of coupling additives A DFT study supported by experiment. J Am Chem Soc 131(10):3650–3655

Chapter 4
Metal Complexes with Anionic Polyphosphorus Chains as Potential Precursors for the Synthesis of Metal Phosphides

Santiago Gómez-Ruiz and Evamarie Hey-Hawkins

Abstract While the synthesis, reactivity and properties of organic oligophosphanes have already been intensively studied, the number of metal complexes of the related anionic species described in the literature is still small. This chapter reviews the different synthetic methods for the preparation of metal complexes of *catena*-oligophosphanediides, as well as the reactivity of the $(P_4R_4)^{2-}$ and $(P_4HR_4)^{-}$ ions. In addition, a brief review on the potential application of metal oligophosphanides as precursors for the preparation of metal-rich phosphides (MP_x, where $x < 1$), monophosphides (MP) and phosphorus-rich polyphosphides (MP_x, where $x > 1$) is given.

4.1 Introduction

The chemistry of polyphosphorus compounds has developed impressively over the last four decades. The development of several preparative techniques and above all the progress made in ^{31}P NMR spectroscopy has enabled systematic studies of the structures and reactivity of this class of compounds. Thus, a great number of cyclic and catenated polyphosphanes (both as hydrides and as organic derivatives) have been synthesised and successfully characterised [1–8]. The chemistry of these

S. Gómez-Ruiz
Departamento de Química Inorgánica y Analítica, E.S.C.E.T., Universidad Rey Juan Carlos, Calle Tulipán sn, 28933 Móstoles, Spain
e-mail: santiago.gomez@urjc.es

E. Hey-Hawkins (✉)
Institut für Anorganische Chemie der Universität Leipzig, Johannisallee 29, 04103 Leipzig, Germany
e-mail: hey@uni-leipzig.de

M. Peruzzini and L. Gonsalvi (eds.), *Phosphorus Compounds*, Catalysis by Metal Complexes, 37, DOI: 10.1007/978-90-481-3817-3_4,
© Springer Science+Business Media B.V. 2011

compounds can be analogous to that of related carbon compounds [9]. Among other things, this analogy is due to constitutional and configurational isomerism and valence tautomerism as well as the existence of mixed P–C ring systems. The isolobal analogy of the fragments P/CR, PR/CR_2 and PR_2/CR_3, based on similar properties of their frontier orbitals, has been used to rationalise their similar behaviour [1–9]. On the other hand, phosphorus shows a notable propensity to form a wide variety of P_n frameworks due to the comparatively high bond energy of P–P single bonds (ca. 200 kJ/mol, the highest value within group 15) [10].

While the synthesis, reactivity, and properties of organic cyclooligophosphanes have already been intensively studied, the number of metal complexes of these species described in the literature is still small. However, the few known examples have shown that (in contrast to their mostly unstable isolobal carbon counterparts) cyclic [11] and catenated oligophosphanide anions exhibit a rich coordination chemistry, because each P atom can be involved in coordination via its free electron pair. Additionally, metal complexes with anionic polyphosphorus ligands may be an alternative for the development of rational syntheses of binary metal phosphides (M_xP_y), which are a fascinating class of compounds with unusual structures and interesting properties for materials science [12, 13]. Thus, metal phosphides may behave as metallic or semimetallic conductors or (in most cases) as semiconductors. In addition, rare earth metal phosphides have been extensively investigated due to their interesting magnetic properties [14, 15].

Up to now, metal phosphides have mainly been obtained either by solid-state synthetic techniques, under extreme conditions with long reaction times, or via the molecular phase to enable their use in the preparation of new materials. However, the renaissance and subsequent development of the chemistry of catenated oligophosphanide anions and their metal complexes may open up novel routes for the preparation of metal phosphides by thermal treatment of phosphorus-rich metal complexes.

4.2 Synthesis of Metal Complexes with Oligophosphanide Anions: An Old Task

Metal complexes with oligophosphanide anions were previously obtained either serendipitously or as mixtures of compounds, as summarised below:

Method 1: The reaction of cyclooligophosphanes *cyclo*-(P_nR_n) (R = alkyl, aryl; n = 3–6) with complexes of valence electron-rich metals, which led to P–P cleavage.

Method 2: Reaction of halophosphanes with phosphane or phosphanide complexes via HX or salt elimination.

Method 3: Oligomerisation of phosphanes or phosphanides to form metal complexes with triphosphanediide ligands.

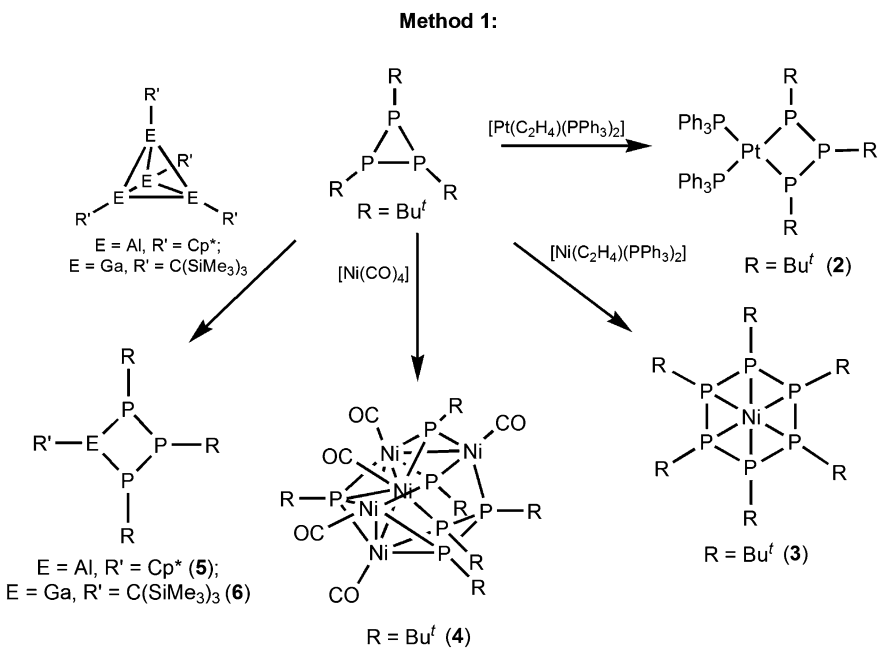


Fig. 4.1 Method 1 for the preparation of metal oligophosphanides

Method 4: Reduction of cyclooligophosphanes with alkali metals and subsequent transmetallation of the formed alkali metal oligophosphanedides $M_2(P_nR_n)$ (n = 2–4) with metal halides.

An example of synthetic method 1 is the reaction of *cyclo*-(P_5R_5) (R = Me, Et, Ph) with $[Fe(CO)_5]$ described by West and Rheingold [16]. This reaction led to the formation of the dinuclear iron complex $[Fe_2(\mu\text{-}P_4R_4)(CO)_6]$ (**1**) with a bridging $(P_4R_4)^{2-}$ ligand.

Fenske and co-workers isolated some transition metal complexes with $(P_3R_3)^{2-}$ ligands from the reaction of *cyclo*-(P_3R_3) (R = Bu^t, Pr^i) with transition metal complexes in low oxidation states. In these reactions formation of bridging *catena*-$(P_nR_n)^{2-}$ ligands (n = 1–6) or ring expansion were observed (compounds **2**–**4**, Fig. 4.1) [17–22]. Similarly, other authors prepared main group [23, 24] (complexes **5** and **6**, Fig. 4.1) and transition metal compounds [25–27] using analogous reactions.

Similar compounds to those described by West and Rheingold have been prepared by method 2 via the reaction of dinuclear phosphanido-bridged complexes with $PhPCl_2$ (compound **7**, Fig. 4.2) [28–30]. Additionally, we could obtain the complexes $[Cp°MoCl_2(\eta^3\text{-}P_4Cy_4H)]$ (**8**) and $[Cp°_2Mo_2(\mu\text{-}Cl)_2(\mu\text{-}P_4Ph_4)]$ (**9**) in low yield by reaction of the paramagnetic phosphane complexes $[Cp°MoCl_4(PH_2R)]$ ($Cp° = \eta^5\text{-}C_5EtMe_4$, R = Cy or Ph) with two equivalents of NEt_3 [31].

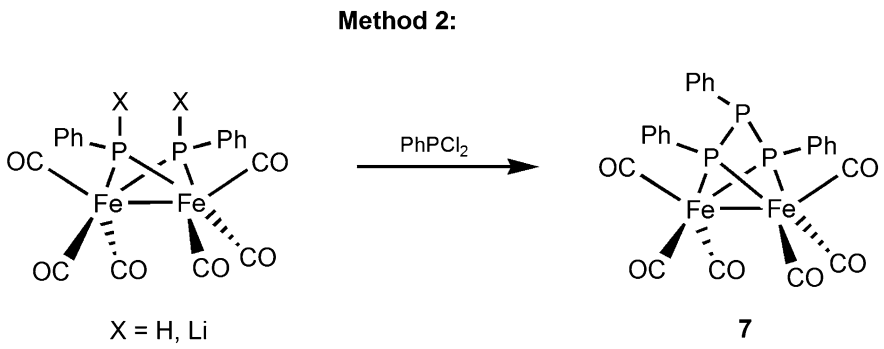


Fig. 4.2 An example of method 2 for the preparation of metal oligophosphanides

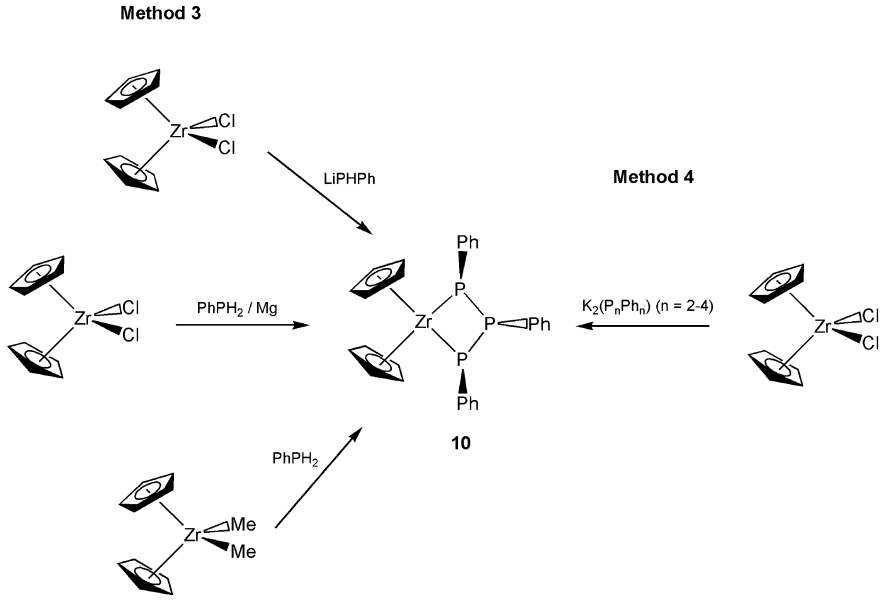


Fig. 4.3 Synthesis of $[Zr(\eta^5\text{-}C_5H_5)_2(P_3Ph_3)]$ (**10**) by methods 3 and 4

Another synthetic procedure (method 3) for the preparation of metal complexes with linear anionic P_nR_n units is the reaction of primary phosphanes and anionic primary phosphanes with metal complexes [32–34]. For example, the reaction of LiPHPh with $[Zr(\eta^5\text{-}C_5H_5)_2Cl_2]$ gave $[Zr(\eta^5\text{-}C_5H_5)_2(P_3Ph_3)]$ (**10**) (Fig. 4.3) [32].

Methods 1–3 have the disadvantage that the chain length of the oligophosphanediide ligands bound to the metal can be poorly controlled. In this respect the transmetallation reaction of alkali metal oligophosphanediides $M_2(P_nR_n)$ ($n = 2$–4) with metal halides (method 4) [35–40] is an interesting starting point, as each ligand has a certain chain length. Thus, in the reaction of $K_2(P_4Bu^t_4)$ with R_2ECl_2, the P_4

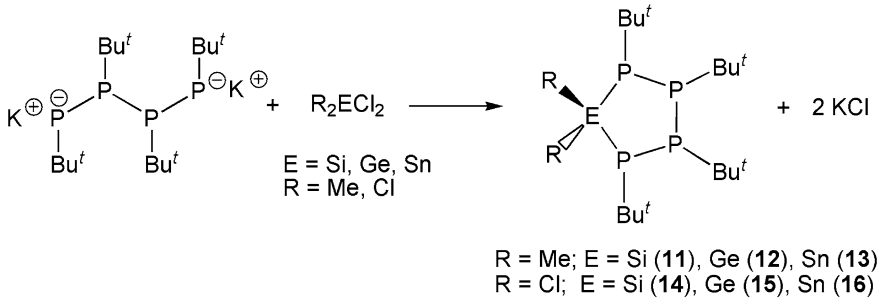


Fig. 4.4 Synthesis of complexes of the type *cyclo*-($P_4Bu^t_4ER_2$) (E = Si, Ge, Sn; R = Bu^t, Cl) using method 4

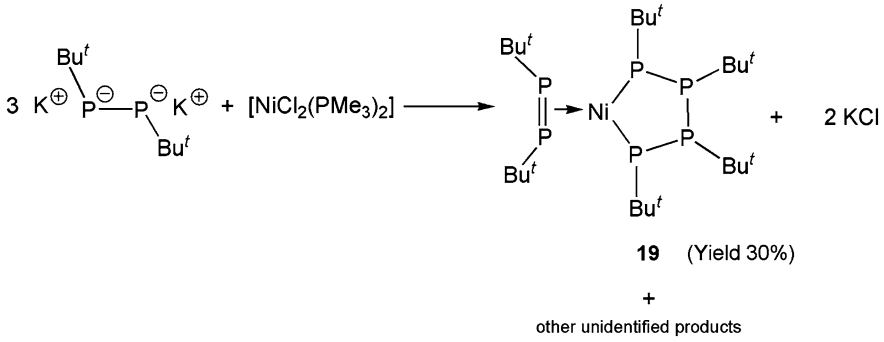


Fig. 4.5 Synthesis of [Ni(η^2-$P_2Bu^t_2$)($P_4Bu^t_4$)] (**19**) by method 4

chain remains intact and *cyclo*-($P_4Bu^t_4ER_2$) [R = Me, E = Si (**11**), Ge (**12**), Sn (**13**); R = Cl, E = Si (**14**), Ge (**15**), Sn (**16**)] is obtained (Fig. 4.4) [41–47].

However, the chain does not always stay intact, as was observed by Köpf and Voigtländer in the reaction of $M_2(P_nPh_n)$ (n = 2–4) with [M(η^5-C_5H_5)$_2$$Cl_2$] (M = Ti, Zr, Hf), which always gave only the compounds [M(η^5-C_5H_5)$_2$(P_3Ph_3)] [M = Ti (**17**), Zr (**10**, Fig. 4.3), Hf (**18**)] [48].

Another example is the reaction of the diphosphanediide $K_2(P_2Bu^t_2)$ with [$NiCl_2(PMe_3)_2$] to give the complex [Ni(η^2-$P_2Bu^t_2$)($P_4Bu^t_4$)] (**19**), in which coupling of two $(P_2Bu^t_2)^{2-}$ units gave the tetraphosphanediide $(P_4Bu^t_4)^{2-}$ as ligand for nickel(II) (Fig. 4.5) [49].

Thus, while method 4 seems to be the most efficient synthesis for metal oligophosphanides, targeted synthesis of the alkali metal oligophosphanediide starting materials $M_2(P_nR_n)$ (n = 2–4) is strictly necessary. In this context, a series of linear oligophosphanediides of different chain lengths were obtained more than

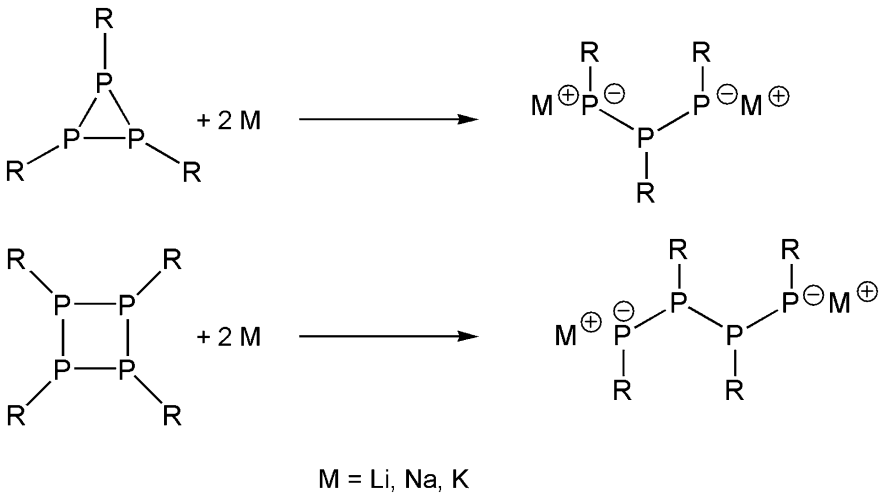


Fig. 4.6 General scheme for the preparation of linear $(P_3R_3)^{2-}$ and $(P_4R_4)^{2-}$ ions

40 years ago from their corresponding cyclooligophosphanes by reductive cleavage with s-block metals (Li, Na, K; Fig. 4.6) [35–40].

With this synthetic method it was possible to vary the chain length by judicious choice of the stoichiometric ratio between metal and oligophosphane. Thus far, these compounds were investigated by X-ray crystallography and their structures were elucidated with the aid of ^{31}P NMR spectroscopy [50–52]. However, these precursors were often obtained as mixtures of products which were very difficult to separate and isolate in pure form.

However, the elegant synthesis of a wide variety of sodium *catena*-oligophosphanediides such as $[Na_2(tmeda)_3(P_3Ph_3)]$ (**20**) and $[Na_2(tmeda)_2(P_4Ph_4)]$ (**21**) (tmeda = $Me_2NCH_2CH_2NMe_2$) (Fig. 4.7) with a different number of phosphorus atoms starting from the appropriate stoichiometric ratio of $PhPCl_2$ and Na allowed the design and synthesis of novel starting materials for the preparation of metal complexes with phosphorus-rich anions [53–56].

4.3 Renaissance of the Chemistry of Metal Complexes with *Catena*-Oligophosphanediides

Inspired by previous work of Baudler, Issleib and Fritz, we set out to develop targeted syntheses for transition metal *catena*-oligophosphanediides as potential precursors for the preparation of metal phosphides [57, 58].

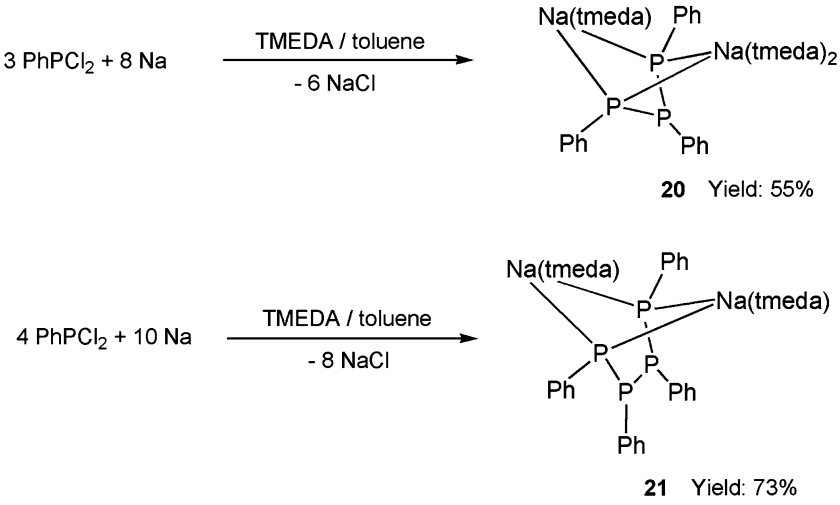


Fig. 4.7 Synthesis of $[Na_2(tmeda)_3(P_3Ph_3)]$ (**20**) and $[Na_2(tmeda)_2(P_4Ph_4)]$ (**21**)

4.3.1 Synthesis of Novel Alkali Metal Oligophosphanediides

We have developed an improved synthesis of alkali metal tetraphosphane-1,4-diides such as $[Na_2(thf)_5(P_4Ph_4)]$ (**22**), $[Na_2(thf)_4(P_4Mes_4)]$ (**23**), $[Na_2(thf)_4(P_4Bu^t_4)]$ (**24**) and $[K_2(thf)_6(P_4Mes_4)]$ (**25**) (Mes = 2,4,6-$Me_3C_6H_2$) by reactions of the corresponding dichlorophosphane $RPCl_2$ and sodium or potassium in stoichiometric ratio 4:10 [59].

In the solid state, these compounds form isolated ion-contact complexes, in which the P_4 chain of the $(P_4R_4)^{2-}$ ligand has a *syn* arrangement and is coordinated to two alkali metal cations. The coordination spheres of the alkali metal cations are completed by two or three THF molecules. The $M_2P_4R_4$ moieties have different arrangements. Whereas for **23** and **25** the phosphorus–alkali metal distances are in the typical range for related sodium and potassium phosphanides for both the internal and terminal phosphorus atoms of the chain, in **22** and **24** the Na cations are exclusively coordinated by the terminal phosphorus atoms (Fig. 4.8). Thus, in **23** and **25**, the phosphorus atoms in the 1,3-positions coordinate and four-membered MP_3 chelate rings are formed. Additionally, longer contacts can be observed between the alkali metal and the second terminal phosphorus atom (Fig. 4.8).

Using similar synthetic methods the preparation of $[K_2(pmdeta)_2(P_4Ph_4)]$ (**26**) and $[K_2(pmdeta)(P_4Bu^t_4)]_2$ (**27**) (pmdeta = $Me_2NCH_2CH_2NMeCH_2CH_2NMe_2$) was also achieved [60].

The AA′BB′ coupling pattern in the ^{31}P NMR spectra of **22**–**27** were analysed, and the resulting coupling constants indicated that the basic structural features observed for these species in the solid state are also preserved in solution [57–60].

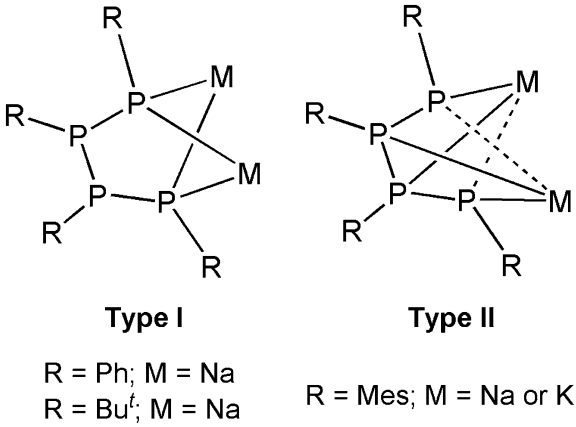


Fig. 4.8 Different coordination modes of alkali metal tetraalkyl- or tetraaryltetraphosphanediides

4.3.2 *Reactivity of $M_2(P_4R_4)$ (M = Na or K; R = Ph, Mes or Bu^t)*

The reactivity of the $(P_4R_4)^{2-}$ anion towards a wide variety of transition metal compounds was studied. One of the first studies was carried out on copper salts [61, 62]. Thus, the reaction of CuCl with $[Na_2(thf)_5(P_4Ph_4)]$ (**22**) or $K_2(P_4Bu^t_4)$ led only to a black precipitate consisting of elemental copper, NaCl and the cyclophosphanes *cyclo*-(P_nPh_n) (n = 4–6) or *cyclo*-$(P_4Bu^t_4)$, respectively. However, the transmetallation reaction of $[CuCl(PCyp_3)_2]$ (Cyp = *cyclo*-C_5H_9) with $[Na_2(thf)_5(P_4Ph_4)]$ (**22**) yielded the tetranuclear copper(I) complex $[Cu_4(P_4Ph_4)_2(PCyp_3)_3]$ (**28**) (Fig. 4.9) and avoided the reduction of the metal cation which was observed in the reaction with CuCl.

The molecular structure of **28** (Fig. 4.10) revealed that this complex consists of a tetranuclear aggregate of four Cu^+ cations with two bridging $(P_4Ph_4)^{2-}$ anions. Some of the Cu^+ cations are additionally coordinated by tricyclopentylphosphane ligands, building a Cu_4P_{11} core with fused five- and six-membered rings in which three of the copper(I) atoms present a distorted trigonal planar geometry while one copper(I) centre has a distorted tetrahedral environment.

Compound **28** displays a complicated $^{31}P\{^1H\}$ NMR spectrum at room temperature with several broad peaks of different intensity, as was expected for an unsymmetric spin system of 11 different phosphorus nuclei if the solid-state structure of **28** were retained in solution (Table 4.1). In addition, the spectrum becomes even more complicated at −80 °C with broader multiplets indicating that line broadening at room temperature may not exclusively be caused by coupling between phosphorus and the quadrupolar $^{63}Cu/^{65}Cu$ nuclei, but also by a fluxional process.

The analogous complex $[Cu_4(P_4Ph_4)_2(PH_2Ph)_2(PCyp_3)_2]$ (**29**) was obtained from the reaction of one equivalent of $K_2(P_4Ph_4)$ or $[Na_2(thf)_5(P_4Ph_4)]$ (**22**) with one equivalent of HCl [63] followed by subsequent reaction with one equivalent of

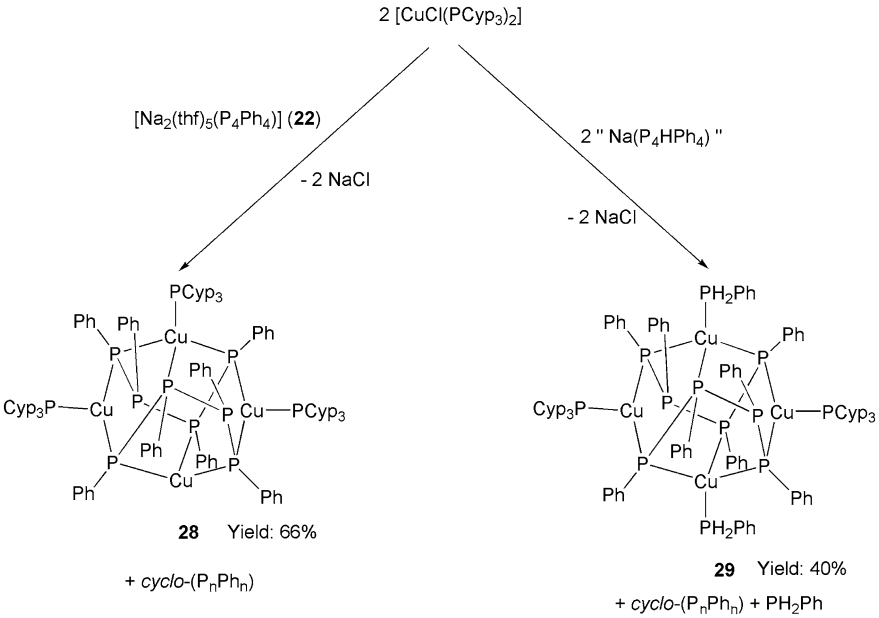


Fig. 4.9 Synthesis of $[Cu_4(P_4Ph_4)_2(PCyp_3)_3]$ (**28**) and $[Cu_4(P_4Ph_4)_2(PH_2Ph)_2(PCyp_3)_2]$ (**29**)

$[CuCl(PCyp_3)_2]$ (Fig. 4.9) when formation of the intermediate $(P_4HPh_4)^-$ and its reaction with copper(I) salts was attempted [64]. Compound **29** is presumably formed via rearrangement of the "in situ"-generated $(P_4HPh_4)^-$ to $(P_4Ph_4)^{2-}$ and $P_4H_2Ph_4$. The latter is very unstable in solution and decomposes rapidly to give a mixture of phosphanes [4, 5] including PH_2Ph, which then coordinates to copper. The molecular structure of **29** determined by X-ray diffraction shows a centrosymmetric arrangement of the Cu_4P_{12} cluster core which differs slightly from that in $[Cu_4(P_4Ph_4)_2(PCyp_3)_3]$ (**28**) (for selected structural data see Table 4.2). Compound **29** consists of a tetranuclear aggregate of four Cu^+ ions with two bridging $(P_4Ph_4)^{2-}$ dianions (Fig. 4.11), but in this case two copper(I) atoms are coordinated in a tetrahedral fashion (selected structural data are given in Table 4.2).

As observed previously for $[Cu_4(P_4Ph_4)_2(PCyp_3)_3]$ (**28**), the room-temperature $^{31}P\{^1H\}$ NMR spectrum of **29** is very complicated, displaying several broad peaks of varying intensity. This indicates that it is rather unlikely that the molecular structure of **29** is retained in solution (Table 4.1).

In a similar reaction, $K_2(P_4Mes_4)$ or $[Na_2(thf)_4(P_4Mes_4)]$ (**23**) was treated with one equivalent of HCl and the $(P_4HMes_4)^-$ anion formed "in situ" was then treated with half an equivalent of $[\{RhCl(cod)\}_2]$ (cod = 1,5-cyclooctadiene) to give a mixture of rhodium-containing products, from which the desired complex $[Rh(P_4HMes_4)(cod)]$ (**30**) and $[Rh_2(\mu\text{-}P_2HMes_2)(\mu\text{-}PHMes)(cod)_2]$ (**31**) could be isolated (Fig. 4.12) [64].

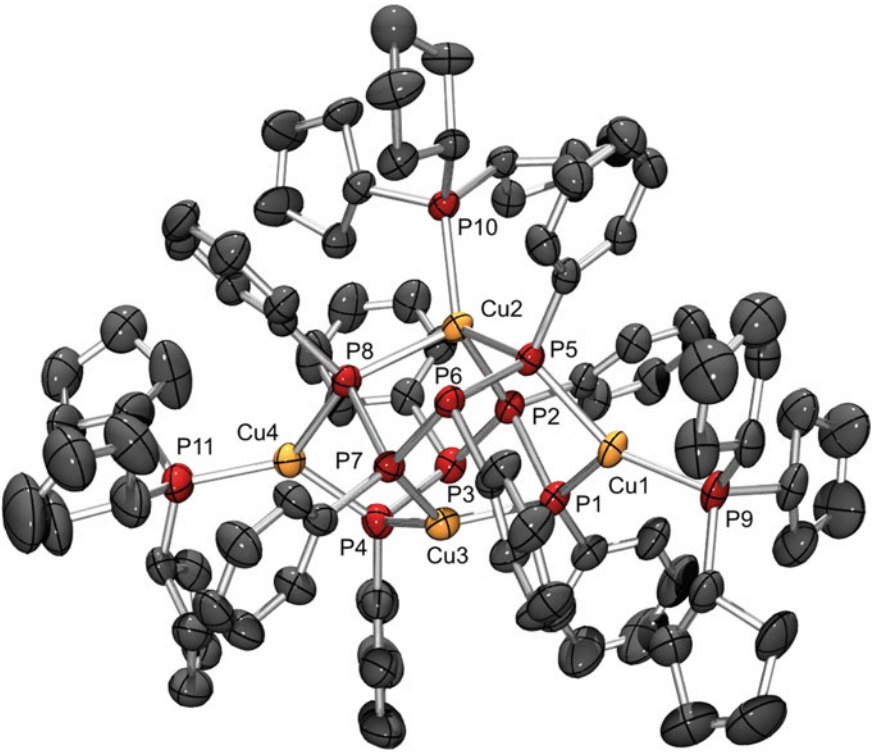


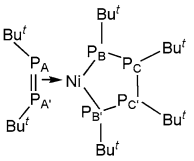
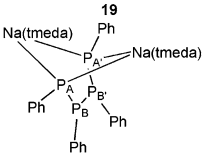
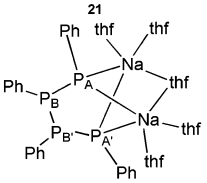
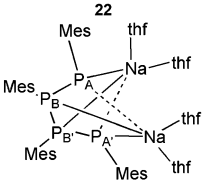
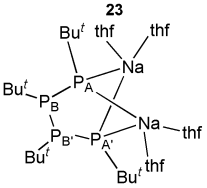
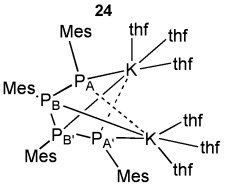
Fig. 4.10 Molecular structure of $[Cu_4(P_4Ph_4)_2(PCyp_3)_3]$ (**28**). Hydrogen atoms are omitted for clarity

The X-ray crystal structure determination revealed that the $(P_4HR_4)^-$ anion acts as a chelating ligand via its two terminal phosphorus atoms P1 and P4 (Table 4.2). This structure seems to be retained in solution, as the proton-coupled ^{31}P NMR spectrum of **30** shows an ABCDXY spin system (Fig. 4.13), in which one of the signals (P_B) is more complex due to coupling to hydrogen with a very large $^1J_{PH}$ coupling constant of 335.2 Hz. In addition, the terminal phosphorus atoms of the P_4 chain have coupling constants $^1J_{PRh}$ of ca. 160 and 85 Hz (for a detailed analysis of the chemical shifts and coupling constants see Table 4.1).

Interestingly, in the FAB-MS of **30**, organyl-free fragments such as $[Rh_2P_3]^+$ and $[Rh_2P_2]^+$ were observed, which may indicate the suitability of this complex to act as molecular precursor for binary metal phosphides.

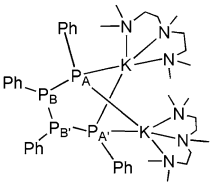
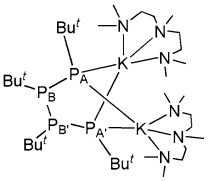
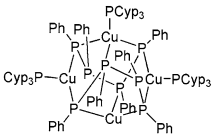
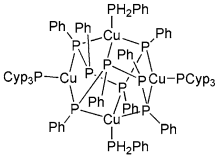
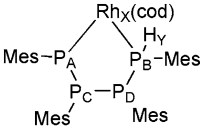
During our studies on the reactivity of the $(P_4R_4)^{2-}$ ion, we unexpectedly observed formation of Ni^0 and Pd^0 dimesityldiphosphene complexes $[Ni(\eta^2\text{-}P_2Mes_2)(PEt_3)_2]$ (**32**), $[Ni(\eta^2\text{-}P_2Mes_2)(PMe_2Ph)_2]$ (**33**), $[Pd(\eta^2\text{-}P_2Mes_2)(PBu^n_3)_2]$ (**34**) and $[Pd(\eta^2\text{-}P_2Mes_2)(PMe_2Ph)_2]$ (**35**) in the reaction of $Na_2(P_4Mes_4)$ with the corresponding nickel and palladium complexes (Fig. 4.14) [65].

Table 4.1 $^{31}P\{^{1}H\}$ NMR data of complexes with linear oligophosphanide anions (25 °C, δ in ppm, J in Hz)

Compound	Spin system	Chemical shift (ppm)	Coupling constants (Hz)	References
	AA′BB′CC′	$\delta_{AA'} = +45.0$ $\delta_{BB'} = +53.6$ $\delta_{CC'} = +29.2$	$^{1}J_{AA'} = 275$ $^{1}J_{BC} = 225$ $^{1}J_{CC'} = 325$ $^{2}J_{AB} = 1$ $^{2}J_{AB'} = 22$	[49]
19 	AA′BB′	$\delta_{AA'} = -89.1$ $\delta_{BB'} = -24.9$	$^{1}J_{AB} = {}^{1}J_{A'B'} = 322$ $^{1}J_{BB'} = 310$ $^{2}J_{AB'} = {}^{2}J_{A'B} = 11$ $^{3}J_{AA'} = 306$	[53, 54]
21 	AA′BB′	$\delta_{AA'} = -91.4$ $\delta_{BB'} = -26.6$	$^{1}J_{AB} = {}^{1}J_{A'B'} = -323.1$ $^{1}J_{BB'} = -310.2$ $^{2}J_{AB'} = {}^{2}J_{A'B} = -12.3$ $^{3}J_{AA'} = +310.6$	[59]
22 	AA′BB′	$\delta_{AA'} = -113.1$ $\delta_{BB'} = -13.7$	$^{1}J_{AB} = {}^{1}J_{A'B'} = -309.8$ $^{1}J_{BB'} = -118.3$ $^{2}J_{AB'} = {}^{2}J_{A'B} = +120.3$ $^{3}J_{AA'} = +3.3$	[59]
23 	AA′BB′	$\delta_{AA'} = -78.1$ $\delta_{BB'} = -5.2$	$^{1}J_{AB} = {}^{1}J_{A'B'} = -341.1$ $^{1}J_{BB'} = -305.5$ $^{2}J_{AB'} = {}^{2}J_{A'B} = -12.6$ $^{3}J_{AA'} = +200.9$	[59]
24 	AA′BB′	$\delta_{AA'} = -110.5$ $\delta_{BB'} = -12.6$	$^{1}J_{AB} = {}^{1}J_{A'B'} = -328.5$ $^{1}J_{BB'} = -127.6$ $^{2}J_{AB'} = {}^{2}J_{A'B} = +107.2$ $^{3}J_{AA'} = +1.5$	[59]
25				

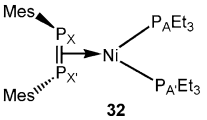
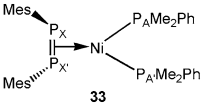
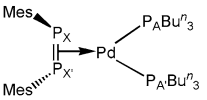
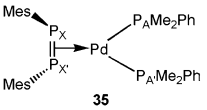
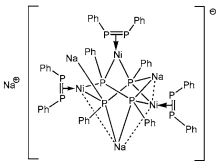
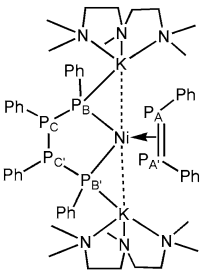
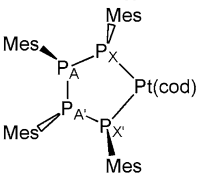
(continued)

Table 4.1 (continued)

Compound	Spin system	Chemical shift (ppm)	Coupling constants (Hz)	References
 **26**	AA′BB′	$\delta_{AA'} = -70.0$ $\delta_{BB'} = -21.3$	$^1J_{AB} = {}^1J_{A'B'} = -323.1$ $^1J_{BB'} = -301.8$ $^2J_{AB'} = {}^2J_{A'B} = +30.8$ $^3J_{AA'} = +82.8$	[60]
 **27**	AA′BB′	$\delta_{AA'} = -59.4$ $\delta_{BB'} = +4.0$	$^1J_{AB} = {}^1J_{A'B'} = -360.9$ $^1J_{BB'} = -307.3$ $^2J_{AB'} = {}^2J_{A'B} = -11.0$ $^3J_{AA'} = +102.6$	[60]
 **28**	[a]	$\delta = +32.5$ $\delta = +18.2$ $\delta = +10.0$ $\delta = +5.4$ $\delta = +2.9$ $\delta = -20.4$ $\delta = -23.8$ $\delta = -71.2$ $\delta = -88.8$	[a]	[61, 62]
 **29**	[a]	$\delta = +19.9$ $\delta = +11.3$ $\delta = +10.0$ $\delta = -5.0$ $\delta = -9.7$ $\delta = -24.7$ $\delta = -46.5$ $\delta = -70.3$ $\delta = -79.5$ $\delta = -94.0$	[a]	[64]
 **30**	ABCDXY[b]	$\delta_A = +39.3$ $\delta_B = -23.3$ $\delta_C = -34.4$ $\delta_D = -61.2$	$^1J_{AC} = +167.6$ $^1J_{AX} = +85.3$ $^1J_{BD} = +272.7$ $^1J_{BX} = +160.6$ $^1J_{BY} = +335.2$ $^1J_{CD} = +205.6$ $^2J_{AD} = +58.0$ $^2J_{BC} = +55.3$ $^3J_{AB} = +16.5$	[64]

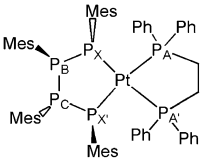
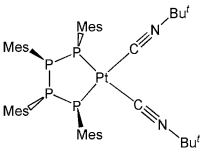
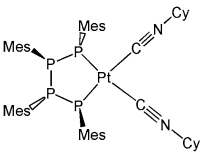
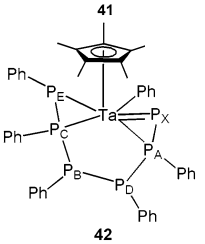
(continued)

Table 4.1 (continued)

Compound	Spin system	Chemical shift (ppm)	Coupling constants (Hz)	References
 **32**	AA′XX′	$\delta_A = +14.9$ $\delta_X = +3.9$	$^2J_{AX'} = +42.3$ $^2J_{AX} = +1.7$	[65]
 **33**	AA′XX′	$\delta_A = +14.9$ $\delta_X = +12.2$	$^2J_{AX'} = +51.8$ $^2J_{AX} = +1.5$	[65]
 **34**	AA′XX′	$\delta_A = +4.3$ $\delta_X = +41.1$	$^2J_{AX'} = +50.4$ $^2J_{AX} = +2.1$	[65]
 **35**	AA′XX′	$\delta_A = -12.8$ $\delta_X = +49.7$	$^2J_{AX'} = +57.7$ $^2J_{AX} = +1.0$	[65]
 **36**	a	$\delta = +11$ $\delta = -9$ $\delta = -15$ $\delta = -29$ $\delta = -52$	a	[68]
 **37**	AA′BB′CC′	$\delta_{AA'} = -3.8$ $\delta_{BB'} = +7.6$ $\delta_{CC'} = -7.5$	c	[68]
 **38**	AA′XX′	$\delta_{AA'} = +2.4$ $\delta_{XX'} = -37.3$	$^1J_{AX} = {}^1J_{A'X'} = +109.7$ $^1J_{AA'} = +165.4$ $^2J_{AX'} = {}^2J_{A'X} = +14.8$ $^3J_{XX'} = +12.6$ $^1J_{XPt} = 1146$	[79]

(continued)

Table 4.1 (continued)

Compound	Spin system	Chemical shift (ppm)	Coupling constants (Hz)	References
 **39**	AA′BCXX′	$\delta_{AA'} = +44.8$ $\delta_B = -39.0$ $\delta_C = -39.8$ $\delta_{XX'} = -53.3$	$^1J_{BX} = +141.4$ $^1J_{CX'} = +140.8$ $^2J_{AX} = +52.0$ $^2J_{AX'} = +17.2$ $^2J_{A'X} = +17.3$ $^2J_{A'X'} = +52.1$ $^1J_{APt} = 2261$ $^1J_{XPt} = 780$	[79]
 **40**	[d]	$\delta = -43.7$ to -34.2	[d]	[79]
 **41**	[d]	$\delta = -36.8$ to -35.2	[d]	[79]
 **42**	ABCDEX	$\delta_A = +34.0$ $\delta_B = +24.9$ $\delta_C = -1.8$ $\delta_D = -57.6$ $\delta_E = -127.7$ $\delta_X = +370.3$	$^1J_{AX} = \pm 471$ $^1J_{BD} = \pm 204$ $^1J_{BC} = \pm 391$ $^1J_{AD} = \pm 355$ $^1J_{CE} = \pm 444$	[80]

[a]Severe line broadening precluded numerical analysis of the coupling patterns
[b]Refers to its ^{31}P NMR spectrum
[c]Due to the presence of more than one isomer in solution, the signals reported are those corresponding to the major isomer, presumably the all-*trans* isomer. The coupling constants could not be obtained by simulation of the spectrum without ambiguity due to the presence of signals corresponding to the other isomers
[d]Severe overlap of the signals precluded numerical analysis of the coupling constants

A plausible mechanism for the formation of **32**–**35** includes prior formation of the corresponding nickel(II) or palladium(II) tetraphosphanediide species, which give the Ni^0 or Pd^0 bis(dimesityldiphosphene) complexes after an intramolecular redox reaction. These intermediates eliminate a diphosphene ligand to give the observed products **32**–**35** (Fig. 4.14).

The $^{31}P\{^1H\}$ NMR spectra of **32**–**35** show two triplets with additional signals of low intensity indicating an AA′XX′ spin system with $^2J_{(P,P)cis}$ coupling constants close to zero (Table 4.1). These results are in agreement with previous work by Pidcock and co-workers reporting slow rotation (on the NMR timescale) of the

Table 4.2 P–P and M–P bond lengths in complexes with linear oligophosphanide anions (determined by single-crystal X-ray diffraction studies)

Compound	P–P	M–P[a]	References
$[Ni(\eta^2\text{-}P_2Bu^t_2)(P_4Bu^t_4)]$ (**19**)	211.0(5)	214.9(4)	[49]
	219.6(4)	225.7(4)	
	223.7(5)		
$[Na_2(tmeda)_2(P_4Ph_4)]$ (**21**)	216.7(4)	289.4(6)	[53, 54]
	216.8(4)	291.6(6)	
	219.0(4)	293.3(6)	
		296.0(6)	
$[Na_2(thf)_5(P_4Ph_4)]$ (**22**)	216.6(1)	289.2(2)	[59]
	220.7(2)	290.1(2)	
$[Na_2(thf)_4(P_4Mes_4)]$ (**23**)	217.7(1)	289.6(1)	[59]
	218.3(1)	296.1(1)	
	225.1(1)	305.3(1)	
		316.6(1)	
		317.3(1)	
		331.6(2)	
$[Na_2(thf)_4(P_4Bu^t_4)]$ (**24**)	215.8(1)	281.9(1)	[59]
	217.0(2)	284.0(1)	
	222.2(2)	290.1(2)	
		291.1(2)	
$[K_2(thf)_6(P_4Mes_4)]$ (**25**)	215.0(2)	331.4(3)	[59]
	215.9(2)	341.1(2)	
	225.2(2)	343.2(3)	
		359.8(2)	
		382.3(3)	
		385.1(2)	
$[K_2(pmdeta)_2(P_4Ph_4)]$ (**26**)	217.2(1)	324.5(2)	[60]
	217.2(2)	327.9(2)	
	220.7(2)	330.1(2)	
		337.2(2)	
		376.7(2)	
		381.5(2)	
$[K_2(pmdeta)(P_4Bu^t_4)]_2$ (**27**)	217.4(1)	308.0(2)	[60]
	219.0(2)	313.3(2)	
	224.8(3)	323.1(2)	
		341.7(2)	
		342.2(2)	
$[Cu_4(P_4Ph_4)_2(PCyp_3)_3]$ (**28**)	218.0(2)	225.8(2)	[61, 62]
	220.0(3)	227.1(2)	
	220.6(3)	228.1(2)	
	221.3(2)	229.0(2)	
	222.1(2)	229.9(2)	
	224.2(3)	231.5(2)	
		232.0(2)	
		239.8(2)	
		240.0(2)	
		240.3(2)	

(continued)

Table 4.2 (continued)

Compound	P–P	M–P[a]	References
$[Cu_4(P_4Ph_4)_2(PH_2Ph)_2(PCyp_3)_2]$ (**29**)	218.6(1) 218.6(1) 220.5(1)	222.6(2) 222.7(1) 227.6(2) 228.5(2) 230.1(1) 233.4(1)	[64]
$[Rh(P_4HMes_4)(cod)]$ (**30**)	219.9(1) 221.2(1) 222.3(1)	225.7(2) 229.9(1)	[64]
$[Ni(\eta^2\text{-}P_2Mes_2)(PEt_3)_2]$ (**32**)	213.6(2)	226.1(1) 226.3(1)	[65]
$[Ni(\eta^2\text{-}P_2Mes_2)(PMe_2Ph)_2]$ (**33**)	213.7(1)	224.9(1) 226.0(1)	[65]
$[Pd(\eta^2\text{-}P_2Mes_2)(PBu^n{}_3)_2]$ (**34**)	214.2(2)	237.7(1) 238.2(1)	[65]
$[Pd(\eta^2\text{-}P_2Mes_2)(PMe_2Ph)_2]$ (**35**)	214.1(1)	236.9(1) 238.1(1)	[65]
$[Na(Et_2O)_3][Na_3(Et_2O)_2Ni_3(\mu\text{-}P_2Ph_2)_2(\eta^2\text{-}P_2Ph_2)_3]$ (**36**)	211.5(3) 213.4(4) 213.5(3) 218.5(3) 219.2(3)	219.4(2)[b] 219.5(2)[b] 219.9(3)[b] 220.9(2)[b] 221.0(3)[b] 221.5(2)[b] 221.5(3)[b] 222.2(3)[b] 222.5(3)[b] 223.1(3)[b] 225.0(3)[b] 226.1(3)[b] 290.5(5)[c] 298.6(4)[c] 298.7(4)[c] 299.6(4)[c] 300.1(4)[c]	[68]
$[K(pmdeta)]_2[Ni(P_4Ph_4)(P_2Ph_2)]$ (**37**)	211.2(2) 218.9(2) 220.7(2) 221.0(2)	218.7(2)[b] 219.7(2)[b] 223.1(2)[b] 224.1(2)[b] 354.5(2)[d] 362.0(3)[d]	[68]
$[Pt(P_4Mes_4)(cod)]$ (**38**)	221.4(2) 222.4(2)	232.8(2)	[79]
$[Pt(P_4Mes_4)(dppe)]$ (**39**)	219.5(3) 221.4(3) 223.6(3)	233.8(2) 234.7(2)	[79]

(continued)

Table 4.2 (continued)

Compound	P–P	M–P[a]	References
$[Pt(P_4Mes_4)(C{\equiv}NBu^t)_2]$ (**40**)	221.3(2) 221.3(2) 222.1(2)	231.9(1) 233.9(1)	[79]
$[Pt(P_4Mes_4)(C{\equiv}NCy)_2]$ (**41**)	221.1(2) 221.2(2) 221.5(2)	233.1(2) 233.1(2)	[79]
$[Ta(\eta^5\text{-}C_5Me_5)(Ph)(P_6Ph_5)]$ (**42**)	209.6(3) 213.3(3) 218.5(3) 221.1(3) 221.3(3)	241.6(2) 252.8(2) 256.1(2) 265.9(2)	[80]

[a]Refers to M–P bond of the P_n chain
[b]Ni–P bond
[c]Na–P bonds
[d]K–P bonds

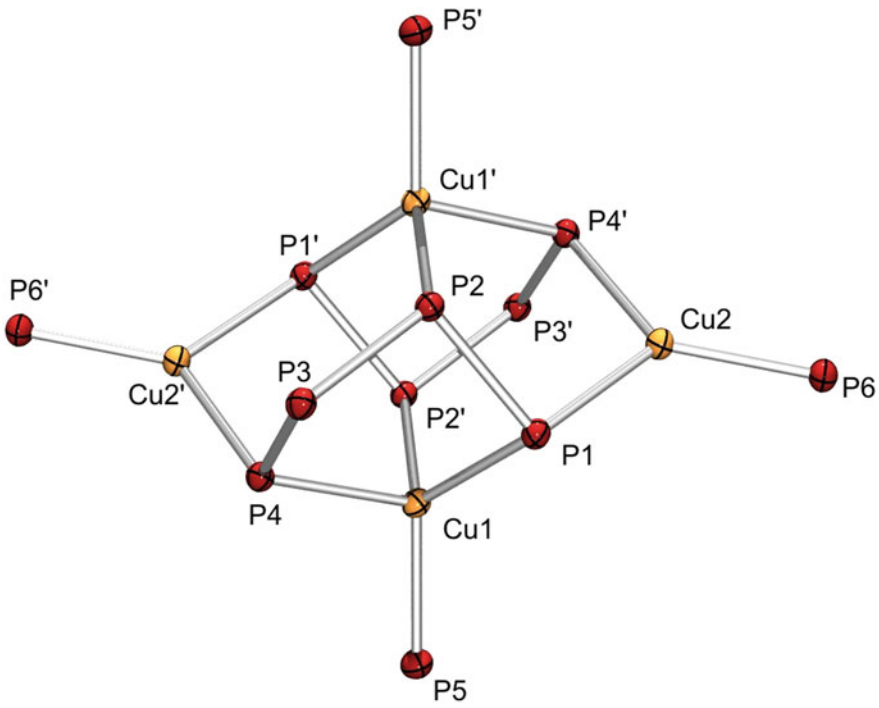


Fig. 4.11 Cu_4P_{12} core structure of $[Cu_4(P_4Ph_4)_2(PH_2Ph)_2(PCyp_3)_2]$ (**29**)

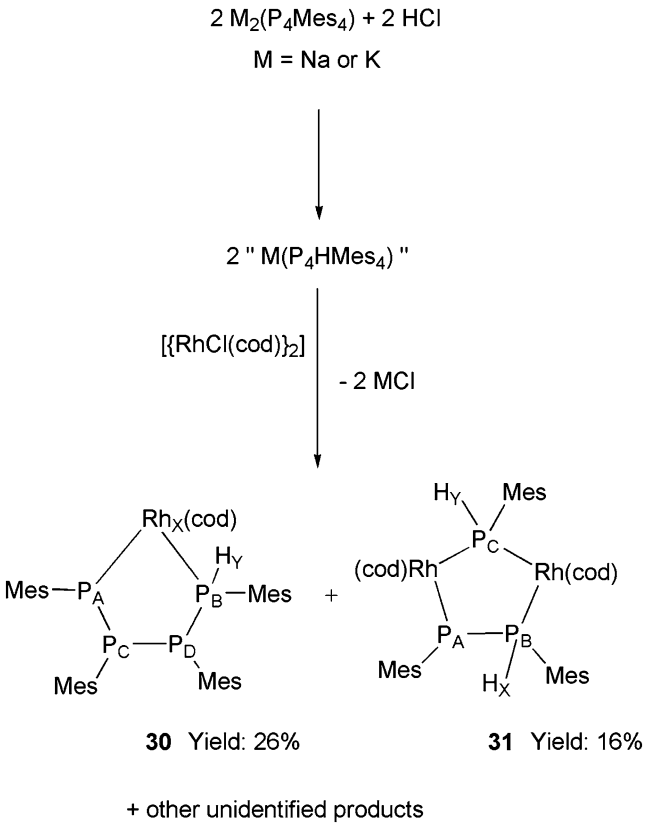


Fig. 4.12 Synthesis of [Rh(P_4HMes_4)(cod)] (**30**) and [Rh_2(μ-P_2HMes_2)(μ-PHMes)$(cod)_2$] (**31**)

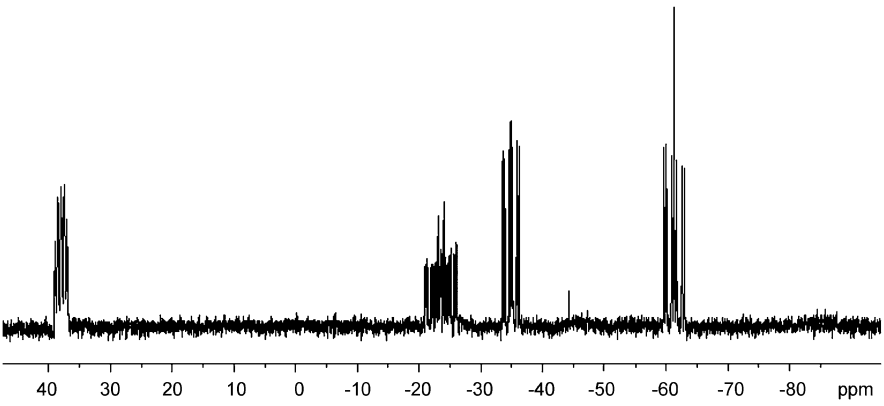


Fig. 4.13 ^{31}P NMR spectrum of [Rh(P_4HMes_4)(cod)] (**30**)

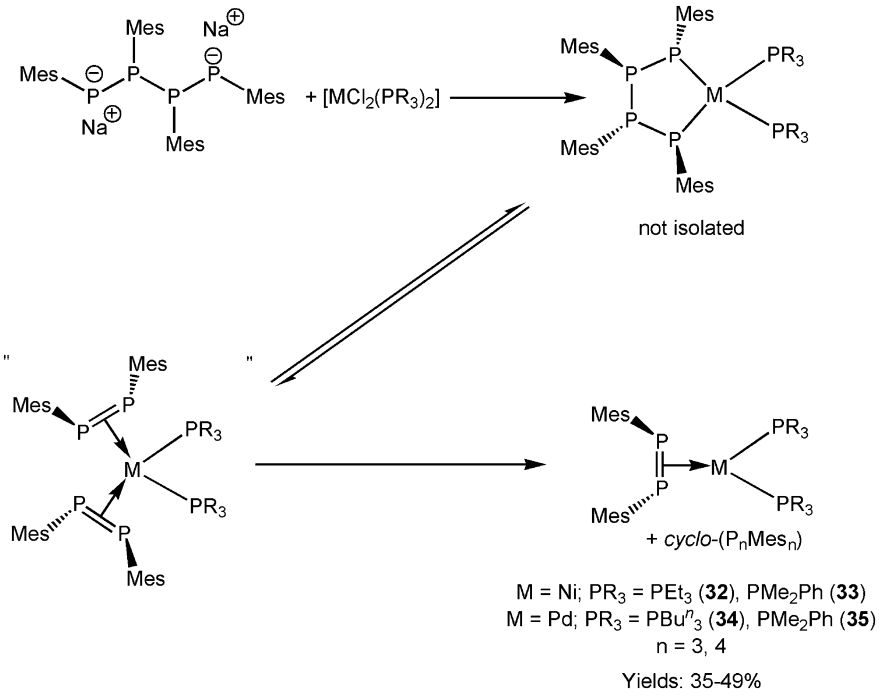


Fig. 4.14 Synthesis of Ni^0 and Pd^0 dimesityldiphosphene complexes **32–35**

diphosphene ligand around the C_2 axis for similar compounds [66, 67]. The X-ray structure determinations of compounds **32–35** showed similar structural parameters to those described in previously reported nickel, palladium and platinum diphosphene derivatives (for some selected structural parameters of **32–35** see Table 4.2) [66, 67].

Recently, we also observed P–P bond cleavage of tetraphenyltetraphosphane-1, 4-diide by nickel(0) in the reaction of $[Na_2(thf)_5(P_4Ph_4)]$ (**22**) with one equivalent of $[Ni(cod)_2]$ to give the ionic compound $[Na(Et_2O)_3][Na_3(Et_2O)_2Ni_3(\mu\text{-}P_2Ph_2)_2(\eta^2\text{-}P_2Ph_2)_3]$ (**36**) presumably via reduction of the $(P_4Ph_4)^{2-}$ ion to give two $(P_2Ph_2)^{2-}$ ions and oxidation of $(P_4Ph_4)^{2-}$ to give two diphenyldiphosphene ligands (Fig. 4.15) [68]. This reaction also generates $Na_2P_2Ph_2$ as by-product as well as a mixture of oligophosphanes and oligophosphanides.

A subsequent reaction between the less reactive $[K_2(pmdeta)_2(P_4Ph_4)]$ (**26**) and $[Ni(cod)_2]$ (ratio 1:1 or 2:1), which gave as a major product the ionic complex $[K(pmdeta)]_2[Ni(P_4Ph_4)(\eta^2\text{-}P_2Ph_2)]$ (**37**) (Fig. 4.16), clarified the mechanism of formation of **36**. Thus, **37** can be considered as the potassium analogue of the possible intermediate in the formation of **36**, in which K–P and K–Ni interactions stabilise the NiP_4 framework. In both reactions P–P bond cleavage of tetraphenyltetraphosphane-1,4-diide by nickel(0) is highly surprising, since nickel(0) and nickel(II) complexes have been widely used as catalysts for olefin oligomerisation reactions and formation of C–C bonds from olefins (isolobal to diphosphenes) [69–75]. However, assuming

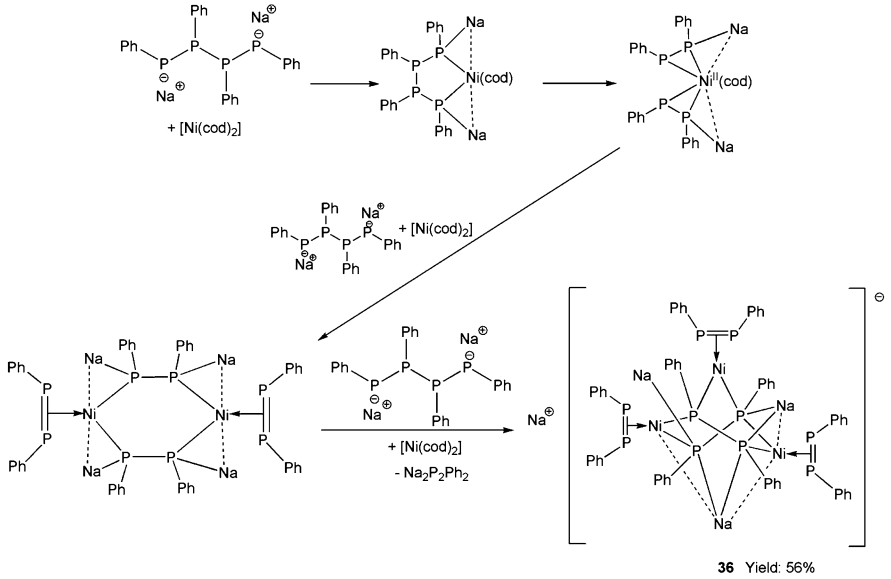


Fig. 4.15 Proposed mechanism for the formation of $[Na(Et_2O)_3][Na_3(Et_2O)_2Ni_3(\mu\text{-}P_2Ph_2)_2(\eta^2\text{-}P_2Ph_2)_3]$ (**36**)

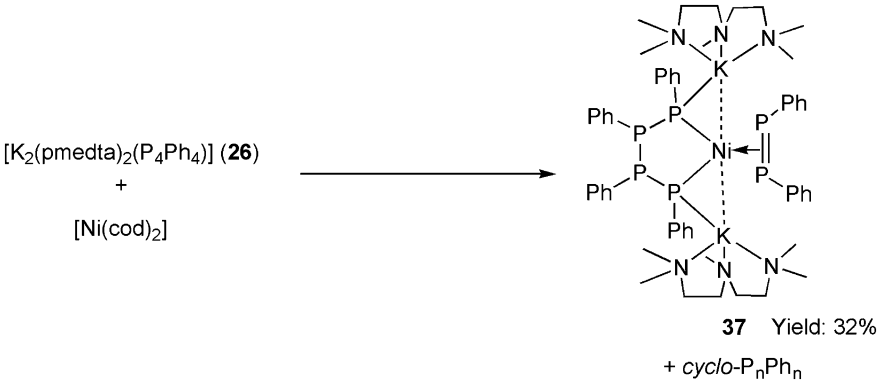


Fig. 4.16 Synthesis of $[K(pmdeta)]_2[Ni(P_4Ph_4)(\eta^2\text{-}P_2Ph_2)]$ (**37**)

that nickel(0) facilitates the reduction and nickel(II) the oxidation, as observed previously by us [65], the reaction seems to be catalysed by nickel(0). Nevertheless, when the reaction of $[Na_2(thf)_5(P_4Ph_4)]$ (**22**) or $[K_2(pmdeta)_2(P_4Ph_4)]$ (**26**) was carried out with catalytic amounts (3%) of $[Ni(cod)_2]$ and monitored by $^{31}P\{^1H\}$ NMR only signals of *cyclo*-(P_nPh_n) ($n = 4$ and 5) and $(P_4Ph_4)^{2-}$ were observed in the spectrum, that is, the nickel(0) centres exhibit no catalytic action. Thus, it seems clear that P–P bond cleavage was facilitated by stoichiometric amounts of $[Ni(cod)_2]$, and in the case of $[K_2(pmdeta)_2(P_4Ph_4)]$ (**26**) the reaction stopped at

$[K(pmdeta)]_2[Ni(P_4Ph_4)(\eta^2\text{-}P_2Ph_2)]$ (**37**) because the Ni–K and Ni–P interactions apparently stabilise the complex and prevent further reaction to the corresponding potassium analogue of $[Na(Et_2O)_3][Na_3(Et_2O)_2Ni_3(\mu\text{-}P_2Ph_2)_2(\eta^2\text{-}P_2Ph_2)_3]$ (**36**).

The $^{31}P\{^1H\}$ NMR spectra of **36** (Table 4.1) exhibited very broad signals at room and low temperature (down to −80 °C) which were very similar to those found in its solid-state $^{31}P\{^1H\}$ CP MAS NMR spectrum, suggesting that the solid-state structure of **36** is retained in solution. The molecular structure of **36** determined by X-ray diffraction revealed that this ionic complex consists of a core in which bridging of three nickel(0) atoms by two diphenyldiphosphanediide ligands results in a norbornane-like Ni_3P_4 metallabicyclic framework. Each nickel atom is additionally coordinated in an η^2-fashion by a *trans*-diphenyldiphosphene ligand. Three of the four negative charges of the two dianionic bridging ligands are counterbalanced by three sodium cations which interact with the phosphorus atoms of the diphenyldiphosphanediide ligands as well as the nickel atoms giving rise to a monoanionic $Na_3Ni_3P_{10}$ core (Fig. 4.17; for comparison of some selected structural parameters, see Table 4.2).

On the other hand, the $^{31}P\{^1H\}$ NMR spectrum of **37** consists of a set of three signals corresponding to an AA′BB′XX′ spin system (Table 4.1), which indicates that the dianionic P_4 chain with the expected all-*trans* conformation is retained in solution, as was observed in its molecular structure determined by X-ray diffraction. In the solid state, the nickel atom and the four phosphorus atoms of the chain form a puckered five-membered ring (Table 4.2). Interestingly, the nickel atom has pseudo-octahedral coordination, with the diphosphene ligand (P5 and P6) and the terminal phosphorus atoms of the $(P_4Ph_4)^{2-}$ ligand (P1 and P4) in the equatorial positions, and the potassium atoms (K1 and K2) in the axial positions with short K···Ni distances of 318.5(2) pm for K1 and 310.7(2) pm for K2, which are the shortest distances reported for an Ni···K interaction in a complex (Fig. 4.18).

Based on previous studies of the reactivity of the $(P_4R_4)^{2-}$ ion with group 10 metal salts [65–68] and the wide variety of platinum diphosphene complexes described in the literature [66, 67, 76–78], we expected that the reaction of $Na_2(P_4Mes_4)$ with platinum(II) salts would lead to formation of the corresponding platinum(II) dimesityldiphosphene complexes via reduction of the metal centre and oxidation of the dianion, as was observed for nickel(II) and palladium(II) salts [65]. However, the higher stability of the oxidation state +2 for platinum compared to nickel and palladium resulted in the formation of the corresponding transmetallation product [79], which could not be isolated for nickel and palladium [65].

Thus, the reaction of $[Na_2(thf)_4(P_4Mes_4)]$ (**23**) with one equivalent of $[PtCl_2(cod)]$ or $[PtCl_2(dppe)]$ (dppe = bis(diphenylphosphino)ethane) gave the corresponding platinum(II) tetramesityltetraphosphane-1,4-diide complexes $[Pt(P_4Mes_4)(cod)]$ (**38**) and $[Pt(P_4Mes_4)(dppe)]$ (**39**) (Fig. 4.19). This reaction was the first targeted synthesis of a platinum complex containing a tetramesityltetraphosphane-1,4-diide ligand.

The $^{31}P\{^1H\}$ NMR spectra of **38** and **39** showed higher order AA′XX′ and AA′BCXX′ (Fig. 4.20; Table 4.1) spin systems, respectively, which indicate that the P_4 ligand is retained in solution. In addition, platinum satellites were observed

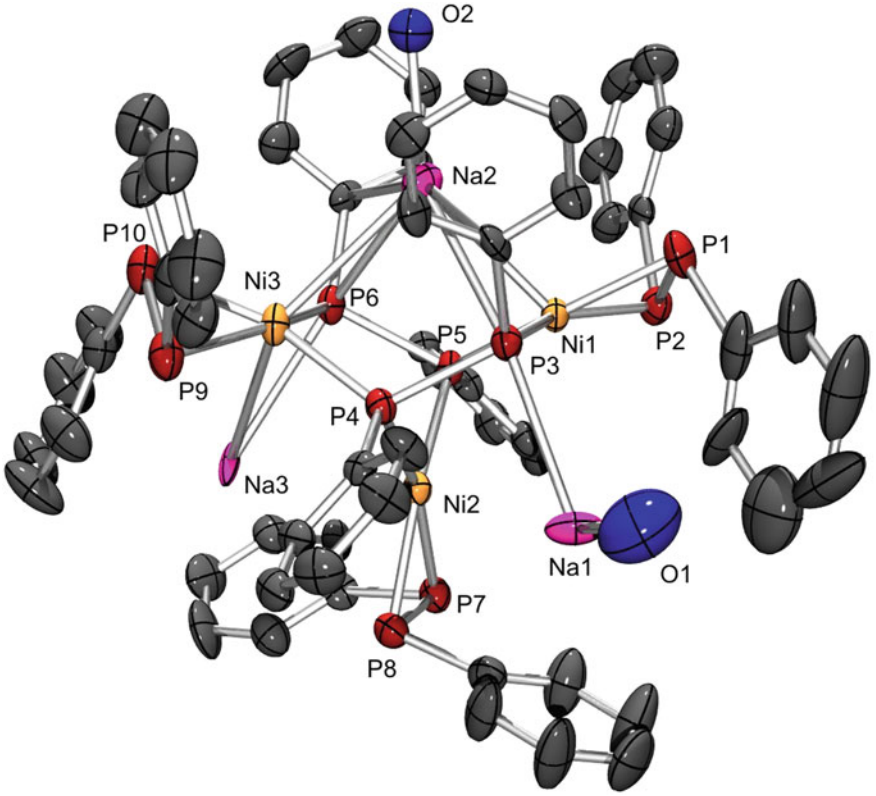


Fig. 4.17 Anionic part of the molecular structure of $[Na(Et_2O)_3][Na_3(Et_2O)_2Ni_3(\mu\text{-}P_2Ph_2)_2(\eta^2\text{-}P_2Ph_2)_3]$ (**36**). Hydrogen atoms and carbon atoms of the coordinated ether molecules have been omitted for clarity

with $^1J(^{31}P–^{195}Pt)$ values of ca. 1146 Hz for **38** and 2261 and 780 Hz for **39** (Table 4.1). In the mass spectrum of **38**, the organyl-free fragment $[PtP_4]^+$ was observed, and hence this complex may be a suitable molecular precursor for the synthesis of binary phosphorus-rich platinum phosphides.

In the molecular structures of **38** and **39** determined by X-ray diffraction the P_4 chain shows a *syn* arrangement with pyramidal geometry of the phosphorus atoms of the ligand, and the five-membered PtP_4 rings are in an envelope conformation (Fig. 4.21). Furthermore, the Pt–P bond lengths in **38** and **39** are close to 233 pm, as expected for platinum(II) phosphanido complexes (for some selected structural parameters of **38** and **39** see Table 4.2) [21].

The Pt–P bonds of these complexes are very stable, as there was no evidence of insertion of CO, CS_2, white phosphorus or ethyl diazoacetate into the Pt–P bonds or reaction with MeI. These reactions led either to formation of *cyclo*-(P_4Mes_4) and *cyclo*-(P_3Mes_3) or to unidentified products with no apparent insertion reaction. In addition, the proposed insertion reaction of **38** and **39** with *tert*-butyl isocyanide and

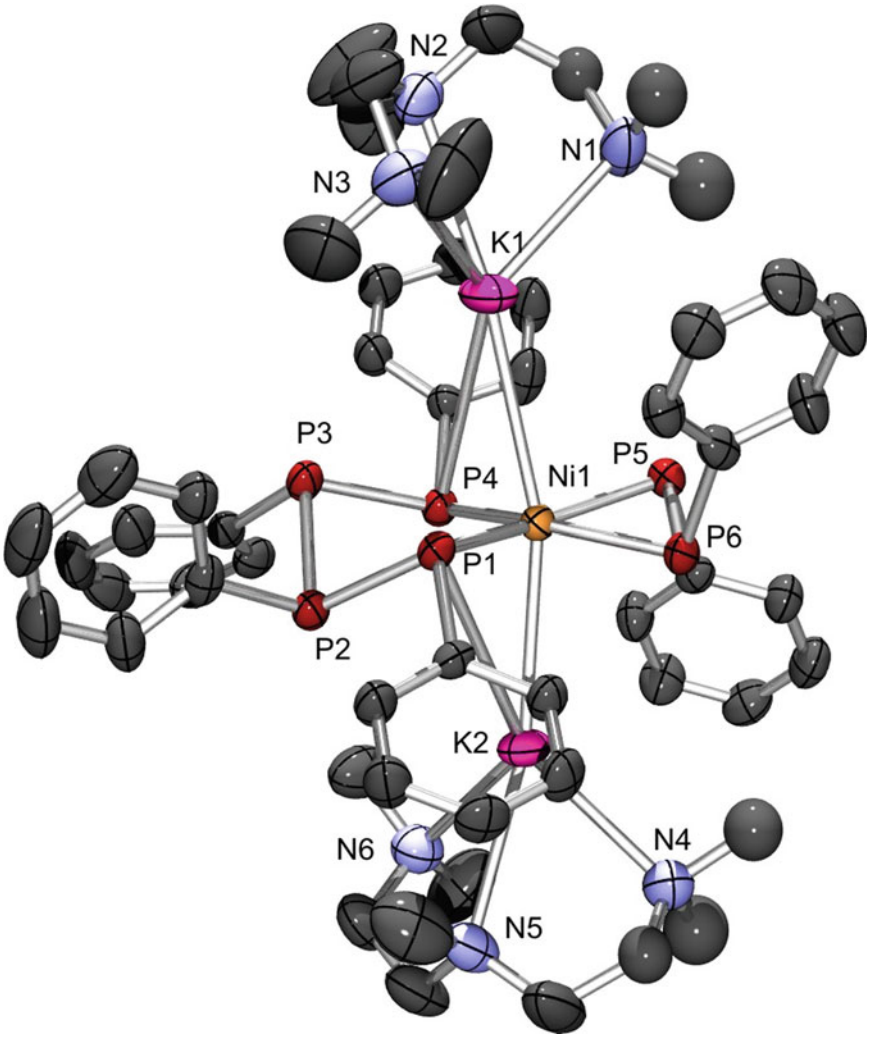


Fig. 4.18 Molecular structure of $[K(pmdeta)]_2[Ni(P_4Ph_4)(\eta^2\text{-}P_2Ph_2)]$ (**37**). Hydrogen atoms are omitted for clarity

cyclohexyl isocyanide led to ligand transfer instead to give $[Pt(P_4Mes_4)(C{\equiv}NBu^t)_2]$ (**40**) and $[Pt(P_4Mes_4)(C{\equiv}NCy)_2]$ (**41**), respectively, even at high temperatures (up to 110 °C) or after prolonged reaction times (2–150 h; Fig. 4.19). In contrast to the expected AA′XX′ spin system (observed for similar metal complexes with a P_4 chain), the $^{31}P\{^1H\}$ NMR spectra of **40** and **41** gave only one multiplet at ca. −40 ppm, which showed no changes with varying temperature (Table 4.1); however, the molecular structure of **40** and **41** determined by X-ray diffraction showed similar structural parameters to those found in **38** and **39** (Table 4.2).

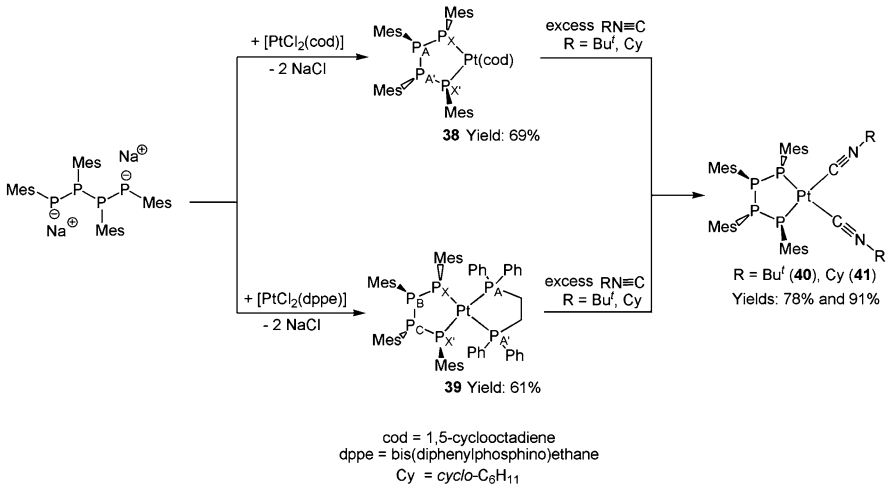


Fig. 4.19 Synthesis of platinum(II) complexes **38**–**41**

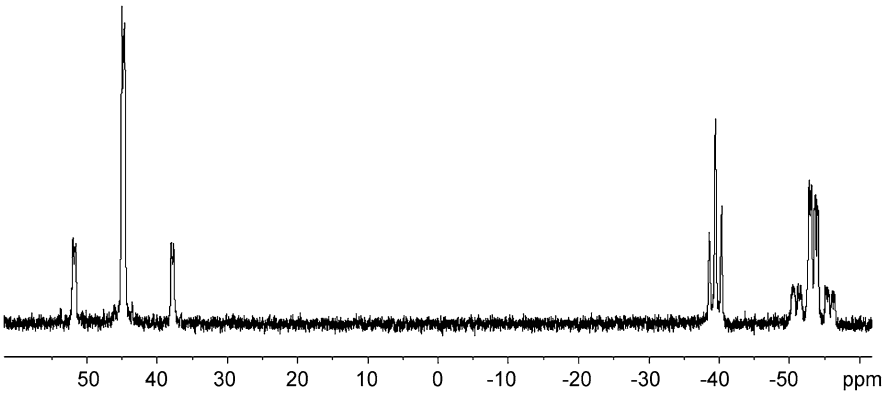


Fig. 4.20 $^{31}P\{^{1}H\}$ NMR spectrum of $[Pt(P_4Mes_4)(dppe)]$ (**39**)

Finally, when we attempted the transmetallation reaction of the sodium salt of $(P_4Ph_4)^{2-}$ with early transition metal halides such as $[Ta(\eta^5\text{-}C_5Me_5)Cl_4]$, we obtained, serendipitously, the complex $[Ta(\eta^5\text{-}C_5Me_5)(Ph)(P_6Ph_5)]$ (**42**) [80], which contains an unprecedented oligophosphanide trianion $(P_6Ph_5)^{3-}$ acting as a terminal phosphanyl phosphinidene ligand (Fig. 4.22).

Formation of this complex may occur via an initial formation of a low-valent tantalum intermediate which oxidatively adds one terminal $P–C_{Ph}$ bond to the metal centre resulting in transfer of the phenyl ligand to the metal and formation of complex **42**. The ^{31}P NMR spectrum of the reaction mixture showed formation of a mixture of cyclooligophosphanes, the phosphinidene-bridged complex $[\{Ta(\eta^5\text{-}C_5Me_5)Cl(\mu\text{-}PPh)\}_2]$ as well as numerous low-intensity multiplets which could not

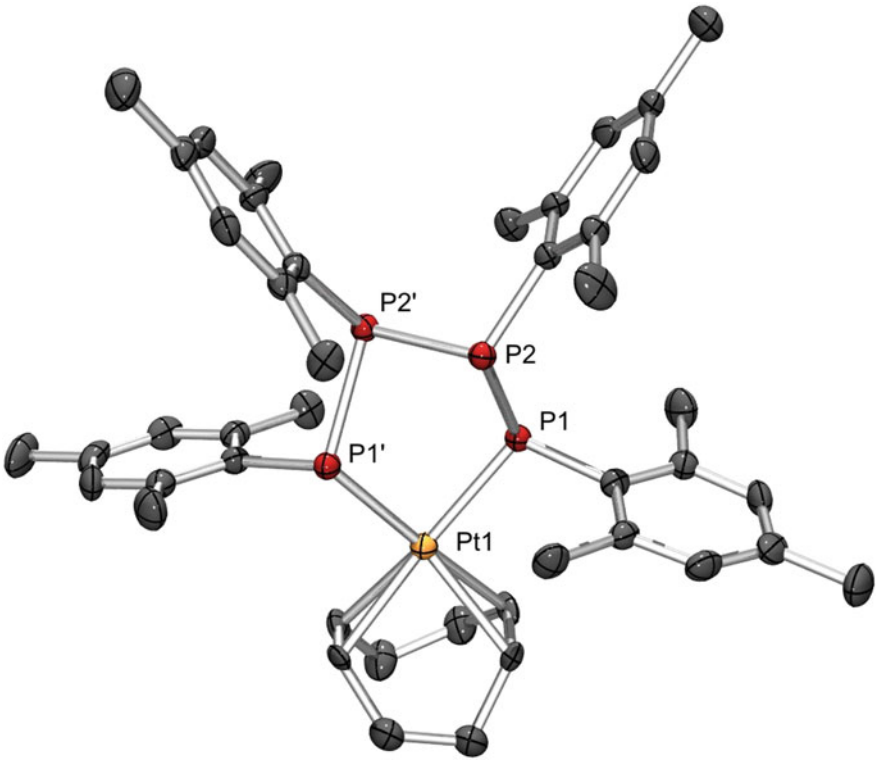


Fig. 4.21 Molecular structure of [Pt(P_4Mes_4)(cod)] (**38**). Hydrogen atoms are omitted for clarity

be assigned. As no further tantalum-containing products other than [Ta(η^5-C_5Me_5)(Ph)(P_6Ph_5)] (**42**) were isolated from the reaction mixture even under different reaction conditions and with other stoichiometric ratios, the reaction mechanism remained totally unclear.

The X-ray crystal structure of **42** revealed a mononuclear complex with a tetradentate trianionic $(P_6Ph_5)^{3-}$ ligand coordinating to the tantalum atom through the two terminal and their adjacent phosphorus atoms of the P_6 chain (P1, P2, P5 and P6; Fig. 4.23). This coordination mode of the trianionic ligand together with an η^5-coordinating pentamethylcyclopentadienyl ligand and an η^1-bound phenyl ligand leads to a highly distorted octahedral complex. Interestingly, the Ta–P bond of the phosphorus atom of the phosphinidene moiety (Ta1–P1 241.6(2) pm) is more than 10 pm shorter than the remaining Ta–P bond lengths, but slightly longer than those reported in bridging tantalum phosphinidene complexes [81, 82] and significantly longer than in terminal phosphinidene complexes [83–85]. In addition, the P1–P2 bond length of 209.6(3) pm between the phosphorus atom of the phosphinidene group and the adjacent one is shorter than those observed for P–P single bonds (Table 4.2), that is, the bonding situation in this complex may be described by a superposition of different mesomeric structures [86–92].

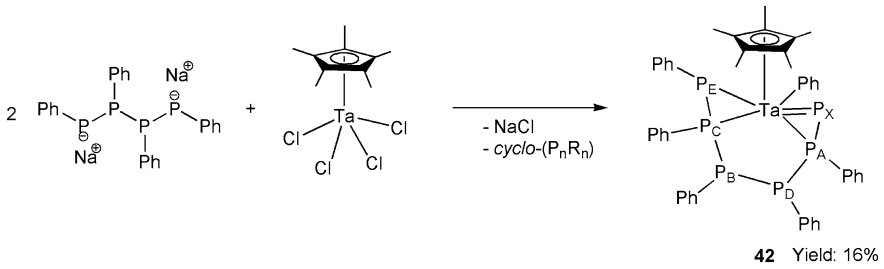


Fig. 4.22 Synthesis of [Ta(η^5-C_5Me_5)(Ph)(P_6Ph_5)] (**42**)

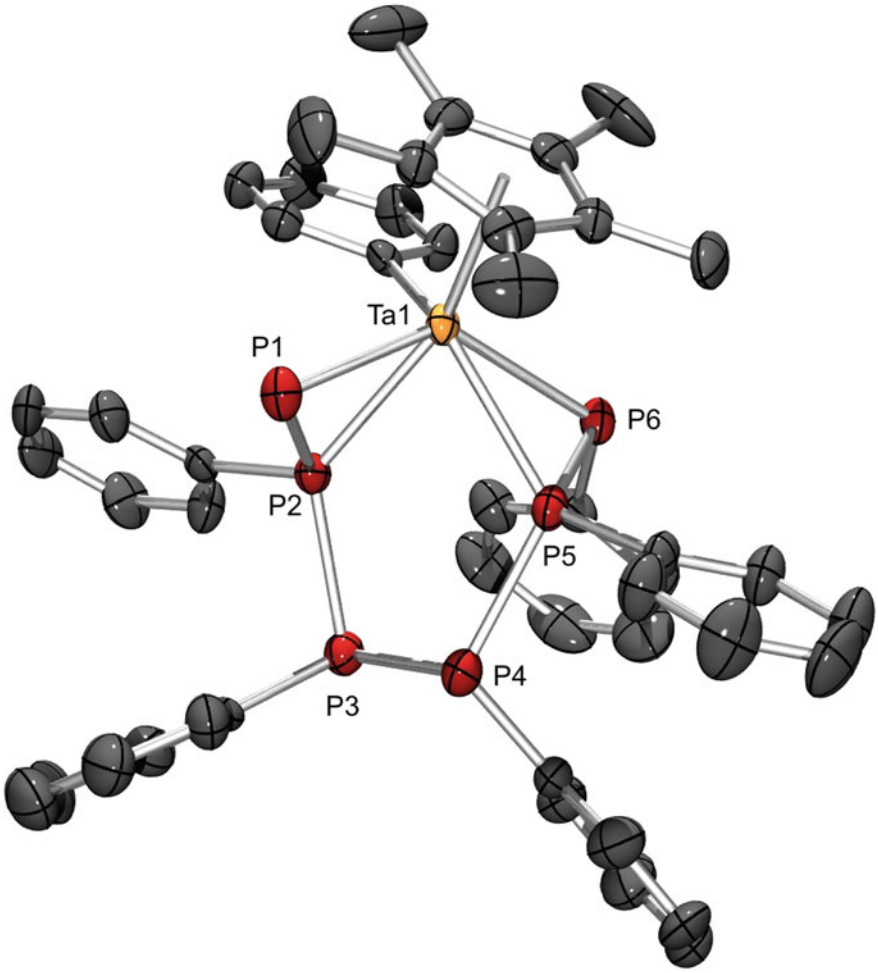


Fig. 4.23 Molecular structure of [Ta(η^5-C_5Me_5)(Ph)(P_6Ph_5)] (**42**). Hydrogen atoms are omitted for clarity

As expected, the $^{31}P\{^{1}H\}$ NMR spectrum of **42** shows a first-order ABCDEX spin system, with the signal of the phosphorus atom of the terminal phosphinidene group shifted to ca. 370 ppm (Table 4.1).

In view of the highly versatile reactivity of the $(P_4R_4)^{2-}$ and $(P_4HR_4)^{-}$ ions and the rareness of investigations on early transition metals, future work should now be centred on the exploration of different synthetic routes for the preparation of early transition metal or rare earth metal oligophosphanides as well as on the thermal decomposition of known complexes in order to find novel synthetic procedures for the preparation of binary metal phosphides.

4.4 Potential Application of Metal Oligophosphanides as Precursors in the Preparation of Metal Phosphides

The ability of phosphorus to exist as isolated anions or larger anionic polyphosphide networks with P–P bonds enables possible formation of transition metal phosphides [14], which are an important class of binary metal/non-metal compounds with a wide variety of structures, compositions and properties. For example, phosphorus-to-metal ratios in these compounds have a wide range, from metal-rich (MP_x, where $x < 1$) to monophosphides (MP) and phosphorus-rich polyphosphides (MP_x, where $x > 1$) [93].

Metal phosphides have been extensively studied for many applications, for example, corrosion-resistant materials [94], catalysts for hydrodesulfurisation and hydrodenitrogenation of petroleum fuels [95–100] and oxygen barriers in capacitors [101]. In addition, applications associated with the magnetic properties of these compounds have been also studied in depth [102–105].

Synthetic methods for the preparation of metal-rich metal phosphides and monophosphides are very different depending on the morphology and the conditions of use of the final products. For example, metal phosphides can be obtained as bulk materials from high-temperature elemental reactions, as films by chemical deposition techniques and as nanoparticles by molecular solvothermal reactions [14, 15, 94, 102–126].

Reports on phosphorus-rich metal phosphides are rare compared to their metal-rich analogues. This may be due to the problems associated with the preparation of these materials, which are caused by the lower thermal stability compared to metal-rich phosphides. The stability problems limit the possibility to make metal-rich phosphides by simply heating a mixture of the elements at elevated temperature [101, 127–129].

Some of the reported phosphorus-rich metal phosphides have been synthesised from the elements (powdered metal and red phosphorus) at elevated temperatures (700–1,200 °C), or at moderate temperatures for extended periods of time in tin fluxes (up to 550 °C, more than 10 days) [110, 127, 130–132]. These species can also be prepared by heating the elements in the presence of a chemical transport agent such as Cl_2 or I_2 in sealed ampoules (between 600 and 800 °C)

[127, 131, 133]. These compounds have been also synthesised by non-conventional methods such as high-energy ball-milling and high-pressure anvil syntheses [134–136]. All of these routes do not control the morphology and size of the obtained products, and most of them require high energy input and long reaction times.

The syntheses of metal phosphides under solvothermal conditions using molecular precursors leads to metal-rich phases, probably due to hydrolysis or oxidation of the phosphorus reagents at elevated temperatures [96, 103, 124, 129]. However, a straightforward, solvent-free, moderate-temperature synthetic method for the production of several phosphorus-rich transition-metal phosphides has been recently developed by Gillan and co-workers [137, 138]. The general synthetic strategy involves direct reaction of anhydrous metal dichloride pellets with molecular P_4 vapour or solid–solid reactions between the metal dichloride and red phosphorus. Both reactions require the evolution of volatile PCl_3 as by-product and give crystalline MP_x ($x \geq 2$) at moderate temperatures of 500–700 °C [139, 140].

Alternative routes that seem feasible are decomposition of the corresponding phosphorus-rich metal oligophosphanide complexes under mild conditions, and reactions of metal salts and neutral phosphorus-rich phosphanes under solvothermal conditions. These studies may lead to the preparation of novel phosphorus-rich metal phosphides whose potential as anode materials for lithium–ion batteries [134–136, 141–146] and thermoelectric materials may be studied [139, 140]. One of the principal processes for the preparations of metal phosphides starting from phosphorus-rich metal oligophosphanide complexes is removal of the R group, which should be possible by thermal decomposition of the compounds, to give organyl-free species such as M_xP_y. These species have already been observed in the mass spectra of several of these complexes.

However, with this synthetic method the control of the morphology of the resulting materials may be difficult and intensive investigations in this area must therefore be carried out.

References

1. Baudler M (1980) Three-membered phosphorus ring compounds. Pure Appl Chem 52:755–769
2. Baudler M (1982) Ketten- und ringförmige Phosphorverbindungen – Analogien zwischen Phosphor- und Kohlenstoffchemie. Angew Chem 94:520–539
3. Baudler M (1982) Chain and ring phosphorus compounds—analogies between phosphorus and carbon chemistry. Angew Chem Int Ed Engl 21:492–512
4. Baudler M (1987) Polyphosphorverbindungen – neue Ergebnisse und Perspektiven. Angew Chem 99:429–451
5. Baudler M (1987) Polyphosphorus compounds—new results and perspectives. Angew Chem Int Ed Engl 26:419–441
6. Baudler M, Glinka K (1993) Monocyclic and polycyclic phosphanes. Chem Rev 93:1623–1667
7. Etkin N, McFermin MC, Stephan DW (1997) Catalytic synthesis of the P_{16} macrocycle: $(C_6H_4P_8)$. J Am Chem Soc 119:2954–2955

8. Moser C, Belaj F, Pietschnig R (2009) Diphospha[2]ferrocenophane and 1,4-dihydrotetraphosphane—stereoselective formation via hydrolytic P–P bond formation. Chem Eur J 15:12589–12591
9. Dillon KB, Mathey F, Nixon JF (1998) Phosphorus the carbon copy: from organophosphorus to phospha-organic chemistry. Wiley, Chichester
10. Luo YR (2007) Comprehensive handbook of chemical bond energies. CRC Press, Boca Raton
11. Gómez-Ruiz S, Hey-Hawkins E (2010) The versatile reactivity of anionic polyphosphorus rings. New J Chem 34:1525–1532
12. Hoffmann R (1982) Brücken zwischen Anorganischer und Organischer Chemie. Angew Chem 94:725–739
13. Hoffmann R (1982) Bridges between Inorganic and Organic Chemistry. Angew Chem Int Ed Engl 21:711–724
14. von Schnering H-G, Hönle W (1988) Bridging chasms with polyphosphides. Chem Rev 88:243–273
15. Brook SL, Perera SC, Stamm KL (2004) Chemical routes for production of transition-metal phosphides on the nanoscale: implications for advanced magnetic and catalytic materials. Chem Eur J 10:3364–3371
16. West BO (1977) In: Rheingold AL (ed) Homoatomic rings, chains and macromolecules of main-group elements. Elsevier, Amsterdam
17. Ahlrichs R, Fenske D, Oesen H, Schneider U (1992) Synthese und Struktur von $[Ni(PtBu)_6]$ und $[Ni_5(PtBu)_6(CO)_5]$ sowie Rechnungen zur elektronischen Struktur von $[Ni(PtBu)_6]$ und $(PR)_6$, R = *t*Bu, Me. Angew Chem 104:312–314
18. Ahlrichs R, Fenske D, Oesen H, Schneider U (1992) Synthesis and Structure of $[Ni(PtBu_6)]$ and $[Ni_5(PtBu)_6(CO)_5]$ and Calculations on the Electronic Structure of $[Ni(PtBu)_6]$ and $(PR)_6$, R = *t*Bu, Me. Angew Chem Int Ed Engl 31:323–326
19. Queisser J, Fenske D (1994) Neue Phosphor-verbrückte Übergangsmetallcarbonyl-Komplexe Die Kristallstrukturen von $[Re_2(CO)_7(P^tBu)_3]$, $[Co_4(CO)_{10}(P^tBu)_2]$, $[Ir_4(CO)_6(P^tBu)_6]$ und $[Ni_4(CO)_{10}(P^iPr)_6]$. Z Anorg Allg Chem 620:58–66
20. Queisser J, Oesen H, Fenske D, Lehari B (1994) Synthese und Struktur der Phosphor-verbrückten Übergangsmetallkomplexe $[Fe_2(CO)_6(PR)_6]$ (R = ^{t}Bu, ^{i}Pr), $[Fe_2(CO)_4(P^iPr)_6]$, $[Fe_2(CO)_3Cl_2(P^tBu)_5]$, $[Co_4(CO)_{10}(P^iPr)_3]$, $[Ni_5(CO)_{10}(P^iPr)_6]$ und $[Ir_4(C_8H_{12})_4Cl_2(PPh)_4]$. Z Anorg Allg Chem 620:1821–1831
21. Fenske D, Queisser J, Schottmüller H (1998) Neue Untersuchungen zum Reaktionsverhalten von Triorganylcyclotriphosphanen. Die Kristallstrukturen von $[(PPh_3)_2Pt(P^tBu)_3]$, $[(PPh_3)_2Pd(P^tBu)_2]$, $[(CO)_4Cr\{(P^iPr)_3\}_2]$, $[RhCl(PPh_3)(P^tBu)_3]$, $[(NiCO)_6(\mu_2\text{-}CO)_3\{(P^tBu)_2\}_2]$ und $[(CpFeCO)_2(\mu\text{-}CO)(\mu\text{-}PH^tBu)]^+$ $[FeCl_3(thf)]^-$. Z Anorg Allg Chem 624:443–451
22. Fenske D, Queisser J, Schottmüller H (1996) Neue Phosphor-verbrückte Übergangsmetall-Komplexe Die Kristallstrukturen von $[Co_4(CO)_{10}(P^iPr)_2]$, $[Fe_3(CO)_9(P^tBu)(PPh)]$, $[Cp_3Fe_3(CO)_2(PP^tBu)(P^tBu)]$, $[(NiPPh_3)_2(P^iPr)_6]$, $[(NiPPh_3)Ni\{(P^tBu)_3\}_2]$ und $[Ni_8(P^tBu)_6(PPh_3)_2]$. Z Anorg Allg Chem 622:1731–1739
23. Üffing C, von Hänisch C, Schnöckel H (2000) Der erste viergliedrige Al/P-Ring, der von drei Phosphoratomen und einem Aluminiumatom gebildet wird: Synthese und Kristallstruktur von $[Cp^*Al(PtBu)_3]$. Z Anorg Allg Chem 626:1557–1560
24. Uhl W, Benter M (2000) Formation of a gallium triphosphorus heterocycle by reaction of the alkylgallium(I) compound $Ga_4[C(SiMe_3)_3]_4$ with tri(*tert*-butyl)cyclotriphosphane. J Chem Soc Dalton Trans 3133–3135
25. Geier SJ, Stephan DW (2008) Activation of P_5R_5 (R = Ph, Et) by a Rh-β-diketiminate complex. Chem Commun 2779–2781
26. Geier SJ, Stephan DW (2008) Rh-catalyzed P–P bond activation. Chem Commun 99–101
27. Bai G, Wei P, Das AK, Stephan DW (2006) P–H and P–P bond activation by Ni(I) and Fe(I) β-diketiminato-complexes. Dalton Trans 1141–1146

28. Bartsch R, Hietkamp S, Morton S, Stelzer O (1981) Reaktionen koordinierter Liganden: X. Reaktivität zweikerniger Eisencarbonylkomplexe mit sekundären Phosphidobrücken μ-RPH. J Organomet Chem 222:263–273
29. Weber L, Bungardt D, Reizig K, Boese R, Benn R (1987) Übergangsmetall-substituierte Diphosphene, IV. Cyclotriphosphane und Cyclotetraphosphane mit Eisen- und Rutheniumkomplexsubstituenten. Chem Ber 120:451–456
30. Weber L, Sonnenberg U (1991) Übergangsmetall-substituierte Diphosphene, XXIII. Studien zur Synthese und Reaktivität von Dihalogenphosphido-Komplexen des Eisens und Rutheniums. Chem Ber 124:725–728
31. Felsberg R, Blaurock S, Junk P, Kirmse R, Voigt A, Hey-Hawkins E (2004) Organometallic molybdenum(V) complexes with primary phosphine ligands. Syntheses, spectroscopic properties and molecular structures of $[Cp^{\circ}MoCl_4(PH_2R)]$ (R = ^{t}Bu, 1-Ad, Cy, Ph, 2,4,6-$Me_3C_6H_2$, 2,4,6-$Pr^i_3C_6H_2$, $Cp^{\circ} = C_5EtMe_4$). Z Anorg Allg Chem 630:806–816
32. Hey E, Bott SG, Atwood JL (1988) Synthese von Bis(η^5-cyclopentadienyl)(1,2,3-triphenyltriphosphan-1,3-diyl)zirconium(IV) und -hafnium(IV), (M = Zr, Hf) und Struktur des Hafnocenderivates. Chem Ber 121:561–563
33. Hey E (1988) Neuer Syntheseweg und Molekülstruktur von (1,2,3-Triphenyltriphosphan-1,3-diyl)zirkonocen(IV), [(η^5-$C_5H_5)_2$Zr(PPh-PPh-PPh)]. Z Naturforsch 43B:1271–1273
34. Beswick MA, Choi N, Hopkins AD, McPartlin M, Mosquera MEG, Raithby PR, Rothenberger A, Stalke D, Wheatley AJ, Wright DS (1998) Direct synthesis of heterocyclic $[(RP)_nE]^-$ anions using $[E(NMe_2)_3]$ (E = Sb, As); implications to the mechanism of formation of Zintl compounds. Chem Commun 2485–2486
35. Issleib K, Krech K (1965) Alkali-Phosphorverbindungen und ihr reaktives Verhalten, XXXVII: Spaltung des Tetraäthyl- und Tetracyclohexyl-cyclotetraphosphins mit Alkalimetallen. Chem Ber 98:2545–2550
36. Fluck E, Issleib K (1965) Untersuchungen der kernmagnetischen Resonanz von Phosphorverbindungen. X. ^{31}P-Resonanzspektren von Alkalimetallphosphiden. Z Anorg Allg Chem 339:274–280
37. Issleib K, Krech K (1966) Alkali-Phosphorverbindungen und ihr reaktives Verhalten, XXXIX. Spaltung von "Phosphobenzol" mit Alkalimetallen. Chem Ber 99:1310–1315
38. Issleib K, Hoffmann M (1966) Alkali-Phosphorverbindungen und ihr reaktives Verhalten, XLI. Tetra-tert.-butyl-biphosphin und Tetra-tert.-butyl-cyclotetra-phosphin. Chem Ber 99:1320–1324
39. Issleib K, Rockstroh Ch, Duchek I, Fluck E (1968) Alkali-Phosphorverbindungen und ihr reaktives Verhalten. Alkalimetall- bzw. Magnesium-tetra- und -pentaalkylphosphine. Z Anorg Allg Chem 360:77–87
40. Issleib K, Krech K (1969) Alkali-phosphorverbindungen und ihr reaktives Verhalten. LX. Zur Spaltung der P–P-Bindung mit Lithium-phosphides $LiPR_2$ bzw. Li_2PR. J Prakt Chem 311:463–471
41. Riegel B, Pfitzner A, Heckmann G, Fluck E, Binder H (1994) Phosphorus-boron and phosphorus-silicon ring systems functionalization of phosphorus ring systems. Phosphorus Sulfur Silicon 93–94:173–176
42. Riegel B, Pfitzner A, Heckmann G, Binder H, Fluck E (1994) Synthese und Strukturbestimmung von $(i\text{-}Pr)_2NB(t\text{-}BuP)_3$ und $(i\text{-}Pr)_2NB(t\text{-}BuP)_4$. Z Anorg Allg Chem 620:8–15
43. Riegel B, Pfitzner A, Heckmann G, Binder H, Fluck E (1995) Synthese der Silatetraphospholane $(t\text{BuP})_4SiMe_2$, $(t\text{BuP})_4SiCl_2$ und $(t\text{BuP})_4Si(Cl)SiCl_3$ Molekül- und Kristallstruktur von $(t\text{BuP})_4SiCl_2$. Z Anorg Allg Chem 621:1989–1994
44. Bongert D, Heckmann G, Schwarz W, Hausen HD, Binder H (1995) Synthese und Strukturbestimmung von $(t\text{BuP})_4Sn(CH_3)_2$ und $(CH_3)_2Sn[(t\text{Bu})P\text{–}P(t\text{Bu})]_2Sn(CH_3)_2$. Z Anorg Allg Chem 621:1358–1364
45. Bongert D, Heckmann G, Schwarz W, Hausen HD, Binder H (1996) Synthese der Stannatetraphospholane $(t\text{BuP})_4SnR_2$ (R = tBu, nBu, C_6H_5) und $(t\text{BuP})_4Sn(Cl)n\text{Bu}$ Molekül- und Kristallstruktur von $(t\text{BuP})_4Sn(t\text{Bu})_2$. Z Anorg Allg Chem 622:1167–1672

46. Bongert D, Heckmann G, Hausen HD, Schwarz W, Binder H (1996) Synthese und Struktur von Hexa-t-butyl-1,4-dichloro-1,4-distanna-2,3,5,6,7,8-hexaphosphabicyclo[2.2.2]octan—Eine neue Käfigverbindung mit dem $Sn(P_2)_3Sn$-Gerüst. Z Anorg Allg Chem 622: 1793–1798
47. Binder H, Schuster B, Schwarz W, Klinkhammer KW (1999) 1,1-Diethyl-1-germa-2,3,4,5-tetra-*tert*-butyl-2,3,4,5-tetraphospholan $(C_2H_5)_2Ge(t\text{BuP})_4$, Molekül- und Kristallstruktur. Z Anorg Allg Chem 625:699–701
48. Köpf H, Voigtländer R (1981) Anionoide Polyphosphane als Chelatliganden: Triphosphanato-P^1,P^3-Komplexe des Titanocen-, Zirconocen- und Hafnocen-Systems. Chem Ber 114: 2731–2743
49. Jones RA, Seeberger MH, Whittlesey BR (1985) Reactions of coordinated ligands: coupling of two diphosphenes (P=P) at a metal center to give a coordinated phosphametallo cyclopentane. Synthesis and X-ray structure of (t-BuPP-t-Bu)Ni(t-BuP-t-BuP-t-BuP-t-BuP): a square-planar Ni(II) geometry imparted by sterically demanding ligands. J Am Chem Soc 107:6424–6426
50. Baudler M, Koch D (1976) Beiträge zur Chemie des Phosphors. 64 [1]. Zur quasicyclischen Konformation der Organylphosphide $M_2(PR)_n'$ [M = K, Na]. Z Anorg Allg Chem 425:227–235
51. Baudler M, Koch D, Tolls E, Diederich KM, Kloth B (1976) Beiträge zur Chemie des Phosphors. 61. Zur Struktur der Salze $M_2(PC_6H_5)_3$, [M = K, Na]. Z Anorg Allg Chem 420:146–154
52. Hoffmann PR, Caulton KG (1975) Structure and dynamics of catenated phosphorus(III) dianions. J Am Chem Soc 97:6370–6374
53. Geier J, Rüegger H, Wörle M, Grützmacher H (2003) Synthese und Struktur von Natriumoligophosphandiiden im System $PhPCl_2$/Na. Angew Chem 115:4081–4085
54. Geier J, Rüegger H, Wörle M, Grützmacher H (2003) Sodium oligophosphanediide ions in the $PhPCl_2$/Na system: syntheses and structural characterization. Angew Chem Int Ed 42:3951–3954
55. Geier J, Harmer J, Grützmacher H (2004) "Naked" phosphanediide chains and their fragmentation into diphosphene radical anions. Angew Chem 116:4185–4189
56. Geier J, Harmer J, Grützmacher H (2004) "Naked" phosphanediide chains and their fragmentation into diphosphene radical anions. Angew Chem Int Ed 43:4093–4097
57. Schisler A (2003) Dissertation, Universität Leipzig
58. Wolf R (2005) Dissertation, Universität Leipzig
59. Wolf R, Schisler A, Lönnecke P, Jones C, Hey-Hawkins E (2004) Syntheses and molecular structures of novel alkali metal tetraorganylcyclopentaphosphanides and tetraorganyltetraphosphane-1,4-diides. Eur J Inorg Chem 3277–3286
60. Wolf R, Hey-Hawkins E (2006) Oligophosphanid-Anionen: Synthesen und Molekülstrukturen von $[K_2(PMDETA)_2(P_4Ph_4)]$, $[K_2(PMDETA)(P_4t\text{Bu}_4)]_2$ und $[K(PMDETA)(THF)\{cyclo\text{-}(P_5t\text{Bu}_4)\}]$ (PMDETA = $NMe(CH_2CH_2NMe_2)_2$). Z Anorg Allg Chem 632:727–734
61. Wolf R, Hey-Hawkins E (2005) Synthese und Molekülstruktur der Cu_4P_8-Käfigverbindung $[Cu_4(P_4Ph_4)_2(PCyp_3)_3]$. Angew Chem 117:6398–6401
62. Wolf R, Hey-Hawkins E (2005) Synthesis and molecular structure of the Cu_4P_8 cage compound $[Cu_4(P_4Ph_4)_2(PCyp_3)_3]$. Angew Chem Int Ed 44:6241–6244
63. Wolf R, Gómez-Ruiz S, Böhlmann W, Reinhold J, Hey-Hawkins E (2006) The (P_4HMes_4)-anion: lability, fluxionality, and structural ambiguity (Mes = 2,4,6-$Me_3C_6H_2$). Inorg Chem 45:9107–9113
64. Gómez-Ruiz S, Wolf R, Hey-Hawkins E (2008) Different transmetallation behaviour of $[M(P_4HR_4)]$ salts toward rhodium(I) and copper(I) (M = Na, K; R = Ph, Mes; Mes = 2,4,6-$Me_3C_6H_2$). Dalton Trans 1982–1988
65. Gómez-Ruiz S, Hey-Hawkins E (2007) Oxidative cleavage of tetraaryltetraphosphane-1,4-diides by nickel(II) and palladium(II): formation of unusual Ni^0 and Pd^0 diaryldiphosphene complexes. Dalton Trans 5678–5683

66. Chatt J, Hitchcock PB, Pidcock A, Warrens CP, Dixon KR (1982) Synthesis and ^{31}P n.m.r. spectroscopy of platinum and palladium complexes containing side-bonded diphenyldi phosphene. The X-ray crystal and molecular structure of [Pd(PhP = PPh){bis(diphenyl-phosphino)ethane}]. J Chem Soc Chem Commun 932–933
67. Chatt J, Hitchcock PB, Pidcock A, Warrens CP, Dixon KR (1984) The nature of the co-ordinate link. Part 11. Synthesis and phosphorus-31 nuclear magnetic resonance spectroscopy of platinum and palladium complexes containing side-bonded (*E*)-diphenyldiphosphene. *X*-Ray crystal and molecular structures of [Pd{(*E*)-PhP = PPh}($Ph_2PCH_2CH_2PPh_2$)] and [Pd{[(*E*)-PhP = PPh][$W(CO)_5$]$_2$}($Ph_2PCH_2CH_2PPh_2$)]. J Chem Soc Dalton Trans 2237–2244
68. Gómez-Ruiz S, Zahn S, Kirchner B, Böhlmann W, Hey-Hawkins E (2008) P–P bond cleavage of tetraphenyltetraphosphane-1,4-diide facilitated by Nickel(0). Chem Eur J 14:8980–8985
69. Weng Z, Teo S, Hor TS (2006) Stabilization of nickel(0) by hemilabile P,N-ferrocene ligands and their ethylene oligomerization activities. Organometallics 25:4878–4882
70. Carlini C, Marchionna M, Galletti AMR, Sbrana G (2001) Olefin oligomerization by novel catalysts prepared by oxidative addition of carboxylic acids to nickel(0) precursors and modified by phosphine ancillary ligands and organoaluminum compounds. J Mol Catal A 169:79–88
71. Eisch JJ, Ma X, Han KI, Gitua JN, Kruger C (2001) Mechanistic comparison of the nickel(0)-catalyzed homo-oligomerization and co-oligomerization of alkynes and nitriles. Eur J Inorg Chem 77–88
72. Cermak J, Soukupova L, Chvalovsky V (1993) Propadiene oligomerization catalysed by nickel(0) phosphine complexes immobilized on phosphinated poly(styrene-divinylbenzene) support. J Mol Catal 80:181–188
73. Sun W-H, Zhang D, Zhang S, Jie S, Hou J (2006) Ethylene polymerization promoted by nickel complexes. Kinet Catal 47:278–283
74. Speiser F, Braunstein P, Saussine L (2005) Catalytic ethylene dimerization and oligomerization: recent developments with nickel complexes containing P,N-chelating ligands. Acc Chem Res 38:784–793
75. Zhang Z (2005) Nickel(0) catalysts in organic synthesis. Synlett 877–878
76. Bartsch R, Carmichael D, Hitchcock PB, Meidine MF, Nixon JF, Sillet GJD (1988) First examples of η^1-ligated 1,2,4-triphosphacyclopentadienyl ring systems. Synthesis and fluxional behaviour of *trans*-[$MCl(C_2R_2P_3)(PEt_3)_2$], (R = ^{t}Bu, adamantyl), (M = Pd, Pt); crystal and molecular structures of *trans*-[$PtX(C_2^tBu_2P_3)(PR_3)_2$], (X = Cl, R = Et; X = I, R = Ph). J Chem Soc Chem Commun 1615–1617
77. Philips IG, Ball RG, Cavell RG (1992) Reactions of perfluoromethyl-substituted cyclopolyphosphines with zerovalent group 10 metal complexes. Crystal and molecular structure of a palladium complex with a coordinated diphosphene, [Pd(η^2-$CF_3P{=}PCF_3$)(PPh_3)$_2$]. Inorg Chem 31:1633–1641
78. Nixon JF, Sillet GJD (1993) ^{31}P and ^{195}Pt NMR studies on fluxional η^1-ligated 1,2,4-triphosphacyclopentadienyl palladium(II) and platinum(II) complexes. J Organomet Chem 461:237–245
79. Gómez-Ruiz S, Gallego B, Hey-Hawkins E (2009) Platinum(II) tetramesityltetraphosphane-1,4-diides. Dalton Trans 2915–2920
80. Wolf R, Hey-Hawkins E (2006) Synthesis and molecular structure of [Cp*Ta(Ph)(P_6Ph_5)]: a terminal phosphinidene complex of the $(P_6Ph_5)^{3-}$ ligand (Cp* = C_5Me_5). Eur J Inorg Chem 1348–1351
81. Blaurock S, Hey-Hawkins E (2002) Syntheses, crystal structures and reactivity of organometallic tantalum(IV) phosphinidene complexes: *trans*-[{Cp*TaCl(μ-PR)}$_2$] (Cp* = C_5Me_5, R = Cy, *t*Bu, Ph), *cis*- and *trans*-[{Cp*TaCl(μ-PMes)}$_2$] (Mes = 2,4,6-$Me_3C_6H_2$) and *cis*-[{Cp′TaCl(μ-PMes)}$_2$] (Cp′ = C_5H_4Me). Eur J Inorg Chem 2975–2984
82. Hadi GAA, Fromm K, Blaurock S, Jelonek S, Hey-Hawkins E (1997) Organometallic tantalum complexes with phosphine, phosphanido and phosphinidene ligands. Syntheses

and crystal structures of $[Cp'TaCl_4\{PH_2(2,4,6\text{-}Pr^i_3C_6H_2)\}]$, $[Cp'Ta(\mu\text{-}PPh_2)(PPh_2)]_2{\cdot}C_7H_8$ and $[Cp'TaCl\{\mu\text{-}P(2,4,6\text{-}Pr^i_3C_6H_2)\}]_2{\cdot}C_7H_8$($Cp' = C_5H_4Me$). Polyhedron 16:721–731
83. Cummins CC, Schrock RR, Davis WM (1993) Phosphinidentantal(v)-Komplexe des Typs [(N_3N)TaPR] als Phospha-Wittig-Reagentien (R = Ph, Cy, *t*Bu; $N_3N = (Me_3SiNCH_2CH_2)_3N$). Angew Chem 105:758–761
84. Cummins CC, Schrock RR, Davis WM (1993) Phosphinidenetantalum(V) complexes of the type [(N_3N)Ta=PR] as phospha-Wittig reagents. Angew Chem Int Ed Engl 32:756–759
85. Bonanno JB, Wolczanski PT, Lobkovsky EB (1994) Arsinidene, phosphinidene, and imide formation via 1,2-H_2-elimination from $(silox)_3HTaEHPh$ (E = N, P, As): structures of $(silox)_3Ta{=}EPh$ (E = P, As). J Am Chem Soc 116:11159–11160
86. Olkowska-Oetzel J, Pikies J (2003) Chemistry of the phosphinophosphinidene $^t Bu_2P{-}P$, a novel π-electron ligand. Appl Organomet Chem 17:28–35
87. Krautscheid H, Matern E, Kovacs I, Fritz G, Pikies J (1997) Komplexchemie P-reicher Phosphane und Silylphosphane. XIV. Phosphinophosphiniden $^t Bu_2P{-}P$ als Ligand in den Pt-Komplexen $[\{\eta^2\text{-}^tBu_2P{-}P\}Pt(PPh_3)_2]$ und $[\{\eta^2\text{-}^tBu_2P{-}P\}Pt(PEtPh_2)_2]$. Z Anorg Allg Chem 623:1917–1924
88. Matern E, Pikies J, Fritz G (2000) Komplexchemie P-reicher Phosphane und Silylphosphane. XXI Zum Einfluß der PR_3-Liganden auf Bildung und Eigenschaften der Phosphinophosphiniden-Komplexe $[\{\eta^2\text{-}^tBu_2P{-}P\}Pt(PR_3)_2]$ und $[\{\eta^2\text{-}tBu_2P^1{-}P^2\}Pt(P^3R_3)(P^4R'_3)]$. Z Anorg Allg Chem 626:2136–2142
89. Figueroa JS, Cummins CC (2004) Diorganophosphanylphosphinidenes as complexed ligands: synthesis via an anionic terminal phosphide of niobium. Angew Chem 116: 1002–1006
90. Figueroa JS, Cummins CC (2004) Diorganophosphanylphosphinidenes as complexed ligands: synthesis via an anionic terminal phosphide of niobium. Angew Chem Int Ed 43:984–988
91. Cummins CC (2006) Anionische Übergangsmetallkomplexe mit terminalen Carbid-, Nitrid- und Phosphidliganden als Synthesebausteine für niederkoordinierte Phosphorverbindungen. Angew Chem 118:876–884
92. Cummins CC (2006) Terminal, anionic carbide, nitride, and phosphide transition-metal complexes as synthetic entries to low-coordinate phosphorus derivatives. Angew Chem Int Ed 45:862–870
93. Corbridge DEC (1990) Phosphorus: an outline of its chemistry, biochemistry and technology, 4th edn. Elsevier, New York
94. Liu J, Chen X, Shao M, An C, Yu W, Qian Y (2003) Surfactant-aided solvothermal synthesis of dinickel phosphide nanocrystallites using red phosphorus as starting materials. J Cryst Growth 252:297–301
95. Abu II, Smith KJ (2007) HDN and HDS of model compounds and light gas oil derived from Athabasca bitumen using supported metal phosphide catalysts. Appl Catal A 328:58–67
96. Senevirathne K, Burns AW, Bussell ME, Brock SL (2007) Synthesis and characterization of discrete nickel phosphide nanoparticles: effect of surface ligation chemistry on catalytic hydrodesulfurization of thiophene. Adv Funct Mater 17:3933–3939
97. Shu Y, Oyama ST (2005) Synthesis, characterization, and hydrotreating activity of carbon-supported transition metal phosphides. Carbon 43:1517–1532
98. Prins R, Pirngruber G, Weber T (2001) Metal phosphides and zeolite-like mesoporous materials as catalysts. Chimia 55:791–795
99. Zuzaniuk V, Prins R (2003) Synthesis and characterization of silica-supported transition-metal phosphides as HDN catalysts. J Catal 219:85–96
100. Rodriguez JA, Kim J-Y, Hanson JC, Sawhill SJ, Bussell ME (2003) Physical and chemical properties of MoP, Ni_2P, and MoNiP hydrodesulfurization catalysts: time-resolved X-ray diffraction, density functional, and hydrodesulfurization activity studies. J Phys Chem B 107:6276–6285
101. Stinner C, Prins R, Weber T (2001) Binary and ternary transition-metal phosphides as HDN catalysts. J Catal 202:187–194

102. Chiriac H, Moga A-E, Urse M, Paduraru I, Lupu N (2004) Preparation and magnetic properties of amorphous NiP and CoP nanowire arrays. J Magn Magn Mater 272–276:1678–1680
103. Park J, Koo B, Yoon KY, Hwang Y, Kang M, Park JG, Hyeon T (2005) Generalized synthesis of metal phosphide nanorods via thermal decomposition of continuously delivered metal–phosphine complexes using a syringe pump. J Am Chem Soc 127:8433–8440
104. Boyanov S, Bernardi J, Gillot F, Dupont L, Womes M, Tarascon JM, Monconduit L, Doublet ML (2006) FeP: another attractive anode for the Li-ion battery enlisting a reversible two-step insertion/conversion process. Chem Mater 18:3531–3538
105. Gu Z, Parans Paranthaman M, Pan Z (2009) Vapor-phase synthesis of gallium phosphide nanowires. Cryst Growth Des 9:525–527
106. Xie Y, Su HL, Qian XF, Liu XM, Qian YT (2000) A mild one-step solvothermal route to metal phosphides (metal = Co, Ni, Cu). J Solid State Chem 149:88–91
107. Muller TKT, Labardi M, LuxSteiner M, Marti O, Mlynek J, Krausch G (1996) Scanning force and friction microscopy at highly oriented polycrystalline graphite and CuP_2(100) surfaces in ultrahigh vacuum. J Vac Sci Technol B 14:1296–1301
108. Blackman CS, Carmalt CJ, O'Neill SA, Parkin IP, Apostolico L, Molloy KC (2004) Atmospheric-pressure chemical vapor deposition of group IVb metal phosphide thin films from tetrakisdimethylamidometal complexes and cyclohexylphosphine. Chem Mater 16:1120–1125
109. Blackman CS, Carmalt CJ, O'Neill SA, Parkin IP, Molloy KC, Apostolico L (2003) Chemical vapour deposition of group Vb metal phosphide thin films. J Mater Chem 13:1930–1935
110. Kanatzidis MG, Pöttgen R, Jeitschko W (2005) Metallische Schmelzen – Reaktionsmedien zur Präparation intermetallischer Verbindungen. Angew Chem 117:7156–7184
111. Kanatzidis MG, Pöttgen R, Jeitschko W (2005) The metal flux: a preparative tool for the exploration of intermetallic compounds. Angew Chem Int Ed 44:6996–7023
112. Kaner R, Castro CA, Gruska RP, Wold A (1977) Preparation and characterization of the platinum metal phosphides RuP_2 and IrP_2. Mater Res Bull 12:1143–1147
113. Chen L, Luo T, Huang M, Gu Y, Shi L, Qian Y (2004) A mild reduction–phosphidation approach to nanocrystalline GaP. Solid State Commun 132:667–671
114. Kim YK, Cho YW (2005) Synthesis of transition metal pnictide nanocrystalline powders by mechanochemical reaction. J Alloys Compd 393:211–218
115. Hou H, Yang Q, Tan C, Ji G, Gu B, Xie Y (2004) One-pot solution-phase synthesis of paramagnetic Co_2P nanorods. Chem Lett 33:1272–1273
116. Henkes AE, Vasquez Y, Schaak RE (2007) Converting metals into phosphides: a general strategy for the synthesis of metal phosphide nanocrystals. J Am Chem Soc 129:1896–1897
117. Kleinke H, Franzen HF (1996) Das binäre Phosphid Hf_7P_4 – ein unerwartetes Syntheseprodukt. Angew Chem 108:2062–2064
118. Kleinke H, Franzen HF (1996) Hf_7P_4: a new binary phosphide synthesized by a surprising route. Angew Chem Int Ed 35:1934–1936
119. Kher SS, Wells RL (1994) A straightforward, new method for the synthesis of nanocrystalline GaAs and GaP. Chem Mater 6:2056–2062
120. Trentler TJ, Hickman KM, Goel SC, Viano AM, Gibbons PC, Buhro WE (1995) Solution–liquid–solid growth of crystalline III–V semiconductors: an analogy to vapor–liquid–solid growth. Science 270:1791–1794
121. Hector AL, Parkin IP (1994) Self-propagating routes to transition-metal phosphides. J Mater Chem 4:279–283
122. Treece RE, Conklin JA, Kaner RB (1994) Metathetical synthesis of binary and ternary antiferromagnetic gadolinium pnictides (P, As, and Sb). Inorg Chem 33:5701–5707
123. Carmalt CJ, Morrison DE, Parkin IP (2000) Liquid-mediated metathetical synthesis of binary and ternary transition-metal pnictides. Polyhedron 19:829–833

124. Lukehart CM, Milne SB, Stock SR (1998) Formation of crystalline nanoclusters of Fe_2P, RuP, Co_2P, Rh_2P, Ni_2P, Pd_5P_2, or PtP_2 in a silica xerogel matrix from single-source molecular precursors. Chem Mater 10:903–908
125. Jarvis RF Jr, Jacubinas RM, Kaner RB (2000) Self-propagating metathesis routes to metastable group 4 phosphides. Inorg Chem 39:3243–3246
126. Gregg KA, Perera SC, Lawes G, Shinozaki S, Brock SL (2006) Controlled synthesis of MnP nanorods: effect of shape anisotropy on magnetization. Chem Mater 18:879–886
127. Odile JP, Soled S, Castro CA, Wold A (1978) Crystal growth and characterization of the transition-metal phosphides copper diphosphide, nickel diphosphide, and rhodium triphosphide. Inorg Chem 17:283–286
128. Takacs L, Mandal SK (2001) Preparation of some metal phosphides by ball milling. Mater Sci Eng A 304–306:429–433
129. Henkes AE, Schaak RE (2007) Trioctylphosphine: a general phosphorus source for the low-temperature conversion of metals into metal phosphides. Chem Mater 19:4234–4242
130. Shatruk MM, Kovnir KA, Shevelkov AV, Popovkin BA (2000) Ag_3SnP_7: ein Polyphosphid mit einer einzigartigen (P_7)-Kette und einem neuartigen Ag_3Sn-Heterocluster. Angew Chem 112:2561–2562
131. Shatruk MM, Kovnir KA, Shevelkov AV, Popovkin BA (2000) Ag_3SnP_7: a polyphosphide with a unique (P_7) chain and a novel Ag_3Sn heterocluster. Angew Chem Int Ed 39:2508–2509
132. Braun DJ, Jeitschko W (1978) Über Polyphosphide von Chrom, Mangan, Ruthenium und Osmium. Synthese und Kristallstruktur von RuP_4 und OsP_4. Z Anorg Allg Chem 445:157–166
133. Kloc C, Lux-Steiner MC, Keil M, Baumann JR, Doell G, Bucher E (1990) Growth and characterization of CuP_2 single crystals. J Cryst Growth 106:635–642
134. Zhang Z, Yang J, Nuli Y, Wang B, Xu J (2005) CoP_x synthesis and lithiation by ball-milling for anode materials of lithium ion cells. Solid State Ion 176:693–697
135. Park C-M, Sohn H-J (2008) Tetragonal zinc diphosphide and its nanocomposite as an anode for lithium secondary batteries. Chem Mater 20:6319–6324
136. Jeitschko W, Donohue PC (1975) High-pressure MnP_4, a polyphosphide with Mn–Mn pairs. Acta Crystallogr B31:574–580
137. Barry BM, Gillan EG (2008) Low-temperature solvothermal synthesis of phosphorus-rich transition-metal phosphides. Chem Mater 20:2618–2620
138. Barry BM, Gillan EG (2009) A general and flexible synthesis of transition-metal polyphosphides via PCl_3 elimination. Chem Mater 21:4454–4461
139. Loevvik OM, Prytz O (2004) Density-functional band-structure calculations for La-, Y- and Sc-filled CoP_3-based skutterudite structures. Phys Rev B 70:195119/1–195119/6
140. Watcharapasorn A, DeMattei RC, Feigelson RS, Caillat T, Borshchevsky A, Snyder GJ, Fleurial JP (1999) Preparation and thermoelectric properties of some phosphide skutterudite compounds. J Appl Phys 86:6213–6217
141. Wang K, Yang J, Xie J, Wang B, Wen Z (2003) Electrochemical reactions of lithium with CuP_2 and $Li_{1.75}Cu_{1.25}P_2$ synthesized by ball-milling. Electrochem Commun 5:480–483
142. Tirado JL (2003) Inorganic materials for the negative electrode of lithium-ion batteries: state-of-the-art and future prospects. Mater Sci Eng R40:103–136
143. Alcantara R, Tirado JL, Jumas JC, Monconduit L, Olivier-Fourcade J (2002) Electrochemical reaction of lithium with CoP_3. J Power Sources 109:308–312
144. Silva DCC, Crosnier O, Ouvrard G, Greedan J, Safa-Sefat A, Nazar LF (2003) Reversible lithium uptake by FeP_2. Electrochem Solid-State Lett 6:A162–A165
145. Pralong V, Souza DCS, Leung KT, Nazar LF (2002) Reversible lithium uptake by CoP_3 at low potential: role of the anion. Electrochem Commun 4:516–520
146. Gillot F, Boyanov S, Dupont L, Doublet ML, Morcrette M, Monconduit L, Tarascon JM (2005) Electrochemical reactivity and design of NiP_2 negative electrodes for secondary Li-ion batteries. Chem Mater 17:6327–6337

Chapter 5
Phosphine-Containing Planar Chiral Ferrocenes: Synthesis, Coordination Chemistry and Applications to Asymmetric Catalysis

Eric Manoury and Rinaldo Poli

Abstract Chiral ferrocenyl phosphino ligands are certainly one of the most developed and successful classes of chiral ligands used in asymmetric catalysis. The literature describing their synthetic and coordination chemistry, as well as their metal-mediated applications in the field of catalysis, is extremely rich and varied. Moreover, they represent a rare example in which enantioselective chemical catalysts were used in industrial processes. The present chapter provides an account of the planar-chiral ferrocene ligands developed in the Authors' laboratory, including their coordination chemistry with various metals as well as their use in different asymmetric catalytic reactions (allylic substitution, Suzuki coupling, methoxycarbonylation of alkenes, hydrogenation of ketones).

5.1 Introduction

Over the last few decades, homogenous asymmetric catalysis by transition metals has received considerable attention and numerous chiral ligands and complexes allowing

E. Manoury (✉) · R. Poli (✉)
CNRS, LCC (Laboratoire de Chimie de Coordination), 205, route de Narbonne, 31077 Toulouse, France
e-mail: manoury@lcc-toulouse.fr

R. Poli
e-mail: poli@lcc-toulouse.fr

E. Manoury · R. Poli
UPS, INPT, LCC, Université de Toulouse, 31077, Toulouse, France

R. Poli
Institut Universitaire de France, 103, bd Saint-Michel, 75005 Paris, France

M. Peruzzini and L. Gonsalvi (eds.), *Phosphorus Compounds*, Catalysis by Metal Complexes, 37, DOI: 10.1007/978-90-481-3817-3_5,
© Springer Science+Business Media B.V. 2011

high efficiency reactions have been reported [1–3]. Among these chiral ligands, ferrocene—containing ligands [4–8] are of particular interest because of their stability, the easy introduction of planar chirality [9–12] and the peculiar stereoelectronic properties of the ferrocene moiety. Amongst the chiral ferrocene-based ligands, enantiopure 1,2-disubstituted ferrocene derivatives played a major role. Examples comprise P,P ligands like TRAP [13–19], Josiphos [18], and particularly the industrially important Xyliphos [19], Taniaphos [20–22] and Walphos-type [23] ligands, P,N ligands [24] like pyrazoline-phosphines [25–27] or phosphine-oxazolines such as DIPOFs [28], and more recently P,S ligands such as Fesulphos [29]. These ligands have been so largely used that it is difficult to select the most important achievements. However, it is worth pointing out that they have been particularly efficient, for instance, in asymmetric hydrogenation [30, 31], asymmetric alkenes hydroboration [25, 32], asymmetric hydrophosphination [33], asymmetric Heck reaction [34, 35], asymmetric ring opening of oxo or azabicyclic alkenes [36, 37], and Diels–Alder and hetero Diels–Alder reactions [38–40]. In addition, it should be highlighted that the most important industrial process using asymmetric catalysis, namely the synthesis of grass herbicide (*S*)-metolachlor, uses the ferrocene-based Xyliphos ligand in an imine asymmetric hydrogenation step [19]. This chapter will focus on planar-chiral ferrocene ligands developed in our laboratory, mostly comprising a PPh_2 and a second CH_2X function with different donor groups X in relative 1,2 positions where the only element of asymmetry is the ferrocene planar chirality.

5.2 Synthesis of Ligands

The common intermediates of all syntheses are the planar chiral alcohols having the general formula shown in Fig. 5.1.

5.2.1 Synthesis of Intermediates Alcohols

5.2.1.1 Synthesis of Racemic Alcohols

The racemic thiophosphine–alcohol **1** was synthesized in high yields by optimizing a literature procedure (the overall yield from *N*,*N*-dimethylaminomethylferrocene of 84%, see Scheme 5.1) [41]. The first step is an *ortho*-lithiation of $FcCH_2NMe_2$ followed by an electrophilic trapping and then by the protection of the phosphine by

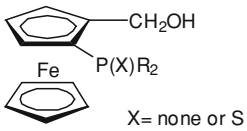
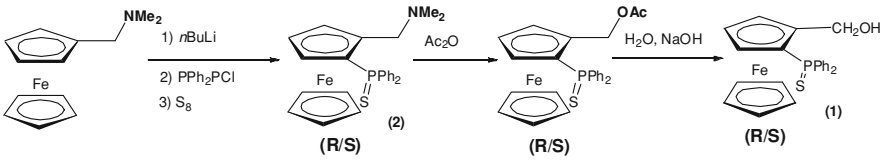
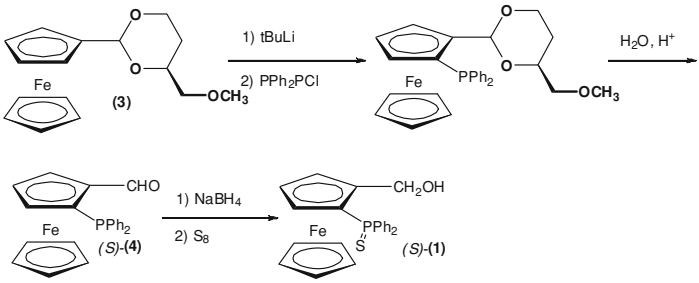


Fig. 5.1 General structure of chiral alcohol intermediates



Scheme 5.1 Synthesis of the racemic thiophosphine–alcohol **1**



Scheme 5.2 Synthesis of the enantiomerically pure (*S*)-**1** via Kagan's acetal

sulfuration to yield the thiophosphine-amine **2** with high efficiency (91% yield). This compound is then transformed by classical methods into an acetate by nucleophilic substitution and finally into the alcohol *rac*-**1** by a saponification step (Scheme 5.1). The overall yield from dimethylaminomethylferrocene was 84%.

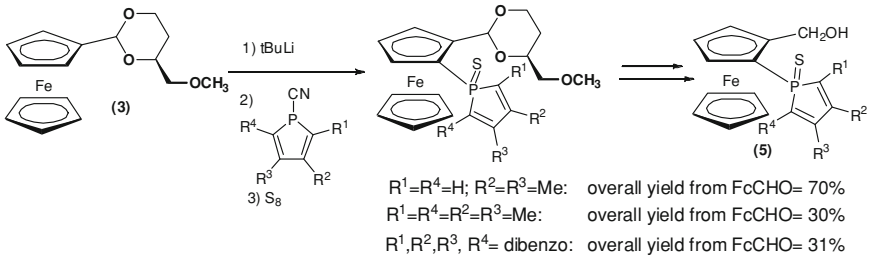
5.2.1.2 Synthesis of Enantiomerically Pure Alcohols

We used two synthetic methods to access these chiral alcohols, the first one being a diastereoselective synthesis using a chiral acetal developed by Kagan et al. [42, 43], the second one being a resolution via separation of a diastereoisomeric mixture as developed by Weissensteiner et al. [44].

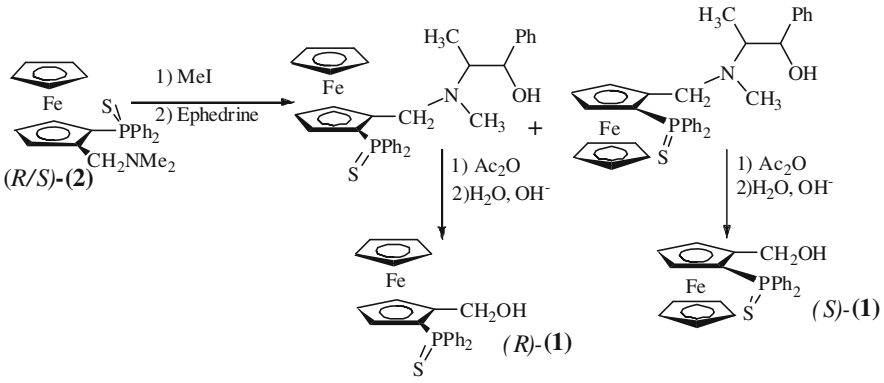
5.2.1.3 Synthesis Using Chiral Acetals

The acetal **3** has been used to access the alcohol **1** in a straightforward way (Scheme 5.2). The first step is a diastereoselective lithiation of compound **3**, which is directed in only one position on the substituted Cp ring by the acetal moiety. Electrophilic quenching of the lithiated intermediate by Ph_2PCl yields a diastereoisomerically pure phosphine–acetal which can be efficiently hydrolyzed under acidic conditions to yield the aldehyde *(S)*-**4** [42, 43]. The desired alcohol could be obtained after reduction by $NaBH_4$ and protection of the phosphine by S_8.

The overall yield for *(S)*-**1** from commercially available ferrocenecarboxaldehyde was 49%. This method is therefore efficient but has two major drawbacks:



Scheme 5.3 Synthesis of the enantiomerically pure phosphole–alcohols **5** via Kagan's acetal



Scheme 5.4 Synthesis of the enantiomerically pure (S)-**1** and (*R*)-**1**

first, the commercial availability of the enantiomerically pure butanetriol, needed for the synthesis of **3**, is erratic; secondly, only one enantiomer of the desired compound can be obtained. The same method has been used to obtain various enantiomerically pure ferrocenyl phosphole–alcohol (Scheme 5.3) [45, 47].

5.2.1.4 Synthesis via Resolution

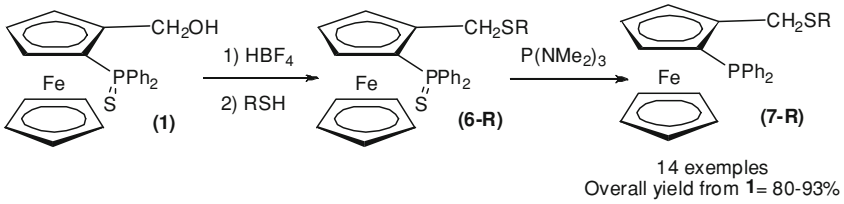
In 1998, Weissensteiner described an efficient method to obtain both pure enantiomers of 2-bromo-(dimethylaminomethylferrocene) using ephedrine for the resolution step [44]. We used a similar methodology to obtain both pure enantiomers of alcohols **1** in a highly efficient manner (overall yield from dimethylaminomethylferrocene of 72%, Scheme 5.4) [47].

5.2.2 Synthesis of Phosphine–Thioether and Related Ligands

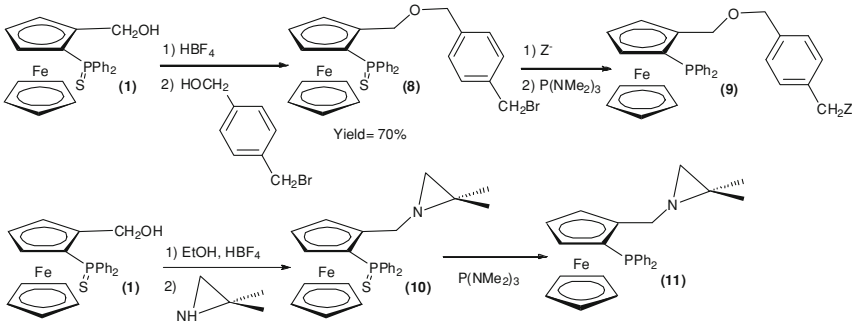
A large number of ligands bearing various combinations of heteroelements (in particular, P–P, P–N or N–N ligands) have been extensively used in catalysis [1].

On the other hand, in spite of their rich coordination chemistry [48, 49], sulfur-containing ligands have been much less involved in homogenous asymmetric catalysis and are now raising growing interest [50–54]. We have decided to investigate phosphine–thiother ligands with planar chirality as the only element of asymmetry. As a few examples of direct transformation of ferrocenyl alcohols into corresponding thiothers under acidic conditions had already been described [55–57], we considered that compounds **6-R** (for instance, R = Et, Ph, *t*Bu, etc.) could be accessed from alcohol **1** via the carbocationic intermediate that is easily generated by protonation with HBF_4 in CH_2Cl_2 [58–63]. By rapidly adding an excess of thiol to the carbocation solution, the expected thiophosphine–thioethers **6-R** could be obtained in high yields (Scheme 5.5) [64]. These reactions are very fast (2 min for the two steps) and the purification is straightforward by a simple filtration on a silicagel column. The desired phosphine–thioether ligands **7-R** could be easily and efficiently obtained by desulfuration by classical sulfur atom transfer with $P(NMe_2)_3$ (3 equivalents) [64].

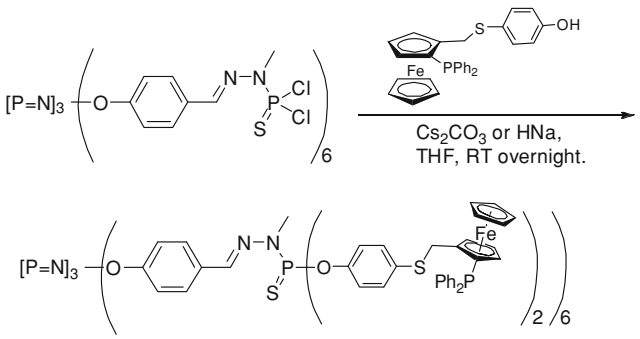
This synthetic method can also be applied to other nucleophiles like amines (Sect. 5.2.4) or alcohols [65] (Scheme 5.6). With poorer nucleophiles such as 2,2′-dimethylaziridine, the nucleophilic trapping of the carbocationic intermediate is not fast enough to prevent decomposition. However, using EtOH instead of CH_2Cl_2 as solvent provides sufficient stabilization to the carbocation to afford the thiophosphine–aziridine **10** in good yields [66], even though contaminated by the



Scheme 5.5 Synthesis of the phosphine–thioethers **7-*R***



Scheme 5.6 Synthesis of the phosphine-ethers **9** and phosphine-aziridines **11**



Scheme 5.7 Synthesis of the dendrimeric ligands $\mathbf{G_1}$**-7**

thiophosphine–ethoxy compound derived by the addition of EtOH to the carbocation.

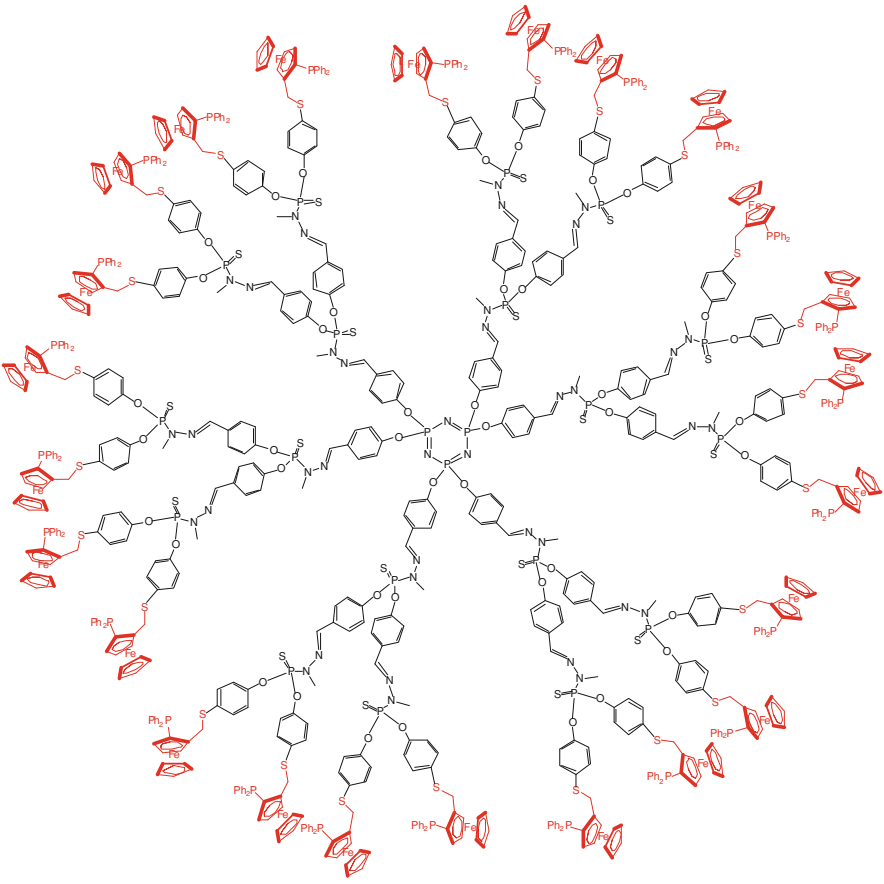
The ligands **7** with R = 4-hydroxyphenyl have been grafted to the periphery of phosphorus-based dendrimers [67–71] by reaction of the phenol function with the surface P–Cl bonds as exemplified for the first generation in Scheme 5.7 [72]. Dendrimers of generation 1–4 ($\mathbf{G_n}$**-7**, n = 1–4) have been synthesized, the structure of $\mathbf{G_2}$**-7** being shown in the Scheme 5.8.

5.2.3 Synthesis of Phosphole-Based Ligands

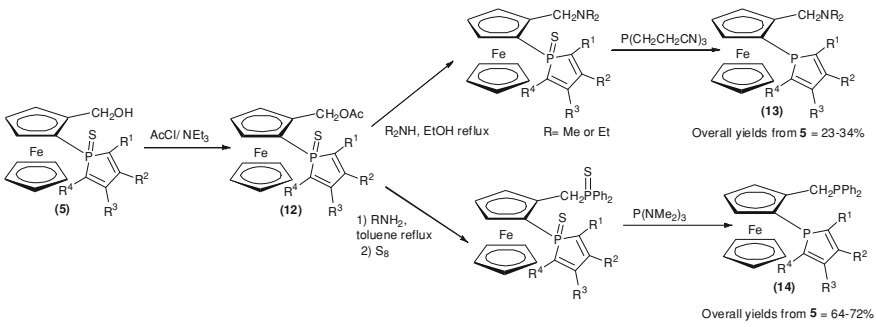
The thiophosphole–alcohols **5** (Scheme 5.3) have been used for further functionalization. However, the protonation method described in Sect. 5.2.1 could not be applied because of the reactivity of the dienic part of phospholes. An alternative method consists in the replacement of the hydroxyl group by the better leaving group acetoxy (Scheme 5.9), even though the primary nature of the acetoxy derivative **12** required harsh conditions for the subsequent nucleophilic substitution. Nevertheless, phosphole–amines **13** [45] and phosphole–phosphines **14** [46, 73] could be obtained in good to moderate yields.

5.2.4 Synthesis of Phosphine-N-Heterocyclic Carbene Ligands Precursors

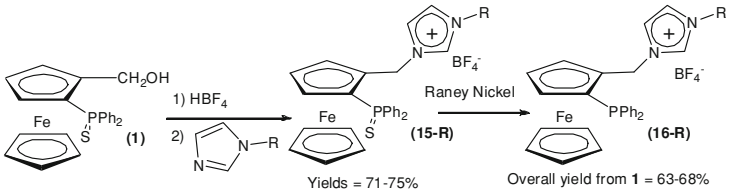
Using the same synthetic method shown in Sect. 5.2.1, the reaction of **1** with imidazoles yielded imidazolium salts **15-R** (R = Me or mesityl) in good yields (Scheme 5.10). The desulfuration with $P(NMe_2)_3$ was not effective in this case, but the free phosphine-imidazoliums **16-R**, which are precursors of phosphine-*N*-



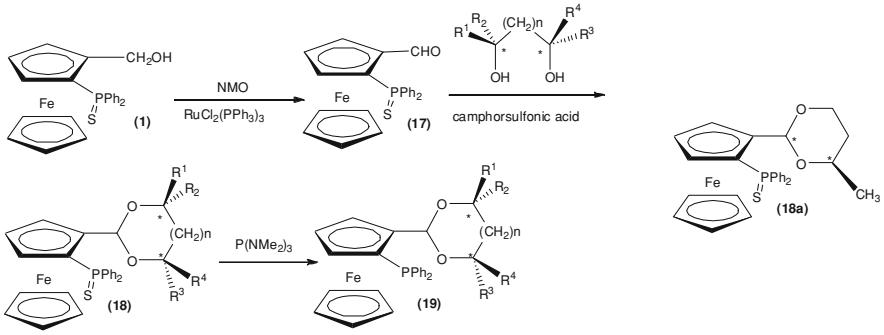
Scheme 5.8 Ligand G_2-**7**



Scheme 5.9 Synthesis of the phosphole–amines **13** and phosphole–phosphines **14**



Scheme 5.10 Synthesis of phosphine-*N*-heterocyclic carbene ligand precursors



Scheme 5.11 Synthesis of phosphine–acetal ligands

heterocyclic carbenes by deprotonation, could be efficiently obtained using Raney nickel as desulfurating agent [74].

5.2.5 *Synthesis of Phosphine–Acetal Ligands*

The alcohol **1** was selectively oxidized into the corresponding aldehyde **17** (Scheme 5.11). Amongst several literature methods to efficiently convert benzylic alcohols to the corresponding benzaldehydes, the only successful one in our case was that described by Sharpless et al. [75], using *N*-methylmorpholine oxide (NMO) as oxidant in the presence of $RuCl_2(PPh_3)_3$ [47]. The reaction of the aldehyde **17** with various 1,2 and 1,3-diols yields various thiophosphine–acetals **18**, which led to the P,O ligands **19** upon desulfuration [47]. Since both enantiomers of aldehyde **17** are accessible, using one particular chiral diol, the two diastereoisomeric ligands **19** could be obtained. For a specific catalytic reaction, it is especially interesting to be able to test both diastereoisomers in order to identify the matched and mismatched ligands. When using the unsymmetrical *(R)*-1,3-butanediol ($R^1 = R^2 = R^3 = H$; $R^4 = Me$), leading to acetal **18a**, the absolute configuration of the new asymmetric carbon created during the synthesis was fully controlled (only one single diastereoisomer was observed).

5.3 Coordination Chemistry

Ligands or pro-ligands **1–19** have been used to generate several coordination compounds with a variety of catalytic metals. A comprehensive coverage of this coordination chemistry will be given below using the metal group classification. A general phenomenon that is valid for all the phosphine thioether ligands **7** (Scheme 5.5) concerns the diastereoselectivity of the coordination reaction. The sulfur atom of the thioether function becomes a new center of chirality upon coordination, thus a mixture of two diatereoisomers may be obtained in principle. However, only one product was observed in all cases, corresponding to the stereoisomer where the lone pair of the pyramidalized sulfur atom points towards the CpFe group while the S substituent points away (left on Fig. 5.2). This means that the planar chirality fully controls the absolute configuration at the sulfur atom during the ligand coordination process. The great steric discrimination between the S substituent and the lone pair at such short distance from the catalytic metal atom is perhaps a reason for the good performance of these ligands in enantioselective catalysis (Sect. 5.4).

5.3.1 Rhodium Complexes

When ligands **7-R** (R = Et, Ph, *t*Bu, Scheme 5.5) were treated with $[Rh(COD)Cl]_2$ in a 2:1 molar ratio, a single product with the stoichiometry RhCl(COD)(**7-R**) was obtained [76]. In contrast to the behaviour observed for the Ir system (vide infra), all three complexes exhibited a ^{31}P resonance at similar values, strongly indicating the same coordination mode for the three ligands with respect to Rh^{I}. When the reaction was carried out in a 1:1 molar ratio, a ^{31}P resonance at a slightly different chemical shift was obtained and attributed to complex $[Rh(COD)(\mathbf{7\text{-}R})]^{+}[Rh(COD)Cl_2]^{-}$ by analogy with the Ir system. These complexes were only characterized spectroscopically in solution.

The pro-ligands **16-R** (Scheme 5.10) led to (carbene)rhodium(I) complexes upon deprotonation in the presence of potassium *tert*-butoxide and $[RhCl(COD)]_2$ in THF (Scheme 5.12), followed by chloride abstraction, which could also be carried out with $AgBF_4/CH_2Cl_2$ without oxidization of the ferrocene unit. While the selectivity for **20-Mes** was almost total, complex **20-Me** was obtained along with another carbene/phosphane complex in a 85:15 ratio, the minor species

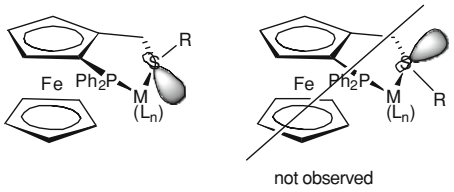
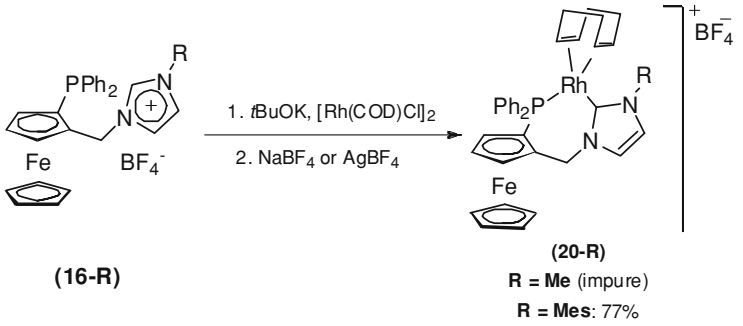


Fig. 5.2 Diastereoselective coordination of phosphine–thioether ligands **7**



(16-R)

(20-R)
R = Me (impure)
R = Mes: 77%

Scheme 5.12 Synthesis of phosphine–carbene rhodium complexes

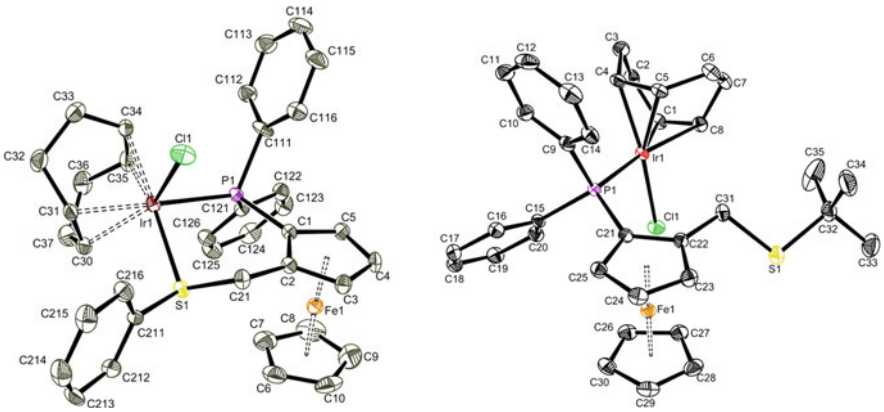


Fig. 5.3 Structure of [IrCl(COD)(**7-*R***)] complexes. *Left* R = Ph. *Right* R = *t*Bu

possibly corresponding to a rhodium complex bearing two carbene/phosphane ligands and no COD ligand. The products are air stable and could be purified by filtration through silica gel [74].

5.3.2 Iridium Complexes

The coordination chemistry of ligands **7-R** (Scheme 5.5) with iridium has been studied in some detail. Addition to $[IrCl(COD)]_2$ (one equivalent of ligand per Ir atom) in CH_2Cl_2 yields a product the structure of which depends on the nature of R. For less sterically encumbering R groups (Et, Ph, Bz) the product has a pentacoordinated structure, as shown in Fig. 5.3 (left) for the Ph derivative (the solid state structure of the Et derivative has also been determined), whereas the bulkier *t*Bu derivative features a 4-coordinate square planar geometry with a dangling thioether function (Fig. 5.3, right). This difference appears to be maintained also in

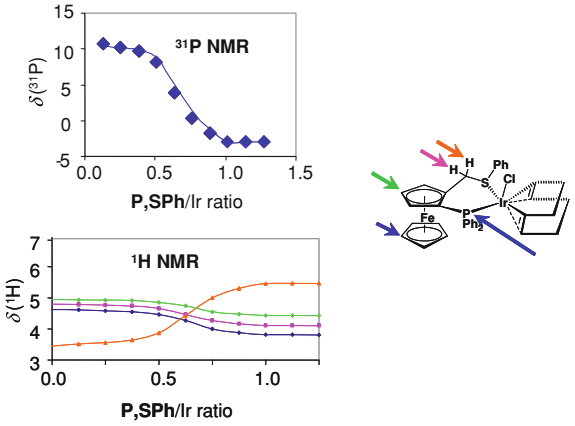
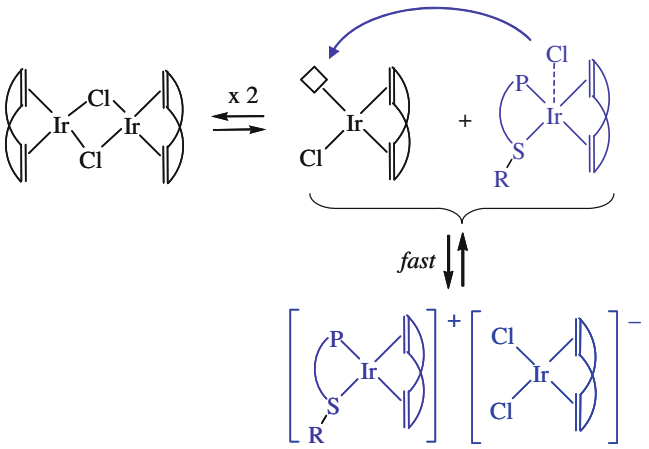


Fig. 5.4 ^{31}P and ^{1}H NMR titration of the addition of **7-Ph** to $[IrCl(COD)]_2$

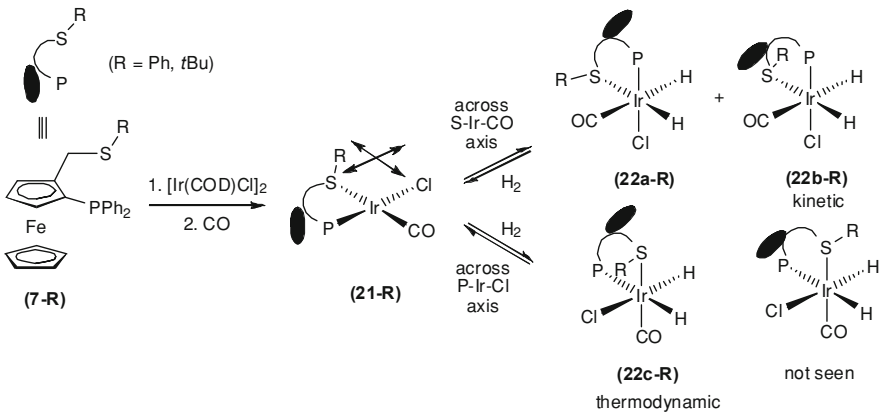
solution, as shown by the different ^{31}P resonances (δ +15.6 for the *t*Bu derivative, vs. −2.9 for Ph, −4.6 for Et and −6.1 for Bz). The structure of the 5-coordinate compounds features an exceedingly long Ir–Cl bond (2.5576(12) Å for the Ph derivative and 2.5739(19) Å for the Et derivative, vs. 2.3625(8) Å for the *t*Bu derivative), suggesting that these derivatives have an important contribution from the ionic $[Ir(COD)(\mathbf{7\text{-}R})]^+Cl^-$ limiting form and should thus be prone to dissociate a chloride ion. This is indeed shown by the solution behaviour [74].

When the addition of **7-R** was carried out in toluene rather than in CH_2Cl_2, a different product was obtained, corresponding to the formulation $[Ir(COD)(\mathbf{7\text{-}R})]^+[IrCl_2(COD)]^-$ (**7-R**/Ir ratio of 0.5), which was structurally characterized for R = Ph. This is not a byproduct, due to a bad stoichiometry control; half the ligand remained unreacted. When the reaction was carried out with a **7-R**/Ir ratio of 0.5, the same ionic product was obtained from toluene, whereas the neutral complex $[IrCl(COD)(\mathbf{7\text{-}R})]$ was obtained from dichloromethane (and half the $[Ir(COD)Cl]_2$ starting material remained unreacted. This suggests the presence of solution equilibria and the nature of the crystallized product was dictated by relative solubility in different solvents. An NMR titration experiment (Fig. 5.4) showed the presence of only one signal at a concentration-dependent chemical shift for each type of resonating nucleus, indicating rapid exchange between two different species. The proposed mechanism of this exchange is illustrated in Scheme 5.13. The same process also occurs for the 4-coordinate *t*Bu system [74]. Metal competition experiments using $[IrCl(COD)]_2$ and $[RhCl(COD)]_2$ and ligand **7-Ph** gave predominantly complex $[IrCl(COD)(\mathbf{7\text{-}Ph})]$, in equilibrium with a small amount of $[Ir(COD)(\mathbf{7\text{-}Ph})]^+[Rh(COD)Cl_2]^-$, suggesting that the iridium ion forms stronger bonds with the phosphorus and sulfur atoms of the **7-Ph** ligand than does the rhodium ion.

When the solution obtained upon treatment of $[Ir(COD)Cl]_2$ with two equivalents of the ligand **7-Ph** or **7-*t*Bu** was exposed to CO, the corresponding complexes **21-R** (Scheme 5.14) were obtained in high yields. Both products were structurally characterized. Subsequent treatment of these complexes with H_2 led to oxidative



Scheme 5.13 Coordination equilibriums of iridium complex **7**-Ph in solution



Scheme 5.14 Addition of pH_2 on iridium complexes **21-*R***

addition along both *trans* L–Ir–L′ vectors (as indicated by the double-pointed arrows in Scheme 5.14) to yield a mixture of isomeric dihydridoiridium(III) derivatives **22-*R***, which evolved with time as a consequence of isomerization processes. The initially obtained **22b-*R*** rapidly equilibrated with **22a-R** and then more slowly with the more stable isomer **22c-R** [77].

5.3.3 Palladium Complexes

Several palladium complexes of functionalized diphenylphosphinoferrocenes have been used in the catalyzed allylic substitution reactions (Sect. 5.4.1). These complexes have typically been generated in situ upon addition of the appropriate

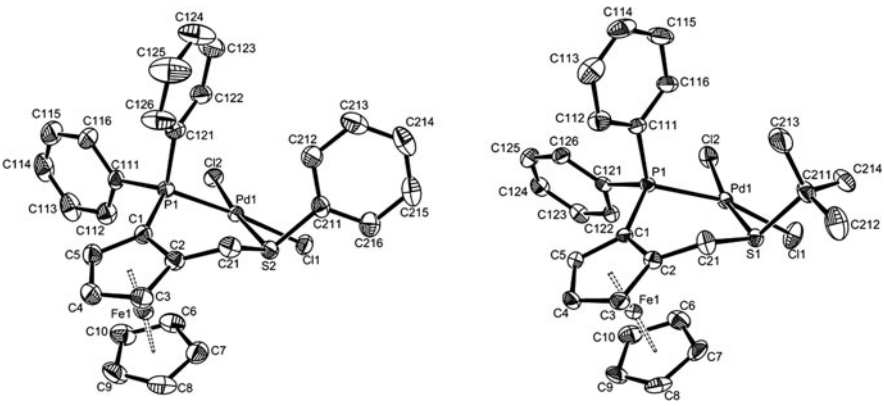


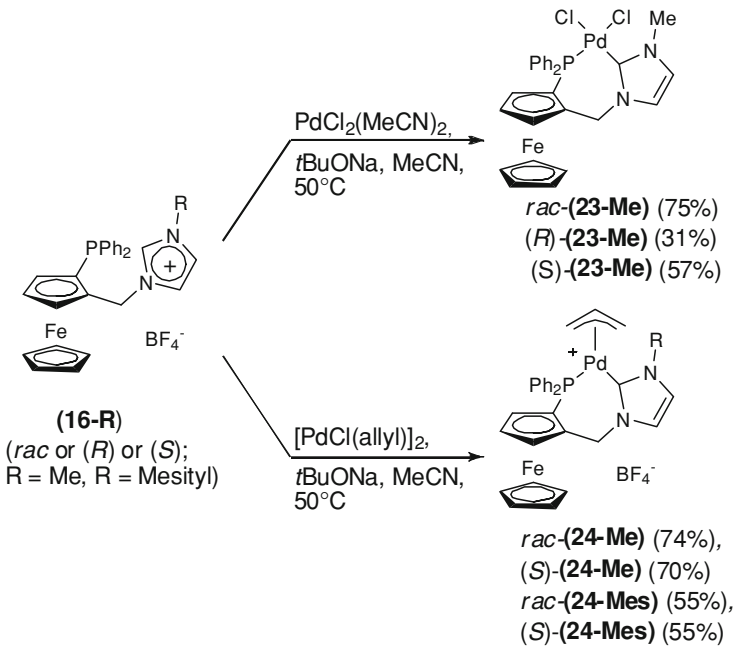
Fig. 5.5 Structures of [$PdCl_2$(**7-Ph**)] and [$PdCl_2$(**7-*t*Bu**)] [40]

ligand to appropriate Pd^{II} precatalysts. However, a few of these complexes have been isolated and fully characterized. Ligand **14** ($R_1 = R_2 = R_3 = R_4 =$ Me, Scheme 5.9) rapidly adds to [$PdCl_2(CH_3CN)_2$] at room temperature to afford the corresponding adduct, which has been structurally characterized and used as an allylic substitution precatalyst [46]. Related complexes containing ligands **7-R** (R = Ph, Et, *t*Bu) have also been isolated and characterized in solution and in the solid state [76, 79] (Fig. 5.5).

Functionalized *N*-heterocyclic carbenes generated from the pro-ligands **16-R**, either in racemic or enantiomerically pure form, have been coordinated to Pd^{II} through the reaction with either [$PdCl_2(MeCN)_2$], to yield products **23-Me**, or [$PdCl(allyl)]_2$; to yield products **24-R** (R = Me or Mesityl; see Scheme 5.15). NMR data of the allylic compounds indicated the presence of two species in a 55:45 (**24-Me**) or 75:25 (**24-Mes**) ratio, which we can attribute to *exo* and *endo* configurational isomers. Crystallographic characterization was presented for complexes *rac*-(**23-Me**), *(R)*-(**23-Me**), *rac*-(**24-Me**) and *rac*-(**24-Mes**) [80].

5.3.4 Platinum Complexes

The addition of the **7-R** ligands (R = Ph, Et, *t*Bu) to [$PtCl_2(MeCN)_2$] afforded Pt^{II} complexes of formula [$PtCl_2$(**7-R**)], which adopt slightly distorted square planar geometries very close to those of the corresponding palladium analogues [78]. The subsequent reaction of complex [$PtCl_2$(**7-Ph**)] with one equivalent of $SnCl_2 \cdot H_2O$ in refluxing toluene results in clean insertion of SnCl2 into one Pt–Cl bond, leading to [$PtCl(SnCl_3)$(**7-Ph**)] in good yields (90%) [81]. Several systems associating a platinum dichloride complex and tin dichloride have been used in the hydroformylation reaction of alkenes and, particularly, in its asymmetric version



Scheme 5.15 Synthesis of phosphine–carbene palladium complexes **23** and **24**

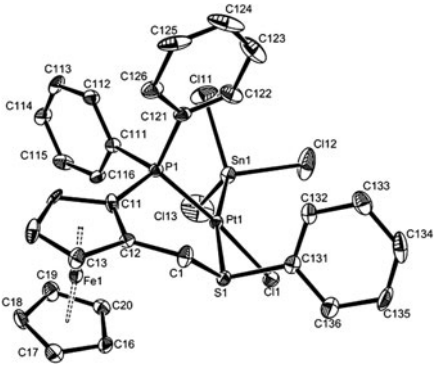


Fig. 5.6 Structure of [PtCl(SnCl$_3$)(**7-Ph**)] [42]

and platinum complexes bearing one chloro ligand and one trichlorotin ligand are considered to be important catalytic intermediates. Complex [PtCl(SnCl$_3$)(**7-Ph**)] is one of few examples of such system to be isolated and crystallographically characterized (Fig. 5.6).

The coordination chemistry of the **7-Ph** ligand was also investigated with respect to Pt^0. Reduction of the above-mentioned complex [PtCl$_2$(**7-Ph**)] by sodium tris(methoxy)-borohydride in the presence of diphenylacetylene in THF at room temperature for 2 h yielded the expected product [Pt(PhC≡CPh)(**7-Ph**)] in

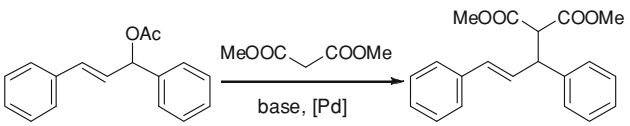
89% yield. This complex was also crystallographically characterized, showing the expected distorted trigonal planar geometry at the metal centre with the alkyne ligand in the P–Pt–S plane. The elongated C–C bond [1.278(15) and 1.290(14) Å in two crystallographically independent molecules] and the pronounced bending of the C≡C–C angles [144(1)–147(1)°], reflect the major contribution of π^* back-donation [81].

5.4 Asymmetric Catalysis

The different ligands and complexes that we have synthesized have been tested in a few selected reactions, like the asymmetric allylic substitution, the asymmetric methoxycarbonylation, the asymmetric Suzuki coupling, and the asymmetric hydrogenation.

5.4.1 Asymmetric Allylic Substitution

The asymmetric allylic substitution has become a popular method for the synthesis of enantiomerically pure molecules [82–84]. The palladium-catalyzed allylic substitution of acetate in *rac*-1,3-diphenylprop-2-enyl acetate with dimethylmalonate is a benchmark reaction for chiral ligands (Scheme 5.16). Ligands **7** yielded good catalytic activities and high enantioselectivities (e.e. up to 93%, see Table 5.1) [64], proving amongst the most efficient P,S ligands for this reaction [51–54].



Scheme 5.16 Palladium-catalyzed allylic substitution of *rac*-1,3-diphenylprop-2-enyl acetate with dimethylmalonate

Table 5.1 Allylic substitution reactions with ligands **7**

Entry	R	Yield (%)	e.e. (%)
1	tBu	93	80
2	iPr	94	81
3	Et	96	83
4	Cy	93	80
5	$PhCH_2$	95	78
6	Ph	97	93

Reaction run with 0.5 mmol of *rac*-1,3-diphenylprop-2-enyl acetate, 1 mmol of dimethylmalonate, 1 mmol of BSA, a catalytic amount of LiOAc, 0.02 mmol of ligand (4 mol%) and 0.02 mol of palladium (4 mol% as$[PdCl(allyl)]_2$) in 3 mL of dichloromethane at RT during 2 h

Table 5.2 Allylic substitution reactions with dendrimeric ligands $\mathbf{G_n}$**-7**

Entry	Ligand	Reaction time	Conversion (%)	Yield (%)	e.e. (%)
1	**S-7-Ph**	2h30	100	96	93
2	**G1-7**	3 h	100	89	93
3	**G2-7**	3 h	100	93	92
4	**G3-7**	3 h	100	94	90
5	**G4-7**	2h30	100	92	91

Reaction run with 0.5 mmol of *rac*-1,3-diphenylprop-2-enyl acetate, 1 mmol of dimethyl malonate, 1 mmol of BSA, a catalytic amount of LiOAc, the ligand and 0.01 mol of dimeric palladium precursor (2 mol% in palladium as $[PdCl(allyl)]_2$) in 2 mL of dichloromethane at RT; with a P,S ligand/Pd ratio of 1.05

Table 5.3 Allylic substitution reactions with thiophosphine–thioether ligands **6**

Entry	R	Yield (%)	e.e. (%)
1	tBu	90	93
2	iPr	91	88
3	Et	97	90
4	Cy	90	87
5	$PhCH_2$	88	91
6	Ph	93	88

Reaction run with 0.5 mmol of *rac*-1,3-diphenylprop-2-enyl acetate, 1 mmol of dimethyl malonate, 1 mmol of BSA, a catalytic amount of LiOAc, 0.02 mmol of ligand (4 mol%) and 0.02 mol of palladium (4 mol% as$[PdCl(allyl)]_2$) in 3 mL of dichloromethane at RT during 2 h

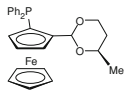
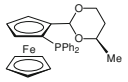
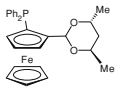
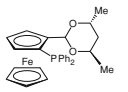
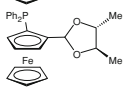
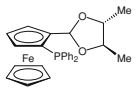
The dendrimeric ligands $\mathbf{G_n}$**-7** have been also tested in the same reaction: catalytic activities and enantioselectivities are essentially the same as with corresponding monomeric ligand **7-Ph** whatever the generation of the involved dendrimer (Table 5.2) [72].

The chiral compounds **6** have also been considered as potential ligands for palladium-catalyzed allylic substitution. Thiophosphines have been very rarely used in asymmetric catalysis [85–89]. These compounds represent, to the best of our knowledge, only the second example of thiophosphine–thioether ligands used in asymmetric catalysis [64, 85–89]. Good catalytic activities and enantioselectivities were obtained (e.e. up to 93% for R = *t*Bu, Table 5.3). Ligands **6** are amongst the few best S,S ligands for this reaction [90–93].

Phosphole–amine **13** and phosphole–phosphine ligands **14** have also been tested. High catalytic activities were obtained but with only moderate enantioselectivities (e.e. up to 65% for ligand **13** (R = Me, R1 = R4 = H, R2 = R3 = Me))[45, 46].

P,O ligands have seldom been used in asymmetric allylic substitution [94–98] but have already proved to be good ligands for this reaction. We therefore tested phosphine acetal ligands **19**, which combine planar chirality and central chirality.

Table 5.4 Allylic substitution reactions with phosphine acetals **19**

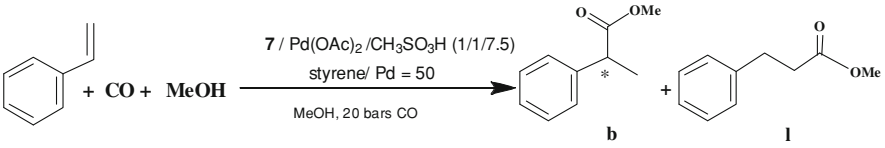
Entry	Ligand	Yield (%)	e.e. (%)	Configuration
1		90	8	R
2		94	53	S
3		89	41	S
4		93	64	S
5		95	18	S
6		97	77	R

Reactions run with 0.5 mmol of *rac*-1,3-diphenylprop-2-enyl acetate, 1 mmol of dimethylmalonate, 1 mmol of BSA and a catalytic amount of base, 0.015 mol of $[PdCl(allyl)]_2$ and 0.03 mol of ligand in 20 mL of ichloromethane at RT during 16 h

For every ligand studied, good catalytic activities was observed (Table 5.4). The enantioselectivities difference observed between the matched and mismatched diastereoisomers is high for the three couples of diasteroisomers (Table 5.4, entries 1–2, 3–4 and 5–6), indicating that both elements of chirality have a strong influence on the stereochemical outcome of the catalytic reaction [47]. In addition, it is worth pointing out that with one ligand the catalytic system already reached promising levels of enantioselectivity (e.e. = 77%) before any optimisation attempt (solvent, temperature, base, ligand/metal ratio, …).

5.4.2 Asymmetric Methoxycarbonylation

The asymmetric alkoxycarbonylation of alkenes is a reaction of particular interest, especially for vinylarenes, because it gives a two steps access (alkoxycarbonylation, ester hydrolysis) to enantiomerically pure carboxylic acids from alkenes. For instance, a few arylpropionic acids such as *(S)*-Ibuprofen, *(S)*-Ketoprofen, and *(S)*-Naproxen, are popular non-steroidal anti-inflammatory agents [99]. Although good regio- and enantioselectivities have already been reported for asymmetric alkoxycarbonylation, no systems, to the best of our knowledge, possesses both types of selectivities [100–104]. We tested ligands **7** in the asymmetric



Scheme 5.17 Palladium-catalyzed asymmetric methoxycarbonylation of styrene

Table 5.5 Asymmetric methoxycarbonylation of styrene (Scheme 5.17) with phosphine–thioethers **7**

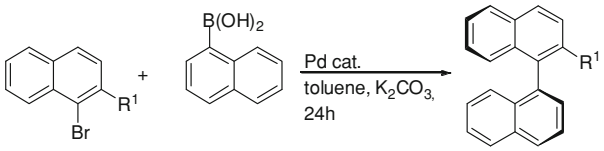
Entry	R	*T* (°C)	*t* (h)	Conv. (%)	Yield (%)	*b*/*l*	e.e. (%)
1	*t*Bu	50	24	83	80	98/2	10
2	*t*Bu[a]	50	24	60	58	99/1	13
3	*t*Bu	25	48	20	19	99/1	17
4	Ph	50	24	50	42	99/1	7.5
5	Ph	30	50	62	57	98/2	13
6	Et	55	48	75	69	97/3	2

Conditions: substrate = styrene; substrate/catalyst = 50; L/Pd = 1; acid (CH_3SO_3H)/catalyst = 7.5; acid/substrate = 0.015; 20 bar CO in MeOH
[a] substrate/catalyst = 50; L/Pd = 2

methoxycarbonylation of styrene (Scheme 5.17; Table 5.5). Good catalytic activities could be obtained under mild conditions (20 bars of CO, 50 °C, 7.5 equivalents of methanesulfonic acid per palladium atom) with excellent chemoselectivities (up to 97%), excellent diastereoselectivities (d.e. up to 98%), but low enantioselectivities (e.e. up to 17%) [105].

5.4.3 Asymmetric Suzuki Coupling

The asymmetric Suzuki coupling reaction is a method of choice to access chiral enantiomerically pure atropoisomeric biaryls. An efficient access to axially chiral biaryl compounds is highly desirable because some of them are biologically important molecules like the famous antibiotic vancomycin, the anti-HIV alkaloid Michellamine B, etc. [106–108] In addition, the axially chiral ligands based on the binaphthalene framework, like BINAP [109, 110], BINOL [111, 112] or MOP [113], are certainly among the most successful ligands in asymmetric catalysis [114–116]. Because efficient asymmetric catalytic systems are still rather rare [108, 117–124], we tested complexes **23-R** in this reaction (Scheme 5.18). This is, to the best of our knowledge, the first use of phosphine–carbene ligands in such reaction. Catalytic activities were good: the amount of catalyst could be limited to 0.1% when the reaction was carried out at 70 °C and to 0.5% at 40 °C (Table 5.6). However, enantioselectivities was moderate (e.e. up to 42%) [80].



Scheme 5.18 Palladium-catalyzed asymmetric Suzuki coupling

Table 5.6 Asymmetric Suzuki coupling (Scheme 5.18) with complexes **23**

Entry	Cat (mol%)	R^1	*T* (°C)	Yield (%)	e.e. (%)
1	0.1	Me	70	89	38
2	0.1	OMe	70	86	33
3	0.1	OEt	70	89	30
4	0.5	Me	40	88	42
5	0.5	Me	40	57[a]	39[a]
6	0.5	OMe	40	93	33
7	0.5	OEt	40	92	24

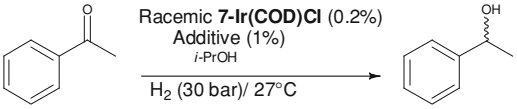
Reagents and conditions: naphthyl bromide (1.0 equiv), boronic acid (1.2 equiv), Pd cat., K_2CO_3 (2.4 equiv), toluene, 24 h
[a] Reaction stopped after 8 h

5.4.4 Asymmetric Hydrogenation of Ketones

5.4.4.1 Catalytic Results

Complexes **7-Ir(COD)Cl** have been tested in the asymmetric iridium-catalyzed hydrogenation of ketones [125]. The racemic complexes were first used in order to optimize the reaction conditions [126]. In the presence of a strong base like MeONa, tBuOK or KOH, but not NEt_3, full conversions were obtained for the hydrogenation of acetophenone in isopropanol as solvent (Scheme 5.19, Table 5.7, entries 1–6). We also carried out the reaction in the absence of hydrogen, leading to no reactivity (Table 5.7, entry 7). Hydrogen is thus necessary but it was not possible to conclude, at this stage, whether hydrogen (hydrogenation) or isopropanol was the reducing agent (transfer hydrogenation) because the role of H_2 may be restricted to the precatalyst activation (hydrogenation of the COD ligand).

The reaction works in various solvents (Table 5.8), although with a strong dependence on the nature of the solvent (see, for instance, entries 1–4). In solvents such as toluene or benzene (Table 5.8, entries 5–8) no transfer hydrogenation may be operating, proving that hydrogenation must take place in that case. The solvent dependence observed for this catalytic system is at variance from that observed for other hydrogenation and transfer hydrogenation catalysts, for which the activity is often zero in aromatic hydrocarbons. A closely related complex, [Ir(COD){Ph_2PhCH(Ph)-CH(Me)NHMe}]$^+$, for instance, was described as inactive in aprotic solvents and its activity is greater in MeOH relative to *i*PrOH [127, 128].



Scheme 5.19 Iridium-catalyzed hydrogenation of acetophenone

Table 5.7 Hydrogenation of acetophenone (Scheme 5.19) with complexes **7-Ir(COD)Cl**

Entry	R	Additive (5 eq.)	Time (h)	Conversion (%)
1	Et	–	5	0
2	Et	NaOMe	2	94
3	Et	KOtBu	5	>99
4	Et	KOH	5	>99
5	Et	NEt_3	5	0
6	Et	NaOMe	2	1[a]
7	Ph	NaOMe	2	>99
8	tBu	NaOMe	5	>99
9	Bz	NaOMe	5	>99

Reaction conditions: racemic catalyst, 6.4×10^{-3} mmol; additive, 3.2×10^{-2} mmol; acetophenone, 3.2 mmol; (1/5/500) under 30 bars at room temperature in 2 mL of isopropanol
[a] Reaction run without H_2

Table 5.8 Hydrogenation of acetophenone in various solvents

Entry	R	Additive	Solvent	Time (h)	Conversion (%)
1	Ph	NaOMe	iPrOH	2	>99
2	Ph	NaOMe	EtOH	2	16
3	Ph	NaOMe	MeOH	2	68
4	Et	NaOMe	tBuOH	2	1
5	Et	NaOMe	Toluene	5	44
6	Et	KOtBu	Toluene	5	94
7	Et	NaOMe	Benzene	5	5
8	Et	KOtBu	Benzene	5	11
9	Et	KOtBu	CH_3CN	5	52

Conditions as in Table 5.7

The enantiomerically pure complexes **(*S*)-7-Ir(COD)Cl** were then used for the asymmetric hydrogenation of acetophenone and aryl substituted analogues (Scheme 5.20). Enantioselectivities were moderate to good, especially for R = Bz (see Table 5.9, e.e. = 47–77%). By limiting the reaction temperature to 10 °C, high yields were still obtained after 8 h with 0.2% catalyst, accompanied by a strong increase of enantioselectivities (e.e. up to >99%). To the best of our knowledge, this catalytic system is the most active and the most enantioselective homogeneous iridium-based system for the asymmetric hydrogenation of ketones [126].

Scheme 5.20 Iridium-catalyzed asymmetric hydrogenation of acetophenone derivatives

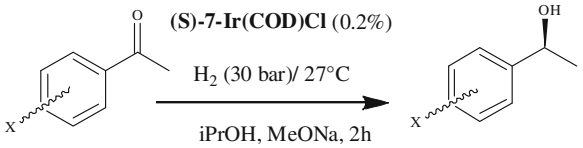


Table 5.9 Asymmetric hydrogenation of acetophenone derivatives (Scheme 5.20) with complexes **7**-Ir(COD)Cl

Entry	R	X	T = 25 °C[a]		T = 10 °C[a, b]	
			Conversion (%)	e.e. (%)	Conversion (%)	e.e. (%)
1	Et	H	94	68	>99	78
2	Ph	H	>99	43		
3	*t*Bu	H	92	59		
4	Bz	H	95	77	99	87
9	Et	2-F	71	37		
10	Ph	2-F	>99	11		
11	*t*Bu	2-F	47	17		
12	Bz	2-F	82	47		
17	Et	4-CH_3	85	67	86	93
18	Ph	4-CH_3	97	72		
19	*t*Bu	4-CH_3	72	68		
20	Bz	4-CH_3	81	73	84	93
25	Et	4-F	16	61	>99	>99
26	Ph	4-F	>99	74		
27	*t*Bu	4-F	72	57		
28	Bz	4-F	64	75	96	>99

[a] Reaction conditions: catalyst, 6.4×10^{-3} mmol; NaOMe, 3.2×10^{-2} mmol; substrate, 3.2 mmol (1/5/500) at room temperature

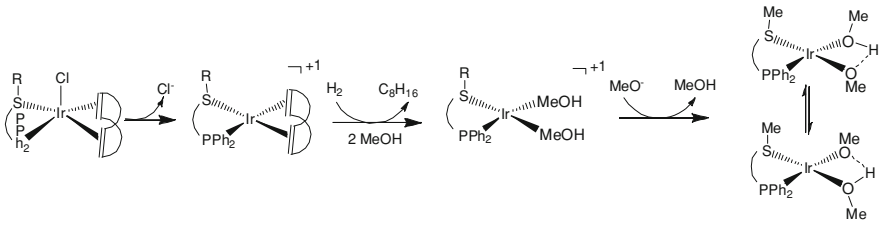
[b] Reaction temperature: 10 °C

5.4.4.2 Mechanistic Studies

As mentioned in the previous section, although the substrate takes the reducing equivalents from H_2 when the reaction is conducted in a non reducing solvent such as benzene, toluene or MeCN, there is the possibility of interference between hydrogenation and transfer hydrogenation when the reaction is conducted in an alcohol solvent. One clear evidence that transfer hydrogenation from *i*PrOH is competitive with hydrogenation by H_2 is the observation by GC and by ^{1}H NMR of the presence of acetone at the end of the reaction, although in very small quantities (ca. 0.5% relative to the starting PhCOMe). This observation, however, does not provide quantitative information on the competition between H_2 and *i*PrOH as reducing agents, because part of the acetone produced by hydrogen transfer may in turn be reduced by H_2 back to isopropanol during the reaction. Indeed, a control experiment run with acetone as substrate showed catalytic

reduction by H_2 and a competition experiment using a 1:1 (mol/mol) mixture of acetone and acetophenone shows that the former is consumed more rapidly (ca. 4 times faster). Finally, the hydrogenation of acetophenone in the presence of the optically pure precatalyst **(*S*)-7-Et-IrCl(COD)** was run under standard conditions for a limited period (1 h) in order to achieve only partial conversion (21.5%), then the autoclave was depressurized and washed with argon, followed by continued monitoring over several hours. After depressurization, only hydrogen transfer may occur. Only an additional 7.5% of substrate was hydrogenated in the next 22 h, proving that hydrogen transfer from *i*PrOH does take place, but much more slowly than hydrogenation with H_2. Furthermore, the enantiomeric excess of the alcohol product obtained after 1 h (69.0%), dropped to 57.2% after 23 h of reaction, indicating a lower enantioselectivity for the hydrogen transfer process (calculated as ca. 30% from the data). An independent experiment showed that the enantioselectivity of the hydrogenation process was constant as a function of conversion, with no erosion over longer reaction times. Hence, this experiment shows that the **7-IrCl(COD)**/NaOMe system catalyzes both the hydrogenation and the hydrogen transfer reduction of acetophenone in isopropanol, with the former being at the same time faster and more enantioselective [129].

Further mechanistic investigations showed that the chloride ligand does not play any role in the enantio-discriminating step, because use of $[Ir(COD)(OMe)]_2$/**7-Et**/NaOMe as a catalyst led to an identical e.e. (67%) to that observed for the reaction catalyzed by **7-Et-IrCl(COD)**/NaOMe under the same conditions. The catalytic activity is lower, however, when using the methoxido pre-catalyst. Furthermore, a GC monitoring experiment shows that the COD ligand of the precatalyst is eliminated as cyclooctene (no evidence of cyclooctane) during the initial stages of the catalysis. One additional mechanistic question is the possibility of hydrogenation through the enol tautomer by H_2 transfer to the C=C bond rather than direct reduction of the C=O bond. This mechanism was in fact proposed for a rhodium system on the basis of a computation investigation [130], following the experimental observations of a cooperative effect leading to much higher activities for the catalyst in the form of Langmuir–Blodgett films relative to the solution [129]. This mechanistic variant, however, seems unnecessary to rationalize the activity of this Ir catalytic system, because good activities were also observed for the reduction of two non enolizable ketones, PhC(O)R with R = CF_3 and *t*Bu. Conversions for these two substrates were 42 and 25% after 2 h when using **7-Et-IrCl(COD)**/NaOMe under the same condition of Table 5.7, and an enantiomeric excess of 62% was obtained for the second substrate by using the optically pure catalyst. The current mechanistic hypothesis is that the precatalyst is activated by the base as shown in Scheme 5.21. Two H atoms (either from H_2 or from *i*PrOH) are then used to convert the methoxido derivatives into hydride derivatives, of either Ir^{I} or Ir^{III}, which are then able to reduce the carbonyl substrate either by an inner sphere or by an outer sphere mechanism. A theoretical investigation by DFT on model systems is currently ongoing to elucidate these mechanistic details [129].



Scheme 5.21 Proposed pathway to the precatalyst

5.4.5 Conclusions

Various planar chiral ferrocene ligands (P,S; P,O; P,P; P,NHC, …) have been synthesized and the coordination of these ligands with various metals of catalytic interest (Rh, Ir, Pd, Pt) has been investigated. The first applications of these ligands in asymmetric catalysis have been presented: asymmetric allylic substitution (e.e. up to 93%), asymmetric methoxycarbonylation (branched/linear up to 99/1, e.e. up to 17%), asymmetric Suzuki coupling (e.e. up to 42%), iridium-catalyzed asymmetric hydrogenation of unfunctionalized ketones (high activities and e.e. >99% for selected substrates). These initial results have shown the potential of the various ligands in catalysis and especially in asymmetric catalysis. The extension of these studies to new reactions, substrates and reaction conditions, as well as better mechanistic understanding, holds promise for meeting new challenges in asymmetric catalysis.

References

1. Jacobsen EN, Pfalz A, Yamamoto H (eds) (1999) Comprehensive asymmetric catalysis, vols 1–3. Springer, Berlin
2. Ojima I (ed) (2000) Catalytic asymmetric synthesis. Wiley-VCH, New York
3. Börner A (ed) (2008) Phosphorus ligands in asymmetric catalysis, vols 1–3. Wiley-VCH, Weinheim
4. Togni A, Hayashi H (eds) (1995) Ferrocenes. VCH, Weinheim
5. Stepnicka P (ed) (2008) Ferrocenes. Wiley, Chichester
6. Gomez Arrayas R, Adrio J, Carretero JC (2006) Recent applications of chiral ferrocene ligands in asymmetric catalysis. Angew Chem Int Ed 45:7674–7715
7. Atkinson RCJ, Gibson VC, Long NJ (2004) The synthesis and catalytic applications of unsymmetrical ferrocene ligands. Chem Soc Rev 33:313–328
8. Colacot TJ (2003) A concise update on the applications of chiral ferrocenyl phosphines in homogeneous catalysis leading to organic synthesis. Chem Rev 103:3101–3118
9. Richards CJ, Locke AJ (1998) Recent advances in the generation of non-racemic ferrocene derivatives and their application to asymmetric synthesis. Tetrahedron Asym 9:2377–2407
10. Balavoine GGA, Daran J-C, Iftime G, Manoury E, Moreau-Bossuet C (1998) Selective synthesis of ferrocenes. J Organomet Chem 567:191–198

11. Riant O, Kagan HB (1997) In: Hassner A (ed) Advances in asymmetric synthesis, vol 1. Jai Press, Greenwich, p 189
12. Togni A (1996) Planar-chiral ferrocenes: synthetic methods and applications. Angew Chem Int Ed 35:1475–1477
13. Sawamura M, Nakayama Y, Kato T, Ito Y (1995) Gold(I)-catalyzed asymmetric aldol reaction of *N*-methoxy-*N*-methyl-alpha-isocyanoacetamide (alpha-isocyano Weinreb amide)—an efficient synthesis of optically-active beta-hydroxy-alpha-amino aldehydes and ketones. J Org Chem 60:1727–1732
14. Sawamura M, Sudoh M, Ito Y (1996) An enantioselective two-component catalyst system: Rh–Pd-catalyzed allylic alkylation of activated nitriles. J Am Chem Soc 118:3309–3310
15. Kuwano R, Miyazaki H, Ito Y (1998) Asymmetric aldol reaction of 2-cyanopropionates catalysed by *trans*-chelating chiral diphosphine ligand TRAP-rhodium(I) complex. Chem Commun 71–72
16. Kuwano R, Uemura T, Saitoh M, Ito Y (1999) Synthesis of a trans-chelating chiral diphosphine ligand with only planar chirality and its application to asymmetric hydrosilylation of ketones. Tetrahedron Lett 40:1327–1330
17. Kuwano R, Sato K, Kurokawa T, Karube D, Ito Y (2000) Catalytic asymmetric hydrogenation of heteroaromatic compounds, indoles. J Am Chem Soc 122:7614–7615
18. Blaser H-U, Brieden W, Pugin B, Spindler F, Studer M, Togni A (2002) Solvias Josiphos ligands: from discovery to technical applications. Top Catal 19:3–16
19. Blaser H-U (2002) The chiral switch of (*S*)-metolachlor: a personal account of an industrial odyssey in asymmetric catalysis. Adv Synth Catal 344:17–31
20. Ireland T, Grossheimann G, Wieser-Jeunesse C, Knochel P (1999) Ferrocenyl ligands with two phosphanyl substituents in the alpha, epsilon positions for the transition metal catalyzed asymmetric hydrogenation of functionalized double bonds. Angew Chem Int Ed 38:3212–3215
21. Lotz M, Polborn K, Knochel P (2002) New ferrocenyl ligands with broad applications in asymmetric catalysis. Angew Chem Int Ed 41:4708–4711
22. Spindler F, Malan C, Lotz M, Kesselgruber M, Pittelkow U, Rivas-Nass A, Briel O, Blaser HU (2004) Modular chiral ligands: the profiling of the Mandyphos and Taniaphos ligand families. Tetrahedron Asym 15:2299–2306
23. Sturm T, Weissensteiner W, Spindler F (2003) A novel class of ferrocenyl-aryl-based diphosphine ligands for Rh- and Ru-catalysed enantioselective hydrogenation. Adv Synth Catal 345:160–164
24. McManus A, Guiry PJ (2004) Recent developments in the application of oxazoline-containing ligands in asymmetric catalysis. Chem Rev 104:4151–4202
25. Schnyder A, Hintermann L, Togni A (1995) Strong electronic effects on enantioselectivity in rhodium-catalyzed hydroborations with novel pyrazole-containing ferrocenyl ligands. Angew Chem Int Ed 34:931–933
26. Togni A, Buckardt U, Gramlich V, Pregosin PS, Salzman R (1996) Palladium-catalyzed asymmetric allylic amination using ferrocenyl pyrazole ligands: steric control of eta(3)-allyl configuration and site-selective nucleophilic attack. J Am Chem Soc 118:1031–1037
27. Pioda G, Togni A (1998) Highly enantioselective palladium-catalyzed hydrosilylation of norbornene with trichlorosilane using ferrocenyl ligands. Tetrahedron Asym 9:3903–3910
28. Sutcliffe OB, Bryce MR (2003) Planar chiral 2-ferrocenyloxazolines and 1,1′-bis(oxazolinyl)ferrocenes-syntheses and applications in asymmetric catalysis. Tetrahedron Asym 14:2297–2325
29. Cabrera S, Mancheno OG, Arrayas RG, Alonso I, Mauleon P, Carretero JC (2006) Sulfenylphosphinoferrocenes: novel planar chiral ligands in enantioselective catalysis. Pure Appl Chem 78:257–265
30. Hu XP, Zheng Z (2005) Practical Rh(I)-catalyzed asymmetric hydrogenation of *β*-(acylamino) acrylates using a new unsymmetrical hybrid ferrocenylphosphine–

phosphoramidite ligand: crucial Influence of an N−H Proton in the ligand. Org Lett 7:419–422
31. Kuwano R, Kaneda K, Ito T, Sato K, Kurokawa T, Ito Y (2004) Highly enantioselective synthesis of chiral 3-substituted indolines by catalytic asymmetric hydrogenation of indoles. Org Lett 6:2213–2215
32. Kloetzing RJ, Lotz M, Knochel P (2003) New P,N-ferrocenyl ligands for rhodium-catalyzed hydroboration and palladium-catalyzed allylic alkylation. Tetrahedron Asym 14:255–264
33. Sadow AD, Togni A (2005) Enantioselective addition of secondary phosphines to methacrylonitrile: catalysis and mechanism. J Am Chem Soc 127:17012–17024
34. Tu T, Deng W-P, Hou X-L, Dai L-X, Dong X-W (2003) The regioselectivity of the asymmetric intermolecular Heck reaction with planar chiral diphosphine-oxazoline ferrocenyl ligands. Chem Eur J 9:3073–3081
35. Tu T, Hou X-L, Dai L-X (2003) Highly regio- and enantioselective Heck reaction of *N*-methoxycarbonyl-2-pyrroline with planar chiral diphosphine-oxazoline ferrocenyl ligands. Org Lett 5:3651–3653
36. Lautens M, Fagnou K, Yeng D (2003) Rhodium-catalyzed asymmetric ring opening reactions of oxabicyclic alkenes: application of halide effects in the development of a general process. J Am Chem Soc 125:14884–14892
37. Cho Y-H, Zunic V, Senboku H, Olsen M, Lautens M (2006) Rhodium-catalyzed ring-opening reactions of *N*-Boc-azabenzonorbornadienes with amine nucleophiles. J Am Chem Soc 128:6837–6848
38. Garcia Mancheno O, Gomez Arrayas R, Carretero J-C (2005) Palladium complexes of chiral planar 1-phosphino-2-sulfenylferrocenes as efficient catalysts in enantioselective Diels-Alder reactions. Organometallics 24:557–561
39. Fukuzawa S-I, Yahara Y, Kamiyana A, Hara M, Kikuchi S (2005) Stereoselective pinacol coupling of chiral formylferrocene using divalent samarium triflate: preparation of a new chiral bisferrocenyl oxazoline ligand and its application to asymmetric Diels–Alder reactions. Org Lett 7:5809–5812
40. Garcia Mancheno O, Gomez Arrayas R, Carretero J-C (2004) Chiral copper complexes of phosphino sulfenyl ferrocenes as efficient catalysts for enantioselective formal Aza Diels–Alder reactions of *N*-sulfonyl imines. J Am Chem Soc 126:456–457
41. Hayashi T, Mise T, Fukushima M, Kagotani M, Nagashima N, Hamada Y, Matsumoto A, Kawakami S, Konishi M, Yamamoto K, Kumada M (1980) Asymmetric synthesis catalyzed by chiral ferrocenylphosphine-transition metal complexes. I. Preparation of chiral ferrocenylphosphines. Bull Chem Soc Jpn 53:1138–1151
42. Riant O, Samuel O, Kagan HB (1993) A general asymmetric synthesis of ferrocenes with planar chirality. J Am Chem Soc 115:5835–5836
43. Riant O, Samuel O, Flessner T, Taudien S, Kagan HB (1997) An efficient asymmetric synthesis of 2-substituted ferrocenecarboxaldehydes. J Org Chem 62:6733–6745
44. Xiao L, Mereiter K, Weissensteiner W, Wildham M (1999) A practicable synthesis of enantiopure 2-aminomethyl-1-bromo- and 2-aminomethyl-1-iodoferrocenes. Synthesis 8:1354–1362
45. Mourgues S, Serra D, Lamy F, Vincendeau S, Daran J-C, Manoury E, Gouygou M (2003) Chiral [(dialkylamino)methyl](phospholyl)ferrocene ligands as a new class of 1,2-disubstituted ferrocene ligands. Eur J Inorg Chem 2820–2826
46. Lopez Cortes JG, Ramon O, Vincendeau S, Serra D, Lamy F, Daran J-C, Manoury E, Gouygou M (2006) New chiral ferrocenyl phosphole–phosphane ligands. Eur J Inorg Chem 5148–5157
47. Mateus N, Routaboul L, Daran J-C, Manoury E (2006) Synthesis and catalytic applications of new chiral ferrocenyl P,O ligands. J Organomet Chem 691:2297–2310
48. Murray SG, Hartley FR (1981) Coordination chemistry of thioethers, selenoethers, and telluroethers in transition–metal complexes. Chem Rev 81:365–414
49. Dilworth JR, Wheatley N (2000) The preparation and coordination chemistry of phosphorus–sulfur donor ligands. Coord Chem Rev 199:89–158

50. Bayon JC, Claver C, Masdeu-Bulto AM (1999) Homogeneous catalysis with transition metal complexes containing sulfur ligands. Coord Chem Rev 193–195:73–145
51. Masdeu-Bulto AM, Dieguez M, Martin E, Gomez M (2003) Chiral thioether ligands: coordination chemistry and asymmetric catalysis. Coord Chem Rev 242:159–201
52. Mellah M, Voituriez A, Schulz E (2007) Chiral sulfur ligands for asymmetric catalysis. Chem Rev 107:5133–5209
53. Pellissier H (2007) Chiral sulfur-containing ligands for asymmetric catalysis. Tetrahedron 63:1297–1330
54. Malacea R, Manoury E (2008) Phosphorus–sulfur ligands. In: Börner A (ed) Phosphorus ligands in asymmetric catalysis, vols 1–3. Wiley-VCH, Weinheim
55. Combs CS, Ashmore CI, Bridges AF, Swanson CR, Stephens W (1969) Reactions of hydroxymethylferrocene. II. Sulfides. J Org Chem 34:1511–1512
56. Ratajczaj A, Krzykawski J (1987) Synthesis of dithia-(1,2)ferrocenophanes and tetrathia-(1,2)Ferrocenophanes by the reactions of 1,2-di(hydroxymethyl)ferrocene with alpha, omega, alpha, omega-alkanedithiols. Gazz Chim Ital 117:533–537
57. Beer PD, Nation JE, Harman ME, Hursthouse MB (1992) Synthesis, electrochemistry and complexation studies of new redox active bisferrocene acyclic and macrocyclic thioethers. J Organomet Chem 441:465–477
58. Cais M, Eisenstadt A (1965) Organometallic studies. X. Reductive dimerization of alpha-metallocenylcarbonium ions. I. J Org Chem 30:1148–1154
59. Allenmark S (1974) Synthetic use of alpha-ferrocebylcarbonium tetrafluoroborates. Tetrahedron Lett 13:371–374
60. Ceccon A, Gambaro A, Paolucci D, Venzo A (1983) Nucleophilic-addition of the thiocyanate ion to ferrocenyl-stabilized carbocations. Polyhedron 2:183–184
61. Richards CJ, Hibbs D, Hursthouse MB (1994) Stereoselective addition of silyl enol ethers to alpha-ferrocenylcarbenium ions. Tetrahedron Lett 35:4215–4218
62. Taudien S, Riant O, Kagan HB (1995) Synthesis of chiral carbocations linked to a ferrocene unit. Tetrahedron Lett 36:3513–3516
63. Brunner H, Taudien S, Riant O, Kagan HB (1997) Stereoselective synthesis of some chiral alpha-ferrocenyl carbenium ions. Chirality 9:478–486
64. Routaboul L, Vincendeau S, Daran J-C, Manoury E (2005) New ferrocenyl P,S and S,S ligands for asymmetric catalysis. Tetrahedron Asym 16:2685–2690
65. Audin C, Daran J-C, Deydier E, Manoury E, Poli R (2010) New ferrocenyl P,O ligands with polar substituents. R C R Chimie 13:890–899
66. Midura WH, Krysiak J, Manoury E, Daran J-C, manuscript in preparation
67. Majoral J-P, Caminade A-M (1999) Dendrimers containing heteroatoms (Si, P, B, Ge, or Bi). Chem Rev 99:845–880
68. Turrin C-O, Chiffre J, de Montauzon D, Daran J-C, Caminade A-M, Manoury E, Balavoine GGA, Majoral J-P (2000) Phosphorus-containing dendrimers with ferrocenyl units at the core within the branches and on the periphery. Macromolecules 33:7328–7336
69. Turrin C-O, Chiffre J, de Montauzon D, Daran J-C, Caminade A-M, Manoury E, Balavoine GGA, Majoral J-P (2001) New chiral phosphorus-containing dendrimers with ferrocenes on the periphery. Tetrahedron 57:2521–2536
70. Turrin C-O, Chiffre J, de Montauzon D, Balavoine G, Manoury E, Caminade A-C, Majoral J-P (2002) Behavior of an optically active ferrocene chiral shell located within phosphorus-containing dendrimers. Organometallics 21:1891–1897
71. Turrin C-O, Chiffre J, de Montauzon D, Balavoine G, Manoury E, Caminade A-C, Majoral J-P (2002) New phosphorus-containing dendrimers with ferrocenyl units in each layer. Comptes Rendus Chimie 5:309–318
72. Routaboul L, Vincendeau S, Turrin C-O, Caminade A-M, Majoral J-P, Daran J-C, Manoury E (2007) New phosphorus dendrimers with chiral ferrocenyl phosphine-thioether ligands on the periphery for asymmetric catalysis. J Organomet Chem 692:1064–1073

73. Lopez Cortes JG, Vincendeau S, Daran J-C, Manoury E, Gouygou M (2006) New enantiomerically pure ferrocenyl phosphole compounds. Acta Crystallogr C C62:m188–m191
74. Labande A, Daran J-C, Manoury E, Poli R (2007) 1,1′- and 1,2-ferrocenyl phosphine-diaminocarbene ligands: synthesis, Rh(I) complexes. Eur J Inorg Chem 1205–1209
75. Sharpless KB, Akashi K, Oshima K (1976) Ruthenium catalyzed oxidation of alcohols to aldehydes and ketones by amine-*N*-oxides. Tetrahedron Lett 29:2503–2506
76. Malacea R, Manoury E, Routaboul L, Daran J-C, Poli R, Dunne JP, Withwood AC, Godard C, Duckett SB (2006) Coordination chemistry and diphenylacetylene hydrogenation catalysis of planar chiral ferrocenylphosphine-thioether ligands with cyclooctadiene iridium(I). Eur J Inorg Chem 1803–1816
77. Malacea R. Daran J-C, Duckett SB, Dunne JP, Manoury E, Poli R, Withwood AC (2006) Parahydrogen studies of H_2 addition to Ir(I) complexes containing chiral phosphine-thioether ligands: implications for catalysis. Dalton Trans 3350–3359
78. Malacea R, Routaboul L, Manoury E, Daran J-C, Poli R (2008) Palladium and platinum complexes with planar chiral 1,2-disubstituted ferrocenes containing phosphine and thioether donor groups. J Organomet Chem 693:1469
79. Diab L, Daran J-C, Gouygou M, Manoury E, Urrutigoity M (2007) Dichlorido[(S, RS)-diphenyl-phosphino-2-(ethylsulfanylmethyl)-ferrocene]palladium(II)]. Acta Crystallogr C63:m586–m588
80. Debono N, Labande A, Manoury E, Daran J-C, Poli R (2010) Palladium complexes of planar chiral ferrocenyl phosphine-NHC ligands: new catalysts for the asymmetric Suzuki–Miyaura reaction. Organometallics 29:1879–1882
81. Malacea R, Routaboul L, Manoury E, Daran J-C, Poli R (2008) Synthesis, characterization and crystal structures of two new platinum complexes with planar chiral 1,2-disubstituted ferrocenes containing phosphine and thioether donor groups. J Mol Struct 890:249–254
82. Trost BM, van Vranken DL (1996) Asymmetric transition metal-catalyzed allylic alkylations. Chem Rev 96:395–422
83. Pfalz A, Yamamoto H (2000) In: Ojima I (ed) Catalytic asymmetric synthesis, 2nd edn. Wiley-VCH, New York, pp 834–884
84. Trost BM, Crawley ML (2003) Asymmetric transition-metal-catalyzed allylic alkylations: applications in total synthesis. Chem Rev 103:2921–2943
85. Zhang W, Xu Q, Shi M (2004) Palladium-catalyzed asymmetric allylic substitutions by axially chiral P,S-, S,S-, and S,O-heterodonor ligands with a binaphthalene framework. Tetrahedron Asym 15:3161–3169
86. Faller JW, Wilt JC, Parr J (2004) Kinetic resolution and unusual regioselectivity in palladium-catalyzed allylic alkylations with a chiral P,S ligand. Org Lett 6:1301–1304
87. Faller JW, Wilt JC (2005) Palladium/BINAP(*S*)-catalyzed asymmetric allylic amination. Org Lett 7:633–636
88. Faller JW, Wilt JC (2005) Regioselectivity in the palladium/(*S*)-BINAP(S)-catalyzed asymmetric allylic amination: reaction scope, kinetics, and stereodynamics. Organometallics 24:5076–5083
89. Robé E, Perlikowska W, Lemoine C, Diab L, Vincendeau S, Mikolajczyk M, Daran J-C, Gouygou M (2008) Diphosphine sulfides derived from 2,2′-biphosphole: novel chiral *S*,*S* ligands for palladium-catalyzed asymmetric allylic substitution. Dalton Trans 2894–2898
90. Okuyama Y, Nakano H, Takahashi K, Hongo H, Kabuto C (2003) Novel and efficient chiral sulfideoxathiane ligands for palladium-catalyzed asymmetric allylic alkylation. Chem Commun 524–525
91. Khiar N, Araujo CS, Alvarez E, Fernandez I (2003) C-2-symmetric bis-thioglycosides as new ligands for palladium-catalyzed allylic substitutions. Tetrahedron Lett 44:3401–3404
92. Okuyama Y, Nakano H, Saito Y, Takahashi K, Hongo H (2005) Chiral sulfideoxathiane ligands for palladium-catalyzed asymmetric allylic alkylation. Tetrahedron Asym 16:2551–2557
93. Khiar N, Araujo CS, Alvarez E, Fernandez I (2006) Sulfur-sulfur-based ligands derived from D-sugars: synthesis of Pd-II complexes, application in palladium-catalyzed allylic

alkylation for the synthesis of both members of enantiomer pairs, and structural studies. Eur J Org Chem 1685-1700
94. Dai W-M, Yeung KKY, Liu J-T, Zhang YY, Williams ID (2002) A novel class of nonbiaryl atropisomeric P,O-ligands for palladium-catalyzed asymmetric allylic alkylation. Org Lett 4:1615–1618
95. Tollabi M, Framery E, Goux-Henry C, Sinou D (2003) Palladium-catalyzed asymmetric allylic alkylation using chiral glucosamine-based monophosphines. Tetrahedron Asym 14:3329–3333
96. Gladiali S, Taras R, Ceder RM, Rocamora M, Muller G, Solans X, Font-Bardia M (2004) Asymmetric allylic alkylation catalyzed by Pd(II)-complexes with (S)-BINPO, a hemilabile axially chiral P,O-heterodonor inducer. Tetrahedron Asym 14:1477–1485
97. Jiang B, Huang Z-G (2007) Chiral P,O-ligands derived from N,O-phenylene prolinols for palladium-catalyzed asymmetric allylic alkylation. Tetrahedron Lett 48:1703–1706
98. Marinho VR, Rodrigues AI, Burke AJ (2008) Novel chiral P,O-ligands for homogeneous Pd(0) catalysed asymmetric allylic alkylation reactions. Tetrahedron Asym 19:454–458
99. Gerharzt W (ed) (1985) Ullmann's encyclopedia of industrial chemistry, vol 3. VCH Weinheim, p 41
100. Wang L, Kwok WH, Chan ASC, Tu T, Hou X, Dai L (2003) Asymmetric hydroesterification of styrene using catalysts with planar-chiral ferrocene oxazoline ligands. Tetrahedron Asym 14:2291–2295
101. Munoz B, Marinetti A, Ruiz A, Castillon S, Claver C (2005) Enhanced regioselectivity in palladium-catalysed asymmetric methoxycarbonylation of styrene using phosphetanes as chiral ligands. Inorg Chem Commun 8:1113–1115
102. Godard C, Ruiz A, Claver C (2006) Systematic study of the asymmetric methoxycarbonylation of styrene catalyzed by palladium systems containing ferrocenyl diphosphine ligands. Helv Chim Act 89:1610–1622
103. Munoz BK, Godard C, Marinetti A, Ruiz A, Benet-Buchholz J, Claver C (2007) Pd-catalysed methoxycarbonylation of vinyl arenes using chiral monodentate phosphetanes and phospholane as ligands; effect of substrate substituents on enantioselectivity. Dalton Trans 5524–5530
104. Godard C, Munoz BK, Ruiz A, Claver C (2008) Pd-catalysed asymmetric mono- and bis-alkoxycarbonylation of vinylarenes. Dalton Trans 853–860
105. Diab L, Gouygou M, Manoury E, Kalck P, Urrutigoïty M (2008) Higly regioselective Palladium-catalyzed methoxycarbonylation of styrene using chiral ferrocene- and biphosphole-based ligands. Tet Lett 49:5186-5189
106. Bolm C, Hildebrand JP, Muniz K, Hermanns N (2001) Catalyzed asymmetric arylation reactions. Angew Chem Int Ed 40:3285–3308
107. Bringmann G, Price Mortimer AJ, Keller PA, Gresser MJ, Garner J, Breuning M (2005) Atroposelective synthesis of axially chiral biaryl compounds. Angew Chem Int Ed 44:5384–5427
108. Baudoin O (2005) The asymmetric Suzuki coupling route to axially chiral biaryls. Eur J Org Chem 20:4223–4229
109. Noyori R (2003) Asymmetric catalysis: science and opportunities (Nobel lecture 2001). Adv Synth Catal 345:15–32
110. Kumobayashi H, Miura T, Sayo N, Saito T, Zang X (2001) Recent advances of BINAP chemistry in the industrial aspects. Synlett 1055–1064
111. Chen Y, Yekta S, Yudin AK (2003) Modified BINOL ligands in asymmetric catalysis. Chem Rev 103:3155–3211
112. Brunel JM (2005) BINOL: a versatile chiral reagent. Chem Rev 105:857–897
113. Hayashi T (2000) Chiral monodentate phosphine ligand MOP for transition-metal-catalyzed asymmetric reactions. Acc Chem Rev 33:354–362
114. Kocovsky P, Vyskocil S, Smrcina M (2003) Non-symmetrically substituted 1,1′-binaphthyls in enantioselective catalysis. Chem Rev 103:3213–3245

115. McCarthy M, Guiry PJ (2001) Axially chiral bidentate ligands in asymmetric catalysis. Tetrahedron 57:3809–3844
116. Shimizu H, Nagasaki I, Saito T (2006) Recent advances in biaryl-type bisphosphine ligands. Tetrahedron 61:5405–5432
117. Cammidge AN, Crépy KVL (2000) The first asymmetric Suzuki cross-coupling reaction. Chem Commun 1723–1724
118. Yin JJ, Buchwald SL (2000) A catalytic asymmetric Suzuki coupling for the synthesis of axially chiral biaryl compounds. J Am Chem Soc 122:12051–12052
119. Genov M, Almorín A, Espinet P (2006) Efficient synthesis of chiral 1,1′-binaphthalenes by the asymmetric Suzuki-Miyaura reaction: dramatic synthetic improvement by simple purification of naphthylboronic acids. Chem Eur J 12:9346–9352
120. Bronger RPJ, Guiry PJ (2007) Aminophosphine-oxazoline and phosphoramidite-oxazoline ligands and their application in asymmetric catalysis. Tetrahedron Asym 18:1094–1102
121. Sawai K, Tatumi R, Nakahodo T, Fujihara H (2008) Asymmetric Suzuki–Miyaura coupling reactions catalyzed by chiral palladium nanoparticles at room temperature. Angew Chem Int Ed 47:6917–6919
122. Bermejo A, Ros A, Fernández R, Lassaletta JM (2008) C-2-symmetric bis-hydrazones as ligands in the asymmetric Suzuki–Miyaura cross-coupling. J Am Chem Soc 130:15798–15799
123. Mori K, Kondo Y, Yamashita H (2009) Synthesis and characterization of FePd magnetic nanoparticles modified with chiral BINAP ligand as a recoverable catalyst vehicle for the asymmetric coupling reaction. Phys Chem Phys 11:8949–8954
124. Uozumi Y, Matsuura Y, Arakawa T, Yamada YMA (2009) Asymmetric Suzuki–Miyaura coupling in water with a chiral palladium catalyst supported on an amphiphilic resin. Angew Chem Int Ed 48:2708–2710
125. Malacea R, Manoury E, Poli R (2010) Asymmetric hydrosilylation, transfer hydrogenation and hydrogenation of ketones catalyzed by iridium complexes. Coord Chem Rev 254:729–752
126. Le Roux E, Malacea R, Manoury E, Poli R, Gonsalvi L, Peruzzini M (2007) Highly efficient asymmetric hydrogenation of alkyl aryl ketones catalyzed by iridium complexes with chiral planar ferrocenyl phosphino-thioether ligands. Adv Synth Catal 349:309–313
127. Dahlenburg L, Goetz R (2004) Iridium complexes with chiral and achiral β-aminophosphane ligands: catalysts for C=O hydrogenation and H/D exchange involving both homo- and heterolytic H_2 activation. Eur J Inorg Chem 888–905
128. Dahlenburg L, Goetz R (2004) Functional phosphines. Part XIV. Cationic (P,N)2-coordinated hydrides of iridium(III): catalysts for C=O hydrogenation or transfer hydrogenation? Inorg Chim Acta 357:2875–2880
129. Hayes JM, Ujaque G, Lledós A, Malacea R, Manoury E, Vincendeau S, Poli R, in preparation
130. Iron MA, Sundermann A, Martin JML (2003) Catalytic reduction of acetone by (bpy)Rh (+): a theoretical mechanistic investigation and insight into cooperativity effects in this system. J Am Chem Soc 125:11430–11441
131. Tollner K, Popovitzbiro R, Lahav M, Milstein D (1997) Impact of molecular order in Langmuir–Blodgett films on catalysis. Science 278:2100–2102

Chapter 6
Phosphinine-Based Ligands in Homogeneous Catalysis: State of the Art and Future Perspectives

Christian Müller and Dieter Vogt

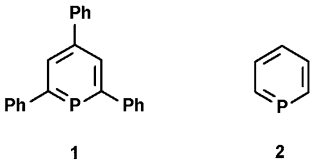
Abstract Despite the fact that phosphinines are known for more than 40 years and possess a rich and versatile coordination chemistry, investigations on their application as ligands in homogeneous catalysis are still comparatively rare. Nevertheless, their particular electronic and steric properties compared to classical phosphorus ligands, as well as the facile access to the related bicyclic phosphabarrelenes might lead to significant breakthroughs in homogeneous catalysis in the near future. So far, studies are limited to only a few examples but several promising results have recently emerged. State-of-the-art synthetic methodologies allow nowadays a straightforward derivatization and functionalization of phosphinine-based ligands and systems with tailored properties can thus be expected. This chapter exclusively focuses on phosphinines and phosphabarrelenes. Selected synthetic procedures for the preparation of functionalized ligands are presented and examples of their coordination chemistry towards catalytically relevant transition metals are provided. A detailed overview on their application as ligands in homogeneous catalysis is given.

6.1 Introduction

Homogeneous catalysis is a research area that has grown enormously in recent years and contributes nowadays significantly to both intermediates and fine chemicals production [1]. Homogeneous catalysts are uniquely amenable to

C. Müller (✉) · D. Vogt
Department of Chemical Engineering and Chemistry, Homogeneous Catalysis and Coordination Chemistry, Eindhoven University of Technology,
5600 MB Eindhoven, The Netherlands
e-mail: c.mueller@tue.nl

M. Peruzzini and L. Gonsalvi (eds.), *Phosphorus Compounds*,
Catalysis by Metal Complexes, 37, DOI: 10.1007/978-90-481-3817-3_6,
© Springer Science+Business Media B.V. 2011



1 2

Fig. 6.1 2,4,6-Triphenylphosphinine **1** and parent phosphinine **2**

modifications at the molecular level; steric and electronic properties can be tailored and chirality can be introduced with high precision. This molecular engineering can currently be achieved with such sophistication that tailor-made catalysts for specific chemical transformations become feasible. Research in late-transition-metal mediated homogeneous catalysis has focused mainly on a few ligand classes, such as phosphines, phosphites, pyridine-derivatives, carbenes and carbocyclic (e.g. cyclopentadienyl) ligands, while phosphorus undoubtedly plays a key role in the development of modern ligand systems for a range of homogeneous catalytic reactions. Yet, nearly all phosphorus containing ligands have in common that they are based on trivalent phosphorus centers. In contrast, the application of λ^3-phosphinines (phosphabenzenes), which contain a low-coordinated and formally sp^2-hybridized phosphorus atom, have received much less attention. With the synthesis of 2,4,6-triphenylphosphinine (**1**) by Märkl in 1966 and the parent phosphinine C_5H_5P (**2**) by Ashe III, in 1971, the stabilization of reactive P=C double bonds by incorporation into aromatic systems opened up the access to phosphorus systems with significantly different electronic and steric properties compared to classical ligands based on trivalent phosphorus (Fig. 6.1) [2, 3].

Phosphinines have long been regarded as "chemical curiosities" but state-of-the-art synthetic methodologies, developed mainly by the groups of Mathey and Le Floch, allow nowadays specific derivatization and functionalization [4–6]. In the last few years, our group has focused on the design of (donor-)functionalized and chiral 2,4,6-triaryl-substituted phosphinines, which turned out to be accessible via the original pyrylium salt route. These derivatives often show a considerable kinetic stability and are often inert towards water, oxygen and many acids and bases, which facilitates their preparation and functionalization [7].

6.2 Phosphinines—Electronic Properties

Phosphinines are planar, aromatic systems. Theoretical calculations suggest their aromaticity to be as high as 88% of benzene [8, 9]. The electronic properties of phosphinines differ from pyridines, as shown by photoelectron and electron transmission spectroscopy as well as by theoretical calculations [10–13]. The $HOMO^{-2}$ orbital has a large coefficient at the phosphorus atom and represents essentially the lone-pair at the heteroatom. The phosphorus lone-pair occupies a more diffuse, partly delocalized, and less directional orbital than that of pyridine. While the $HOMO^{-1}$ and HOMO orbitals contribute to π-donation, the LUMO

orbital, with a large coefficient at the phosphorus atom, enables the heterocycle to act as a π-acceptor ligand, once coordinated to the metal center via the phosphorus atom (Fig. 6.2). In pyridines, the LUMO is located higher in energy compared to phosphinines, while the HOMO represents the lone pair located at the nitrogen atom. Consequently, phosphinines are much better π-acceptor ligands, but less good σ-donors compared to pyridines. The phosphorus atom in λ^3-phosphinines has a strong 3*s*-orbital character, which is about 63.8%, versus 29.1% found for the nitrogen atom in pyridines [14]. This reflects the poor hybridization ability of phosphorus, that leads to a very low basicity of the phosphorus center (pK_a ($C_5H_6P^+$) $= -16.1 \pm 1.0$ in aqueous solution) [15].

Phosphinines show a typical downfield shift of about $\delta = +200$ ppm in the $^{31}P\{^1H\}$ NMR spectrum, and all peripheral protons show chemical shift values downfield from benzene in the ^1H NMR spectrum. These phenomena can be attributed to the presence of a diamagnetic ring current typical for aromatic systems. Nucleus-independent chemical shift values (NICS) of phosphinines lead to the same conclusion [14]. In order to quantify the electronic properties of ligands, Tolman's electronic parameter χ (chi) can be used to compare different monodentate systems [16]. These values are usually obtained using the IR stretching frequencies of the corresponding $LNi(CO)_3$ complexes, with L = P(*t*-Bu)$_3$ as the reference. While a large χ value indicates strong π-acceptor properties of the ligand due to a reduced π-back donation from the metal center to the CO ligand, a small value of χ is indicative of strong σ-donation. An ideal probe for determining the electronic properties of monodentate phosphinine ligands is the IR stretching frequency of the CO ligand in *trans*-$L_2Rh(CO)Cl$ complexes. In fact, the synthesis

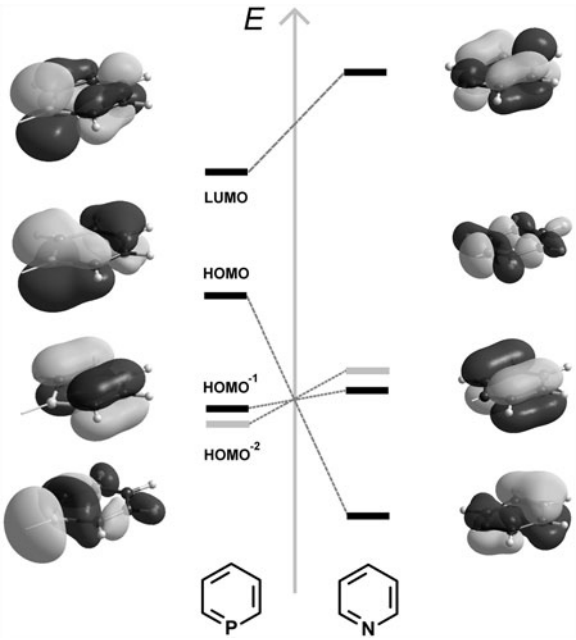


Fig. 6.2 Qualitative MO-diagram of the frontier orbitals of phosphinine and pyridine. *Light grey* MO representing the lone-pair

Table 6.1 Selected χ-values of P-Ligands

Ligand	χ	$\nu_{CO(Ni)}$ (cm^{-1})	$\nu_{CO(Rh)}$[b] (cm^{-1})
Phosphinine[a]	24[15]	–	1999
PPh_3	12.9	2069	1979
PEt_3	5.6	2062	1958
$P(OPh)_3$	29.1	2085	2016 [18]
$P(OMe)_3$	23.3	2076	2006 [19]
$P[O(2\text{-}t\text{-}BuC_6H_4)]_3$	30	2086	2013

[a] 2,4,6-Triphenylphosphinine
[b] *Trans*-$L_2Rh(CO)Cl$ complex

of $LNi(CO)_3$ complexes attracts nowadays much less attention due to the extreme toxicity and inconvenience of Ni-carbonyls and correlations between values derived from $LNi(CO)_3$ complexes and various metal carbonyl species exist [17].

Table 6.1 shows typical values for phosphinines in comparison with phosphines and phosphites, which suggest that phosphinines are electron withdrawing ligands (π-acceptors) with properties similar to phosphites as already anticipated from the corresponding MO scheme (Fig. 6.2).

6.3 Phosphinines—Structural Characteristics and Steric Properties

Several λ^3-phosphinines have been characterized crystallographically [20]. Figure 6.3 shows part of the molecular structure of phosphinine **3** [7]. The thienyl-substituents in *ortho*- and the phenyl group in *para*-position have been excluded for clarity and only the corresponding *ipso*-carbon atoms (C6, C12, C16) of those substituents are shown. The phosphorus heterocycle is essentially planar and can best be described as a distorted hexagon due to the larger size of the phosphorus atom in comparison to a carbon atom. The P–C_α bond lengths lie in-between a P–C single bond (triphenylphosphine: 1.83 Å [21]) and a P–C double bond (diphenylmethylenephosphaalkene: 1.66 Å [22]). There is no bond alternation between the C–C ($\sim$1.39 Å) and the P–C ($\sim$1.75 Å) bond lengths, which indicates delocalization of the π-system and the presence of an aromatic system. The internal C–P–C angle of approximately 100° is somewhat smaller compared to the C–N–C angle in pyridine (117°) [23]. This phenomenon is attributed mainly to the poor ability of phosphorus orbitals to hybridize, rather than to the lengthening of the heteroatom-carbon bond. From the planarity of the P-heterocycle it becomes obvious that the steric demand of such ligand systems is significantly different compared to trivalent phosphines. Tolman's steric parameter θ (cone angle), which provides a measure of the volume around a metal center occupied by a ligand, is not appropriate to describe the steric properties of phosphinines. In fact, the occupancy angles α and β along the two orthogonal planes x and y, show that the steric demand in the y plane is relatively small, while very large in the x plane.

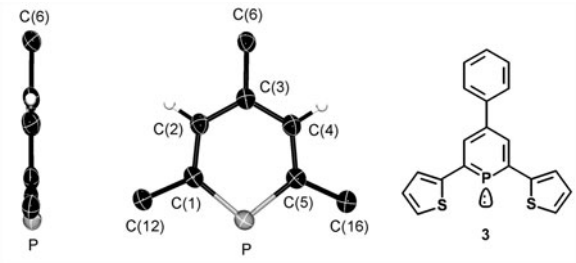


Fig. 6.3 Molecular structure of the bis-thienyl-substituted phosphinine **3**. Only part of the structure is shown. Side-view (*left*), front view (*middle*). Selected bond lengths (Å) and angles (°): P–C(1): 1.749, P–C(5): 1.750, C(1)–(C2): 1.398, C(2)–C(3): 1.394, C(3)–C(4): 1.394, C(4)–C(5): 1.392. C(1)–P–C(5): 101.37

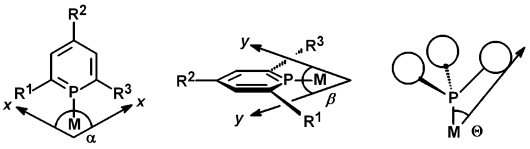


Fig. 6.4 Occupancy angles α and β of a phosphinine and cone-angle θ of a phosphine

This leads to a flattened rather than a symmetrical cone and the steric demand of phosphinines can thus be better described by the occupancy angles α and β rather than by the cone angle θ (Fig. 6.4) [24].

6.4 Synthetic Access to Phosphinines

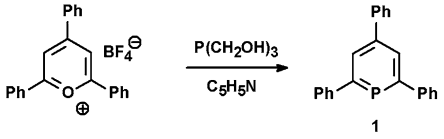
The first reported phosphinine was prepared from 2,4,6-triphenylpyrylium tetrafluoroborate and $P(CH_2OH)_3$ in refluxing pyridine, and was obtained as a yellow air- and moisture stable solid in 24–30% yield (Scheme 6.1) [2].

Although largely neglected in phosphinine-research, this route is a highly flexible and modular procedure. Our group showed, that starting from functionalized benzaldehydes and acetophenones, the stepwise assembly of the phosphorus containing heterocycle via pyrylium salts allows the incorporation of various (donor-) substituents into specific positions of the 2,4,6-triarylphosphinine core [7]. In this way, the steric and electronic properties of phosphinine-based ligands can be varied to a certain extend.

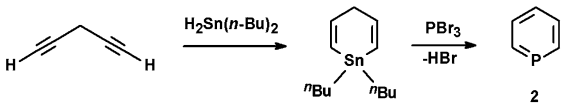
A synthetic access to the unsubstituted parent compound C_5H_5P has been developed by Ashe III, in 1971. Hydrostannation of 1,4-pentadiyne with $H_2Sn(n\text{-}Bu)_2$ yields 1,4-dihydro-l,l-dibutylstannabenzene in good yields. Reaction with PBr_3 gives C_5H_5P under loss of HBr (Scheme 6.2) [3].

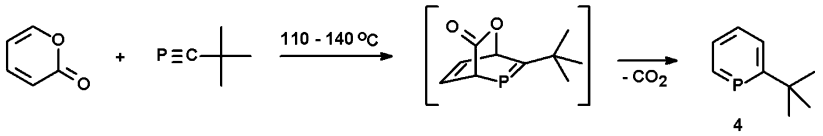
Regitz et al. described [4 + 2] cycloaddition reactions of phosphaalkynes with cyclopentadienones or pyrones under subsequent exclusion of CO and CO_2, respectively. In this way, alkyl-substituted phosphinines, such as **4**, are synthetically accessible (Scheme 6.3) [25, 26].

Scheme 6.1 2,4,6-Triphenylphosphinine synthesis via pyrylium salt

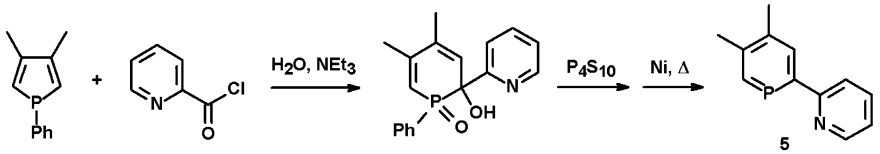


Scheme 6.2 Synthesis of the parent phosphinine **2** from 1,4-pentadiyne

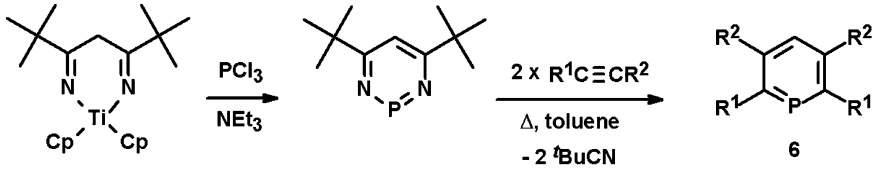




Scheme 6.3 Synthesis of phosphinines from pyrones



Scheme 6.4 Synthesis of phosphinines via ring-expansion



Scheme 6.5 Synthesis of phosphinines from diazaphosphinines

Ring-expansion reactions of phospholes by formal insertion of methylene fragments lead to 2-substituted phosphinines as described by Mathey et al. In this way, the first phosphinine derivative of 2,2′-bipyridine (NIPHOS, **5**) was synthesized (Scheme 6.4) [27].

The use of (di)azaphosphinines as precursors has been investigated by Le Floch and Mathey and co-workers and is especially suitable for the introduction of substituents into the 2- and 6-position of the heterocyclic framework (Scheme 6.5) [28].

6.5 Chiral Phosphinines

The planarity of phosphinines and the formal sp^2-hybridization of the phosphorus atom do not allow the introduction of P-stereogenic centers within the heterocycle, as it is common for classical phosphines based on a trivalent phosphorus atom.

Until recently, the implementation of chirality to phosphinines was in fact limited to the introduction of chiral auxiliaries within the phosphinine-framework, such as (+) camphor (**7**), oxazoline– (**8**), dicyclohexyl-1,2-ethanediol (**9**) or binaphthyl-groups (**11**) (Fig. 6.5) [29–32].

Our group started to investigate the synthetic access to polymethyl-substituted phosphinines in order to generate axial chirality. The introduction of an *o*-xylyl group in 6-position and an additional $-CH_3$ group in 5-position of the heterocycle via the pyrylium salt route gave a racemic mixture of the (S_a) and (R_a) enantiomer of phosphinine **10** (Fig. 6.5, only the S_a enantiomer is shown) [33, 34]. Chiral resolution could be achieved by chiral HPLC. The rotational barrier of $\Delta G^{\#} = 109.5$ kJ/mol was determined experimentally by means of racemization experiments.

The first C_2-symmetrical chiral phosphinine **12** was recently reported by Garner and co-workers and prepared from the corresponding biscamphorpyrylium salt and $P(SiMe_3)_3$ (Scheme 6.6) [35].

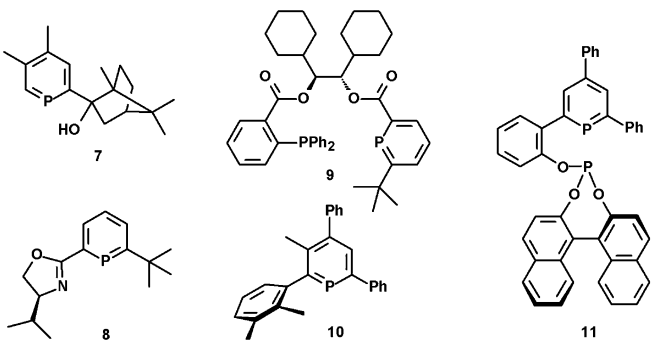
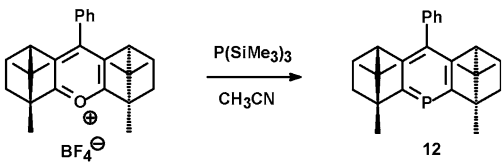


Fig. 6.5 Chiral phosphinines

Scheme 6.6 Chiral C_2-symmetric phosphinine



6.6 Transition Metal Complexes and Coordination Modes

Due to their particular electronic properties, phosphinines are especially suitable for the stabilization of late transition metal centers in low oxidation states. Phosphinines as ambidentate ligands possess two different potential coordination sites, the lone pair of the phosphorus atom and the aromatic π-system. As mentioned above, the $HOMO^{-2}$ of a phosphinine ligand is suitable for σ-coordination towards a metal center. Its energy is close to the energy of the $HOMO^{-1}$ and HOMO orbitals that can participate in η^6-coordination. This leads to a range of coordination modes and Fig. 6.6 represents the most common ones [36–38]. Representative examples with transition metals potentially relevant for homogeneous catalytic reactions are shown in Figs. 6.7, 6.8, 6.9, 6.10, 6.11, 6.12, 6.13, and 6.14.

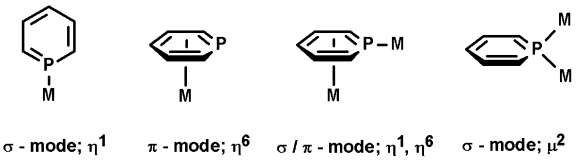


Fig. 6.6 Common coordination modes of phosphinines

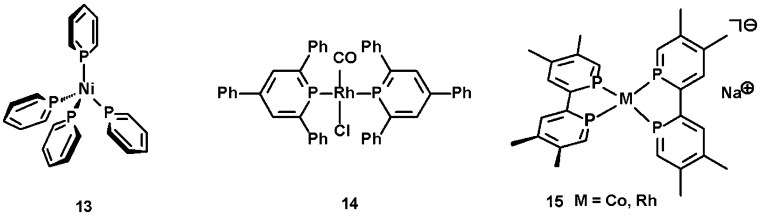


Fig. 6.7 Transition metal complexes of phosphinines (σ-coordination mode)

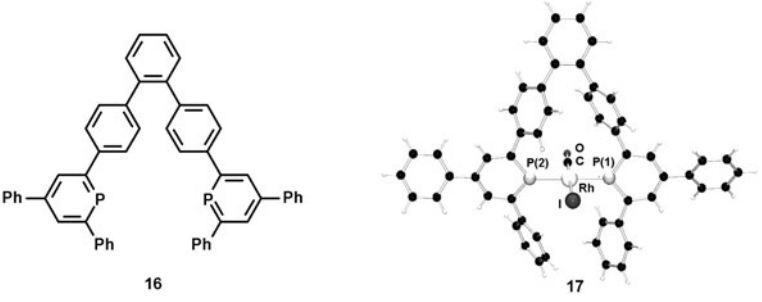


Fig. 6.8 Trans-coordinating di-phosphinine **16** and molecular structure of the corresponding Rh(I) complex **17** in the crystal

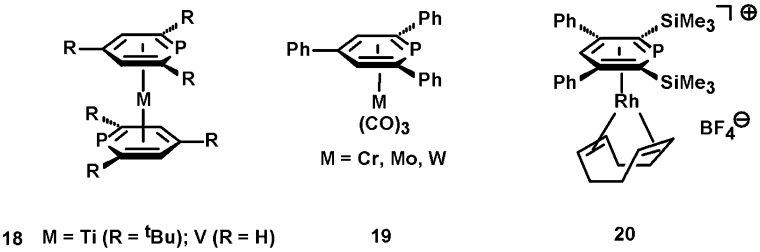


Fig. 6.9 Transition metal complexes of phosphinines (π-coordination mode)

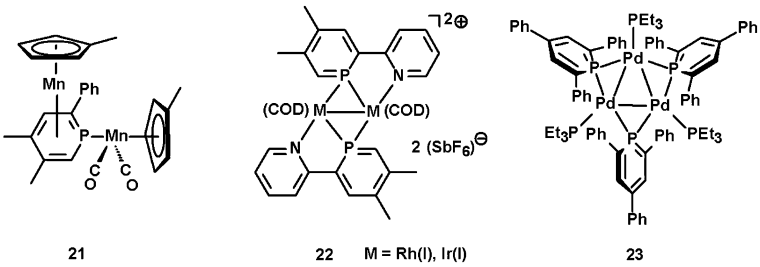


Fig. 6.10 Transition metal complexes of phosphinines (σ/π and bridging coordination mode)

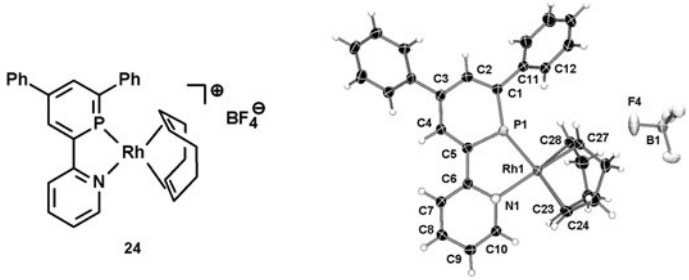


Fig. 6.11 Rh(I) complex containing a phosphinine derivative of 2,2′-bipyridine and the molecular structure of **24** in the crystal

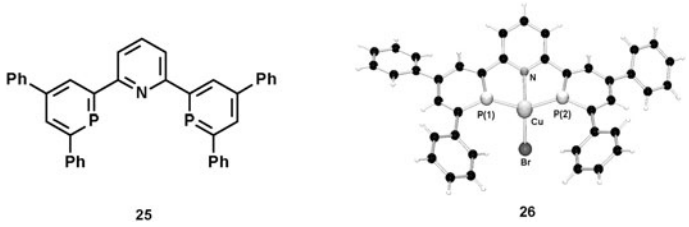


Fig. 6.12 Neutral PNP pincer ligand **25** and molecular structure of the corresponding Cu(I) complex **26** in the crystal

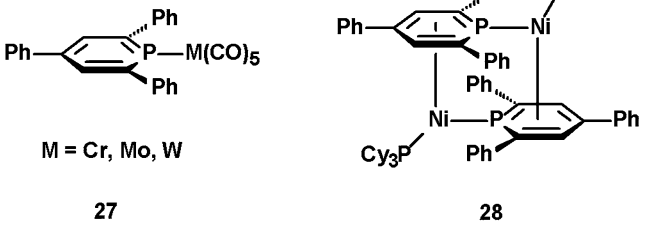
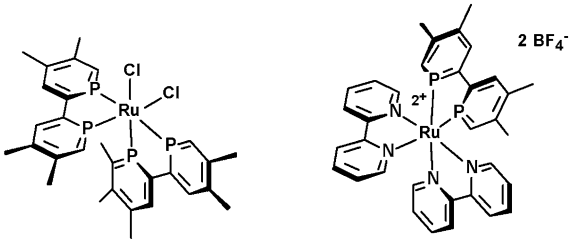


Fig. 6.13 Transition metal complexes of phosphinines (σ- and σ/π-coordination mode)

Fig. 6.14 Ru(II) complexes containing the tmbp ligand



The coordination mode through the phosphorus atom (σ-coordination, $2e^-$ donation) is the most common one and is generally observed with late transition metals in low oxidation states, due to the strong π-acceptor properties of the phosphinine ligand. This has been shown, for example, in homoleptic η^1-phosphinine complexes of the type [Ni(η^1-$C_5H_5P)_4$] (**13**) and [Fe(η^1-$C_5H_5P)_5$], reported by Elschenbroich et al. or in the Rh(I) complex $L_2Rh(CO)Cl$ ($L = C_5H_2(Ph)_3P$) (**14**) described by Breit et al. (Fig. 6.7) [39–41]. The stabilization of reduced transition metal complexes has been reported by Le Floch et al. and realized in structurally characterized Rh(1-) and Co(1-) complexes of 2,2′-bisphosphinines of the type **15** (Fig. 6.7) [42].

In cooperation with the group of van Leeuwen, we have started to investigate the access to *trans*-coordinating di-phosphinines via the classical and modular pyrylium salt route. Compound **16** is based on a terphenyl-backbone and the corresponding Rh(I) complex **17** was characterized crystallographically (Fig. 6.8) [43].

The η^6-coordination mode is typically observed in early transition metal complexes in order to compensate for the electron deficiency of the metal center (Fig. 6.9). This has been reported, for example, for Ti(0) and V(0) complexes (**18**), or in combination with additional π-acceptor ligands as in $LM(CO)_3$ complexes (M = Cr, Mo, W) (**19**) [44–47]. Moreover, the η^6-coordination mode can be imposed by steric effects as it has been found in complexes containing phosphinines with sterically demanding substituents, such as *t*-butyl– or Me_3Si– groups in *ortho*-position (**20**), which prevents σ-coordination via the lone-pair [48, 49].

The mixed η^1–η^6 binding mode in which the phosphinine behaves as an $8e^-$ donor, has been found for metals in the center of the transition series, such as the manganese complex **21** depicted in Fig. 6.10 [50].

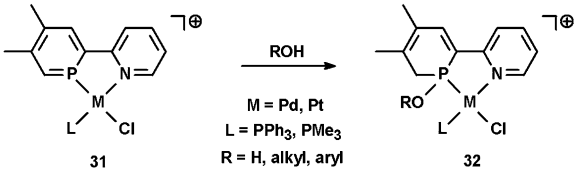
A very unusual coordination mode has been reported by Venanzi et al. In the cationic dinuclear complexes (NIPHOS)-Rh(I) and (NIPHOS)-Ir(I) of the type **22** the phosphinine acts as a bridging ligand for two metal centers, while the phosphorus atom is still considered as a two-electron donor [51]. This is attributed to the nature of the lone-pair, which has a strong 3*s*-orbital character and is more diffuse and less directed compared to pyridines and could therefore give rise to the formation of formally two M–P bonds. A similar coordination mode was observed in the *triangulo* Pd_3 cluster **23**, reported by Reetz et al., which contains three bridging phosphinines. The analysis of MO interactions shows that the bonding between the phosphinine ligands and the metal core involves both σ-and π-orbitals [52]. A mononuclear Rh(I) complex containing 2-(2′-pyridyl)-4,6-diphenyl-phosphinine as a chelating P,N-hybrid ligand has been reported by our group (Fig. 6.11) [53]. The metal center in **24** is not located in the ideal axis of the phosphorus lone-pair and clearly shifted towards the nitrogen atom. Obviously, this non-directional coordination mode is necessary for a proper complexation of the Rh atom by the ligand and enabled by the more diffuse lone pair of the low-coordinated phosphorus atom compared to the sp^2-hybridized nitrogen atom in pyridines. Consequently, this phenomenon is not observed for the N1–Rh interaction. A *trans* influence of the P-atom can further be noticed in the longer Rh–cod bonds compared to the corresponding Rh–cod bonds *trans* to the N-atom.

The di-phosphinine derivative of terpyridine (**25**), recently developed by us, consists both of a σ-donative pyridine group and of two π-accepting phosphinine donors (Fig. 6.12) [54]. This compound was also synthesized according to the classical and modular pyrylium salt route. Due to the presence of electronically rather inequivalent donor atoms, these compounds represent therefore a new class of π-accepting PNP-pincer ligands. As a matter of fact neutral PNP-pincers with such electronic properties are very rare. In contrast to its terpyridine analogue facile coordination of **25** towards a neutral Cu(I) center was observed and the corresponding Cu(I)Br complex **26** was characterized crystallographically. The molecular structure in the crystal revealed a distorted tetrahedral coordination geometry of the metal center as a result of an unusual coordination mode of the two phosphinine ligands (Fig. 6.12). These results might lead to transition-metal complexes with new properties and applications, especially in homogeneous catalysis and as optoelectronic devices in the near future.

Coordination modes which differ from the above mentioned "rule-of-thumb" have also been observed, for example, in complex **27**, in which the phosphinine is η^1-coordinated to a $M(CO)_5$ fragment (M = Cr, Mo, W) [55, 56]. In the Nickel complex **28**, reported by Lehmkuhl et al., the phosphinine ligands both coordinate to the metal centers in a σ- and π- coordination mode (Fig. 6.13) [57].

The stabilization of higher oxidation states by phosphinines is possible by making use of the chelate effect. 4,4′,5,5′-tetramethylbiphosphinine (tmbp) has

Scheme 6.7 Formation of dihydrophosphinines



been applied to prepare phosphorus analogs of $[Ru(bipy)_n]^{2+}$ and the Ru(II) complexes **29** and **30** were isolated and characterized (Fig. 6.14) [37, 58].

Cationic Pd(II) and Pt(II) complexes of the type **31** containing the bidentate NIPHOS ligand have been reported by Venanzi and co-workers, but not isolated. These species are highly sensitive towards water and alcohols, demonstrating the fact that phosphinine complexes are prone to nucleophilic attack on the phosphorus atom (Scheme 6.7) [59]. This reactivity, however, has not been fully rationalized, yet. Because state-of-the-art synthetic methodologies allow nowadays a straightforward derivatization and functionalization of phosphinines, a kinetic stabilization of these complexes might be feasible.

6.7 Phosphinines in Homogeneous Catalysis

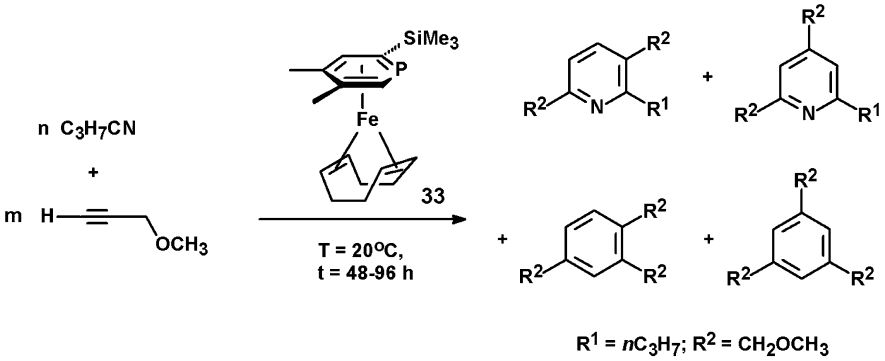
6.7.1 Fe-Catalyzed Cyclotrimerizations and Cyclodimerizations

The first application of a phosphinine-based catalyst in homogeneous catalysis was reported in 1996 by Zenneck et al. The η^6-phosphinine-iron complex **33** was used in the catalytic [2 + 2 + 2] cyclotrimerization of the electron-poor alkyne dimethyl acetylenedicarboxylate to give $C_6(CO_2Me)_6$ and in the co-cyclotrimerization of methyl propargylether with butyronitrile affording functionalized pyridine derivatives (Scheme 6.8) [60]. Turnover-numbers of up to 160 for the pyridine derivatives and chemoselectivities of up to 1.4:1 (pyridines:arenes) were observed. Nevertheless, the efficiency of **33** is significantly lower compared to classical CpCo catalysts [61, 62].

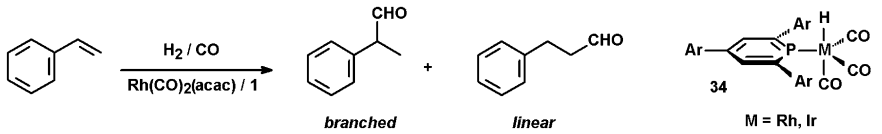
The same group reported on the catalytic cyclodimerization of 1,3-butadiene towards cyclooctadiene (COD) and vinyl cyclohexene (VCH) using (DAD)-η^6-phosphinine-iron(0) complexes (DAD = diazadiene) and $[(Et_2AlOEt)_2]$ as cocatalyst. The reaction produces 64% COD ([4 + 4] cycloaddition) and 36% VCH ([4 + 2] cycloaddition) but the turnover-numbers for their formation are relatively low (COD: TON = 94; VCH: TON = 54) [63].

6.7.2 Rh-Catalyzed Hydroformylations

An important contribution has been described by Breit et al. who explored the application of phosphinines in the Rh-catalyzed hydroformylation of various



Scheme 6.8 Cyclotrimerization reaction with an η^6-phosphinine-Fe(0) complex



Scheme 6.9 Rh-catalyzed hydroformylation of styrene and hydrido-carbonyl Rh(I) and Ir(I) complexes

alkenes [64–66]. These are probably the most prominent examples for the use of phosphinines as ligands in homogeneous catalytic reactions. While α-unsubstituted phosphinines inhibit the catalytic cycle, 2,4,6-trisubstituted ligands showed both high activity and high regioselectivity in the formation of the branched product in the Rh-catalyzed hydroformylation of styrene (Scheme 6.9).

While the regioselectivity towards the branched product is comparable to PPh_3 and P(O(*o*,*p*-*t*Bu)Ph)$_3$ as representatives of classical phosphines and phosphites ($\sim$20:1; b:l), the activity of the phosphinine-based system is much higher under very mild hydroformylation conditions (T = 25 °C; p = 20 bar CO/H_2; Rh: L = 1:5; TOF/h^{-1}: 28.7 (2,4,6-triphenylphosphinine 1) vs 16.4 (phosphite) and 7.5 (phosphine), respectively). The high activity of the Rh-phosphinine complex nicely reflects the electronic and steric situation of the ligand system: electron-withdrawing substituents or π-acceptor ligands generally favour CO-dissociation from the metal center, leading consequently to higher activities. High pressure NMR studies (p = 40 bar CO/H_2) on analogous and more stable iridium(I) systems revealed the presence of a trigonal bipyramidal hydrido complex of the type **34**, which is also expected for the corresponding Rh(I) complex. These experiments show, that most likely only one phosphinine ligand is coordinated to the transition metal center under hydroformylation conditions due to the substituents in C_α-position of the heterocycle. The subtle combination of electronic and steric properties seems to account for very high hydroformylation activities.

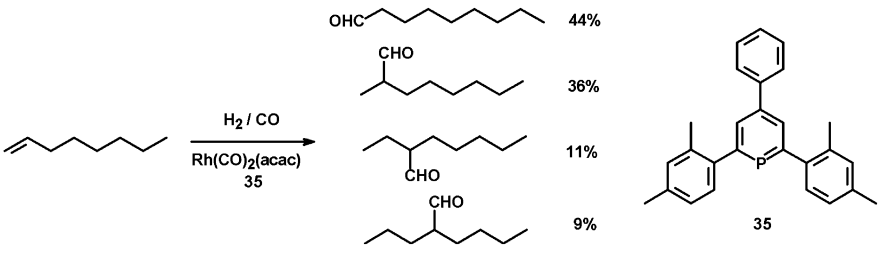
In this respect, 2,4,6-triphenylphosphinine **1** was also successfully applied in the hydroformylation of less reactive internal alkenes, such as cyclohexene. It was

demonstrated that the corresponding Rh-catalyst is as active as catalysts based on monodentate bulky triarylphosphites, which belong to one of the most active ligand-modified hydroformylation catalysts known to date (T = 90 °C; p = 20 bar CO/H_2; Rh:L = 1:10; TOF/h^{-1}: 214 (phosphinine) vs 216 (P(O(*o*-^{t}Bu)Ph)$_3$)).

Based on the results obtained with monodentate ligands, Breit et al. described the synthesis of chiral bidentate phosphinine-based systems with electronic differentiation of the two binding sites and their application in the Rh-catalyzed hydroformylation of styrene in comparison with PPh_3. The phosphine-phosphinine combination as represented by ligand **9** (Fig. 6.5) is electronically similar to a phosphine-phosphite ligand, while the oxazoline fragment in ligand **8** (Fig. 6.5) represents a hard σ-donor site. Under the same reaction conditions (T = 20 °C; p = 50 bar CO/H_2; t = 22 h), the PPh_3-Rh systems showed 31% conversion and a regioselectivity of 25.8:1 (b/l; Rh:L = 1:20). This is comparable with the **9**-Rh catalyst, which gave a conversion of 42% and a good regioselectivity of 21.4:1 (b/l; Rh:L = 1:2). Interestingly, quantitative conversion of styrene to phenylpropionaldehyde with a good regioselectivity of 25:1 (b/l; Rh:L = 1:2) was achieved with the system **8**-Rh. However, even though chiral ligands were applied in the hydroformylation reaction, no significant enantiomeric excess of any of the two 2-phenylpropionaldehyde enantiomers could be detected.

In the screening of various monodentate phosphinines for the Rh-catalyzed hydroformylation of 1-octene, the substituted bulky 2,4,6-triphenylphosphinine derivative 35 (Scheme 6.10) was found to show superior performance over classical PPh_3-based catalysts. Turnover frequencies of up to 45370 h^{-1} have been determined (T = 130 °C; p = 40 bar CO/H_2; Rh:L = 1:20), although the selectivity towards the linear product nonanal is low, as anticipated for a monodentate ligand (l/b ~ 2). Nevertheless, complete and rapid consumption of internal octenes, which have been formed by isomerization reaction prior to hydroformylation, occurred, showing the potential of these catalyst systems for the hydroformylation of less-reactive and internal alkenes (Scheme 6.10).

The hydroformylation of internal and substituted alkenes with **35**-Rh, such as 2-octene, cyclohexene, isobutene and methallyl alcohol showed better performance compared to the PPh_3-Rh catalyst. Most strikingly, selective hydroformylation of α-pinene and tetramethylethylene, which undergoes a tandem isomerization-hydroformylation, can be achieved with **35**-Rh, although with low



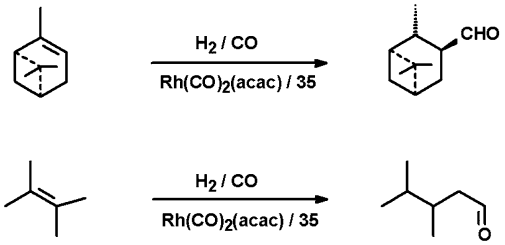
Scheme 6.10 Rh-catalyzed hydroformylation of 1-octene

rates (Scheme 6.11). These substrates are among the least reactive substrates and cannot be hydroformylated with the PPh_3-Rh system.

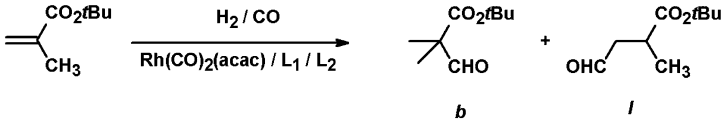
These impressive examples demonstrate that phosphinines have great potential as ligands in the hydroformylation reaction. As described above, the high activity in the hydroformylation of 1-octene as well as the isomerization activity and hydroformylation activity of less reactive alkenes can be attributed to the presence of monoligated Rh-species in combination with the strong π-acceptor capabilities of the ligand. Future developments in this area will most likely focus on the design and application of bidentate phosphinines, which should lead especially to more regioselective catalysts. It should be mentioned here that $^{31}P\{^{1}H\}$ NMR analysis of the hydroformylation mixtures showed that no phosphinine degradation had occurred during the catalytic runs indicating the stability of phosphinines under the applied hydroformylation conditions.

Recent work of Reetz et al. describes combinatorial approaches in homogeneous catalysis, such as the use of mixtures of achiral monodentate ligands (L_1, L_2) for catalytic reactions [67]. The authors suggest that appropriate mixtures may affect catalytic parameters, such as activity, selectivity and/or regioselectivity in non enantioselective reactions. Thus, a new and different catalytic profile may emerge if the heterocombination of ligands attached to the metal center leads to a more reactive species than the two homo-combinations. During the course of their investigations, also 1:1 mixtures of **35** and PPh_3 were used in the Rh-catalyzed hydroformylation of *tert*-butyl methacrylate (Scheme 6.12).

The homo-combinations of PPh_3 and phosphinine **35** both lead to the linear aldehyde as the major product (PPh_3: b/l = 0.72; **35**: b/l = 0.76; T = 50 °C, p = 60 bar CO/H_2, t = 22 h, S:Rh = 200:1). Moreover, a considerable amount of hydrogenated byproduct (6–13%) was observed. Interestingly, the application of the hetero-combination leads to a *reversed* regioselectivity and the branched aldehyde becomes the major product (PPh_3/**35**: b/l = 8.4). Much less hydrogenation was

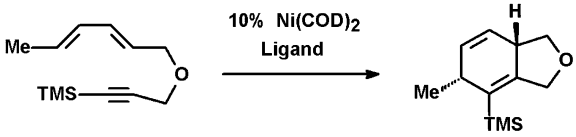


Scheme 6.11 Hydroformylation of substituted (less-reactive) alkenes



Scheme 6.12 Hydroformylation of *tert*-butyl methacrylate

Scheme 6.13 [4 + 2] Cycloaddition of a dieneyne



observed (1%), although the activity of the catalyst decreased substantially (conversion PPh_3: 72%; **35**: 72%; PPh_3/**35**: 39% after 22 h). Nevertheless further variation of the reaction conditions (T = 40 °C, p = 80 bar CO/H_2, t = 30 h) leads to a higher conversion (45%) and a b/l ratio of 20, which corresponds to 95% regioselectivity for the branched product.

6.7.3 Ni-Catalyzed Cycloisomerization

Due to the strong π-acceptor properties of phosphinines and their preference to stabilize late-transition metals in low oxidation states, successful applications of these ligands might be anticipated in reactions in which the rate determining step leads to an increase in the electron density at the metal center. This has been explored in the Ni-catalyzed intramolecular [4 + 2] cycloaddition of dieneynes, in which the reductive elimination of the product from the metal center is most likely the rate determining step (Scheme 6.13) [24].

Using a **1**/Ni catalyst, a maximum conversion of 92% within 20 h in cyclohexane could indeed be observed (T = 80 °C, 10% $Ni(COD)_2$). Under the same reaction conditions, lower conversions (70–89%) were achieved with the bulky phosphite $P(O–o–C_6H_4Ph)_3$. The reaction is strongly solvent dependent and a significant increase in rate was observed for the phosphinine/Ni system in passing from a coordinating solvent (THF, 7% conversion) to the non-coordinating solvent cyclohexane (63–92% conversion).

6.7.4 Rh- and Ir-catalyzed Hydrogenations

The above mentioned concept of combinatorial homogeneous catalysis has been extended by Reetz et al. to the use of mixtures of chiral and achiral monodentate phosphorus ligands for asymmetric transition metal catalysis. In the Rh-catalyzed asymmetric hydrogenation of acetamidoacrylate (Scheme 6.14) the homo-combination of a chiral phosphonite based on (*R*)-BINOL leads to an enantiomeric excess of *ee* = 93% of the (*S*)-enantiomer, while the homo-combination of the achiral phosphinine **35** gives essentially an inactive catalyst under the applied reaction conditions (T = 25 °C; p = 1.3 bar H_2; CH_2Cl_2; $Rh(cod)_2BF_4$ as Rh-precursor) [68]. Intriguingly, a reversal of enantioselectivity is observed with the heterocombination **35**/phosphonite and an enantiomeric excess of *ee* = 58.6% of the (*R*) enantiomer was found. According to the authors, a mixture of three different catalysts has to be considered in such systems, while the hetero-combination

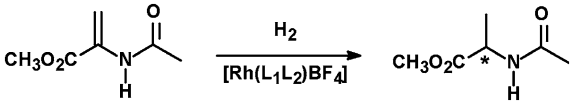
seems to be the most reactive one and essentially determines the catalytic profile of the catalyst.

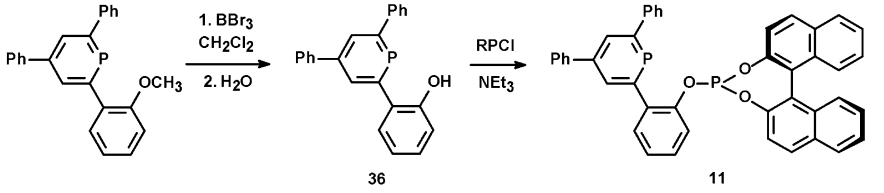
The first successful asymmetric reaction using a chiral phosphinine-based ligand was reported by our group [32]. The chiral BINOL-substituted phosphinine-phosphite **11** (Fig. 6.5) was obtained quantitatively from the hydroxy-substituted phosphinine **36** by reaction with the corresponding phosphorchloridite in the presence of an amine (Scheme 6.15).

Upon reaction of 11 with one equivalent of $[Rh(cod)_2]BF_4$ the loss of cyclooctadiene can be observed by NMR spectroscopy and the corresponding chiral rhodium complex $[(P^1P^2)Rh(cod)]BF_4$ (P^1: phosphinine-P; P^2: phosphite-P) was formed quantitatively. Figure 6.15 shows the $^{31}P\{^1H\}$ NMR spectrum of $[(\mathbf{11})Rh(cod)]BF_4$ and reveals that the phosphinine-phosphite ligand coordinates to the metal center in a bidentate fashion: a doublet of doublets (J_{Rh-P1} = 172.9 Hz, J_{P1-P2} = 68.8 Hz) at δ = 160.5 ppm is observed in the phosphinine region P^1 as well as in the phosphite region P^2 at δ = 136.5 ppm (J_{Rh-P2} = 243.2 Hz, J_{P2-P1} = 68.8 Hz).

The cationic Rh(I) complex was further applied in the asymmetric hydrogenation of dimethyl itaconate and methyl 2-(*N*-acetylamino)cinnamate, showing turnover frequencies of up to 2500 h^{-1} and enantioselectivities of up to 79% of

Scheme 6.14 Rh-catalyzed asymmetric hydrogenation





Scheme 6.15 Synthesis of chiral phosphinine-phosphites

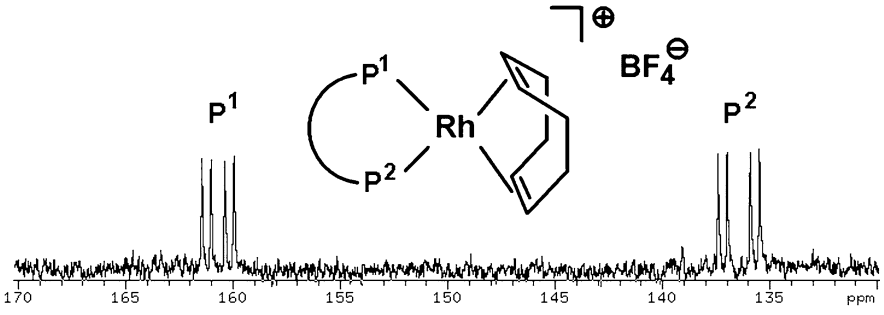
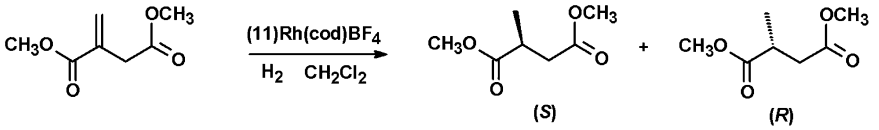
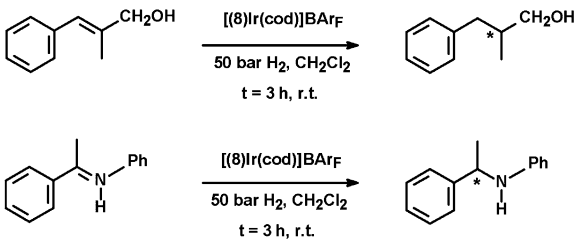


Fig. 6.15 $^{31}P\{^1H\}$ NMR spectrum of complex $[(\mathbf{11})Rh(cod)]BF_4$



Scheme 6.16 Rh-catalyzed hydrogenation of dimethyl itaconate with [(**11**)Rh(cod)]BF_4

Scheme 6.17 Ir-catalyzed hydrogenation of allyl alcohols and imines



(*S*)-methyl-succinate at T = 25 °C and a H_2 pressure of p = 10 bar (0.1 mol%, c_{Rh} = 1.25 mM, CH_2Cl_2). It should be mentioned, however, that although hydrogenation of the phosphinine ligand was not observed in the above mentioned catalytic transformations but cannot be excluded especially under more drastic hydrogenation conditions (Scheme 6.16).

A very recent example on the application of phosphinines in homogeneous catalysis was reported by Neumann [69]. The chiral oxazoline-functionalized phosphinine **8** (Fig. 6.5), first reported by Breit et al., was applied in the Ir-catalyzed hydrogenation of several highly substituted unfunctionalized and functionalized alkenes and imines (Scheme 6.17).

Among the different substrates which were tested, the allylic alcohol and the imine shown in Scheme 6.17 were hydrogenated with full conversion. Interestingly, [(**8**)Ir(cod)]BAr_F was hydrogenated with high enantioselectivity (92%), while an *ee* of 37% (*R*) was observed in the hydrogenation of the imine. Both examples show that the stereogenic information of the catalyst can efficiently be conferred to the substrates. Nevertheless, the nature of the catalytic species remains unknown. It is questionable, whether the phosphinine moiety is still part of the catalytically active species, since both alcohols and amines can react with transition metal complexes of phosphinines, leading quantitatively to addition products (vide supra). This also counts for the Ir-catalyzed transfer hydrogenations of acetophenone with potassium methoxide in *iso*-propanol, which gave complete conversion to 2-phenylethanol within several minutes and with an enantioselectivity of *ee* = 65%.

6.7.5 Ir- and Pd-Catalyzed Hydrosilylation

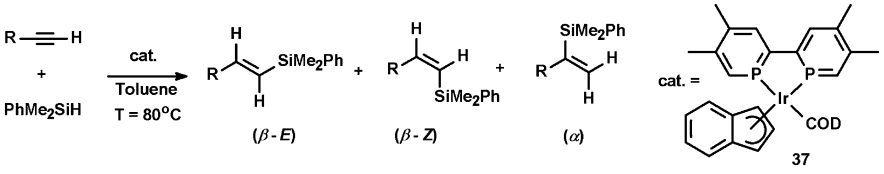
The application of the chelating bisphosphinine 4,4′,5,5′-tetramethylbiphosphinine (tmbp) in the Ir-catalyzed hydrosilylation of alkynes with **37** has been explored by Iyoda and co-workers [70]. In the presence of tmbp *β*-(*E*)-vinylsilanes were formed

selectively in moderate yields (Scheme 6.18). Comparable hydrosilylation reactions in the absence of tmbp produced selectively *β*-(*Z*)-vinylsilanes. The stereoselectivity of the reported catalytic reactions suggest the importance of the electron-withdrawing properties of the phosphinine-based ligand coordinated to iridium.

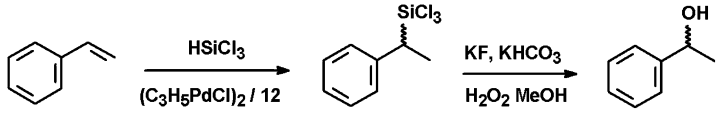
Garner and co-workers applied the first chiral C_2-symmetric phosphinine **12** (Scheme 6.6) in the Pd-catalyzed asymmetric hydrosilylation of styrene (Scheme 6.19) [35]. The trichlorosilane product was converted to 1-phenylethanol by Tamao-Fleming oxidation and showed an enantiomeric excess of 27% by chiral GC analysis. The relatively low level of asymmetric induction is attributed to the size and orientation of the bridgehead methyl groups.

6.8 Phosphinine-Based Ligands: Phosphabarrelenes

The phosphinine heterocycle can also serve as the basis for the development of very promising new classes of phosphorus containing ligand systems for homogeneous catalysis. In 1971 Märkl reported on the Diels–Alder-type [4 + 2] cycloaddition of benzyne with phosphinines to give the corresponding phosphabarrelenes of the type **38** (Scheme 6.20) [71]. Phosphabarrelenes have mainly *σ*-donating character with some *π*-acceptor properties due to low lying *π** orbitals of the P–C bonds [72].

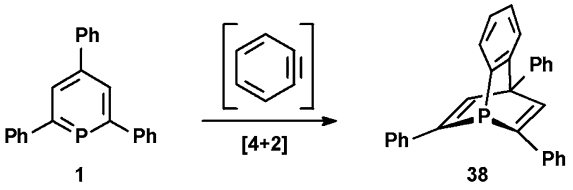


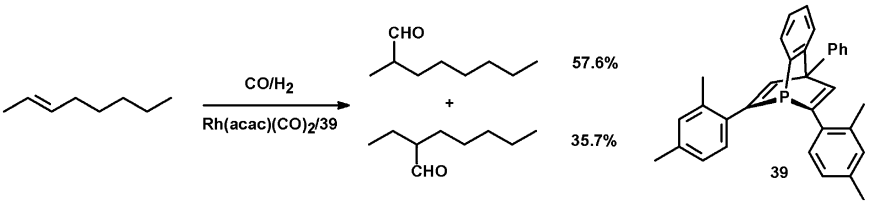
Scheme 6.18 Ir-catalyzed hydrosilylation of alkynes



Scheme 6.19 Pd-catalyzed hydrosilylation of styrene

Scheme 6.20 Synthesis of phosphabarrelenes by [4 + 2] cycloaddition reaction





Scheme 6.21 Rh-catalyzed hydroformylation of 2-octene

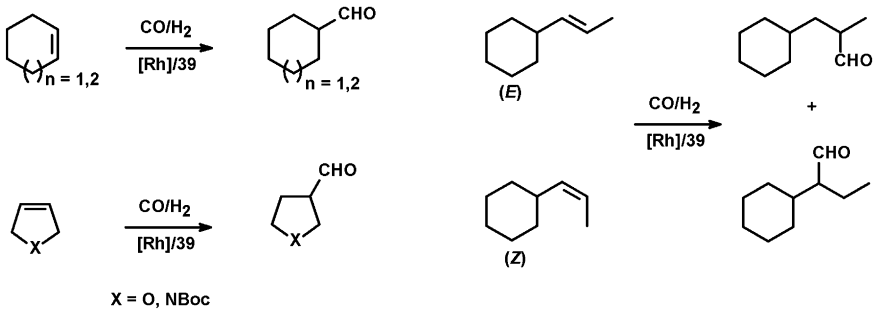
6.8.1 Rh-Catalyzed Hydroformylations

Breit and co-workers showed that very active hydroformylation catalysts could be generated in combination with $[Rh(CO)_2(acac)]$. Remarkably, internal alkenes were converted essentially free of alkene-isomerization towards internal aldehydes. This was impressively demonstrated in the hydroformylation of 2-octene [73, 74]. While Rh/phosphite and Rh/phosphinine complexes show a very high activity for the hydroformylation of 2-octene with complete consumption of the starting material, isomerization prior to hydroformylation leads to the formation of 2-propylhexanal and *n*-nonanal as well. In contrast, the Rh/phosphabarrelene system Rh/**39** gives almost exclusively the internal aldehydes 2-methyloctanal (57.6 mol %) and 2-ethylheptanal (35.7 mol %). Some starting material (6.5 mol %) and 2-propylhexanal (0.2 mol %) (toluene; T = 70 °C; p = 10 bar CO/H_2; t = 4 h; 2-octene:L:Rh = 7187:20:1) could be detected at the end of the reaction (Scheme 6.21). With Rh/**39** turnover frequencies of up to 12,000 h^{-1} were also reached for the hydroformylation of internal cyclic olefins, (*E*)- and (*Z*)-1-cyclohexylpropenes.

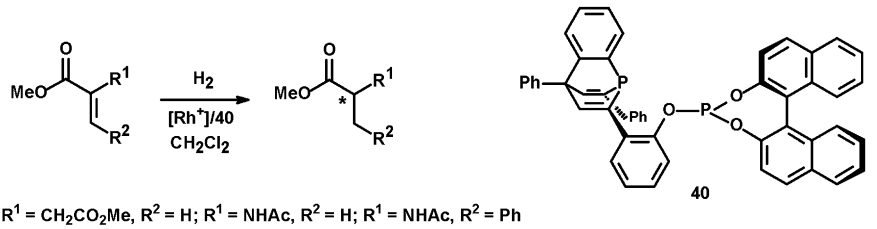
Also heterocyclic alkenes, which are known to isomerize easily, can be hydroformylated efficiently with Rh/phosphabarrelene systems. Thus, in the hydroformylation of 2,5-dihydrofuran with Rh/**39**, the tendency towards isomerization is very low and 79 mol % of the desired 3-aldehyde is formed (6-mol % 2-aldehyde, 15 mol % starting material; toluene; T = 50 °C; p = 10 bar CO/H_2; t = 4 h). More strikingly, in the case of N-Boc-pyrroline as starting material, the 3-aldehyde was formed exclusively in 72 mol % yield (28 mol % substrate; toluene, T = 50 °C; p = 10 bar CO/H_2; t = 4 h; Scheme 6.22) [74]. In contrast, phosphite-based Rh-catalysts produces substantial amounts of 2-aldehydes, due to isomerization prior to hydroformylation.

6.8.2 Rh-Catalyzed Hydrogenations

Bidentate, diasteriomerically pure phosphabarrelene-phosphites of the type **40** have recently been described by Breit and co-workers (Scheme 6.23) [75]. These compounds were prepared by reaction of the corresponding hydroxy-functionalized phosphabarrelenes with (*S*)-(1,1′-binaphthyl-2,2′-dioxy)chlorophosphine,



Scheme 6.22 Rh-catalyzed hydroformylation of internal and heterocyclic alkenes



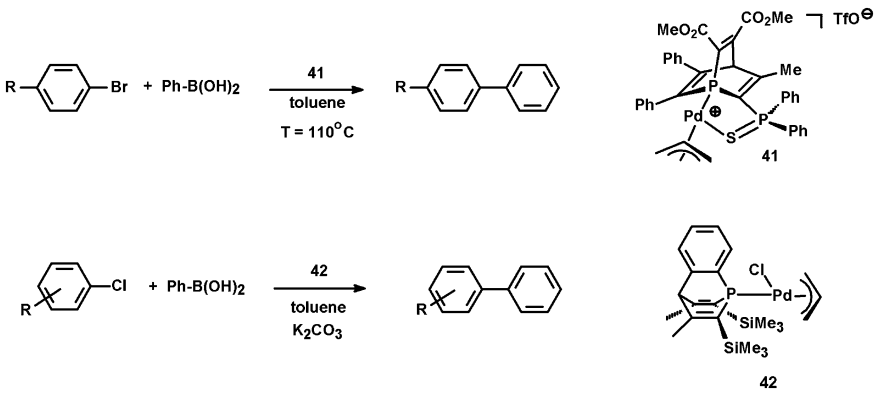
Scheme 6.23 Rh-catalyzed asymmetric hydrogenation of prochiral substrates

similar to the procedure reported by us for the preparation of the analogues phosphinine-phosphites. They contain both a stereogenic phosphorus atom as well as a chiral binaphthol-based chiral auxiliary.

These ligands were applied in the Rh-catalyzed asymmetric hydrogenation of prochiral substrates, indicating a strong influence of the stereogenic phosphorus atom on the chiral induction. While the enantiopure phosphinine-phosphite **11**/Rh(I) catalyst (Scheme 6.15) gives an enantiomeric excess of 79% (*S*) in the hydrogenation of dimethyl itaconate (*vide supra*), an *ee* of only 19% (*S*) was found applying the diastereomerically pure system **40**/Rh(I) (1 mol %; $c_{Rh} = 0.8$ mM; RT; CH_2Cl_2; t = 20 h, full conversion). In the asymmetric hydrogenation of methyl 2-(*N*-acetylamino)cinnamate, an enantiomeric excess of 88% (*S*) was found with **40**/Rh^+. In comparison, a moderate *ee* of 62% (*R*) was found for the catalyst **11**/Rh(I) (*vide supra*). Unfortunately, no comparison with the complementary diastereoisomer can be made here for these analogous reactions. However, using methyl acetamido acrylate as substrate, enantioselectivities of *ee* = 9% (*R*) and as high as 90% (*S*), respectively, were found with the system **40**/Rh(I) depending on the configuration of the phosphorus atom incorporated into the cyclic framework.

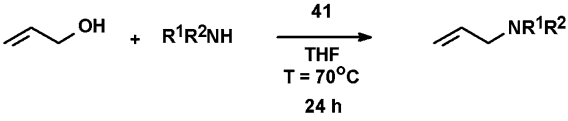
6.8.3 Pd-Catalyzed Suzuki–Miyaura Cross-Coupling Reactions

Very efficient Pd-catalysts (**41**) containing bidentate phosphabarrelene-based P,S ligands have been applied by Le Floch and co-workers in the Pd-catalyzed



Scheme 6.24 Pd-catalyzed Suzuki–Miyaura cross-coupling reaction

Scheme 6.25 Pd-catalyzed allylation of primary and secondary amines



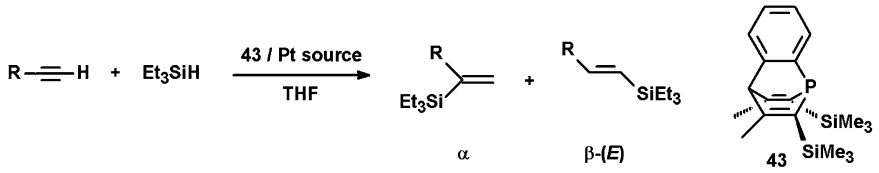
Suzuki–Miyaura cross-coupling reaction (Scheme 6.24). Conversions of up to 90% (TON = 90,000) within 2 h were achieved in toluene under reflux [76]. The same group reported on Pd-complexes of the type **42** that form efficient room temperature catalytic systems for the Suzuki–Miyaura coupling of poorly reactive aryl-chlorides (Scheme 6.24) [77].

6.8.4 Pd-Catalyzed Allylation of Amines

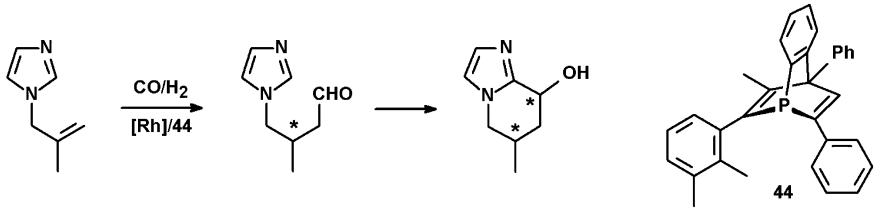
Pd-catalyst **41** was also found to be active in the allylation of primary amines (Scheme 6.25) [76]. Interestingly and in contrast to the classical Tsuij-Trost process [78], this reaction did not require the activation of the OH-functionality via derivatization. Complex **41** could also convert secondary amines efficiently, a reaction which is usually difficult to catalyze. Good yields were obtained by heating allylic alcohol and secondary amines in the presence of 2% **41** in THF at T = 70 °C.

6.8.5 Pt-Catalyzed Hydrosilylations

Le Floch and co-workers reported on the application of the bulky phosphabarrelene ligand **43** in the Pt(0)-catalyzed hydrosilylation of alkynes under mild reaction conditions (Scheme 6.26). Ligand **43** turned out to be very efficient in the stabilization of electron-deficient complexes and a rare example of a 14-VE



Scheme 6.26 Pt-catalyzed hydrosilylation of alkynes



Scheme 6.27 Tandem hydroformylation-cyclization reaction to bicyclic imidazole-derivatives

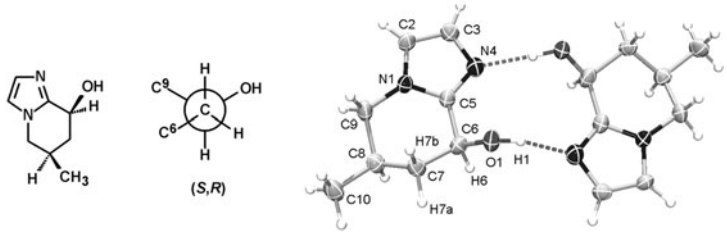


Fig. 6.16 Hydroxy-functionalized bicyclic imidazole and molecular structure in the crystal

platinum(0) complex (Pt(**43**)$_2$) could be isolated and crystallographically characterized [79].

6.8.6 Tandem Reactions: Hydroformylation-Cyclizations

Our group has developed a new route towards functionalized bicyclic imidazole derivatives consisting of a one-pot tandem reaction sequence under hydroformylation conditions using the catalyst system Rh/**44** [80]. 8-Hydroxy-6-methyl-5,6,7,8-tetrahydroimidazo-[1,2-a]pyridine as a mixture of 2 stereoisomers was formed selectively in high yield by hydroformylation of *N*-(*β*-methallyl)imidazole and subsequent intramolecular cyclization (Scheme 6.27).

Yet not trivial to achieve, these multistep reactions are powerful tools for the construction of more complex molecular structures by making economical use of available functional groups within the same molecule (Fig. 6.16).

6.9 Future Perspectives

State-of-the-art synthetic methodologies allow nowadays a straightforward derivatization and functionalization of phosphinines, leading to ligands with tailored properties and substitution pattern not easily accessible with classical phosphorus ligands. An extensive screening of such phosphinines in homogeneous catalytic reactions is desirable and could lead to unexpected results in terms of activity, reactivity and selectivity in the future [7, 81]. It should be kept in mind, however, that the application of phosphinines in catalysis might be restricted to specific transformations as metal complexes of phosphinines can be prone to nucleophilic attack on the phosphorus atom. Nevertheless, this reactivity has not been fully rationalized yet and needs further detailed investigations. Transition metal complexes containing 2,4,6-triarylphosphinines as ligands seem to be kinetically more stable than complexes based on less substituted phosphinines. As an example, the P,N hybrid ligand NIPHOS forms highly moisture sensitive Pd(II) and Pt(II) complexes of the type [MCl(L)(NIPHOS)][MCl_3(L)] (Scheme 6.7) [59]. In contrast, the additional phenyl-substituents in 2-(2′-pyridyl)-4,6-diphenylphosphinine (Fig. 6.11) apparently contribute to a kinetic stabilization, as no particularly high sensitivity towards water was observed for the corresponding Rh(I), Pt(II), Pd(II) and Ru(II) complexes [53]. The application of such P,N hybrid ligands in homogeneous catalysis has so far remained elusive and needs further investigations.

6.9.1 Di-Phosphinines: Control of Coordination Modes

Phosphinines have electronic properties and structural elements which are significantly different compared to classical phosphines. This allows the design and preparation of chelating ligands with controlled coordination modes via the modular pyrylium salt route. In combination with a suitable metal center, a P–M–P angle of 180° is present in metal-complex **I**, which has been shown for the *trans*-coordinating di-phosphinine and the corresponding $L_2Rh(CO)I$ complex depicted in Fig. 6.8 [43]. Alternatively, a P–M–P angle of 120° is realized in metal-complex **II** (Fig. 6.17).

Taking the special electronic and steric properties of the phosphorus-heterocycles into account, the design of di-phosphinines and di-phosphabarrelenes with natural bite angles close to 120° are expected to give very active and selective catalysts in

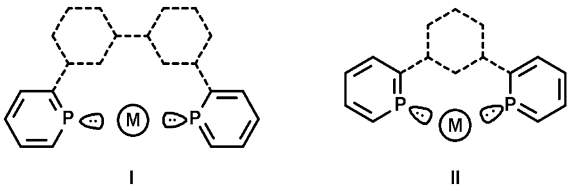


Fig. 6.17 Bidentate di-phosphinines with fixed coordination geometry

the Rh-catalyzed hydroformylation of 1-alkenes. Breit and co-workers prepared the bidentate di-phosphinine **45**, which is based on a 1,3-substituted phenyl-backbone (Fig. 6.18) [65]. The system Rh/**45**, however, is inactive in the hydroformylation of 1-octene, which can most likely be attributed to a C–H activation process in the backbone by the adjacent metal center, leading to stable, catalytically inactive Rh-species. Other inert backbones of the type **III** and **IV** have consequently to be chosen for the design of suitable ligand systems (Fig. 6.18). Keeping in mind the high price of rhodium, the investigation of Co-catalyzed hydroformylation reactions employing phosphinine-based ligands seems to be an attractive alternative. Especially the influence of the steric and electronic properties of these ligands on the selectivity and activity of the corresponding metal complexes, as well as on the reaction conditions might lead to interesting observations.

6.9.2 Pincer-Type Phosphinines

PNP and PCP pincer ligands and their complexes have attracted considerable interest due to their stability, activity and variability [82]. Pincer complexes have been extensively explored as catalysts in various transition metal mediated reactions, sensors and building blocks for supramolecular structures [83]. The most widely used class of pincer ligands contains phosphines or phosphites as additional donor group. Interestingly, the modularity of the phosphinine synthesis via pyrylium salts allows the preparation of analogous PNP and PCP pincer ligands containing π-accepting phosphinine-donors. The first example of a PNP pincer complex of the type **V** has been described by us (see Fig. 6.12), while the preparation, characterization and investigation of PCP pincer complexes of the type **VI** has so far remained elusive (Fig. 6.19). The synthetical access to such systems and the evaluation of the catalytic properties of the corresponding complexes is an intriguing task for future investigations.

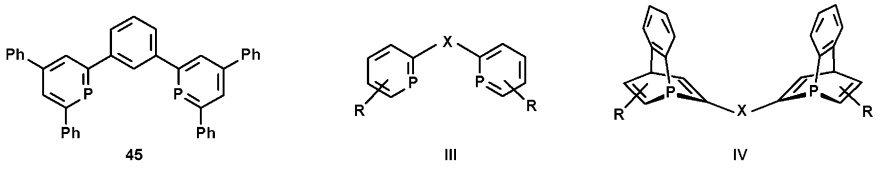
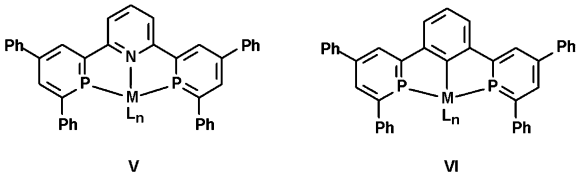


Fig. 6.18 Di-phosphinines and phosphabarrelenes

Fig. 6.19 PNP and PCP pincer complexes containing phosphinine donors



6.9.3 Chiral Phosphinine-Based Ligands for Asymmetric Catalysis

The development of chiral phosphinines and phosphabarrelenes with the chiral information close to the phosphorus center is a very challenging research topic and could lead to interesting developments in asymmetric homogeneous catalysis. As described above, phosphinines and phosphabarrelenes have shown to be efficient ligands for the hydroformylation of internal and less reactive alkenes. The hydroformylation products are potentially chiral aldehydes and are therefore interesting building blocks for the fine-chemicals and pharmaceutical industry (*vide supra*). The chiral atropisomeric phosphinine **10** (Fig. 6.5) and phosphabarrelene **44** (Scheme 6.27) have recently been reported by our group [33, 34]. However, the barrier for internal rotation is still too low for applications as efficient ligands in asymmetric homogeneous catalysis, especially at higher temperature. Modification of the substitution pattern for the development of suitable systems (**VII/VIII**) is therefore necessary (Fig. 6.20).

6.9.4 C–C Bond Formation Reactions

In view of their particular electronic and steric properties we recently became interested in the use of phosphinine ligands in Ni- and Pd-catalyzed Suzuki–Miyaura cross-coupling reactions. It was anticipated that these π-accepting ligands might stabilize efficiently Pd(0) and Ni(0) species, which play a crucial role in C–C bond formation reactions. Indeed, good activities and high selectivities to the cross-coupling products were especially achieved with the Ni systems, also with less reactive arylchlorides as substrates (Scheme 6.28). This opens up new perspectives in this highly important research area.

6.9.5 Gold Catalysis

Yoshifuji and co-workers have recently investigated low-coordinated organophosphorus compounds in Au-catalyzed transformations [84]. Apparently, the

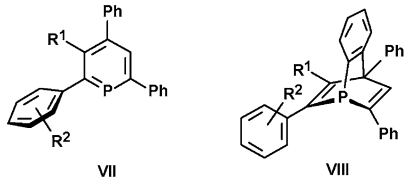
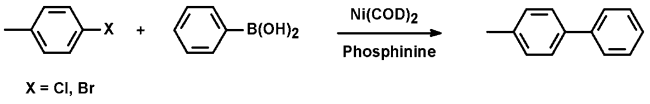


Fig. 6.20 Axially chiral phosphinines and phosphabarrelenes



Scheme 6.28 Ni-catalyzed Suzuki–Miyaura reaction using phosphinine ligands

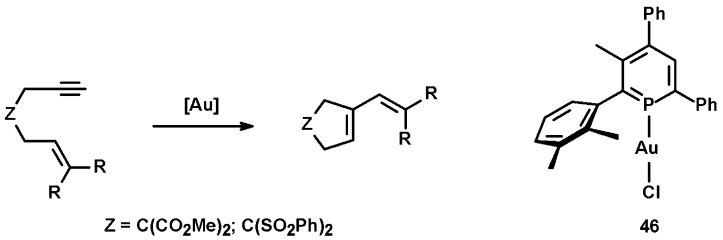


Fig. 6.21 Gold-catalyzed 1,6-enyne cyclization and Au(I)Cl complex containing the axially chiral phosphinine ligand **10**

highly π-accepting properties of phosphaalkenes is beneficial for increasing the Lewis acidity of the gold centers. Moreover, the soft properties of low-coordinated phosphorus centers in such systems is advantageous for a moderate stabilization of putative cationic Au intermediates. In the cyclotrimerization of 1,6-enynes (Fig. 6.21) the formation of vinylcyclopentenes were even observed in the absence of the typical silver co-catalyst. The analogy between phosphaalkenes and phosphinines is obvious. In fact, phosphinines can stabilize Au(I) centers efficiently [85, 86]. Figure 6.21 shows the Au(I)Cl complex **46** recently prepared by us, that contains the chiral phosphinine ligand **10**. An investigation of phosphinines in gold catalysis and the elucidation of ligand effects in such reactions is currently carried out in our laboratories.

References

1. van Leeuwen PWNM (2004) Homogeneous catalysis-understanding the art. Kluwer, Dordrecht
2. Märkl G (1966) 2,4,6-Triphenylphosphabenzene. Angew Chem Int Ed 5:846–847
3. Ashe AJ III (1971) Phosphabenzene and arsabenzene. J Am Chem Soc 93:3293–3295
4. Mathey F, Le Floch P (2005) Product class 13: 1λ^3-phosphinines. Sci Synth 15:1097–1155
5. Le Floch P (2001) In: Mathey F (ed) Phosphorus-carbon heterocyclic chemistry: the rise of a new domain. Pergamon, Palaiseau
6. Märkl G (1990) Chapter D.5: λ^3-Phosphinines, Aza-λ^3-Phosphinines, and λ^3, λ^3-Diphosphinines. In: Regitz M, Scherer OJ (eds) Multiple bonds and low coordination in phosphorus chemistry. Thieme, Stuttgart
7. Müller C, Vogt D (2007) Phosphinines as ligands in homogeneous catalysis: recent developments, concepts and perspectives. Dalton Trans 5505–5523
8. Baldridge KK, Gordon MS (1988) Potentially aromatic heterocycles. J Am Chem Soc 110:4204–4208
9. Nyulászi L, Veszprémi T, Réffi J, Burkhardt B, Regitz M (1992) Electronic structure and aromaticity of azaphospholes. J Am Chem Soc 114:9080–9084
10. Burrow PD, Ashe AJ III, Bellville DJ, Jordan KD (1982) Temporary anion states of phosphabenzene, arsabenzene, and stibabenzene. trends in the π and π^* orbital energies. J Am Chem Soc 104:425–429
11. Nyulászi L (2001) Aromaticity of phosphorus heterocycles. Chem Rev 101:1229–1246
12. Nyulászi L, Veszprémi TJ (1996) Nature of bonding in cyclic conjugated ylides. J Phys Chem 100:6456–6462

13. Modelli A, Hajgató B, Nixon JF, Nyulászi L (2004) Anionic states of six-membered aromatic phosphorus heterocycles as studied by electron transmission spectroscopy and ab initio methods. J Phys Chem A 108:7440–7447
14. Frison G, Sevin A, Avarvari N, Mathey F, Le Floch P (1999) The CH by N replacement effects on the aromaticity and reactivity of phosphinines. J Org Chem 64:5524–5529
15. Pham-Tran NN, Bouchoux G, Delaere D, Nguyen MT (2005) Theoretical and experimental reevaluation of the basicity of λ^3-phosphinine. J Phys Chem A 109:2957–2963
16. Tolman CA (1977) Steric effects of phosphorus ligands in organometallic chemistry and homogeneous catalysis. Chem Rev 77:313–348
17. Kühl O (2005) Predicting the net donating ability of phosphines—do we need sophisticated theoretical methods? Coord Chem Rev 249:693–704
18. Muller A, Meijboom R, Roodt A (2006) A crystallographic and DFT study on Vaska-type *trans*-[Rh(CO)Cl$(PR_3)_2$] complexes containing flexible ligands: the molecular structure of *trans*-[Rh(CO)Cl$\{P(OC_6H_5)_3\}_2$]. J Organomet Chem 691:5782–5789
19. Serron S, Nolan SP, Moloy KG (1996) Solution thermochemical study of tertiary phosphine ligand substitution reactions in the RhCl(CO)$(PR_3)_2$ system. Organometallics 15:4301–4306
20. Müller C, Lutz M, Spek AL, Vogt D (2006) 4-(*p*-Methylthio)phenyl-2,6-diphenyl phosphinine: the first X-ray crystal structure of a λ^3-triaryl-phosphabenzene. J Chem Crystallogr 36:869–874
21. Bart JCJ, Daly JJ (1968) Kristallstruktur von 2,6-dimethyl-4-phenylphosphabenzol. Angew Chem 20:843–844
22. Bart JCJ (1968) An X-ray study of non-stabilized ylids. Angew Chem Int Ed 7:730
23. Ashe AJ III (1996) In: Katritzky AR, Rees CW, Scriven EFV (eds) Comprehensive heterocyclic chemistry II. Pergamon, New York
24. DiMauro EF, Kozlowski MC (2001) Phosphabenzenes as electron withdrawing phosphine ligands in catalysis. J Chem Soc Perkin Trans 1:439–444
25. Rösch W, Regitz M (1986) Z Naturforsch B 41:931
26. Regitz M, Binger P (1988) Phosphaalkine–Synthesen, Reaktionen, Koordinationsverhalten. Angew Chem 100:1541–1565
27. Alcaraz JM, Breque A, Mathey F (1982) Acces aux [pyriyl-2′]-2 phosphorines. Tetrahedron Lett 2323:1565–1568
28. Avarvari N, Le Floch P, Mathey F (1996) 1,3,2-Diazaphosphinines: new, versatile precursors of 1,2-azaphosphinines and polyfunctional phosphinines. J Am Chem Soc 118:11978–11979
29. Rosa P, Le Floch P, Ricard L, Mathey F (1997) 1,3,2-Diazaphosphinines: new, versatile precursors of 1,2-azaphosphinines and polyfunctional phosphinines. J Am Chem Soc 119:9417–9423
30. Breit B (1996) Highly regioselective hydroformylation under mild conditions with new classes of π-acceptor ligands. Chem Commun 2071–2072
31. Breit B (1999) Probing new classes of π-acceptor ligands for rhodium catalyzed hydroformylation of styrene. J Mol Catal A Chem 143:143–154
32. Müller C, Guarrotxena-Lopéz L, Kooijman H, Spek AL, Vogt D (2006) Chiral bidentate phosphabenzene-based ligands: synthesis, coordination chemistry, and application in Rh-catalyzed asymmetric hydrogenations. Tetrahedron Lett 47:2017–2020
33. Müller C, Pidko EA, Totev D, Lutz M, Spek AL, van Santen RA, Vogt D (2007) Atropisomeric phosphinines: design and synthesis. Dalton Trans 5372–5375
34. Müller C, Pidko EA, Staring AJPM, Lutz M, Spek AL, van Santen RA, Vogt D (2008) Developing a new class of axial chiral phosphorus ligands: preparation and characterization of enantiopure atropisomeric phosphinines. Chem Eur J 14:4899–4905
35. Bell JR, Franken A, Garner CM (2009) Synthesis of the first C_2-asymmetric phosphinine and its pyrylium precursor. Tetrahedron 65:9368–9372
36. Le Floch P, Mathey F (1998) Transition metals in phosphinine chemistry. Coord Chem Rev 179–180:771–791
37. Mézailles N, Mathey F, Le Floch P (2001) The coordination chemistry of phosphinines, their polydentate and macrocyclic derivatives. Prog Inorg Chem 49:455

38. Le Floch P (2006) Phosphaalkene, phospholyl and phosphinine ligands: new tools in coordination chemistry and catalysis. Coord Chem Rev 250:627–681
39. Elschenbroich C, Nowotny M, Behrendt A, Massa W, Wocadlo S (1992) Tetrakis(η^1-phosphabenzol)nickel. Angew Chem 104:1388–1390
40. Elschenbroich C, Nowotny M, Behrendt A, Harms K, Wocadlo S, Pebler J (1994) Pentakis(η^1-phosphinine)iron: synthesis, structure, and mode of formation. J Am Chem Soc 116:6217–6219
41. Breit B, Winde R, Mackewitz T, Paciello R, Harms K (2001) Phosphabenzenes as monodentate π-acceptor ligands for rhodium-catalyzed hydroformylation. Chem Eur J 7:3106–3121
42. Mézailles N, Rosa P, Ricard L, Mathey F, Le Floch P (2000) Bisphosphinine rhodium and cobalt(−1) complexes. Organometallics 19:2941–2943
43. Müller C, Freixa Z, Lutz M, Spek AL, Vogt D, van Leeuwen PWNM (2008) Wide-bite-angle diphosphinines: design, synthesis, and coordination properties. Organometallics 27:834–838
44. Elschenbroich C, Nowotny M, Metz B, Graulich J, Massa W, Wocadlo S (1991) Bis(η^6-phosphabenzene)vanadium: synthesis, structure, redox properties, and conformational flexibility. Angew Chem Int Ed 30:547–550
45. Deberitz J, Nöth H (1970) Triphenylphosphorin-chrom(0)-tricarbonyl. Chem Ber 103:2541–2547
46. Vahrenkamp H, Nöth H (1972) Heteroaromatische Komplexliganden. Die Struktur von 2,4,6-Triphenyl-phosphorin-chrom(0)-tricarbonyl. Chem Ber 105:1148–1157
47. Deberitz J, Nöth H (1973) Tricarbonyl(triphenylphosphorin)molybdän(0). Chem Ber 106:2222–2226
48. Doux M, Ricard L, Mathey F, Le Floch P, Mézailles N (2003) Synthesis and reactivity of the first η^6-rhodium(I) and η^6-iridium(I) complexes of 2,6-bis(trimethylsilyl)phosphinines. Eur J Inorg Chem 687–698
49. Mézailles N, Ricard L, Mathey F, Le Floch P (2001) (η^5-pentamethylcyclopentadienyl) phosphineruthenium(II) complexes: η^1- vs η^6-coordination. Organometallics 20:3304–3307
50. Nief F, Charrier C, Mathey F, Simalty M (1980) Reaction des phosphorines avec les cymantrenes. Synthese d'un complexe sandwich η^5-cyclopentadienyl-η^6-phosphorine-manganese. J Organomet Chem 187:277–285
51. Schmid B, Venanzi LM, Gerfin T, Gramlich V, Mathey F (1992) Synthesis and spectroscopic properties of the complexes $[M_2(DIEN)_2(NIPHOS)_2][SbF_6]_2$ (M = Ir, DIEN = 1,5-cyclooctadiene, COD; M = Rh, DIEN = norbornadiene, NBD; NIPHOS = 2-(2′-pyridyl)-4,5-dimethylphosphinine). X-ray crystal structure of $[Ir_2(COD)_2(NIPHOS)_2][SbF_6]_2$. Inorg Chem 31:5117–5122
52. Reetz MT, Bohres E, Goddard R, Holthausen MC, Thiel W (1999) Synthesis, solid-state structure, and electronic nature of a phosphinine-stabilized *triangulo* palladium cluster. Chem Eur J 5:2101–2108
53. Campos-Carrasco A, Pidko EA, Masdeu-Bultó AM, Lutz M, Spek AL, Vogt D, Müller C (2010) 2-(2′-pyridyl)-4,6-diphenylphosphinine versus 2-(2′-pyridyl)-4,6-diphenylpyridine: an evaluation of their coordination chemistry towards Rh(I). New J Chem 34:1547–1550
54. Müller C, Pidko EA, Lutz M, Spek AL, Vogt D (2008) Diphosphinine derivatives of terpyridine: a new class of neutral π-accepting PNP-pincer ligands. Chem Eur J 14:8803–8807
55. Deberitz J, Nöth H (1973) 2,4,6-Triphenylphosphorin-Metall(0)Carbonyle des Chroms, Molybdäns und Wolframs. J Organometal Chem 49:453–467
56. Vahrenkamp H, Nöth H (1973) Die Kristallstruktur von Pentacarbonyl(2,4,6-triphenyl-phosphorin)chrom(0). Chem Ber 106:2227–2235
57. Lehmkuhl H, Paul R, Mynott R (1981) Phosphabenzolnickel-Komplexe. Liebigs Ann Chem 1139–1146
58. Carmichael D, Le Floch P, Ricard L, Mathey F (1992) Ruthenium(II) complexes of 2,2′-bisphosphinine. Inorg Chim Acta 198–200:437–441

59. Schmid B, Venanzi LM, Albinati A, Mathey F (1991) Synthesis and reactivity of platinum and palladium complexes with a phosphorus analogue of 2,2′-bipyridine, NIPHOS. X-ray crystal structure of [PtCl(NIPHOSH·OMe)(PMe_3)][SbF_6]. Inorg Chem 30:4693–4699
60. Knoch F, Kremer F, Schmidt U, Zenneck U, Le Floch P, Mathey F (1985) (η^4–1,5-Cyclooctadiene)(η^6-phosphinine)iron(0): novel room-temperature catalyst for pyridine formation. Organometallics 15:2713–2719
61. Bönnemann H (1985) Organocobalt compounds in the synthesis of pyridines—an example of structure-effectivity relationships in homogeneous catalysis. Angew Chem Int Ed 24:248–262
62. Heller B, Oehme G (1995) First cobalt(I)-catalysed heterocyclotrimerization of ethyne with nitriles to pyridines in water under mild conditions. J Chem Soc Chem Commun 179–180
63. Le Floch P, Knoch F, Kremer F, Mathey F, Scholz J, Scholz W, Thiele KH, Zenneck U (1998) [(Arene)(Diene)Fe] and [(Arene)(Diazadiene)Fe] complexes: preparation, reactivity, and catalytic properties. Eur J Inorg Chem 119–126
64. Breit B, Winde R, Harms K (1997) Phosphabenzene–rhodium catalysts for the efficient hydroformylation of terminal and internal olefins. J Chem Soc Perkin Trans 18:2681–2682
65. Paciello R, Zeller E, Breit B, Röper M (1999) DE 197 43 197 A1 (to BASF)
66. Mackewitz T, Röper M (2000) EP 1 036 796 A1 (to BASF)
67. Reetz MT, Li X (2005) The influence of mixtures of monodentate achiral ligands on the regioselectivity of transition-metal-catalyzed hydroformylation. Angew Chem Int Ed 44:2962–2964
68. Reetz MT, Mehler G (2003) Mixtures of chiral and achiral monodentate ligands in asymmetric Rh-catalyzed olefin hydrogenation: reversal of enantioselectivity. Tetrahedron Lett 44:4593–4596
69. Neumann E (2006) PhD Thesis, Universität Basel, Switzerland
70. Miyake Y, Isomura E, Iyoda M (2006) Chem Lett 35:836–837
71. Märkl G, Lieb F (1968) Substituted 1-phosphabarrelenes (1-phospha[2.2.2]octa-2,5,7-trienes). Angew Chem Int Ed 7:733
72. Blug M (2009) Phosphinines as precursors for phosphinine anions and phosphabarrelenes: coordination chemistry, catalysis and stabilisation of nanoparticles. PhD Thesis, Ecole Polytechnique, France
73. Breit B, Fuchs E (2004) Phosphabarrelene–rhodium complexes as highly active catalysts for isomerization free hydroformylation of internal alkenes. Chem Commun 694–695
74. Fuchs E, Keller M, Breit B (2006) Phosphabarrelenes as ligands in rhodium-catalyzed hydroformylation of internal alkenes essentially free of alkene isomerization. Chem Eur J 12:6930–6939
75. Breit B, Fuchs E (2006) Chiral phosphabarrelene ligands: synthesis and evaluation in rhodium-catalyzed asymmetric hydrogenation. Synthesis 13:2121–2128
76. Piechaczyk O, Doux M, Ricard L, Le Floch P (2005) Synthesis of 1-phosphabarrelene phosphine sulfide substituted palladium(II) complexes: application in the catalyzed suzuki cross-coupling process and in the allylation of secondary amines. Organometallics 24:1204–1213
77. Blug M, Guibert C, Le Goff XF, Mézailles N, Le Floch P (2009) 1-Phosphabarrelene complexes of palladium and their use in Suzuki–Miyaura coupling reactions. Chem Commun 201–203
78. Tsuji J (2000) Transition metal reagents and catalysts. Wiley, New York
79. Blug M, Le Goff XF, Mézailles N, Le Floch P (2009) A 14-VE platinum(0) phosphabarrelene complex in the hydrosilylation of alkynes. Organometallics 28:2360–2362
80. Bäuerlein PS, Arenas Gonzalez I, Weemers JJM, Lutz M, Spek AL, Vogt D, Müller C (2009) Phosphabarrelene-modified Rh-catalysts: a new and selective route towards hydroxy-functionalized bicyclic imidazoles via tandem reactions. Chem Commun 4944–4946
81. Kollár L, Keglevich G (2010) *P*-Heterocycles as ligands in homogeneous catalytic reactions. Chem Ber 110:4257–4302
82. Benito-Garagorri D, Kirchner K (2008) Modularly designed transition metal PNP and PCP pincer complexes based on aminophosphines: synthesis and catalytic applications. Acc Chem Res 41:201–213

83. Albrecht M, van Koten G (2001) Platinum group organometallics based on “pincer” complexes: sensors, switches and catalysts. Angew Chem Int Ed 40:3750–3781
84. Ito S, Kusano S, Morita N, Mikami K, Yoshifuij M (2010) Ligand effect of bulky 2,2-dialkyl-1-phosphaethenes on Au-catalyzed cycloisomerization of 1,6-enynes and lactonization of pent-4-ynoic acids. J Organometal Chem 695:291–296
85. Dash KC, Eberlein J, Schmidbaur H (1973) Gold(I) halide complexes of 2,4,6-triphenyl-phosphabenzene. Synth Inorg Metalorg Chem 3:375–380
86. Mézailles N, Ricard L, Mathey F, Le Floch P (1999) Synthesis, X-ray crystal structures and reactivity towards alkynes of gold(I)-phosphinine complexes. Eur J Inorg Chem 2233–2241

Chapter 7
Aqueous Phase Reactions Catalysed by Transition Metal Complexes of 7-Phospha-1,3,5-triazaadamantane (PTA) and Derivatives

Luca Gonsalvi and Maurizio Peruzzini

Abstract The possibility to run selective catalytic transformations in water has fascinated generations of chemists working in the field of homogenous catalysis. One of the most common approaches has been so far to translate organic phase transition metal complex catalyzed processes into water phase by replacing ancillary ligands such as phosphines with their water soluble analogs. A class of neutral, stable, easy-to-handle and functionally versatile monodentate phosphines is represented by 7-phospha-1,3,5-triazacyclo-[3.3.1.1]decane (PTA) whose application has witnessed a true renaissance in the first decade of the present century after some interest starting from its discovery in 1974. This chapter summarizes the most relevant applications of transition metal complexes of PTA in catalysis, from C=C and C=O bond hydrogenation, to olefin hydroformylation and various C–C and C-element bond forming reactions.

7.1 Introduction

In order to reduce the environmental impact of organic solvents in industrial scale applications, water is a possible alternative as it is cheap, most of the times readily available, non flammable and non-toxic. Moreover, in a biphasic water/organic solvent system, it is often possible to recycle expensive water soluble catalysts and separate them from organic reagents and products by simple phase separation and

L. Gonsalvi (✉) · M. Peruzzini
Consiglio Nazionale delle Ricerche (CNR), Istituto di Chimica dei Composti Organometallici (ICCOM), Via Madonna del Piano 10 Sesto Fiorentino, 50019 Florence, Italy
e-mail: l.gonsalvi@iccom.cnr.it

M. Peruzzini and L. Gonsalvi (eds.), *Phosphorus Compounds*, Catalysis by Metal Complexes, 37, DOI: 10.1007/978-90-481-3817-3_7,
© Springer Science+Business Media B.V. 2011

filtration. Recent efforts have thus focused on the development of metal complexes with water-soluble ligands, in particular phosphines.

Among neutral water soluble phosphines, PTA (PTA = 1,3,5-triaza-7-phosphatricyclo[3.3.1.1]decane) has received increasing attention in past and recent literature due to its versatility in synthetic modifications, use as ligands and interesting properties as either free compound or as ancillary ligand to metals, with applications covering homogeneous catalysis, material science, luminescence and medicinal chemistry [1, 2].

PTA and analogues have been applied as water soluble ligands especially for platinum group transition metals. Some of the complexes obtained have been used as catalysts for reactions in water or biphasic water/organic solvent systems. These reactions include olefin, aldehyde, ketone chemoselective hydrogenations and transfer hydrogenations (Ru, Rh, Ir), olefin hydroformylations (Rh), bicarbonate hydrogenation to formate (Ru, Ir), benzonitrile hydration to benzamide (Ru), cyclization of 4-pentyn-1-amine to 2-methyl-pyrroline (Pd, Pt, Ir), Sonogashira coupling of aryl chlorides and bromides with terminal alkynes (Pd), alkyne hydrations (Ru) and allylic alcohol isomerization (Ru), as recently reviewed [1, 2].

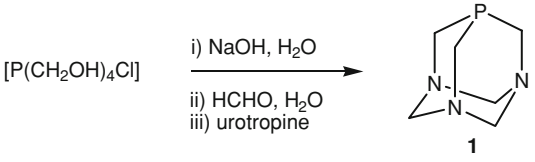
7.1.1 PTA Synthesis and Structural Modifications

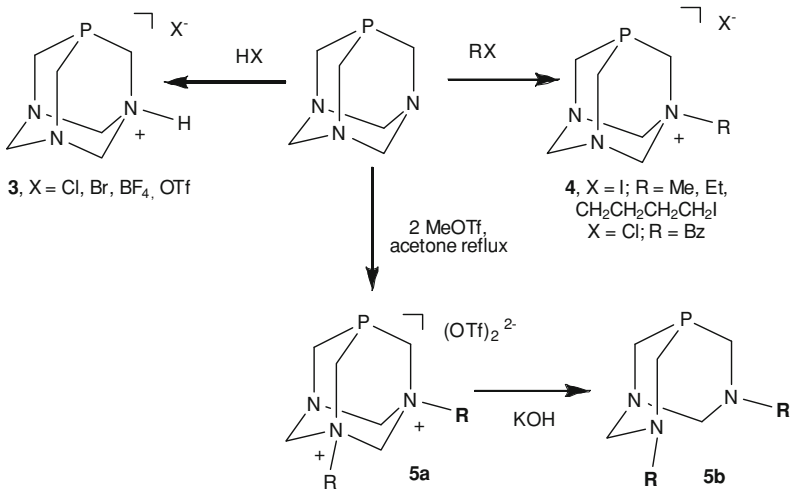
In this section, the synthesis of PTA and its analogues will be described, only if the compounds so obtained have found use as ligands in catalytic applications. All other synthetic modifications which have so far appeared in the literature have been recently reviewed [1, 2].

The synthesis of the water soluble aminophosphine PTA (**1**) was originally published by Daigle et al. [3] and modified later by Fluck and Forster [4]. Ammonia, hexamethylenetetraamine (urotropine) or ammonium acetate were reacted with *tris*-(hydroxymethyl)phosphine (THP) in the air to give **1** in ca. 40% yield (Scheme 7.1) [3]. An optimised one-pot synthesis was reported by Daigle, generating THP from the cheaper *tetrakis*-(hydroxymethyl)phosphonium chloride (THPC) by reaction with an excess of NaOH and using urotropine as nitrogen source [5], obtaining PTA in 65% yield and 97% purity, the oxide PTA(O) (**2**) being the main by-product.

The basicity of PTA was measured in water at $pK_a = 5.70$. At pH lower than 6.5, **1** is *N*-protonated as the ammonium-phosphine [PTAH]X, (**3**). Further *N*-protonation is disfavored, as the increase in cage strain of PTA decreases its stability due to a change in hybridization of nitrogen centers [6].

Scheme 7.1 Synthesis of PTA



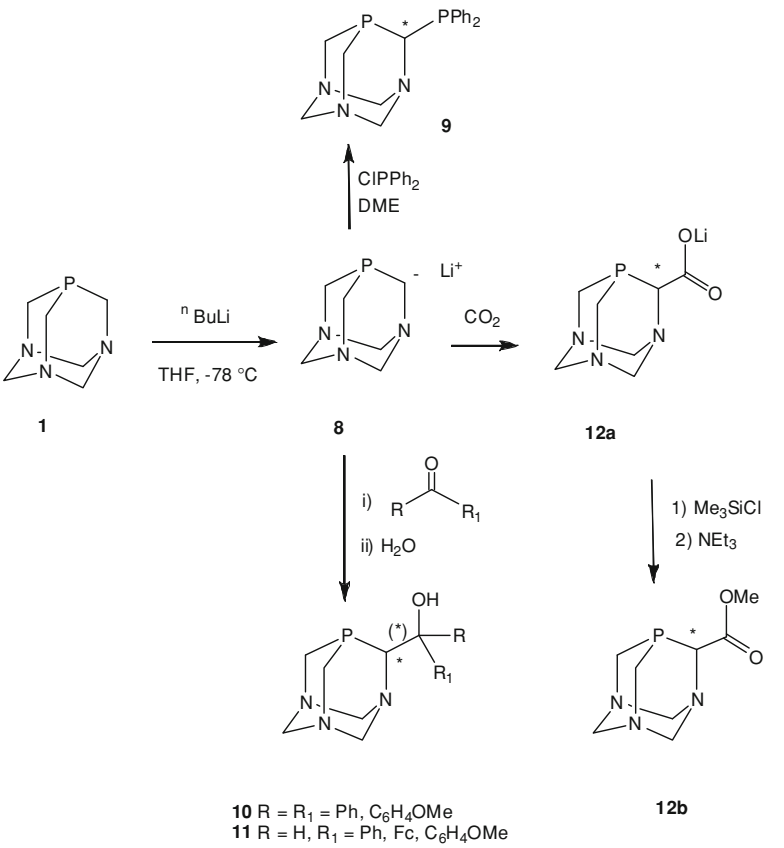


Scheme 7.2 "Lower rim" PTA functionalizations

PTA can be alkylated at one nitrogen (Scheme 7.2) using MeI [7], EtI, $PhCH_2Cl$ [8], or $I(CH_2)_4I$ [9] in acetone or methanol under reflux conditions. The resulting cationic R-PTA, (R = alkyl, benzyl), (**4**) are air stable and water soluble compounds, generally less soluble in organic solvents than **1**. The *N*-methylated species, $[mPTA]^+$, (**4a**) can be recrystallized MeOH/EtOAc, and dissolves in water and DMSO [5]. Bis-methylation of PTA was obtained by reaction of **1** with 2 equivalents of MeOTf in refluxing acetone, yielding *N,N′*-dimethyl-1,3,5-triaza-7-phosphaadamantane (dmPTA, **5a**) as triflate salt [10].

By refluxing $[RP(CH_2OH)_3]Cl$ (R = Me, Et, Ph, Bz, Cy) in acetone with ammonium acetate and formaldehyde, the corresponding phosphonium salts [R-*P*-PTA]Cl, (**6**) are obtained in variable yields [11–13]. *N*-alkyl-PTA halides [R-PTA]X (R = ^{n}Bu, ^{n}Pr, Et; X = I^-, Br^-) undergo C–C bond cleavage at the alkyl pending arm to give **4a** and the corresponding aldehyde, running the reaction in water under heating [14]. Reaction of **1** with 2-bromo methylpyridine gave the *N*-functionalized PTA derivative [pymePTA]Br (**7**) [15]. The compound is soluble in halogenated solvents and is more soluble in water (2.4 M) than PTA (1.5 M).

The introduction of functional groups on the C atoms adjacent to the P donor (6-position) is a powerful key to bidentate ligands for transition metals and to introduce one or more stereogenic centres on carbons close to phosphorus ("upper rim" functionalizations). The chirally pure complexes so obtained may in principle be used for applications in enantioselective catalytic processes. Selective α-C-lithiation of PTA with *n*-BuLi [16] yields the key reagent for this class of reaction, i.e. PTA-Li (**8**), which can be isolated as an off-white highly pyrophoric powder (Scheme 7.3). Compound **8** can be reacted with electrophiles at low to room temperature in THF slurries to yield various derivatives. Reaction of PTA-Li

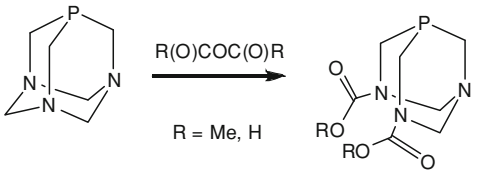


Scheme 7.3 "Upper rim" PTA functionalizations

with $ClPPh_2$ in 1,2-dimethoxyethane gives the racemic bidentate phosphine PTA-PPh_2 (**9**) in ca. 10% yield. Other electrophiles [17, 18] such as ketones, aldehydes and CO_2 were reacted with **8** giving β-phosphino alcohols PTA-CR_2OH (**10**, R = Ph, C_6H_4OMe) with one stereocenter at the C atom, secondary alcohols PTA-CH(R)OH (**11**, R = Ph, C_6H_4OMe, Fc = ferrocenyl) having two sterogenic carbon atoms, and carboxylates PTA-CO_2Li (**12a**), respectively (Scheme 7.3). Reaction of **12a** with Me_3SiCl/NEt_3 yields the ester PTA-CO_2Me (**12b**) [18].

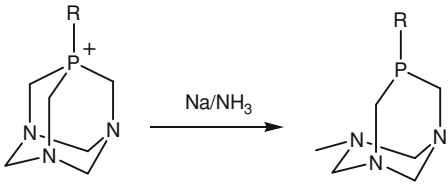
An interesting class of "lower rim" functionalized PTA analogues is represented by open versions of **1** which can be obtained by cleavage of a N–C bond of the triazacyclohexane ring. Darensbourg et al. showed that reaction of **1** with acetic anhydride gives the highly water soluble (7.4 vs 1.5 mol L^{-1} for **1**) 3,7-diacetyl-1,3,7-triaza-5-phosphabicyclo[3.3.1]nonane (DAPTA, **13**) (Scheme 7.4) [19]. The formyl analogue of **13**, i.e. 3,7-diformyl-1,3,7-triaza-5-phosphabicyclo[3.3.1]nonane (DFPTA, **14**) is obtained as expected by reaction of **1** with formic anhydride [15].

Scheme 7.4 Synthesis of DAPTA and DFPTA



13 R = Me, DAPTA
14 R = H, DFPTA

Scheme 7.5 Synthesis of PTN(R) ligands



R = Me, Et, Ph, Bz, Cy

15

The formal analogue of DAPTA, having two methyl groups instead of acetyl groups was obtained by Romerosa and coworkers [10]. Compound 3,7-dimethyl-1,3,7-triaza-5-phosphabicyclo[3.3.1]nonane (dmoPTA, **5b**, Scheme 7.2) was obtained by reaction of dmPTA (**5a**) with KOH by elimination of one of the methylenes of the triazacyclohexane lower rim.

Finally, the selective cleavage of a N–CH_2–N methylene bridge in phosphonium chlorides [R-*P*-PTA]Cl (Scheme 7.5) with Na chunks in liquid ammonia at low temperature produces a mixture of **1** and 7-phospha-3-methyl-1,3,5-triazabicyclo[3.3.1]nonane [**15**, R = Me (a), Ph (b), Et (c), Bz (d), Cy (e)]. The desired products can be generally isolated as pure compounds by sublimation under reduced pressure, albeit in low yields [13]. Compounds **15a** and **15b**, i.e. PTN(R) (R = Me, Ph) have found application as ligands to Rh(I) precursors and the corresponding complexes were used as catalysts for olefin hydroformylation with some success (see Sect. 7.3). The synthesis of PTN(Me) has been recently rivisited and improved [20].

7.2 Hydrogenation Reactions

The homogeneous hydrogenation of carbonyl groups from organic compounds is a valuable tool for the synthesis of alcohols, often bearing other functionalities such as C=C double bonds. Thus, early reports of transition metal catalyzed hydrogenation have focused on α,β-unsaturated carbonyl compounds as test substrates for chemo- and regioselective catalysts. The hydrogenation protocols used have included hydrogen gas and transfer hydrogenation conditions as terminal reducing agents, and the relevant examples of complexes containing PTA used as catalysts

for these methods will be described in the Sect. 7.2.1. Some late transition metal complexes containing PTA have been used successfully to hydrogenate carbon dioxide and hydrogen carbonate to formate. This topic will be highlighted in Sect. 7.2.2.

7.2.1 C=O and C=C Bond Hydrogenation

C=O bond reduction. Ru-PTA complexes $[RuCl_2(PTA)_4]$ (**16**) and $[RuCl_2(CO)(PTA)_3]$ (**17**) catalyze the hydrogenation of substituted benzaldehydes into alcohols and terminal aldehydes [6, 21–24]. Under biphasic conditions using sodium formate as the hydrogen source, $[RuCl_2(PTA)_4]$ gave 95.1% conversion of benzaldehyde into benzyl alcohol at 80 °C (TOF = 22 h^{-1}) [24]. In the presence of an *ortho* substituent on the phenyl group of the substrate, as for 2-methoxybenzaldehyde, the conversion decreased to 23.6%. For α,β-unsaturated aldehydes, hydrogenation is usually selective to the unsaturated alcohol [24]. Saturated and unsaturated acyclic aldehydes were hydrogenated using **16** with sodium formate, with conversions ranging from a maximum of 87.6% for 2-butenal to 23.0% for 1-hexanal (Table 7.1). Long chain aldehydes such as 1-decenal are not hydrogenated in the presence of **16** [24]. The biphasic hydrogenation of benzaldehyde (0.80 M) using **16** (0.03 mmol) with aqueous $NaHCO_2$ proceeds with a rate of 1.01×10^{-2} min^{-1} (80 °C in chlorobenzene). Deuterium labeling experiments performed by Joó and co-workers demonstrated that the source of hydrogen is sodium formate instead of water in the presence of **16**. Three benzaldehyde hydrogenation tests using **16** were carried out using $D_2O/NaHCO_2$, $H_2O/NaDCO_2$

Table 7.1 Catalytic hydrogenation of aryl aldehydes to alcohols using $[RuCl_2(PTA)_4]$ (**16**) [24]

Substrate (mmol)	Conversion (%)[a]
Benzaldehyde(4.92)	64.0
	7.1[b]
	0.4[c]
4-Methylbenzaldehyde (4.24)	23.6
4-Methoxybenzaldehyde (4.11)	26.7
4-Bromobenzaldehyde (1.35)	16.3
2-Hydroxybenzaldehyde (4.69)	0
1-Hexanal (4.16)	23.0
2-Butenal (6.04)	87.6
3-Phenyl-2-propenal (3.96)	21.2
1-Propanal (6.93)	81.6
1-Butanal (5.55)	72.8
1-Pentanal (4.70)	46.1
1-Hexanal (4.16)	23.0

[a] *Conditions* **16**, 0.0625 mmol, chlorobenzene 5 ml/H_2O 5 ml; 5 M $NaCO_2H$, 5 ml; 80 °C, 3 h
[b] Under an atmosphere of CO
[c] 10 equiv PTA added

and $D_2O/NaDCO_2$, respectively [24]. Mass spectroscopy analysis demonstrated that the level of deuterium incorporation in the benzyl alcohol was higher using $H_2O/NaDCO_2$, whereas 100% C_6H_4CDHOH was obtained as expected with $D_2O/NaDCO_2$.

Catalyst **16** was efficiently recycled without loss of activity and it was demonstrated that it does not transfer into the organic phase. Interestingly, transfer hydrogenation conditions seem to be the choice for this kind of catalysts. By replacing sodium formate with H_2 pressure, 400 psi at least are needed to obtain modest TOFs. For example, conversion of benzaldehyde using 14 psi of H_2 resulted in a 2.6% conversion whereas using 400 psi of H_2 increased the conversion to 45.9%.

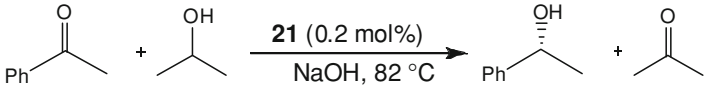
Ruthenium(II) and rhodium(III) complexes of mPTA such as *trans*-$[RuI_4(mPTA)_2]$ (**18**), *mer*-$[RuI_2(mPTA)_3(H_2O)]I_3$ (**19**) and $[RhI_4(mPTA)_2]I$ (**20**) are active catalysts for the hydrogenation of cinnamaldehyde [25]. Different chemoselectivity was observed for these catalysts: whereas **18** and **20** are selective to C=O bond hydrogenation, **20** gives selective reduction of the C=C double bond under biphasic water/toluene or chlorobenzene mixtures and H_2 pressure. Average TOFs were measured at 40 (**19**) to 183 (**18**) and 190 h^{-1} (**20**) respectively. Cinnamaldehyde was reduced to $PhCH_2CH_2CHO$ using **20** (95% conversion and 84% selectivity). The highest selectivity to cinnamol was observed in the presence of **18** (84% yield at 89% conversion). Transfer hydrogenations using these catalysts gave in general lower conversions (see Table 7.2). Recycling of the catalyst showed no loss of activity upon three cycles.

Complex *fac*-$[RuCl_2(PTA)_2\{\kappa^2(P,N)\text{-FcPN}\}]$ (**21**) is a moderately active catalyst for the asymmetric transfer hydrogenation (ATH) of acetophenone [26]. Moderate conversions and *ee*'s were obtained in the presence of **21** (0.2 mol %) using 0.1 M acetophenone, 50 mL iPrOH, 4.8 mol % NaOH. The maximum conversion was measured at 54% corresponding to a TOF of 1633 h^{-1} and accompanied by a *ee*(R) of 23% (Scheme 7.6). Figure 7.1 shows drawings of catalysts **18**–**21**.

Table 7.2 Hydrogenation of cinnamaldehyde using catalysts **18**, **19** and **20** [25]

Catalyst	Conv. (%)	TOF (h^{-1})	Products (yield %)
18	89[a]	40	$PhCH{=}CHCH_2OH$ (84) $Ph(CH_2)_3OH$ (5)
18	4[b]	8	$PhCH{=}CHCH_2OH$ (2.5) $Ph(CH_2)_2CHO$ (1)
19	45[a]	183	$PhCH{=}CHCH_2OH$ (36) $Ph(CH_2)_2CHO$ (5) $Ph(CH_2)_3OH$ (4)
19	2[b]	4	$PhCH{=}CHCH_2OH$ (2)
20	95[a]	190	$PhCH{=}CHCH_2OH$ (2.5) $Ph(CH_2)_2CHO$ (84) $Ph(CH_2)_3OH$ (8)
20	13[b]	25	$Ph(CH_2)_2CHO$ (13)
18	17[c]	4	$PhCH{=}CHCH_2OH$ (17)

Conditions [a]Toluene/water, $p(H_2) = 3.0$ Mpa, [catalyst] 0.01 mmol, 333 K
[b]Chlorobenzene/water, 5 M $NaCO_2H$, [catalyst] 0.01 mmol, 348 K
[c]Toluene/water, $p(H_2) = 0.1$ Mpa, [catalyst] 0.01 mmol, 293 K



Scheme 7.6 Asymmetric transfer hydrogenation of acetophenone catalyzed by a Ru-PTA complex

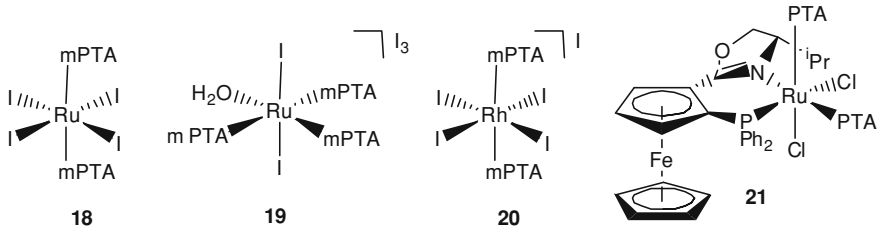


Fig. 7.1 Ru and Rh-PTA complexes **18**–**21**, active catalysts for C=O bond reduction

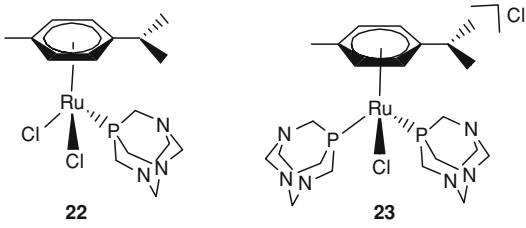


Fig. 7.2 RAPTA Ru(II) arene complexes **22**–**21**

C=C bond reduction. Hydrogenation of substituted arenes into saturated cyclohexanes was demonstrated by Dyson et al. using arene-Ru complexes [Ru(η^6-*p*-cymene)Cl_2(PTA)] (**22**) and [Ru(η^6-*p*-cymene)Cl(PTA)$_2$]Cl (**23**) as catalysts under biphasic conditions [27, 28]. This class of compounds is also known in the literature as RAPTA complexes (Fig. 7.2) [1, 2]. The homogeneous nature of the catalysts was demonstrated by the lack of influence of added elemental Hg on the performance. Catalyst **22** was slightly more active than **23** (Table 7.3), but both were significantly less active than the analogous [Ru(*p*-cymene)(TPPMS)Cl_2] complex, for which however the addition of Hg hinders hydrogenation, suggesting that Ru colloidal particles may be the active catalytic species. Hydrogenation of chlorobenzene results in extremely poor TOFs. Arene hydrogenation catalyzed by **22** in ionic liquids such as [bmim]BF_4, (bmim = 1-butyl-3-methylimidazolium) was carried out later on by the same authors. In this system, a 50% increase was observed for the conversion of benzene compared to catalytic tests run in water [29].

A detrimental effect of the presence of trace amounts of chloride salts was also shown (see Table 7.3). Recycling of the catalyst was possible and the turnovers remained constant in [bmim][BF_4] and Cl-free [bmim][BF_4], decreasing slightly in water after 5 cycles.

Table 7.3 Hydrogenation of various arenes using catalytic amounts of **22** and **23** [27, 29]

Catalyst	Substrate	TOF (h^{-1})	Conditions
22	Benzene	170	H_2O
22	Benzene	140	[bmim]BF_4/Cl[a]
22	Benzene	137	[hmim]BF_4/Cl[a]
22	Benzene	141	[omim]BF_4/Cl[a]
22	Benzene	206	[bmim]BF_4
22	Benzene	54	CH_2Cl_2
22	Toluene	130	H_2O
22	Toluene	54	[bmim]BF_4/Cl[a]
22	Toluene	136	[bmim]BF_4
22	Ethylbenzene	122	H_2O
22	Ethylbenzene	53	[bmim]BF_4/Cl[a]
22	Ethylbenzene	145	[bmim]BF_4
22	Chlorobenzene	11	H_2O
22	Chlorobenzene	6	[bmim]BF_4/Cl[a]
22	Chlorobenzene	18	[bmim]BF_4
23	Benzene	150	H_2O
23	Toluene	129	H_2O
23	Ethylbenzene	72	H_2O

bmim = 1-butyl-3-methylimidazolium, hmim = 1-hexyl-3-methyl imidazolium,omim = 1-octyl-3-methylimidazolium. *Conditions* $p(H_2)$ 60 atm, 90 °C, 1 h. Catalyst, 30 mg; solvent, 10 ml; substrate, 1 ml

[a]Trace amounts

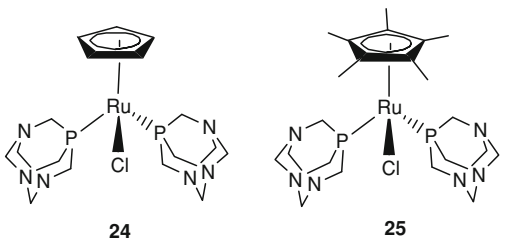


Fig. 7.3 Cyclopentadienyl (Cp) and pentamethylcyclopentadienyl (Cp*) Ru(II) PTA complexes **24** and **25**

The synthesis and application of a series of Ru-PTA cyclopentadienyl (Cp) and pentamethylcyclopentadienyl (Cp*) complexes was reported by Peruzzini and coworkers (Fig. 7.3) [30]. Complexes [CpRuCl(PTA)$_2$] (**24**) and [Cp*RuCl(PTA)$_2$] (**25**) were found to be active catalysts for the chemoselective C=C bond hydrogenation of benzylidene acetone (BZA).

Under moderate H_2 pressure (450 psi) in a biphasic water/octane solvent mixture, conversions ranging from 39.1% (3 h, 130 °C) to 99.7% (21 h, 130 °C), were obtained. Catalyst recycling under these conditions was found to be limited to the third cycle. The mechanism of formation of catalytically active Ru hydrido-complexes was investigated by HPNMR spectroscopy. Complex **24** was observed to react at 50 °C with H_2 (450 psi) in H_2O/THF-d_8 to form the mono-hydrido complex [CpRuH(PTA)$_2$](**26**), stable upon heating to 80 °C. In contrast,

25 activates H_2 at 50 °C to form a dihydride complex [Cp*RuH_2(PTA)$_2$]Cl which converts to the monohydride [Cp*RuH(PTA)$_2$] after heating to 80 °C. The reason for this behavior was recently explained using DFT calculations [31]. Complexes **24** and **25** were also applied as catalysts for BZA and cinnamaldehyde reduction under transfer hydrogenation conditions. For BZA, conversions ranged from moderate (36%, 6 h) using **24** to excellent (97%, 6 h) in the presence of **25** (conditions: substrate, 0.75 mmol; catalyst, 7.5×10^{-3} mmol; HCO_2Na, 7.5 mmol; MeOH, 3 ml; H_2O, 3 ml; 90 °C) was observed [32].

Later on, Frost et al. showed that the chemoselectivity in the reduction of BZA by [CpRuH(PTA)$_2$] (**26**) in a biphasic H_2O/Et_2O solvent system at room temperature and low pressures of H_2 (10-150 psi) is dramatically influenced by pH. At pH >7 and pH <3.6 a poor catalytic performance was observed, and highest activity was measured at pH = 4.7. Although the reduction is generally selective to C=C double bond hydrogenation, at pH 2.1 the selectivity changes with the type of buffer used (HBF_4/NaH_2PO_4, 99% of 4-phenylbutan-2-one; HCl/NaH_2PO_4, 77.5% of 4-phenylbut-3-en-2-ol). Another factor affecting conversion is the addition of salts such as KCl, $NaNO_3$, $NaBF_4$, or $NaPF_6$, in particular BF_4^- was the one that gave the highest conversion [33, 34].

The same authors later expanded on these results to explore the effect of the nature of the arene ligand on the transfer hydrogenation of CNA, BZA and chalcone. Ruthenium bis-PTA or mixed PPh_3/PTA complexes bearing cyclopentadienyl ($C_5H_5^-$, Cp), 1,2-dihydropentalenyl ($C_8H_9^-$, Dp) and indenyl ($C_9H_7^-$, Ind) as ancillary ligands (**27**–**31**) were tested in aqueous media using either sodium formate or formic acid (pH ≤3). The indenyl complex was less active than either the Cp or Dp analogues. The results of BZA reduction are summarized in Table 7.4 [35].

Rh(I) complexes bearing PTA were also tested as catalysts for C=C bond hydrogenations. The complex Rh(acac)(CO)(PTA) (**32**) was tested for catalytic hydrogenation of alkenes and allyl alcohol [36]. Under biphasic conditions water/substrate and H_2 pressure, initial TOF values ranged from 26 h^{-1} for hydrogenation of allyl alcohol into *n*-propanol (selectivity 90%) to 143 h^{-1} for the hydrogenation of 1-hexene. The activity of **32** was compared to other [Rh(acac)(CO)L] derivatives with hydrophilic phosphines (L) such as trisulfonated triphenylphosphine, TPPTS. It was observed that the complexes were active for alkene and allyl alcohol hydrogenations, although **32** shows lower initial TOFs for conversion of 1-hexene than [Rh(acac)(CO)(TPPTS)] (260 h^{-1}). The hydrogenation of allyl alcohol resulted in partial isomerization to propanal, and in D_2O the incorporation of deuterium was observed at the a-position followed by acetalyzation to $CH_3CHDCH(OD)_2$, see Scheme 7.7.

Complexes [RhI(CO)(mPTA)$_2$]I_2 (**33**) and [RhI(CO)(mPTA)$_3$]I_3·$4H_2O$ (**34**) found applications as catalysts for olefin hydroformylation (see Sect. 7.3) and alkene hydrogenation under biphasic or aqueous phase conditions [37]. The hydrogenation of C=C double bond in unsaturated carboxylic acids such as maleic and fumaric acid was also tested successfully, see Table 7.5. Acetalyzation products were also formed in the case of aldehyde hydrogenations. When terminal

Table 7.4 Transfer hydrogenation of BZA using either HCOOH or HCOONa as the reducing agents

Entry	Catalyst	% conv	TOF (h^{-1})	% sel saturated ketone	% sel unsaturated alcohol	% sel saturated alcohol
1	[CpRu(PTA)(PPh_3)Cl] (**27**)	79.4	0.7	55.9	0.0	34.7
2	[CpRu(PTA)$_2$Cl] (**24**)	66.7	0.6	100.0	0.0	0.0
3[a,b]	[CpRu(PTA)$_2$Cl] (**24**)	78.9	0.6	>99.0	<1.0	0.0
4[c,d]	[CpRu(PTA)$_2$Cl] (**24**)	36.1	6.0	93.9	6.1	0.0
5[c]	[DpRu(PTA)(PPh_3)Cl] (**28**)	51.1	1.7	100	0.0	0.0
6	[DpRu(PTA)$_2$Cl] (**29**)	81.4	0.8	58.7	41.3	0.0
7[a]	[DpRu(PTA)$_2$Cl] (**29**)	83.7	0.8	100.0	0.0	0.0
8[e]	[IndRu(PTA)(PPh_3)Cl] (**30**)	48.9	0.41	100.0	0.0	0.0
9[f]	[CpRu(PTA)(PPh_3)H] (**31**)	38.5	0.64	100.0	0.0	0.0

General conditions catalyst, 5 mmol; BZA, 4.3 mg; 88% HCO_2H, 40 μL; H_2O, 2 mL; 24 h; 80 °C; pH ≈ 3

[a] HCO_2Na, 0.9 mmol, pH ≈ 9

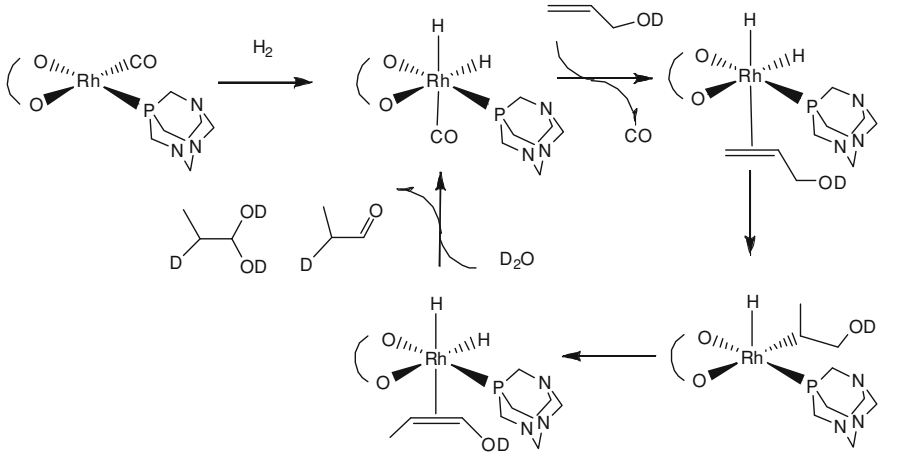
[b] 25 h

[c] 6 h

[d] substrate, 0.75 mmol; catalyst, 7.5×10^{-3} mmol; HCO_2Na, 7.5 mmol; MeOH, 3 mL; H_2O, 3 mL; 90 °C, 6 h

[e] HCOOH, 150 μL; H_2O, 2 mL; MeOH, 1 mL

[f] HCOOH, 100 μL; 12 h



Scheme 7.7 Proposed mechanism for allyl alcohol hydrogenation in D_2O in the presence of [Rh(acac)(CO)(PTA)] (**32**)

Table 7.5 Hydrogenation tests with **34** and **34** [37]

Catalyst	Substrate	Product distribution (yield %)	Average TOF (h^{-1})	Conv (%)
33	n-C_3H_7CHO[a]	n-BuOH (6) n-PrCH=C(Et)CHO (6) $BuEtCHCH_2OH$(2) $EtC(n\text{-}PrCHOH)_2CHO$ (77) n-PrCOO(n-Bu) (1)	109	98
34	n-C_4H_9CHO[a]	n-$C_5H_{11}OH$ (80) n-$BuCH=C(n\text{-}Pr)CHO$ (3) Other (14)	108	97
34	n-$C_5H_{11}CHO$[a]	n-$C_6H_{13}OH$ (84) n-$C_5H_{11}CH=C(n\text{-}Bu)CHO$ (6) n-$C_6H_{13}CH(n\text{-}Bu)CH_2OH$ (2) Other (8)	108	97
34	n-$C_6H_{13}CHO$[a]	n-$C_7H_{15}OH$ (78) n-$C_6H_{13}CH=C(n\text{-}C_5H_{11})CHO$ (12) n-$C_7H_{15}CH(n\text{-}C_5H_{11})CHO$ (2) Other (3)	109	95
34	Maleic acid[b]	$HO_2C(CH_2)_2CO_2H$	110[c]	>99
34	Fumaric acid[c]	$HO_2C(CH_2)_2CO_2H$	210[c]	>99
34	$CH_2=CHCH_2OH$[c]	C_3H_7OH	160[c]	>99

Conditions [a] Substrate 20 mmol; catalyst 0.01 mmol; H_2O 15 ml; $p(H_2)$ 8.0 Mpa; 353 K
[b] Substrate 10 mmol; catalyst 0.01 mmol; H_2O 15 ml; $p(H_2)$ 0.1 Mpa; 293 K
[c] Initial TOF

saturated aldehydes were used as substrates, C=O bond hydrogenation to primary alcohols was observed as expected.

[RhCl(PTAH)$(PTA)_2$]Cl (**35**) catalyzed the conversion of *trans*-cinnamaldehyde with high selectivity for C=C double bond (93.3%) under biphasic conditions using sodium formate as the hydrogen source [38]. The nature of the catalytically active species was however thought to be heterogeneous, as suggested by a decrease in conversion upon addition of cylcooctatetraene and elemental Hg. Complex **35** is also a transfer hydrogenation catalyst for allylbenzene. This reduction is poorly selective, as it gives extensive isomerization to *cis*- and *trans*-propenylbenzene, somehow improved replacing sodium formate with H_2 pressure, which leads to faster reactions and decreased isomerization. Catalyst recycling for **35** was limited to the fourth cycle.

Complexes κ^1-*P*-[RhCl(cod){PTN(R)}] (R = Me, **36**; R = Ph, **37**) and κ^2-*P*,*N* -[Rh(cod){PTN(R)}](BAr^F_4) (R = Me, **38**; R = Ph, **39**, Fig. 7.4) were tested as catalysts for olefin hydroformylation (Sect. 7.3) and transfer hydrogenations of BZA and acetophenone [39].

High chemoselectivity to C=C bond hydrogenation was obtained with all complexes in the transfer reduction of BZA using $NaHCO_2$ as hydrogen source in water (Table 7.6), with complex **39** showing the highest conversion (>95%). Transfer hydrogenation of acetophenone was achieved using the KOH/Pr^iOH protocol. In this case, the κ^1-*P* complexes **36**–**37** showed higher conversions (57–69%) than the

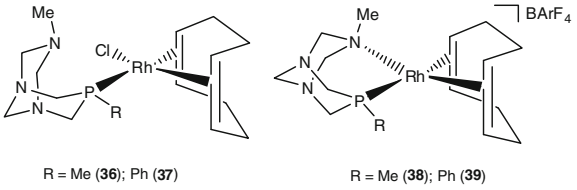


Fig. 7.4 Rh(I) complexes bearing the water soluble PTN(R) ligand (R = Me, Ph)

Table 7.6 Transfer hydrogenation of BZA and acetophenone in the presence of **36–39**

Catalyst	Substrate	% conversion	% sel. A[a]	% sel. B[a]	% sel. C[a]	Av. TON
36	BZA	59.9	98.6	1.4	0.0	60
36	PhC(O)Me	69.3	–	–	100	347
37	BZA	96.4	99.8	0.2	0.0	97
37	PhC(O)Me	57.7	–	–	100	288
38	BZA	59.3	98.8	1.2	0.0	60
38	PhC(O)Me	22.3	–	–	100	112
39	BZA	100	100	0.0	0.0	100
39	PhC(O)Me	17.4	–	–	100	87

Conditions BZA:catalyst:$NaHCO_2$ (100:1:1000); MeOH (3 ml); H_2O (3 ml); 80 °C, 5 h
Conditions catalyst:acetophenone:KOH (1:500:5); Pr^i OH (10 ml); 80 °C, 6 h
[a]GC values based on pure samples. A = 4-phenyl-2-butanone; B = 4-phenyl-3-buten-2-ol; C = 1-phenyethanol

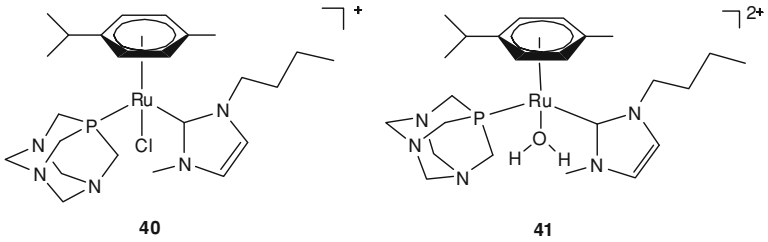


Fig. 7.5 Imidazolyl-arene Ru(II) PTA complexes **40** and **41**

κ^2-P,N chelated complexes **38–39**. Higher substrate/catalyst ratio (1000:1) was tested for transfer hydrogenation of acetophenone giving lower conversions (20%, TON 198).

Finally, PTA complexes derived (Fig. 7.5) from chloride substitution in [$RuCl_2$(*p*-cymene)L] (L = 1-butyl-3-methylimidazol-2-ylidene), namely [RuCl(*p*-cymene)L(PTA)]Cl (**40**) and [Ru(*p*-cymene)(H_2O)L(PTA)]$^{2+}$ (**41**) were able to catalyze the hydrogenation of cinnamaldehyde, BZA to the C=C bond and acetophenone (C=O reduction) under a hydrogen pressure of 10 bar, with a catalyst concentration of 4.73 mM, substrate concentration 667 mM, after 1 h at 80°C in buffered water solution (pH 6.9, phosphate buffer), albeit with low conversions. For cinnamaldehyde, conversion reached 27% using **40** and 42% with **41**, whereas

for BZA it ranged from 21% with **40** to 42% using **41**. In the case of acetophenone, 29% conversion was obtained with **40** and 46% in the presence of **41** [40].

7.2.2 CO_2 and HCO_3^- Hydrogenation

Carbon dioxide is often seen as a potential tool offered by nature for C1-chemistry, and its capture from the environment is an issue linked to greenhouse effect control. Under the chemical point for view, CO_2 hydrogenation to formate can in principle represent a cheap feedstock (carbonate rocks) for a useful building block, providing that mild and selective conditions are available for such transformation. In a comparative study, Laurenczy et al. have tested the efficiency of a series of water-soluble Ru(II) and Rh(I) complexes such as $[RuCl_2(PTA)_4]$ (**16**) $[RuCl_2(TPPTS)_3]$, $[RuCl_2(TPPMS)_2]_2$, $[RhCl(TPPTS)_3]$ as catalysts for CO_2 and HCO_3^- reduction under mild conditions (60 bar CO_2, 30 bar H_2). It was observed that the initial TOF increases linearly with H_2 pressure, with maximum initial value of 7260 h^{-1} under 81 °C and 40 atm total pressure CO_2/H_2 (1:1) [41]. Additives such as amines are required to achieve efficient hydrogenation, although it was observed that Na_2CO_3 1 M can replace Me_2NH 0.5 M causing an increase in the overall TOF from 0.13 h^{-1} to 116 h^{-1} at 24 °C, by formation of $NaHCO_3$ which is more easily hydrogenated. $[RuCl_2(TPPTS)_2]_2$ catalyses the hydrogenation of CO_2 to formic acid (TOF 6 h^{-1}, 23 °C) in the presence of amines. The increase of CO_2 pressure has negative effect on the rate of hydrogenation of bicarbonate using $[RuCl_2(TPPTS)_2]_2$, whereas with **16** an increase of the rate is observed under these conditions. In the presence of $CaCO_3$ as a base, TOFs ranged from 26.6 h^{-1} with $[RuCl_2(TPPTS)_2]_2$ to 18.7 h^{-1} using $[RhCl(TPPTS)_3]$, to 2.5 h^{-1} with **16** [42].

The mechanism involving **16** was studied in details by ^1H and ^{13}C HPNMR. An aqueous solution of $NaHCO_3$ (1.6 mmol) $NaH^{13}CO_3$ (0.4 mmol) and a catalytic amount of **16** (5.4×10^{-3} mmol) was pressurized with H_2 [43]. Three new species were observed in solution, and they were identified as the monohydride $[RuHCl(PTA)_4]$ (**42**), the hydrido aquo cation $[RuH(H_2O)(PTA)_4]^+$ (**43**) and the dihydride $[RuH_2(PTA)_4]$ (**44**). The relative stability of these hydrido complexes and their formation strongly depend on pH. At pH 12.0, only **44** was observed by ^1H NMR as a typical multiplet resonance at –11.40 ppm. At pH 2.0, the monohydride **42** is formed, as indicated by a doublet of quartets at –8.31 ppm in the ^1H NMR spectra. In the presence of an excess of PTA, the new species $[RuH(PTA)_5]^+$ (**45**) was identified. The catalytic reaction does not require the addition of amines, but can be promoted with inorganic bases such as NaOH or $CaCO_3$. High pressure ^1H and ^{13}C NMR measurements under different H_2 pressures show that the reaction rate is first order in H_2 pressure. HCO_3^- is the substrate which is hydrogenated, and the initiation time observed with **16** may be due to the formation of such species in solution, accompanied by ligand exchange and formation of the corresponding hydride complex as the active catalytic species. An overall

activation energy of 86 kJ mol^{-1} was calculated, higher than the 25 kJ mol^{-1} observed for the $RuCl(TPPTS)_3$ system.

Complexes $[CpRuCl(PTA)_2]$ (**24**), $[Cp^*RuCl(PTA)_2]$ (**25**) [44], and $[Cp^*IrCl(PTA)_2]Cl$ (**46**) [45], were tested as catalysts for CO_2/HCO_3^- reduction to formate, in the absence of additives and under mild conditions, in the pH range 5.3–10.5 and in the temperature range 30–100 °C (Table 7.7). Complex **46** showed the highest activity at higher temperature and in slightly basic conditions (pH 9). The active species was determined to be the cationic complex $[Cp^*IrH(PTA)_2]^+$ (**47**).

The presence of arene or cyclopentadienyl ligands does not seem to be mandatory for the hydrogenation of CO_2/bicarbonate under mild conditions, as demonstrated by tests using $[RuCl_2(PTA)([9]aneS_3)]$ (**48**), where they are replaced by the facial trithiane $[9]aneS_3$ ligand [46]. In aqueous solutions, $NaH^{13}CO_3$ (0.15 M) is reduced to sodium formate under a hydrogen pressure of 100 bar at 303 K, albeit **48** gave low activity in absence of amines as additives. No induction period

Table 7.7 Catalyst screening for aqueous hydrogenation of bicarbonate at different pH values and temperatures

Catalyst	T (°C)	pH	Initial TOF (h^{-1})[a]
$[CpRuCl(PTA)_2]$ (**24**)	50	10.54	0.04
	50	7.87	1.2
	50	5.94	1.56
	65	7.87	4.5
	80	10.54	0.05
	80	9.46	1.4
	80	7.87	5.2
$[Cp^*RuCl(PTA)_2]$ (**25**)	25	10.2	1.0
	25	9.4	7.4
	25	6.24	12.1
	30	9.46	0.4
	30	8.14	2.3
	30	5.60	5.0
	50	9.46	3.9
	62	10.3	11.4
	80	12.2	16.0
$[Cp^*IrCl(PTA)_2]Cl$ (**46**)	70	8.4	4.0
	80	8.4	10.7
	90	8.4	16.5
	100	8.4	22.6
	80	5.9	6.5
	80	9.0	12.7
	80	9.2	9.1
	80	9.5	6.5
	80	9.8	5.4
	80	10.3	2.3

[a]TOF (mol formate/mol catalyst/h^{-1}) were calculated by non linear least-square fits of the experimental data from the initial part of the reactions

is required probably due to the rapid hydrolysis of the compound in water. [Ru(H)(CO_3H)(PTA)([9]aneS_3)] was identified as a key species being formed during the catalytic reactions (Scheme 7.8).

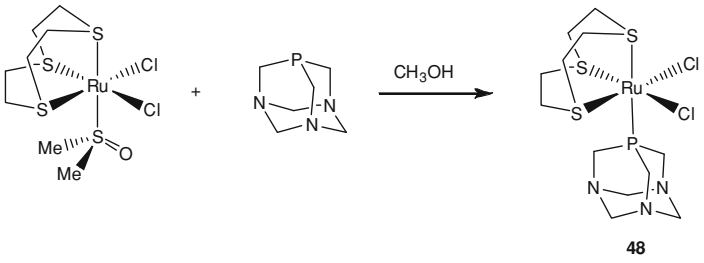
7.3 Olefin Hydroformylation

A few complexes of transition metals, especially Rh(I), bearing PTA as ancillary ligand able to impart water solubility, found applications in biphasic olefin hydroformylation reactions. [RhI_4(mPTA)$_2$]I (**20**) was found to be active for the hydroformylation of 1-hexene under 3.5 MPa total pressure (CO/H_2 = 1:1), 60 °C, using 0.01 mmol of catalyst, H_2O 15 cm^3 and 30 mmol of 1-hexene. The TOF was measured as 138 h^{-1}, corresponding to a final conversion of 93%. The regioselectivity was however found to be very modest with a l/b ratio of 1.7 [25].

The complex [Rh(acac)(CO)(PTA)] (**61**) was also tested for the hydroformylation of 1-hexene [36]. The substrate (0.02 mol) was hydroformylated using 10^{-5} mol of catalyst in H_2O (15 mL) under a CO/H_2 (1:1) total pressure of 3.0 MPa at 60 °C. The average TOF was measured at 61 h^{-1} and after 18 h the conversion reached 64.9%, however poor selectivity was observed as the product distribution included isomerization products and l/b ratio of 2.5, i.e. n-heptanal 34.1%, i-heptanal 13.6%, 2-hexene 11.0% and 3-hexene 6.2%.

Complexes [RhI(CO)(mPTA)$_2$]I_2 (**33**) and [RhI(CO)(mPTA)$_3$]I_3·4H_2O (**34**) were tested for alkene hydroformylation under biphasic or aqueous phase conditions [37]. For the hydroformylation of 1-hexene, l/b ratio was found to be *ca.* 1 in the presence of **33**, with extensive isomerization. Although fast rates were observed, the activity of **33** and **34** are lower than for the corresponding TPPTS analogues. The catalytic tests were repeated using **34** together with an excess of free mPTA. Both conversion (from 70 to 91%) and TOF (from 117 to 150 h^{-1}) increased, however in this case by-products coming from hydrocarboxylation and hydrogenation side reactions were obtained (Table 7.8).

Complexes κ^1-*P*-[RhCl(cod){PTN(R)}] (R = Me, **36**; R = Ph, **37**) and κ^2-*P*,*N*-[Rh(cod){PTN(R)}](BAr^F_4) (R = Me, **38**; R = Ph, **39**, Fig. 7.4) were tested as catalysts for 1-hexene hydroformylation in homogeneous phase (either THF or



48

Scheme 7.8 Synthesis of [$RuCl_2$(PTA)([9]aneS_3)] (**48**)

Table 7.8 Biphasic 1-hexene hydroformylation using **33** and **34**

Catalyst	Substrate	Product distribution (yield %)	Average TOF (h^{-1})	Conv (%)
33	1-Hexene	*n*-$C_6H_{13}CHO$ (29) $C_4H_9CH(CH_3)CHO$ (25) $CH_3CH{=}CHC_3H_7$ (10) $CH_3CH_2CH{=}CHC_2H_5$ (6)	117	70
34	1-Hexene + 6 equiv mPTA	*n*-$C_6H_{13}CHO$ (39) $C_4H_9CH(CH_3)CHO$ (25) *n*-$C_6H_{13}COOH$ (14) $C_4H_9CH(CH_3)COOH$ (13)	150	91

Conditions substrate 30 mmol; catalyst 0.01 mmol; H_2O 15 ml; p(CO) = p(H_2) 3.0 MPa; 353 K

Table 7.9 1-Hexene hydroformylation under homogeneous conditions in the presence of complexes **36–39**

Catalyst	Conv. % (h)	Linear %	Branched %	l/b	Isom %	Hydrog %
36	20.2 (1)	12.2	3.9	3.13	4.0	0.1
36	61.5 (4)	31.9	13.4	2.38	16.1	0.1
36[a]	83.0 (4)	43.5	20.9	2.08	18.4	0.2
36[b]	92.5 (4)	50.7	26.2	1.94	15.5	0.1
37	63.4 (1)	33.6	12.3	2.73	17.4	0.1
37	99.3 (4)	48.3	26.1	1.85	20.9	4.0
37[b]	82.5 (4)	33.5	24.9	1.35	19.9	4.2[c]
38	27.4 (1)	14.8	5.5	2.69	7.0	0.1
38	70.0 (4)	35.8	15.8	2.27	17.6	0.8
39	52.6 (1)	29.8	11.3	2.64	11.3	0.2

1-Hexene: 2.5 mmol; cat 0.01 mmol; H_2:CO (2:1), 600 psi; THF: 30 ml; 60° C; 4 h
[a] CO/H_2 (1:1) 600 psi
[b] $CHCl_3$ 30 ml, 55 °C, CO/H_2 (1:1) 600 psi
[c] Including alcohols

$CHCl_3$) under relatively mild conditions and the results are summarized in Table 7.9.

As expected, the linear aldehyde was found to be the favored product, with l/b ratio ranging from 1.35 (**37** in $CHCl_3$, 4 h) to 3.13 (**36** in THF, 1 h). The best conversion was achieved with **37** (99%), although a larger amount of isomerized alkenes were formed. Interestingly, in THF the systems afford very little amounts of hydrogenation products. Styrene hydroformylation tests were also carried out both under homogeneous and biphasic *n*-octane/water conditions. High conversions and chemoselectivity to the branched aldehydes (>94%) were achieved (Table 7.10) and only traces of hydrogenated product (ethylbenzene, <0.5%) were formed under these conditions. Phosphine-free $[Rh(cod)Cl_2]_2$ was used for comparison. In this case, running the reactions in $CHCl_3$ at 55 °C, a slightly higher l/b ratio was obtained at almost complete conversion compared to runs using complexes **36–39** (0.11, corresponding to 88.9% branched and 9.9% linear aldehyde),

Table 7.10 Styrene hydroformylation under homogeneous and biphasic conditions using complexes **36–39**

Complex	Conv. (%)	Branched (%)	Linear (%)	l/b	EtPh (%)
36[a]	99.3	95.4	3.7	0.039	0.2
36[b]	57.7	52.9	2.3	0.043	1.9
37[a]	88.4	84.5	3.7	0.044	0.2
37[b]	71.0	66.9	3.2	0.047	0.9
38[a]	80.8	74.7	5.5	0.074	0.5
39[b]	99.9	95.3	4.7	0.049	0.0

[a]Styrene: 2.5 mmol; cat: 0.01 mmol; H_2:CO (1:1), 600 psi; CH_3Cl: 40 ml; 55 °C; 6 h (Homogeneous conditions)
[b]As above, except H_2O/*n*-octane (2/1), 60 °C (Biphasic conditions)

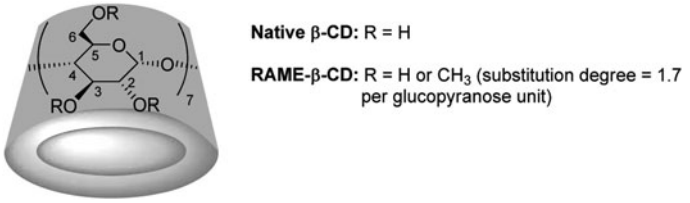


Fig. 7.6 Sketch view of the toroidal structure of β-CDs

whereas in *n*-octane/water at 60 °C a higher amount of ethylbenzene is produced (5.9% against 0.1 in $CHCl_3$).

PTA and the *N*-benzylated derivative 7-phospha-1-benzyl-1,3,5-triazaadamantanyl chloride (*N*-Bz-PTA)Cl were used as ligands for Rh(I) precursors and tested for the hydroformylation of long-chain terminal aldehydes such as 1-decene in water, in the presence of randomly methylated β-cyclodextrin (RAME-β-CD, Fig. 7.6) as mass transfer promoters [47].

Results showed that both ligands could be considered as non-interacting phosphines with respect to RAME-β-CD, contrary to what observed for sulfonated aryl phosphines such as TPPTS for which a large inclusion constant ($K_i = 10^4$ M^{-1}) was calculated. It was observed (Table 7.11) that the chemoselectivities in aldehydes obtained in the presence of PTA and (*N*-Bz-PTA)Cl were very high at higher temperatures (>98%), without a decrease in regioselectivity as observed with TPPTS. Moreover, high conversions and selectivities were observed already at 100 °C with (*N*-Bz-PTA)Cl, being slightly less basic than PTA, without a dramatic change in the l/b ratio.

7.4 C–C and C-Element Bond Formation

Among catalytic processes, those entailing the formation of C–C or C-element bonds have received large attention due to the potential in synthetic organic chemistry, bringing about carbon chain elongations, cyclizations and related

Table 7.11 Biphasic rhodium-catalyzed hydroformylation of 1-decene in the presence of randomly methylated β-cyclodextrins (RAME-β-CD) and water soluble phosphines

Phosphine	CD	T (°C)	Conv. (%)[a]	Selectivity (%)[b]	l/b ratio[c]
TPPTS	–	80	3	59	2.8
TPPTS	–	100	28	42	2.9
TPPTS	–	120	50	30	3.0
TPPTS	RAME-β-CD	80	95 (65[d])	96	1.8
TPPTS	RAME-β-CD	100	100 (74[d])	88	1.9
TPPTS	RAME-β-CD	120	100 (85[d])	73	2.2
PTA	–	80	<1	n.d.	n.d.
PTA	–	100	2	90	1.9
PTA	–	120	81	96	1.9
PTA	RAME-β-CD	80	<1	n.d.	n.d.
PTA	RAME-β-CD	100	11	98	1.9
PTA	RAME-β-CD	120	94	99	1.7
(N-Bz-PTA)Cl	–	80	19	98	1.9
(N-Bz-PTA)Cl	–	100	77	99	1.8
(N-Bz-PTA)Cl	RAME-β-CD	80	24	98	1.9
(N-Bz-PTA)Cl	RAME-β-CD	100	86	96	1.8

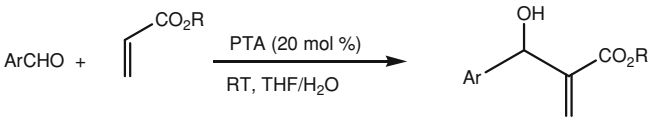
$Rh(acac)(CO)_2$ (4.07×10^{-2} mmol), water-soluble ligand (0.21 mmol), CD (0.48 mmol), H_2O (11.5 mL), 1-decene (20.35 mmol), CO/H_2 (1/1) 50 bar, 6 h

[a] Based on starting olefin

[b] Calculated as (mol. of aldehydes)/(mol of converted olefins) × 100

[c] l/b aldehyde ratio

[d] After 3 h

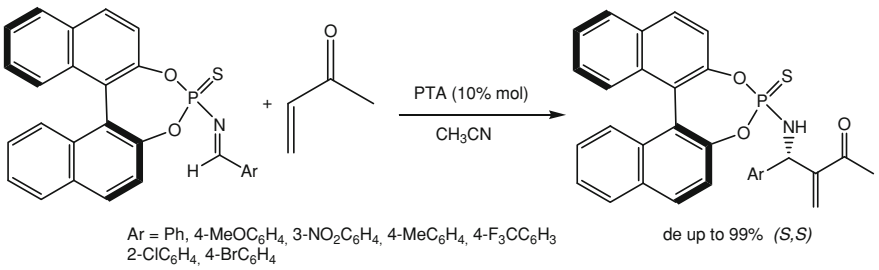


Ar = 2-$NO_2C_6H_4$, 3-$NO_2C_6H_4$, 4-$NO_2C_6H_4$, 2,4-$Cl_2C_6H_3$
2-F-4-ClC_6H_3, 2-pyridyl, 2-$NO_2C_6H_4$, 4-$NO_2C_6H_4$

Scheme 7.9 Morita–Baylis–Hillman (MBH) reaction catalyzed by PTA

reactions, often endowed with stereoselectivity at the C atom which takes part to the new bond forming metal mediated mechanism. Although a huge amount of literature deals with this important class of reactions, only few cases are run in water of biphasic systems [48]. Among these, very few cases are described either in the presence of PTA complexes or PTA as organic base and are hereby summarized.

PTA was used as an organic base to catalyze Morita-Baylis–Hillman type reactions (Scheme 7.9) [49–51]. Variously substituted aryl aldehydes ArCHO were reacted with ethyl acrylate in THF/H_2O (4:1, v/v) at room temperature in the presence of a catalytic amount of **1** (20 mol %) giving the addition products after 5–19 h in yields ranging from 59 to 93%.



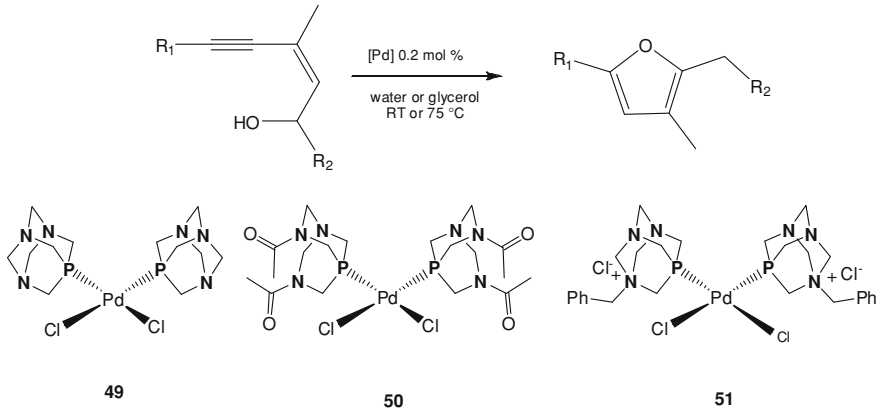
Scheme 7.10 An example of aza-Morita–Baylis–Hillman (AMBH) diastereoselective reaction catalyzed by PTA

Also for the diastereoselective aza-MBH reaction (Scheme 7.10) between chiral *N*-thiophenyl imines and methyl vinyl ketone, PTA was found to be an active catalyst. The products were obtained in good yields (>80%) with excellent diastereoselectivities (>99% *de*, Ar = 4-$F_3CC_6H_4$), albeit at long reaction times (up to 5 days) [52]. PTA is also an effective catalyst in the [3 + 2] cycloaddition of activated allenes with *N*-thiophosphoryl imines to give 3-pyrrolines [53].

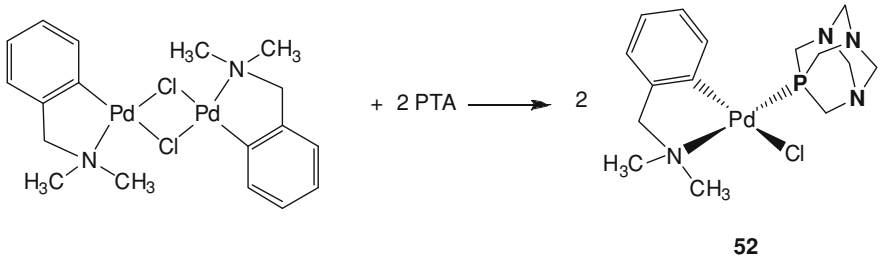
A recent example of C-E (E=O) bond formation is the heteroannulation (cycloisomerization) reactions of (Z)-2-en-4-yn-1-ol derivatives into furans, which have been performed in water and glycerol using *cis*-[$PdCl_2$(PTA)$_2$] (**49**), *cis*-[$PdCl_2$(PTA-Bz)$_2$]Cl_2 (**50**) *cis*-[$PdCl_2$(DAPTA)$_2$] (**51**) as catalysts (Scheme 7.11). In the case of 1,4-substituted (R_1 = alkyl, aryl, alkenyl groups, R_2 = H, Ph) 3-methyl-2-penten-4-yn-1-ol, complex **51** gave complete conversions at 75 °C in both water and glycerol as solvents, with TOFs ranging from 3 h^{-1} (R_1 = H, R_2 = Ph) to 1980 h^{-1} (R_1 = R_2 = H). Also the other catalysts were found to be effective catalysts for this class of reactions, giving almost complete conversions albeit at longer reaction times (3–9 h) running the tests at room temperature. Higher activities were generally observed in an aqueous medium, however recycling of the catalysts was more effectively achieved in glycerol (up to 17 cycles, maximum TON 8190) [54].

Complex κ^2-C,N-[Pd(dmba)Cl(PTA)] (**52**, dmba = dimethylbenzylamine, Scheme 7.12) and $Pd(OAc)_2$/PTA (1:3 molar ratio) were tested for catalytic Sonogashira cross-coupling reactions of aryl bromides and chlorides with terminal alkynes without the need of added copper or amines (Scheme 7.13) [55].

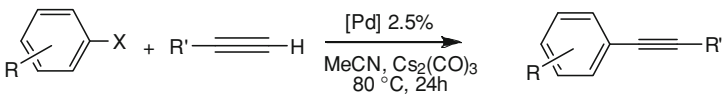
The two catalytic systems gave comparable results under the conditions applied, i.e. 1.0 equiv of aryl bromide RC_6H_4Br, 1.5 equiv of alkyne $R'C_2H$, 1.5 equiv of Cs_2CO_3, 4.0 mL of CH_3CN, 2.5 mol % of [Pd], 80 °C, 24 h. When **52** was used as catalyst, the yields ranged from 45% (R = Mes, R′ = Cy) to 100% (R = MeO, R′ = Ph, ^{t}Bu, Cy, 1-cyclohexene; R = H, R′ = Cy, ^{t}Bu; R = Me, MeO, R′ = *t*Bu). In the case of (activated) aryl chlorides RC_6H_4Cl the yields with both catalytic systems were high using MeCN as solvent, under the conditions described above and adding 1.5 equivalents of tetrabutylammonium chloride. The lowest yield was observed for R = H, R′ = Ph (50%) while 100% yields were



Scheme 7.11 Pd(II) catalysts for cycloisomerization of (Z)-2-en-4-yn-1-ols into furans



Scheme 7.12 Synthesis of [Pd(dmba)Cl(PTA)] (**52**)



Scheme 7.13 Pd-catalyzed Sonogashira couplings of aryl bromides and chlorides with terminal alkynes (X = Br; R = H, Me, Mes, MeO; R′ = Ph, Cy, 1-cyclohexene, ^{t}Bu. X = Cl; R = H, MeO, HOOC, NC, 4-py; R′ = Ph, Cy, 1-cyclohexene, ^{t}Bu)

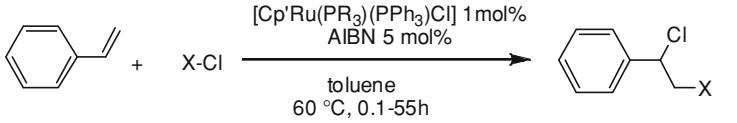
observed for other combinations of activating groups (R = MeOC, HO_2C, NC, 4-py; R′ = Ph, Cy, 1-cyclohexene, ^{t}Bu).

Intramolecular hydroamination is an atom efficient cyclization reaction which finds use for the synthesis of pharmaceutically relevant intermediates such as *N*-heterocycles. Krogstad and co-workers [56] tested as series of Pd, Pt and Ir-PTA complexes as catalysts for the hydroamination of 4-pentyn-1-amine to 2-methyl-pyrroline and studied the reaction mechanism mainly by NMR techniques in solution using various deuterated solvents (Table 7.12). Palladium complexes *cis*-$[PdCl_2(PTA)_2]$ (**49**) and *cis*-$[PdBr_2(PTA)_2]$ (**53**) outperformed the Pt analogs *cis*-$[PtCl_2(PTA)_2]\cdot H_2O$ (**54**), *cis*-$[PtBr_2(PTA)_2]$ (**55**),

Table 7.12 Hydroamination (cyclization) of 4-pentyn-1-amine to 2-methyl-pyrroline

Catalyst	Solvent	% Conv.[a]	TOF (h^{-1})[b]
49	D_2O	97	6.0
49	CD_3OD	92	4.5
49	d_6-DMSO	49	1.0
53	D_2O	96	5.6
53	CD_3OD	89	3.9
53	d_6-DMSO	40	0.75
54	D_2O	27	0.35
54	CD_3OD	25	0.33
54	d_6-DMSO	8.7	0.021
55	D_2O	28	0.36
55	CD_3OD	27	0.38
55	d_6-DMSO	6.3	0.023
56	D_2O	26	0.34
56	CD_3OD	20	0.25
56	d_6-DMSO	6.8	0.023
57	D_2O	24	0.33
58	D_2O	28	0.36
59	D_2O	23	0.32

[a] Determined by integration of the ^1H NMR spectra after 48 h
[b] Calculated as the number of moles of product/moles of catalyst/h at 50% conversion



Scheme 7.14 Ru-catalyzed Kharasch addition of chloro substrates to styrene

and *cis*-$[PtI_2(PTA)_2]$ (**56**). Iridium complexes $[Ir(cod)(PTA)_3]Cl$ (**57**), $[IrCl(CO)(PTA)_3]$ (**58**) and $[Ir(CO)(PTA)_4]Cl$ (**59**) were also tested and found to be less active than Pd(II)-PTA complexes [57, 58].

A series of ruthenium mixed phosphine complexes of general formula $[Cp'Ru(PR_3)(PPh_3)Cl]$ [Cp′ = Cp*, Dp, Ind, Cp, Tp (Tp = tris(pyrazolyl)borate); PR_3 = PTA, PMe_3, PPh_3] were used by Frost and co workers [59] to catalyze the atom transfer radical addition (Kharasch reaction) of various chloro substrates [CCl_4, $CHCl_3$, and TsCl (Ts = tosyl)] to styrene and/or 1-hexene in the presence of AIBN [AIBN = azobis(isobutyronitrile)]. Cp*Ru(PTA)(PPh_3)Cl (**60**) and Cp*Ru$(PMe_3)(PPh_3)$Cl under the conditions described in Scheme 7.14 were found to be very active for the addition of CCl_4 to styrene with TOF of 1060 and 933 h^{-1}, respectively. The latter reaction were also performed at room temperature, where $Cp^*Ru(PPh_3)_2Cl$ was the most active with TOF > 960 h^{-1}. Total turnovers (TTO) higher than 8×10^4 were obtained for the addition of CCl_4 to 1-hexene.

Water soluble ruthenium(II) complexes [$RuCl_2(\eta^6$-arene)(L)] [L = PTA (**61**), (PTA-Bz)Cl (**62**), DAPTA (**63**), TPPMS (**64**); η^6-arene = C_6Me_6 (a), 1,3,5-$C_6H_3Me_3$ (b), *p*-cymene (c), C_6H_6 (d)] were used by Cadierno et al. [60] as catalysts for the synthesis of β-oxo esters, important precursors for industrially relevant α-hydroxy ketones, by addition of terminal propargylic alcohols to carboxylic acids in aqueous medium. As a model reaction, 1-phenyl-2-propyn-1-ol (1 mmol) was reacted with benzoic acid (1 mmol) in 1 mL of water in the presence of 2 mol % of Ru complex and stirred at 60 °C for 24 h. The best results were obtained with the TPPMS complexes (76–87% yields) whereas lower yields (14–71%, the latter in the presence of **61a**) were observed for the PTA-type catalysts.

7.5 Alkyne and Nitrile Hydration

Water soluble ruthenium(II) complexes **61**–**64** were also used as catalysts for the hydrogenation of nitriles to amides in pure aqueous media and under neutral conditions [61]. All complexes gave benzamide from benzonitrile in almost quantitative yield. TOFs were observed to depend on the nature of the arene ligand, in the order C_6Me_6 > 1,3,5-$C_6H_3Me_3$ > *p*-cymene > C_6H_6 suggesting that higher performances are obtained for the more sterically demanding and electron-rich arenes (Table 7.13). Among the complexes studied, **62a** was the most active and was efficiently applied for the hydration of a large number of nitriles RCN (R = Ph, C_6H_4F, C_6H_4Br, 3-$C_6H_4NO_2$, C_6H_4OH, C_6H_4OMe, 4-$C_6H_4C(=O)OEt$, C_6F_5 etc.).

Table 7.13 Ru-PTA type complexes for catalytic hydration of benzonitrile to benzamide in water

Catalyst[a]	t (h)	% Yield[b]	TOF (h^{-1})[c]
61a	4	99	5.0
61b	5	99	4.0
61c	8	99	2.5
61d	9	98	2.2
62a	2	99	9.9
62b	4	99	5.0
62c	4	99	5.0
62d	10	99	2.0
63a	9	98	2.2
63b	8	98	2.5
63c	9	98	2.2
63d	19	99	1.0

[a] Substrate/Ru = 20:1; N_2, 100 °C, 1 mmol benzonitrile (0.33 M in water)
[b] Yield of benzamide determined by GC
[c] Turnover frequencies (mol product/mol Ru/time)

The same authors expanded on the concept of Ru-PTA catalyzed selective hydration of several organonitriles to the corresponding amides and compared the activites of a class of Ru(IV) complexes of general formula $[RuCl_2(\eta^3{:}\eta^3\text{-}C_{10}H_{16})(L)]$ [L = PTA (**65**), (PTA-Bz)Cl (**66**), DAPTA (**67**), TPPMS (**68**)] under pure aqueous media under neutral conditions [62]. Also in this case, fast reactions (1–24 h) and complete conversions were obtained for the substrates described above. The combination of microwave irradiation (MW, 80 W) and water allowed to decrease the reaction times down to 20 min without significant loss of efficiency.

Ru-arene PTA complexes were recently used as decorating ending groups on dendrimers of various generations (Fig. 7.7) by Servin et al. [63]. The complexes (5 mol % based on Ru) were used in phenylacetylene hydration in water/isopropanol mixtures at 90 °C running the reactions for 48 h. The first generation **5-G$_1$** gave higher conversion than the monomer, and the efficiency was observed to decrease with generations 2 and 3 (**5-G$_2$** and **5-G$_3$** respectively). On the other hand, the selectivity for methylphenyl ketone increases from the monomer to the third generation from 91 to 98%, showing a slightly positive dendritic effect (Fig. 7.8).

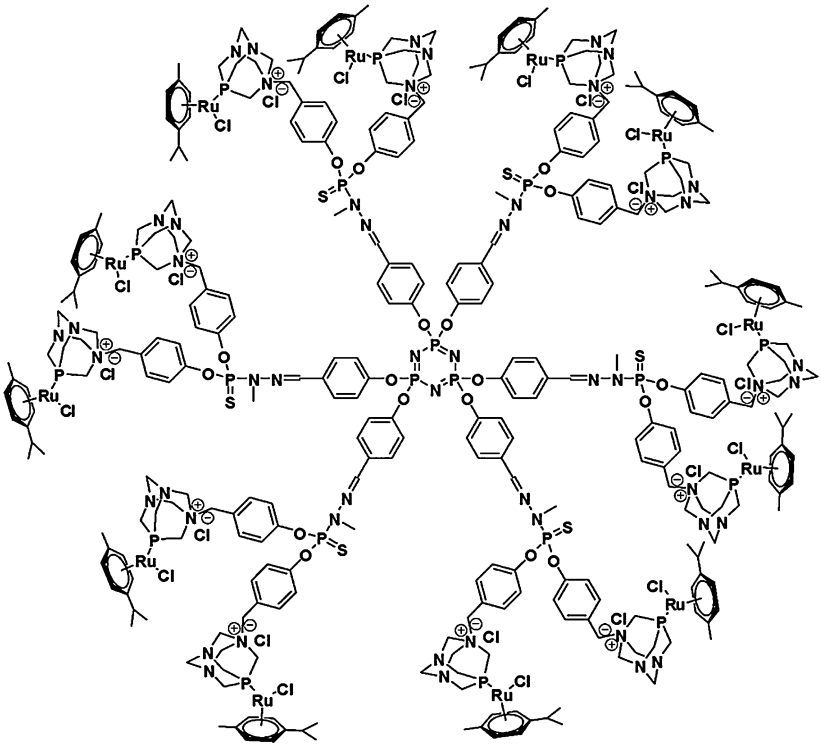


Fig. 7.7 A sketch view of [RuCl(*p*-cymene)PTA]-decorated dendrimer **5-G$_1$**

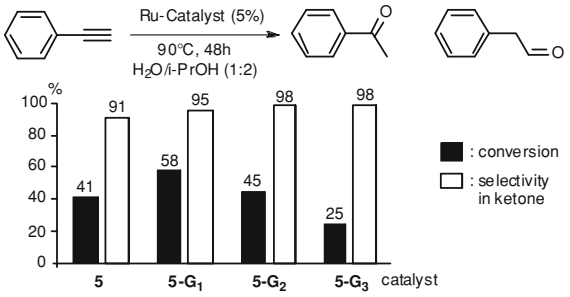
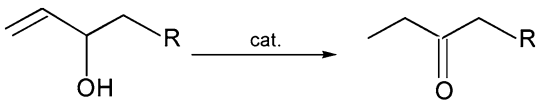


Fig. 7.8 Hydration of phenylacetylene using monomer **5** and dendrimers **5-Gn** ($n = 1$–3)



Scheme 7.15 Allylic alcohol isomerization

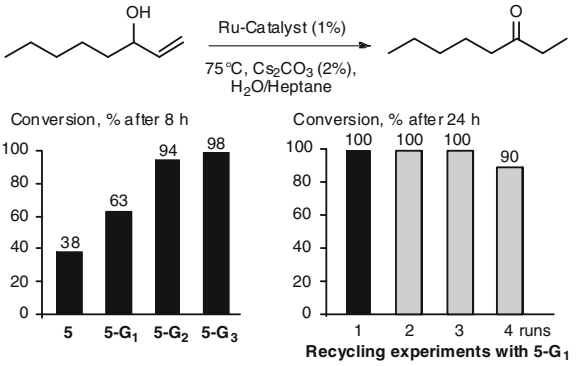


Fig. 7.9 Isomerization of 1-octen-3-ol using monomer **5** and dendrimers **5-Gn** ($n = 1$–3) as catalysts (1 mol% based on Ru). On the right: recycling experiments with **5-G$_1$**

7.6 Allylic Alcohol Isomerization

Catalytic isomerization of allylic alcohols (Scheme 7.15) is an attractive strategy for the synthesis of the corresponding ketones and aldehydes. Such internal redox reactions show 100% atom economy and for this reason they have found large attention in the literature.

$[CpRuCl(mPTA)_2](OSO_2CF_3)_2$ (**69**) and $[CpRu(mPTA)_2(H_2O)](OSO_2CF_3)_3$ (**70**) were found to be effective catalysts of the redox isomerization of 1-octen-3-ol to the corresponding ketones in water at 80 °C, with initial TOF of 162 h^{-1} (**70**) and 9.6 h^{-1} (**69**). The eaction rate was monitored against pH, showing the presence of A with **69** in phosphate buffer solutions. A combination of kinetic and ^{31}P NMR analyses allowed to establish that the buffer component HPO_4^{2-} strongly interacts with the catalysts causing in turn a decrease in activity [64].

The dendrimer-supported catalysts described in Sect. 7.5 were also tested in allylic alcohol isomerization. Isomerization of 1-octen-3-ol into octan-3-one was

carried out in the presence of 1 mol% of Ru catalysts and 2 mol% of Cs_2CO_3 in water/heptane at 75 °C for. At the end of the reaction phase separation allowed for efficient recycling of the catalyst up to 4 runs (Fig. 7.9) [63]. Interestingly, a positive dendritic effect was clearly evident for this kind of reactions, as the conversion increased from the monomer (38%) to the third generation (98%) under the same conditions.

Finally, the combination of $[Rh(cod)(MeCN)_2]BF_4$ (5 mol%) with 2 equivalents of PTA proved to be an efficient catalyst for the redox isomerization of a series of allylic alcohols to the corresponding ketones in water running the tests in the temperature range 25–80 °C [65]. The system was screened for catalyst loading effect and functional groups tolerance with good to excellent results in yields and selectivities. The work is complemented by deuterium labelling mechanistic studies, leading to a enone-centered proposed mechanism.

Acknowledgments The authors thank support by EC through MC Actions RTN n° HPRN-CT-2002-00176 (Hydrochem) and MRTN-CT-2003-503864 (Aquachem); Ente Cassa di Risparmio di Firenze through the FIRENZE HYDROLAB project; COST Actions D29 and C0802 (PhoSciNet); Italian Ministries MIUR and MATTM through projects PRIN 2007and PIRODE; GDRE project "*Catalyse Homogène pour le Développement Durable* (*CH2D*)".

References

1. Phillips AD, Gonsalvi L, Romerosa A, Vizza F, Peruzzini M (2004) Coordination chemistry of 1,3,5-triaza-7-phosphaadamantane (PTA). Transition metal complexes and related catalytic, medicinal and photo-luminescent applications. Coord Chem Rev 248:955–993
2. Bravo J, Bolaño S, Gonsalvi L, Peruzzini M (2010) Coordination chemistry of 1,3,5-triaza-7-phosphaadamantane (PTA) and derivatives. Part II. The quest for tailored ligands, complexes and related applications. Coord Chem Rev 254:555–607
3. Daigle DJ, Pepperman AB Jr, Vail SL (1974) Synthesis of a monophosphorus analog of hexamethylenetetramine. J Heterocycl Chem 11:407–408
4. Fluck E, Forster JE (1975) 1,3,5-Triaza-7-phosphaadamantan. Chem Zeit 99:246–248
5. Daigle DJ (1998) 1,3,5-Triaza-7-phosphatricyclo[3.3.1.1^{3,7}]decane and derivatives. Inorg Synth 32:40–45
6. Darensbourg DJ, Decuir RJ, Reibenspies JH (1995) In: Horvath IT, Joó F (eds) Aqueous organometallic chemistry and catalysis. Kluwer, Dordrecht, pp 61–80
7. Forward JM, Staples RJ, Liu CW, Fackler JP (1997) Luminescent tris(3-ethyl-1,5-diaza-3-azonia-7-phosphatricyclo[3.3.1.1^{3,7}]decane-P)gold(I) tetraiodide trihydrate, $[(EtTPA)_3Au]I_4{\cdot}3H_2O$. Acta Cryst C 53:195–197
8. Fluck E, Förster JE, Weidlein J, Hädicke E (1977) 1,3,5-triaza-7-phosphaadamantan (Monophospha-urotropin). Z Naturforsch 32b:499–506
9. Forward JM, Staples RJ, Fackler JP Jr (1996) Crystal structure of 1-*n*-butyliodo-1-azonia-3,5-diaza-7-phosphaadamantane iodide, $(C_6H_{12}PN_3(CH_2)_4I)I$. Z Kristallogr 211:129–130
10. Mena-Cruz A, Lorenzo-Luis P, Romerosa A, Saoud M, Serrano-Ruiz M (2007) Synthesis of the water soluble ligands dmPTA and dmoPTA and the complex $[RuClCp(HdmoPTA)(PPh_3)](OSO_2CF_3)$ (dmPTA = *N*,*N*′-dimethyl-1,3,5-triaza-7-phosphaadamantane, dmoPTA = 3,7-dimethyl-1,3,7-triaza-5-phosphabicyclo[3.3.1]nonane, HdmoPTA = 3,7-H-3,7-dimethyl-1,3,7-triaza-5-phosphabicyclo[3.3.1]nonane). Inorg Chem 46:6120–6128
11. Fluck E, Weissgraber HJ (1977) 7-Methyl-1,3,5-triaza-7-phosphaadamantan-7-ium iodide P-methyl-phospha-urotropinium iodide. Chem Ztg 101:304–307

12. Assmann B, Angermaier K, Schmidbaur H (1994) Synthesis, structure and complexes of a new bicyclic N,P-ligand derived from phosphatriazaadamantane. J Chem Soc Chem Commun 941–942
13. Assmann B, Angermaier K, Paul M, Riede J, Schmidbaur H (1995) Synthesis of 7-alkyl/aryl-1,3,5-triaza-7-phosphonia-adamantane cations and their reductive cleavage to novel *n*-methyl-*p*-alkyl/aryl[3.3.1]bicyclononane ligands. Chem Ber 128:891–900
14. Kirillov AM, Smoleński P, Haukka M, Guedes da Silva MFC, Pombeiro AJL (2009) Unprecedented metal-free C(*sp*(3))-C(*sp*(3)) bond cleavage: switching from *N*-alkyl- to *N*-methyl-1,3,5-triaza-7-phosphaadamantane. Organometallics 28:1683–1687
15. Krogstad DA, Ellis GS, Gunderson AK, Hammrich AJ, Rudolf JW, Halfen JA (2007) Two new water-soluble derivatives of 1,3,5-triaza-7-phosphaadamantane (PTA): synthesis, characterization, X-ray analysis and solubility studies of 3,7-diformyl-1,3,7-triaza-5-phos phabicyclo[3.3.1]nonane and 1-pyridylmethyl-3,5-diaza-1-azonia-7-phosphatricyclo [3.3.1.1] decane bromide. Polyhedron 26:4093–4100
16. Wong GW, Harkreader JL, Mebi CA, Frost BJ (2006) Synthesis and coordination chemistry of a novel bidentate phosphine: 6-(diphenylphosphino)-1,3,5-triaza-7-phosphaadamantane (PTA-PPh_2). Inorg Chem 45:6748–6755
17. Erlandsson M, Gonsalvi L, Ienco A, Peruzzini M (2008) Diastereomerically enriched analogues of the water soluble phosphine PTA. Synthesis of phenyl-(1,3,5-triaza-7-phosphatricyclo [3.3.1.$1^{3,7}$]dec-6-yl)methanol (PZA) and the Sulfide PZA(S) and X-ray crystal structures of the oxide PZA(O) and [Cp*$IrCl_2$(PZA)]. Inorg Chem 47:8–10
18. Wong GW, Lee WC, Frost BJ (2008) Insertion of CO_2, ketones, and aldehydes into the C-LI bond of 1,3,5-triaza-7-phosphaadamantan-6-yllithium. Inorg Chem 47:612–620
19. Darensbourg DJ, Ortiz CG, Kamplain JW (2004) A new water-soluble phosphine derived from 1,3,5-triaza-7-phosphaadamantane (PTA), 3,7-diacetyl-1,3,7-triaza-5-phosphabicyclo[3.3.1] nonane. Structural, bonding, and solubility properties. Organometallics 23:1747–1754
20. Caporali M, Gonsalvi L, Zanobini F, Peruzzini M (2010) Synthesis of the water soluble bidentate (P,N) ligand PTN(Me) [PTN(Me) = 7-phospha-3-methyl-1,3,5-triazabicyclo[3.3.1] nonane]. Inorg Synth 35:96–101
21. Darensbourg DJ, Robertson JB, Larkins DL, Reibenspies JH (1999) Water-soluble organometallic compounds. 7. Further studies of 1,3,5-triaza-7-phosphaadamantane derivatives of group 10 metals, including metal carbonyls and hydrides. Inorg Chem 38:2473–2478
22. Fisher KJ, Alyea EC, Shahnazarian N (1990) A P-NMR study of the water-soluble derivatives of 1,3,5-triaza-7-phosphaadamantane (PTA). Phosphorus Sulfur 48:37–40
23. Darensbourg DJ, Joó F, Kannisto M, Kathó A, Reibenspies JH, Daigle DJ (1994) Water-soluble organometallic compounds. 4. Catalytic-hydrogenation of aldehydes in an aqueous 2-phase solvent system using a 1,3,5-triaza-7-phosphaadamantane complex of ruthenium. Inorg Chem 33:200–208
24. Darensbourg DJ, Joó F, Kannisto M, Kathó A, Reibenspies JH (1992) Water-soluble organometallic compounds. 2. Catalytic-hydrogenation of aldehydes and olefins by new water-soluble 1,3,5-triaza-7-phosphaadamantane complexes of ruthenium and rhodium. Organometallics 11:1990–1993
25. Smolenski P, Pruchnik FP, Ciunik Z, Lis T (2003) New rhodium(III) and ruthenium(II) water-soluble complexes with 3,5-diaza-1-methyl-1-azonia-7-phosphatricyclo [3.3.1.$1^{3,7}$]decane. Inorg Chem 42:3318–3322
26. Madrigal CA, García-Fernández A, Gimeno J, Lastra E (2008) Asymmetric transfer hydrogenation of ketones catalyzed by ruthenium(II) complexes bearing a chiral phosphinoferrocenyloxazoline ligand. J Organomet Chem 693:2535–2540
27. Dyson PJ, Ellis DJ, Laurenczy G (2003) Minor modifications to the ligands surrounding a ruthenium complex lead to major differences in the way in which they catalyse the hydrogenation of arenes. Adv Synth Catal 345:211–215
28. Allardyce CS, Dyson PJ, Ellis DJ, Heath SL (2001) [Ru(η^6-p-cymene)Cl_2(pta)] (pta = 1,3,5-triaza-7-phosphatricyclo[3.3.1.1]decane): a water soluble compound that exhibits pH dependent DNA binding providing selectivity for diseased cells. Chem Commun 1396–1397

29. Dyson PJ, Ellis DJ, Henderson W, Laurenczy G (2003) A comparison of ruthenium-catalysed arene hydrogenation reactions in water and 1-alkyl-3-methylimidazolium tetrafluoroborate ionic liquids. Adv Synth Catal 345:216–221
30. Akbayeva DN, Gonsalvi L, Oberhauser W, Peruzzini M, Vizza F, Brüggeller P, Romerosa A, Sava G, Bergamo A (2003) Synthesis, catalytic properties and biological activity of new water soluble ruthenium cyclopentadienyl PTA complexes $[(C_5R_5)Ru(PTA)_2Cl]$ (R = H, Me; PTA = 1,3,5-triaza-7-phosphaadamantane). Chem Commun 264–265
31. Kovacs G, Rossin A, Gonsalvi L, Lledos A, Peruzzini M (2010) Comparative DFT analysis of ligand and solvent effects on the mechanism of H_2 activation in water mediated by half-sandwich complexes $[Cp'Ru(PTA)_2Cl]$ ($Cp' = C_5H_5$, C_5Me_5; PTA = 1,3,5-triaza-7-phosphaadamantane). Organometallics 29:5121–5131
32. Bolaño S, Gonsalvi L, Zanobini F, Vizza F, Bertolasi V, Romerosa A, Peruzzini M (2004) Water soluble ruthenium cyclopentadienyl and aminocyclopentadienyl PTA complexes as catalysts for selective hydrogenation of α,β-unsaturated olefins. (PTA = 1,3,5-triaza-7-phosphaadamantane). J Mol Catal A Chem 224:61–70
33. Mebi CA, Frost BJ (2005) Effect of pH on the biphasic catalytic hydrogenation of benzylidene acetone using $CpRu(PTA)_2H$. Organometallics 24:2339–2346
34. Frost BJ, Mebi CA (2004) Aqueous organometallic chemistry: synthesis, structure, and reactivity of the water-soluble metal hydride $CpRu(PTA)_2H$. Organometallics 23:5317–5323
35. Mebi CA, Nair RP, Frost BJ (2007) pH-dependent selective transfer hydrogenation of α,β-unsaturated carbonyls in aqueous media utilizing half-sandwich ruthenium(II) complexes. Organometallics 26:429–438
36. Pruchnik FP, Smolenski P, Wajda-Hermanowicz K (1998) Rhodium(I) acetylacetonato complexes with functionalized phosphines. J Organomet Chem 570:63–69
37. Pruchnik FP, Smolenski P, Galdecka E, Galdecki Z (1998) New water-soluble rhodium(I) complexes containing 1-methyl-1-azonia-3,5-diaza-7-phosphaadamantane iodide. New J Chem 22:1395–1398
38. Darensbourg DJ, Stafford NW, Joó F, Reibenspies JH (1995) Water-soluble organometallic compounds. 5. The regioselective catalytic-hydrogenation of unsaturated aldehydes to saturated aldehydes in an aqueous 2-phase solvent system using 1,3,5-triaza-7-phosphaadamantane complexes of rhodium. J Organomet Chem 488:99–108
39. Phillips AD, Bolaño S, Bosquain SS, Daran J-C, Malacea R, Peruzzini M, Poli R, Gonsalvi L (2006) A new class of rhodium(I) κ^1-P and κ^2-P,N complexes with rigid PTN(R) ligands (PTN = 7-phospha-3-methyl 1,3,5-triazabicyclo[3.3.1]nonane). Organometallics 25:2189–2200
40. Csabai P, Joó F (2004) Synthesis and catalytic properties of new water-soluble ruthenium(II)-*N*-heterocyclic carbene complexes. Organometallics 23:5640–5643
41. Laurenczy G, Joó F, Nadasdi L (2000) Towards an easy carbon dioxide reduction in aqueous solution. High Press Res 18:251–255
42. Joó F, Laurenczy G, Karady P, Elek J, Nadasdi L, Roulet R (2000) Homogeneous hydrogenation of aqueous hydrogen carbonate to formate under mild conditions with water soluble rhodium(I)- and ruthenium(II)-phosphine catalysts. Appl Organomet Chem 14:857–859
43. Laurenczy G, Joó F, Nadasdi L (2000) Formation and characterization of water-soluble hydrido-ruthenium(II) complexes of 1,3,5-triaza-7-phosphaadamantane and their catalytic activity in hydrogenation of CO_2 and HCO_3^- in aqueous solution. Inorg Chem 39:5083–5088
44. Bosquain SS, Dorcier A, Dyson PJ, Erlandsson M, Gonsalvi L, Laurenczy G, Peruzzini M (2007) Aqueous phase carbon dioxide and bicarbonate hydrogenation catalysed by cyclopentadienyl ruthenium complexes. Appl Organomet Chem 21:947–951
45. Erlandsson M, Landaeta VR, Gonsalvi L, Peruzzini M, Phillips AD, Dyson PJ, Laurenczy G (2008) Methylcyclopentadienyl iridium PTA complexes and their application in catalytic water phase carbon dioxide hydrogenation (PTA = 1,3,5-triaza-7-phosphaadamantane). Eur J Inorg Chem 620–627

46. Laurenczy G, Jedner S, Alessio E, Dyson PJ (2007) In situ NMR characterisation of an intermediate in the catalytic hydrogenation of CO_2 and HCO_3^- in aqueous solution. Inorg Chem Commun 10:558–562
47. Legrand FX, Hapiot F, Tilloy S, Guerriero A, Peruzzini M, Gonsalvi L, Monflier E (2009) Aqueous rhodium-catalyzed hydroformylation of 1-decene in the presence of randomly methylated β-cyclodextrin and 1,3,5-triaza-7-phosphaadamantane derivatives. Appl Catal A Gen 362:62–66
48. Shaughnessy KH (2009) Hydrophilic ligands and their application in aqueous-phase metal-catalyzed reactions. Chem Rev 109:643–710
49. Xu X, Wang C, Zhou Z, Tang X, He Z, Tang C (2007) The aza-Morita–Baylis–Hillman reaction of *N*-thiophosphoryl imines catalyzed by 1,3,5-triaza-7-phosphaadamantane (PTA)—convenient synthesis of alpha-methylene-beta-amino ketone or acid derivatives. Eur J Org Chem 4487–4491
50. He Z, Tang X, Chen Y, He Z (2006) Adv Synth Catal 348:413
51. Tang X, Zhang B, He Z, Gao R, He Z (2007) 1,3,5-Triaza-7-phosphaadamantane (PTA): a practical and versatile nucleophilic phosphine organocatalyst. Adv Synth Catal 349:2007–2017
52. Lu A, Xu X, Gao P, Zhou Z, Song H, Tang C (2008) Chiral *N*-thiophosphoryl imine-induced diastereoselective aza-Morita–Baylis–Hillman reaction. Tetrahedron Asymmetry 19:1886–1890
53. Zhang B, He Z, Xu S, Wu G, He Z (2008) Nucleophilic phosphine-catalyzed [3 + 2] cycloaddition of allenes with *N*-(thio)phosphoryl imines and acidic methanolysis of adducts *N*-(thio)phosphoryl 3-pyrrolines: a facile synthesis of free amine 3-pyrrolines. Tetrahedron 64:9471–9479
54. Francos J, Cadierno V (2010) Palladium-catalyzed cycloisomerization of (Z)-enynols into furans using green solvents: glycerol vs. water. Green Chem 12:1552–1555
55. Ruiz J, Cutillas N, López F, López G, Bautista D (2006) A copper- and amine-free Sonogashira reaction of aryl halides catalyzed by 1,3,5-triaza-7-phosphaadamantane palladium systems. Organometallics 25:5768–5773
56. Krogstad DA, DeBoer AJ, Ortmeier WJ, Rudolf JW, Halfen JA (2005) 1,3,5-Triaza-7-phosphaadamantane (PTA) ligated iridium(I) complexes as catalysts for the intramolecular hydroamination of 4-pentyn-1-amine in water. Inorg Chem Commun 8:1141–1144
57. Krogstad DA, Owens SB, Halfen JA, Young VG Jr (2005) Intramolecular hydroamination of alkynylamines in aqueous media catalyzed by platinum(II) 1,3,5-triaza-7-phosphaadamantane (PTA) complexes. Inorg Chem Commun 8:65–69
58. Krogstad DA, Cho J, DeBoer AJ, Klitzke JA, Sanow WR, Williams HA, Halfen JA (2006) Platinum(II) and palladium(II) 1,3,5-triaza-7-phosphaadamantane (PTA) complexes as intramolecular hydroamination catalysts in aqueous and organic media. Inorg Chim Acta 359:136–148
59. Nair RP, Kim TH, Frost BJ (2009) Atom transfer radical addition reactions of CCl_4, $CHCl_3$, and *p*-tosyl chloride catalyzed by $Cp'Ru(PPh_3)(PR_3)Cl$ complexes. Organometallics 28:4681–4688
60. Cadierno V, Francos J, Gimeno J (2010) Ruthenium-catalyzed synthesis of β-oxo esters in aqueous medium: scope and limitations. Green Chem 12:135–143
61. Cadierno V, Francos J, Gimeno J (2008) Selective ruthenium-catalyzed hydration of nitriles to amides in pure aqueous medium under neutral conditions. Chem Eur J 14:6601–6605
62. Cadierno V, Diez J, Francos J, Gimeno J (2010) Bis(allyl)ruthenium(IV) complexes containing water-soluble phosphane ligands: synthesis, structure, and application as catalysts in the selective hydration of organonitriles into amides. Chem Eur J 16:9808–9817
63. Servin P, Laurent R, Gonsalvi L, Tristany M, Peruzzini M, Majoral JP, Caminade AM (2009) Grafting of water-soluble phosphines to dendrimers and their use in catalysis: positive dendritic effects in aqueous media. Dalton Trans 4432–4434
64. González B, Lorenzo-Luis P, Serrano-Ruiz M, Papp E, Fekete M, Csépkec K, Oszc K, Kathó A, Joó F, Romerosa (2010) Catalysis of redox isomerization of allylic alcohols

by [RuClCp(mPTA)$_2$](OSO$_2$CF$_3$)$_2$ and [RuCp(mPTA)$_2$(OH$_2$-kappa*O*)](OSO$_2$CF$_3$)$_3$ (H$_2$O)(C$_4$H$_{10}$O)$_{0.5}$. Unusual influence of the pH and interaction of phosphate with catalyst on the reaction rate. A J Mol Catal A Chem 326:15–20

65. Ahlsten N, Lundberg H, Martin-Matute B (2010) Rhodium-catalyzed isomerisation of allylic alcohols in water at ambient temperature. Green Chem 12:1628–1633

Chapter 8
Synthesis of Phosphorus Compounds via Metal-Catalyzed Addition of P–H Bond to Unsaturated Organic Molecules

Irina P. Beletskaya, Valentine P. Ananikov and Levon L. Khemchyan

Abstract In the present chapter we discuss transition-metal-catalyzed phosphorus-hydrogen (P–H) bond addition to the triple bond of alkynes and to the double bond of alkenes, dienes, imines, aldehydes and ketones. Main attention is paid to highlight the factors responsible for development of highly efficient catalytic systems and to carry out the addition reaction with high stereo-, regio- and enantioselectivity.

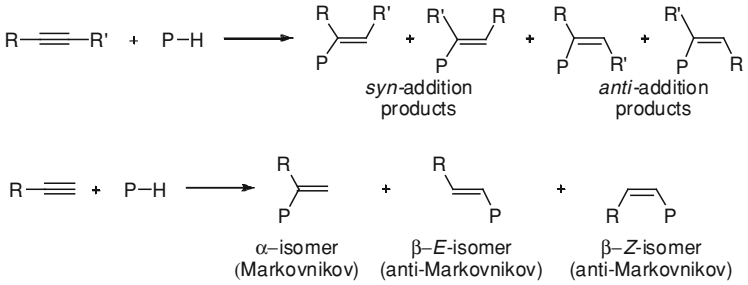
8.1 Introduction

Development of synthetic procedures for carbon–phosphorus (C–P) bond formation has made outstanding progress in recent years. Transition-metal-catalyzed phosphorus-hydrogen (P–H) bond addition to unsaturated compounds is a rapidly developing area of synthetic phosphorus chemistry for constructing C–P bonds in an atom-economic manner [1–7]. In such case high atom efficiency of the addition reaction can be combined with high selectivity of the catalytic transformation leading to environmentally friendly and cost-efficient synthetic procedure in agreement with requirements of modern Green Chemistry [1–7].

I. P. Beletskaya (✉)
Chemistry Department, Lomonosov Moscow State University,
Vorob'evy gory, 119899 Moscow, Russia
e-mail: beletska@org.chem.msu.ru

V. P. Ananikov · L. L. Khemchyan
Russian Academy of Sciences, Zelinsky Institute of Organic Chemistry,
Leninsky Prospect 47, 119991 Moscow, Russia
e-mail: val@ioc.ac.ru

M. Peruzzini and L. Gonsalvi (eds.), *Phosphorus Compounds*,
Catalysis by Metal Complexes, 37, DOI: 10.1007/978-90-481-3817-3_8,
© Springer Science+Business Media B.V. 2011



Scheme 8.1 Possible products in a P–H bond addition reaction to alkynes

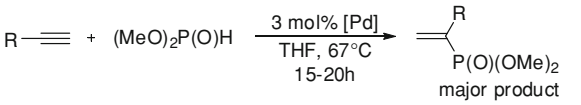
Using a general framework of P–H bond addition reaction to double and triple bonds several important products can be accessible, but the key issue is reaction selectivity. In the case of internal alkynes *E*- and *Z*- isomers may be obtained in the reaction (Scheme 8.1). P–H bond addition to terminal alkynes may lead to three different isomers (Scheme 8.1). Stereoselectivity should be controlled in case of addition reaction to symmetrical internal alkynes ($R = R'$) and both stereo- and regioselectivity should be controlled in the reaction with terminal alkynes and non-symmetrical internal alkynes ($R \neq R'$). Indeed, in a typical case of non-catalytic addition reaction (or poor efficiency of a catalyst) a mixture of the isomers is formed. Similar issues should be taken into account for P-H bond addition to other unsaturated organic molecules as well.

Therefore, finding an appropriate catalytic system—transition metal complex, ligand and reaction conditions—are the key-questions for successful application of this methodology in order to selectively prepare desired products.

Various phosphorus compounds can be synthesized by P–H bond addition to unsaturated organic molecules (alkynes, alkenes, dienes, aldehydes and imines). The target products are in demand as biologically active compounds [8–26], useful compounds in nucleic acid chemistry [27–31], versatile reagents in synthesis [32–36] and building blocks in polymer sciences [37–43]. In the area of biologically active compounds antifungal and antibacterial properties of vinyl phosphonates were considered as well as their anticancer and antiviral activity was evaluated [44–47]. Practical application includes utilization of phosphorus compounds in fuel cell membranes, optical materials and flame retardants [48–55].

Special application of phosphorus compounds, which cannot be underestimated, is utilizations as ligands in catalytic reactions [56–60]. Increasing requirements for preparing new ligands for high performance catalytic systems represent one of the major driving forces of this area of synthetic chemistry. As it will be discussed in the present chapter P–H bond addition to unsaturated molecules is an excellent approach to new phosphorus ligands either in direct synthetic route or using further known transformation pathways. Particularly, chiral ligands were synthesized via the enantioselective P–H bond addition to alkenes or via P–H bond addition to alkynes followed by asymmetric hydrogenation.

Scheme 8.2 Pd-catalyzed hydrophosphorylation of terminal alkynes



[Pd]=*cis*-$PdMe_2(PPh_2Me)_2$

R	yield,%	α/β
n-C_6H_{13}	95	>95/5
Ph	93	>92/8
p-Tol	90	>92/8
$NC(CH_2)_3$	94	>95/5
	89	96/4

8.2 Catalytic Addition of P–H Bond to Unsaturated Molecules

8.2.1 Addition of H-Phosphonates $(RO)_2P(O)H$ to Alkynes

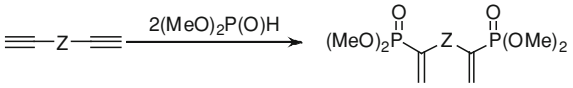
Base-promoted or radical-initiated reaction between dialkyl phosphites and alkynes is known to give a mixture of *cis-trans*-stereoisomers according to addition reaction in anti-Markovnikov fashion [61–64]. Catalytic reactions were of much interest in this regard in order to provide a better control of reaction regio- and stereoselectivity.

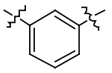
The first example of a transition-metal-catalyzed addition of a P–H bond to the triple bond of alkynes was described in 1972 [65]. The reaction was carried out under harsh conditions resulting in low selectivity and from low to medium product yields.

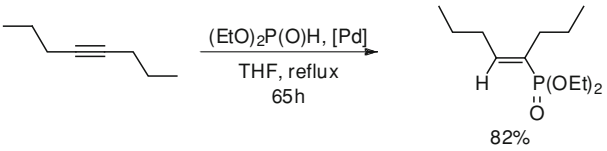
Tanaka et al. were the pioneers of the synthetic application of catalytic hydrophosphorylations and hydrophosphinylations of multiple carbon–carbon bonds. Addition to alkynes was catalyzed by Pd complexes and led to vinylphosphonates in high yields under relatively mild conditions (Scheme 8.2) [66]. In some cases an excellent α-regioselectivity was reported. As an exception, trimethylsilylacetylene gave trans-*β*-trimethylsilyl-vinylphosphonate in the addition reaction presumably due to steric hindrance. Various α-substituted vinylphosphonates were synthesized from terminal alkynes in 80–95% yield and 92–96% regioselectivity using *cis*-$PdMe_2(PPh_2Me)_2$ as the catalyst precursor.

The catalytic P–H bond addition to enynes showed selective reactions, which involved the triple bond only. The presence of two triple bonds in diynes resulted in bis-hydrophosphorylation product under these conditions (Scheme 8.3).

Scheme 8.3 Pd-catalyzed hydrophosphorylation of diynes

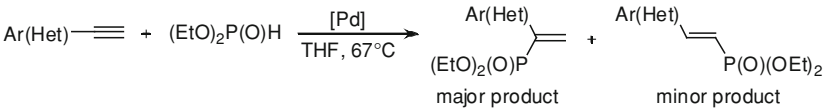


Z	yield,%	αα/αβ
$(CH_2)_5$	83	>95/5
	87	>92/8



[Pd] = *cis*-$PdMe_2(PPh_2Me)_2$

Scheme 8.4 Pd-catalyzed hydrophosphorylation of 4-octyne



[Pd] = $Pd_2dba_3 \times 4PPh_3$

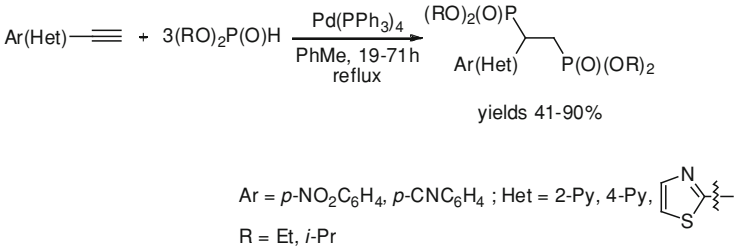
Ar = Ph, *p*-$MeOC_6H_4$, 6-MeO-2-Nf, Py

Scheme 8.5 Pd-catalyzed hydrophosphorylation of aryl(hetaryl) substituted alkynes

Internal alkynes were also involved in the reaction, however, required longer reaction time—more than 60 h instead of 15–20 h for the terminal alkynes (Scheme 8.4). The products were formed in very good yields in stereoselective *syn*-addition reaction [66].

Various α-arylvinyldiethylphosphonates, including heteroaryl derivatives, were synthesized utilizing a simple catalytic system $Pd_2(dba)_3$ 4 × PPh_3 [67, 68]. In all studied cases the formation of α-isomer was observed as a major product in >90% yield and *β*-isomer was formed as a minor product (Scheme 8.5).

Reduction of α-arylvinylphosphonates in the $HCOONH_4$-Pd/C system led to α-arylethylphosphonates, which represent phosphorus-substituted analogs of α-arylpropionic acids (including Naproxen and Ibuprofen). These derivatives are in demand in pharmaceutical applications due to their biological activity [69].



Scheme 8.6 Pd-catalyzed double hydrophosphorylation of aryl(hetaryl) substituted alkynes

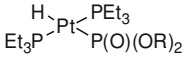
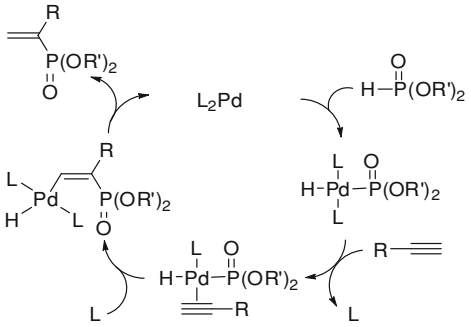


Fig. 8.1 *Trans*-Pt(II) complex with phosphonate group bound to the Pt(0) center

Scheme 8.7 Proposed mechanism of Pd-catalyzed hydrophosphorylation of alkynes

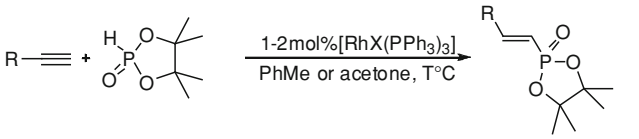


Asymmetric hydrogenation of vinylphosphorus acids as well as their esters was carried out by molecular hydrogen using Ru catalyst with chiral ligands [67, 69] and chiral Ir complexes [70].

The addition of the second phosphorus group to the β-position of vinylphosphonate was observed in the presence of electron withdrawing aryl (heteroaryl) substituent, if an excess of dialkyl phosphite was employed (Scheme 8.6) [71].

Pt complexes did not catalyze this reaction, however, the reaction of $Pt(PEt_3)_3$ with dialkyl phosphites led to the formation of *trans*-Pt(II) complex as a result of oxidative addition to the Pt(0) center (Fig. 8.1). Alkyne insertion involving this complex was observed under harsh conditions at 100 °C with phenylacetylene (R = Et) and resulted in the formation of α-isomer in 63% yield and >99% regioselectivity [66].

The mechanism of the catalytic cycle was proposed to include the following steps: (1) oxidative addition of dialkyl phosphite to the zero-valent metal complex; (2) alkyne coordination to the metal and alkyne insertion; (3) reductive elimination

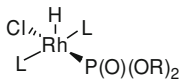


(*E*)-β–isomer >98%

solvent	X	T,°C (t, h)	R	yield, %
acetone	Br	25 (20)	H	81
			Ph	93
			n-C_6H_{13}	95
			t-Bu	79
PhMe	Cl	100-110 (2-6)	Ph	91
			n-C_6H_{13}	93
			t-Bu	92

Scheme 8.8 Rh-catalyzed hydrophosphorylation of terminal alkynes

Fig. 8.2 Rh complex with phosphonate group bound to the metal center



(Scheme 8.7). It was proposed that alkyne insertion into the metal–phosphorus bond took place in the Pd system.

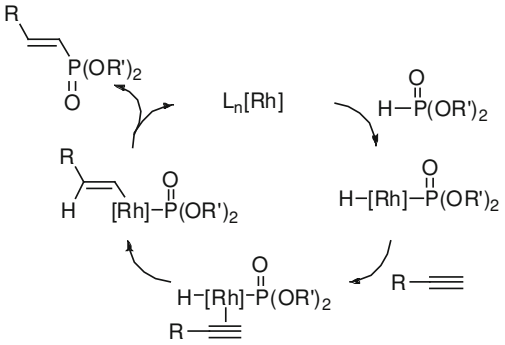
Cyclic five-membered H-phosphonates were found to be much more active in the addition reaction to the multiple carbon–carbon bonds compared to acyclic phosphorus derivatives [72] Rh-catalyzed addition of the five-membered H-phosphonate to alkynes was carried out under mild conditions at room temperature and results in high yield of the *β*-isomer with *E*-configuration (Scheme 8.8). It should be pointed out that Pd- and Rh-catalyzed reactions were complementary to each other providing the access to α-(Markovnikov) and trans-*β*-(anti-Markovnikov) isomers, respectively (cf. Schemes 8.5 and 8.8).

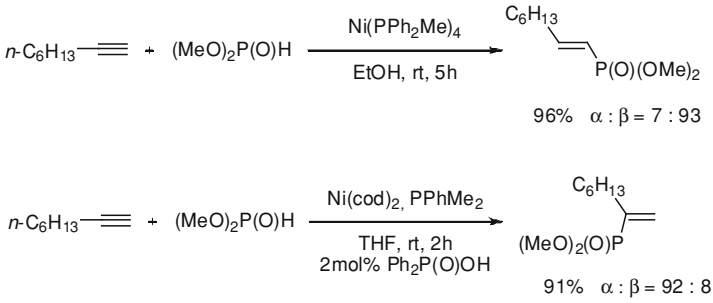
The cyclic H-phosphonate easily reacted with the Wilkinson complex at room temperature under formation of five-coordinated Rh derivatives (Fig. 8.2).

Different regioselectivity observed in Pd-catalyzed and Rh-catalyzed reaction originates from reaction mechanisms, which involve alkyne insertion into the metal-phosphorus bond in case of Pd (Scheme 8.7) and alkyne insertion into the metal–hydrogen bond in case of Rh (Scheme 8.9). In both cases stereoselectivity remains the same and the reactions proceeds as *syn*-addition. In case of Rh-mediated transformation this results in selective formation of a single product with *E*-configuration of the double bond.

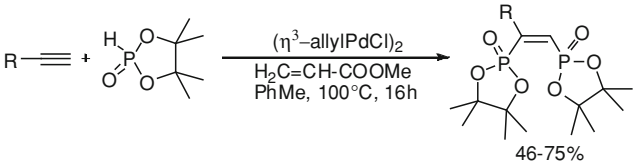
Han et al. have studied hydrophosphorylation of alkynes catalyzed by Ni complexes (Scheme 8.10) [73]. The influence of diphenylphosphinic acid $Ph_2P(O)OH$ on the reaction selectivity was found using different Ni systems with phosphorus

Scheme 8.9 Proposed mechanism of Rh-catalyzed hydrophosphorylation of alkynes





Scheme 8.10 Ni-catalyzed hydrophosphorylation of 1-octyne

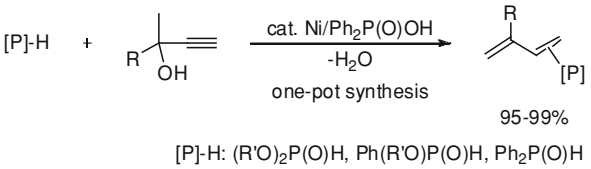


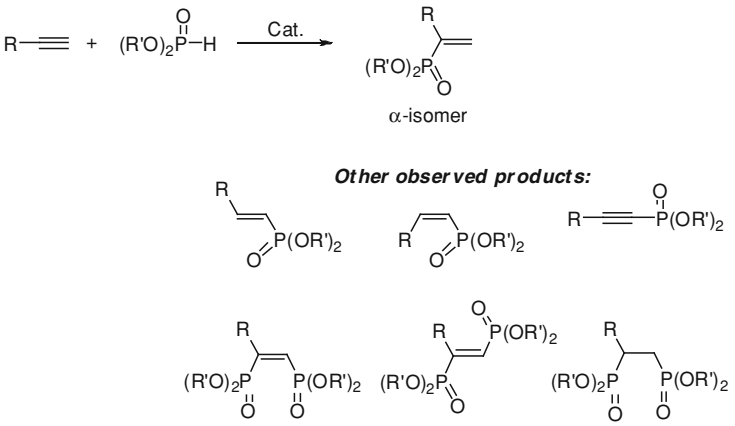
Scheme 8.11 Pd-catalyzed "dehydrogenative *cis* double phosphorylation" of alkynes

ligands. It was reported that regioselectivity of addition can be changed by varying reaction conditions. Unfortunately, it was not possible to understand the key-factor controlling selectivity of P–H bond addition, since the reactions were carried in different solvents (THF or EtOH), with and without acid using different catalyst precursors and ligands (Scheme 8.10) [73].

Pd-catalyzed reaction was reported to proceed via the "dehydrogenative *cis* double phosphorylation" and led to the formation of (*Z*)-bis-phosphoryl alkenes (Scheme 8.11) [74]. High product yield was obtained in the presence of additional equivalent of olefin for hydrogen absorption.

Scheme 8.12 Ni-catalyzed addition/dehydration reactions of P–H bond with propargyl alcohols



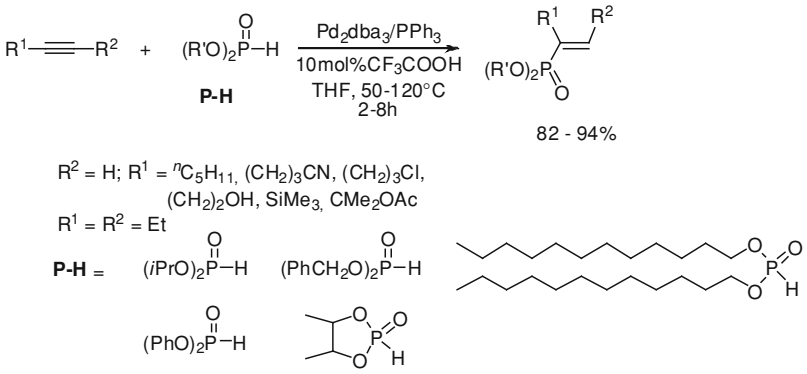


Scheme 8.13 Hydrophosphorylation of alkynes leading to α-isomer and possible by-products

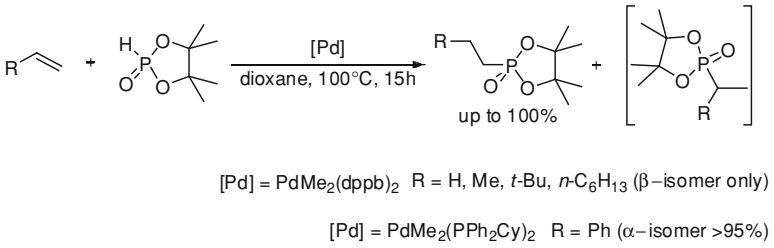
Various reagents with P–H bond (H-phosphonates, H-phosphinates and diphenylphosphine oxide) were shown to undergo addition/dehydration reactions with propargyl alcohols (Scheme 8.12) [75]. The synthetic procedure was carried out in one pot and gave good product yields of phosphinoyl 1,3-dienes.

Detailed study of the outcome of alkynes hydrophosphorylation reaction have revealed rather complicated picture with several by-products depending on the structure of alkyne, H-phosphonate, catalytic system and reaction conditions (Scheme 8.13) [76].

A novel catalytic system was developed to accomplish regio- and stereoselective (>99/1) hydrophosphorylation of terminal and internal alkynes with high yields (up to 96%). Utilization of low-ligated Pd/2xPPh_3 catalytic system in the presence of catalytic amount of trifluoroacetic acid suppressed by-products formation. The developed catalytic system has been applied successfully to synthesize diverse alkenylphosphonates from a variety of available H-phosphonates and alkynes (Scheme 8.14). The catalytic system developed was tolerant to typical organic functional groups in alkynes and to the nature of H-phosphonates. Excellent selectivity and yields were found over the large temperature range of 50–120 °C even for difficult substrates, thus, expanding the scope of preparative synthesis of alkenylphosphonates [76].



Scheme 8.14 Regioselective hydrophosphorylation of alkynes using [Pd]/CF_3COOH system



Scheme 8.15 Pd-catalyzed hydrophosphorylation of alkenes

8.2.2 Addition of H-Phosphonates $(RO)_2P(O)H$ to Alkenes

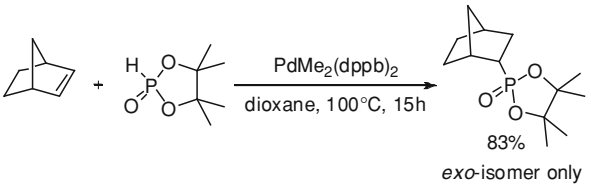
It was possible to carry out hydrophosphorylation of non-activated alkenes only with cyclic five-membered P–H substrate using cis-$PdMe_2L_2$ as catalyst precursor (Scheme 8.15) [77]. Neither six-membered analogs of the substrate, nor non-cyclic dialkyl phosphites were active in this catalytic addition reaction.

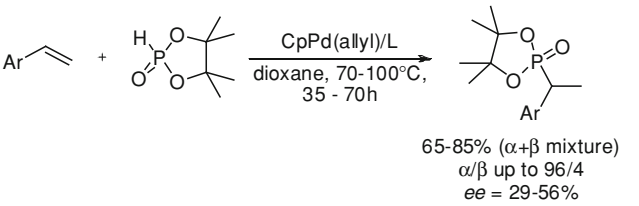
In contrast to the addition reaction involving alkynes, β-isomer was the only product in the case of P–H bond addition to aliphatic alkenes. An exception was reported in the case of styrene, where a mixture of α- and β-isomers in 1:1 ratio was formed. Changing the direction of the addition reaction towards formation of the α-isomer in the reaction with styrene was achieved using PPh_2Cy as a ligand.

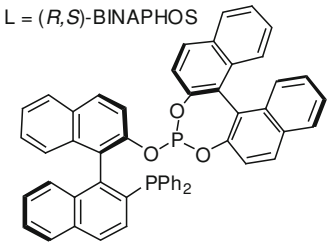
Internal alkenes were found inactive in the P–H bond addition reaction, however, cyclic strained alkenes did show some reactivity and led to the product formation (Scheme 8.16). Important to point out that Ni and Rh complexes were less efficient catalysts in the reaction compared to Pd complexes.

Substituted styrenes reacted with pinacol H-phosphonate and gave Markovnikov isomer in the Pd-catalyzed reaction with CpPd(allyl)/L catalyst precursor (Scheme 8.17) [78]. With bidentate (*R*,*S*)-binaphos ligand the reaction was carried out with 96% regioselectivity and 56% e.e.

Scheme 8.16 Pd-catalyzed hydrophosphorylation of 2-norbornene







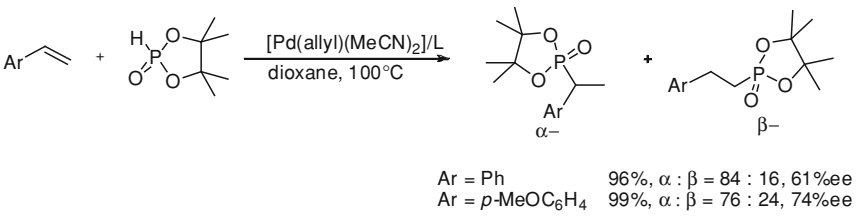
Scheme 8.17 Pd-catalyzed hydrophosphorylation of styrenes with (*R*,*S*)-BINAPHOS as ligand

In the case of styrene regioselectivity strongly depended on the ligand. With dppb a mixture of α:β isomers (branched/linear isomers) was obtained, while using $PCyPh_2$ gave 95:5 selectivity. The formation of the H–Pd(L_2)–P complex with L = PCy_3 was reported and the reaction with styrene gave the addition products with 88% yield and α:β = 18:82 selectivity [1, 2, 77]. It was reported that cyclic H-phosphonates did undergo this transformation, but $(MeO)_2P(O)H$ was found inactive. The difference in reactivity was presumed to originate on the reductive elimination stage, rather than alkene insertion. The difference in reactivity on the reductive elimination step was also observed with PEt_3 ligand, while addition of PPh_3 facilitated the reaction [79].

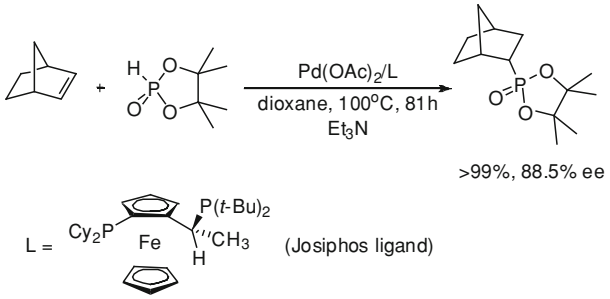
Using a new chiral ligand enantiomeric excess was increased to 74% e.e., however, the ratio of α:β isomers was decreased to 76:24 (Scheme 8.18) [80].

Enantioselective addition of cyclic H-phosphonates to norbornene was carried out with $Pd(OAc)_2$ as catalyst precursor and Josiphos ligand (Scheme 8.19) [81]. It was reported that addition of the base (Et_3N) increased the value of enantiomeric excess.

Rh complexes were found to catalyze addition of the cyclic H-phosphonates to the double bond of alkenes. Moreover, even simple terminal alkenes may be involved in the reaction. For example, addition of pinacol-H-phosphonate to



Scheme 8.18 Pd-catalyzed hydrophosphorylation of styrenes with (*R*,*S*)-2′-trifluoro-methanesulfonyl-[P(*p*-anisyl)$_2$]-BINAPHOS as ligand



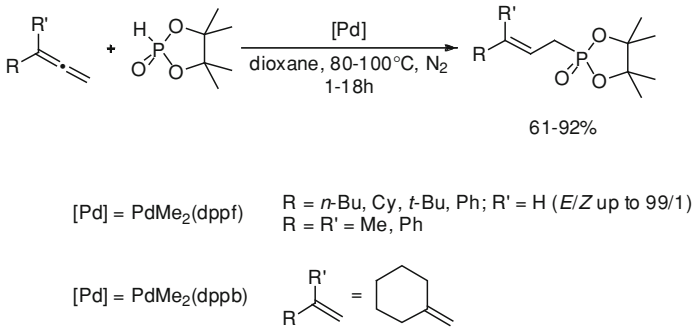
Scheme 8.19 Enantioselective Pd-catalyzed hydrophosphorylation of 2-norbornene

1-octene catalyzed by $(PPh_3)_3RhCl$/dppb (5:5 mol%) gave anti-Markovnikov product in 95% yield [82] Interesting to note that in the case of enynes with terminal triple bond only that triple bond undergoes the addition reaction, while the addition to the double bond was not observed. If substituted internal alkyne unit was present in the enyne molecule, the addition reaction involved double bond, while addition to the triple bond was not observed.

Vinylarenes with electron donating or electron accepting substituents reacted with pinacol-H-phosphonate with excellent anti-Markovnikov selectivity >99% in dioxane at 100 °C using Wilkinson complex as catalyst precursor [78]. Changing the ligand in the $RhClL_3$ complex it was possible to find a catalytic system, which selectively reacts with the terminal double bond (L = PCy_3), while the addition reaction to the internal double bond did not take place [82].

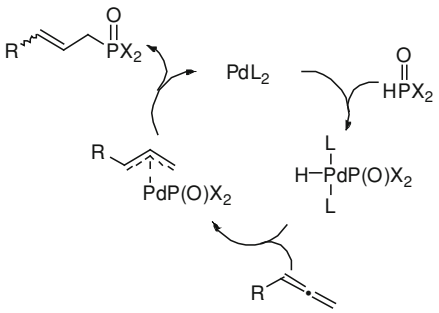
8.2.3 Addition of H-Phosphonates $(RO)_2P(O)H$ to 1,2- and 1,3-Dienes

The first example of $(EtO)_2P(O)H$ addition to isoprene was described by Hirao et al. [83]. The yield of the product was <10% (150 °C, 20 h).



Scheme 8.20 Pd-catalyzed hydrophosphorylation of allenes

Scheme 8.21 Proposed mechanism of the P–H bond addition to allenes

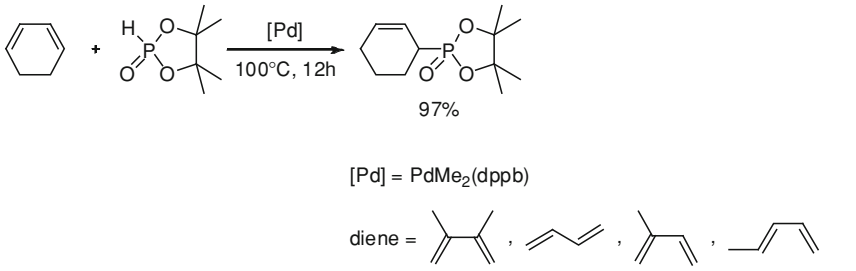


Utilization of activated five-membered H-phosphonate led to successful hydrophosphorylation of various allenes (Scheme 8.20) [84, 85]. High product yields and high regio- and stereoselectivity were found using $PdMe_2$(dppf) as catalyst precursor. Based on this addition reaction a convenient route to allylphosphonates was developed.

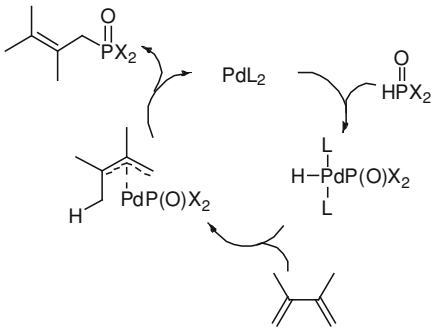
A generally accepted mechanistic framework with allenes as substrates involves formation of π-allyl-Pd complex. The formation of the allyl derivatives in the P–H bond addition reaction agrees well with the mechanism of hydropalladation (Scheme 8.21).

Tetrasubstituted allene 2,4-diethyl-2,3-pentadiene was also reacted with H-phosphonate, but the addition reaction was accompanied with double bond isomerization leading to a mixture of allyl- and vinylphosphonates.

Cyclic five-membered pinacol-H-phosphonate was found to react with conjugated dienes similar to alkenes and allenes discussed above. The [$PdMe_2L$] complex with bidentate ligands (L = dppb, dppf, BINAP) were used as catalyst precursors (Scheme 8.22) [85]. Depending on the nature of diene reaction temperature was varied in the range of 60–100 °C. Allylphosphonates were prepared in high yields and good *E*-stereoselectivity. It was reported that Pd complexes with triphenylphosphine ligands were unable to catalyze the reaction with high stereoselectivity.



Scheme 8.22 Pd-catalyzed hydrophosphorylation of 1,3-dienes



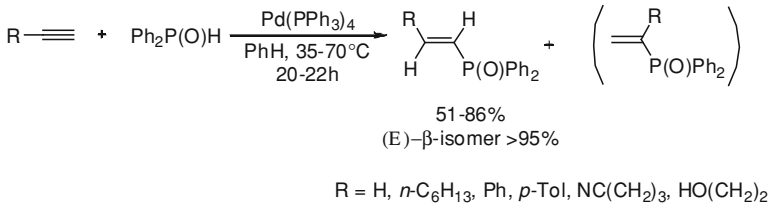
Scheme 8.23 Proposed mechanism of the P–H bond addition to 1,3-dienes

The plausible mechanism of the catalytic reaction involves: (1) oxidative addition; (2) double bond insertion into the Pd–H bond with formation of η^3-allyl palladium intermediate and (3) reductive elimination (Scheme 8.23) [85]. In a similar way allene insertion into the Pd–H bond as a key-step of the catalytic cycle was suggested earlier (Scheme 8.21).

8.2.4 Addition of Phosphine Oxides $R_2P(O)H$ to Alkynes

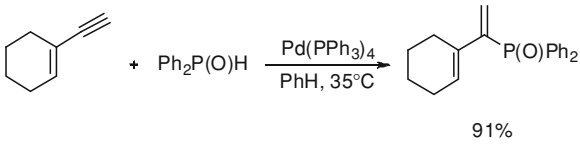
Conventionally used palladium complex $Pd(PPh_3)_4$ was utilized as catalyst precursor in the addition of diphenylphosphine oxide to alkynes [86]. Highly selective syn-addition was observed in good yields for various substituents R in the terminal alkynes (Scheme 8.24). Inspite of several similarities between this reaction and addition of phosphites, the reversed regioselectivity was observed leading to the formation of the β-isomer as a major product (>95%).

Hydrophosphinylation of diynes led to the formation of bis(β-phosphine oxide) derivatives. Reaction with the enyne (1-ethynyl-1-cyclohexene) gave the product of triple bond functionalization, while the double bond remained untouched (Scheme 8.25). Surprisingly, the reaction with enyne resulted in the Markovnikov product (α-isomer). Presumably, a directed addition took place due to presence of the double bond.

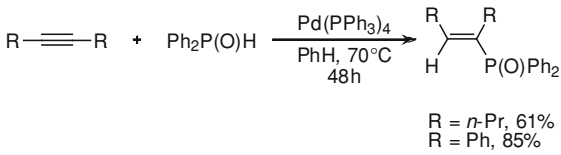


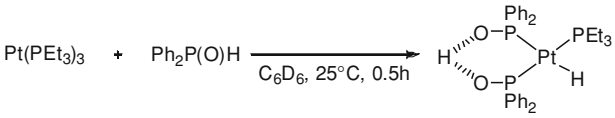
Scheme 8.24 Pd-catalyzed hydrophosphinylation of terminal alkynes

Scheme 8.25 Pd-catalyzed hydrophosphinylation of 1-ethynylcycloxene



Scheme 8.26 Pd-catalyzed hydrophosphinylation of internal alkynes



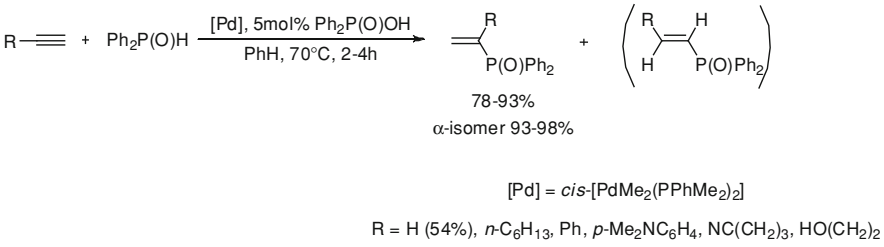


Scheme 8.27 Oxidative addition of diphenylphosphine oxide to $Pt(PEt_3)_3$

Reaction with internal alkynes required higher temperature, but retained high selectivity and led to *E*-adduct, indicating that expected *syn*-addition is taking place (Scheme 8.26).

Oxidative addition of diphenylphosphine oxide to $M(PEt_3)_3$ (M = Pd, Pt) was studied by ^{31}P NMR and showed three different signals in the phosphorus NMR spectrum in a 1:1:1 ratio [86]. Isolated metal complex was characterized by means of X-ray crystal structure analysis, which revealed two $Ph_2P(O)H$ fragments in *cis*-orientation and one coordinated PEt_3 ligand (Scheme 8.27).

Stoichiometric reaction of the above mentioned Pd complex with 1-octyne gave a mixture of α- and β-isomers in 65% total yield. Different ratio of the α- and β-isomers was observed in the stoichiometric reaction, which could be attributed to the changes in reaction conditions (temperature, concentration, etc.). It was proposed that catalytic cycle involves alkyne insertion into the Pd–H bond—i.e. hydropalladation [86].



Scheme 8.28 Hydrophosphinylation of terminal alkynes using [Pd]/$Ph_2P(O)OH$ catalytic system

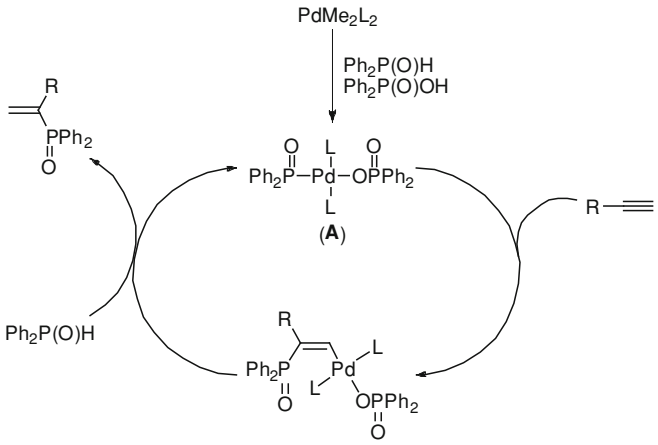
Tanaka et al. were able to change the regioselectivity of the addition reaction by adding a small amount of diphenylphosphinic acid, 1 mol% of $Ph_2P(O)OH$ (Scheme 8.28) [87]. In addition to the change of reaction selectivity, the additive also increased the activity of the catalyst. Even $PdMe_2$(dmpe) catalyst precursor (which is inactive without the acid) did catalyze the addition reaction: high product yields (>93%) and excellent regioselectivity (α:β = 92:8) were observed in the reaction carried out at 100 °C. Somehow unusual that as small as 1 mol% of the acid was enough to influence the reaction with 5 mol% of the catalyst. This may be explained, if we assume that Pd catalyst formed in the presence of acid is much more active compared to Pd complex formed from the catalyst precursor and $Ph_2P(O)H$.

Trimethylsilylacetylene again was an exception in terms of reaction selectivity (see also the addition of dialkyl phosphites discussed earlier). Addition to internal alkynes was also improved in this catalytic system, although the reaction was slower than the similar transformation involving terminal alkynes.

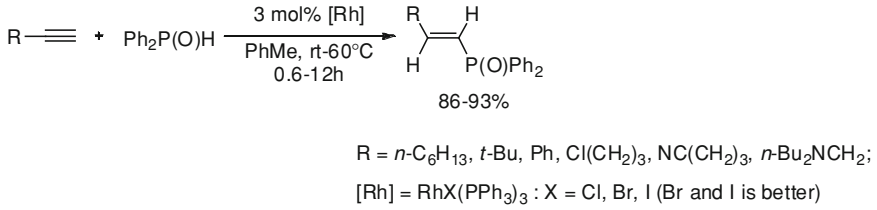
To explain the fact of regioselectivity change by diphenylphosphinic acid, the authors have proposed catalytic cycle involving alkyne insertion into the Pd–P bond of the intermediate metal complex (Scheme 8.29). Suggested catalytic cycle raised some important questions. Complex (A) may be formed after cleavage of the Pd–Me bond, while the other Pd(0) complexes were inactive. Next, it is hardly to expect the protonolysis of the Pd–C bond by oxide, rather than acid (even taking into account their concentrations). The question appears whether all the acid is strongly bound to the metal without being released to the solution. Very likely, that exchange reaction (σ-bond metathesis) took place with formation of [Pd]-$P(O)Ph_2$.

Ni-catalyzed reaction led to the formation of a mixture of products in the addition of $Ph_2P(O)H$ to 1-octyne (α:β = 12:88) [73] In agreement with the data reported for Pd-catalyzed reaction discussed above, high selectivity with the Ni catalyst was obtained in the presence of $Ph_2P(O)OH$ acid (see also Scheme 8.10).

Commercially available diphenylphosphine oxide $Ph_2P(O)H$ usually contains noticeable amount of the diphenylphosphinic acid $Ph_2P(O)OH$ as impurity due to easy oxidation of the former one. Therefore, investigation of the acid effect requires careful purification of the phosphorus substrate. It also means that it would be difficult to reproduce this synthetic procedure using commercially available phosphorus substrate.



Scheme 8.29 Proposed mechanism of hydrophosphinylation of alkynes using [Pd]/$Ph_2P(O)OH$ catalytic system

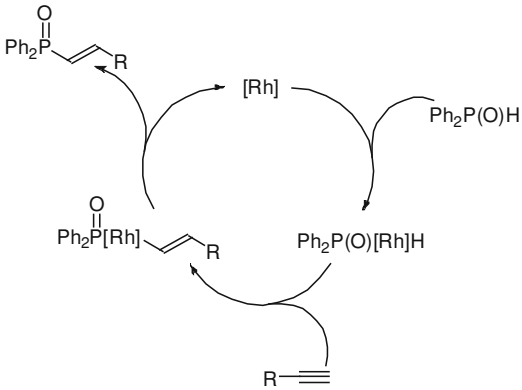


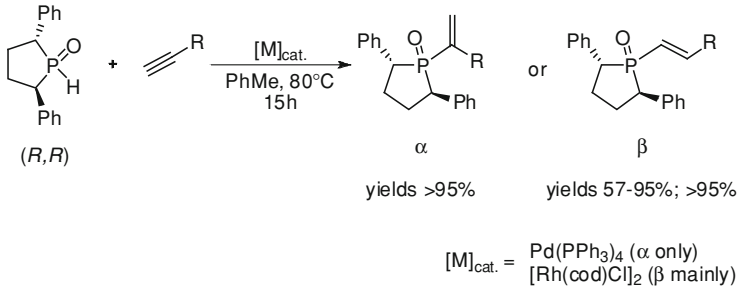
Scheme 8.30 Rh-catalyzed hydrophosphinylation of terminal alkynes

Efficient catalyst for addition of diphenylphosphine oxide was reported based on Rh complexes (Scheme 8.30) [88]. Regioselective formation of the trans-β-isomer was observed for terminal alkynes and stereoselective *syn*-addition was found for internal alkynes. High yields were reported for various alkynes with electron donating or electron withdrawing substituents; with aromatic, heteroaromatic or aliphatic radicals; with or without conjugated multiple bonds. For some alkynes the reaction was carried out in mild conditions at the room temperature. High yield of the addition product was observed at 110 °C with Rh/C source of the metal catalyst. Interestingly, that catalytic activity of RhCl(cod) was also found indicating that phosphine ligand free catalytic reaction may also take place. As far as Rh-catalyzed reaction is discussed, we would like also to mention $Ru_3(CO)_{12}$-mediated addition of diphenylphosphinic acid to terminal alkynes [89]. Formally this reaction did not involve P–H bond addition step and alkenylphenylphosphinates are formed instead.

For the Rh catalyst the catalytic cycle was reported to involve alkyne insertion into the metal–hydrogen bond (Scheme 8.31). Thus, this reaction is a suitable synthetic route for the preparation of *E*-alkenylphosphine oxides. In contrast,

Scheme 8.31 Proposed mechanism of Rh-catalyzed hydrophosphinylation of alkynes





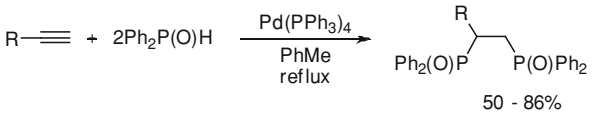
Scheme 8.32 Catalytic addition of 1r-oxo-2c,5t-diphenylphospholane to terminal alkynes

Pd-catalyzed transformations were proposed to involve alkyne insertion into the metal–phosphorus bond and were best suitable for the synthesis of Markovnikov products (Scheme 8.29).

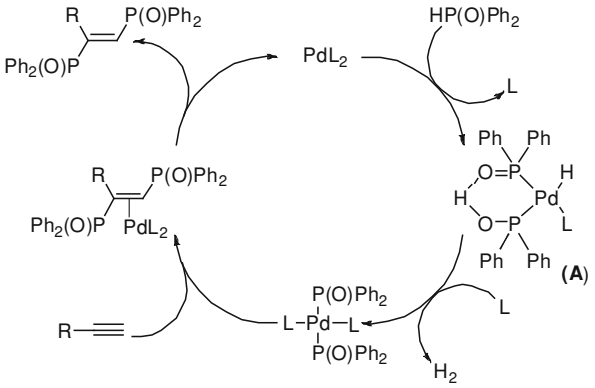
This observation was also confirmed in the addition of chiral enantiopure 1r-oxo-2c,5t-diphenylphospholane to terminal alkynes: *E*-*β*- and Markovnikov α- isomers were formed in Rh- and Pd-catalyzed reactions, respectively (Scheme 8.32) [90]. Surprisingly, it was reported that corresponding acid $R_2P(O)OH$ has no influence on the regioselectivity of the catalytic reaction. Moreover, a higher conversion was observed in Pd-catalyzed reaction without the acid.

Another useful Rh-catalyzed reaction includes $Ph_2P(O)H$ addition to the triple bond of ethynyl steroids as air and water insensitive microwave-assisted hydrophosphinylation [91]. The reaction proceeded via the anti-Markovnikov addition, leading to the *E*-*β*-isomer. Rhodium complexes with hydrotris(3,5-dimethylpyrazolyl)borate ligand (Tp*) have shown catalytic activity in alkynes hydrophosphinylation with diphenylphosphine oxide [92]. Anti-Markovnikov products (*E*-*β*-isomers) were formed in this reaction in moderate yields of 17–51%. Catalytic performance of $Tp^*Rh(PPh_3)_2$ and Tp*Rh(cod) complexes was less efficient than $[ClRh(PPh_3)_4]$ catalyst in the same conditions.

Scheme 8.33 Pd-catalyzed double hydrophosphinylation of terminal alkynes



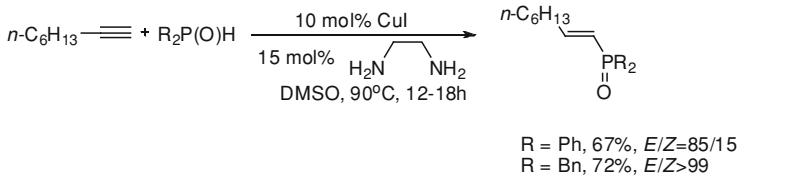
Scheme 8.34 Proposed mechanism of Pd-catalyzed dehydrogenative double phosphinylation of terminal alkynes with diphenylphosphine oxide



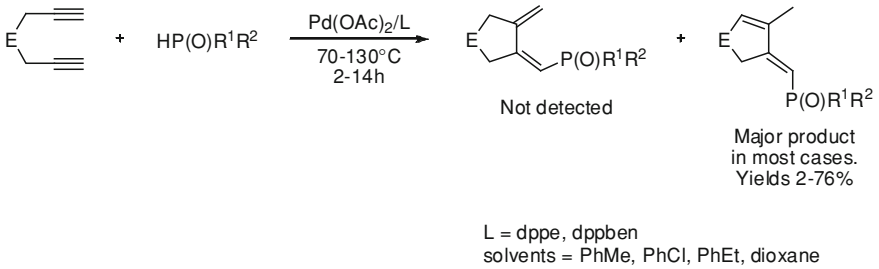
Double hydrophosphinylation of alkynes was performed by Lin et al. (Scheme 8.33) [93]. Bis(phosphineoxide)s were prepared with $[Pd(PPh_3)_4]$ catalyst and an excess of diphenylphosphine oxide (2.4 equiv.). The further studies have resulted in development of microwave assisted synthetic procedure, where a very fast reactions (few minutes) and good yields (60–90%) were found [94]. Mechanistic study has shown that the first hydrophosphinylation step was carried out under metal-catalyzed conditions and the second addition stage did not require a metal catalyst [94]. Double addition under mild conditions (40 °C) in high yields (>95%, 1 h) was reported with dinuclear and trinuclear Pd/M catalysts (M = Ti, Zr, Hf), which were able to promote activation of intermediate vinyl phosphorus derivatives in cooperative manner [95].

Important study was carried out recently by Tanaka et al. to understand the relationship between regioselective Markovnikov addition reaction and dehydrogenative double phosphinylation of terminal alkynes with diphenylphosphine oxide [96]. In the presence of chelate ligand (dppe) the formation of Markovnikov product was observed in good yields (64–88%) and high selectivity (95–99%). If PAr_3 ligands were added to the catalytic system a significant contribution of dehydrogenative double phosphinylation was observed, particularly 48% with L = $P(o\text{-}Tol)_2Ph$. Proposed reaction mechanism involves dehydrogenation of the intermediate cyclic Pd complex (A) and formation of $[PdL_2(P(O)Ph_2)_2]$ complex (Scheme 8.34) [96]. Alkyne insertion into the Pd–P bond of the latter complex and reductive elimination gives the final product with two C–P bonds.

In addition of Ni, Pd and Rh-catalyzed reactions, Fu et al. have reported Cu-catalyzed addition to alkynes (Scheme 8.35) [97]. Not only $Ph_2P(O)H$, but also $(PhCH_2)_2P(O)H$ was successfully utilized as the substrate in the addition reaction.



Scheme 8.35 Cu-catalyzed hydrophosphinylation of 1-octyne



Scheme 8.36 Pd-catalyzed carbocyclization of α,ω-diynes

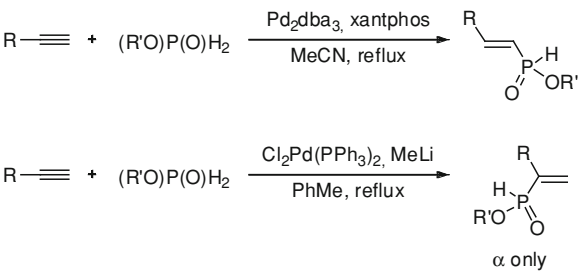
Carbocyclization of α,ω-diynes was observed in Pd-catalyzed addition reaction (Scheme 8.36) [98]. Utilization of chelate phosphine ligand was of key importance to carry out this transformation: only 5% of product was observed with PPh_3, while 70% with dppe (100 °C, 1 h).

8.2.5 Addition of Phosphinates $(RO)P(O)H_2$ to Alkynes

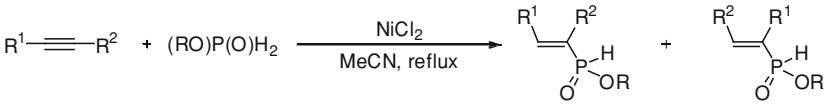
Montchamp et al. have made an important contribution to this field in recent years [4]. Regioselectivity of catalytic addition of phosphinates to alkynes was shown to depend on the nature of the ligand and solvent (Scheme 8.37) [99]. In Pd-catalyzed reaction using xantphos ligand in MeCN resulted in the *E*-*β*-isomer, but PPh_3 ligand in toluene gave the α-isomer.

Using $NiCl_2$ without ligand resulted in development of efficient catalytic system for addition of alkylphosphinates not only to terminal, but also to internal alkynes (Scheme 8.38) [100]. For terminal alkynes a mixture of α and *β* isomers was obtained with different substituents. Addition reaction to alkenes was more difficult compared to the same reaction involving alkynes [100]. For example in reaction with 1-octene 100% yield was found with Pd catalyst, but only 25% with $NiCl_2$. In the presence of phosphine ligand the yield was increased to 69% (L = dppf). Some other reactions of phosphinates addition to the multiple bonds have been also studied [101–104].

Scheme 8.37 Pd-catalyzed addition of phosphinates to terminal alkynes



cat	R	R'	yield, %	α/β
Pd_2dba_3	Oct	Et	75	1/3.7
		Bu	78	1/5
$Cl_2Pd(PPh_3)_2$	Oct	Bu	70	
	Ph		85	



$R^1 = R^2 = n$-Pr 75-100% (2.5-38h)
R = Et; $R^1 = R^2 = n$-Bu 76% (12h)

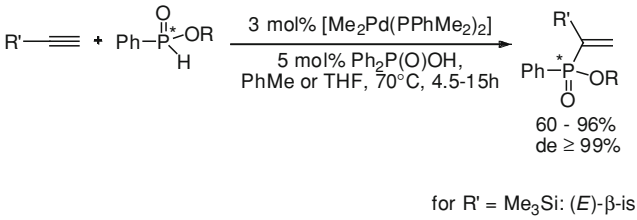
R_2	R	R_1	t,h	yield, %	α/β
		Ph	5	100	1/1
H	Et	EtO	18	42	3/1
		n-Hex	13	100	1/3

Scheme 8.38 Ni-catalyzed phosphine-free addition of phosphinates to alkynes

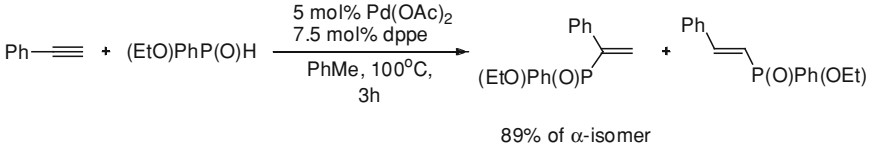
8.2.6 Addition of H-Phosphinates (RO)(R′)P(O)H to Alkynes

There are a few examples of H-phosphinates addition to the triple bond of alkynes and all of them utilize phenyl-H-phosphinates as the substrates. Pd-catalyzed transformation resulted in good product yields and high selectivity (Scheme 8.39) [105]. The configuration of the phosphorus atom was retained during the addition reaction. As in the case of addition of H-phosphonates (see above), the $Ph_2P(O)OH$ additive was utilized to control reaction selectivity towards the formation of α-isomer. The formation of the *β*-isomer was reported for alkynes bearing $SiMe_3$ substituent, where the $Ph_2P(O)OH$ additive was not efficient.

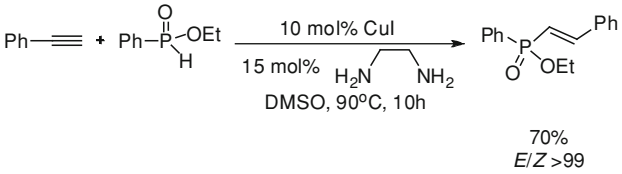
Similar studies were carried out for the Ni-catalyzed reaction [73]. $Ni(PMe_2Ph)_4$ in THF at rt gave α-isomer in the Ph(EtO)P(O)H addition to 1-octyne and phenylacetylene, 88 and 98% yields for R = C_6H_{13} and Ph, respectively. However, *β*-isomer with 92% yield was formed if R = $SiMe_3$.



Scheme 8.39 Addition of H-phosphinates to terminal alkynes using [Pd]/$Ph_2P(O)OH$ catalytic system



Scheme 8.40 Pd-catalyzed hydrophosphonylation of phenylacetylene



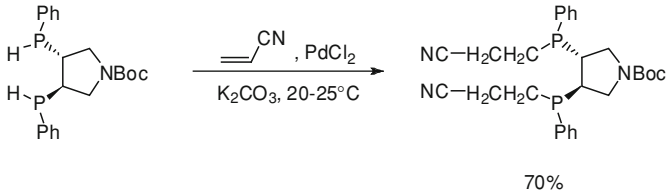
Scheme 8.41 Cu-catalyzed phosphine-free hydrophosphonylation of phenylacetylene

Tanaka et al. have found that high selectivity in the formation of Markovnikov-type α-isomer can be achieved in Pd-catalyzed reaction without addition of the acid (Scheme 8.40) [106]. Excellent selectivity and good yields were observed with bidentate ligand (dppe) and $Pd(OAc)_2$.

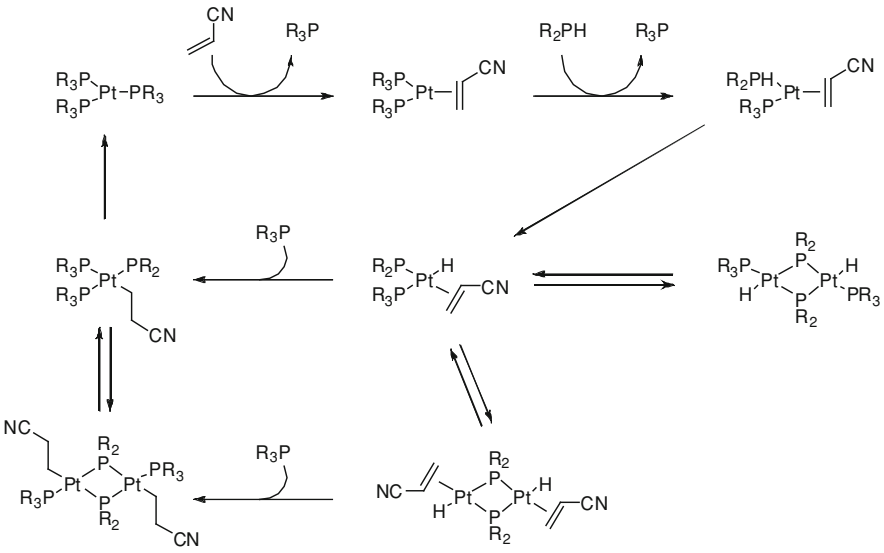
Cu-catalyzed reaction in the CuI/ethylenediamine catalytic system was studied for the phenyl-H-phosphinate addition to phenylacetylene (Scheme 8.41) [97]. Selective formation of anti-Markovnikov *β*-isomer was found in the reaction.

8.2.7 Addition of phosphines $R_{3-n}PH_n$ to Alkenes

Non-catalytic addition of the phosphines $R_{3-n}PH_n$ ($n = 1$–3) to activated olefins is known under acid or base catalyzed conditions, or in the presence of radical initiator [107–109]. The first transition-metal-catalyzed reaction was shown by addition of 3,4-bis-(phenylphosphino)pyrrolidine to acrylonitryle and methyl acrylate in the presence of 2 mol% of $PdCl_2$ (Scheme 8.42) [110].



Scheme 8.42 Pd-catalyzed hydrophosphination of acrylonitrile

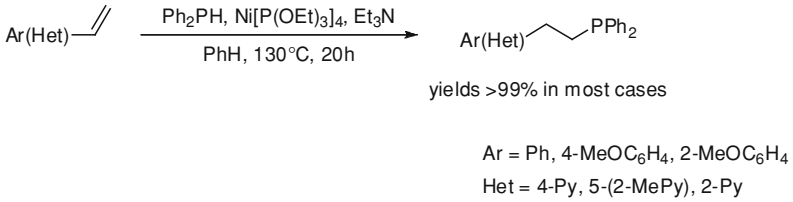


Scheme 8.43 Proposed mechanism of Pt-catalyzed hydrophosphination of acrylonitrile

Pringle et al. have reported Pt-mediated hydrophosphination of acrylonitrile as the first example of transition-metal-catalyzed hydrophosphination of alkenes [111]. Tris(cyanoethyl)phosphine complex of Pt catalyzed addition of H–P(CH_2CH_2CN)$_2$ with formation of the P(CH_2CH_2CN)$_3$. The reaction in acetonitrile was carried out at RT. Kinetic measurements and NMR studies suggested two parallel reaction pathways including mononuclear and dinuclear Pt intermediates (Scheme 8.43) [111–113].

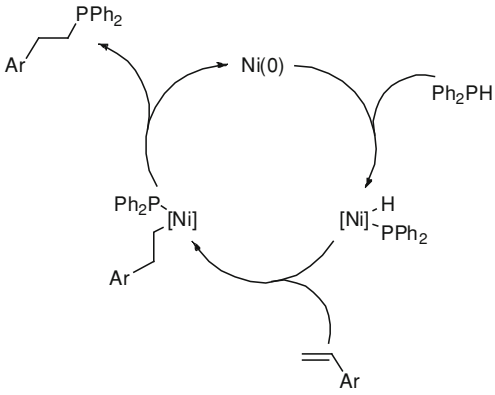
Several studies have highlighted the advantages of metal-catalyzed hydrophosphination of activated alkenes compared to the radical initiating reaction [114, 115]. For example, tris-adduct with 90% selectivity was formed in the reaction of PH_3 and ethyl acrylate, while in the same reaction, initiated by AIBN, a mixture of mono:bis:tris adducts in the ratio of 1:1:1 was formed [116].

Later Glueck et al. have shown that Pt-catalyzed hydrophosphination of acrylonitrile took place via the catalytic cycle, which includes (1) oxidative addition of P–H bond to the metal; (2) olefin insertion into the Pt–P bond; and (3) reductive



Scheme 8.44 Ni-catalyzed hydrophosphination of aryl(hetaryl) substituted alkenes

Scheme 8.45 Proposed mechanism of Ni-catalyzed hydrophosphination of alkenes



elimination [117–119]. Phosphine–alkene intermediates formed in the Pt-catalyzed addition of diethylphosphine to dienes were detected and characterized by NMR spectroscopy [120].

Glueck et al. have reported the addition reaction to activated alkenes (Michael acceptors) and have carried out detailed mechanistic studied [121, 122]. An important mechanistic study was also carried out for the palladium catalyzed asymmetric phosphination [123, 124]. Hydrophosphination of less activated olefins was achieved for the first time by Ni-catalyzed reaction using phosphite ligands (Scheme 8.44) [125].

Regioselective transformation was observed leading to the β-adduct as a sole product. Involvement of the π-allylic intermediate (similar to Pd-catalyzed hydroamination of styrene) in the catalytic cycle was excluded, since the α-adduct was not formed in Ph_2P–H addition to styrene and vinyl pyridine [126]. The plausible catalytic cycle of alkenes hydrophosphination involves oxidative addition of the phosphine to Ni(0) leading to the formation of H–Ni–P complex, followed by alkene insertion into the Ni–H bond and reductive elimination (Scheme 8.45).

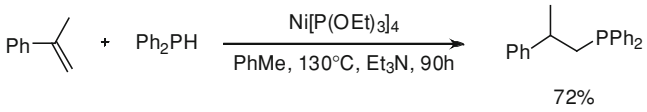
Hydrophosphination of α-methyl styrene is of special interest (Scheme 8.46), since it can be a convenient route to chiral ligands (if asymmetric addition reaction is carried out) [125].

Intramolecular hydrophosphination of phosphinealkenes was carried out as $Cp'LnE(TMS)_2$ catalyzed reaction (where Ln = La, Sm, Y, Lu; E = CH, N;

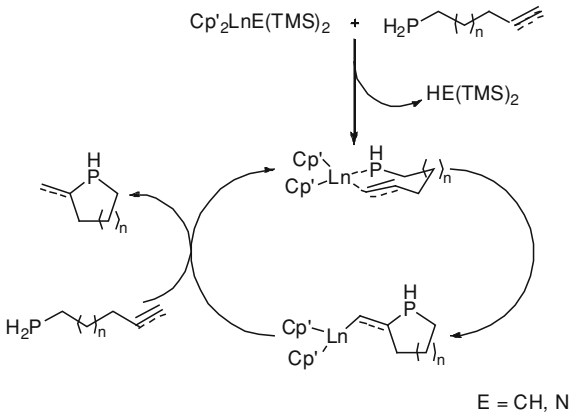
TMS = $SiMe_3$) [127–130]. The reaction starts with cleavage of the Ln–Alk bond by the phosphine resulting in formation of the phosphide derivative of the metal (Scheme 8.47). After insertion of the multiple carbon–carbon bond into the Ln–P bond five-membered heterocycle with two chiral centers was formed. On the next step phosphorus heterocycle is released as a final product and catalytically active Ln species were regenerated. Multiple carbon–carbon insertion into the Ln–P bond was found as rate limiting step of the reaction [129].

Rather unusual hydrophosphination of alkenes was reported using calcium-catalyzed transformation [131]. The reaction was carried out in benzene at 25–75 °C for 13–36 h and resulted in 78–95% conversion. Anti-Markovnikov addition products were formed with high selectivity. Proposed reaction mechanism involves insertion of the C=C bond into the Ca–P bond followed by metathesis stage (Scheme 8.48). The metathesis stage was found as rate determining for the catalytic cycle. Thus, if an activated alkene is utilized in the reaction insertion a more rapid insertion stage compared to slow metathesis stage results in formation phosphine-terminated polymers [131].

Togni et al. have carried out highly enantioselective hydrophosphination of methacrylonitrile (Scheme 8.49) [132]. In the addition reaction a dicationic nickel complex containing (*R*)–(*S*)-Pigiphos ligand was utilized as a catalyst. Up to 89% e.e. was observed in the tBu_2PH addition to methacrylonitrile for reaction carried out in acetone at –25 °C. The higher values of enantiomeric excess (94% e.e.) was found in the addition of Ad_2PH to methacrylonitrile (Ad = 1-adamantyl).

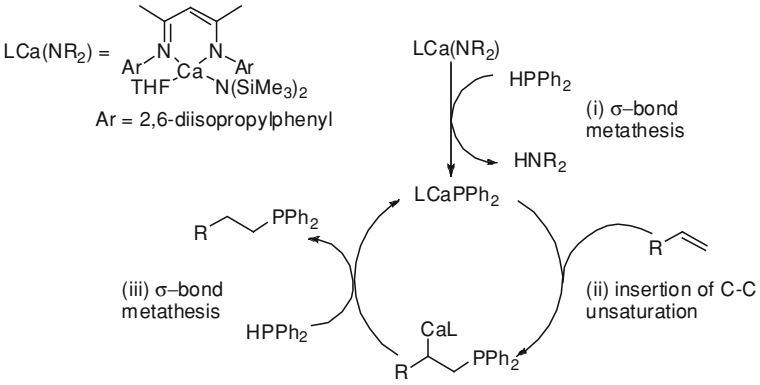


Scheme 8.46 Ni-catalyzed hydrophosphination of α-methyl styrene

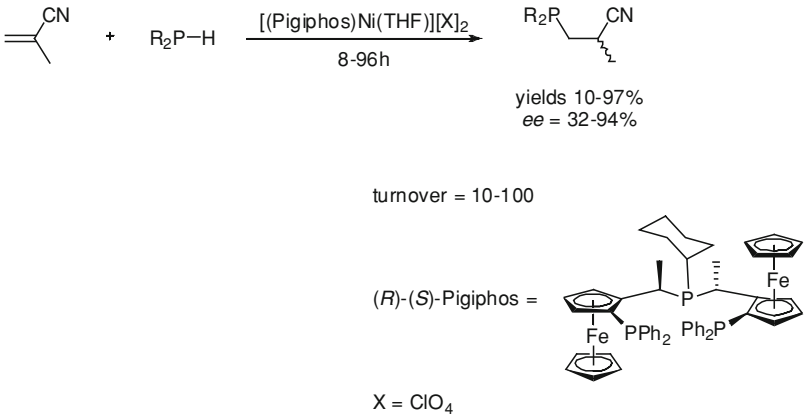


Scheme 8.47 Proposed mechanism of intramolecular hydrophosphination of phosphinealkenes using Cp′LnE(TMS)$_2$

Proposed mechanism of the catalytic reaction starts with coordination of methacrylonitrile to the metal via CN group (Scheme 8.50). Phosphorus–carbon bond was formed on the second 1,4-conjugate addition stage. Proton transfer and

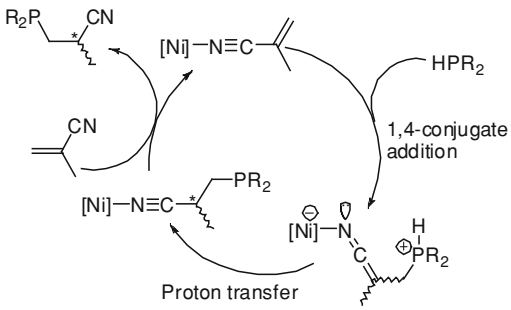


Scheme 8.48 Proposed mechanism of Ca-catalyzed hydrophosphination of alkenes



Scheme 8.49 Enantioselective hydrophosphination of methacrylonitrile using [Ni]/Pigiphos

Scheme 8.50 Proposed mechanism of hydrophosphination of methacrylonitrile using [Ni]/Pigiphos



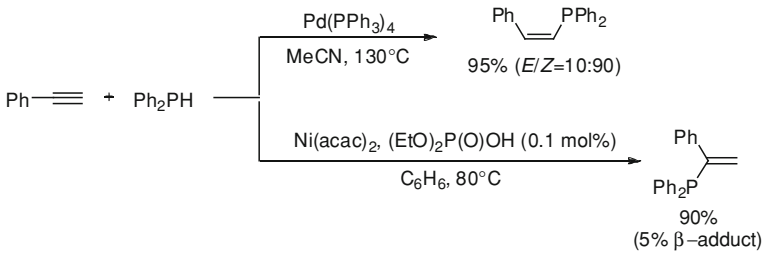
decoordination of product are the last stages of the catalytic cycle [132]. More detailed mechanistic study has shown that proton transfer is the rate-determining step of the catalytic cycle [133].

8.2.8 Addition of Phosphines $R_{3-n}PH_n$ to Alkynes

The first example of Pd and Ni-catalyzed hydrophosphination of terminal and internal alkynes was reported in 2001 (Scheme 8.51) [134]. Regioselectivity of the reaction depended on the catalytic system used and the nature of the alkyne. Hydrophosphination of phenylacetylene in acetonitrile solution in the presence of Pd(0) complexes led to the β-adduct, while $Ni(acac)_2$ in the presence of $(EtO)_2P(O)OH$ gave nearly pure α-adduct ($\alpha:\beta = 95:5$).

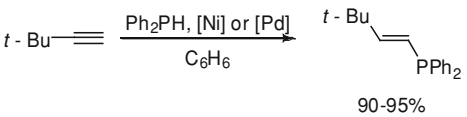
Steric hindrance governed the addition reaction towards β-adduct if *t*-butylacetylene and diphenylphosphine were used as substrates (Scheme 8.52).

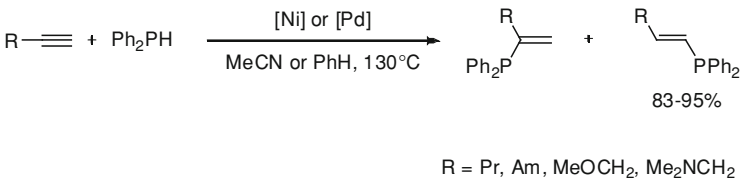
In some cases addition of diphenylphosphine was less selective and the structure of the products (regio- and stereoselectivity of P–H bond addition) strongly depended on the reaction conditions (Scheme 8.53).



Scheme 8.51 Catalytic hydrophosphination of phenylacetylene

Scheme 8.52 Catalytic hydrophosphination of *t*-butylacetylene



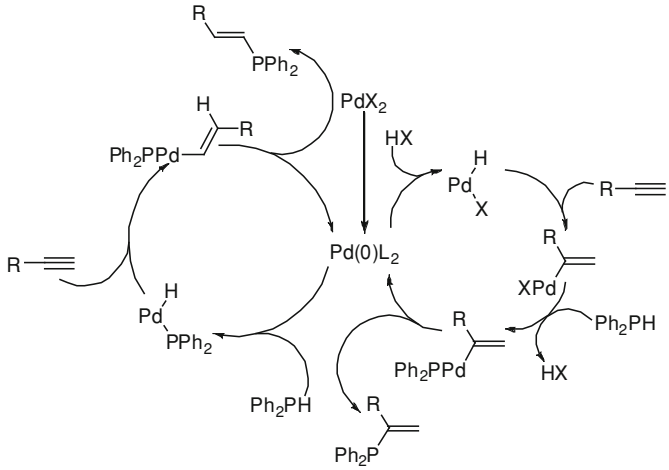


Scheme 8.53 Catalytic hydrophosphination of terminal alkynes

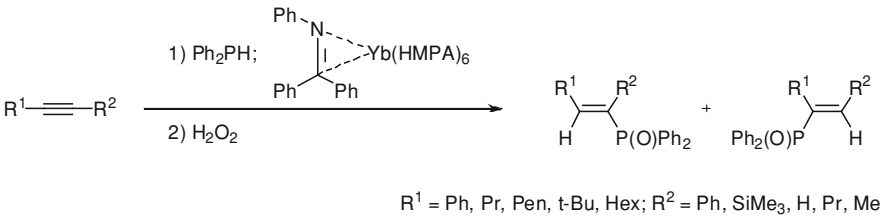
Important mechanistic difference in the reactions using Pd(0)/Ni(0) or PdX_2/NiX_2 species as catalyst precursors is highlighted on Scheme 8.54. In the latter case a small amount of HX (HOAc or HBr) were formed on the catalyst precursor activation step. This catalytic amount of the acid initiated the second catalytic cycle, which led to another isomer as a final product (Scheme 8.54).

Ogawa et al. have reported a novel regioselective hydrophosphination of terminal alkynes with diphosphine in the presence of Pd catalyst [135]. Surprisingly, the reaction resulted not in the corresponding bisphosphination product, but in the formation of Markovnikov-type hydrophosphination product [135]. Rh-catalyzed transformation in the presence of hydrosilanes afforded anti-Markovnikov-type hydrophosphination product [136].

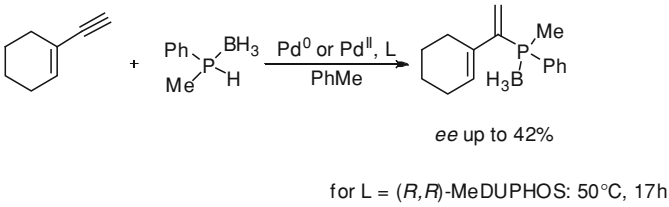
Ytterbium/imine complex [Yb(η^2-Ph_2CNPh)$(HMPA)_6$] was reported as a catalyst for hydrophosphination of alkynes (Scheme 8.55) [137]. From 52% to quantitative product yields were found in the reaction. Regio- and stereoselective transformation was observed in case of internal alkynes, but the reaction with terminal alkynes gave a mixture of α- and β-adducts with the former being



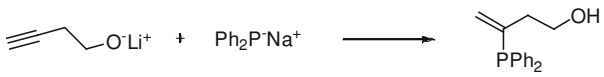
Scheme 8.54 Mechanistic difference in the hydrophosphination reactions using Pd(0)/Ni(0) or PdX_2/NiX_2 species as catalyst precursors



Scheme 8.55 Yb-catalyzed hydrophosphination of alkynes



Scheme 8.56 Pd-catalyzed hydrophosphination of 1-ethynylcyclohexene



Scheme 8.57 Direct hydrophosphination of terminal alkynols

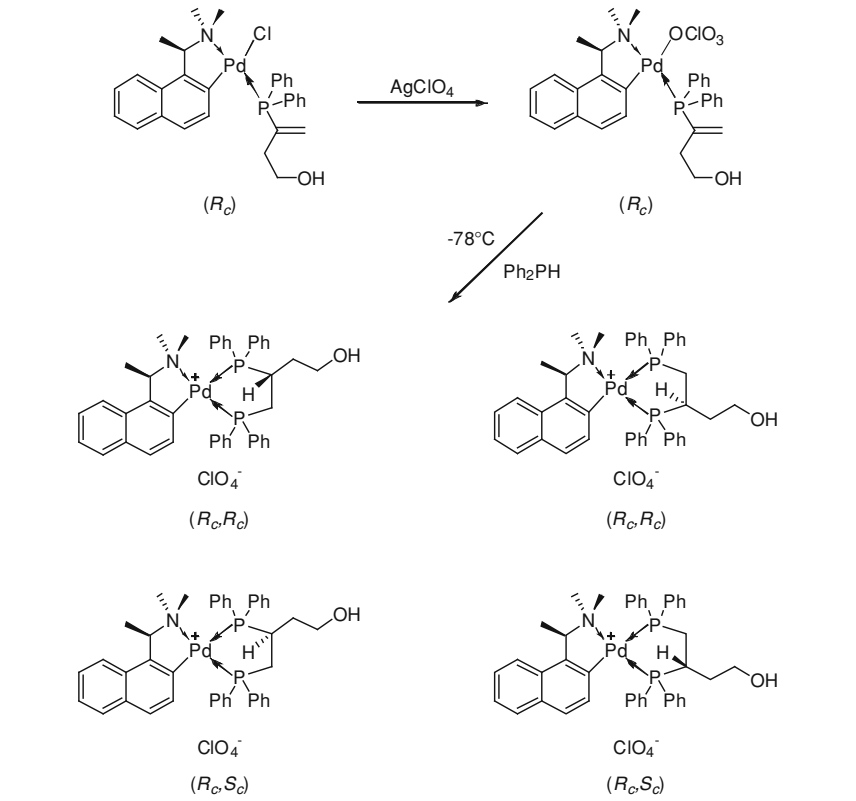
dominating. This Yb-catalyzed reaction was further developed to increase the scope of hydrophosphination of various C–C multiple bonds with diphenylphosphine [138].

Various chiral ligands were studied in the Pd-catalyzed reaction of methylphenylphosphine with 1-ethynylcyclohexene (Scheme 8.56) [139] (for racemic version of the reaction see Ref. [140]). P-Stereogenic vinyl phosphines were prepared with enantiomeric excess up to 30% e.e. The best results were achieved with (*R*,*R*)-Me-Duphos and (*R*,*R*)-*i*-Pr-Duphos in toluene at 35 °C. Increasing the temperature to 50 °C led to better conversion of the reagents and slightly better enantioselectivity. It should be pointed out that hydrophosphination of the double bond of alkenes with phosphine-borane complex did not require a catalyst and was carried out under regular thermal or microwave heated conditions [141].

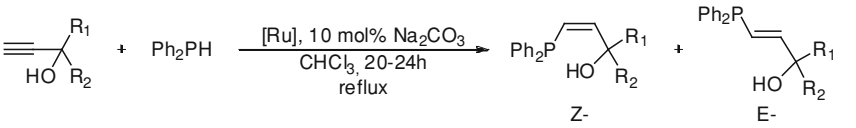
An interesting approach towards formation of functionalized chiral diphosphines was developed based on two-stage hydrophosphination of terminal alkynols [142]. At the first stage the alkynols were subjected to direct hydrophosphination under mild conditions to give the corresponding Markovnikov addition products (Scheme 8.57). At the second stage asymmetric hydrophosphination was carried out employing an organopalladium complex containing the orthometalated (*R*)-(1-(dimethylamino)ethyl)naphthalene as a chiral auxiliary (Scheme 8.58). All four possible stereoisomeric products were generated stereoselectively (in the ratio of 1:2:4:18) for the reaction with 3-diphenylphosphanyl-but-3-en-1-ol. The major isomer was isolated and structure determination was performed by means of X-ray crystal structure analysis [142].

Hydrophosphination of propargylic alcohols with ruthenium catalysts RuCl$(PPh_3)_2$Cp* and RuCl(cod)Cp* resulted in the product formation with the phosphorus atom attached to terminal position (Scheme 8.59) [143]. The reaction mechanism was proposed to involve intermediate ruthenium vinylidene species.

Synthesis of (*Z*)-bis-diphenylphosphino-alkenes was successfully carried out by Oshima et al. by addition of Ph_2PH to 1-alkynylphosphines (Scheme 8.60) [144]. The reaction was carried out in Cu-catalyzed conditions in DMF in the presence of



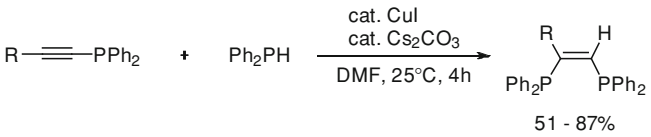
Scheme 8.58 Asymmetric hydrophosphination of diphenylphosphinoalkenols using organo palladium complex



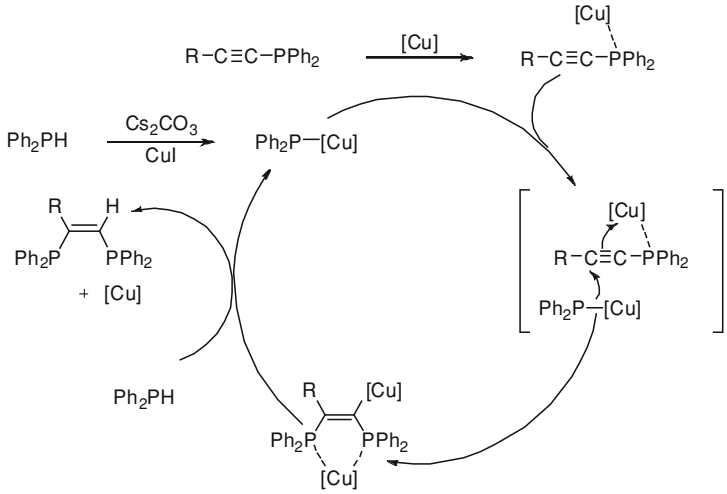
[Ru] = RuCl(cod)(C_5Me_5)

	yield [%]	(Z) / (E)
R_1=R_2=-$(CH_2)_5$-	70	95 / 5
R_1=R_2=Me	81	75 / 25
R_1=R_2=Et	55	75 / 25
R_1=Me; R_2=*i*-Bu	50	80 / 20

Scheme 8.59 Ru-catalyzed hydrophosphination of propargylic alcohols



Scheme 8.60 Cu-catalyzed hydrophosphination of 1-alkynylphosphines



Scheme 8.61 Proposed mechanism of Cu-catalyzed hydrophosphination of 1-alkynylphosphines

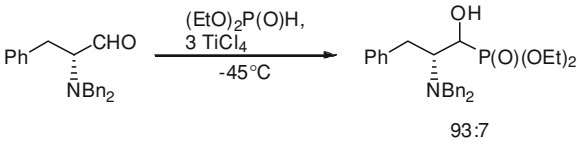
Cs_2CO_3. Asymmetric hydrogenation of the reaction product in the $RuCl_2(PPh_3)_3$-(*R*)-BINAP system led to chiral bidentate phosphine ligand. Plausible reaction mechanism was proposed to involve triple bond activation by CuI as well as nucleophilic attack of the Cu phosphide species (Scheme 8.61) [144].

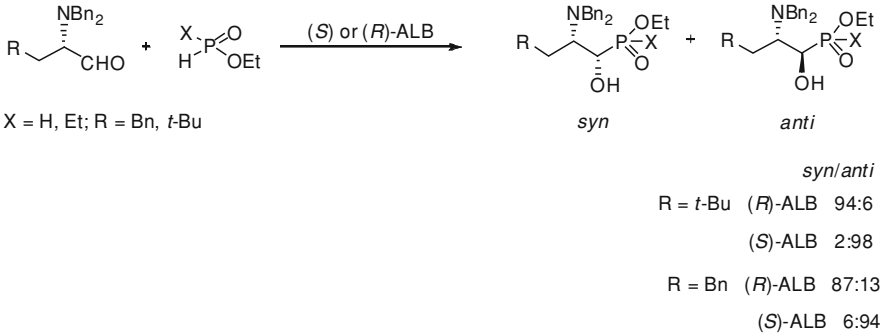
Hydrophosphination of the triple bond leading to anti-Markovnikov products in case of terminal alkynes and *syn*-addition products in case of internal alkynes was reported using $Co(acac)_2$ as catalyst precursor [145].

8.2.9 Addition of H-Phosphonates $(RO)_2P(O)H$ to Aldehydes

Addition of dialkyl phosphites to aldehydes and imines are important synthetic methods for the preparation of α-hydroxyl and α-amino phosphonates, which represent phosphorus analogs of α-hydroxyl and α-amino acids. These compounds were investigated in terms of their biological activity [146–156], especially the role of the chiral center configuration on the biological activity [157–170]. Both transition-metal-catalyzed as well as thermal additions were studied. Utilization of

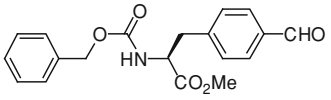
Scheme 8.62 $TiCl_4$-catalyzed hydrophosphorylation of α-amino aldehyde





Scheme 8.63 Hydrophosphonylation of chiral α-amino aldehydes using (ALB) catalyst

Fig. 8.3 The compound for the synthesis of β-amino -α-hydroxyphosphinic acids



chiral catalyst opened the way to asymmetric synthesis of these important phosphorus derivatives.

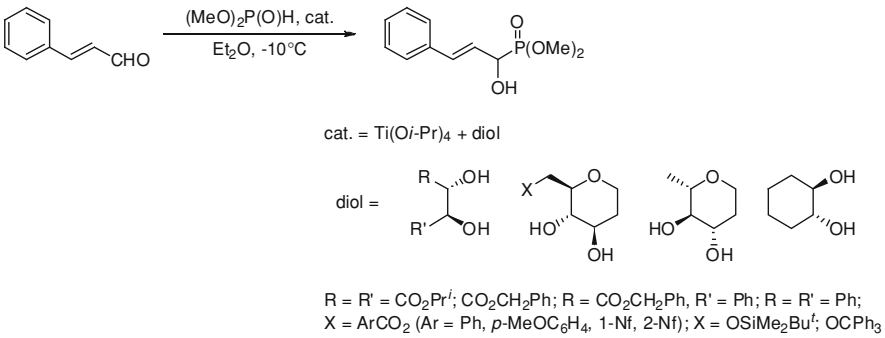
Earlier it was shown that $TiCl_4$-catalyzed reaction of chiral α-amino aldehyde with diethylphosphite took place with high diastereoselectivity (Scheme 8.62) [171].

High diastereoselectvity was achieved in the hydrophosphonylation reaction of chiral α-amino aldehydes using 20 mol% of the Al/Li/BINOL catalyst (ALB) developed by Shibasaki (Scheme 8.63) [172]. The ratio of *syn*-/*anti*-isomers was easily controlled by chirality of the ALB catalyst.

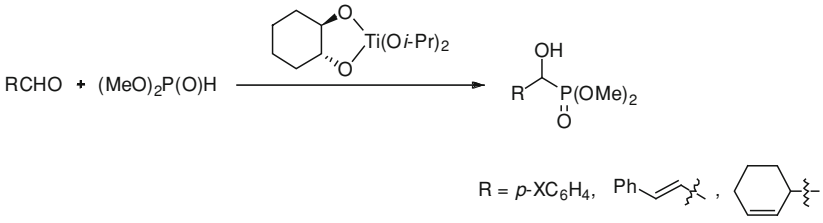
Diastereoselective reaction of the chiral aldehyde (Fig. 8.3) with diethylphosphite was mediated by LLB catalytic system (Ln/Li/BINOL) with the diastereoisomers ratio 75:25, same transformation catalyzed by ALB system gave 80:20 ratio of the diastereoisomers [173]. Synthesized β-amino-α-hydroxyphosphinic acids were considered as key intermediates in the preparation of potential inhibitors of human renin and HIV-protease.

The influence of various chiral diols on the performance of Ti catalysts was studied on the model reaction involving cinnamaldehyde and dimethylphosphite (Scheme 8.64) [174].

The best result with ~70% e.e. was found in the catalyst with cyclohexyl diol (Scheme 8.65). Using this catalyst in the reaction with aromatic aldehydes also gave similar values of enantiomeric excess (50–65% e.e.).



Scheme 8.64 Hydrophosphorylation of cinnamaldehyde using Ti catalyst



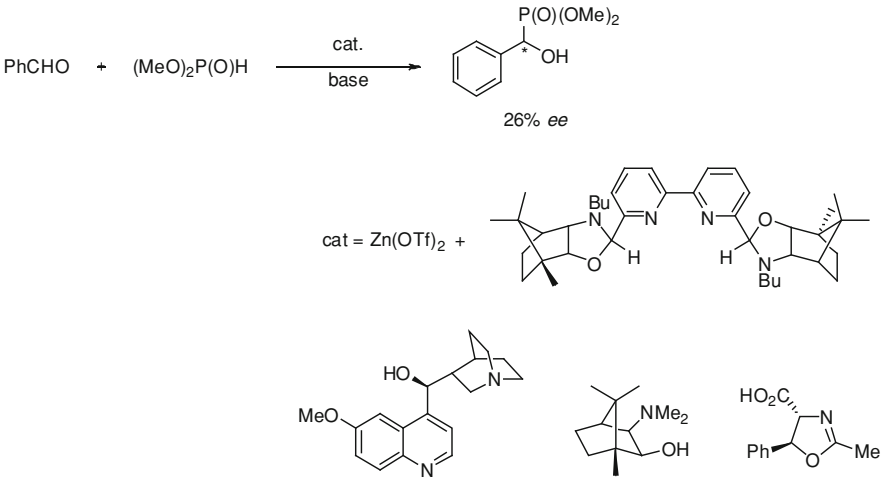
Scheme 8.65 Hydrophosphorylation of aromatic aldehydes using [Ti]/cyclohexyl diol catalytic system

Rather small enantiomeric excess was observed in the reaction between the dimethylphosphite and benzaldehyde (Scheme 8.66) catalyzed by zinc salt with *N*,*O*-chiral ligands (or other chiral aminoalcohols) [175].

Chiral Al complexes with SALEN ligands (Fig. 8.4) showed 10–54% e.e. depending on the type of substituents and nature of X in the ligand [176]. Mechanistic study revealed dimer–monomer equilibrium of catalyst in solution and discussed the possible influence on the values of enantiomeric excess [177] Small values of enantioselectivity ($\sim$30% e.e.) were observed in the reaction of cinnamaldehyde with dimethylphosphite using La/Li/BINOL as a catalyst [176].

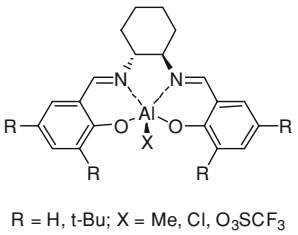
Addition reaction with Sharpless catalyst (Ti tartrate) gave the highest value of 53% e.e. in diethylether solution for the reaction between aromatic aldehyde and diethylphosphite (Scheme 8.67) [178]. Strong dependence of enantiomeric excess from the solvent was reported for this transformation.

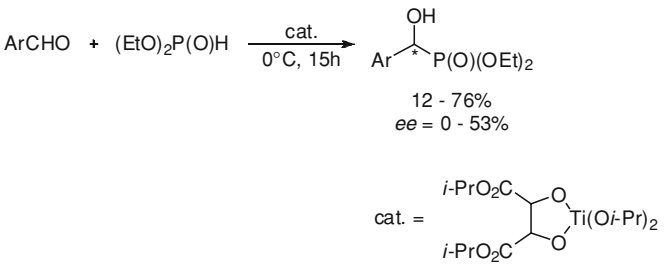
The influence of various factors was addressed in the enantioselective reaction catalyzed by La/Na/BINOL (LSB) catalytic systems (Scheme 8.68) [179]. The nature of the aldehyde (aromatic or α,β-unsaturated), substituents in the benzene ring, type of solvent, reaction temperature and substituents in the BINOL ligand were found to effect strongly the outcome of the reaction. The presence of the phenyl groups in 6,6′ positions increased e.e., compared to the unsubstituted BINOL, while the present of EtO-group in the 3,3′ positions decreased e.e. The



Scheme 8.66 Zn-catalyzed hydrophosphorylation of benzaldehyde

Fig. 8.4 Chiral Al complexes with SALEN ligands

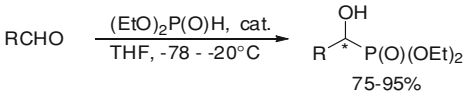




Scheme 8.67 Hydrophosphorylation of aromatic aldehydes using Sharpless catalyst

following representative results were found carrying out the reaction at −40 °C in THF with 20 mol% 6,6′-diphenylBINOL as a catalyst (Scheme 8.68).

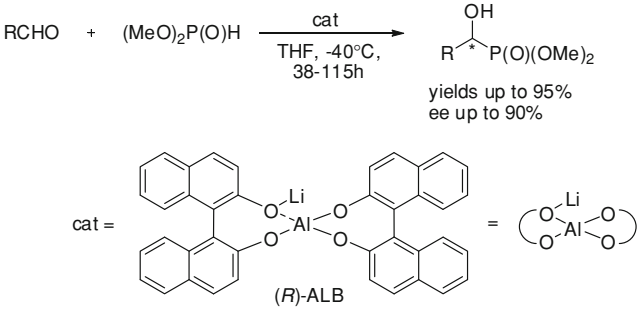
Important achievement in the field was reported by Shibasaki et al. using heterobimetallic catalysts. It should be pointed out that complexation of BINOL and La was suggested in the presence of Li or Na and desired structure of the catalyst was formed under carefully optimized conditions.



cat = La/Na/6,6'-diphenylBINOL

RCHO	% *ee*	RCHO	% *ee*
PhCHO	39	PhCH=CHCHO	41
p-MeC_6H_4CHO	69	1-NfCHO	35
p-$MeOC_6H_4CHO$	74	$PhCH_2CH_2CHO$	0
p-ClC_6H_4CHO	52		

Scheme 8.68 Hydrophosphorylation of aldehydes using LSB catalyst



R = *p*-ZC_6H_4 (Z = H, Cl, Me, MeO, NO_2, $(CH_3)_2N$), (*E*)-PhCH=CH, (*E*)-PhCH=CH(CH_3), (*E*)-$CH_3(CH_2)_2CH$=CH, $CH_3(CH_2)_3CH_2$

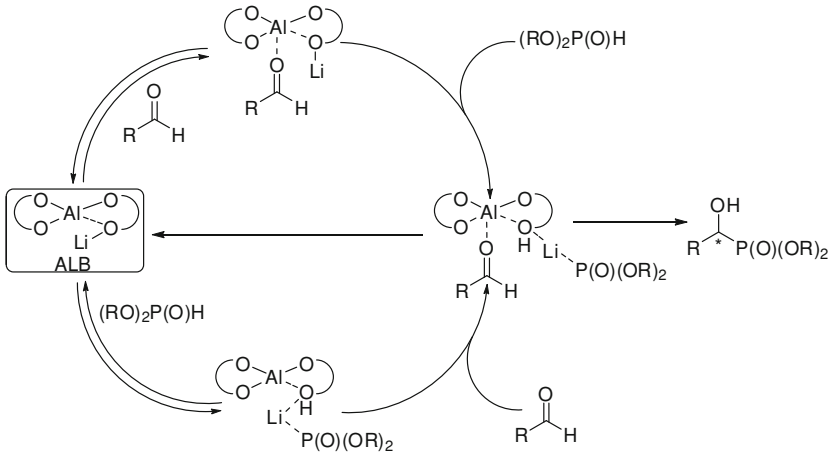
Scheme 8.69 Hydrophosphorylation of aldehydes using ALB catalyst

Hydrophosphorylation of aldehydes catalyzed by LnMB complex (where Ln = La, Pr, Sm, Gd, Dy, Yb; M = Li, Na, K; B = BINOL) made it possible to synthesize α-hydroxyphosphonates with e.e. up to 98% [180, 181]. Catalytic asymmetric synthesis of α-hydroxyphosphonates using the Al–Li-BINOL complex (ALB) was also carried out (Scheme 8.69) [181].

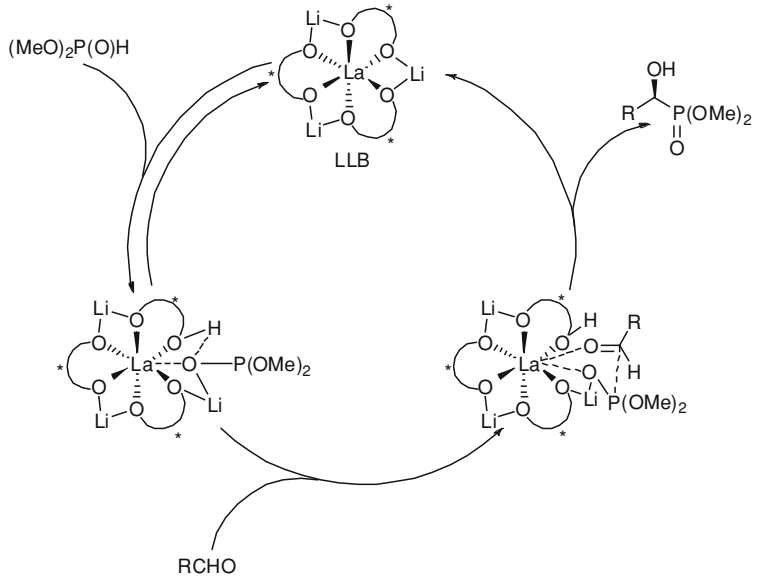
Lithium naphthoxide was suggested to act as a Brønsted base and aluminium center—as a Lewis acid. Thus, both the electrophile and nucleophile were activated in the same complex (Scheme 8.70) [180, 181].

The enantioselective addition of dialkylphosphites $(RO)_2P(O)H$ to aldehydes was catalyzed by a lanthanum (*R*)-binaphthoxide complex (10 mol %) and resulted in formation of (*S*)-hydroxyphosphonates in good yield (51–100%) and modest enantioselectivity (6–33% e.e.) [182].

Shibasaki et al. have reported excellent La/Li/BINOL (LLB) catalytic system prepared from the $LaCl_3 \times 7H_2O$ and BINOL–dilithium salt in the presence of *t*-BuONa in THF at 50 °C [183]. Using this catalytic system enantiomeric excess in the reaction of dimethylphosphite and aldehydes was increased to 95% (for *p*-dimethylaminobenzaldehyde). For the aliphatic aldehydes also a better



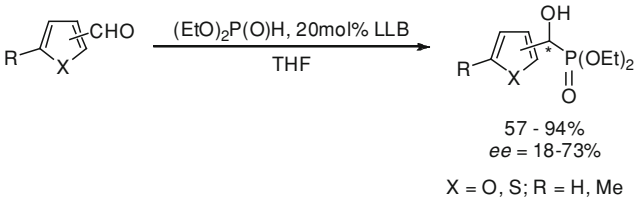
Scheme 8.70 Proposed mechanism of hydrophosphorylation of aldehydes using ALB catalyst



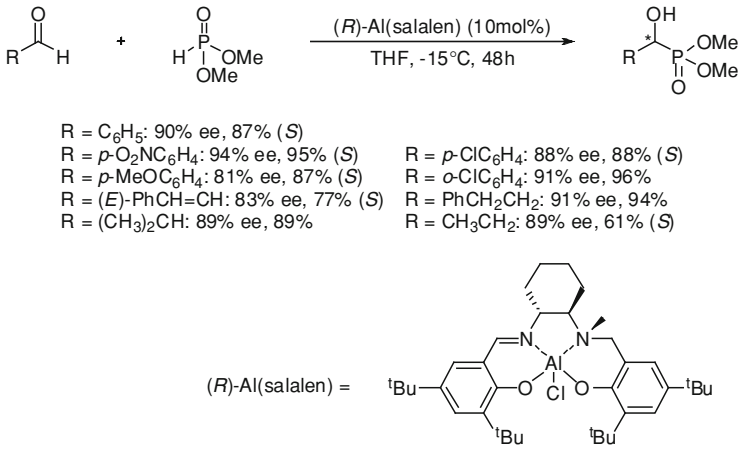
Scheme 8.71 Proposed mechanism of hydrophosphorylation of aldehydes using LLB catalyst

performance was observed compared to ALB catalyst. Proposed mechanism of the catalytic reaction involves simultaneous activation of the aldehyde and phosphite by La and Li (Scheme 8.71).

However, such significant enhancement of the catalyst efficiency of LLB compared to ALB was observed only for some selected aldehydes. For benzaldehyde and its *p*-NO_2 and *p*-Cl derivatives the reversed relationship was observed.



Scheme 8.72 LLB-catalyzed hydrophosphorylation of heteroaromatic aldehydes



Scheme 8.73 Hydrophosphorylation of aldehydes using (*R*)-Al(salalen) complex

The values of e.e. obtained with ALB were significantly higher than those obtained with LLB (for example, for PhCHO 90 and 79% e.e. were observed for ALB and LLB, respectively) [180, 183]. The nature of the metal also effected the value of e.e. [184].

Using LLB the addition reaction to heteroaromatic aldehydes was also carried out (Scheme 8.72) [178]. The highest value of enantiomeric excess (73%) was observed for the 5-methyl-2-thiophenecarbaldehyde (cf. with the 41% e.e. for the 2-thiophenecarbaldehyde).

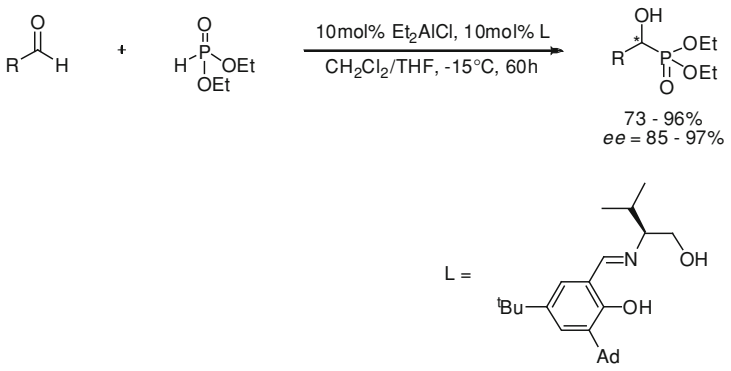
Catalytic hydrophosphorylation of aldehydes was studied by Katsuki et al. with optically active salalen ligands (Scheme 8.73) [185, 186]. Excellent yields (up to 96%) and enantiomeric excess (up to 96% e.e.) were achieved in the addition reaction. An efficient catalyst was developed for enantioselective reactions with both aromatic and aliphatic aldehydes (up to 84 and 86% e.e., respectively) [187].

Feng et al. have reported highly enantioselective hydrophosphorylation of aldehydes catalyzed by aluminum complexes with tridentate Schiff base (Scheme 8.74) [188]. Excellent yields (up to 96%) and enantiomeric excess (up to 97%) were found in the addition reaction. Same authors have also studied asymmetric hydrophosphorylation of aldehydes catalyzed by bifunctional chiral aluminum complexes [189] and Lewis acid-catalyzed hydrophosphonylation of ketones [190].

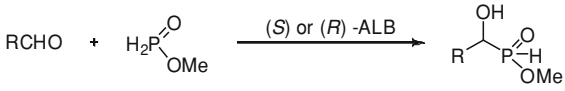
8.2.10 Other P–H Bond Addition Reactions Involving Aldehydes

Shibuya et al. have shown the reaction of aldehydes with methyl phosphinate catalyzed by ALB (Scheme 8.75) [191]. No reaction was observed with LLB, while LPB did not give acceptable stereochemical outcome. In a best case with ALB 62% yield and 85% e.e. was found. In the presence of an excess of the aldehyde double phosphonylation was observed. Arylation product was formed with 61–82% e.e.

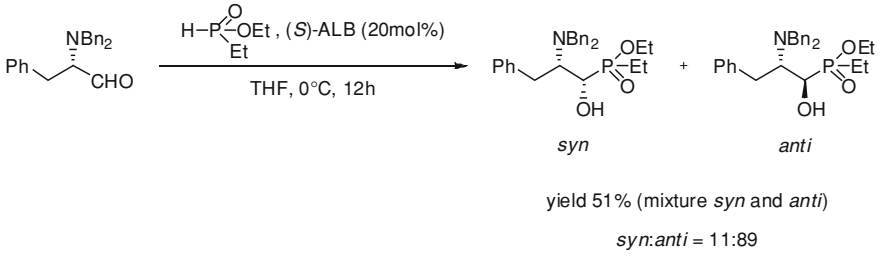
This reaction was utilized for (*S*)-ALB catalyzed diastereoselective synthesis *β*-amino-α-hydroxyphosphinates by hydrophosphonylation of *N*,*N*-dibenzyl-α-aminoaldehydes with (EtO)EtP(O)H (Scheme 8.76) [192].



Scheme 8.74 Hydrophosphorylation of aldehydes using [Al]/Schiff base catalytic system



Scheme 8.75 Addition of methyl phosphinate to aldehydes using ALB catalyst



Scheme 8.76 Hydrophosphonylation of *N*,*N*-dibenzyl-α-aminoaldehydes using (*S*)-ALB catalyst

8.2.11 Addition of H-Phosphonates $(RO)_2P(O)H$ to Imines

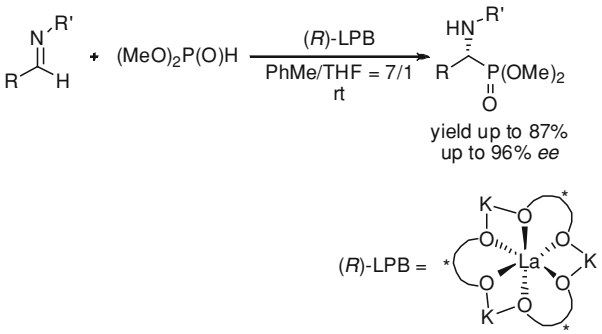
Excellent results were reported in asymmetric hydrophosphorylation of imines by heterobimetallic catalysts (Scheme 8.77) [193]. Although the yield and enantiomeric excess were affected by nature of the imine, solvent, temperature and catalyst, as high as 96% e.e. was achieved. The catalyst with potassium ions showed the best performance under studied conditions. This synthetic approach is of potential interest for industrial applications in the synthesis of chiral α-aminophosphonic acids [194].

Proposed mechanism of the catalytic reaction includes deprotonation of the phosphite and oxygen coordination to La, followed by nucleophilic attack of phosphorus center to carbon atom of the imine group and nitrogen coordination to the metal (Scheme 8.78). Proton shift yields the product and regenerates the catalyst.

Cyclic imines were reacted in a similar manner under catalysis by Ti and Ln-complexes [195]. The best result in this study was reported for the YbPB complex (5 mol%) at 50 °C in the 1:7 mixture of THF-toluene for 48 h – 88% yield and 95% e.e. (Scheme 8.79).

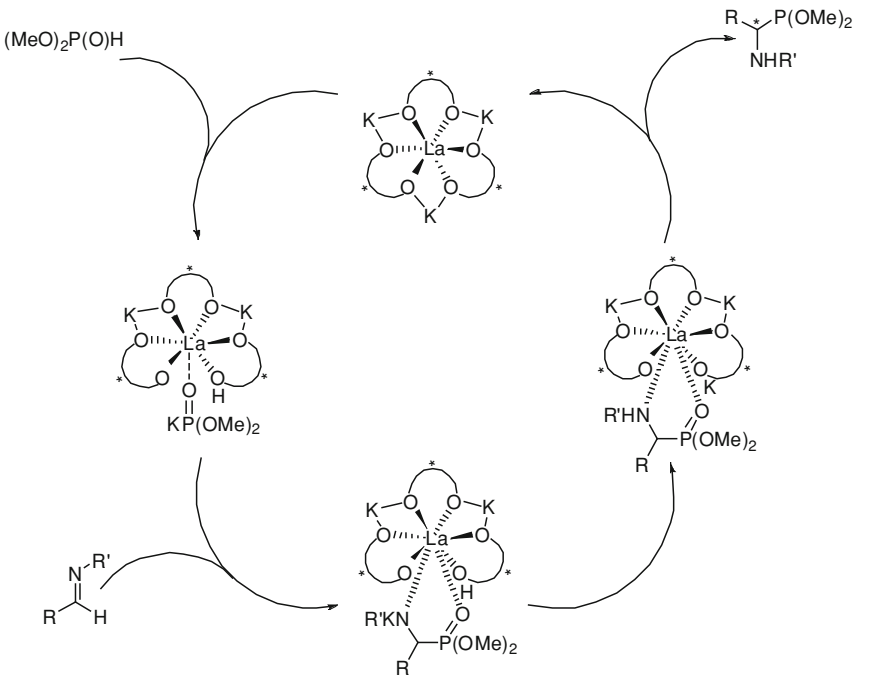
Catalytic hydrophosphorylation of imines was studied by Katsuki et al. with optically active salalen ligands (the same system was used for hydrophosphonylation of aldehydes, see Scheme 8.73) [186]. High yields (up to 93%) and good enantiomeric excess (up to 87%) were found.

It was reported that iron salts catalyzed the oxidative α-phosphonation of *N*,*N*-dimethylanilines with $(RO)_2P(O)H$ in the presence of *tert*-butylhydroperoxide [196]. In the study electrochemical C–H bond activation was utilized to generate iminium species, followed by C–P bond formation. An efficient dehydrogenative coupling reaction involving iminium salt as a possible intermediate was also reported with copper salt as catalyst and molecular oxygen as oxidant [197].

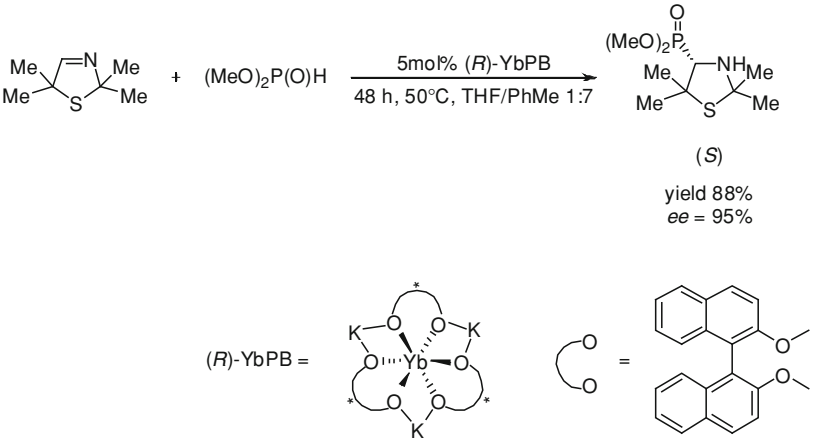


imine	yield, %	*ee* %
R = *i*-Pr; R' = $CH(C_6H_4OMe\text{-}p)_2$	70	96
R = Et, R' = Ph_2CH	80	91
R = C_5H_{11}; R' = Ph_2CH	87	85

Scheme 8.77 Hydrophosphorylation of imines using (*R*)-LPB catalyst



Scheme 8.78 Proposed mechanism of hydrophosphorylation of imines using (*R*)-LPB catalyst



Scheme 8.79 Hydrophosphorylation of cyclic imines using (*R*)-YbPB catalyst

8.2.12 Addition of Phosphine Oxides $R_2P(O)H$ to Imines

Addition of diphenylphosphine oxide was carried out in high yields of 50–96% with high e.e. values of 75–93% (Scheme 8.80) [198]. Praseodymium complex PrPB was reported as the best catalyst for the studied conditions.

8.2.13 Addition of Phosphines $R_{3-n}PH_n$ to Aldehydes and Imines

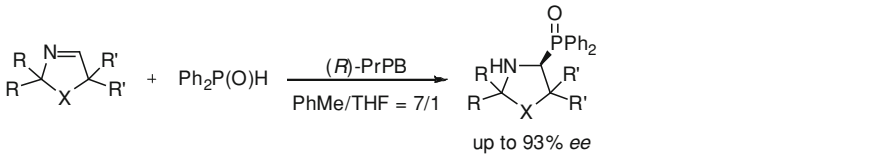
Transition metal catalysts facilitated the addition reaction of phosphines to aldehydes. For example, Pt(II)-catalyzed reaction between phosphine and aldehyde led to the formation of water soluble product $P(CH_2OH)_3$. The corresponding metal complexes $[M(PCH_2CH_2OH)_3)_4]$ (M = Ni, Pd, Pt) also catalyzed the reaction in water solutions (Scheme 8.81) [199–201].

Transition-metal-free P–H bond addition of phosphines to aldehydes, ketones and imines can be carried out by activating the substrate with borane (Scheme 8.82) [201–203].

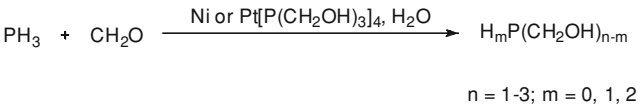
Double addition of the Ph_2PH to α,β-unsaturated carbonyl compounds was carried out using stoichiometric amounts of niobium (V) chloride $NbCl_5$-$BF_3 \times Et_2O$ (Scheme 8.83) [204]. Various enones were involved in the reaction leading to 71–80% product yields.

Catalytic addition of Ph_2PH to aldehydes was possible to carry out with $NbCl_5$ catalyst precursor and was furnished as redox-process (Scheme 8.84) [204].

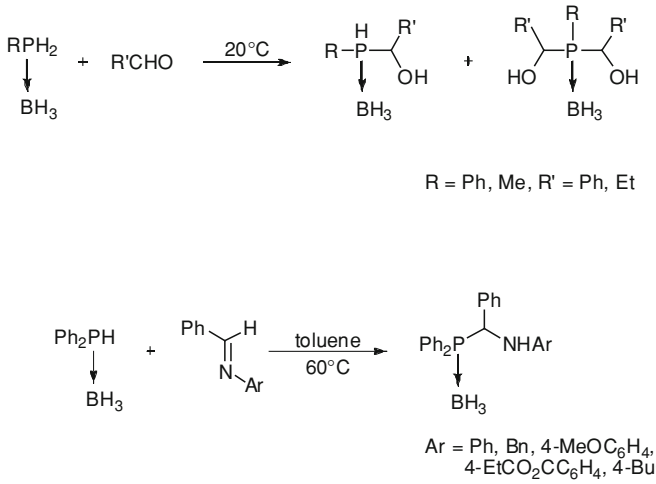
Although the present review deals with transition-metal-catalyzed addition reactions, we would like to point out that recent development of organocatalysis made it a very efficient tool for facilitating P–H bond addition reactions. As a selected representative examples we can mention hydrophosphination of



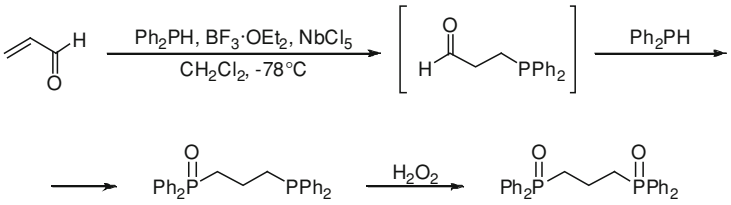
Scheme 8.80 Hydrophosphinylation of cyclic imines using (*R*)-PrPB catalyst



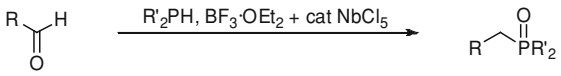
Scheme 8.81 Catalytic hydrophosphination of formaldehyde



Scheme 8.82 BH_3-mediated transition-metal-free hydrophosphination of aldehydes and imines



Scheme 8.83 Hydrophosphination of α,β-unsaturated carbonyl compounds using $NbCl_5$-$BF_3 \times Et_2O$



Scheme 8.84 Addition of diphenylphosphine to aldehydes using $NbCl_5$

α,β-unsaturated aldehydes [205], thiourea-catalyzed enantioselective hydrophosphonylation of imines [206] and asymmetric synthesis of α-amino phosphonates [207, 208].

8.3 Conclusions

Important to point out that discussed catalytic P–H bond addition reactions represent relatively young area, which appears to be on an early stage of development.

Noteworthy, even at this stage catalytic reactions have provided outstanding tool to control stereo-, regio- and enantioselectivity of P–H bond addition to unsaturated molecules discussed in this chapter. Several synthetic procedures were developed for C–P bond formation in atom-economic manner with high yields and excellent selectivity.

In spite of several successful catalytic systems reported for each class of unsaturated molecules, in most cases little is known about reaction mechanism and several reports appear controversial. Another important question concerns strong dependence of selectivity and yields of the reaction on the nature of P–H substrate. In fact, most catalytic systems were developed for particular phosphorus substrates and have to be re-optimized to extend the scope to another specific substrate. Inability to create flexible catalytic system for different P–H substrates as well as difficulties in predicting the direction of the addition reaction for different metals and ligands (and additives) also reflects poor knowledge on understanding reaction mechanism.

As far as mechanistic aspects are considered, the catalytic P–H bond addition reaction is a "hot" area, where several studies are anticipated in the near future to make a better insight into this fascinating subject.

References

1. Alonso F, Beletskaya IP, Yus M (2004) Transition-metal-catalyzed addition of heteroatom–hydrogen bonds to alkynes. Chem Rev 104:3079–3160
2. Beletskaya IP, Kazankova MA (2002) Catalytic methods for building up phosphorus–carbon bond. Russ J Org Chem 38:1391–1430
3. Tanaka M (2004) Homogeneous catalysis for H–P bond addition reactions. Top Curr Chem 232:25–54
4. Coudray L, Montchamp J-L (2008) Recent developments in the addition of phosphinylidene-containing compounds to unactivated unsaturated hydrocarbons: phosphorus–carbon bond formation by hydrophosphinylation and related processes. Eur J Org Chem 3601–3613
5. Merino P, Marqués-López E, Herrera R (2008) Catalytic enantioselective hydrophosphonylation of aldehydes and imines. Adv Synth Catal 350:1195–1208
6. Baillie C, Xiao J (2003) Catalytic synthesis of phosphines and related compounds. Curr Org Chem 7:477–514
7. Delacroix O, Gaumont AC (2005) Hydrophosphination of unactivated alkenes, dienes and alkynes: a versatile and valuable approach for the synthesis of phosphines. Curr Org Chem 9:1851–1882
8. Quntar AAAA, Gallily R, Katzavian G, Srebnik M (2007) Potent anti-inflammatory activity of 3-aminovinylphosphonates as inhibitors of reactive oxygen intermediates, nitric oxides generation, and tumor necrosis factor-alpha release. Eur J Pharm 556:9–13
9. Doddridge ZA, Bertram RD, Hayes CJ, Soultanas P (2003) Effects of vinylphosphonate internucleotide linkages on the cleavage specificity of exonuclease III and on the activity of DNA polymerase I. Biochemistry 42:3239–3246
10. Jung K-Y, Hohl RJ, Wiemer AJ, Wiemer DF (2000) Synthesis of phosphonate derivatives of uridine, cytidine, and cytosine arabinoside. Bioorg Med Chem 8:2501–2509
11. Cermak DM, Wiemer DF, Lewis K, Hohl RJ (2000) 2-(Acyloxy)ethylphosphonate analogues of prenyl pyrophosphates: synthesis and biological characterization. Bioorg Med Chem 8:2729–2737

12. Amori L, Costantino G, Marinozzi M, Pellicciari R, Gasparini F, Flor PJ, Kuhn R, Vranesic I (2000) Synthesis, molecular modeling and preliminary biological evaluation of 1-amino-3-phosphono-3-cyclopentene-1-carboxylic acid and 1-amino-3-phosphono-2-cyclopentene-1-carboxylic acid, two novel agonists of metabotropic glutamate receptors of group III. Bioorg Med Chem Lett 10:1447–1450
13. Vidil C, Morere A, Garcia M, Barragan V, Hamdaoui B, Rochefort H, Montero J-L (1999) Synthesis and biological activity of phosphonate analogs of mannose 6-phosphate (M6P). Eur J Org Chem 447–450
14. Tian W, Zhu Z, Liao Q, Wu Y (1998) A practical synthesis of 3-substituted Δ3, 5(6)-steroids as new potential 5α-reductase inhibitor. Bioorg Med Chem Lett 8:1949–1952
15. Dragovich PS, Webber SE, Babine RE, Fuhrman SA, Patick AK, Matthews DA, Lee CA, Reich SH, Prins TJ, Marakovits JT, Littlefield ES, Zhou R, Tikhe J, Ford CE, Wallace MB, Meador JW, Ferre RA, Brown EL, Binford SL, Harr JEV, DeLisle DM, Worland ST (1998) Structure-based design, synthesis, and biological evaluation of irreversible human rhinovirus 3C protease inhibitors. 1. Michael acceptor structure—activity studies. J Med Chem 41:2806–2818
16. Lazrek HB, Khaïder H, Rochdi A, Barascut J-L, Imbach J-L (1996) Synthesis of new acyclic nucleoside phosphonic acids by Michael addition. Tetrahedron Lett 37:4701–4704
17. Wang D-Y, Hu X-P, Huang J-D, Deng J, Yu S-B, Duan Z-C, Xu X-F, Zheng Z (2007) Highly enantioselective synthesis of α-hydroxy phosphonic acid derivatives by Rh-catalyzed asymmetric hydrogenation with phosphine–phosphoramidite ligands. Angew Chem Int Ed 46:7810–7813
18. Hayashi T, Senda T, Takaya Y, Ogasawara M (1999) Rhodium-Catalyzed asymmetric 1,4-addition to 1-alkenylphosphonates. J Am Chem Soc 121:11591–11592
19. Giordano C, Castaldi G (1989) First asymmetric synthesis of enantiomerically pure (1R,2S)-(-)-(1,2-Epoxypropyl)phosphonic acid (Fosfomycin). J Org Chem 54:1470–1473
20. Thomas AA, Sharpless KB (1999) The Catalytic asymmetric aminohydroxylation of unsaturated phosphonates. J Org Chem 64:8379–8385
21. Burk MJ, Stammers TA, Straub JA (1999) Enantioselective synthesis of α-hydroxy and α-amino phosphonates via catalytic asymmetric hydrogenation. Org Lett 1:387–390
22. Sulzer-Mossé S, Tissot M, Alexakis A (2007) First enantioselective organocatalytic conjugate addition of aldehydes to vinyl phosphonates. Org Lett 9:3749–3752
23. Yokomatsu T, Yoshida Y, Suemune K, Yamagishi T, Shibuya S (1995) Enantioselective synthesis of threo-α,β-dihydroxyphosphonates by asymmetric dihydroxylation of vinylphosphonates. An application to the stereocontrolled synthesis of (4S,5S)-4-diethylphosphono-5-hydroxymethyl-2,2-dimethyl-1,3-dioxolane. Tetrahedron Asym 6:365–368
24. Cravotto G, Giovenzana GB, Pagliarin R, Palmisano G, Sisti M (1998) A straightforward entry into enantiomerically enriched β-Amino-α-hydroxyphosphonic acid derivatives. Tetrahedron Asym 9:745–748
25. Vieth S, Costisella B, Schneider M (1997) Tandem Michael addition alkylation of vinylphosphonates. Tetrahedron 53:9623–9628
26. Henry J-C, Lavergne D, Ratovelomanana-Vidal V, Genet J-P, Beletskaya IP, Dolgina TM (1998) Asymmetric hydrogenation of vinylphosphonic acids and esters with chiral Ru(II) Catalysts. Tetrahedron Lett 39:3473–3476
27. Zmudzka K, Johansson T, Wojcik M, Janicka M, Nowak M, Stawinski J, Nawrot B (2003) Novel DNA analogues with 2-, 3- and 4-pyridylphosphonate internucleotide bonds: synthesis and hybridization properties. New J Chem 27:1698–1705
28. Abbas S, Bertram RD, Hayes CJ (2001) Commercially available 5′-DMT phosphoramidites as reagents for the synthesis of vinylphosphonate-linked oligonucleic acids. Org Lett 3:3365–3367
29. Harnden MR, Parkin A, Parratt MJ, Perkins RM (1993) Novel acyclonucleotides: synthesis and antiviral activity of alkenylphosphonic acid derivatives of purines and a pyrimidine. J Med Chem 36:1343–1355

30. Lazrek HB, Rochdi A, Khaider H, Barascut J-L, Imbach J-L, Balzarini J, Witvrouw M, Pannecouque C, De Clercq E (1998) Synthesis of (*Z*) and (*E*) α-Alkenyl phosphonic acid derivatives of purines and pyrimidines. Tetrahedron 54:3807–3816
31. Agarwal KL, Riftina F (1979) Synthesis and enzymatic properties of deoxyribooligonucleotides containing methyl and phenylphosphonate linkages. Nucleic Acids Res 6:3009–3024
32. Minami T, Motoyoshiya J (1992) Vinylphosphonates in organic synthesis. Synthesis 333–349
33. Dembitsky VM, Quntar AAAA, Haj-Yehia A, Srebnik M (2005) Recent synthesis and transformation of vinylphosphonates. Mini Rev Org Chem 2:91–109
34. Failla S, Finocchiaro P, Consiglio GA (2000) Syntheses, characterization, stereochemistry and complexing properties of acyclic and macrocyclic compounds possessing α-Amino- or α-hydroxyphosphonate units: a review article. Heteroatom Chem 11:493–504
35. Maffei M (2004) Transition metal-promoted syntheses of vinylphosphonates. Curr Org Synth 1:355–375
36. Nagaoka Y (2001) Carbon–carbon bond formation based on alkenylphosphonates. Yakugaku Zasshi 121:771–779
37. Parvole J, Jannasch P (2008) Polysulfones grafted with poly(vinylphosphonic acid) for highly proton conducting fuel cell membranes in the hydrated and nominally dry state. Macromolecules 41:3893–3903
38. Sato T, Hasegawa M, Seno M, Hirano T (2008) Radical polymerization behavior of dimethyl vinylphosphonate: homopolymerization and copolymerization with trimethoxyvinylsilane. J Appl Polym Sci 109:3746–3752
39. Schmider M, Müh E, Klee JE, Mülhaupt R (2005) A versatile synthetic route to phosphonate-functional monomers, oligomers, silanes, and hybrid nanoparticles. Macromolecules 38:9548–9555
40. Senhaji O, Robin JJ, Achchoubi M, Boutevin B (2004) Synthesis and characterization of new methacrylic phosphonated surface active monomer. Macromol Chem Phys 205:1039–1050
41. Ebdon JR, Price D, Hunt BJ, Joseph P, Gao F, Milnes GJ, Cunliffe LK (2000) Flame retardance in some polystyrenes and poly(methyl methacrylate)s with covalently bound phosphorus-containing groups: initial screening experiments and some laser pyrolysis mechanistic studies. Polym Degrad Stab 69:267–277
42. Jin S, Gonsalves KE (1998) Synthesis and characterization of functionalized poly(ε-caprolactone) copolymers by free-radical polymerization. Macromolecules 31:1010–1015
43. Hertler WR (1991) vinylphosphonic esters as end-capping agents in group transfer polymerization. J Polym Sci A Polym Chem 29:869–873
44. Holstein SA, Cermak DM, Wiemer DF, Lewis K, Hohl RJ (1998) Phosphonate and bisphosphonate analogues of farnesyl pyrophosphate as potential inhibitors of farnesyl protein transferase. Bioorg Med Chem 6:687–694
45. Megati S, Phadtare S, Zemlicka J (1992) Unsaturated phosphonates as acyclic nucleotide analogs. Anomalous Michaelis-Arbuzov and Michaelis-Becker reactions with multiple bond systems. J Org Chem 57:2320–2327
46. Smeyers YG, Laguna AH, Romero-Sanchez FJ, Fernandez-Ibanez M, Galyez-Ruano E, Arias-Perez S (1987) Self-consistent field-molecular orbital (SCF-MO) calculations and nuclear magnetic resonance measurements for fosfomycin and related compounds. J Pharm Sci 76:753–756
47. Smith PW, Chamiec AJ, Chung G, Cobley KN, Duncan K, Howes PO, Whittington AR, Wood MR (1995) Synthesis and biological activity of novel cephalosporins containing a (*Z*)-vinyl dimethylphosphonate group. J Antibiot (Tokyo) 48:73–82
48. Bock T, Möhwald H, Mülhaupt R (2007) Arylphosphonic acid-functionalized polyelectrolytes as fuel cell membrane material. Macromol Chem Phys 208:1324–1340
49. Ogawa T, Usuki N, Ono N (1998) A new synthesis of π-electron conjugated phosphonates and phosphonic bis(diethylamides) and their SHG activities. J Chem Soc Perkin Trans 1:2953–2958

50. Zakeeruddin SM, Nazeeruddin MK, Pechy P, Rotzinger FP, Humphry-Baker R, Kalyanasundaram K, Grätzel M, Shklover V, Haibach T (1997) Molecular engineering of photosensitizers for nanocrystalline solar cells: synthesis and characterization of Ru dyes based on phosphonated terpyridines. Inorg Chem 36:5937–5946
51. Belfield KD, Chinna C, Schafer KJ (1997) New NLO stilbene derivatives bearing phosphonate ester electron-withdrawing groups. Tetrahedron Lett 38:6131–6134
52. Welch CM, Gonzales EJ, Guthrie JD (1961) Derivatives of unsaturated phosphonic acids. J Org Chem 26:3270–3273
53. Welch FJ, Paxton HJ (1965) Preparation and polymerization of addition compounds of unsaturated tertiary phosphine oxides. J Polym Sci Part A Gen Pap 3:3427–3437
54. Welch FJ, Paxton HJ (1965) Preparation and polymerization of propenyldiphenylphosphine oxide isomers. J Polym Sci Part A Gen Pap 3:3439–3449
55. Levchik SV, Weil ED (2005) Flame retardancy of thermoplastic polyesters-a review of the recent literature. Polym Int 54:11–35
56. Defieber C, Grützmacher H, Carreira EM (2008) Chiral olefins as steering ligands in asymmetric catalysis. Angew Chem Int Ed 47:4482–4502
57. Laporte C, Böhler C, Schönberg H, Grützmacher H (2002) Strain in organometallics: synthesis of rhodium and iridium complexes with a novel rigid tetrachelating phosphine olefin ligand and their redox properties. J Organomet Chem 641:227–234
58. Shi W, Luo Y, Luo X, Chao L, Zhang H, Wang J, Lei A (2008) Investigation of an efficient palladium-catalyzed C(sp)–C(sp) cross-coupling reaction using phosphine–olefin ligand: application and mechanistic aspects. J Am Chem Soc 130:14713–14720
59. Maire P, Deblon S, Breher F, Geier J, Böhler C, Rüegger H, Schönberg H, Grützmacher H (2004) Olefins as steering ligands for homogeneously catalyzed hydrogenations. Chem Eur J 10:4198–4205
60. Shintani R, Duan W-L, Okamoto K, Hayashi T (2005) Palladium/chiral phosphine–olefin complexes: X-ray crystallographic analysis and the use in catalytic asymmetric allylic alkylation. Tetrahedron Asym 16:3400–3405
61. Tayama O, Nakano A, Iwahama T, Sakaguchi S, Ishii Y (2004) Hydrophosphorylation of alkenes with dialkyl phosphites catalyzed by Mn(III) under air. J Org Chem 69:5494–5496
62. Beaufils F, Dénès F, Renaud P (2005) Dimethyl phosphite mediated hydrogen atom abstraction: a tin-free procedure for the preparation of cyclopentane derivatives. Angew Chem Int Ed 44:5273–5275
63. Gusarova NK, Sukhov BG, Malysheva SF, Kazantseva TI, Smetannikov YuV, Tarasova NP, Trofimov BA (2001) Reactions of elemental phosphorus and phosphines with electrophiles in superbasic systems: XIII. phosphorylation of phenylacetylene with active modifications of elemental phosphorus. Russ J Gen Chem 71:721–723
64. Malysheva SF, Sukhov BG, Larina LI, Belogorova NA, Gusarova NK, Trofimov BA (2001) Reaction of phenylacetylene with primary phosphines as a convenient way to nonsymmetric tertiary phosphines and their derivatives. Russ J Gen Chem 71:1907–1911
65. Preparation of vinyl organo-phosphorus compounds (1972), US Patent no 3673285. Chem Abstr (1972) 77, no 140290j
66. Han L-B, Tanaka M (1996) Palladium-catalyzed hydrophosphorylation of alkynes via oxidative addition of $HP(O)(OR)_2$. J Am Chem Soc 118:1571–1572
67. Goulioukina NS, Dolgina TM, Beletskaya IP, Henry J-Ch, Lavergne D, Ratovelomanana-Vidal V, Genet J-P (2001) A practical synthetic approach to chiral α-aryl substituted ethylphosphonates. Tetrahedron Asym 12:319–327
68. Gulykina NS, Dolgina TM, Bondarenko GN, Beletskaya IP (2003) Hydrophosphorylation of terminal alkynes catalyzed by palladium. Russ J Org Chem 39:797–807
69. Gulyukina NS, Dolgina TM, Bondarenko GN, Beletskaya IP, Bondarenko NA, Henry JC, Lavergne D, Ratovelomanana-Vidal V, Genet J-P (2002) Synthesis of biologically active 1-arylethylphosphonates. Russ J Org Chem 38:573–587

70. Beletskaya IP, Goulioukina NS, Dolgina TM, Bondarenko GN, Bondarenko NA, Genet J-P (2001) Asymmetric hydrogenation of vinylphosphorus acids. Abstracts of Papers, XXth Int Chugaev Conf on Coordination Chemistry, Rostov-on-Don, 538
71. Allen A Jr, Manke DR, Lin W (2000) Synthesis of functional bisphosphonates via new palladium-catalyzed bis-hydrophosphorylation reactions. Tetrahedron Lett 41:151–154
72. Zhao Ch-Q, Han L-B, Goto M, Tanaka M (2001) Rhodium-catalyzed hydrophosphorylation of terminal alkynes leading to highly selective formation of (*E*)-alkenylphosphonates: complete reversal of regioselectivity to the palladium-catalyzed counterpart. Angew Chem Int Ed 40:1929–1932
73. Han L-B, Zhang C, Yazawa H, Shimada S (2004) Efficient and selective nickel-catalyzed addition of H–P(O) and H–S bonds to alkynes. J Am Chem Soc 126:5080–5081
74. Han L-B, Ono Y, Shimada S (2008) Palladium-catalyzed dehydrogenative cis double phosphorylation of alkynes with H-phosphonate leading to (*Z*)-bisphosphoryl-1-alkenes. J Am Chem Soc 130:2752–2753
75. Han L-B, Ono Y, Yazawa H (2005) Nickel-catalyzed addition of P(O)–H bonds to propargyl alcohols: one-pot generation of phosphinoyl 1,3-butadienes. Org Lett 7:2909–2911
76. Ananikov VP, Khemchyan LL, Beletskaya IP (2009) Celebrating 20 years of SYNLETT—special essay: general procedure for the palladium-catalyzed selective hydrophosphorylation of alkynes. Synlett 2375–2381
77. Han L-B, Mirzaei F, Ch-Q Zhao, Tanaka M (2000) High reactivity of a five-membered cyclic hydrogen phosphonate leading to development of facile palladium-catalyzed hydrophosphorylation of alkenes. J Am Chem Soc 122:5407–5408
78. Shulyupin MO, Franciò G, Beletskaya IP, Leitner W (2005) Regio- and enantioselective catalytic hydrophosphorylation of vinylarenes. Adv Synth Catal 347:667–672
79. Levine AM, Stockland RA, Clark R, Guzei I (2002) Direct observation of P(O)–C bond formation from (N⌒N)PdMe(P(O)(OPh)$_2$) complexes. Rate enhancement of reductive elimination by addition of triarylphosphines. Organometallics 21:3278–3284
80. Barta K, Franciò G, Leitner W, Lloyd-Jones GC, Shepperson IR (2008) A new class of 3′-sulfonyl BINAPHOS ligands: modulation of activity and selectivity in asymmetric palladium-catalysed hydrophosphorylation of styrene. Adv Synth Catal 350:2013–2023
81. Xu Q, Han L-B (2006) Palladium-catalyzed asymmetric hydrophosphorylation of norbornenes. Org Lett 8:2099–2101
82. Reichwein JF, Patel MC, Pagenkopf BL (2001) Rhodium-catalyzed regioselective olefin hydrophosphorylation. Org Lett 3:4303–4306
83. Hirao T, Masunaga T, Yamada N, Ohshiro Y, Agawa T (1982) Palladium-catalyzed new carbon-phosphorus bond formation. Bull Chem Soc Jpn 55:909–913
84. Zhao Ch-Q, Han L-B, Tanaka M (2000) Palladium-catalyzed hydrophosphorylation of allenes leading to regio- and stereoselective formation of allylphosphonates. Organometallics 19:4196–4198
85. Mirzaei F, Han L-B, Tanaka M (2001) Palladium-catalyzed hydrophosphorylation of 1,3-dienes leading to allylphosphonates. Tetrahedron Lett 42:297–299
86. Han L-B, Choi N, Tanaka M (1996) Oxidative addition of HP(O)Ph$_2$ to platinum(0) and palladium(0) complexes and palladium-catalyzed regio- and stereoselective hydrophosphinylation of alkynes. Organometallics 15:3259–3261
87. Han L-B, Hua R, Tanaka M (1998) Phosphinic acid induced reversal of regioselectivity in Pd-catalyzed hydrophosphinylation of alkynes with Ph$_2$P(O)H. Angew Chem Int Ed 37:94–96
88. Han L-B, Zhao Ch-Q, Tanaka M (2001) Rhodium-catalyzed regio- and stereoselective addition of diphenylphosphine oxide to alkynes. J Org Chem 66:5929–5932
89. Hua R, Tanaka M (1998) Ruthenium-catalyzed addition reaction of diphenylphosphinic acid to terminal alkynes: regioselective synthesis of alkenyl diphenylphosphinates. Chem Lett 27:431–432

90. Duraud A, Toffano M, Fiaud J-C (2009) Regioselective metal-catalyzed hydrophosphinylation of alkynes: synthesis of enantiopure α-or β-substituted vinylphosphane oxides. Eur J Org Chem 4400–4403
91. Stockland RA Jr, Lipman AJ, Bawiec JA III, Morrison PE, Guzei IA, Findeis PM, Tamblin JF (2006) Remarkable tolerance of ethynyl steroids to air and water in microwave-assisted hydrophosphinylation: reaction scope and limitations. J Organomet Chem 691:4042–4053
92. Van Rooy S, Cao C, Patrick BO, Lam A, Love JA (2006) Alkyne hydrophosphinylation catalyzed by rhodium pyrazolylborate complexes. Inorg Chim Acta 359:2918–2923
93. Allen A Jr, Ma L, Lin W (2002) Facile synthesis of chelating bisphosphine oxides and bisphosphines via palladium-catalyzed bishydrophosphinylation reactions. Tetrahedron Lett 43:3707–3710
94. Stone JJ, Stockland RA Jr, Reyes JM Jr, Kovach J, Goodman CC, Tillman ES (2005) Microwave-assisted solventless single and double addition of $HP(O)Ph_2$ to alkynes. J Mol Catal A 226:11–21
95. Mizuta T, Miyaji C, Katayama T, Ushio J, Kubo K, Miyoshi K (2009) Bi- and trinuclear complexes of group 4 metal and palladium bridged by $OPPh_2$ groups: synthesis and high catalytic activities in double hydrophosphinylation of 1-octyne. Organometallics 28:539–546
96. Dobashi N, Fuse K, Hoshino T, Kanada J, Kashiwabara T, Kobata C, Nune SK, Tanaka M (2007) Palladium-complex-catalyzed regioselective Markovnikov addition reaction and dehydrogenative double phosphinylation to terminal alkynes with diphenylphosphine oxide. Tetrahedron Lett 48:4669–4673
97. Niu M, Fu H, Jiang Y, Zhao Y (2007) Copper-catalyzed addition of H-phosphine oxides to alkynes forming alkenylphosphine oxides. Chem Commun 272–274
98. Kanada J, Yamashita K, Nune SK, Tanaka M (2009) Pd-catalyzed addition–carbocyclization of α,ω-diynes with $H–P(O)R_2$ compounds. Tetrahedron Lett 50:6196–6199
99. Deprèle S, Montchamp J-L (2002) Palladium-catalyzed hydrophosphinylation of alkenes and alkynes. J Am Chem Soc 124:9386–9387
100. Ribière P, Bravo-Altamirano K, Antczak MI, Hawkins JD, Montchamp J-L (2005) $NiCl_2$-catalyzed hydrophosphinylation. J Org Chem 70:4064–4072
101. Deprèle S, Montchamp J-L (2004) Environmentally benign synthesis of H-phosphinic acids using a water-tolerant, recyclable polymer-supported catalyst. Org Lett 6:3805–3808
102. Bravo-Altamirano K, Abrunhosa-Thomas I, Montchamp J-L (2008) Palladium-catalyzed reactions of hypophosphorus compounds with allenes, dienes, and allylic electrophiles: methodology for the synthesis of allylic *H*-phosphinates. J Org Chem 73:2292–2301
103. Bravo-Altamirano K, Montchamp J-L (2007) A Novel approach to phosphonic acids from hypophosphorus acid. Tetrahedron Lett 48:5755–5759
104. Coudray L, Montchamp J-L (2008) Green, Palladium-catalyzed synthesis of benzylic H-phosphinates from hypophosphorus acid and benzylic alcohols. Eur J Org Chem 4101–4103
105. Han L-B, Zhao C-Q, Onozawa S-Y, Goto M, Tanaka M (2002) Retention of configuration on the oxidative addition of P–H bond to platinum (0) complexes: the first straightforward synthesis of enantiomerically pure P-chiral alkenylphosphinates via palladium-catalyzed stereospecific hydrophosphinylation of alkynes. J Am Chem Soc 124:3842–3843
106. Nune SK, Tanaka M (2007) Palladium-catalysed regioselective addition reaction of ethyl phenylphosphinate with terminal acetylenes: ligand- and solvent-dependent regioselectivity. Chem Commun 2858–2860
107. Wolfsberger W (1985) Chem-Ztg 109:317
108. Wolfsberger W (1988) Chem-Ztg 112:53
109. Wolfsberger W (1988) Chem-Ztg 112:215
110. Nagel U, Rieger B, Bublewitz A (1989) Enantioselektive katalyse: VII. Komplexe von (P(R,S),3R,4R,P′(R,S))-3,4-bis(phenylphosphino)pyrrolidinen. Die darstellung optisch reiner 1,2-bisphosphanliganden mit vier stereozentren, die zusätzliche funktionnelle gruppen enthalten. J Organomet Chem 370:223–239

111. Pringle PG, Smith MB (1990) Platinum(0)-catalysed hydrophosphination of acrylonitrile. J Chem Soc, Chem Commun 1701–1702
112. Costa E, Pringle PG, Smith MB, Worboys K (1997) Self-replication of Tris(cyanoethyl)phosphine catalysed by platinum group metal complexes. J Chem Soc Dalton Trans 4277–4282
113. Orpen AG, Pringle PG, Smith MB, Worboys K (1998) Synthesis and properties of new tris(cyanoethyl)phosphine complexes of platinum (0,II), palladium (0,II), iridium (I) and rhodium (I): conformational analysis of tris(cyanoethyl)phosphine ligands. J Organomet Chem 550:255–266
114. Pringle PG, Brewin D, Smith MB, Worboys K (1995) Aqueous organometallic chemistry and catalysis. In: Horvath IT, Joo F (eds) vol 5. Kluwer, Dordrecht, pp 111–122
115. Costa E, Pringle PG, Worboys K (1998) chemoselective platinum(0)-catalysed hydrophosphination of ethyl acrylate. Chem Commun 49–50
116. Rauhut MM, Currier HA, Semsel AM, Wystrach VP (1961) The free radical addition of phosphines to unsaturated compounds. J Org Chem 26:5138–5145
117. Wicht DK, Kourkine IV, Lew BM, Nthenge JM, Glueck DS (1997) Platinum-catalyzed acrylonitrile hydrophosphination via olefin insertion into a Pt–P bond. J Am Chem Soc 119:5039–5040
118. Wicht DK, Kourkine IV, Kovacik I, Glueck DS, Concolino TE, Yap GPA, Incarvito CD, Rheingold AL (1999) Platinum-catalyzed acrylonitrile hydrophosphination. P–C bond formation via olefin insertion into a Pt–P bond. Organometallics 18:5381–5394
119. Kovacik I, Wicht DK, Grewal NS, Glueck DS, Incarvito CD, Guzei IA, Rheingold AL (2000) Pt(Me-Duphos)-catalyzed asymmetric hydrophosphination of activated olefins: enantioselective synthesis of chiral phosphines. Organometallics 19:950–953
120. Kovacik I, Scriban C, Glueck DS (2006) Regiochemistry of platinum-catalyzed hydrophosphination of a diene. Formation of the chiral diphosphine $Et_2PCH(CN)CH(CH_2CH_2CN)PEt_2$ via monophosphine intermediates. Organometallics 25:536–539
121. Scriban C, Kovacik I, Glueck DS (2005) A Protic Additive suppresses formation of byproducts in platinum-catalyzed hydrophosphination of activated olefins. Evidence for P–C and C–C bond formation by Michael addition. Organometallics 24:4871–4874
122. Scriban C, Glueck DS, Zakharov LN, Kassel WS, DiPasquale AG, Golen JA, Rheingold AL (2006) P–C and C–C bond formation by Michael addition in platinum-catalyzed hydrophosphination and in the stoichiometric reactions of platinum phosphido complexes with activated alkenes. Organometallics 25:5757–5767
123. Scriban C, Glueck DS (2006) Platinum-catalyzed asymmetric alkylation of secondary phosphines: enantioselective synthesis of P-stereogenic phosphines. J Am Chem Soc 128:2788–2789
124. Blank NF, Moncarz JR, Brunker TJ, Scriban C, Anderson BJ, Amir O, Glueck DS, Zakharov LN, Golen JA, Incarvito CD, Rheingold AL (2007) Palladium-catalyzed asymmetric phosphination. scope, mechanism, and origin of enantioselectivity. J Am Chem Soc 129:6847–6858
125. Shulyupin MO, Kazankova MA, Beletskaya IP (2002) Catalytic hydrophosphination of styrenes. Org Lett 4:761–763
126. Nettekoven U, Hartwig JF (2002) A new pathway for hydroamination. mechanism of palladium-catalyzed addition of anilines to vinylarenes. J Am Chem Soc 124:1166–1167
127. Giardello M, King WA, Nolan SP, Porchia M, Sishta C, Marks TJ (1992) Energetics of organometallic species. In: Martinho Simoes JA (ed) Kluwer, Dordrecht, pp 35–51
128. Douglass MR, Marks TJ (2000) Organolanthanide-catalyzed intramolecular hydrophosphination/cyclization of phosphinoalkenes and phosphinoalkynes. J Am Chem Soc 122:1824–1825
129. Douglass MR, Stern ChL, Marks TJ (2001) Intramolecular hydrophosphination/cyclization of phosphinoalkenes and phosphinoalkynes catalyzed by organolanthanides: scope, selectivity, and mechanism. J Am Chem Soc 123:10221–10238
130. Douglass MR, Ogasawara M, Hong S, Metz MV, Marks TJ (2002) "Widening the Roof": synthesis and characterization of new chiral c_1-symmetric octahydrofluorenyl

organolanthanide catalysts and their implementation in the stereoselective cyclizations of aminoalkenes and phosphinoalkenes. Organometallics 21:283–292
131. Crimmin MR, Barrett AGM, Hill MS, Hitchcock PB, Procopiou PA (2007) Calcium-catalyzed intermolecular hydrophosphination. Organometallics 26:2953–2956
132. Sadow AD, Haller I, Fadini L, Togni A (2004) Nickel(II)-catalyzed highly enantioselective hydrophosphination of methacrylonitrile. J Am Chem Soc 126:14704–14705
133. Sadow AD, Togni A (2005) Enantioselective addition of secondary phosphines to methacrylonitrile: catalysis and mechanism. J Am Chem Soc 127:17012–17024
134. Kazankova MA, Efimova IV, Kochetkov AN, Afanas'ev VV, Beletskaya IP, Dixneuf PH (2001) New approach to vinylphosphines based on Pd- and Ni-catalyzed diphenylphosphine addition to alkynes. Synlett 497–500
135. Nagata S, Kawaguchi S-i, Matsumoto M, Kamiya I, Nomoto A, Sonoda M, Ogawa A (2007) A Highly regioselective hydrophosphination of terminal alkynes with tetraphenyldiphosphine in the presence of palladium catalyst. Tetrahedron Lett 48:6637–6640
136. Kawaguchi S-i, Kotani M, Ohe T, Nagata S, Nomoto A, Sonoda M, Ogawa A (2010) Rhodium-catalyzed anti-Markovnikov–type hydrophosphination of terminal alkynes with diphosphines and hydrosilanes in the presence of oxygen. Phosphorus, Sulfur, Silicon 185:1090–1097
137. Takaki K, Takeda M, Koshoji G, Shishido T, Takehira K (2001) Intermolecular hydrophosphination of alkynes and related carbon—carbon multiple bonds catalyzed by ytterbium–imine complexes. Tetrahedron Lett 42:6357–6360
138. Takaki K, Koshoji G, Komeyama K, Takeda M, Shishido T, Kitani A, Takehira K (2003) Intermolecular hydrophosphination of alkynes and related carbon–carbon multiple bonds catalyzed by organoytterbiums. J Org Chem 68:6554–6565
139. Join B, Mimeau D, Delacroix O, Gaumont A-C (2006) Pallado-catalysed hydrophosphination of alkynes: access to enantio-enriched P-stereogenic vinyl phosphine–boranes. Chem Commun 3249–3251
140. Mimeau D, Gaumont A-C (2003) Regio- and Stereoselective hydrophosphination reactions of alkynes with phosphine–boranes: access to stereodefined vinylphosphine derivatives. J Org Chem 68:7016–7022
141. Mimeau D, Delacroix O, Gaumont A-C (2003) Regioselective uncatalysed hydrophosphination of alkenes: a facile route to P-alkylated phosphine derivatives. Chem Commun 2928–2929
142. Pullarkat SA, Yi D, Li Y, Tan G-K, Leung P-H (2006) A novel approach toward asymmetric synthesis of alcohol functionalized C-chiral diphosphines via two-stage hydrophosphination of terminal alkynols. Inorg Chem 45:7455–7463
143. Jérôme F, Monnier F, Lawicka H, Dérien S, Dixneuf PH (2003) Ruthenium catalyzed regioselective hydrophosphination of propargyl alcohols. Chem Commun 696–697
144. Kondoh A, Yorimitsu H, Oshima K (2007) Copper-catalyzed anti-hydrophosphination reaction of 1-alkynylphosphines with diphenylphosphine providing (Z)-1,2-diphosphino-1-alkenes. J Am Chem Soc 129:4099–4104
145. Ohmiya H, Yorimitsu H, Oshima K (2005) Cobalt-catalyzed *syn* hydrophosphination of alkynes. Angew Chem Int Ed 44:2368–2370
146. Patel DV, Rielly-Gauvin K, Ryono DE (1990) Preparation of peptidic α-hydroxy phosphonates a new class of transition state analog renin inhibitors. Tetrahedron Lett 31:5587–5590
147. Patel DV, Rielly-Gauvin K, Ryono DE (1990) Peptidic α-hydroxy phosphinyls C-terminal modification methodology. Tetrahedron Lett 31:5591–5594
148. Sikorski JA, Miller MJ, Braccolino DS, Cleary DG, Corey SD, Font JL, Gruys KJ, Han CY, Lin KC, Pansegrau PD, Ream JE, Schnur D, Shah A, Walker MC (1993) EPSP Synthase: the design and synthesis of bisubstrate inhibitors incorporating novel 3-phosphate mimics. Phosphorus, Sulfur, Silicon Relat Elem 76:115–118

149. Stowasser B, Budt K-H, Jian-Qi L, Peyman A, Ruppert D (1992) New hybrid transition state analog inhibitors of HIV protease with peripheric C_2-symmetry. Tetrahedron Lett 33:6625–6628
150. Moore ML, Dreyer GB (1993) Substrate-based inhibitors of HIV-1 protease. Perspect Drug Discovery Des 1:85–108
151. Hammerschmidt F, Vollenkle H (1989) Justus Liebigs Ann Chem 577
152. Yokomatsu T, Shibuya S (1992) Enantioselective synthesis of α-amino phosphonic acids by an application of stereoselective opening of homochiral dioxane acetals with triethyl phosphite. Tetrahedron Asym 3:377–378
153. Baraldi PG, Guarneri M, Moroder F, Pollini GP, Simoni D (1982) Synthesis of 1-phthalimidoalkanephosphonates. Synthesis 653–655
154. Maier L (1993) Aminooxyalkylphosphonic acids and derivatives. Phosphorus, Sulfur, Silicon Relat Elem 76:119–122
155. Öhler E, Kotzinger S (1993) Thermal rearrangement of trichloroacetimidic esters of allylic α-hydroxyphosphonates: a convenient way to (3-amino-1-alkenyl)phosphonic acids. Synthesis 497–502
156. Kafarski P, Lejczak B (1991) Biological activity of aminophosphonic acids. Phosphorus, Sulfur, Silicon Relat Elem 63:193–215
157. Kametani T, Kigasawa K, Hiiragi M, Wakisaka K, Haga S, Sugi H, Tanigawa K, Suzuki Y, Fukawa K, Irino O, Saita O, Yamabe S (1981) Studies on the synthesis of chemotherpeutics. Part XI. Synthesis and antibacterial activities of phosphonopeptides. Heterocycles 16:1205–1242
158. Atherton FR, Halli MJ, Hassall CH, Lambert RW, Ringrose PS (1979) Phosphonopeptides as antibacterial agents: mechanism of action of alaphosphin. Antimicrob Agents Chemother 15:696–705
159. Allen JG, Atherton FR, Hall MJ, Hassall CH, Holmes SW, Lambert RW, Nisbet LJ, Ringrose PS (1979) Phosphonopeptides as antibacterial agents: alaphosphin and related phosphonopeptides. Antimicrob Agents Chemother 15:684–695
160. Gordon NJ, Evans SA Jr (1993) Studies on the base-promoted enantioselective aldol reaction between an (S,S)-2-oxo-2-propionyl-1,3,2-oxazaphosphorinane and benzaldehyde. Phosphorus, Sulfur, Silicon Relat Elem 75:47–50
161. Li YF, Hammerschmidt F (1993) Enzymes in Organic Chemistry, part 1: enantioselective hydrolysis of α-(acyloxy)phosphonates by esterolytic enzymes. Tetrahedron Asym 4:109–120
162. Wynberg H, Smaardijk AA (1983) asymmetric catalysis in carbon–phosphorus bond formation. Tetrahedron Lett 24:5899–5900
163. Sum V, Davies AJ, Kee TP (1992) New, chiral silylated organophosphorus(III) reagents: syntheses and applications in the asymmetric phosphorylation of aldehydes. J Chem Soc, Chem Commun 1771–1773
164. Jacques J, Leclercq M, Brienne MJ (1981) La Formation de Sels Augmente-t-elle la Fréquence des Dédoublements Spontanés? Tetrahedron 37:1727–1733
165. Heisler A, Rabiller C, Douillard R, Goalou N, Hägele G, Levayer F (1993) Enzyme catalysed resolution of aminophosphonic acids-I—serine and isoserine analogues. Tetrahedron Asym 4:959–960
166. Hoffmann M (1990) Optically active 1-hydroxy-3-methylbutanephosphonic acid and its derivatives. J Prakt Chem 251–255
167. Gordon NJ, Evans SA Jr (1993) Diastereoselective condensation of oxazaphosphites with aliphatic and aromatic aldehydes. J Org Chem 58:5293–5294
168. Gajda T (1994) Enantioselective synthesis of diethyl 1-hydroxyalkylphosphonates via oxazaborolidine catalyzed borane reduction of diethyl α-ketophosphonates. Tetrahedron Asym 5:1965–1972
169. Blazis VJ, Koeller KJ, Spilling CD (1995) Reactions of chiral phosphorus acid diamides: the asymmetric synthesis of chiral alpha-hydroxy phosphonamides, phosphonates, and phosphonic acids. J Org Chem 60:931–940

170. Yokomatsu T, Yamagishi T, Shibuya S (1995) Stereoselective synthesis of γ,δ-unsaturated α-hydroxyphosphonates through [2,3]-Wittig sigmatropic rearrangement of α-allyloxyphosphonates. Synlett 1035–1036
171. Yokomatsu T, Yamagishi T, Shibuya S (1993) Stereodivergent synthesis of β-amino-α-hydroxyphosphonic acid derivatives by Lewis acid mediated stereoselective hydrophosphonylation of α-amino aldehydes. Tetrahedron Asym 4:1401–1404
172. Arai T, Sasai H, Aoe K, Okamura K, Date T, Shibasaki M (1996) A new multifunctional heterobimetallic asymmetric catalyst for Michael additions and tandem Michael–aldol reactions. Angew Chem Int Ed 35:104–106
173. Yokomatsu T, Yamagishi T, Matsumoto K, Shibuya S (1996) Stereocontrolled synthesis of hydroxymethylene phosphonate analogues of phosphorylated tyrosine and their conversion to monofluoromethylene phosphonate analogues. Tetrahedron 52:11725–11738
174. Groaning MD, Rowe BJ, Spilling CD (1998) New homochiral cyclic diol ligands for titanium alkoxide catalyzed phosphonylation of aldehydes. Tetrahedron Lett 39:5485–5488
175. Davies SR, Mitchell MC, Cain CP, Devitt PG, Taylor RJ, Kee TP (1998) Phospho-transfer catalysis: on the asymmetric hydrophosphonylation of aldehydes. J Organomet Chem 550:29–57
176. Duxbury JP, Cawley A, Thornton-Pett M, Wantz L, Warne JND, Greatrex R, Brown D, Kee TP (1999) Chiral aluminium complexes as phospho-transfer catalysts. Tetrahedron Lett 40:4403–4406
177. Ward CV, Jiang M, Kee TP (2000) New chiral catalysts for phospho-transfer. Tetrahedron Lett 41:6181–6184
178. Yokomatsu T, Yamagishi T, Shibuya S (1997) Enantioselective synthesis of α-hydroxyphosphonates through asymmetric Pudovik reactions with chiral lanthanoid and titaniumalkoxides. J Chem Soc Perkin Trans 1:1527–1534
179. Qian C, Huang T, Zhu C, Sun J (1998) Synthesis of 3,3′-,6,6′- and 3,3′,6,6′-substituted binaphthols and their application in the asymmetric hydrophosphonylation of aldehydes—an obvious effect of substituents of BINOL on the enantioselectivity. J Chem Soc Perkin Trans 1:2097–2104
180. Arai T, Bougauchi M, Sasai H, Shibasaki M (1996) Catalytic asymmetric synthesis of α-hydroxy phosphonates using the Al–Li-BINOL complex. J Org Chem 61:2926–2927
181. Shibasaki M, Sasai H, Arai T (1997) Asymmetric catalysis with heterobimetallic compounds. Angew Chem Int Ed 36:1236–1256
182. Rath NP, Spilling CD (1994) The enantioselective addition of dialkylphosphites to aldehydes: catalysis by a lanthanum binaphthoxide complex. Tetrahedron Lett 35:227–230
183. Sasai H, Bougauchi M, Arai T, Shibasaki M (1997) Enantioselective synthesis of α-hydroxy phosphonates using the $LaLi_3$tris(binaphthoxide) catalyst (LLB), prepared by an improved method. Tetrahedron Lett 38:2717–2720
184. Gröger H, Hammer B (2000) Catalytic concepts for the enantioselective synthesis of α-amino and α-hydroxy phosphonates. Chem Eur J 6:943–948
185. Saito B, Katsuki T (2005) Synthesis of an optically active C_1-symmetric Al(salalen) complex and its application to the catalytic hydrophosphonylation of aldehydes. Angew Chem Int Ed 44:4600–4602
186. Saito B, Egami H, Katsuki T (2007) Synthesis of an optically active Al(salalen) complex and its application to catalytic hydrophosphonylation of aldehydes and aldimines. J Am Chem Soc 129:1978–1986
187. Ito K, Tsutsumi H, Setoyama M, Saito B, Katsuki T (2007) Enantioselective hydrophosphonylation of aldehydes using an aluminum binaphthyl Schiff base complex as a catalyst. Synlett 1960–1962
188. Zhou X, Liu X, Yang X, Shang D, Xin J, Feng X (2008) Highly enantioselective hydrophosphonylation of aldehydes catalyzed by tridentate Schiff base aluminum(III) complexes. Angew Chem Int Ed 47:392–394
189. Gou S, Zhou X, Wang J, Liu X, Feng X (2008) Asymmetric hydrophosphonylation of aldehydes catalyzed by bifunctional chiral Al(III) Complexes. Tetrahedron 64:2864–2870

190. Zhou X, Liu Y, Chang L, Zhao J, Shang D, Liu X, Lin L, Feng X (2009) Highly efficient synthesis of quaternary α-hydroxy phosphonates via Lewis acid-catalyzed hydrophosphonylation of ketones. Adv Synth Catal 351:2567–2572
191. Yamagishi T, Yokomatsu T, Suemune K, Shibuya S (1999) Enantioselective synthesis of α-hydroxyphosphinic acid derivatives through hydrophosphinylation of aldehydes catalyzed by Al–Li-BINOL complex. Tetrahedron 55:12125–12136
192. Yamagishi T, Suemune K, Yokomatsu T, Shibuya S (2002) Asymmetric synthesis of *β*-amino-α-hydroxyphosphinic acid derivatives through hydrophosphinylation of α-amino aldehydes. Tetrahedron 58:2577–2583
193. Sasai H, Arai S, Tahara Y, Shibasaki M (1995) Catalytic asymmetric synthesis of alpha-amino phosphonates using lanthanoid-potassium-BINOL complexes. J Org Chem 60:6656–6657
194. European Patent no 877 028 (1998)
195. Gröger H, Saida Y, Sasai H, Yamaguchi K, Martens J, Shibasaki M (1998) A new and highly efficient asymmetric route to cyclic α-amino phosphonates: the first catalytic enantioselective hydrophosphonylation of cyclic imines catalyzed by chiral heterobimetallic lanthanoid complexes. J Am Chem Soc 120:3089–3103
196. Han W, Ofial AR (2009) Iron-catalyzed dehydrogenative phosphonation of *N*,*N*-dimethylanilines. Chem Commun 6023–6025
197. Baslé O, Li C-J (2009) Copper-catalyzed aerobic phosphonation of sp^3C–H bonds. Chem Commun 4124–4126
198. Yamakoshi K, Harwood SJ, Kanai M, Shibasaki M (1999) Catalytic asymmetric addition of diphenylphosphine oxide to cyclic imines. Tetrahedron Lett 40:2565–2568
199. Hoye PAT, Pringle PG, Smith MB, Worboys K (1993) Hydrophosphination of formaldehyde catalysed by tris-(hydroxymethyl)phosphine complexes of platinum, palladium or nickel. J Chem Soc Dalton Trans 269–274
200. Ellis JW, Harrison KN, Hoye PAT, Orpen AG, Pringle PG, Smith MB (1992) Water-soluble tris(hydroxymethyl)phosphine complexes with nickel, palladium, and platinum. Crystal structure of $[Pd\{P(CH_2OH)_3\}_4].CH_3OH$. Inorg Chem 31:3026–3033
201. Harrison KN, Hoye PAT, Orpen AG, Pringle PG, Smith MB (1989) Water soluble, zero-valent, platinum–, palladium–, and nickel–$P(CH_2OH)_3$ complexes: catalysts for the addition of PH_3 to CH_2O. J Chem Soc Chem Commun 1096–1097
202. Bourumeau K, Gaumont A-C, Denis J-M (1997) P–H bond activation of primary phosphine-boranes: access to α-hydroxy and α,α′-dihydroxyphosphine-borane adducts by uncatalyzed hydrophosphination of carbonyl derivatives. J Organomet Chem 529:205–213
203. Bar-Nir BB-A, Portnoy M (2000) Addition of borane-protected secondary phosphines to imines. A route to protected mono-*N*-substituted-α-aminophosphines. Tetrahedron Lett 41:6143–6147
204. Hashimoto T, Maeta H, Matsumoto T, Morooka M, Ohba S, Suzuki K (1992) Synthesis of 1,3-Bis(diphenylphosphinoyl)alkanes via double addition of diphenylphosphine to α,*β*-unsaturated carbonyl compounds: sequential 1,4- and 1,2-addition promoted by $NbCl_5$-$BF_3{\cdot}OEt_2$. Synlett 340–342
205. Carlone A, Bartoli G, Bosco M, Sambri L, Melchiorre P (2007) Organocatalytic asymmetric hydrophosphination of α,*β*-unsaturated aldehydes. Angew Chem Int Ed 46:4504–4506
206. Joly GD, Jacobsen EN (2004) Thiourea-catalyzed enantioselective hydrophosphonylation of imines: practical access to enantiomerically enriched α-amino phosphonic acids. J Am Chem Soc 126:4102–4103
207. Akiyama T, Morita H, Itoh J, Fuchibe K (2005) Chiral Brønsted acid catalyzed enantioselective hydrophosphonylation of imines:asymmetric synthesis of α-amino phosphonates. Org Lett 7:2583–2585
208. Pettersen D, Marcolini M, Bernardi L, Fini F, Herrera RP, Sgarzani V, Ricci A (2006) Direct access to enantiomerically enriched α-amino phosphonic acid derivatives by organocatalytic asymmetric hydrophosphonylation of imines. J Org Chem 71:6269–6272

Chapter 9
Phosphorus-Containing Dendrimers: Uses as Catalysts, for Materials, and in Biology

Anne-Marie Caminade and Jean-Pierre Majoral

Abstract Dendrimers are macromolecules elaborated step by step, and constituted of branching units emanating radially from a central core. Phosphorus-containing dendrimers constitute a special class of dendrimers having one phosphorus atom at each branching point. They possess numerous properties, depending mainly on the type of their terminal groups. With organometallic complexes as terminal functions, these dendrimers are able to catalyze various types of reactions, in various media including water, with good enantioselectivities, easy recycling of the dendritic catalyst, and excellent catalytic efficiencies in many cases. Phosphorus-containing dendrimers were also used for the elaboration of materials incorporating the dendrimers in their structure, and for modifying the properties of the surface of the materials at the nanometric scale. Very sensitive DNA chips were elaborated in this way. Phosphorus-containing dendrimers have also important biological properties. Among them, the activation of the human immune system, in particular with the specific and unprecedented multiplication of some immune cells is certainly the most promising.

A.-M. Caminade (✉) · J.-P. Majoral
Laboratoire de Chimie de Coordination du CNRS, 205 route de Narbonne, 31077 Toulouse Cedex 4, France
e-mail: caminade@lcc-toulouse.fr

J.-P. Majoral
e-mail: majoral@lcc-toulouse.fr

A.-M. Caminade · J.-P. Majoral
Université de Toulouse, UPS, INP, LCC, 31077 Toulouse, France

M. Peruzzini and L. Gonsalvi (eds.), *Phosphorus Compounds*, Catalysis by Metal Complexes, 37, DOI: 10.1007/978-90-481-3817-3_9,
© Springer Science+Business Media B.V. 2011

9.1 Introduction

Dendrimers [1–3] constitute one of the most important contributions of chemistry to the field of nanosciences, with more than 1,200 publications and 300 patents per year since 4 years. Indeed, after being attractive for their aesthetic structure constituted of branching units emanating radially from a central core, a number of potential applications have now emerged, in particular as catalysts, for the elaboration of nanomaterials, and even in the field of nanomedicine. These very special types of polymers, hyperbranched and multifunctional, are elaborated step by step (generation after generation) from a central core, and not by polymerization reactions. Figure 9.1 illustrates first the most widely used type of synthesis of dendrimers that is a divergent process from the core to the periphery. The convergent process, which consists in the association of dendrons (dendritic wedges) by their core, is less frequently used. In the divergent process, the generations are created by reaction of an increasing number of small molecules with the dendrimer of the previous generation; each generation is isolated. Due to this highly controlled synthesis, dendrimers offer a perfect modularity of size (a few nanometers), functionality, and solubility, mainly depending on the type of their terminal groups.

Among all types of dendrimers, phosphorus-containing dendrimers [4] that are dendrimers having one phosphorus atom at each branching point play more and more an important role. In this chapter, we will focus on their use as catalysts, for materials, and in biology. Besides our own work, a few other groups have reported the synthesis of phosphorus-containing dendrimers. We can mentioned in particular the first example of any type of phosphorus dendrimers (poly(phosphonium)

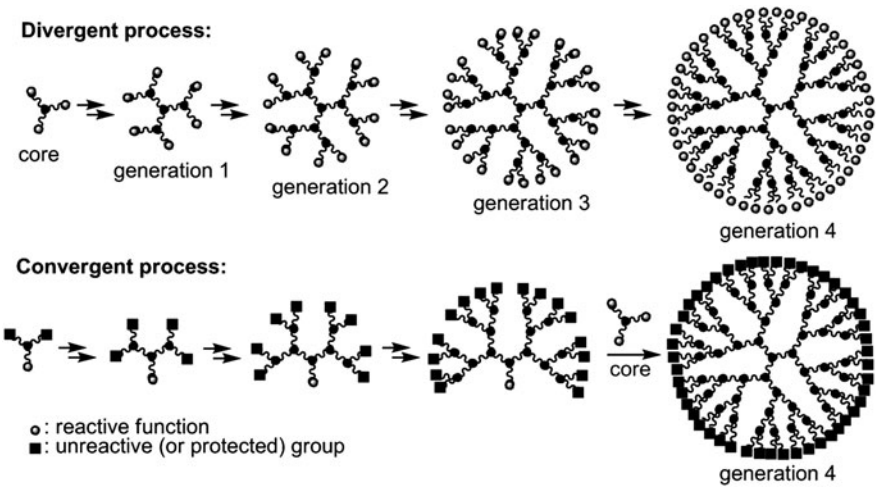


Fig. 9.1 Illustration of the divergent and convergent processes, both usable for the synthesis of dendrimers

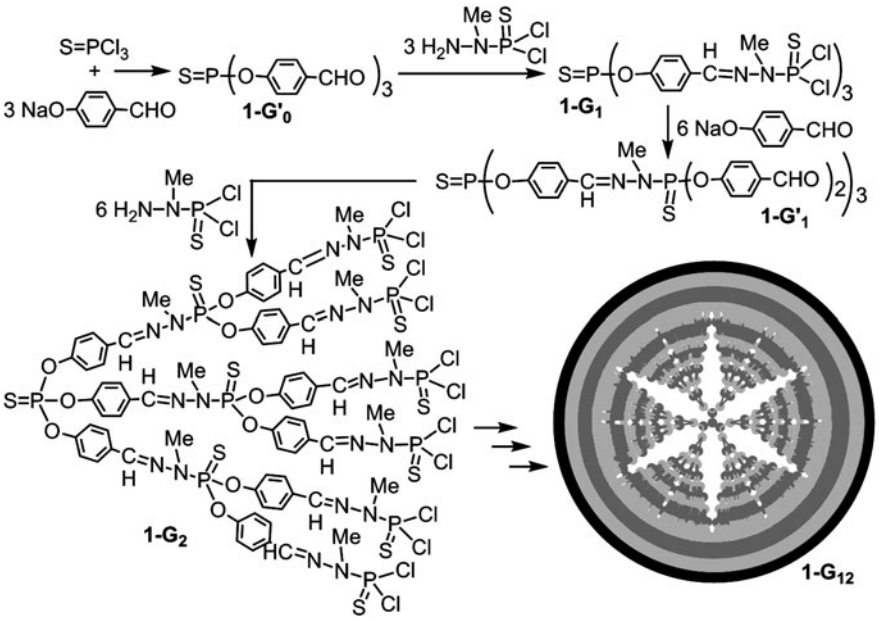


Fig. 9.2 The most widely used method of synthesis of phosphorus dendrimers, applied here to the trifunctional core $P(S)Cl_3$, and up to the twelfth generation **1-G$_{12}$**

dendrimers) reported by Engel [5], small poly(phosphine) dendrimers reported by DuBois [6], and larger ones by Kakkar [7], poly(phosphate) dendrimers developed by Damha [8] in a convergent process, and by Roy [9] and Salamonczyck [10] in divergent processes. However, the most generally used method of synthesis of phosphorus-dendrimers is the one we described in 1994 [11]. It consists in applying a two-step reiterative process using successively 4-hydroxybenzaldehyde in basic conditions and $H_2NNMeP(S)Cl_2$ (Fig. 9.2). Both steps generate only NaCl and H_2O as by-products and are quantitative. This process was first carried out up to the fourth generation [11], then to the seventh generation [12], the ninth [13], and finally to the twelfth generation [14], starting from the trifunctional core $P(S)Cl_3$. This twelfth generation is the highest generation well characterized obtained up to now for any type of dendrimers (**1-G$_{12}$**). It is also the highest generation obtainable from a practical point of view (the twelfth generation is the last one soluble) and from a theoretical point of view (De Gennes dense packing [15]), due to the fact that the number of end groups increases more rapidly than the free space available for them for high generations, preventing full substitution after the dense packing limit.

This two-step method of synthesis can be applied to a large number of different cores, provide they possess either several PCl_2 or CHO functional groups. In particular this reaction was carried out from the hexafunctional cyclotriphosphazene core ($N_3P_3Cl_6$), and up to eighth generation **2-G$_8$′** (Fig. 9.3) [16]. This is presumably not the highest generation obtainable from this core. This core allows

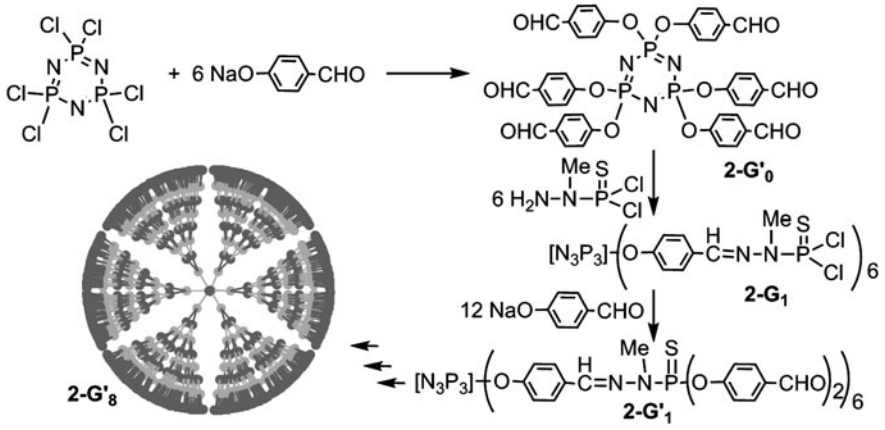


Fig. 9.3 The same method of synthesis as in Fig. 9.2, but applied to the cyclotriphosphazene core

doubling the number of terminal groups at a given generation, when compared to the trifunctional core. For instance, **1-G$_2$** and **2-G$_1$** have the same number of Cl, but have not the same generation number. This method of synthesis of phosphorus dendrimers allows different modifications at all levels, the core [17, 18], the branches [19–23], and even the general shape of the structure [24–26].

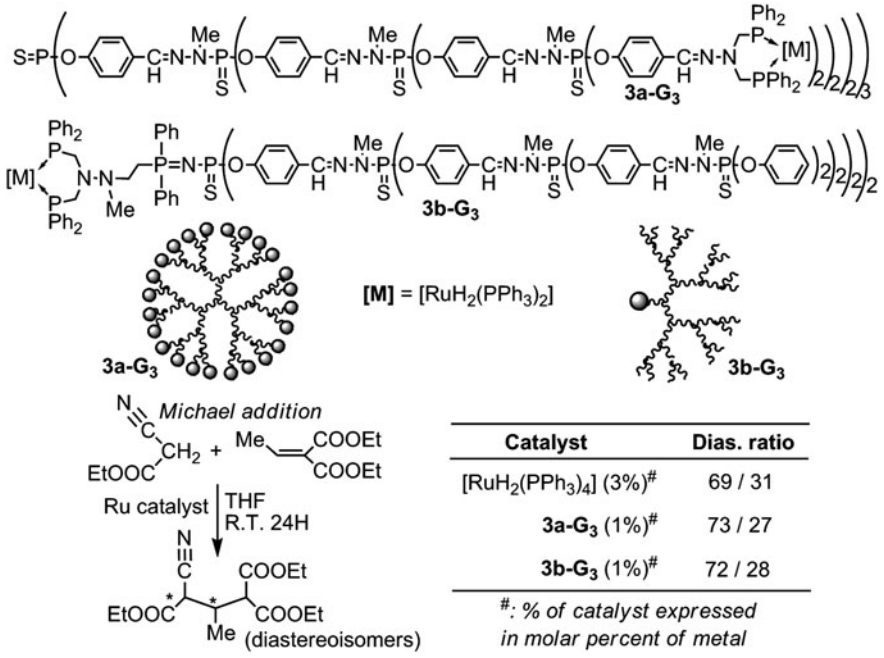
The terminal groups of these dendrimers are either aldehydes or P(S)Cl$_2$, which are among the most versatile and reactive functions in organic chemistry and phosphorus chemistry, respectively. The type of terminal functions is the main determinant for modifying the properties of dendrimers. In the next paragraphs, we will see how, by modifying the terminal groups of dendrimers **1-G$_n$'** and **2-G$_n$'** they become usable as catalysts, for creating or modifying (nano)materials, and for diverse biological purposes.

9.2 Catalysis

Catalysis remains a highly active research area in both academia and industry, despite more than one century of industrial uses of catalysts. Molecular catalysis research is directed towards the discovery or optimization of catalysts that have improved efficiencies, higher enantioselectivities and longer lifetimes, tolerance of air and moisture, and/or easier separation, recovery and recycling. The use of dendrimers as catalysts was recognized very early, with the aim of combining both the advantages of homogeneous catalysts (solubility) and heterogeneous catalysts (easy recovery). Dendritic catalysts have generated a large interest, as emphasized by numerous reviews [27–33]. The first example dates back to 1994, using organic dendrimers [34]. The first example with phosphorus dendrimers concerned the palladium complexes of small polyphosphines, used for the electrocatalyzed reduction of CO_2 to CO [6]. The rhodium complexes of larger polyphosphines are

efficient catalysts for olefin hydrogenation, in a 1:200 metal-to-substrate ratio [7]. We have synthesized early in 1995 organometallic complexes of our phosphorus dendrimers, by grafting phosphines as terminal groups [13], and developed numerous examples of organometallic chemistry with dendrimers [35], but our first report about their use as catalysts dates back to 2000 [36]. It must be emphasized that in all cases of catalysis that will be described now the molar percentage of catalyst is the molar percentage of metal (not of dendrimer), with one metal per ligating site on the dendrimer. In this way it is possible to compare directly the efficiency of a monomer with that of any generation of dendrimer.

In our first example of catalysis, we wanted to compare the catalytic efficiency depending on the location of the catalytic site(s). Amino diphosphine ligands were grafted either at the surface of dendrimers or at the core of dendrons. The $RuH_2(PPh_3)_2$ complex **3a-G$_3$** was used for Knoevenagel condensations and diastereoselective Michael additions, and compared to the dendron **3b-G$_3$** having one $RuH_2(PPh_3)_2$ complex at the core. No difference in the diastereoselectivity was observed between the dendrimer, the dendron, and the monomer (Fig. 9.4). The $PdCl_2$ complex of the third generation dendrimer shown in Fig. 9.4 was used as catalyst in Stille couplings. In all these cases, it was possible to recover and reuse twice the dendritic catalyst, without any significant loss of activity in marked contrast with the behavior of the corresponding monomer [36].



Catalyst	Dias. ratio
$[RuH_2(PPh_3)_4]$ (3%)#	69 / 31
3a-G$_3$ (1%)#	73 / 27
3b-G$_3$ (1%)#	72 / 28

#: % of catalyst expressed in molar percent of metal

Fig. 9.4 Influence of the location of catalytic site(s) on Michael additions

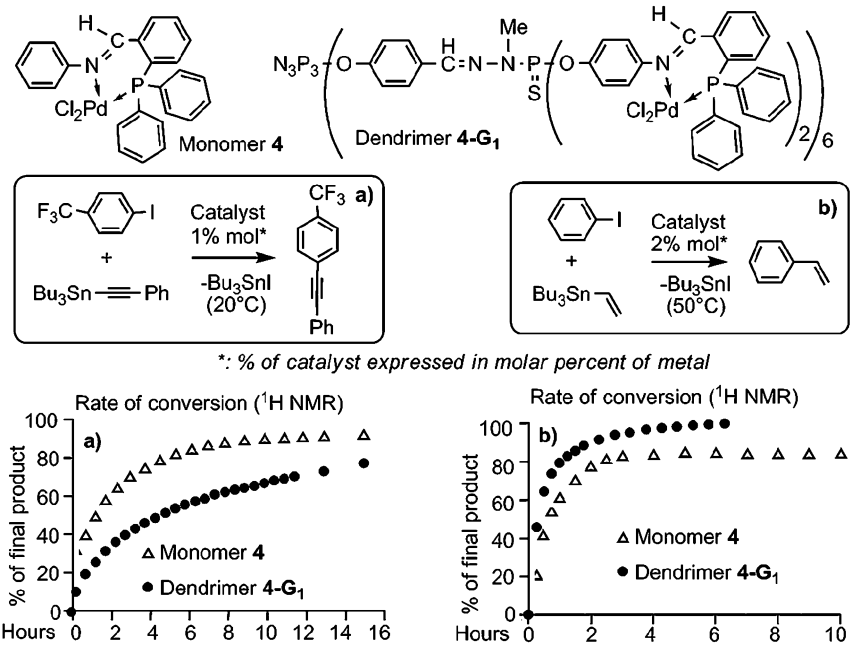


Fig. 9.5 Monomer **4** versus generation 1 dendrimer **4-G$_1$** for catalyzing Stille couplings. Either the dendrimer or the monomer are the most efficient, depending on the reagents used

As shown above, the activity measured for the dendrimers was comparable or slightly higher than that of the monomers in many cases, but no general rules can be deduced concerning the efficiency of a dendritic catalyst. We have synthesized complexed iminophosphine derivatives, such as the monomeric palladium complex **4** and the first generation dendrimer **4-G$_1$**. Comparison of their efficiency for various Stille couplings was really puzzling (Fig. 9.5). Measurements of the rate of conversion by ^{1}H NMR show that in some cases the monomer is more efficient than the dendrimer, in other cases they have the same efficiency, and in still other cases the dendrimer is more efficient. However, the real difference between the monomer **4** and the dendrimer **4-G$_1$** is that the latter can be recovered and reused, but not the former [37].

The influence of the generation on the catalytic efficiency is also interesting to study. Indeed, the closer proximity of the catalytic sites when the generation increases may have a detrimental influence due to problems of steric hindrance, or a positive dendritic effect due to a synergy between two or more catalytic sites, or more generally no influence. We have reported one of the most positive dendritic effects known to date for organometallic derivatives; it concerned the coupling of pyrazole to phenyl iodide or bromide, catalyzed by the copper complexes of pyridineimine-ended phosphorus dendrimers. Copper is a cheap and practically non toxic metal, which is a very attractive alternative to transition metals. However, the monomer **5** is totally inefficient to catalyze this reaction, starting from either iodo-

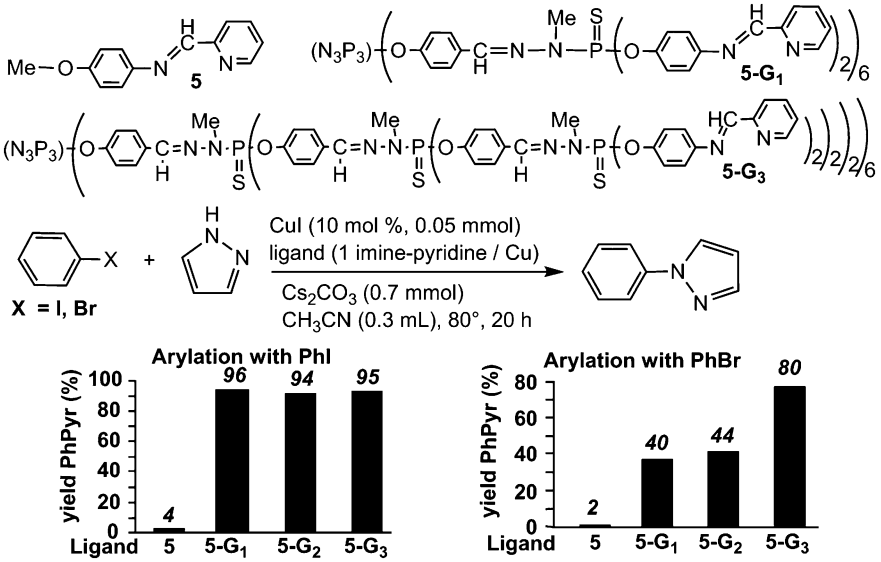


Fig. 9.6 Positive dendritic effect for the catalyzed coupling of pyrazole with copper(I) dendritic complexes **5**-$\mathbf{G_n}$, and monomer **5**

or bromo-benzene. In sharp contrast, dendrimers **5**-$\mathbf{G_n}$ enabled the quantitative conversion of substrate into product within 20 h at 80 °C when starting from iodobenzene. When starting from less reactive bromobenzene, the best catalytic activity was obtained in the presence of the third generation dendritic ligand **5**-$\mathbf{G_3}$, phenylpyrazole being obtained in 80% yield after 20 h at 80 °C (Fig. 9.6). We have also demonstrated specific advantages for copper(I) catalysis of the O- and N-arylation and vinylation of phenol and pyrazole using these copper dendritic complexes, with the highest yields under the mildest conditions known [38].

Very recently, we have reported another largely positive dendritic effect, by grafting the water soluble PTA ligand (1,3,5-triaza-7-phosphaadamantane) as terminal groups of generations 1–3. Their ruthenium complexes (compounds **6**-$\mathbf{G_n}$) were used as catalysts in aqueous media for two types of experiments. A slightly positive dendritic effect on the regioselectivity was observed for hydration of alkynes, and a large positive dendritic effect was observed in the biphasic (water/heptane) catalyzed isomerisation of allylic alcohols to ketones (from 38% of conversion with the monomer **6**, 63% with the first generation dendrimer **6**-$\mathbf{G_1}$, to 98% with the third generation **6**-$\mathbf{G_3}$) strictly in the same conditions. The products were easily isolated and the catalyst could be reused several times, even the first generation **6**-$\mathbf{G_1}$ (Fig. 9.7) [39]. We have also demonstrated that the presence of large amounts of water is fully compatible with various cross-coupling reactions, such as Suzuki, Sonogashira, and Heck reactions catalyzed by palladium complexes of diphosphino terminal groups of dendrimers [40].

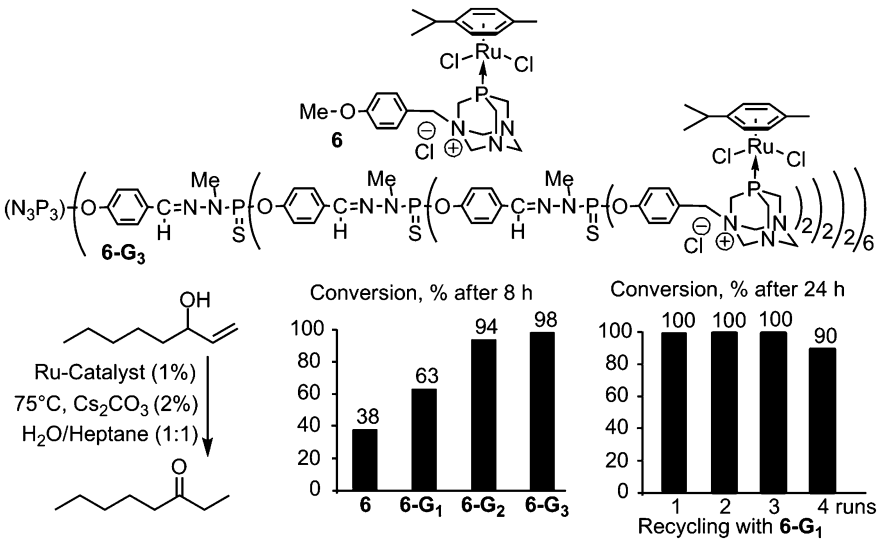


Fig. 9.7 Positive role of the generation and recycling in aqueous media for alcohol isomerisation

An essential component of researches about catalysis in general concerns asymmetric catalysis, which has led to breakthroughs, not only in laboratories but also in industry, particularly in the manufacture of pharmaceuticals and agrochemicals. Thus it appeared tempting to use dendritic complexes for enantioselective catalyses [41]. These experiments necessitate the grafting of chiral entities as terminal groups of dendrimers. In a first example, we have used an iminophosphine derived from (2S)-2-amino-1-(diphenylphosphinyl)-3-methylbutane which was complexed in situ by $[Pd(\eta^3\text{-}C_3H_5)Cl]_2$. This catalyst was used in asymmetric allylic alkylations of *rac*-(E)-diphenyl-2-propenyl acetate and pivalate. The percentage of conversion, the yield of isolated 2-(1,3-diphenylallyl)-malonic acid dimethyl ester, and its enantiomeric excess were found good to very good (ee from 90 to 95%). Furthermore, the dendritic catalyst **7a-G$_3$** can be recovered and reused at least two times, with almost the same efficiency [42] (Fig. 9.8). Chiral (S)-2-diphenylphosphino-(4-hydroxyphenylthiomethyl) ferrocene ligands have been covalently bound on the periphery of phosphorus dendrimers (**7b-G$_n$**, n = 0–4) having a cyclotriphosphazene core. These new dendrimers proved to be efficient ligands for the same palladium-catalyzed asymmetric allylic substitution reaction (ee up to 93%) [43] (Fig. 9.8).

In another example, dendrimers ended by bisoxazoline ligands attached via "click" reactions were used for copper catalyzed asymmetric benzoylations, starting from two different diols. Dendrimers **8-G$_1$** and **8-G$_2$** afford good yields and enantioselectivities in both cases, whereas the third generation has a detrimental influence on the enantioselectivity. The copper(II)-catalysts could be readily recovered and reused in several cycles (Fig. 9.9) [44].

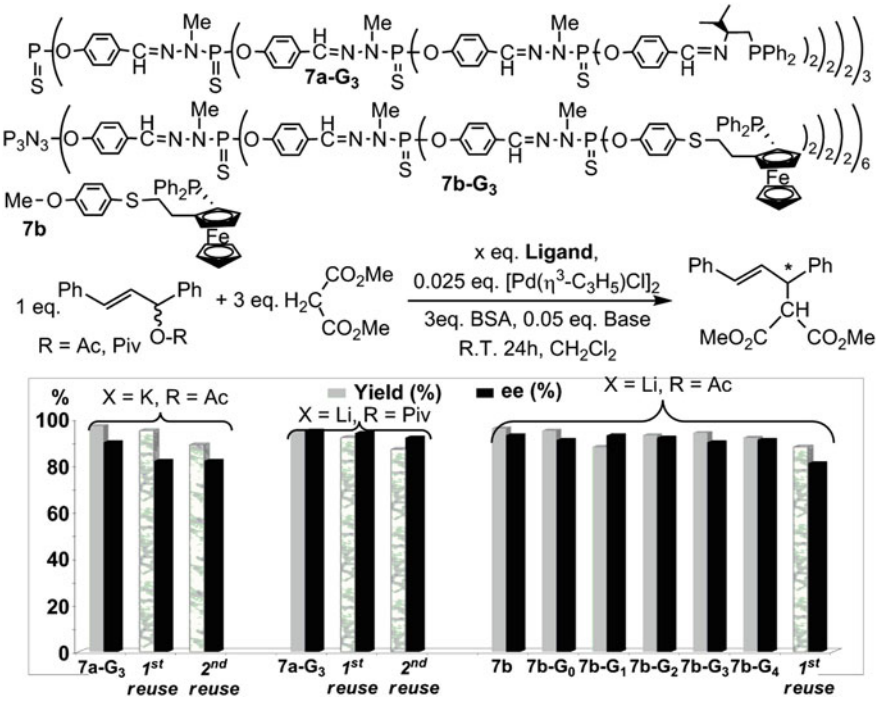


Fig. 9.8 Enantioselective allylic alkylation using two types of chiral phosphino dendritic ligands

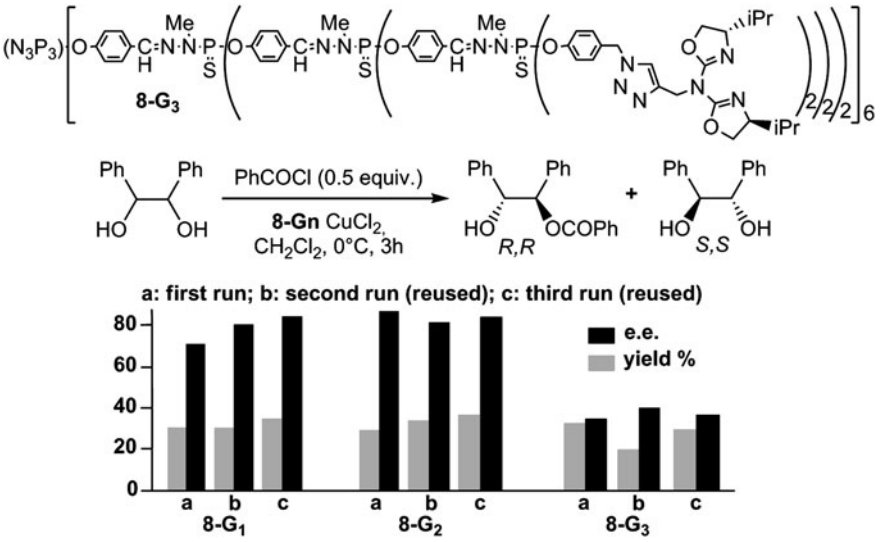


Fig. 9.9 Cu(II) dendritic complexes **8-G$_n$** and their reuse for catalyzed asymmetric benzoylations

9.3 Materials

The development of nanomaterials is one of the main challenges for the development of future technologies. In this perspective, nanosized molecules are attracting a considerable attention, particularly dendrimers [45]. They can be used for the elaboration of new materials including dendrimers in their structure, or for the modification of the surface of materials at the nanometric scale [46]. They are also particularly useful for the elaboration and stabilization of metallic nanoparticles.

9.3.1 Elaboration and Stabilization of Nanoparticles

A particular case concerns the stabilization of metal clusters by suitable ligands to make them isolable compounds, but the presence of this ligand shell modify the electronic properties; thus obtaining and organizing bare clusters appears highly desirable, but also highly challenging. The Au_{55} cluster is in particular very attractive for nanoelectronic devices, but numerous previous attempts to generate it failed and gave only crystals of Au_{13}. In sharp contrast, dendrimers **9-Gn** possessing thiol terminal groups were able to peel off the PPh_3 ligands and the chlorine of $Au_{55}(PPh_3)_{12}Cl_6$, while keeping the Au_{55} structure. It induced also the organization of the bare Au_{55}, which coalesced in nanocrystals of $(Au_{55})\infty$, the dendrimer acting as template for crystallization. The best results were obtained with the fourth generation **9-G_4** (Fig. 9.10) [47]. The same phenomenon was observed later on when the same dendrimer was deposited as thin layer on a silicon surface. Interaction of these dendrimer films with solutions of $Au_{55}(PPh_3)_{12}Cl_6$ also produced nanocrystals of $(Au_{55})\infty$ [48].

Phosphorus dendrimers containing on their surfaces 15-membered azamacrocycles were synthesized (dendrimers **10a**,**b**-G_0, **10b**-G_1, **10b**-G_4) for the elaboration of palladium(0) nanoparticles. Depending mainly on the amount of Pd(0)

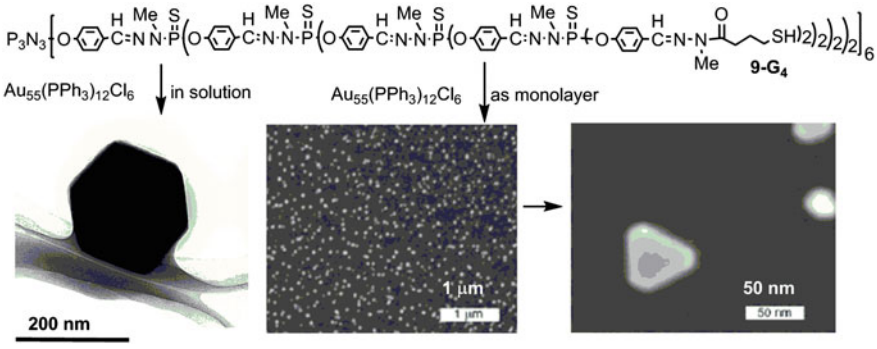


Fig. 9.10 Organization of Au_{55} clusters as nanocrystals induced by the dendrimer **9-G_4**

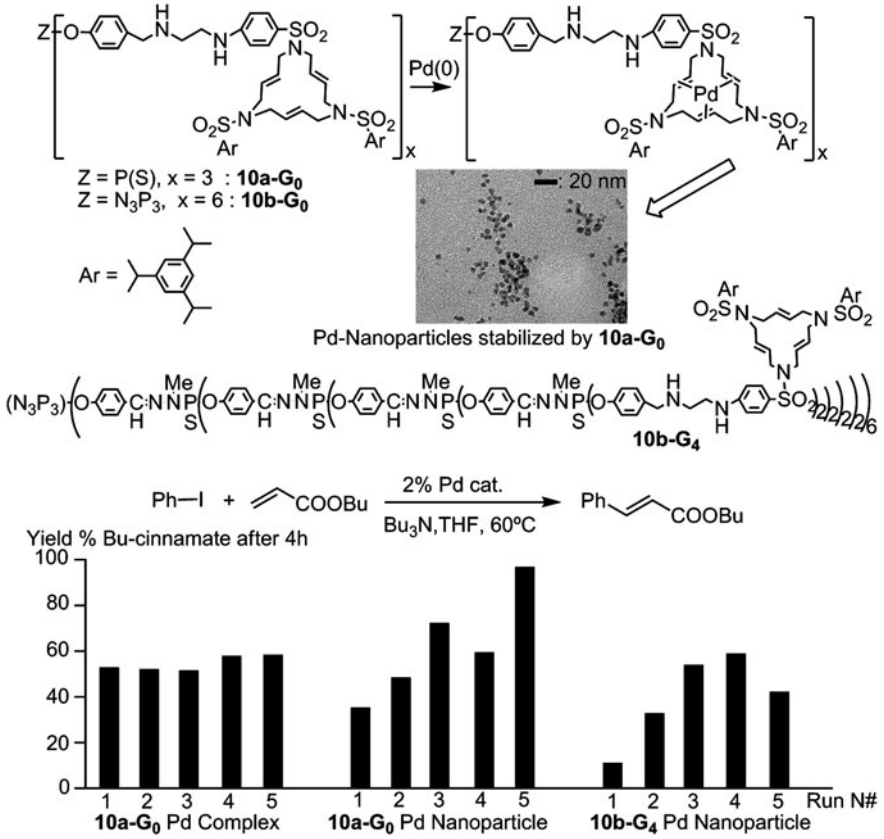


Fig. 9.11 Pd nanoparticles generated by dendrimers **10**-$\mathbf{G_n}$ and used in Mizoroki–Heck reactions

used, either discrete complexes or nanoparticulated materials were obtained. No reduction process of palladium(II) salts was needed to prepare nanoparticles of 2.5–7.9 nm diameter. These complexes and nanoparticles were used for the Mizoroki–Heck reaction; in all cases, the catalyst could be recovered and reused several times. The Pd-complex of **10a**-$\mathbf{G_0}$ displays constant catalytic activity with recycling, whereas the Pd-nanoparticles stabilized with **10a**-$\mathbf{G_0}$ displays an increasing catalytic efficiency with recycling, which could be related to a decrease in the nanoparticles size, observed by electron microscopy (Fig. 9.11) [49].

Very recently, we have used another type of dendrimer (**11**-$\mathbf{G_n}$) [50] ended by macrocycles closely related to **10b**-$\mathbf{G_n}$, for performing also two different organizational roles. When interacting with $Pt(dba)_3$, these dendrimers first induce the formation of Pt(0) nanoparticles, then organize them in hyperbranched networks of coalesced Pt-nanoparticles, intertwined with dendrimers. Surprisingly, both the size and the degree of branching of these networks vary with the generation of the dendrimer. The largest networks were obtained with **11**-$\mathbf{G_4}$ (Fig. 9.12) [51].

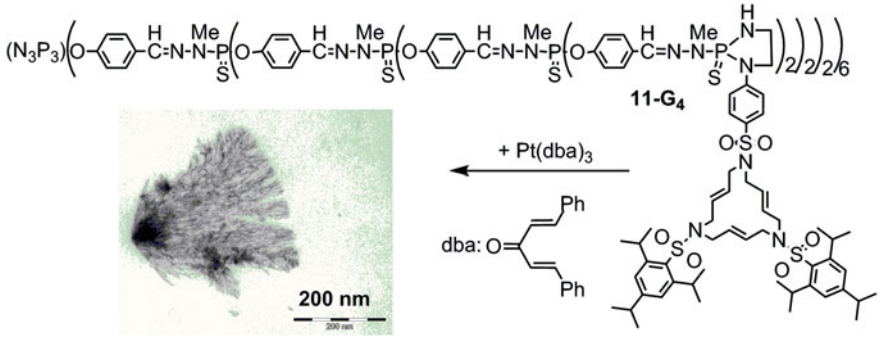


Fig. 9.12 Pt nanoparticles networks induced by the dendrimers **11-G$_n$**

9.3.2 Dendrimers Inside Materials

Silica is a versatile material that can be easily functionalized; phosphorus dendrimers are usable for this purpose. The concomitant use of the positively charged dendrimers **12-G$_n$** or **13-G$_n$** (up to generation 8), with cationic surfactants (Cetyltrimethylammonium bromide (CTAB)) and sodium silicate in water allowed the synthesis of mesostructured nanoporous silica including dendrimers. A relatively important amount of dendrimers (up to 26% in weight) can be incorporated into hexagonal silica phases during the structuring process. In these conditions, the inclusion of dendrimers modified neither the honeycomb structure characteristic of the MCM-41 phase, nor its narrow pore size distribution of about 25 Å and its specific surface (Fig. 9.13, left image). These hybrid nanocomposites possess original properties, in particular the unprecedented possibility to selectively remove the surfactant while keeping the dendrimer inside the material. Furthermore, all the dendrimers, and particularly their end groups are fully accessible [52].

In another approach, dendrons of type **14-G$_3$** functionalized by $Si(OEt)_3$ at their core were covalently grafted inside silica. The cohydrolysis and polycondensation of these dendrons with a defined and varying number of equivalents of tetraethoxysilane (TEOS) was carried out via sol–gel protocol, giving rise to dendron-silica xerogels. The texture (porosity) of materials was determined by BET (Brunauer, Emmett and Teller) measurements. A narrow pore size distribution was obtained in several cases (Fig. 9.13, right image). As the type of terminal groups of the dendrons can be easily varied, this process allowed the synthesis of numerous types of functionalized silica (the R substituents of these dendrons are phosphines, dyes, nitriles, or amines) [53].

Besides silica, less classical periodic hybrid organic–inorganic materials with hierarchical structures and complex forms were obtained using as nanobuilding blocks first generation dendrimers and the structurally well-defined Ti-organo-oxo cluster $Ti_{16}O_{16}(OEt)_{32}$. The hybrid interface is created by trans alcoholysis in the case of the alcohol terminal groups, and by bridging carboxylates in the case of

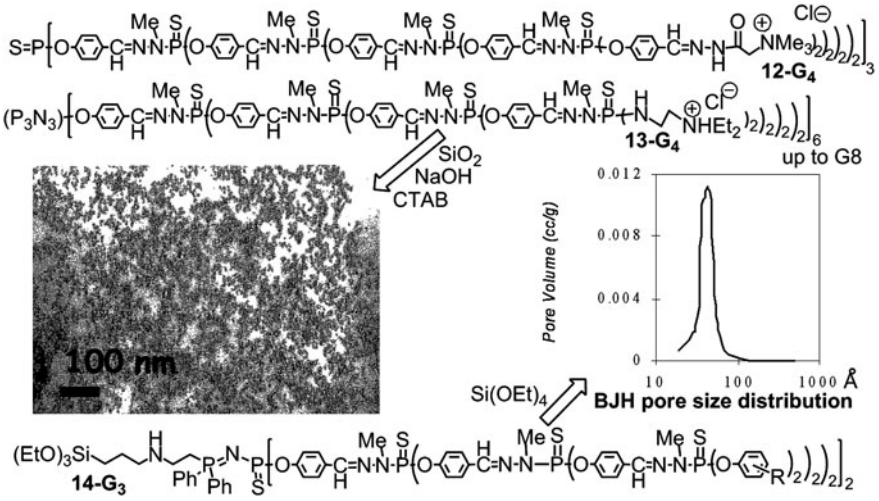


Fig. 9.13 Dendrimers and dendrons used for the elaboration of functionalized silica

acidic terminal groups. In both cases a bicontinuous hybrid gel in which the titanium clusters are regularly spaced by the dendrimers was obtained [54]. Other types of materials were obtained by using metal alkoxides ($Ce(O\text{-}iPr)_4$, $Ti(OR)_4$) as inorganic precursors and acid functionalized dendrimers as organic templates. Chelation by COOH terminal groups was used to control the reactivity of the metal oxide precursors, creating at the same time anchoring points for the nucleation of a gel phase. The bicontinuous gels resulting after solvent evaporation present a "sponge-like" structure with pore size ranging from 10 to 30 nm [55].

A more surprising type of gels was observed with some positively charged dendrimers and water. Solid hydrogels were obtained with dendrimers **15-G_n**, even when using amounts of dendrimers as small as 0.25% in weight in water; the gels are solid at room temperature though they contain 99.75% of water. During the gelation process, large amounts of various types of hydrosoluble substances (for instance up to 30% in weight of nickel acetate) can be incorporated (Fig. 9.14). About 1,200 - 1,400 molecules of water per terminal pyridinium unit were jellified, regardless of the generation considered [56]. The same jellification phenomenon was observed with nanolatexes coated with dendrons possessing the same types of terminal groups [57]. Dendrimers **15-G_n** were also used for obtaining macroscopic fibers, from a concentrated solution (10% in weight) of dendrimer in water (Fig. 9.14). The dendrimer solution in the syringe was continuously injected into a 40-cm-long cell containing a flocculating solution (10 wt% $La(NO_3)_3$ in water). Mechanical measurements showed that dendrimer fibers exhibit an elastic behavior (reversible deformation of 3%, same order of magnitude than nylon and cotton fibers), followed by the rupture of the fiber above 9 GPa, whereas typical polymer fibers exhibit an irreversible deformation before rupture [58].

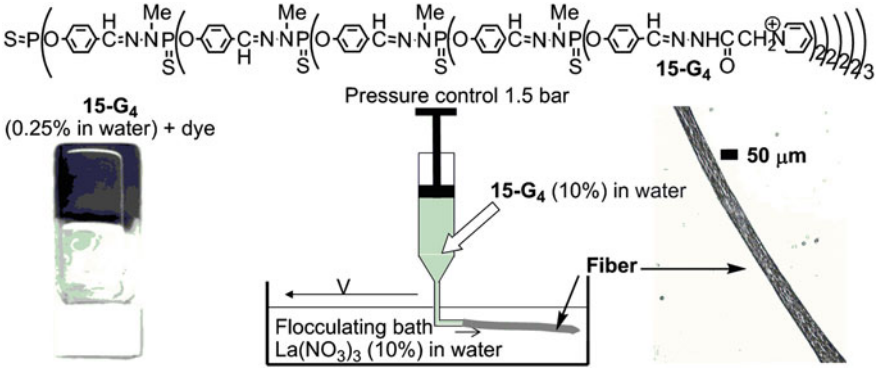


Fig. 9.14 Hydrogels and fibers obtained from pyridinium-ended dendrimers **15-G$_n$**

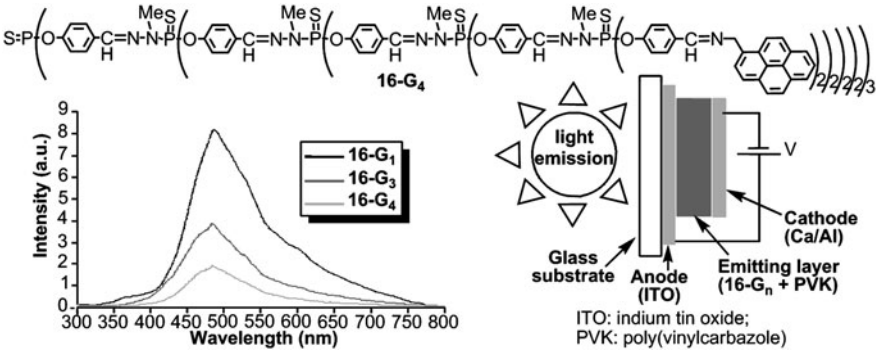


Fig. 9.15 OLEDs elaborated from the fluorescent dendrimers **16-G$_n$**. The fluorescence intensity is in arbitrary units, and cannot be compared within generations

We have synthesized the series of fluorescent dendrimers **16-G$_n$** ($n = 1$–4) bearing pyrene derivatives as terminal groups. The fluorescence measured after excitation at 250 nm displays a single emission band in the blue at 484 nm for all dendrimers **16-G$_n$**. This very broad band corresponds to the emission of excimers of pyrene. No emission of monomeric pyrene could be detected, in accordance with our previous experiments concerning pyrene derivatives included within the interior of dendrimers [59]. Other examples of fluorescent dendrimers will be shown later in the biological section, but this series of compounds **16-G$_n$** was incorporated into poly(vinylcarbazole) (PVK), and used for the elaboration of organic light emitting diodes (OLEDs). The dendrimers incorporated in PVK constitute the emitting (electroluminescent) layer, as shown in Fig. 9.15 [60].

9.3.3 Dendrimers for Modifying the Surface of Materials

Another important field of research in materials chemistry consists in modifying the surface of an existing material by the deposition of organic thin films. Various techniques were already applied using phosphorus dendrimers; for instance, modified electrodes could be obtained using dendrimers possessing electroactive groups in their structure. The bithiophene terminal groups of dendrimers **17-G$_n$** ($n = 0$–4) are electropolymerizable, leading to electrodes irreversibly modified by a dark blue film on the anode, which remains electroactive in aqueous media [61]. On the other hand, the electrodeposition of dendrimers **18-G$_3$** possessing 24 TTF-crown ethers as terminal groups is fully reversible. The modified electrode is usable for the electrochemical sensing of a metal cation (i.e., Ba^{2+}), as shown in Fig. 9.16 which displays the changes of the electrochemical response upon increasing concentrations of Ba^{2+} [62]. Other TTF-terminated dendrimers allowed a deeper insight in the mechanism of electron transfer. Mixed-valence cation radical salts of TTF-terminated dendrimers with closed-shell anion are conducting not only as a result of electron transfer between partially oxidized dendrimers but also due to the presence of interdendrimeric charge transfer (i.e., 3D electronic interactions) [63].

One of the most popular electroactive derivatives is certainly ferrocene, thanks to its robustness and its full electrochemical reversibility in many cases. It has been linked very often to dendrimers, generally as terminal groups [64]. In the particular case of phosphorus dendrimers, we have grafted ferrocene derivatives as terminal groups [65], but also as core [66] and in the interior [67]; in all cases a blue film was reversibly deposited onto the electrode [68]. The most original examples are shown in Fig. 9.17: ferrocenes functionalized by aldehydes were grafted as terminal groups of the third, the fifth and the ninth generation dendrimer **19-G$_n$**, then the aldehydes were reacted as shown previously in Figs. 9.1 and 9.2, to afford the

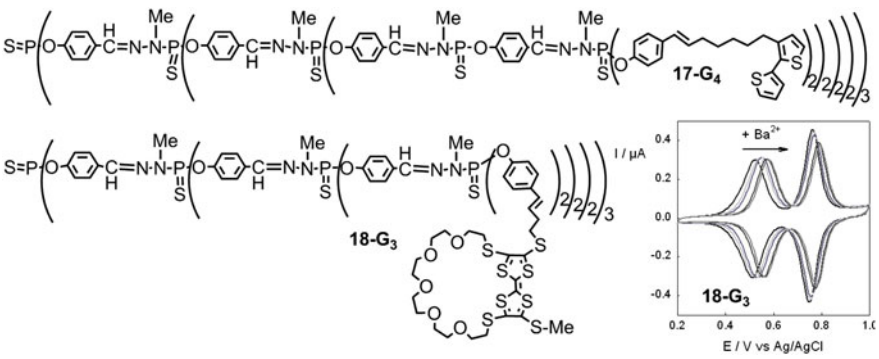


Fig. 9.16 Various types of electrochemically active phosphorus dendrimers, able to modify the surface of electrodes

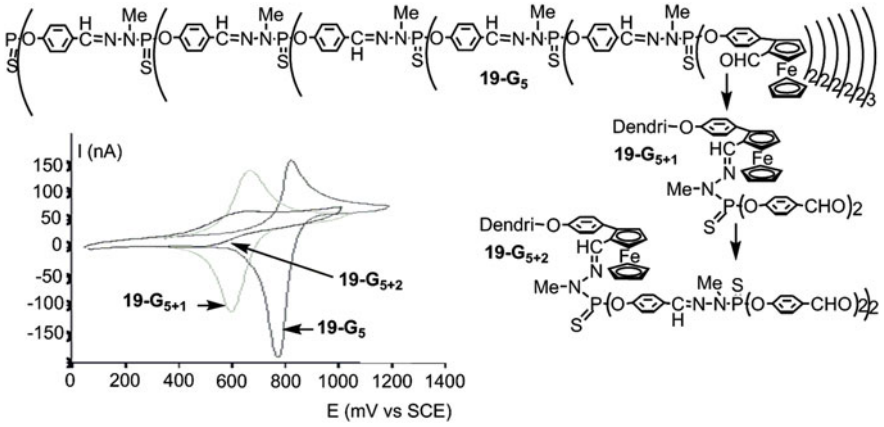


Fig. 9.17 Ferrocenes included at various places inside the structure of dendrimers, able to modify the surface of electrodes, and variation of the electrochemical response

generations $n + 1$ and $n + 2$. This concept is illustrated in Fig. 9.17 for the fifth generation **19-G$_5$**, leading then to the sixth (**19-G$_{5+1}$**), then the seventh (**19-G$_{5+2}$**) generation dendrimers. Progressive burying of the ferrocene inside the dendritic structure induces both a decrease of the rate of the electronic transfer when the redox centers are more confined within the interior of the dendrimer, and a decrease of the reversibility of the system with the increase of the generation of the dendrimer [69].

Another very important way to modify the surface of materials at the nanometric scale consists in using the "layer-by-layer" (LBL) deposition of positively and negatively charged entities [70]. Dendrimers having either positive charges (ammoniums, **13-G$_4$**) or negative charges (carboxylates, **20-G$_4$**) as end groups were used for the coating of various surfaces. Ultrathin (ca. 100 nm) nanoporous gold membranes were used to probe the structural evolution of a layer-by-layer deposition of these charged dendrimers [71]. The phosphorus dendrimers can be associated also to other charged entities. For instance, cationic phosphorus dendrimers (**13-G$_4$**) and anionic hyperbranched polyglycerols were used to elaborate thin films, which formation was monitored by surface plasmon resonance (SPR) spectroscopy and UV–visible spectroscopy. Exposing the supramolecular multilayers to $TiCl_4$ precursors generated hybrid organic-TiO_2 nanostructures, which exhibit characteristic photoluminescence properties [72]. Multilayer thin films of anionic gold nanoparticles (AuNPs) and cationic phosphorus dendrimers **13-G$_4$** were also deposited by layer-by-layer (LbL) assembly driven by electrostatic interactions. The relative amounts of AuNPs and dendrimers in the multilayer films were measured using a quartz crystal microbalance. The localized surface plasmon resonance (LSPR) band of the hybrid films can be tuned by adding NaCl to the dendrimer solution or by removing the organic matrix (the dendrimers) [73]. Very recently, the LbL technique with dendrimers **13-G$_4$** and **20-G$_4$** was also applied onto gold substrates, and a high loading of DNA probes was obtained

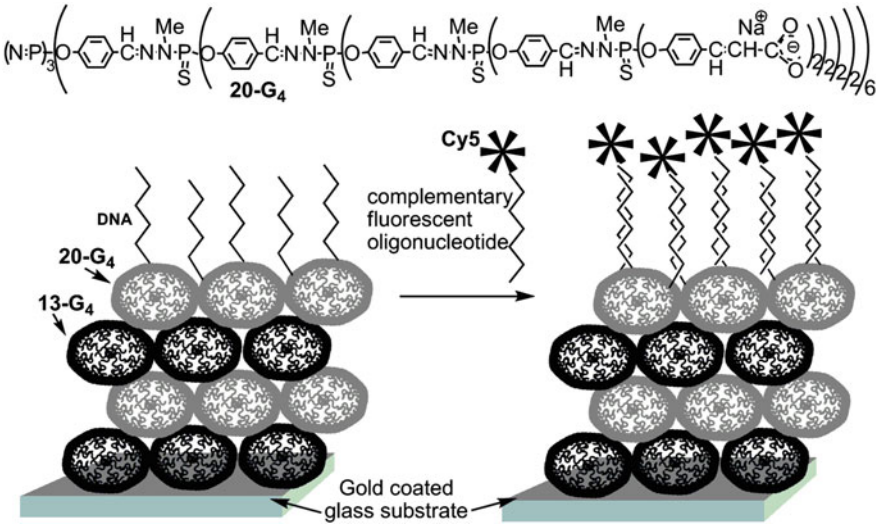


Fig. 9.18 Gold-coated glass substrate modified by LbL deposit of positively (**13-G$_4$**) and negatively (**20-G$_4$**) charged dendrimers (up to four bilayers, here shown with two), then by probe DNA immobilized on the outmost layer, and hybridization with target DNA bearing fluorescent Cy5

through covalent coupling of DNA probe on dendrimers top layer. Hybridization with Cy5-dye labeled complementary target DNA was detected by surface plasmon field-enhanced fluorescence spectroscopy, with a limit detection of 30 pM (Fig. 9.18) [74].

Analogous methods were used for the coating of melamine/formaldehyde microspheres with a radius of $r_0 = 2.0 \pm 0.1$ μm. These spheres were coated by alternating either poly(styrenesulfonate) (PSS) and positively charged dendrimers **13-G$_4$**, or by alternating poly(allylamine hydrochloride) (PAH) and negatively charged dendrimer **20-G$_4$**. Microcapsules were obtained in HCl at pH 1.2–1.6, which dissolved the internal structure while preserving the multilayers of dendrimers and polymers. In the case of the multilayer shell composed of (PSS/**13-G$_4$**)$_4$ (four bilayers), most capsules are broken (Fig. 9.19a); however, in the cases of (PSS/**13-G$_4$**)$_4$(PSS/PAH), or (PAH/**20-G$_4$**)$_4$, or (PAH/**20-G$_4$**)$_4$(PSS/PAH), practically all the microcapsules are intact after this hard treatment (Fig. 9.19b). The mechanical properties of these polyelectrolyte/dendrimer microcapsules were measured from force–deformation curves with the atomic force microscope (AFM). The experiment suggests that they are much softer than PSS/PAH microcapsules; this softening was attributed to an enhanced permeability of the polyelectrolyte/dendrimer multilayer shells as compared with multilayers formed by linear polyelectrolytes [75]. The same concept was applied later on, using positively charged dendrimers **13-G$_3$** and DNA. Contrarily to the previous cases, in which each capsule was isolated, these capsules are aggregated, due to the length of DNA, which is able

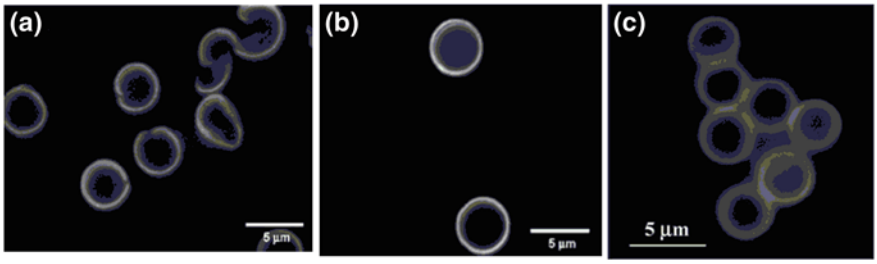


Fig. 9.19 **a** Broken microcapsules from (PSS/**13-G$_4$**)$_4$; **b** intact microcapsules from (PSS/**13-G$_4$**)$_4$(PSS/PAH), or (PAH/**20-G$_4$**)$_4$, or (PAH/**20-G$_4$**)$_4$(PSS/PAH); **c** aggregated microcapsules from (DNA/**13-G$_3$**)$_4$

to link together several capsules (Fig. 9.19c) [76]. In other experiments, the microspheres were coated first with a dye, then by the dendrimers. After removal of the template, it was possible to have the dye encapsulated in the microcapsule, and to study its release [77].

This LbL technique using ionic interactions was also applied to the elaboration of very original nanotubes made of dendrimers [78], which could not be obtained with polymers. Ordered porous alumina templates (Fig. 9.20a) were coated by immersion successively in water solutions of negatively charged dendrimers **20-G$_4$**, then of positively charged dendrimers **13-G$_4$**. Bilayers of dendrimers were deposited by alternately immersing the templates in the corresponding solutions. Removal of the inorganic template was performed without destroying the dendrimers and afforded nanotubes which are the replica of the pores (Fig. 9.20b) [79]. The same methodology was used later on with negatively charged quantum dots (QDs, fluorescent nano-crystals) emitting at 561, 594, and 614 nm, instead of the negatively charged dendrimers. For nanotubes containing a single type of QD, their photoluminescence (PL) emission spectra appear at the expected wavelengths depending on the QDs used. For nanotubes containing multiple types of QDs, their PL emission spectra show exclusively an emission peak centered at 614 nm, originating from QD614, indicating that an efficient excitation energy transfer takes place from the larger bandgap QDs to the ones with lower band energy (Fig. 9.20c) [80]. This is a key feature for the enhanced detection sensitivity of DNA hybridization inside the nanotubes. Hybridization was carried out with amino group-functionalized probe DNA with Cy5-labeled complementary 15-mer DNA oligonucleotides. The measured normalized PL emission spectra display an intense shoulder at about 670 nm, originating from Cy5 which can be attributed to excitation energy transfers by FRET from the QDs to the Cy5. The results suggest that NTs containing a cascaded-energy-transfer architecture have potential utility for the detection of trace amounts of DNA [81].

Using dendrimers instead of simple monomers allows multiplying the number of anchoring points and/or the number of detection groups; both possibilities are particularly interesting for sensor applications. The fluorescent

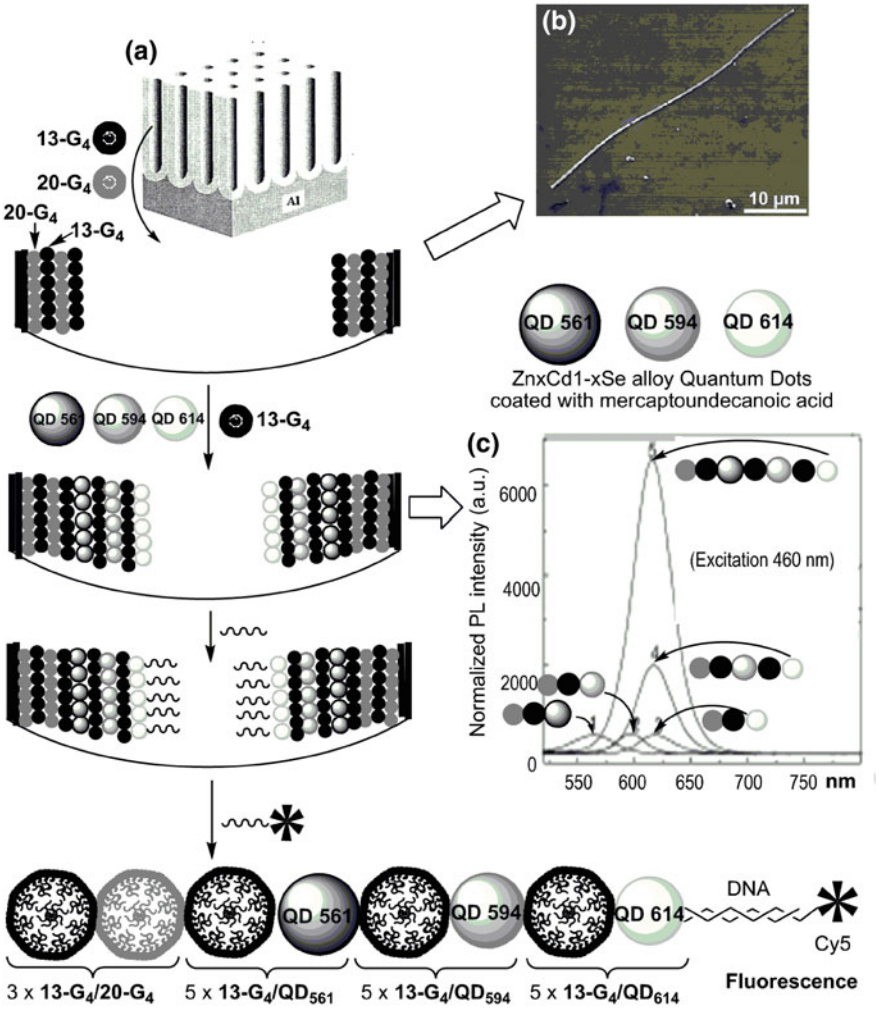


Fig. 9.20 **a** Functionalization of alumina template by LbL deposition of charged dendrimers; **b** nanotubes of dendrimers obtained after removal of the template; **c** nanotubes including one, two, or three types of quantum dots **c** and their use for the detection of trace amounts of DNA

small dendrimer **21-G$_1$** incorporates reactive phosphonate groups able to react with a nano-crystalline titania film. The resulting hybrid functionalized films are brightly fluorescent, but hydrogen bonds between alcohols and the carbonyl groups of the fluo-tag induce a quenching effect. Figure 9.21 shows that the dendrimers grafted to the films display high quenching efficiency towards phenolic OH moieties, especially those from resorcinol and 2-nitroresorcinol, with less than 1% of fluorescence remaining. This effect is attributed to the increased spatial proximity of the fluorescent entities in the film that makes the

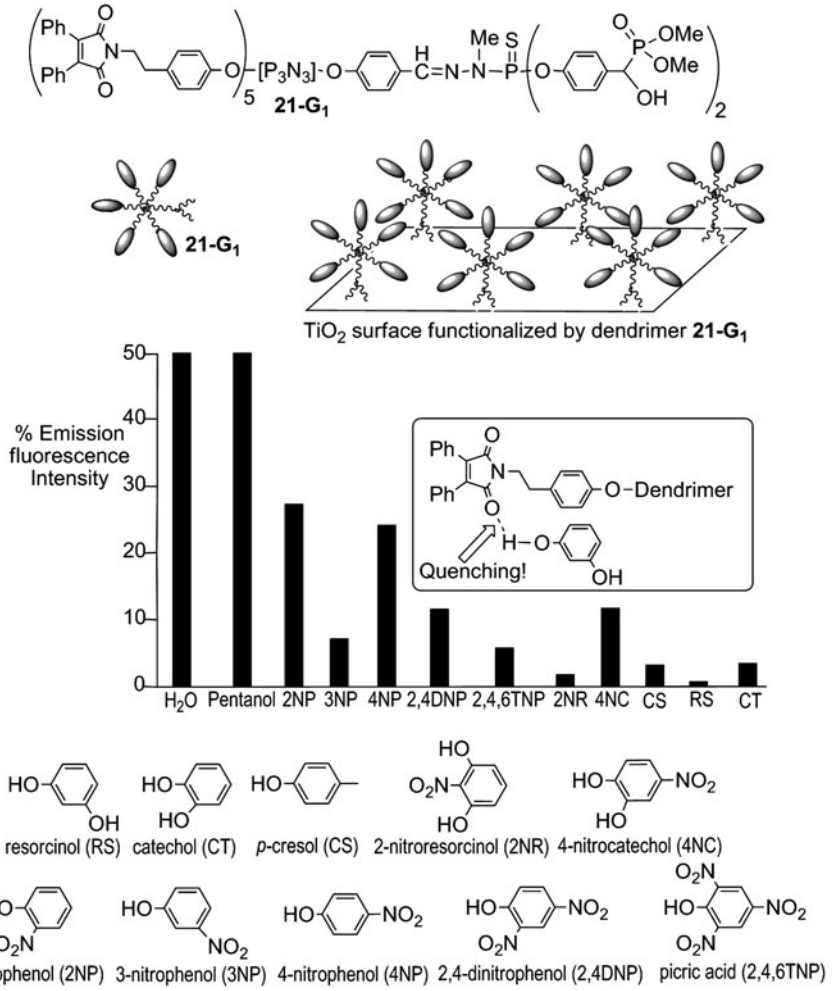


Fig. 9.21 A chemical sensor for phenols, elaborated with the fluorescent dendrimer **21-G$_1$**

formation of hydrogen bonds between the hydroxyl moieties of the quenchers and the carbonyl groups of the dendrimer easier in the film than in solution [82].

There is currently a growing demand of genetic information in molecular medicine, or for genotyping of individuals in forensic applications, but also in analytical chemistry applied in particular to the preservation of food safety and environment quality. Typical biosensors consist of a nucleic acid immobilized at discrete positions on surface activated slides and constituting the probe, and a sample in which the target is among a complex mixture of fluorescently labelled nucleic acids. The supramolecular interaction resulting

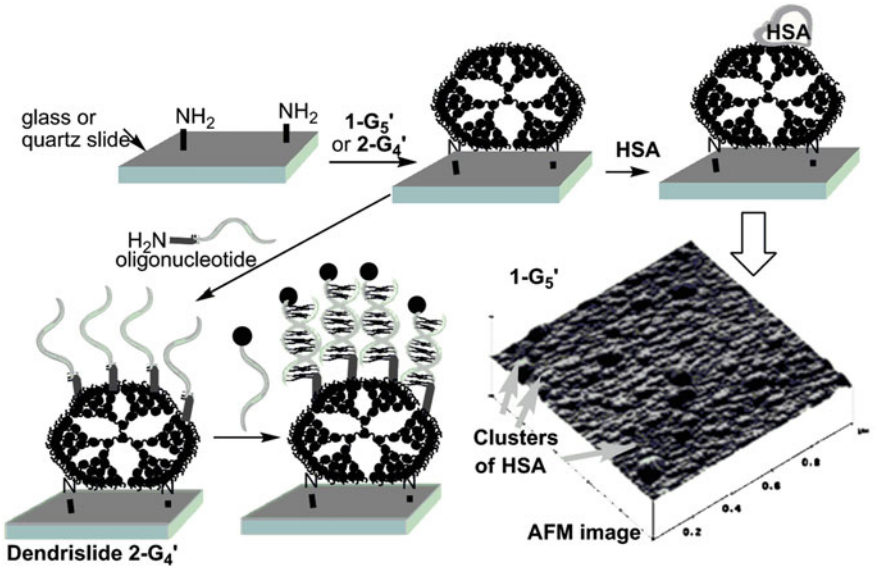


Fig. 9.22 Very sensitive biochips elaborated with dendrimers **2-G_4'** (CHO terminal groups)

in hybridization between the probe and the target is generally quantified by fluorescence [83]. The contribution of our phosphorus dendrimers to the field of bioarrays began in 1999, with the immobilization of a protein (human serum albumin (HSA)) on a quartz slide to which dendrimers **1-G_5'** were covalently linked [84]. AFM (Atomic Force Microscopy) images of the slides showed a total coverage of the surface by dendrimers **1-G_5'** and the presence of HSA clusters [85] (Fig. 9.22). This methodology was later on developed for the elaboration of DNA microarrays. Several generations of dendrimers **2-G_n'** were tested, and the best signal-to-noise ratios were obtained with generations 4–7, thus generation 4 was chosen, because it is more easily synthesized than higher generations.

To quantify the target/probe hybridization sensitivity, "dendrislides" elaborated from **2-G_4'** and 12 commercially available glass slides were spotted with a 35mer oligonucleotide, then hybridized with increasing concentrations of a Cy5-labeled 15mer oligonucleotide complementary to the probe. At target concentrations 0.001 nM of DNA, a fluorescence signal was still quantifiable only using the dendrislides elaborated with **4-G_4'** (Fig. 9.23) [86]. Reusability of the dendrislides was also tested and was found excellent even after 10 hybridization/stripping cycles [87]. The same concept was developed later on for liposomes arrays [88] and for the elaboration of sensitive piezoelectric mass-sensing devices [89].

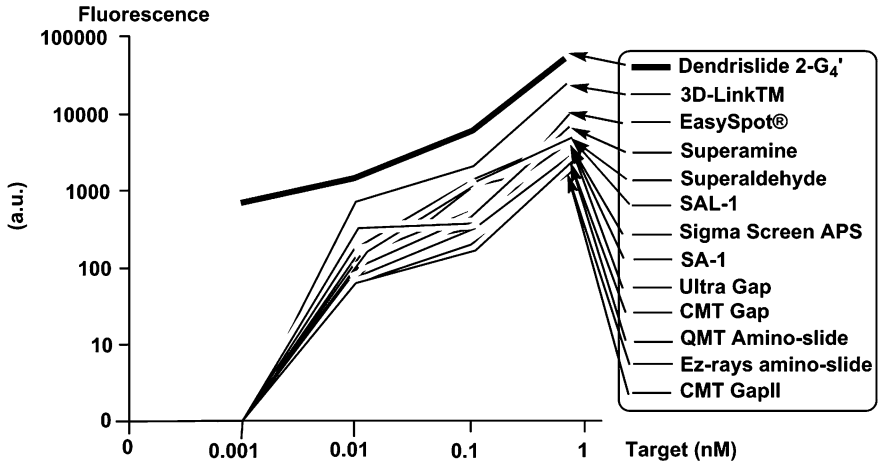


Fig. 9.23 Comparison of the efficiency of dendrislide **2-G_4'** for the detection of fluorescent DNA complementary strand with twelve commercially available glass slides used as DNA chips

9.4 Biology

Biological properties of dendrimers are certainly the most active and attractive area of the researches about dendrimers [90–95]. Obviously, the potential toxicity of dendrimers has to be taken into account. It depends mainly on the type of terminal groups, thus it will be indicated when necessary for each biological property that will be discussed. The use of dendrimers as biosensors, as shown above, pertains both to the field of materials and to biology, but there are other examples of solid materials functionalized by dendrimers and used for biological purposes. For instance, control over the manner in which proteins and cells interact with surfaces is critical for the success of implanted biomedical devices. It has been shown that cellular behaviours on surfaces coated with polymers depend on a combination of several parameters, which include the molecular architecture and chemical nature of the polymers, in particular in terms of rigidity, functionality, surface charge, roughness, hydrophilicity, etc. [96]. Glass substrates covered by multilayer films obtained by LbL deposition of negatively (**20-G_4**) and positively (**13-G_4**) charged generation 4 dendrimers, as shown previously for instance in Fig. 9.13, were used for cultures of foetal cortical rat neurons. The influence of the surface charge of the outermost layer of dendrimers on the adhesion and maturation of these neuronal cells was checked. It was found that neurons attached preferentially and matured slightly faster on film surfaces terminated with positively charged dendrimers (**13-G_4**) than on negatively charged surfaces (Fig. 9.24) [97].

As shown also in the previous section, use of dendrimers for diagnosis is of current high interest, not only as devices, but eventually in vivo. Fluorescent

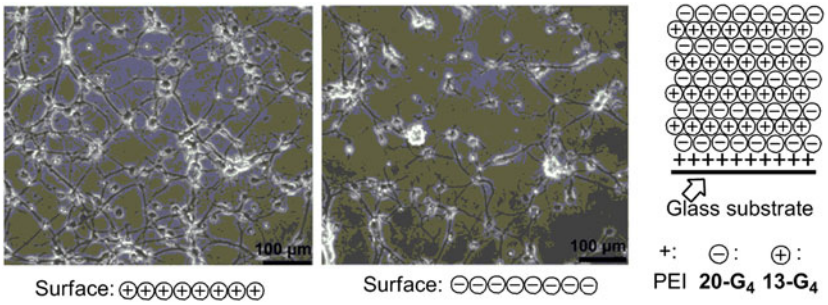


Fig. 9.24 Cortical neurons from foetal rats cultured for 5 days on positively (*left*) and negatively (*right*) charged surfaces. The substrate was coated by the LbL deposition of four bilayers of charged dendrimers **20-G$_4$** and **13-G$_4$**; an additional layer of **20-G$_4$** was deposited in the case of the negatively charged surface

water-soluble dendrimers might afford new tools in this field [98], in particular if they possess chromophores having two-photon excited fluorescence (TPEF) properties. TPEF has a highly spatially confined excitation and intrinsic three-dimensional resolution [99], an increased penetration depth in tissues with reduced photo-damages thanks to excitation in the near-infrared region, which render this technique extremely attractive for biological imaging, in particular of living animals. Quantum dots have been shown to provide a particularly effective approach [100], but they suffer from several drawbacks including toxicity and blinking.

Phosphorus dendrimers having on their periphery optimised two-photon absorption (TPA) chromophores can be considered as an organic alternative to inorganic quantum dots (QDs) [101]. The first attempts were made with a blue fluorophore grafted to the surface of dendrimers **2-G$_n$** ($PSCl_2$ end groups). An additive behaviour depending on the number of fluorophores was observed; the highest generation (generation 4) has a comparable TPA efficiency than the best QDs [102]. The modularity of these fluorescent dendritic systems is very high. For instance, sophisticated architectures allow TPA cooperative enhancement, which can be achieved as a result of purely electrostatic through-space inter-chromophoric interactions; the TPA enhancement was found to depend on the spatial distribution and number of chromophores [103]. Another illustration of the modularity of these systems is also shown by the synthesis of dendrimers possessing one TPA fluorophore as core and surrounded by ammonium groups to ensure the solubility in water. The second generation dendrimer **22a-G$_2$** having a blue fluorophore as core was injected intravenously to a rat. It allowed the imaging of the vascular network in the dorsal part of the rat olfactory bulb, at a depth of about 200 µm (Fig. 9.25) [104]. Analogously, the second generation dendrimer **22b-G$_2$** possessing a green emitter TPA fluorophore as core was used for intra-cardiac injection in a Xenopus tadpole, allowing imaging of the blood vessels of the tail [105].

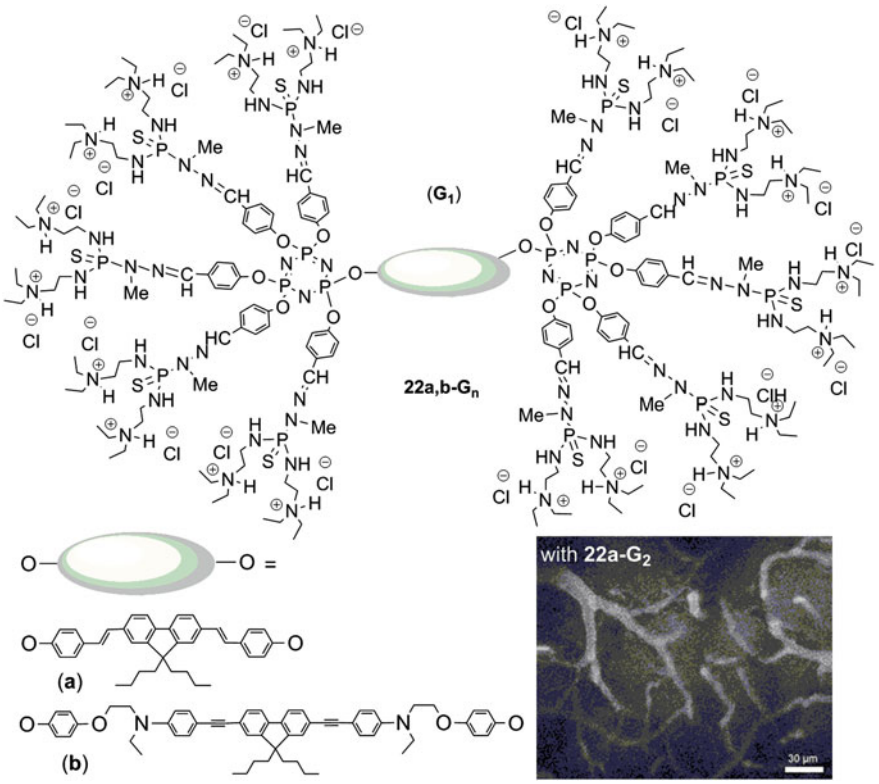


Fig. 9.25 Two-photon imaging (excitation at 710 nm) of the vascular network in the dorsal part of the rat olfactory bulb, after intravenous injection of the dendrimer **22a-G_2** in water

9.4.1 Drug Delivery

The covalent grafting of drugs on the surface of dendrimers necessitates a subtle balance between the stability of the association necessary to reach the target, and the facility to break the link for the delivery. In case of covalent interactions, the second aspect is often difficult to induce, as we have shown for a pesticide grafted to the surface of dendrimers **1-G_n** [106]. Two alternatives to this problem exist: either the dendrimer has its own biological properties, which are not observed for isolated terminal groups, or the dendrimer and the drug possess self-assembling properties in particular by ionic interactions, preferably reinforced with lipophilic interactions. Phosphorus dendrimers were found useful in both cases.

The utility of polycationic dendrimers for interacting with DNA, in particular as synthetic vectors in transfection experiments, has been recognized very early, most experiments in this field being carried out with Poly(AMidoAMine) dendrimers (PAMAM) [91]. Phosphorus-containing dendrimers are also usable as vehicles to transport DNA or plasmids inside cells. Functional tests, to verify if the

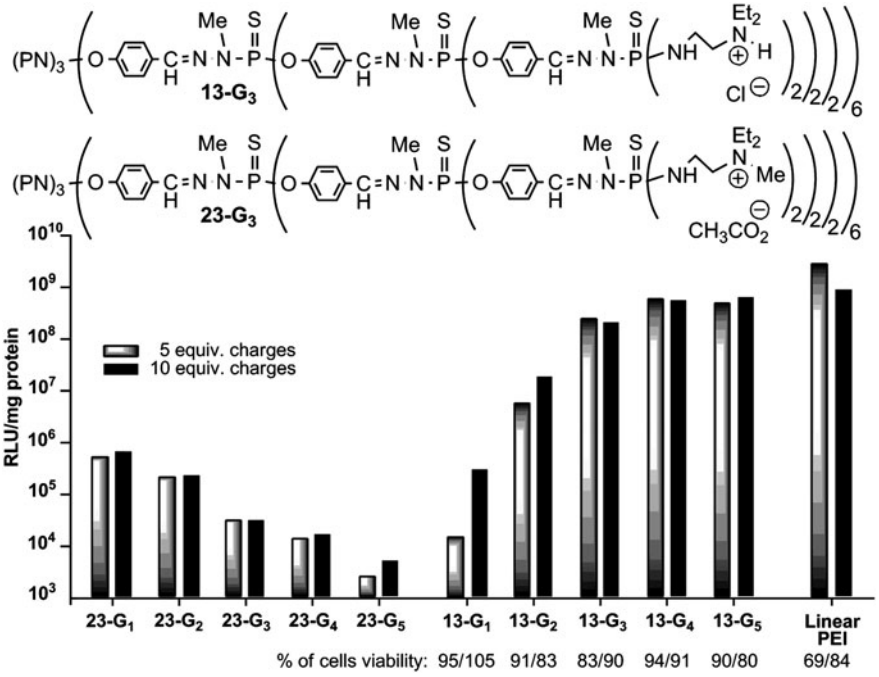


Fig. 9.26 Relative efficiency of generations 1–5 of dendrimers **13-G$_n$** and **23-G$_n$** compared to linear PEI for transfection of 3T3 cells with the luciferase plasmid; cells viability with **13-G$_n$**

delivered genetic material could be active inside the cells, were designed, using the cationic dendrimers **13-G$_n$** and **23-G$_n$**. The first one involved the transfection of eukaryotic 3T3 cells with the pCMV-luc plasmid and generations 1–5 of dendrimers, in the presence of serum. A significant expression of transgene was measured by fluorescence for the series **13-G$_n$**. The transfection efficiency increased with the generation number, then reached a plateau for generations 3–5, comparable to the standard in the field (PEI). In contrast, the corresponding methylated dendrimers **23-G$_n$** were rather toxic and relatively inefficient in transfecting nucleic acids into eukaryotic cells. The contrast between these two types of dendrimers, which differ only by the replacement of H by Me on the ammonium end groups, is possibly due to the presence of a stable positive charge density in the latter case, which may disrupt the cell membrane, leading to cell death (Fig. 9.26) [107]. The same dendrimers **13-G$_n$** are able to efficiently deliver fluorescein-labelled oligodeoxyribonucleotide into HeLa cells (Human epithelioid cervical carcinoma cell line), as well as DNA plasmid containing the functional gene of enhanced green fluorescent protein (EGFP), also into HeLa cells [108].

Continuing this work, three series of phosphorus dendrimers (generations 1 and 4) having various types of amine terminal groups (1-(2-aminoethyl)pyrrolidine, 4-(2-aminoethyl)morpholine, and 1-methylpiperazine) were synthesized, then protonated. Their cytotoxicity towards three cell strains, one healthy (HUVEC: human

umbilical vein endothelial cell), and two cancerous (HEK 293: human transformed primary embryonal kidney, and HeLa) was found low. Then, they were used as transfection agents to deliver single and double-stranded DNA into the three above-mentioned cell strains. The dendrimer having pyrrolidinium groups was found the most efficient in this series [109]. In an attempt to understand better the phenomenon implied in transfection experiments, we have recently synthesized a fluorescent analogue of dendrimer **13-G$_2$** [110].

Transmissible spongiform encephalopathies are fatal neurodegenerative diseases that include Creutzfeldt–Jakob disease in humans, scrapie in sheep and goats and bovine spongiform encephalopathy (BSE), characterized by the accumulation of the abnormal scrapie isoform of the prion protein (PrP^{Sc}) in the brain [111]. While screening anti-prion agents, it was found that the activity of the cationic dendrimers **13-G$_n$** ($n = 3$–5) was strong, decreasing both PrP^{Sc} and infectivity in scrapie-infected cells at non-cytotoxic doses. These dendrimers were able to clear PrP^{Sc} rapidly in ScN2a (infected) cells with an IC_{50} in the nM range. They are effective against pre-existing PrP^{Sc}, as was observed when incubated with brain homogenates infected with different prion strains (including BSE). The most efficient dendrimer is **13-G$_4$** (Fig. 9.27). In view of these important preliminary results, dendrimer **13-G$_4$** was tested with mice infected. Two days after contamination, a series of mice received an injection of 100 µg of **13-G$_4$**, which was repeated every 2 days for 1 month. All treated mice were alive after 1 month, and the amount of PrP^{Sc} detected in the spleen of the treated mice compared to untreated mice shows a diminishing of 80% of the amount of PrP^{Sc}, the best result in this field up to now [112].

Later on, the same dendrimers **13-G$_n$** were found able to interfere with the aggregation process of the prion peptide PrP 185–208 by both slowing down the formation of aggregates and by lowering the final amount of amyloid fibrils, a

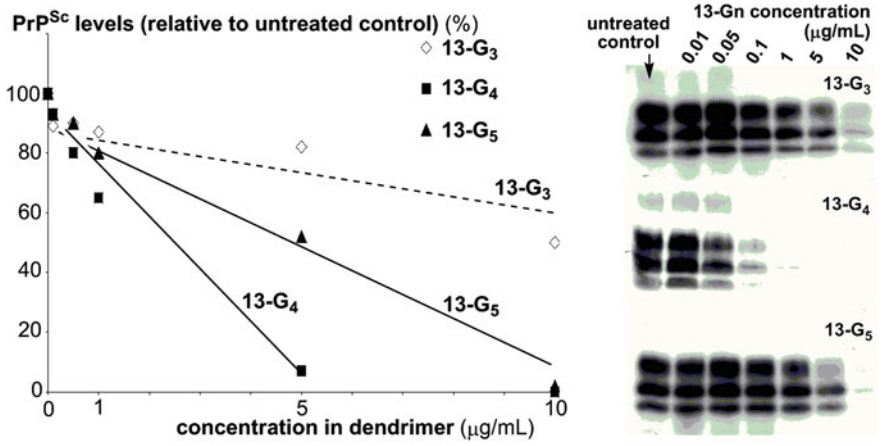


Fig. 9.27 PrP^{Sc} levels relative to untreated control for cells infected with prion 22L, and treated with dendrimers **13-G$_n$**. Detection at day 3 by Western-blot

common hallmark of conformational diseases [113]. This process might imply heparin, which is able to accelerate or inhibit fibrilogenesis depending on its concentration, and the dendrimers **13-G$_n$** were shown to interact with heparin [114]. In addition, the same dendrimers were found able to interact with the Aβ 1–28 peptide involved in Alzheimer disease [115].

As indicated at the beginning of this section about drug delivery, self-assemblies between a dendrimer and the drug might be also a useful alternative. For this purpose, carboxylic acid ended dendrimers (of type **20-G$_n$** built either from a trifunctional or a hexafunctional core) were reacted with an aminolactitol, which is an amphiphilic galactosylceramide (galβ1cer) analogue. Galβ1cer, which is present on the surface of cells, is known to act through its highly specific affinity for the V3 loop region of the gp120 viral envelope protein of HIV-1; this is one of the first events of cells infection. The self-assembly between the carboxylic acid dendrimers and the Galcer analogue gave a chimera of galβ1cer, able to interact strongly with gp120, thus inhibiting the action of galβ1cer, and preventing the infection of cells. In first attempts, ion pair assemblies **24a-G$_1$** were obtained by mixing the first generation dendrimers ended by carboxylic acids with the aminolactitol [116]. Later on, the same process was applied to carboxylic acids ended dendrimers built form the hexafunctional core affording **24b-G$_1$**. The influence of the core functionality of the dendrimers was clearly identified for the series **24a-G$_n$** and **24b-G$_n$**, and the bioactivities were found to be core-dependent but not generation dependent, as shown in Fig. 9.28 [117]. Later on, the same process was applied to a series of phosphonic acid ended dendrimers, affording in particular **25-G$_1$**. Compounds with variable length of the alkyl chain of the phosphonate were synthesized. Dendrimer **25-G$_1$** has the longest chain in this series. The inhibitory assays in this series indicate that the length of the alkyl chain influences the efficiency of these inhibitors [118, 119].

The same principle of interaction was applied recently in vivo for the delivery to rabbits' eyes of carteolol, an ocular anti-hypertensive drug to treat glaucoma. The structure of the dendrimers was especially engineered to fulfill two criteria: the interaction with carteolol, and the limitation of chemical entities in the formulation, obtained by replacing the preservative benzalkonium chloride by a quaternary ammonium as core of dendrimers. For this purpose, dendritic compounds possessing one ammonium salt as core, and carboxylic acids as terminal groups able to interact with the amino function of carteolol were synthesized. After reaction with carteolol, the ion pair species of generation 0 (3 carteolol units) is fairly soluble in water, whereas the first and second generations (6 and 12 carteolol units, respectively) are only poorly soluble. All compounds dissolved in water were instilled in the eyes of rabbits. No irritation was observed, whatever the generation used and even after several hours. Measurements of the quantity of carteolol having penetrated inside the aqueous humor of eyes show practically no difference between carteolol alone and the three carteolol units entrapped with the generation zero. Due to the very low solubility of the second generation, the quantity of carteolol instilled is low, but the quantity of carteolol that penetrates inside the eyes is larger than expected, when compared with carteolol alone (2.5 times larger) [120].

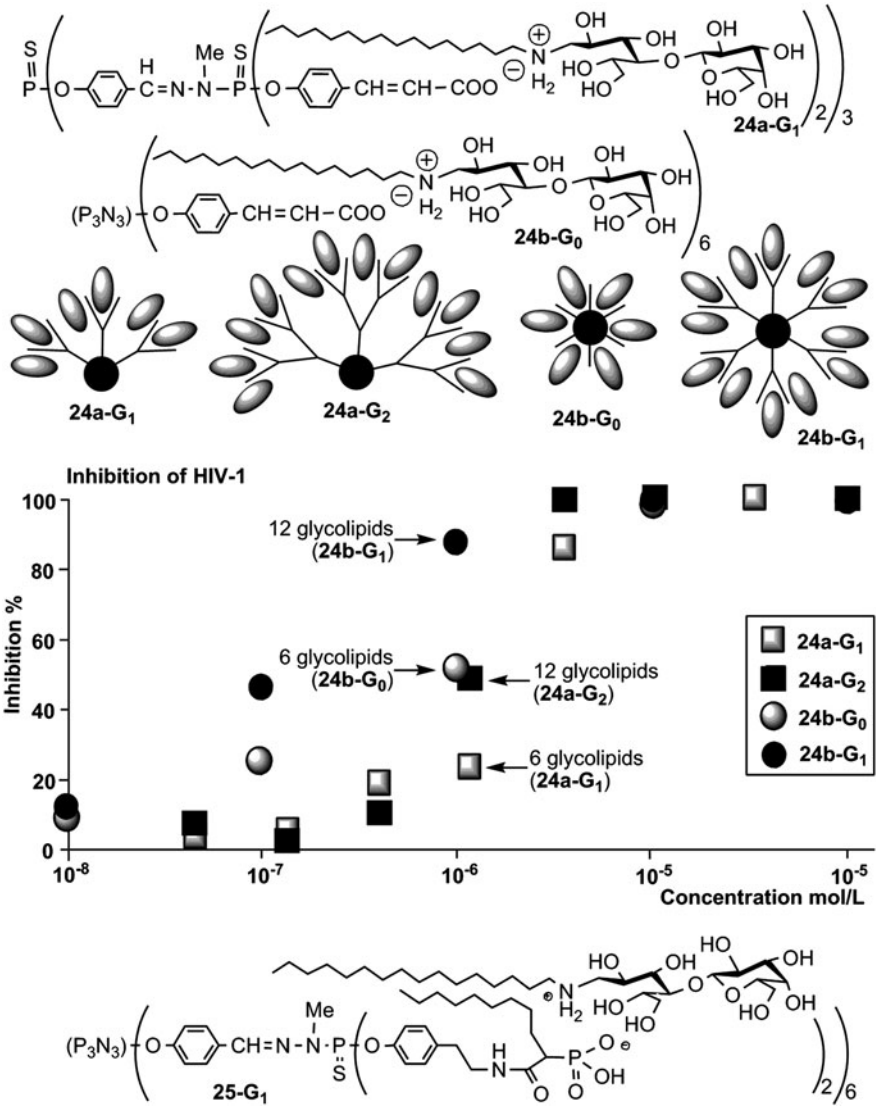


Fig. 9.28 Inhibition of HIV-1 infection of CEM-SS cells by cationic dendrimers **24a,b-G_n**. Compounds **25-G_1**, also against HIV

9.4.2 Interactions with the Human Immune System

Peripheral blood mononuclear cells (PBMCs) are a critical component in the human immune system to fight infections and adapt to external or internal (such as cancers) intruders, which are found within the circulating pool of blood. It is

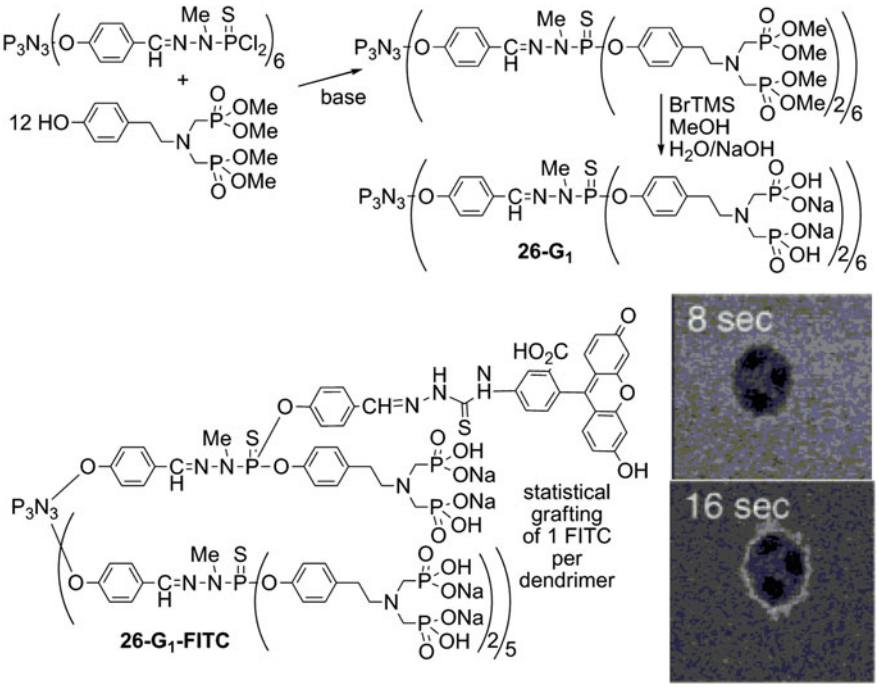


Fig. 9.29 Synthesis of the phosphonic acid salts ended dendrimer **26-G$_1$**, and use of its fluorescent analogue **26-G$_1$-FITC** for visualizing the interaction with monocytes

known that small molecules such as pyrophosphates and amino-bisphosphonates [121] can activate and/or multiply a group of T lymphocytes at the borderline between adaptive and innate immunity. Thus, we thought that amino diphosphonic acids ended dendrimers might interfere with PBMCs. A series of such compounds was synthesized, of which one example, **26-2-G$_1$** , is shown in Fig. 9.29. In order to monitor the possible interactions with PBMCs, a fluorescent analogue was also synthesized, by grafting statistically one FITC (fluorescein isothiocyanate) per dendrimer leading to **26-G$_1$-FITC**. This fluorescent derivative (20 μM) incubated for 30 min with human PBMCs freshly isolated from a healthy donor induced the labeling of monocytes (white blood mononuclear cells, a pivotal cell population of innate immunity). It was the only hematopoietic population labeled. Sequential images of the interaction filmed by confocal video microscopy showed that dendrimer **26-G$_1$-FITC** rapidly bound within a few seconds to monocyte surface (see photos taken after 8 and 16 s in Fig. 9.29) and was progressively internalized within a few minutes and for hours [122].

Within 3–6 days, monocytes in culture with dendrimer **26-G$_1$** underwent morphological changes indicating that they were activated by the dendrimer. They also remained viable over longer periods than control monocytes (in cultures without dendrimers). Analyzing the gene expression of monocytes activated by

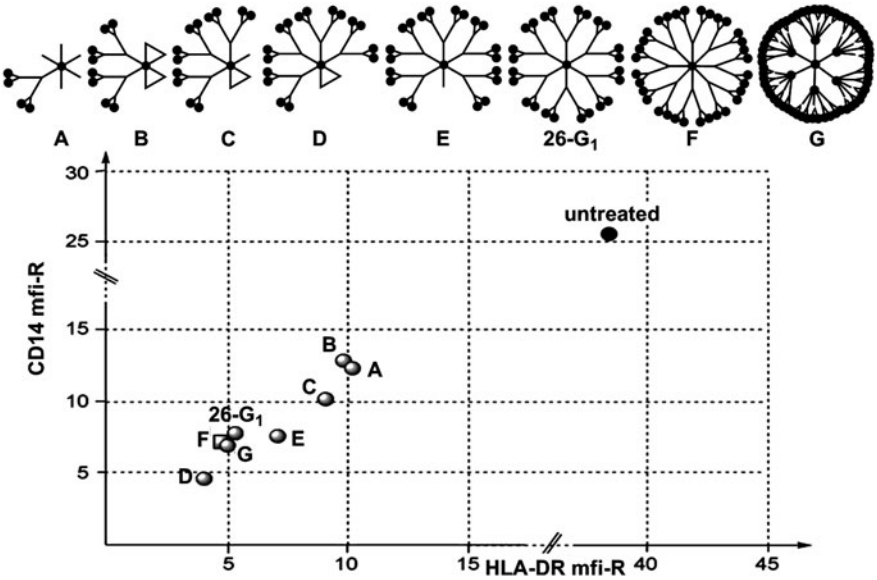


Fig. 9.30 A library of dendrimers ended by aminobis phosphonate salts, and screening of their bioactivity towards human monocytes. The activity increases on going down and left

dendrimer **26-G_1** by comparison with untreated monocytes showed that 78 genes were up-regulated, whereas 62 genes were down-regulated, suggesting an alternative-like, anti-inflammatory activation of human monocytes [123]. The multivalent character of phosphonic acid capped dendrimers is crucial for monocyte targeting and activation; indeed, the corresponding monomeric azadiphosphonic salt displays no activity. Beginning a structure/activity relationship study, we have varied the number of terminal phosphonate functions, using a core-controlled strategy (selective functionalization of 1–5 Cl of the $N_3P_3Cl_6$ core, named **A**–**E** in Fig. 9.30). More dense dendrimers **F** and **G** were also synthesized. This study shows that activation of human monocytes by phosphorus-containing dendrimers depends on the surface density of phosphonic groups, with a neat decrease of the efficiency for compounds with or less than 6 amino-bismethylene phosphonic groups per dendrimer (**A**, **B**, **C**) [124].

Peripheral blood immune cells are present within the circulating pool of blood, easily accessible, and widespread in the whole body, and thus they are a target of choice, in particular for fighting against cancers. In the previous paragraph, we have shown the activation of monocytes by dendrimer **26-G_1** and its derivatives in short term cultures of PBMCs (maximum 6 days, generally one). Very surprisingly, a totally different behavior was observed for longer times of culture. Indeed, an important increase in the number of PBMCs was observed and identification of the cells multiplied in cultures with **26-G_1** revealed the prominence of NK cells (with some T cells). The immune system in blood comprises several kinds of

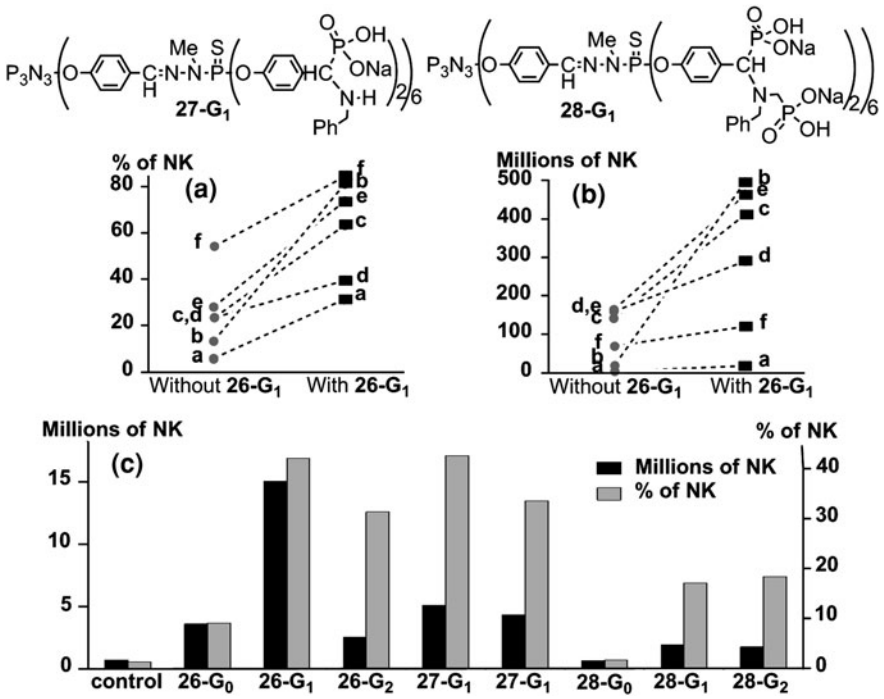


Fig. 9.31 **a** Number and **b** percentage of NK cells from four-week-old cultures without (*gray dots*) or with 20 μM of **26-G$_1$** (*black squares*). a–f represent blood from six healthy donors. **c** Comparison of the efficiency of several dendrimers depending on the generation and the type of phosphonic acid terminal groups

cells derived from stem cells in bone marrow, in particular monocytes as we have seen above, but also natural killer (NK) cells, which are part of the innate immunity.

Experiments with PBMCs obtained from six healthy donors revealed in all cases an important increase in both the percentage (Fig. 9.31a) and the number (Fig. 9.31b) of NK cells. After 4 weeks in culture, a mean multiplication of the number of NK cells by a factor of 105 was achieved in medium containing **26-G$_1$** versus a mean multiplication by a factor of only 7.5 without it. These large-scale prototype cultures of PBMCs comprised 1 million NK cells on average at the beginning; multiplications over 500-fold were obtained with some donors [125].

The multiplication of NK cells observed of up to 500-fold in certain cases is unprecedented. Furthermore, the bioactivity of the NK cells generated in the presence of dendrimers is not modified. Cultures with these dendrimers neither induced activation or inhibition of the NK cells lytic response, nor compromised direct toxicity for their target cells and preserved autologous lymphocytes. In view of this unprecedented result, several variations of the initial structure

were synthesised, in particular a new series of phosphorus-containing dendrimers capped with non-symmetrical azadiphosphonic acids. Their ability to activate human monocytes of healthy individuals was assessed. All of them were found active, but none of them displayed a higher activity than **26-G$_1$** (Fig. 9.31c) [126]. The mechanism of action of this dendrimer is very complex, and is only partly elucidated to date. Phosphonate-capped dendrimers inhibit the activation, and therefore the proliferation of $CD4^+$ T lymphocytes, without affecting their viability. This allows a rapid enrichment of NK cells and further expansion. The dendrimer acts directly on T cells, and it was hypothesized that regulatory activity may signal through a specific receptor that remains to be identified [127].

9.5 Conclusion

Phosphorus-containing dendrimers are now a major class of dendrimers, which have already proved their utility in various fields of researches such as catalysis, materials and biology, as we have demonstrated in this chapter. Several of these properties are shared with other types of dendrimers, but phosphorus affords several specificities. First of all, the presence of phosphorus at each branching point allows an easy characterization by ^{31}P NMR [128]. Indeed, at least the four most external layers can be distinguished by ^{31}P NMR, even for the highest generations; thus any unreacted function is easily detected, with a precision of at least 0.5%. The wealth of the chemistry of phosphorus is also a great tool, which helped us to synthesize among the most original and sophisticated dendritic structures [24], but also to diversify easily the terminal groups, which allowed in particular the specific grafting of 2, 3, and even 4 different terminal functions on the surface of these dendrimers [129].

The presence of phosphorus also plays an important role when considering the potential applications of dendrimers. In the field of catalysis, we have shown in Fig. 9.6 the most positive dendritic effect ever observed for any type of organometallic dendritic catalysts. In the field of materials, the organization in dendritic networks of the nanoparticles generated by the dendrimers (Fig. 9.12) is unprecedented. The nanotubes shown in Fig. 9.20 could not be obtained with polymers, and the phosphorus dendrimers have the suitable equilibrium between rigidity and flexibility to allow their elaboration, and a sufficient stability towards acids and bases to allow their isolation. The sensitivity of biochips elaborated with dendrimers is higher than that of other biochips. Finally, in the field of biology, it can be deduced from all the tests already performed that the phosphorhydrazone dendrimers are biocompatible. The activation of the human immune system with the phosphonate-ended phosphorus dendrimers is totally unprecedented, not only with dendrimers but also with any type of chemical substance, and is of general interest. It should lead in the next years to pharmacokinetic assays, in view of clinical trials.

Thus phosphorus-containing dendrimers have already a rich past, but their story is not finished.

References

1. Fréchet JMJ, Tomalia DA (eds) (2001) Dendrimers and other dendritic polymers. Wiley, Chichester
2. Newkome GR, Moorefield CN, Vögtle F (eds) (2001) Dendrimers and dendrons. Concepts, syntheses, applications. Wiley VCH, Weinheim
3. Newkome GR, Shreiner CD (2008) Poly(amidoamine), polypropylenimine, and related dendrimers and dendrons possessing different 1 → 2 branching motifs: an overview of the divergent procedures. Polymer 49:1–173
4. Majoral JP, Caminade AM (1999) Dendrimers containing heteroatoms (Si, P, B, Ge, or Bi). Chem Rev 99:845–880
5. Rengan K, Engel R (1990) Phosphonium cascade molecules. J Chem Soc Chem Commun 1084–1085
6. Miedaner A, Curtis CJ, Barkley RM, Dubois DL (1994) Electrochemical reduction of CO_2 catalyzed by small organophosphine dendrimers containing palladium. Inorg Chem 33:5482–5490
7. Petrucci-Samija M, Guillemette V, Dasgupta M, Kakkar AK (1999) A new divergent route to the synthesis of organophosphine and metallodendrimers via simple acid-base hydrolytic chemistry. J Am Chem Soc 121:3248
8. Hudson RHE, Damha MJ (1993) Nucleic-acid dendrimers—novel biopolymer structures. J Am Chem Soc 115:2119–2124
9. Roy R (1997) Recent developments in the rational design of multivalent glycoconjugates. Topics Curr Chem 187:241–274
10. Salamonczyk GM, Kuznikowski M, Skowronska A (2000) A divergent synthesis of thiophosphate-based dendrimers. Tetrahedron Lett 41:1643–1645
11. Launay N, Caminade AM, Lahana R, Majoral JP (1994) A general synthetic strategy for neutral phosphorus-containing dendrimers. Angew Chem Int Ed Engl 33:1589–1592
12. Launay N, Caminade AM, Majoral JP (1995) Synthesis and reactivity of unusual phosphorus dendrimers—a useful divergent growth approach up to the 7th generation. J Am Chem Soc 117:3282–3283
13. Slany M, Bardaji M, Casanove MJ, Caminade AM, Majoral JP, Chaudret B (1995) Dendrimer surface-chemistry—facile route to polyphosphines and their gold complexes. J Am Chem Soc 117:9764–9765
14. Lartigue ML, Donnadieu B, Galliot C, Caminade AM, Majoral JP, Fayet JP (1997) Large dipole moments of phosphorus-containing dendrimers. Macromolecules 30:7335–7337
15. de Gennes PG, Hervet H (1983) Statistics of starburst polymers. J De Physique Lett 44:L351–L360
16. Launay N, Caminade AM, Majoral JP (1997) Synthesis of bowl-shaped dendrimers from generation 1 to generation 8. J Organomet Chem 529:51–58
17. Leclaire J, Coppel Y, Caminade AM, Majoral JP (2004) Nanometric sponges made of water-soluble hydrophobic dendrimers. J Am Chem Soc 126:2304–2305
18. Leclaire J, Dagiral R, Fery-Forgues S, Coppel Y, Donnadieu B, Caminade AM, Majoral JP (2005) Octasubstituted metal-free phthalocyanine as core of phosphorus dendrimers: a probe for the properties of the internal structure. J Am Chem Soc 127:15762–15770
19. Galliot C, Prevote D, Caminade AM, Majoral JP (1995) Polyaminophosphines containing dendrimers—syntheses and characterizations. J Am Chem Soc 117:5470–5476

20. Larre C, Caminade AM, Majoral JP (1997) Chemoselective polyalkylations of phosphorus-containing dendrimers. Angew Chem Int Edit Engl 36:596–599
21. Larre C, Donnadieu B, Caminade AM, Majoral JP (1998) Phosphorus-containing dendrimers: chemoselective functionalization of internal layers. J Am Chem Soc 120:4029–4030
22. Brauge L, Magro G, Caminade AM, Majoral JP (2001) First divergent strategy using two AB2 unprotected monomers for the rapid synthesis of dendrimers. J Am Chem Soc 123:8446
23. Maraval V, Caminade AM, Majoral JP, Blais JC (2003) Dendrimer design: how to circumvent the dilemma of a reduction of steps or an increase of function multiplicity? Angew Chem Int Ed 42:1822–1826
24. Galliot C, Larre C, Caminade AM, Majoral JP (1997) Regioselective stepwise growth of dendrimer units in the internal voids of a main dendrimer. Science 277:1981–1984
25. Larre C, Bressolles D, Turrin C, Donnadieu B, Caminade AM, Majoral JP (1998) Chemistry within megamolecules: regiospecific functionalization after construction of phosphorus dendrimers. J Am Chem Soc 120:13070–13082
26. Maraval V, Laurent R, Donnadieu B, Mauzac M, Caminade AM, Majoral JP (2000) Rapid synthesis of phosphorus-containing dendrimers with controlled molecular architectures: first example of surface-block, layer-block, and segment-block dendrimers issued from the same dendron. J Am Chem Soc 122:2499–2511
27. Kreiter R, Kleij AW, Gebbink R, van Koten G (2001) Dendritic catalysts. Dendrimers IV 217:163–199
28. Astruc D, Chardac F (2001) Dendritic catalysts and dendrimers in catalysis. Chem Rev 101:2991–3023
29. Caminade AM, Maraval V, Laurent R, Majoral JP (2002) Organometallic derivatives of phosphorus-containing dendrimers. Synthesis, properties and applications in catalysis. Curr Org Chem 6:739–774
30. Twyman LJ, King ASH, Martin IK (2002) Catalysis inside dendrimers. Chem Soc Rev 31:69–82
31. Helms B, Frechet JMJ (2006) The dendrimer effect in homogeneous catalysis. Adv Synth Catal 348:1125–1148
32. Andres R, de Jesus E, Flores JC (2007) Catalysts based on palladium dendrimers. New J Chem 31:1161–1191
33. Gade L (2006) Topics in Organometallic Chemistry 20. Dendrimer Catalysis. Springer, Berlin
34. Knapen JWJ, Vandermade AW, Dewilde JC, Van Leeuwen PWNM, Wijkens P, Grove DM, Van koten G (1994) Homogeneous catalysts based on silane dendrimers functionalized with arylnickel(II) complexes. Nature 372:659–663
35. Caminade AM, Majoral JP (2005) Phosphorus dendrimers possessing metallic groups in their internal structure (core or branches): syntheses and properties. Coord Chem Rev 249:1917–1926
36. Maraval V, Laurent R, Caminade AM, Majoral JP (2000) Phosphorus-containing dendrimers and their transition metal complexes as efficient recoverable multicenter homogeneous catalysts in organic synthesis. Organometallics 19:4025–4029
37. Koprowski M, Sebastian RM, Maraval V, Zablocka M, Cadierno V, Donnadieu B, Igau A, Caminade AM, Majoral JP (2002) Iminophosphine palladium complexes in catalytic Stille coupling reactions: from monomers to dendrimers. Organometallics 21:4680–4687
38. Ouali A, Laurent R, Caminade AM, Majoral JP, Taillefer M (2006) Enhanced catalytic properties of copper in O- and N-arylation and vinylation reactions, using phosphorus dendrimers as ligands. J Am Chem Soc 128:15990–15991
39. Servin P, Laurent R, Gonsalvi L, Tristany M, Peruzzini M, Majoral JP, Caminade AM (2009) Grafting of water-soluble phosphines to dendrimers and their use in catalysis: positive dendritic effects in aqueous media. J Chem Soc Dalton Trans 4432–4434

40. Servin P, Laurent R, Romerosa A, Peruzzini M, Majoral JP, Caminade AM (2008) Synthesis of dendrimers terminated by bis(diphenylphosphinomethyl)amino ligands and use of their palladium complexes for catalyzing C–C cross-coupling reactions. Organometallics 27:2066–2073
41. Caminade AM, Servin P, Laurent R, Majoral JP (2008) Dendrimeric phosphines in asymmetric catalysis. Chem Soc Rev 37:56–67
42. Laurent R, Caminade AM, Majoral JP (2005) A third generation chiral phosphorus-containing dendrimer as ligand in Pd-catalyzed asymmetric allylic alkylation. Tetrahedron Lett 46:6503–6506
43. Routaboul L, Vincendeau S, Turrin CO, Caminade AM, Majoral JP, Daran JC, Manoury E (2007) New phosphorus dendrimers with chiral ferrocenyl phosphine-thioether ligands on the periphery for asymmetric catalysis. J Organomet Chem 692:1064–1073
44. Gissibl A, Padie C, Hager M, Jaroschik F, Rasappan R, Cuevas-Yanez E, Turrin CO, Caminade AM, Majoral JP, Reiser O (2007) Synthesis and application of phosphorus dendrimer immobilized azabis(oxazolines). Org Lett 9:2895–2898
45. Caminade AM, Majoral JP (2004) Nanomaterials based on phosphorus dendrimers. Acc Chem Res 37:341–348
46. Caminade AM, Majoral JP (2005) Phosphorus dendrimers for the controlled elaboration of organic-inorganic materials. J Mater Chem 15:3643–3649
47. Schmid G, Meyer-Zaika W, Pugin R, Sawitowski T, Majoral JP, Caminade AM, Turrin CO (2000) Naked Au-55 clusters: dramatic effect of a thiol-terminated dendrimer. Chem Eur J 6:1693–1697
48. Schmid G, Emmrich E, Majoral JP, Caminade AM (2005) The Behavior of Au-55 nanoclusters on and in thiol-terminated dendrimer monolayers. Small 1:73–75
49. Badetti E, Caminade AM, Majoral JP, Moreno-Manas M, Sebastian RM (2008) Palladium(0) nanoparticles stabilized by phosphorus dendrimers containing coordinating 15-membered triolefinic macrocycles in periphery. Langmuir 24:2090–2101
50. Franc G, Badetti E, Duhayon C, Coppel Y, Turrin CO, Majoral JP, Sebastián RM, Caminade AM (2010) An efficient synthesis combining phosphorus dendrimers and 15-membered triolefinic azamacrocycles: towards the stabilization of platinum nanoparticles. New J Chem 34:547–555
51. Franc G, Badetti E, Collière V, Majoral JP, Sebastián RM, Caminade AM (2009) Dendritic structures within dendritic structures: dendrimer-induced formation and self-assembly of nanoparticle networks. Nanoscale 1:233–237
52. Reinert P, Chane-Ching JY, Bull L, Dagiral R, Batail P, Laurent R, Caminade AM, Majoral JP (2007) Influence of cationic phosphorus dendrimers on the surfactant-induced synthesis of mesostructured nanoporous silica. New J Chem 31:1259–1263
53. Turrin CO, Maraval V, Caminade AM, Majoral JP, Mehdi A, Reye C (2000) Organic-inorganic hybrid materials incorporating phosphorus-containing dendrimers. Chem Mater 12:3848–3856
54. Soler-Illia G, Rozes L, Boggiano MK, Sanchez C, Turrin CO, Caminade AM, Majoral JP (2000) New mesotextured hybrid materials made from assemblies of dendrimers and titanium(IV)-oxo-organo clusters. Angew Chem Int Ed 39:4250–4254
55. Bouchara A, Rozes L, Soler-Illia GJD, Sanchez C, Turrin CO, Caminade AM, Majoral JP (2003) Use of functional dendritic macromolecules for the design of metal oxo based hybrid materials. J Sol Gel Sci Technol 26:629–633
56. Marmillon C, Gauffre F, Gulik-Krzywicki T, Loup C, Caminade AM, Majoral JP, Vors JP, Rump E (2001) Organophosphorus dendrimers as new gelators for hydrogels. Angew Chem Int Ed 40:2626–2629
57. Larpent C, Genies C, Delgado APD, Caminade AM, Majoral JP, Sassic JF, Leising F (2004) Giant dendrimer-like particles from nanolatexes. Chem Commun 1816–1817
58. El Ghzaoui A, Gauffre F, Caminade AM, Majoral JP, Lannibois-Drean H (2004) Self-assembly of water-soluble dendrimers into thermoreversible hydrogels and macroscopic fibers. Langmuir 20:9348–9353

59. Brauge L, Caminade AM, Majoral JP, Slomkowski S, Wolszczak M (2001) Segmental mobility in phosphorus-containing dendrimers. Studies by fluorescent spectroscopy. Macromolecules 34:5599–5606
60. Brauge L, Veriot G, Franc G, Deloncle R, Caminade AM, Majoral JP (2006) Synthesis of phosphorus dendrimers bearing chromophoric end groups: toward organic blue light-emitting diodes. Tetrahedron 62:11891–11899
61. Sebastian RM, Caminade AM, Majoral JP, Levillain E, Huchet L, Roncali J (2000) Electrogenerated poly(dendrimers) containing conjugated poly(thiophene) chains. Chem Commun 507–508
62. Le Derf F, Levillain E, Trippe G, Gorgues A, Salle M, Sebastian RM, Caminade AM, Majoral JP (2001) Immobilization of redox-active ligands on an electrode: the dendrimer route. Angew Chem Int Ed 40:224–227
63. Kanibolotsky A, Roquet S, Cariou M, Leriche P, Turrin CO, de Bettignies R, Caminade AM, Majoral JP, Khodorkovsky V, Gorgues A (2004) Does charge carrier dimensionality increase in mixed-valence salts of tetrathiafulvalene-terminated dendrimers? Org Lett 6:2109–2112
64. Alonso B, Alonso E, Astruc D, Blais JC, Djakovitch L, Fillaut JL, Nlate S, Moulines F, Rigaut S, Ruiz J, Valério C (2002) Dendrimers containing ferrocenyl or other transition metal sandwich groups. Adv Dendritic Macromol 5:89–127
65. Turrin CO, Chiffre J, Daran JC, de Montauzon D, Caminade AM, Manoury E, Balavoine G, Majoral JP (2001) New chiral phosphorus-containing dendrimers with ferrocenes on the periphery. Tetrahedron 57:2521–2536
66. Turrin CO, Donnadieu B, Caminade AM, Majoral JP (2005) Organometallic derivatives at the core of phosphorus-containing dendrimers. Z Anorg Allg Chem 631:2881–2887
67. Turrin CO, Chiffre J, Daran JC, de Montauzon D, Balavoine G, Manoury E, Caminade AM, Majoral JP (2002) New phosphorus-containing dendrimers with ferrocenyl units in each layer. CR Chim 5:309–318
68. Turrin CO, Chiffre J, de Montauzon D, Daran JC, Caminade AM, Manoury E, Balavoine G, Majoral JP (2000) Phosphorus-containing dendrimers with ferrocenyl units at the core, within the branches, and on the periphery. Macromolecules 33:7328–7336
69. Turrin CO, Chiffre J, de Montauzon D, Balavoine G, Manoury E, Caminade AM, Majoral JP (2002) Behavior of an optically active ferrocene chiral shell located within phosphorus-containing dendrimers. Organometallics 21:1891–1897
70. Decher G (1997) Fuzzy nanoassemblies: toward layered polymeric multicomposites. Science 277:1232–1237
71. Yu F, Ahl S, Caminade AM, Majoral JP, Knoll W, Erlebacher J (2006) Simultaneous excitation of propagating and localized surface plasmon resonance in nanoporous gold membranes. Anal Chem 78:7346–7350
72. Kim DH, Lee OJ, Barriau E, Li X, Caminade AM, Majoral JP, Frey H, Knoll W (2006) Hybrid organic-inorganic nanostructures fabricated from layer-by-layer self-assembled multilayers of hyperbranched polyglycerols and phosphorus dendrimers. J Nanosci Nanotechnol 6:3871–3876
73. Zhao WB, Park J, Caminade AM, Jeong SJ, Jang YH, Kim SO, Majoral JP, Cho J, Kim DH (2009) Localized surface plasmon resonance coupling in Au nanoparticles/phosphorus dendrimer multilayer thin films fabricated by layer-by-layer self-assembly method. J Mater Chem 19:2006–2012
74. Yu YM, Feng CL, Caminade AM, Majoral JP, Knoll W (2009) The detection of DNA hybridization on phosphorus dendrimer multilayer films by surface plasmon field enhanced-fluorescence spectroscopy. Langmuir 25:13680–13684
75. Kim BS, Lebedeva OV, Kim DH, Caminade AM, Majoral JP, Knoll W, Vinogradova OI (2005) Assembly and mechanical properties of phosphorus dendrimer/polyelectrolyte multilayer microcapsules. Langmuir 21:7200–7206
76. Kim BS, Lebedeva OV, Koynov K, Gong HF, Caminade AM, Majoral JP, Vinogradova OI (2006) Effect of dendrimer generation on the assembly and mechanical properties of DNA/phosphorus dendrimer multilayer microcapsules. Macromolecules 39:5479–5483

77. Feng CL, Caminade AM, Majoral JP (2010) Selective encapsulation of dye molecules in microcapsules by DNA hybridization. J Mat Chem 20:1438–1441
78. Caminade AM, Majoral JP (2010) Dendrimers and nanotubes: a fruitful association. Chem Soc Rev 39:2034–2047
79. Kim DH, Karan P, Goring P, Leclaire J, Caminade AM, Majoral JP, Gosele U, Steinhart M, Knoll W (2005) Formation of dendrimer nanotubes by layer-by-layer deposition. Small 1:99–102
80. Feng CL, Zhong XH, Steinhart M, Caminade AM, Majoral JP, Knoll W (2007) Graded-bandgap quantum-dot-modified nanotubes: a sensitive biosensor for enhanced detection of DNA hybridization. Adv Mater 19:1933–1936
81. Feng CL, Zhong XH, Steinhart M, Caminade AM, Majoral JP, Knoll W (2008) Functional quantum-dot/dendrimer nanotubes for sensitive detection of DNA hybridization. Small 4:566–571
82. Martinez-Ferrero E, Franc G, Mazeres S, Turrin UO, Boissiere U, Caminade AM, Majoral JP, Sanchez C (2008) Optical properties of hybrid dendritic-mesoporous titania nanocomposite films. Chem Eur J 14:7658–7669
83. Caminade AM, Padie C, Laurent R, Maraval A, Majoral JP (2006) Uses of dendrimers for DNA microarrays. Sensors 6:901–914
84. Miksa B, Slomkowski S, Chehimi MM, Delamar M, Majoral JP, Caminade AM (1999) Tailored modification of quartz surfaces by covalent immobilization of small molecules (gamma-aminopropyltriethoxysilane), monodisperse macromolecules (dendrimers), and poly(styrene/acrolein/divinylbenzene) microspheres with narrow diameter distribution. Colloid Polym Sci 277:58–65
85. Slomkowski S, Miksa B, Chehimi MM, Delamar M, Cabet-Deliry E, Majoral JP, Caminade AM (1999) Inorganic-organic systems with tailored properties controlled on molecular, macromolecular and microscopic level. React Funct Polym 41:45–57
86. Le Berre V, Trevisiol E, Dagkessamanskaia A, Sokol S, Caminade AM, Majoral JP, Meunier B, Francois J (2003) Dendrimeric coating of glass slides for sensitive DNA microarrays analysis. Nucleic Acids Res 31:e88
87. Trevisiol E, Le Berre-Anton V, Leclaire J, Pratviel G, Caminade AM, Majoral JP, Francois JM, Meunier B (2003) Dendrislides, dendrichips: a simple chemical function-alization of glass slides with phosphorus dendrimers as an effective means for the preparation of biochips. New J Chem 27:1713–1719
88. Chaize B, Nguyen M, Ruysschaert T, le Berre V, Trevisiol E, Caminade AM, Majoral JP, Pratviel G, Meunier B, Winterhalter M, Fournier D (2006) Microstructured liposome array. Bioconjugate Chem 17:245–247
89. Nicu L, Guirardel M, Chambosse F, Rourgerie P, Sinh S, Trevisiol E, Francois JM, Majoral JP, Caminade AM, Cattan E, Bergaud C (2005) Resonating piezoelectric membranes for microelectromechanically based bioassay: detection of streptavidin-gold nanoparticles interaction with biotinylated DNA. Sensors Actuator B Chem 110:125–136
90. Boas U, Heegaard PMH (2004) Dendrimers in drug research. Chem Soc Rev 33:43–63
91. Svenson S, Tomalia DA (2005) Commentary—dendrimers in biomedical applications—reflections on the field. Adv Drug Delivery Rev 57:2106–2129
92. Duncan R, Izzo L (2005) Dendrimer biocompatibility and toxicity. Adv Drug Delivery Rev 57:2215–2237
93. Lee CC, MacKay JA, Frechet JMJ, Szoka FC (2005) Designing dendrimers for biological applications. Nat Biotechnol 23:1517–1526
94. Caminade AM, Turrin CO, Majoral JP (2008) Dendrimers and DNA: combinations of two special topologies for nanomaterials and biology. Chem Eur J 14:7422–7432
95. Rolland O, Turrin CO, Caminade AM, Majoral JP (2009) Dendrimers and nanomedicine: multivalency in action. New J Chem 33:1809–1824
96. Picart C, Elkaim R, Richert L, Audoin F, Arntz Y, Cardoso MDS, Schaaf P, Voegel JC, Frisch B (2005) Primary cell adhesion on RGD-functionalized and covalently crosslinked thin polyelectrolyte multilayer films. Adv Funct Mater 15:83–94

97. Hernandez-Lopez JL, Khor HL, Caminade AM, Majoral JP, Mittler S, Knoll W, Kim DH (2008) Bioactive multilayer thin films of charged N,N-disubstituted hydrazine phosphorus dendrimers fabricated by layer-by-layer self-assembly. Thin Solid Films 516:1256–1264
98. Caminade AM, Hameau A, Majoral JP (2009) Multicharged and/or water-soluble fluorescent dendrimers: properties and uses. Chem Eur J 15:9270–9285
99. Denk W, Strickler JH, Webb WW (1990) Two-photon laser scanning fluorescence microscopy. Science 248:73–76
100. Larson DR, Zipfel WR, Williams RM, Clark SW, Bruchez MP, Wise FW, Webb WW (2003) Water-soluble quantum dots for multiphoton fluorescence imaging in vivo. Science 300:1434–1436
101. Mongin O, Pla-Quintana A, Terenziani F, Drouin D, Le Droumaguet C, Caminade AM, Majoral JP, Blanchard-Desce M (2007) Organic nanodots for multiphotonics: synthesis and photophysical studies. New J Chem 31:1354–1367
102. Mongin O, Krishna TR, Werts MHV, Caminade AM, Majoral JP, Blanchard-Desce M (2006) A modular approach to two-photon absorbing organic nanodots: brilliant dendrimers as an alternative to semiconductor quantum dots? Chem Commun 915–917
103. Terenziani F, Parthasarathy V, Pla-Quintana A, Maishal T, Caminade AM, Majoral JP, Blanchard-Desce M (2009) Cooperative two-photon absorption enhancement by through-space interactions in multichromophoric compounds. Angew Chem Int Ed 48:8691–8694
104. Krishna TR, Parent M, Werts MHV, Moreaux L, Gmouh S, Charpak S, Caminade AM, Majoral JP, Blanchard-Desce M (2006) Water-soluble dendrimeric two-photon tracers for in vivo imaging. Angew Chem Int Ed 45:4645–4648
105. Mongin O, Rouxel C, Robin AC, Pla-Quintana A, Krishna TR, Recher G, Tiaho F, Caminade AM, Majoral JP, Blanchard-Desce M (2008) Brilliant organic nanodots: novel nano-objects for bionanophotonics. Proc SPIE-Int Soc Opt Eng. Nanobiosystems: Processing, Characterization, and Applications 7040:4006
106. Goller R, Vors JP, Caminade AM, Majoral JP (2001) Phosphorus dendrimers as new tools to deliver active substances. Tetrahedron Lett 42:3587–3590
107. Loup C, Zanta MA, Caminade AM, Majoral JP, Meunier B (1999) Preparation of water-soluble cationic phosphorus-containing dendrimers as DNA transfecting agents. Chem Eur J 5:3644–3650
108. Maszewska M, Leclaire J, Cieslak M, Nawrot B, Okruszek A, Caminade AM, Majoral JP (2003) Water-soluble polycationic dendrimers with a phosphoramidothioate backbone: preliminary studies of cytotoxicity and oligonucleotide/plasmid delivery in human cell culture. Oligonucleotides 13:193–205
109. Padie C, Maszewska M, Majchrzak K, Nawrot B, Caminade AM, Majoral JP (2009) Polycationic phosphorus dendrimers: synthesis, characterization, study of cytotoxicity, complexation of DNA, and transfection experiments. New J Chem 33:318–326
110. Kazmierczak-Baranska J, Pietkiewicz A, Janicka M, Wei Y, Turrin CO, Majoral JP, Nawrot B, Caminade AM (2010) Synthesis of a fluorescent cationic phosphorus dendrimer and preliminary biological studies of its interaction with DNA. Nucleosides, Nucleotides and Nucleic Acids 29:155–167
111. Prusiner SB (1982) Novel proteinaceous infectious particles cause scrapie. Science 216:136–144
112. Solassol J, Crozet C, Perrier V, Leclaire J, Beranger F, Caminade AM, Meunier B, Dormont D, Majoral JP, Lehmann S (2004) Cationic phosphorus-containing dendrimers reduce prion replication both in cell culture and in mice infected with scrapie. J Gen Virol 85:1791–1799
113. Klajnert B, Cortijo-Arellano M, Cladera J, Majoral JP, Caminade AM, Bryszewska M (2007) Influence of phosphorus dendrimers on the aggregation of the prion peptide PrP 185–208. Biochem Biophys Res Commun 364:20–25

114. Klajnert B, Cangiotti M, Calici S, Ionov M, Majoral JP, Caminade AM, Cladera J, Bryszewska M, Ottaviani MF (2009) Interactions between dendrimers and heparin and their implications for the anti-prion activity of dendrimers. New J Chem 33:1087–1093
115. Klajnert B, Cangiotti M, Calici S, Majoral JP, Caminade AM, Cladera J, Bryszewska M, Ottaviani MF (2007) EPR study of the interactions between dendrimers and peptides involved in Alzheimer's and prion diseases. Macromol Biosci 7:1065–1074
116. Blanzat M, Turrin CO, Perez E, Rico-Lattes I, Caminade AM, Majoral JP (2002) Phosphorus-containing dendrimers bearing galactosylceramide analogs: Self-assembly properties. Chem Commun 1864–1865
117. Blanzat M, Turrin CO, Aubertin AM, Couturier-Vidal C, Caminade AM, Majoral JP, Rico-Lattes I, Lattes A (2005) Dendritic catanionic assemblies: in vitro anti-HIV activity of phosphorus-containing dendrimers bearing Gal beta(1)cer analogues. Chem Bio Chem 6:2207–2213
118. Pérez-Anes A, Spataro G, Coppel Y, Blanzat M, Turrin C-O, Moog C, Caminade A-M, Rico-Lattes I, Majoral J-P (2009) Phosphonate terminated PPH dendrimers: influence of pendant alkyl chains on the in vitro anti-HIV1 properties. Org Biomol Chem 7:3491–3498
119. Pérez-Anes A, Stefaniu C, Moog C, Majoral JP, Blanzat M, Turrin CO, Caminade AM, Rico-Lattes I (2010) Multivalent catanionic GalCer analogs derived from first generation dendrimeric phosphonic acids. Bioorg Med Chem 18:242–248
120. Spataro G, Malecaze F, Turrin CO, Soler V, Duhayon C, Elena PP, Majoral JP, Caminade AM (2010) Designing dendrimers for ocular drug delivery. Eur J Med Chem 45:326–334
121. Kunzmann V, Bauer E, Feurle J, Weissinger F, Tony HP, Wilhelm M (2000) Stimulation of $\gamma\delta$ T cells by aminobisphosphonates and induction of antiplasma cell activity in multiple myeloma. Blood 96:384–392
122. Poupot M, Griffe L, Marchand P, Maraval A, Rolland O, Martinet L, L'Faqihi-Olive FE, Turrin CO, Caminade AM, Fournie JJ, Majoral JP, Poupot R (2006) Design of phosphorylated dendritic architectures to promote human monocyte activation. FASEB J 20:2339–2351
123. Fruchon S, Poupot M, Martinet L, Turrin CO, Majoral JP, Fournie JJ, Caminade AM, Poupot R (2009) Anti-inflammatory and immunosuppressive activation of human monocytes by a bioactive dendrimer. J Leukocyte Biol 85:553–562
124. Rolland O, Griffe L, Poupot M, Maraval A, Ouali A, Coppel Y, Fournie JJ, Bacquet G, Turrin CO, Caminade AM, Majoral JP, Poupot R (2008) Tailored control and optimisation of the number of phosphonic acid termini on phosphorus-containing dendrimers for the ex vivo activation of human monocytes. Chem Eur J 14:4836–4850
125. Griffe L, Poupot M, Marchand P, Maraval A, Turrin CO, Rolland O, Metivier P, Bacquet G, Fournie JJ, Caminade AM, Poupot R, Majoral JP (2007) Multiplication of human natural killer cells by nanosized phosphonate-capped dendrimers. Angew Chem Int Ed 46: 2523–2526
126. Marchand P, Griffe L, Poupot M, Turrin CO, Bacquet G, Fournie JJ, Majoral JP, Poupot R, Caminade AM (2009) Dendrimers ended by non-symmetrical azadiphosphonate groups: synthesis and immunological properties. Bioorg Med Chem Lett 19:3963–3966
127. Portevin D, Poupot M, Rolland O, Turrin CO, Fournie JJ, Majoral JP, Caminade AM, Poupot R (2009) Regulatory activity of azabisphosphonate-capped dendrimers on human CD4(+) T cell proliferation enhances ex vivo expansion of NK cells from PBMCs for immunotherapy. J Transl Med 7:82
128. Caminade AM, Laurent R, Turrin CO. Rebout C, Delavaux-Nicot B, Ouali A, Zablocka M, Majoral JP (2010) Phosphorus dendrimers as viewed by ^{31}P NMR spectroscopy; synthesis and characterization. CR Chim 13:1006–1027
129. Lartigue ML, Slany M, Caminade AM, Majoral JP (1996) Phosphorus containing dendrimers. Synthesis of multi-tri or tetra-functionalized macromolecules. Chem Eur J 2:1417–1426

Chapter 10
Chiral Phosphorus Ligands for Enantioselective Enyne Cycloisomerizations

Angela Marinetti and Delphine Brissy

Abstract This review intends to highlight the role of phosphorus ligands as chiral auxiliaries in enantioselective enyne cycloisomerizations. A few examples of cycloisomerizations involving polyunsaturated substrates are also discussed. Cycloisomerizations processes are known to follow a variety of reaction pathways according to the nature of the starting materials and the metal used as the catalyst. This implies a specific catalyst design for each class of reactions. Bidentate C2-symmetric diphosphines are the preferred chiral auxiliaries in rhodium and palladium promoted Alder-ene type cyclizations, which are so far the most deeply investigated enantioselective processes. Also, enantioselective variants of cyclizations involving electrophilic activation of the alkyne unit have been reported recently. They have been carried out under Ir, Pt and Au catalysis, by using both bidentate and monodentate chiral phosphines as the ligands. Overall, this literature overview points out the very early stage of development of the field.

10.1 Introduction

Enyne cycloisomerizations are metal promoted rearrangements in which a substrate bearing an alkene and an alkyne unit is isomerised into a cyclic moiety, with no (formal) loss or gain of any atoms. They represent useful catalytic methods for the synthesis of carbo- and heterocycles of increased structural complexity, from relatively simple, acyclic starting materials. These reactions have attracted much attention mainly because of the diversity of molecular scaffolds that they produce.

A. Marinetti (✉) · D. Brissy
Institut de Chimie des Substances Naturelles – CNRS UPR 2301,
Av. de la Terrasse, 91198 Gif-sur-Yvette Cedex, France
e-mail: angela.marinetti@icsn.cnrs-gif.fr

M. Peruzzini and L. Gonsalvi (eds.), *Phosphorus Compounds*,
Catalysis by Metal Complexes, 37, DOI: 10.1007/978-90-481-3817-3_10,
© Springer Science+Business Media B.V. 2011

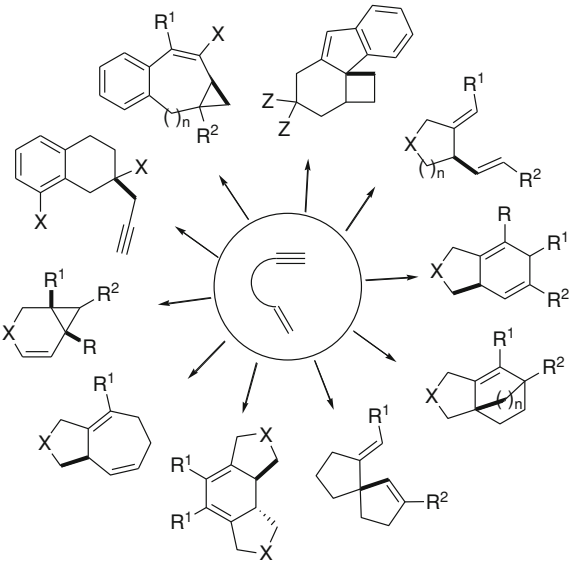


Fig. 10.1 Representative molecular scaffolds produced by enantioselective enyne cycloisomerization reactions

Under transition metal catalysis, different types of skeletal rearrangement can take place indeed, where the original connectivity along the enyne chain can be maintained or not, as a function of the substrate and the catalyst used [1–4]. High selectivity and efficiency are often realized. The field has been exhaustively reviewed in recent papers [5–8]. Surprisingly, asymmetric variants of these reactions [9] are comparatively underdeveloped, in spite of their potential synthetic utility for the construction of chiral cyclic moieties.

This review summarizes recent studies in this field, namely recent investigations on enantioselective enyne cycloisomerizations promoted by Pd, Rh, Pt, Au and Ir complexes bearing chiral phosphorus ligands. The main molecular scaffolds that are produced through these processes are displayed in Fig. 10.1 hereafter.

Tandem reactions combining enyne cycloisomerizations with other processes, induced by additional reactants, are not handled in this paper [10–15].

10.2 Palladium-Catalysed Cycloisomerizations

10.2.1 Alder-Ene Type Cyclizations

Alder-ene cyclizations involve enyne substrates with an allylic hydrogen at the olefinic termini. The pioneering work of Trost initially demonstrated that palladium acetate efficiently promote intramolecular Alder-ene type reactions of 1,6- and 1,7-enynes, leading to 5- or 6-membered rings with exocyclic methylene bonds (Fig. 10.2) [16]. These processes generate a tetrahedral stereogenic centre from a planar sp^2-carbon in the starting material. Therefore, asymmetric variants

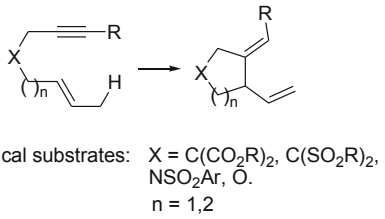


Fig. 10.2 Alder-ene type cycloisomerizations

of these reactions allow the enantioselective construction of intracyclic tertiary or quaternary stereogenic centres.

In the early 90s, Trost demonstrated the catalytic activity of phosphine modified palladium catalysts and also reported the first attempts of setting such asymmetric protocols. These initial experiments involved the use of chiral acid additives in conjunction with Pd(0)/PPh_3 catalysts. (*S*)-Binaphtoic acid was shown to facilitate the reaction as well as to achieve a moderate but encouraging 33% enantiomeric excess in the cycloisomerization of a model substrate [17]. Asymmetric induction could be improved later by using chiral bidentate phosphorus ligands, instead of chiral acids, in the $Pd_2(dba)_3$ [dba = dibenzylidene acetone] promoted reaction shown in Fig. 10.3 [18]. Thus, the Trost's bicyclic diphosphine **L1** first allowed a 50% enantiomeric excess to be attained in example (1), Fig. 10.3. The success of this amidodiphosphane auxiliary, as well as the beneficial effect of acid additives, inspired then the specific design of the C_2-symmetric ligand **L2** which combines a diphosphine function and a carboxylic acid unit. The Pd/**L2** catalyst promoted the ene-type cycloisomerization of an optically active substrate (example 2 in Fig. 10.3) with a good level of diastereoselectivity (52% d.e.). The chiral

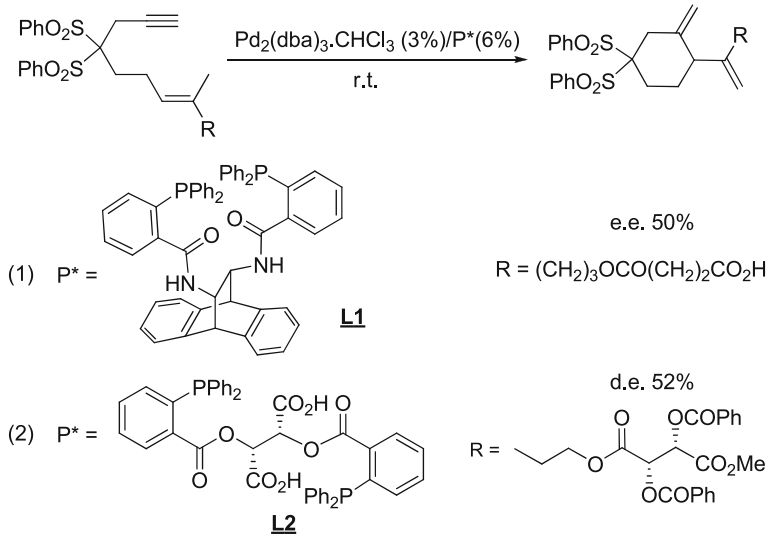
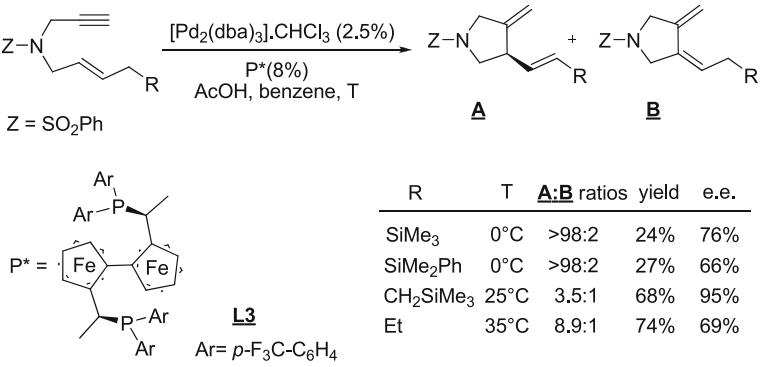


Fig. 10.3 Trost's approach to enantioselective Pd-promoted ene-type cycloisomerizations [18]



R	T	A:B ratios	yield	e.e.
$SiMe_3$	0°C	>98:2	24%	76%
$SiMe_2Ph$	0°C	>98:2	27%	66%
CH_2SiMe_3	25°C	3.5:1	68%	95%
Et	35°C	8.9:1	74%	69%

Fig. 10.4 Representative ene-type isomerizations promoted by TRAP–palladium complexes [19]

phosphorus ligand, and not the chiral substrate, was shown to determine the stereochemistry in this double stereodifferentiation process.

Following to these initial disclosures, in 1996 Ito et al. reported on the first highly successful ene-type cyclizations [19]. Substrates are enynes bearing sulfonamide functions in the tethering chain. Pd^{II} complexes of the trans-coordinating TRAP ligands (**L3**) were generated from $Pd_2(dba)_3$ in the presence of acids. They were found to be particularly effective catalysts, giving good conversion rates in mild conditions (r.t. to 40 °C) and moderate to high enantiomeric excesses (up to 95%). The reactions afforded mainly mixtures of two regioisomeric 1,4- and 1,3-dienes (**A** and **B** in Fig. 10.4).

The challenge of attaining high levels of asymmetric induction as well as high yields in ene-type carbocyclisations was achieved then by Mikami et al. [20] by using catalysts generated in situ from $Pd(O_2CCF_3)_2$ or $(MeCN)_4Pd(BF_4)_2$ and atropisomeric diphosphines such as BINAP, Tol-BINAP, H_8-BINAP, SEGPHOS and Xylyl–SEGPHOS. Especially, the SEGPHOS ligands **L4** attained a nearly perfect enantioselectivity in the Alder-ene cycloisomerization of the 1,6-enyne shown in Fig. 10.5, which displays an ether function in the tethering chain. (*R*)-Configured atropisomeric diphosphines afforded (*S*)-configured tetrahydrofurane moieties.

The postulated mechanism involves palladium(II) hydride complexes as the catalytically active species. They are assumed to initiate the cycloisomerization process through hydrometalation of the acetylenic unit, which converts the intermediate π-complex **I** into the σ-bonded complex **II** (Fig. 10.6). The subsequent step is the conversion of **II** into the cyclic species **III** by carbometalation of the olefin function. This step creates the stereogenic carbon.

The substrate scope of the SEGPHOS–palladium promoted reactions proved to be very restricted, however. This motivated the search for new catalytic systems and the design of more appropriate phosphorus ligands. Thus, C_1-symmetric PN ligands, **L5a**, which combine axially chiral binaphthylphosphine and chiral

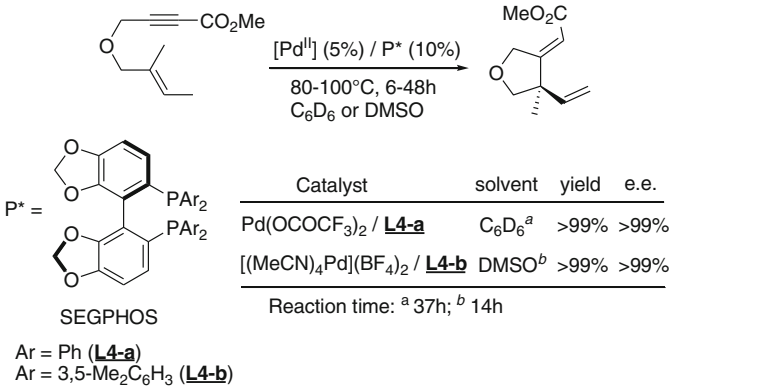


Fig. 10.5 Mikami's catalysts for the enantioselective ene-type cycloisomerizations of a 1,6-enyne [20]

oxazoline units were envisioned as potentially suitable ligands. Ligand **L5-a** showed to be indeed a very effective promoter for the cycloisomerization of a wider range of 1,6-enynes, giving higher enantioselectivity levels than the previously used atropisomeric diphosphines (Fig. 10.7) [21].

From these experiments it appeared that only the axial chirality of the binaphthyl scaffold of **L5-a** is responsible for the chiral induction. Therefore, the simplified ligand **L5-b** could be developed which displays an achiral gem-dimethyl substituted oxazoline ring (Fig. 10.7). This specifically designed ligand performs as good as, or even better than the analogous phosphino-oxazolines bearing two chirality elements. Authors also demonstrated that the double substitution of the 4-position of the oxazoline unit in **L5-b** is essential to the stereochemical control of the cycloisomerization reaction.

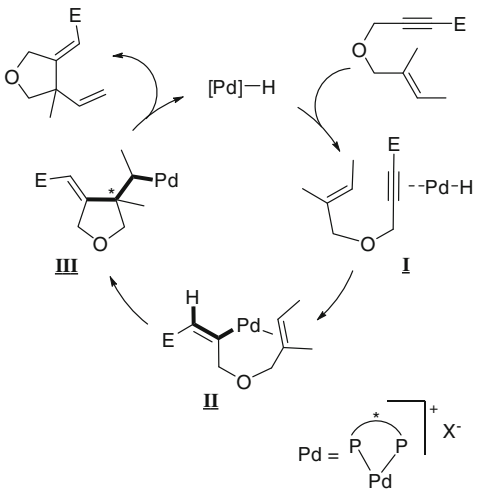
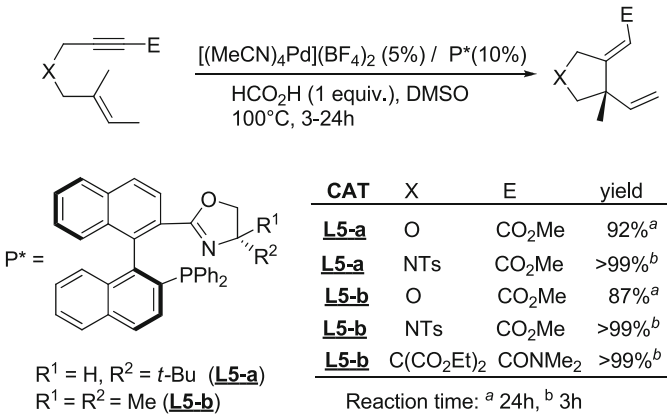


Fig. 10.6 Postulated catalytic cycle for the Pd-promoted Alder-ene type cycloisomerization of 1,6-enynes



CAT	X	E	yield	e.e.
L5-a	O	CO_2Me	92%[a]	87%
L5-a	NTs	CO_2Me	>99%[b]	92%
L5-b	O	CO_2Me	87%[a]	88%
L5-b	NTs	CO_2Me	>99%[b]	93%
L5-b	$C(CO_2Et)_2$	$CONMe_2$	>99%[b]	95%

Reaction time: [a] 24h, [b] 3h

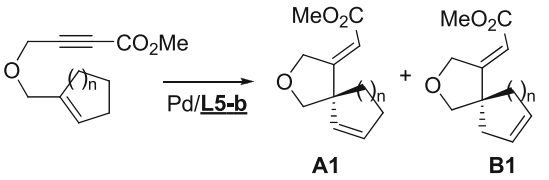
Fig. 10.7 Ene-type isomerizations of 1,6-enynes promoted by a phosphine–oxazoline palladium complex [21]

Ligand **L5-b** has been applied to the cycloisomerization of 1,6-enynes with both oxygen- and nitrogen-containing tethering chain, as well as of enynes with simple carbon chains, leading to the desired cyclopentenes in high yields and enantioselectivities up to 95% ee.

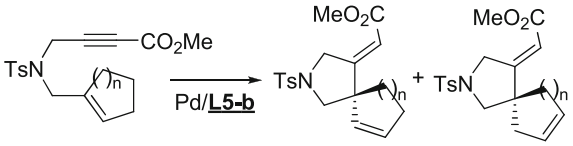
The same catalytic system **L5-b** displayed high efficiency in the enantioselective cyclization of the allyl propargyl ethers and sulfonamides shown in Fig. 10.8, where the alkene function is embedded into a cyclic unit. Propargyl ethers led to the expected spirocyclic derivatives **A1** together with the isomeric side product **B1** which results from double bond migration under palladium catalysis. The enantiomeric excesses of both **A1** and **B1** are in the range 80–90% [22]. Notably, the 15-membered ring system ($n = 11$) afforded the non-isomerized product **A1** as the single isomer, in almost quantitative yield and high enantiomeric excess (83%).

Likewise, the cycloisomerization of the sulfonamide tethered substrates resulted in an efficient synthesis of the spiro-alkaloids **A2** and/or **B2** of various ring sizes, with excellent enantioselectivities and high yields [23]. In this case also, product selectivity depends on the ring size of the cyclic olefin moiety: the 15 membered cyclic substrate ($n = 11$) and the cyclopentene derivative ($n = 1$) afford isomers **A2** selectively, while **B2** is the major product obtained from a cycloheptene derivative ($n = 3$).

The first highly enantioselective synthesis of 6-membered rings via ene-type cyclizations of 1,7-enynes has been reported by Mikami and Hatano [10]. Six-membered rings being more difficult to form than 5-membered derivatives, the only suitable substrates proved to be enynes with *ortho*-substituted benzene scaffolds in the tethering chain (Fig. 10.9). Starting from tosylamides of this class, cationic, BINAP-based palladium catalysts allowed the synthesis of quinolines with quaternary stereogenic carbons, as single enantiomers and in quantitative yields. These reactions were performed in DMSO, in the presence of formic acid.



n	**A1**: yield (e.e.)	**B1**: yield (e.e.)
1	88 (88%)	7
2	63 (84%)	20 (31%)
3	13 (88%)	78 (83%)
4	33 (93%)	61 (80%)
11	>90 (83%)	0



n	**A2**: yield (e.e.)	**B2**: yield (e.e.)
1	90 (96%)	9
2	71 (84%)	29 (35%)
3	6 (95%)	93 (95%)
4	25 (92%)	70 (91%)
11	>95 (84%)	0

Fig. 10.8 Ene-type spirocyclization of 1,6-enyne ethers and tosylamides promoted by the palladium-phosphino-oxazoline complexes **L5-b** (see Fig. 10.7) [22, 23]

Among others, quinolines with spirocyclic structures have been prepared from enynes bearing cyclic olefin units. Very high enantiomeric excesses have been obtained starting from either tetrahydropyran (99% e.e., Eq. (b) in Fig. 10.9) or

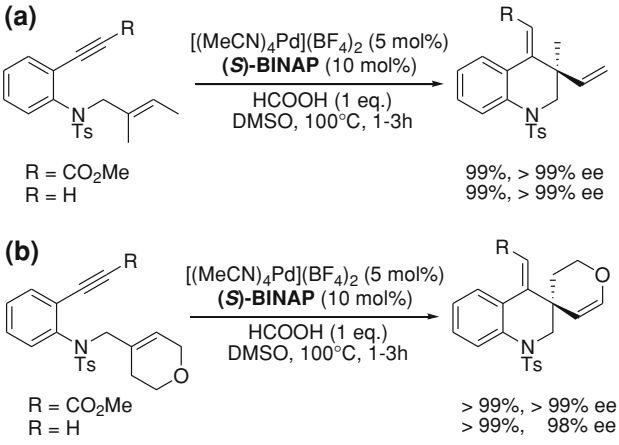


Fig. 10.9 Synthesis of quinolines via Pd-BINAP promoted ene-type cycloisomerizations [10]

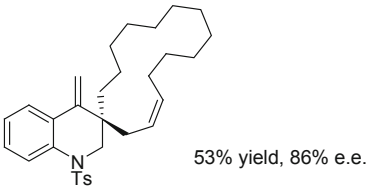


Fig. 10.10 Spiro-macrocyclic quinoline from BINAP-Pd promoted ene-type cyclization [10]

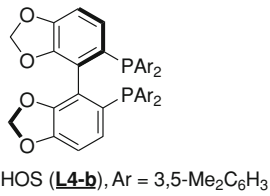
macrocyclic olefins (Fig. 10.10). However, when the olefin function was included in a 5-membered ring, the enantioselectivity level was comparatively low (44–71% e.e.) since an olefin migration processes induced partial racemization of the final product.

10.2.2 Miscellaneous Cyclizations

Beside ene-type cyclizations, chiral phosphine–palladium complexes have been applied to only a few cycloisomerization processes, leading to 6-membered compounds. In all these reactions SEGPHOSs are the preferred ligands (Fig. 10.11).

Thus, for instance, Mikami et al. reported on the enantioselective formation of a tetrahydropyrane ring from the 1,6-enyne in Fig. 10.12. The reaction is assumed to proceed via the same initial key steps as for the ene-type cycloisomerizations shown in Fig. 10.6, that are the generation of a Pd-hydride complex, hydropalladation of the alkyne and subsequent carbopalladation of the olefin unit leading to **III**. The two processes differ from each other in the final rearrangement paths of intermediates **III**, since in the reaction of Fig. 10.12 the phenyl substituent on the olefin unit prevents β-elimination to take place. In this rearrangement, Binap and SEGPHOS palladium(II) complexes displayed moderate efficiency, giving e.e.s of only 26 and 56%, respectively. However, the enantioselectivity could be increased up to a 76% e.e. by using the sterically more demanding (*S*)-xylyl-SEGPHOS ligand [24].

Finally, a conceptually new approach is the application of cycloisomerization processes to the enantioselective synthesis of axially chiral compounds. The method has been introduced by Tanaka [25]. It involves 1,5-enynes with an



Xylyl-SEGPHOS (**L4-b**), Ar = 3,5-$Me_2C_6H_3$

Fig. 10.11 Molecular structure of SEGPHOS ligands

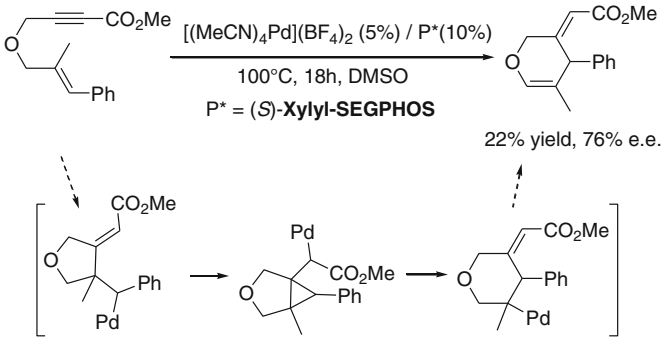


Fig. 10.12 Enantioselective formation of a tetrahydropyran ring from a 1,6-enyne, promoted by a Pd-Xylyl–SEGPHOS catalyst [24]

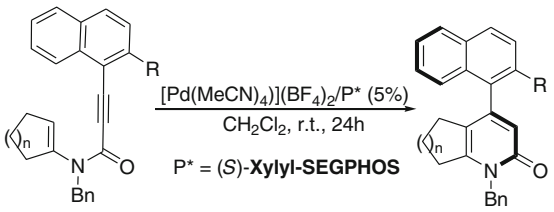
amido group as the connecting chain and an aryl group at the alkyne terminus. *N*-alkenyl ethynylamides are converted into 1-naphthyl substituted 2-pyridones with high e.e. values by using Pd^{II}-(*S*)-Xylyl-SEGPHOS complexes as the catalysts (Fig. 10.13). BINAP and H_8-BINAP afforded lower but still satisfying levels of enantioselectivity (81 and 89%, e.e. respectively) in the cycloisomerization of the amide substrate in Fig. 10.13 (for R = OMe and $n = 2$).

In addition to naphthyl substituted alkynes, 2-methoxy-tetrahydronaphthalen-1-yl- and 2-methoxy-6-methylphenyl alkynes were shown to be suitable substrates affording the corresponding pyridones with e.e.s >90%.

The six-membered rings are assumed to be formed via π-complexation of the triple bond by the electrophilic metal complex, followed by a nucleophilic attack of the olefin moiety on the activated alkyne (Fig. 10.14) and a subsequent H-migration step. The electrophilic activations of enynes by π-complexation are common cycloisomerization pathways especially for platinum and gold catalysts. Other examples are presented in Sects. 10.4 and 10.5 of this book.

Tentative rationales for the chiral induction have been provided so far based on qualitative models only. It is reasonably assumed that the close proximity between

Fig. 10.13 Enantioselective construction of axially chiral compounds by enyne cycloisomerization [25]



n	R	yield	e.e.
1	OMe	93%	91%
2	OMe	96%	94%
2	Me	77%	51%

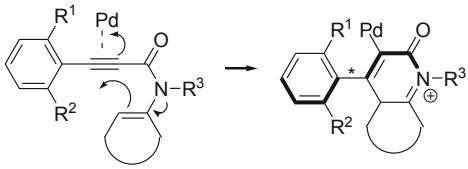


Fig. 10.14 Key intermediates in the cycloisomerization of 1,5-enynes into axially chiral pyridones [25]

the chiral palladium complex and the aryl group adjacent to the triple bond may be a key for the observed enantiocontrol.

10.3 Rhodium-Catalysed Cycloisomerizations

10.3.1 Alder-ene Type Cyclizations

10.3.1.1 1,6-Enynes with Disubstituted Alkene Moieties

Rhodium complexes have been considered as suitable alternatives to palladium catalysts for the enantioselective Alder-ene type cyclizations of 1,6-enynes, following the initial disclosure by Zhang that cationic (diphosphine)$Rh^{+}SbF_6^{-}$ species are efficient achiral precatalysts [26]. The method has been applied to enynes bearing disubstituted *cis*-configured olefins and displaying both all-carbon and heteroatom (N or O) containing linkers.

The Rh-promoted Alder-ene cyclizations are assumed to be mechanistically different from the palladium promoted processes displayed in Sect. 10.2, Fig. 10.6. Unlike palladium-catalyzed pathways, the postulated rhodium-promoted catalytic cycle (Fig. 10.15) does not involve Rh hydride intermediates [16, 27]. The C–C bond is formed via an oxidative coupling which converts **I** into the metallacyclic intermediate **II**. This step generates the stereogenic carbon centre.

The first significant advance toward enantioselective reactions was made in 2000 by Zhang and Cao who achieved chemo-, regio- and enantioselective cycloisomerizations of enynes with oxygen functions in the tethering chain. In these initial studies DuPHOS, BICP ligands had been used [28]. Despite the high levels of asymmetric induction obtained with these diphosphines, further screening proved the superior role of atropisomeric diphosphines such as BINAP or Tunaphos (Fig. 10.16) [29].

Zhang demonstrated that with BINAP as the ligand, the choice of the rhodium precursor is crucial with respect to catalytic activity issues. Thus, the preformed $[(BINAP)RhCl]_2$ complex was inactive, while a catalyst formed in situ from $[Rh(cod)Cl]_2$ and $AgSbF_6$ displayed an excellent catalytic activity: total conversion was attained after only 5 min at room temperature. Almost total enantioselectivities were achieved with most tested substrates, including enynes with functional groups (keto-, hydroxyl- and ester functions) on either the alkyne or the

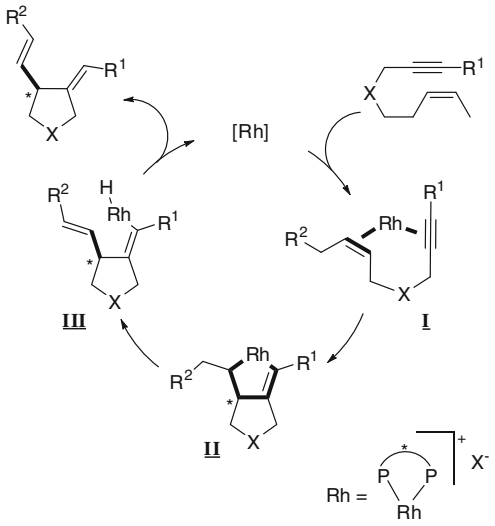
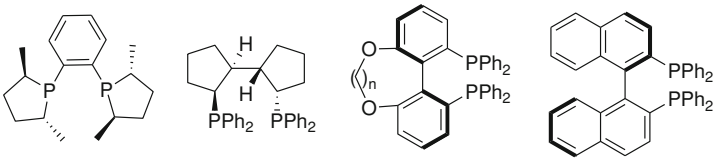
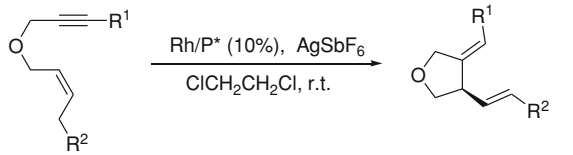


Fig. 10.15 Postulated mechanism for the Rh-promoted Alder-ene cyclization of 1,6-enynes





		yield (e.e.)			
R^1	R^2	DuPHOS[a]	BICP[a]	Tunaphos[b]	BINAP[b]
Ph	H	62 (96%)	73 (74%)		96 (>99.5%)
p-Cl-Ph	H	60 (95%)	24 (83%)	100[c] (>99.9%)	95 (>99.9%)
Bu	H		67 (98%)		89 (>99.9%)
Me	Me				82 (>99.9%)
COPh	Me				99 (>99.9%)
CH_2OH	Me				81 (>99.9%)
Me	OAc				92 (>99.9%)

[a] Rh/P* = $[Rh(P^*)Cl]_2$. [b] $[Rh(cod)Cl]_2$ + P* [c] Conversion rate

Fig. 10.16 Enantioselective synthesis of functionalized tetrahydrofuranes by rhodium promoted Alder-ene type rearrangements of 1,6-enynes [28, 29]

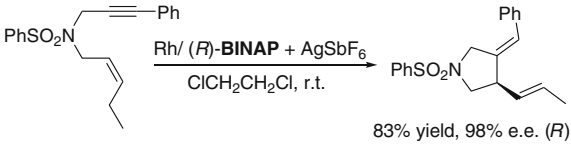


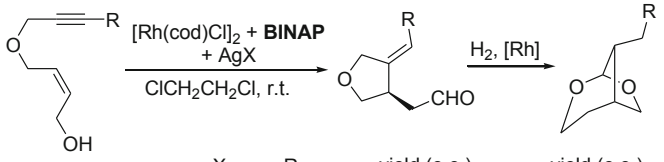
Fig. 10.17 Rh-BINAP promoted Alder-ene cycloisomerization of a sulfonamide tethered enyne [30]

allylic terminus. Thus, the method enabled a highly effective and enantioselective access to a variety of 5-membered heterocycles.

The sense of chiral induction from the Rh-BINAP catalyst was determined by anomalous X-ray crystal diffraction on the 3-benzylidenepyrrolidine obtained by cycloisomerization of a *N*-2-pentenyl-N-(3-phenyl-2-propynyl)sulfonamide (Fig. 10.17). The results showed that the (*R*)-BINAP rhodium complex induces an (*R*)-configuration on the newly formed stereogenic center [30].

Interestingly, cycloisomerizations of 1,6-enynes with a hydroxyl group at the allylic terminus ($R^2 = OH$) generate aldehyde functionalities by virtue of the enol-aldehyde tautomerism in the final product (Fig. 10.18) [29]. The method has been extended recently to a range of 1,6-enynes with various aryl and heteroaryl substituents on the alkyne function, and applied then to a sequential cycloisomerization/isomerisation/hydrogenation/acetalization domino reaction leading to the bicyclic acetals displayed in Fig. 10.18. The rhodium catalyst is assumed to promote the initial cycloisomerization step as well as the isomerisation/hydrogenation process [31].

In later work, Zhang also examined the reactivity of ether substrates with additional substituents at the allylic position (Fig. 10.19) [32] and demonstrated that an highly effective kinetic resolution process takes place in the presence of rhodium/BINAP catalysts. In these cycloisomerization processes, the initial kinetic resolution coupled with a diastereoselective cyclization step allow the synthesis of tetrahydrofurans with two adjacent stereogenic centres, with excellent e.e. and conversion rates. In the representative reaction shown in Fig. 10.19, the *S*-configured BINAP matches the *2R*-configured enyne substrate which is thus quantitatively converted into the expected tetrahydrofurane. The *2S*-configured substrate remains unchanged.



X	R	yield (e.e.)	yield (e.e.)
SbF_6	Ph	98 (99%)	
SbF_6	Me	94 (99.1%)	
BF_4	Ph		69 (>99%)
BF_4	*p*-MeOPh		38 (>99%)
BF_4	*p*-BrPh		54 (>99%)

Fig. 10.18 Cycloisomerizations of 1,6-enynes substituted by an OH function at the allylic terminus [29], and subsequent synthesis of bicyclic acetals [31]

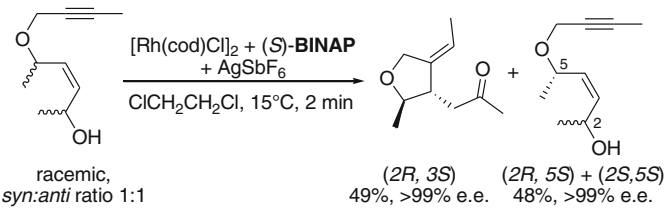
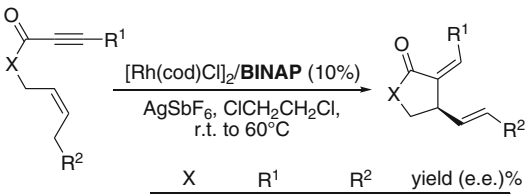


Fig. 10.19 Kinetic resolution of an enyne with stereogenic carbons at the allylic positions [32, 33]

Fig. 10.20 Enantioselective synthesis of lactames and γ-lactones via Rh-BINAP promoted cycloisomerization [27, 34]



X	R^1	R^2	yield (e.e.)%
NBn	Ph	H	90 (99)
NBn	Ph	Et	96 (99)
NBn	n-C_5H_{11}	H	96 (99)
NBn	Ph	OAc	89 (99)
NBn	CH_2OBn	H	92 (99)
NBn	Ph	NR_2[a]	83 (99)
O	Ph	H	94 (99)
O	n-C_5H_{11}	Me	95 (99)
O	Ph	OAc	96 (99)
O	Me	OH	99 (99)

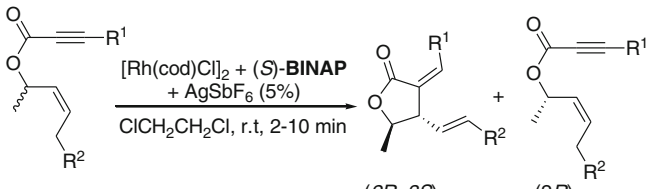
[a] NR_2 = phthalimide

The Zhang's procedure based on the $[Rh(cod)Cl]_2$/BINAP catalyst has been successfully extended to the Alder-ene cyclizations of enynes with amide [27] or ester functions [34] in the tethering chains. This efficient methodology allowed generation of a variety of functionalized lactames and γ-lactones through highly stereoselective carbon–carbon bond formations (Fig. 10.20).

The reaction tolerates a wide range of substituents, including functional groups such as ether, acetate and amide functions on the alkyne (R^1 in Fig. 10.20) as well as at the allylic position (R^2 in Fig. 10.20). The yields and enantioselectivities are impressively high, with e.e.s >99% in most cases.

Enynes with ester functions in the tethering chain and substituted allylic carbons have also been subjected to kinetic resolution experiments, analogous to those mentioned in Fig. 10.19. This strategy affords an efficient and general asymmetric method for the synthesis of polyfunctional lactones with two contiguous stereogenic centres (Fig. 10.21) [33].

Both the products and the unreacted starting materials were isolated in very high yields and e.e. values. The method allowed a convenient formal asymmetric



R^1	R^2	(2*R*, 3*S*) yield (e.e.)	(2*R*) yield (e.e.)
Me	OMe	47 (>99%)	47 (>99%)
C_5H_{11}	C_3H_7	45 (>99%)	48 (>99%)
Ph	H	49 (>99%)	50 (>99%)

Fig. 10.21 Kinetic resolution of ester tethered 1,6-enynes [33]

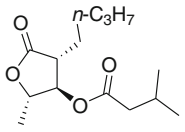
synthesis of (+)-blastmycinone, a degradation product of a class of natural antifungal-antibiotics (Fig. 10.22).

Excellent enantiomeric excesses have been obtained by Zhang et al. also in the synthesis of cyclopentanes and cyclopentanones via cycloisomerization of carbon-tethered enynes promoted by the same cationic Rh/BINAP catalysts (Fig. 10.23) [35]. These structures had been targeted most particularly since they are useful building blocks for the construction of biologically active molecules and industrially relevant compounds such as prostaglandins and jasmonates. Actually, enantiomerically pure (*1S,2S*)-dihydrojasmonate could be prepared indeed by this elegant methodology.

The broad scope and utility of these rhodium-catalyzed cyclizations was demonstrated also by their application to the total synthesis of platensimycin and related natural products, in the work of Nicolaou (Fig. 10.24) [36, 37].

In a preliminary study, Nicolaou adapted the Zhang's procedure to the cycloisomerization of 1,6-enynes with terminal alkyne functions (Fig. 10.24), since the original Zhang catalyst proved unsuitable for this class of substrates [20]. Optimized conditions were found that involve the use of a preformed Rh(BINAP)$^+SbF_6^-$ catalyst, obtained from [Rh(BINAP)(nbd)]SbF_6 under a stream of hydrogen gas [38, 39]. This accurate catalyst optimization process demonstrates that even subtle changes of the phosphine–rhodium complex used as the pre-catalyst may totally change the outcome and selectivity of the catalytic cycloisomerizations. The new catalyst performed well with substrates containing a range of structural motifs linking the two unsaturated functions, namely

Fig. 10.22 Molecular structure of Blastmycinone



(+)-Blastmycinone

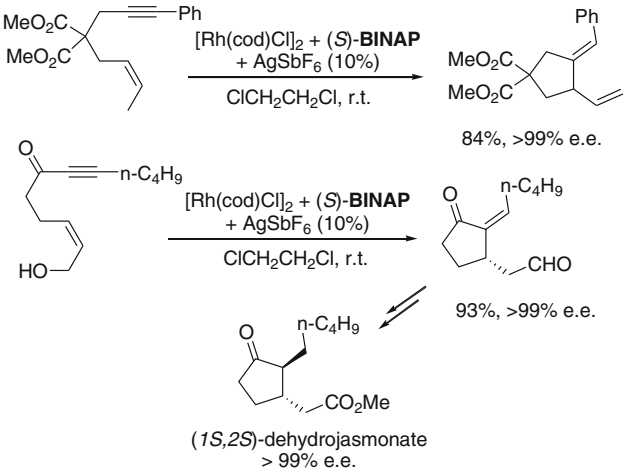
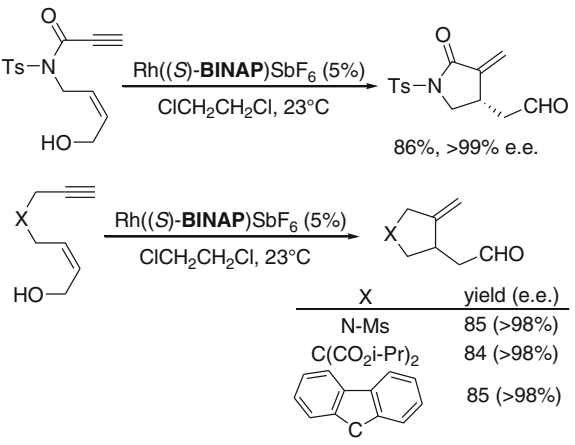


Fig. 10.23 Synthesis of cyclopentanes and cyclopentanones by Rh-promoted cycloisomerizations of 1,6-enynes [35]

1,1-diesters and sulfones, amides, sulfonamides, ether linkages and others (Selected examples are displayed in Fig. 10.24). Preferred substrates were enynes with hydroxyl functions at the allylic position, since they generate a potentially reactive aldehyde functionality in the final product.

Finally, the method was applied to the cycloisomerization of an 1,6-enyne with a cyclohexadienone scaffold which is shown in Fig. 10.25, which produced the corresponding spirocyclic structure in excellent enantiomeric excess. This strategy ensured a suitable enantioselective access to the polycyclic moiety of

Fig. 10.24 $Rh(BINAP)SbF_6$ promoted cycloisomerization of terminal enynes [36, 37]



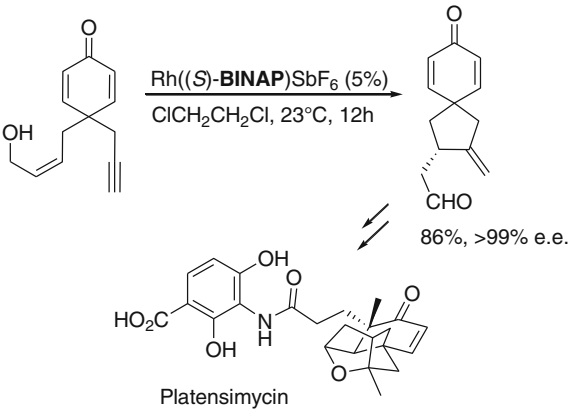


Fig. 10.25 Synthetic approach to Platensimycin [25]

platensimycin, an interesting class of antibiotics whose total synthesis was thus successfully achieved.

10.3.1.2 1,6-Enynes with Trisubstituted Alkene Moieties

As a general trend, only enynes with disubstituted, cis-configured olefin functions undergo cycloisomerization in the presence of the Zhang's BINAP-rhodium catalysts and analogues. To overcome these limitations, Mikami introduced a new catalyst based on Skewphos as the chiral auxiliary [40]. This new catalyst is the dicationic dimeric $[(Skewphos)Rh]_2(SbF_6)_2$ complex **C1** shown in Fig. 10.26 which was formed in situ from (Skewphos)Rh(nbd)SbF_6 by hydrogenation of the norbornadiene ligand.

Catalyst **C1** promoted Alder-ene type cyclizations of 1,6-enynes with sterically congested, trisubstituted double bonds and either ether or amide functions in the tethering chain (Fig. 10.27). These reactions afforded the expected dihydrofuranes and pyrrolines with high levels of enantioselectivity. Minor amounts of the isomerized endo-olefin product **B** were occasionally isolated.

The same catalyst has been applied then to the synthesis of the spirocyclic derivatives **A2** from 1,6-enynes with 6- and 8-membered ring structures shown in Fig. 10.27. High enantiomeric excesses were obtained in this case also.

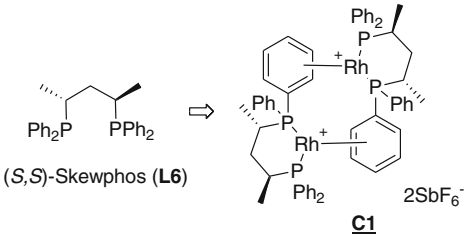


Fig. 10.26 Skewphos-based rhodium catalyst [40]

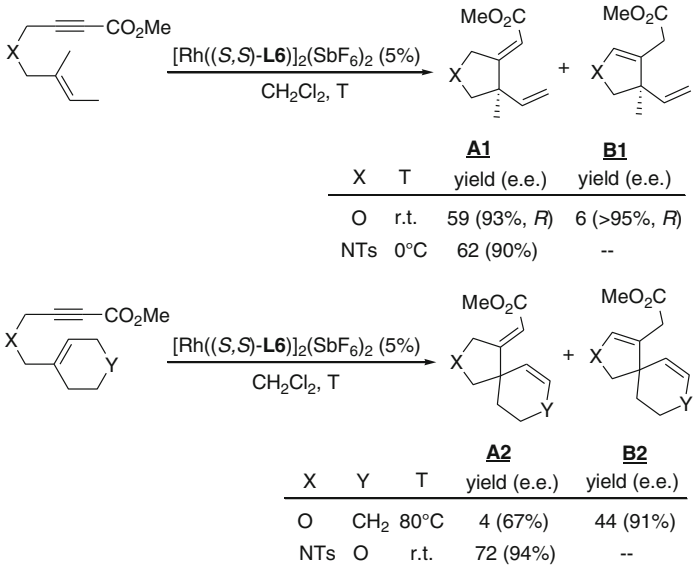


Fig. 10.27 Rh-Skewphos promoted cycloisomerization of 1,6-enynes with trisubstituted double bonds [40]

10.3.1.3 Ene-Type Cyclizations With Chirally Flexible Phosphorus Ligands

An advanced strategy for the generation of chiral metal catalysts is the so-called "asymmetric activation of chirally flexible (*tropos*) ligands" [41]. The method is based on the idea that, in the coordination sphere of a transition metal, a *tropos* ligand can adopt a well defined chiral configuration, under the effect of a suitable chiral 'activator'. Thus, for instance, combining the *tropos* ligand with a chiral, enantiomerically pure ligand will produce, in principle, a pair of diastereomers with opposite configurations of the flexible ligand. In some cases, however, the mixture isomerizes to a single, thermodynamically favoured diastereomer. At this point, experimental conditions must be found where the chiral configuration of the inherently *tropos* ligand can be "frozen" after removal of the chiral 'activator'. This will generate a chirally rigid (*atropos*) transition metal catalyst from a chirally flexible ligand.

Among others, this concept has been demonstrated for rhodium promoted ene-type cycloisomerizations of 1,6-enynes [42]. In these studies, Mikami et al. combined the tropos Xylyl–BIPHEP ligand with the enantiomerically pure (*R*)-1,1′-diaminobinaphthyle (DABN) to produce the cationic rhodium complex **C2** shown in Fig. 10.28. At 80 °C, the initially formed diastereomeric mixture was converted into a single diastereomer which proved to be configurationally stable at lower temperature. Moreover, removal of the chiral amine at 5 °C or below by addition of triflic acid, afforded a configurationally stable Xylyl–BIPHEP rhodium complex. The amine-free, enantiopure Xylyl–BIPHEP complex could be used as

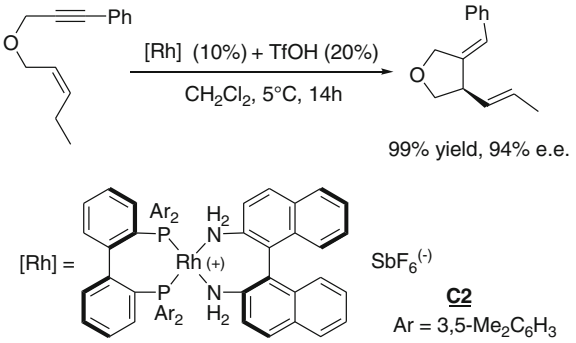


Fig. 10.28 Enantioselective ene-type cyclizations promoted by tropos Rh complexes of the conformationally flexible Xylyl-BIPHEP ligand [42]

the catalyst for the model cycloisomerization reaction in Fig. 10.28. It afforded the expected 3-exo-methylene tetrahydrofuran with an excellent enantiomeric excess (94% e.e.) when the reaction was performed at 5 °C.

The same concept of using tropos ligands as chiral auxiliaries has been illustrated later by the use of bimetallic rhodium catalysts combining a tropos, terphenyl based tetraphosphine and the enantiopure diamine DABN [43]. These bimetallic complexes having higher configurational stability compared to the monometallic analogues, they give highly enantioselective cycloisomerizations even at room temperature.

10.3.2 Cycloisomerization of Dien-ynes: [4 + 2] and [2 + 2 + 2] Cyclisations

10.3.2.1 1,6-Enynes with Unsaturated Substituents at the Olefinic Terminus

1,6-Enynes containing more than one olefinic function can undergo rhodium catalyzed cycloisomerizations involving all of the unsaturated units. The reactions produce bicyclic or tricyclic scaffolds through [4 + 2] or [2 + 2 + 2] annulation processes, depending on the nature of the starting materials. For both [4 + 2] and [2 + 2 + 2] cyclizations, the initial step is assumed to be an oxidative coupling of the enyne functions in the coordination sphere of rhodium, leading to the metallacyclopentene **I**, as shown in Fig. 10.29.

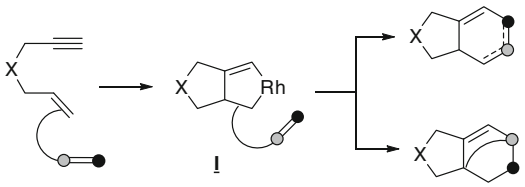
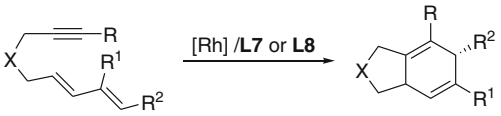
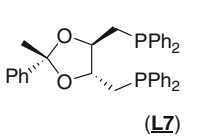


Fig. 10.29 Reaction pathways for dien-yne cycloisomerizations

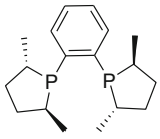


Ligand	X	R	R^1	R^2	yield (e.e.)%
L7	O	$SiMe_3$	Me	H	76 (87)[c]
L8[a]	O	H	H	Me	85 (95)[d]
L8[b]	O	Et	H	Me	76 (88)[d]
L8[b]	$C(CO_2Et)_2$	H	H	Me	78 (91)[d]

[a] Rh(*S,S*-Me-DuPHOS)(hepta-2,5-diene)Cl; [b] catalyst formed *in situ* from Rh(*S,S*-MeDuPHOS)(ndb)$^+SbF_6^-$ under H_2 gas. [c] in CF_3CH_2OH. [d] in CH_2Cl_2/EtOAc at 55°C



(**L7**)



(**L8**)

Fig. 10.30 Enantioselective [4 + 2] cyclizations of dienynes promoted by Rh-diphosphine complexes [44, 45]

The cycloisomerizations of enynes displaying conjugated diene units produce bicycles with cyclohexene subunits through formal [4 + 2], Diels–Alder like reactions. Initial successful attempts of setting asymmetric versions of these rearrangements by means of chiral phosphorus ligands have been reported by Livinghouse by using DIOP type ligands [44]. Later on, another catalytic system has been found by Gilbertson that makes use of Me-DuPHOS as the chiral auxiliary [45]. None of these catalysts have wide scope and general applicability (Fig. 10.30). The substrate limitation is so far the major drawback of these, as well as of most of the enantioselective cycloisomerization processes presented in this review.

Finally, highly enantioselective catalysts have been disclosed by Mikami et al. [46]. They are based on a proper combination of a chiral bidentate phosphine and a chiral diene ligand in the coordination sphere of rhodium. The catalyst design started from the experimental observation that the nature of the diene ligand of the commonly used rhodium precursors (i.e. cyclooctadiene or norbornadiene) affects the enantiodiscrimination in the cyclization process. Therefore, different phosphine/diene pairs were investigated including both chiral and achiral diene ligands and a remarkable increase in enantioselectivity was observed by using chiral dienes. The combination of Me- or Et-DuPHOS with the chiral diene shown in Fig. 10.31 provided a very effective catalyst leading to enantiomeric excesses in the range 81–98% in the cycloisomerization of ether tethered dienynes.

It is proposed that both the phosphine and the chiral diene coordinate to rhodium during the catalytic cycle. The diene is assumed to behave here as a monodentate ligand, since tightly bonding dienes usually inhibit the catalytic activity.

In addition to Diels–Alder type annulations, also enantioselective intramolecular [2 + 2 + 2] cyclization reactions have been carried out on dien-yne

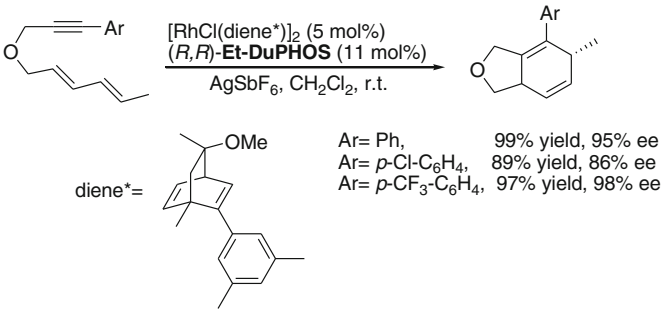
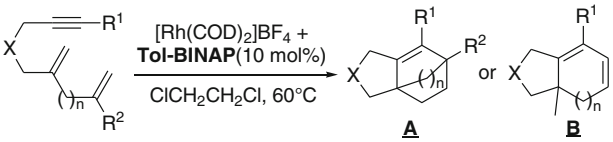


Fig. 10.31 Enantioselective [4 + 2] cyclizations of dienynes promoted by Rh-diphosphine-diene complexes [46]



n	X	R^1	R^2	A yield (e.e.)	B yield (e.e.)
1	NTs	Bu	Me	46 (>99%)	
1	NTs	H	Ph	83 (93%)	
1	$C(CO_2Bn)_2$	H	Me	76 (93%)	
1	O	Ph	Me	40 (92%)	
1	NTs	Me	H		91 (99%)
1	$C(CO_2Bn)_2$	H	H		80 (90%)
1	O	Ph	H		55 (92%)
2	NTs	Me	H		~35 (>99%)
2	$C(CO_2Bn)_2$	H	H		~44 (>99%)

Fig. 10.32 Rhodium-TolBINAP promoted [2 + 2 + 2] annulations of dien-ynes [47, 48]

substrates, in the presence of cationic rhodium complexes. Substrates are 1,6- or 1,7-enynes with an allylic or homoallylic moiety on the olefin terminus, as shown in Fig. 10.32 [47, 48]. They are converted into either bicyclic or tricyclic compounds, depending on the nature of the R^2 substituent of the diene: tricyclic compounds (**A**) are obtained from dien-ynes where R^2 = Me or Ph, while bicyclic compounds (**B**) are formed for R^2 = H.

A ligand screening highlighted (*S*)-TolBINAP as the best chiral ligand for these transformations, leading to the polycyclic species A and B with excellent control of the stereochemistry of their quaternary stereogenic centres (10 examples, e.e.s in the range 88–99%). To facilitate the reaction, COD-free rhodium complexes were used as pre-catalysts. They were prepared from $[Rh(COD)_2]BF_4$ and (*S*)-TolBINAP and pretreated with hydrogen gas to exclude COD by reduction before use.

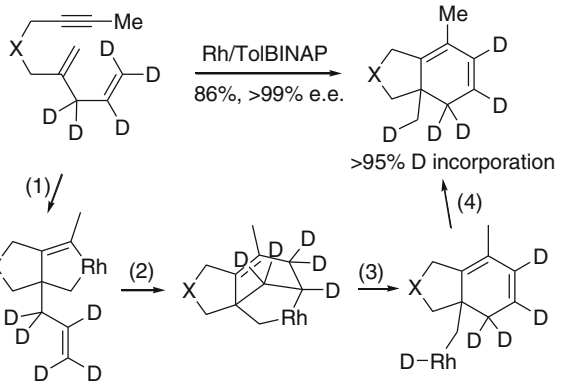


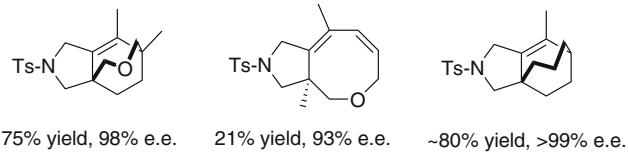
Fig. 10.33 Proposed mechanism for the construction of the cyclohexadiene unit [48]

The assumed mechanism for the reactions leading to the cyclohexadiene derivatives involves an alkyne-alkene oxidative coupling (1), an olefin insertion (2), a β-elimination (3) and an α-elimination steps (Fig. 10.33). Evidences for this mechanism have been provided by studying the cycloisomerization of deuterated 1,4-dien-ynes [48]. The results strongly support the notion that the rearrangement includes a β-hydrogen elimination step (3) and exclude the possibility of a direct intramolecular [4 + 2] cycloaddition of the alkyne with an 1,3-diene moiety generated initially by a double bond migration.

Analogous cycloisomerizations take place on 1,6-dien-ynes with olefin functions tethered by longer chains (n = 3 in Fig. 10.32) which produces the bicyclic or tricyclic compounds shown in Fig. 10.34 in excellent enantiomeric excess.

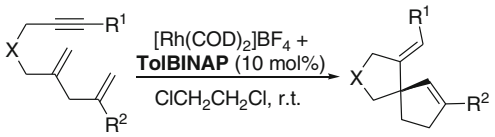
However, dien-ynes with bulky substituents to the alkyne terminus follow a different reaction pathway: under rhodium catalysis, they are efficiently converted into spirocyclic compounds. In these rearrangements also, the Rh-TolBINAP catalyst afforded excellent enantioselectivities (e.e. >90%, Fig. 10.35).

Thus, the comprehensive investigations above demonstrate that a variety of multicyclic compounds with quaternary stereogenic centres can be obtained from this class of dien-ynes, depending on the length of the tethering chain as well as on the substituents of the unsaturated functions. The efficiency of cationic Tol-BINAP/Rhodium complexes as catalysts for many reactions of this class has been assessed.



75% yield, 98% e.e. 21% yield, 93% e.e. ~80% yield, >99% e.e.

Fig. 10.34 Products from dienyne cycloisomerizations promoted by Rh-TolBINAP complexes [48]



X	R^1	R^2	yield (e.e.)
O	2-Ph-C_6H_4	Me	80 (96%)
O	1-naphthyl	Me	82 (97%)
O	1-naphthyl	Ph	78 (93%)
NTs	1-naphthyl	Me	44 (92%)

Fig. 10.35 Enantioselective synthesis of spirocyclic compounds [48]

10.3.2.2 1,6-Enynes with Unsaturated Substituents at the Alkyne Terminus

Dien-ynes with an ene-yne-ene sequence undergo [2 + 2 + 2] cyclizations leading to tricyclic cyclohexenes. An enantioselective process has been carried out by Tanaka by using a Rh/H_8-Binap catalyst (Fig. 10.36) [49].

The cycloadducts were obtained in quantitative yield as mixtures of two diastereoisomers, with the desired C_2-symmetric cyclohexene as the minor product. The enantiomeric excess was almost perfect, however.

10.3.3 Cycloisomerization of En-Diynes: [2 + 2 + 2] Cyclisations

En-diynes where two alkyne moieties are connected to the contiguous carbons of an alkene, are useful substrates for metal promoted cycloisomerizations. Under rhodium catalysis, they undergo formal [2 + 2 + 2] cycloaddition reactions leading to tricyclic cyclohexadienes with two contiguous stereogenic centres. Starting from symmetric en-diynes, the reaction produces C_2-symmetric, dl isomers, provided that the starting olefin has a *Z*-configuration.

Asymmetric versions of these reactions have been carried out by Tanaka [49] and Shibata [50] by using rhodium complexes of modified BINAPs (Fig. 10.37). TolBinap and H_8-Binap were found to be appropriate chiral ligands for the cycloadditions of enynes with oxygen, carbon or nitrogen tethers. In the case of nitrogen-tethered substrates, the substituent of the alkyne unit has a crucial effect

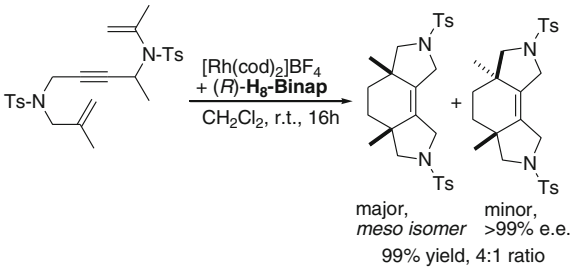
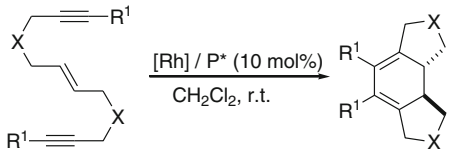
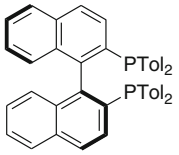
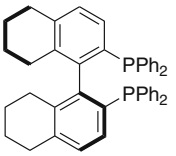


Fig. 10.36 Enantioselective cycloisomerization of dien-ynes into tricyclic cyclohexenes [49]





(*S*)-TolBINAP (**L9**)



(*S*)-H_8-BINAP (**L10**)

P*	X	R^1	yield (e.e.)
L9[a]	O	CO_2Me	95 (59%)
	O	H	78 (48%)
L10[b]	$C(CO_2Me)_2$	CO_2Me	72 (98%)
	$C(CO_2Me)_2$	Br	48 (91%)
	$C(CO_2Me)_2$	Me, CO_2Me	82 (98%)
	$C(SO_2Ph)_2$	H	68 (98%)
	NTs	CO_2Me	69 (21%)
	NTs	Bu	90 (89%)
	NTs, $C(CO_2Me)_2$	Ph, CO_2Me	68 (91%)
	NTs, $C(CO_2Me)_2$	Me	99 (97%)

[a] $[Rh(COD)_2]BF_4$ [b] $[Rh(COD)\{(S)\text{-}H_8\text{-BINAP}\}]BF_4$

Fig. 10.37 Rhodium promoted [2 + 2 + 2] cycloadditions of ene-diynes [49, 50]

on the enantioselectivity levels and especially low enantiomeric excesses were obtained with electron-withdrawing substituents [50].

The authors postulated that these reactions can follow two different reaction pathways involving either alkyne–alkene or alkyne–alkyne oxidative couplings as the initial steps. The alkyne–alkene coupling is assumed to give high levels of stereocontrol, while the alkyne–alkyne coupling initiates low selectivity pathways. Therefore, it is anticipated that alkyne substituents which favour alkyne–alkyne couplings will afford low enantioselectivity levels.

10.3.4 Cycloisomerization of Cyclopropyl Substituted Enynes: [5 + 2] Annulations

Metal-mediated [5 + 2] cyclizations were built based on the hypothesis that the cyclopropyl moiety of cyclopropyl substituted enynes might participate in the rearrangement process as a three atom unit. This approach afforded indeed an efficient process for the formation of 7-membered rings starting from enynes with a cyclopropyl moiety on the olefin terminus [51]. A possible mechanistic model involves coordination of the enyne and oxidative coupling (a), followed by cleavage of the cyclopropyl unit (b) and reductive elimination (Fig. 10.38).

The control of the absolute stereochemistry of the newly generated stereogenic centre has been targeted at first by Wender who investigated the use of cationic rhodium complexes generated from $[Rh(nbd)Cl]_2$, $AgSbF_6$ and (*R*)-BINAP under

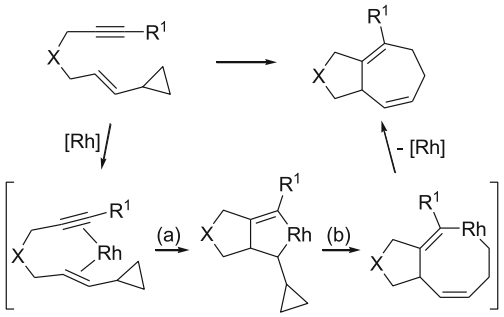
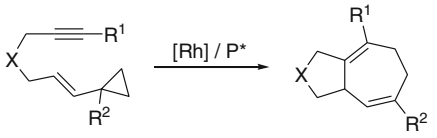


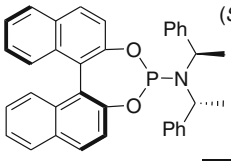
Fig. 10.38 A possible mechanistic model for [5 + 2] annulations of cyclopropyl substituted enynes [51]

H_2 gas (Fig. 10.39, first entry) [38]. In these reactions, only moderate enantioselectivity levels were attained (e.e.s in the range 22–56%), although the same catalyst was found highly suitable for the analogous [5 + 2] annulations of cyclopropyl-substituted dienes.

Further studies from Hayashi et al. [52], including comparative evaluations of several catalysts, allowed the development of an efficient asymmetric variant. The best catalytic system was afforded by chiral monodentate phosphoramidites (Fig. 10.39). The cationic rhodium complexes have been generated in situ from $[(RhCl(C_2H_4)_2]_2$, phosphoramidite (*S,R,R*)-**L11** and $NaBArF_4$ [$NaBArF_4$ = sodium 3,5-bis(trifluoromethyl)phenylborate]. The scope of these catalysts has been illustrated by the cycloisomerization of enynes differing in substitution and tether types. High yields and enantiomeric excesses in the range 83–99% have been obtained for substrates with nitrogen–oxygen- and gem-disubstituted carbon atoms in the linker chain. Selected examples are shown in Fig. 10.39.



P*	X	R^1	R^2	yield (e.e.)
(*R*)-**BINAP**[a]	NTs	H	H	87 (56%)
(*S,R,R*)-**L11**[b]	NTs	H	H	53 (92%)
	NTs	Ph	H	88 (99%)
	NTs	Me	H	87 (>99%)
	O	$(CH_2)_2Ph$	H	90 (95%)
	$C(CO_2Me)_2$	Ph	H	82 (83%)
	NTs	Ph	Me	87 (99%)



(*S,R,R*)-**L11**

[a] (*R*)-BINAP)$Rh^+SbF_6^-$; [b] $[(RhCl(C_2H_4)_2]_2$ 5 mol%, **L11** 7.5 mol% + $NaBAr^F_4$, CH_2Cl_2, 30°C, 5h

Fig. 10.39 Enantioselective [5 + 2] cycloadditions promoted by cationic rhodium complexes [38, 52]

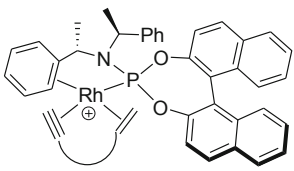


Fig. 10.40 Postulated intermediate of enantioselective [2 + 5] cyclizations promoted by Rh-**L11** complexes [38, 52]

The active catalyst is presumably a cationic complex with a 1:1 phosphine/rhodium ratio. The phenyl substituent of the chiral phosphoramidite ligand **L11** seems to play an important role for stereocontrol. Therefore, it has been postulated that η^2-coordination of the phenyl group takes place during the catalytic cycle and helps to create a well defined chiral environment (Fig. 10.40).

10.4 Platinum Catalysed Cycloisomerizations

10.4.1 Cyclizations Induced by Electrophilic Activation of the Alkyne Unit

The Lewis acid properties of late transition metals, including Pt^{II} species, induce peculiar behaviours in their reactions with enynes. Mainly, the carbophilic metal fragment exhibits high affinity to the π-systems of the substrate and activates the alkyne moiety toward the attack of nucleophilic species [1, 6]. In 1,n-enynes, the alkene unit itself can behave as a nucleophile and its nucleophilic addition to the alkyne terminus initiates a variety of cycloisomerization manifolds. A possible outcome of such skeletal rearrangements is the formation of the bicyclo[4.1.0] heptene structures shown in Fig. 10.41. It is thought that, in these reactions, the olefin terminus gives intramolecular addition to the activated alkyne, leading to the bicyclic intermediates **II**. A proper description of the reactive intermediates **II** might be a carbenoid structure, however, conflicting views can be found in the literature. Theoretical studies suggest that they also exhibit high cationic character [4, 53, 54].

The carbenoid intermediates **II** undergoes then 1,2-hydrogen shift and elimination of the metal catalyst to afford the final bicylo[4.1.0]heptenes.

This type of 6-endo-dig cyclizations has been carried out with π-acidic metal catalysts such as platinum(II) and gold(I) [55–58] as well as with less acidic metals such as Rh(I) or Ir(I) complexes in the presence of electron-acceptor ligands such as CO [59].

Since the whole catalytic cycle involves a single metal–substrate bond, changing from π- to σ-bonds in the successive elementary steps of Fig. 10.41, simultaneous coordination of the alkyne and the alkene to the metal centre is not required. Thus, it was anticipated that metal complexes with even a single vacant coordination site might afford suitable catalysts for these rearrangements. Platinum complexes with a

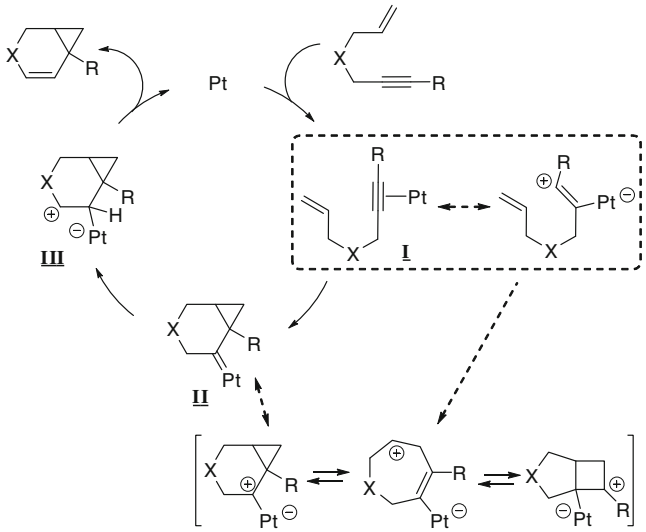


Fig. 10.41 Postulated mechanism for the cycloisomerization of enynes into bicyclo[*n*,1,0] derivatives

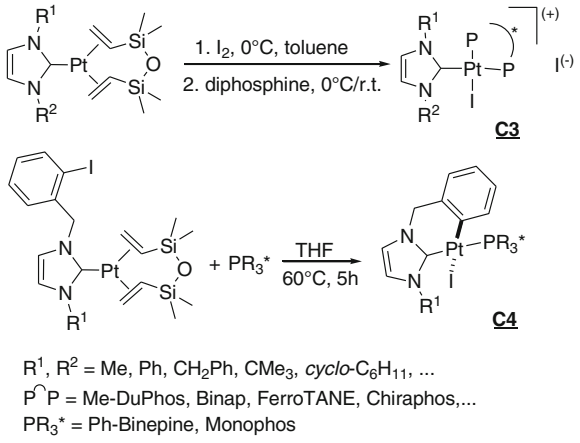


Fig. 10.42 Synthesis of the chiral platinum pre-catalysts **C3** and **C4** [62, 64]

single vacant coordination site were already reported by Gagné as efficient catalysts for the related cycloisomerizations of dienes [60, 61].

Based on this working hypothesis, Marinetti et al. have designed the first series of efficient chiral platinum pre-catalysts for the cycloisomerization of 1,6-enynes, i.e. complexes **C3** and **C4** in Fig. 10.42. These are well defined square planar complexes combining N-heterocyclic carbenes (NHC), chiral phosphorus ligands and an iodide as the arguably labile ligand [62–64].

Complexes **C3** display a monodentate NHC and a chelating diphosphine as the chiral auxiliary, while complexes **C4** are 6-membered platinacycles bearing a

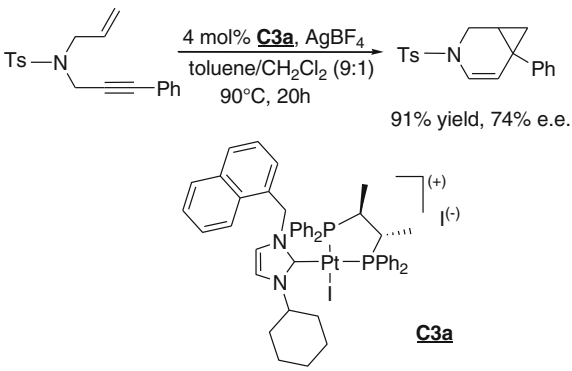
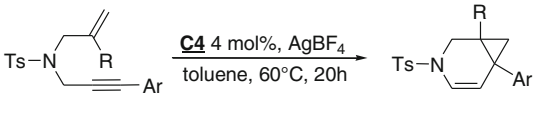
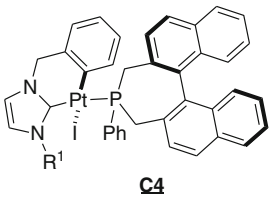


Fig. 10.43 Enantioselective cycloisomerization of 1,6-enynes promoted by cationic (NHC)Pt[(S,S)-chiraphos] complexes [63]

monodentate chiral phosphine. Their syntheses follow the same general strategy, that is the conversion of a platinum(0)-NHC-diene complex into a platinum(II)-NHC derivative via oxidative addition reactions (addition of I_2 or intramolecular oxidative addition of aryl-iodide units). Exchange reactions between the coordinated diene and the chiral phosphine take place then, either after or concomitantly with the oxidative addition step, as shown in Fig. 10.42. Complexes **C3** and **C4** are highly modular, since both the NHC moiety and the chiral phosphine ligand can be varied extensively and independently from each other, thanks to this extremely flexible synthetic method.

Complexes **C3** have been used as pre-catalysts for the cycloisomerization of a model 1,6-enyne which contains a tosylamide function in the tethering chain (Fig. 10.43). The catalytically active species was generated by iodide abstraction from **C3** by addition of a silver salt ($AgBF_4$). The reaction affords the expected 3-azabicyclo[4.1.0]heptene derivative. An extensive catalytic screening highlighted (*S,S*)-Chiraphos as the most effective chiral diphosphine and demonstrated that suitable modulation of the NHC ligand allows increasing of the





R^1 (**C4**)	R	Ar	yield (e.e.)
CH_2Ph	H	Ph	90 (96%)
Me	H	$3,5\text{-}Me_2C_6H_3$	95 (90%)
Et	H	$p\text{-}MeOC_6H_4$	77 (91%)
CH_2Ph	H	$p\text{-}NO_2C_6H_4$	51 (97%)
CH_2Ph	Me	Ph	98 (88%)

Fig. 10.44 Enantioselective cycloisomerizations of 1,6-enynes into bicyclo[4.1.0]heptenes promoted by platinacyclic (S)-Binepine complexes [64]

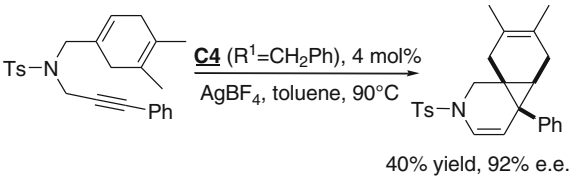


Fig. 10.45 Isomerization of a cyclic 1,6-dien-yne into a tricyclic compound [64]

enantioselectivity levels. Catalyst optimization led to a maximum 74% e.e. for the targeted cyclization reaction.

Complexes **C4** bearing (*S*)-Ph-Binepine as the chiral ligand (Fig. 10.44) proved to be more effective, more enantioselective and more versatile catalysts, compared to **C3**, in the cycloisomerization of the same class of substrates [64]. The catalytic reactions take place in mild conditions (60 °C) and the desired bicyclo[4.1.0]heptenes were obtained in over 90% enantiomeric excesses from a range of substrates. The reaction tolerates various aryl substituents on the alkyne moiety as well as substituted olefin units. Selected examples are given in Fig. 10.44.

Catalysts **C4** also triggered the conversion of the cyclic enyne derivative shown in Fig. 10.45 into the corresponding tricyclic derivative [65] with high stereoselectivity levels (e.e. up to 92%).

Thus, complexes **C4** are the first known, and so far unique class of well defined Pt(II) complexes leading to highly enantioselective enyne skeletal rearrangements.

Recently, the same strategy of using metal complexes containing a single vacant coordination site, has been applied by Hayashi to the design of rhodium-based chiral catalysts [66]. In the case of rhodium, however, chiral bidentate phosphines did not afford active catalysts. Therefore, attention was focused on complexes bearing a C_2-symmetric chiral diene and an achiral monodentate phosphine. This catalyst design allowed high enantiomeric excesses to be obtained in the cycloisomerization of heteroatom-containing enynes (Fig. 10.46).

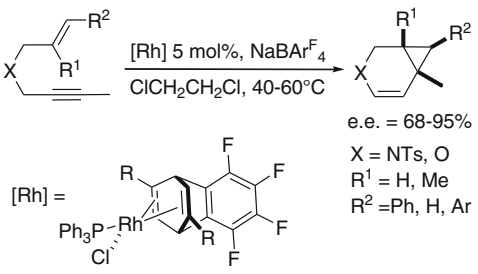


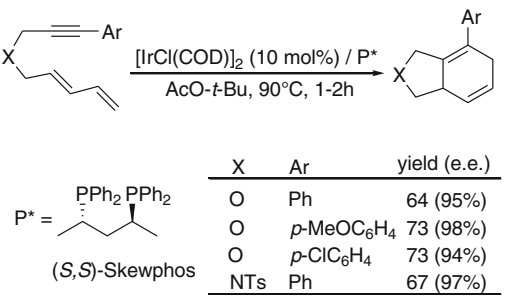
Fig. 10.46 Cycloisomerization of 1,6-enynes promoted by rhodium complexes with a single vacant coordination site [66]

10.5 Iridium Catalysed Cycloisomerizations

The applications of iridium catalysts to enantioselective enyne cycloisomerizations are quite limited. Iridium based catalysts have been investigated by Shibata as chiral promoters for the [4 + 2] cycloadditions of dien-ynes [67]. The preferred catalyst was formed in situ from $[IrCl(COD)]_2$ and (*S,S*)-Skewphos. It gave enantiomeric excesses of over 90% in the cyclizations of both oxygen- and nitrogen containing enynes with unsubstituted diene units (Fig. 10.47). Other chiral phosphines, i.e. BINAP, Me-DuPHOS and DIOP gave only moderate e.e.s in the same cyclizations. Unlike the analogous rhodium complexes (see Sect. 10.3.2), the iridium pre-catalysts do not require activation by silver salts as halide scavengers.

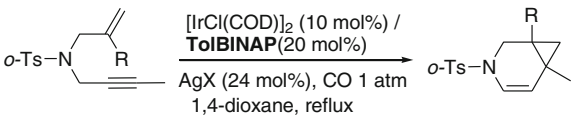
Shibata also reported on the enantioselective cycloisomerization of nitrogen-bridged 1,6-enynes into 3-azabicyclo[4.1.0.]heptenes. In this reaction, Tol-BINAP proved to be the best catalyst, although only moderate enantioselectivity levels could be attained [59](Fig. 10.48).

The catalytically most active species is formed from $[IrCl(COD)]_2$ and TolBinap under a CO atmosphere. Therefore, it is thought that a CO ligand must be coordinated to iridium in the catalytically active complex to increase the Lewis acid character of the metal and to allow the reaction to take place.



X	Ar	yield (e.e.)
O	Ph	64 (95%)
O	*p*-$MeOC_6H_4$	73 (98%)
O	*p*-ClC_6H_4	73 (94%)
NTs	Ph	67 (97%)

Fig. 10.47 Enantioselective [4 + 2] cyclizations of dien-ynes promoted by Ir-Skewphos complexes [67]



R = Ph, 70% yield, 78% e.e.
R = *p*-Cl-C_6H_4, 71% yield, 74% e.e.
R = 2-naphthyl, 57% yield, 64% e.e.

Fig. 10.48 Enantioselective cycloisomerizations of 1,6-enynes into bicyclo[4.1.0]heptenes promoted by iridium TolBINAP complexes [59]

10.6 Gold Catalysed Cycloisomerizations

10.6.1 Alder-Ene Type Cyclizations

The formal Alder-ene cyclizations of 1,6-enynes have been mentioned in Sects. 10.2.1 and 10.3.1 as palladium and rhodium promoted processes. They can be carried out under gold catalysis as well. However, the chiral phosphine (BINAP, MeO–BIPHEP) gold complexes screened so far did not afford significantly high asymmetric induction [58].

10.6.2 Cyclizations Induced by Electrophilic Activation of the Alkyne Unit

Examples of asymmetric gold catalyzed cycloisomerizations of enynes induced by electrophilic activation of the alkyne unit are still scarce. They make use mainly of chiral C_2-symmetric diphosphines.

Thus, for instance, Toste et al. reported a gold catalysed sequential cycloisomerization/ring expansion rearrangement of 1,6-enynes which display a methylene cyclopropane unit (Fig. 10.49) [68]. The method allowed the rapid preparation of polycyclic ring systems with high diastereocontrol.

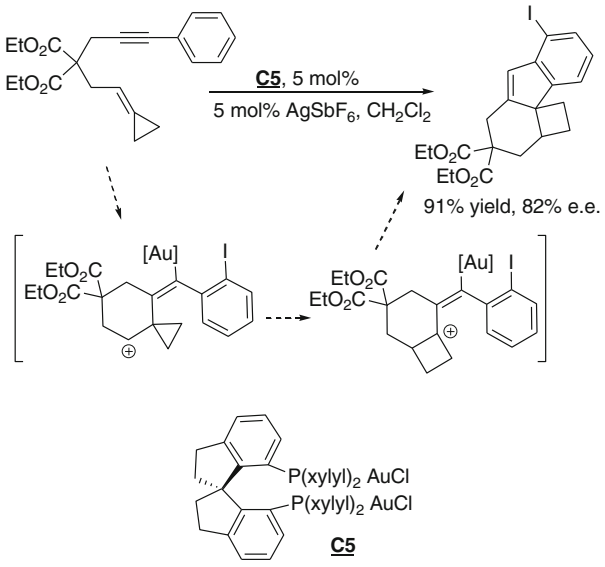
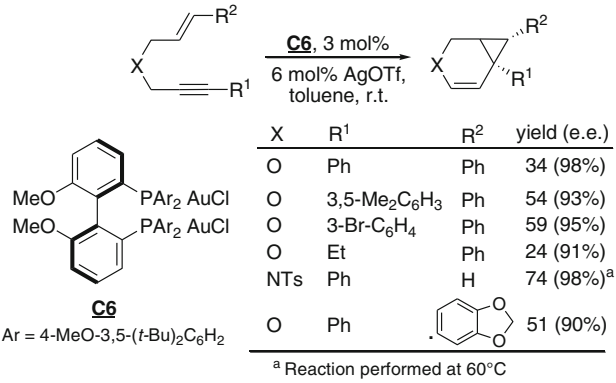


Fig. 10.49 Cycloisomerization of an enyne bearing an alkylidene cyclopropane unit [68]



X	R^1	R^2	yield (e.e.)
O	Ph	Ph	34 (98%)
O	3,5-$Me_2C_6H_3$	Ph	54 (93%)
O	3-Br-C_6H_4	Ph	59 (95%)
O	Et	Ph	24 (91%)
NTs	Ph	H	74 (98%)[a]
O	Ph		51 (90%)

[a] Reaction performed at 60°C

Fig. 10.50 Enantioselective cycloisomerizations of 1,6-enynes into bicyclo[4.1.0]heptenes promoted by gold-diphosphine complexes [69]

According to the postulated reaction pathway, after the initial addition of the olefin to the activated diene, the cyclopropyl unit undergoes a ring enlargement reaction. The gold stabilized allyl cation participates then in a Nazarov-type electrocyclization leading to the final angular tricyclic compound.

The paper discloses one example of enantioselective variant. The catalytically active species is a cationic bimetallic complex generated from the (*R*)-xylyl–SDP–gold pre-catalyst **C5** after addition of a silver salt. The expected polycyclic product could be isolated in good yield, with 82% enantiomeric excess.

Gold complexes have been applied by Michelet et al. to the cycloisomerization of heteroatom-linked 1,6-enynes into bicycle[4.1.0]heptene scaffold [69]. Suitable pre-catalysts are bimetallic gold complexes with MeO-BIPHEP type ligands as the chiral auxiliaries (**C5** in Fig. 10.50).

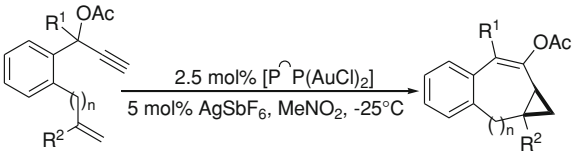
The expected enantiomerically enriched bicyclic products were isolated in moderate to good yields with e.e. values ranging from 90 to 98%.

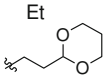
Finally, a last example of enantioselective gold promoted rearrangement is the intramolecular cyclopropanation introduced by Toste et al. as a tool for the synthesis of medium-sized rings (Fig. 10.51) [70]. Favoured substrates are 1,7- and 1,8-enynes with terminal alkyne functions and an acetoxy substituent at the propargylic position. They are converted into bicyclic structures containing a cyclopropane unit.

In this case also, bimetallic complexes of atropisomeric diphosphines proved to be optimal pre-catalysts. (*R*)-Xylyl–BINAP and (*R*)-DTBM–Segphos (**L4-b**) gold(I) complexes have been applied to the synthesis of 8 and 7-membered rings, respectively, with enantiomeric excesses in the range 85–92%. Selected results are given in Fig. 10.51.

The reaction is thought to operate through a gold(I) carbenoid intermediate that is generated by 1,2-shift of the propargylic ester function, as shown in Fig. 10.52.

The carbenoid intermediate which contains an E-configured olefin gives then intramolecular cyclopropanation of the allylic unit leading to the final



P⌒P	n	R^1	R^2	yield (e.e.)
(*R*)-**Xylyl-BINAP**	2	Me	H	94 (92%)
(*R*)-**Xylyl-BINAP**	2	allyl	H	98 (90%)
(*R*)-**Xylyl-BINAP**	2	Et	H	91 (92%)
(*R*)-**Xylyl-BINAP**	2		H	96 (90%)
SegPHOS L4-b	1	H	H	44 (85%)[a]

[a] A pivalate function is used instead of acetate

Fig. 10.51 Gold catalyzed enantioselective cyclopropanations [70]

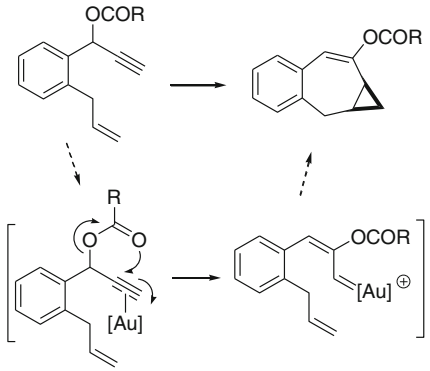


Fig. 10.52 Key postulated intermediates of the intramolecular cyclopropanation reaction [70]

bicyclic structure. Clear evidence for the generation of the carbenoid intermediate has been provided by its trapping in intermolecular cyclopropanation experiments.

10.6.3 Enantioselective Cycloisomerization via Enantiotopos Selection

For all the cycloisomerization reactions we have mentioned so far, the stereodetermining process is an enantiofacial selection taking place during the transformation of an sp^2 centre into an sp^3 chiral centre. Recently Hashmi et al. introduced "enantiotopos selection" as an alternative concept possibly underlying enantioselective cycloisomerizations [71]. The concept consists in using en-diyne substrates which contain two identical and enantiotopic alkynyl groups connected to a prochiral carbon centre. The cycloisomerization process will create a sterogenic carbon at the very first stage of the catalytic cycle, namely the π-coordination of

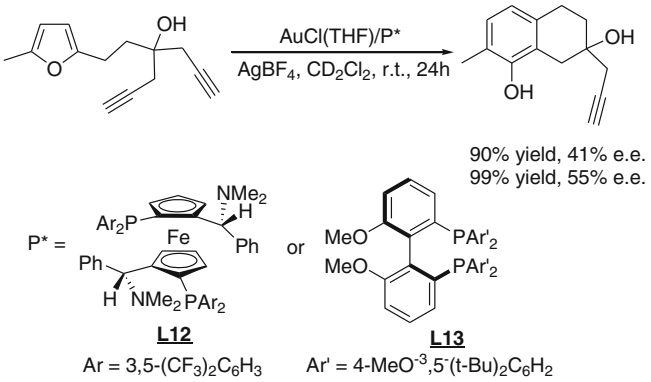


Fig. 10.53 Enantioselective cycloisomerization of prochiral en-diynes [71]

one of the alkynes on the gold complex. This strategy has been typified by the reaction in Fig. 10.53.

The test substrate combines two propargyl units and a furyl group as the ene component. In the presence of Au(I) derivatives, the substrate undergoes a cycloisomerization/ring expansion process leading to a functionalized tetrahydronaphthalene. Despite an extensive screening of chiral phosphines (Josiphos and other ferrocene-based phosphines, BINAP, MeO–Biphep and Monophos type ligands) an e.e. value of only 55% could be attained. Nevertheless, these preliminary experiments highlight enantiotopos selection as a potential strategy for enantioselective cycloisomerizations.

10.7 Conclusions and Outlook

From this short overview it appears that the majority of the recent studies on enantioselective cycloisomerizations have been focused so far on asymmetric Alder-ene type cyclizations with Pd and Rh catalysts, since these reactions represent an economical access into synthetically useful cyclopentene and cyclohexene frameworks (Sects. 10.2.1 and 10.3.1). For these processes, efficient chiral catalysts have been afforded mainly by atropisomeric diphosphines, but also DuPHOS, Skewphos and phosphine-oxazolines can occasionally represent suitable auxiliaries.

Beside Alder-ene cyclizations, only the cycloisomerizations of polyunsaturated substrates (Sects. 10.3.2 and 10.3.3) as well as reactions involving electrophilic activation of the alkyne, notably the conversion of 1,6-enynes into bicyclic scaffolds (Sects. 10.4, 10.5 and 10.6), have been investigated in some depth.

So far, a common limitation of the enantioselective cycloisomerization processes, including the most extensively investigated ones, is the rather restricted substrate scope and the need of specific catalyst–substrate pairs to attain high

levels of enantioselectivity. Thus, expanding the scope of these reactions is expected to be a major concern for future work in this field.

From this overview it also appears that in most cases, catalytic tests have been performed with catalysts formed in situ from a metal precursor and the desired chiral phosphine, according to usual procedures, while specific catalyst design has been done only sporadically. Relevant examples are the DuPHOS/diene rhodium complexes mentioned in Fig. 10.31 (Sect. 10.3.2) and the platinum/NHC/phosphine derivatives **C4** which allowed highly enantioselective platinum promoted cycloisomerizations to be carried out (Fig. 10.44).

Finally, it must be pointed out here that tentative mechanistic rationales for the observed chiral induction are so far mainly speculative and that predictive theoretical models for the selectivity are totally lacking to date. Therefore, it can be anticipated that the mechanistic interpretation of enantioselective enyne cycloisomerization processes and the subsequent appropriate catalyst design will be a key for the development of a wider array of enantioselective rearrangements in the near future.

References

1. Lloyd-Jones GC (2003) Mechanistic aspects of transition metal catalysed 1,6-diene and 1,6-enyne cycloisomerisation reactions. Org Biomol Chem 1:215–236
2. Nieto-Oberhuber C, Lopez S, Jimenez-Nunez E, Echavarren AM (2006) The mechanistic puzzle of transition-metal-catalyzed skeletal rearrangements of enynes. Chem Eur J 12:5916–5923
3. Jiménez-Núñez E, Echavarren AM (2008) Gold-catalyzed cycloisomerizations of enynes: a mechanistic perspective. Chem Rev 108:3326–3350
4. Soriano E, Marco-Contelles JM (2009) Mechanistic insights on the cycloisomerization of polyunsaturated precursors catalyzed by platinum and gold complexes. Acc Chem Res 42:1026–1036
5. Zhang L, Sun J, Kozmin SA (2006) Gold and platinum catalysis of enyne cycloisomerization. Adv Synth Catal 348:2271–2296
6. Fürstner A, Davies PW (2007) Catalytic carbophilic activation: catalysis by platinum and gold p-acids. Angew Chem Int Ed 46:3410–3449
7. Michelet V, Toullec PY, Genet J-P (2008) Cycloisomerization of 1,n-enynes: challenging metal-catalyzed rearrangements and mechanistic insights. Angew Chem Int Ed 47: 4268–4315
8. Lee SI, Chatani N (2009) Catalytic skeletal reorganization of enynes through electrophilicactivation of alkynes: double cleavage of C–C double and triple bonds Chem Commun 371–384
9. Fairlamb IJS (2004) Asymmetric cycloisomerization of 1,6- and 1,7-enynes by transition-metal catalysts. Angew Chem Int Ed 43:1048–1052
10. Hatano M, Mikami K (2003) Highly enantioselective quinoline synthesis via ene-type cyclization of 1,7-enynes catalyzed by a cationic BINAP–palladium(II) complex. J Am Chem Soc 125:4704–4705
11. Charruault L, Michelet V, Taras R, Gladiali S, Genêt J-P (2004) Functionalized carbo- and heterocycles via Pt-catalyzed asymmetric alkoxycyclization of 1,6-enynes Chem Commun 850–851

12. Muñoz MP, Adrio J, Carretero JC, Echavarren AM (2005) Ligand effects in gold- and platinum-catalyzed cyclization of enynes: chiral gold complexes for enantioselective alkoxycyclization. Organometallics 24:1293–1300
13. Toullec PY, Chao C-M, Chen Q, Gladiali S, Genêt J-P, Michelet V (2008) Enantioselective platinum-catalyzed tandem hydroarylation-cycloisomerization of 1,6-enynes. Adv Synth Catal 350:2401–2408
14. Jang H-Y, Hughes FW, Gong H, Zhang J, Brodbelt JS, Krische MJ (2005) Enantioselective reductive cyclization of 1,6-enynes via rhodium-catalyzed asymmetric hydrogenation: C–C bond formation precedes hydrogen activation. J Am Chem Soc 127:6174–6175
15. Corkey BK, Toste FD (2007) Palladium-catalyzed enantioselective cyclization of silyloxy-1, 6-enynes. J Am Chem Soc 129:2764–2765
16. Trost BM (1990) Palladium-catalyzed cycloisomerizations of enynes and related reactions. Acc Chem Res 23:34–42
17. Trost BM, Lee DC, Rise F (1989) A new palladium catalyst for intramolecular carbametalations of enynes. Tetrahedron Lett 30:651–654
18. Trost BM, Czeskis BA (1994) Asymmetric induction in Pd catalyzed enyne cycloisomerizations. Tetrahedron Lett 35:211–214
19. Goeke A, Kuwano R, Ito I, Sawamura M (1996) Enantioselective cycloisomerization of 1,6-enynes catalyzed by chiral diphosphane-palladium complexes. Angew Chem Int Ed 35:662–663
20. Hatano M, Terada M, Mikami K (2001) Highly enantioselective palladium-catalyzed ene-type cyclization of a 1,6-enyne. Angew Chem Int Ed 40:249–253
21. Hatano M, Yamanaka M, Mikami K (2003) A new N,P-ligand with achiral gem-dimethyloxazoline for palladium(II)-catalyzed cyclization of 1,6-enynes: transition state probe for the N/C trans mode in Mizoroki–Heck-type C–C bond formation. Eur J Org Chem 2552–2555
22. Hatano M, Mikami K (2003) Highly enantioselective ene-type spiro-cyclization of allyl propargyl ethers catalyzed by cationic palladium(II) complexes with a new type of PN-ligand bearing achiral gem-dimethyl oxazoline. J Mol Catal A Chem 196:165–169
23. Hatano M, Mikami K (2003) Highly enantioselective alkaloid synthesis via ene-type cyclizations catalyzed by cationic chiral palladium(II) complexes of PN-ligands with an achiral oxazoline unit. Org Biomol Chem 1:3871–3873
24. Mikami K, Hatano M (2004) Palladium-catalyzed carbocyclization of 1,6-enynes leading to six-membered rings or oxidized five-membered trifluoroacetates. Proc Natl Acad Sci USA 101:5767–5769
25. Imase H, Suda T, Shibata Y, Noguchi K, Hirano M, Tanaka K (2009) Highly enantioselective construction of axial chirality by palladium-catalyzed cycloisomerization of N-alkenyl arylethynylamides. Org Lett 11:1805–1808
26. Cao P, Wang B, Zhang X (2000) Rh-catalyzed enyne cycloisomerization. J Am Chem Soc 122:6490–6491
27. Lei A, Waldkirch JP, He M, Zhang X (2002) Highly enantioselective cycloisomerization of enynes catalyzed by rhodium for the preparation of functionalized lactams. Angew Chem Int Ed 41:4526–4529
28. Cao P, Zhang X (2000) The first highly enantioselective Rh-catalyzed enyne cycloisomerization. Angew Chem Int Ed 39:4104–4106
29. Lei A, He M, Wu S, Zhang X (2002) Highly enantioselective Rh-catalyzed Intramolecular Alder–Ene reactions for thesyntheses of chiral tetrahydrofurans. Angew Chem Int Ed 41:3457–3460
30. Hashmi ASK, Haufe P, Rivas Nass A, Bats JW (2004) The absolute configuration of the products of the enantioselective rhodium(I)/BINAP-catalyzed enyne cyclization. Adv Synth Catal 346:421–424
31. Körber N, Rominger F, Müller TJJ (2009) Novel enantioselective sequentially rhodium(I)/BINAP-catalyzed cycloisomerization-hydrogenation-isomerization-acetalization (CIHIA). Adv Synth Catal 351:2921–2935

32. Lei A, He M, Zhang X (2003) Rh-catalyzed kinetic resolution of enynes and highly enantioselective formation of 4-alkenyl-2,3-disubstituted tetrahydrofurans. J Am Chem Soc 125:11472–11473
33. He M, Lei A, Zhang X (2005) Enantioselective syntheses of 3,4,5-trisubstituted γ-lactones: formal synthesis of (−)-blastmycinolactol. Tetrahedron Lett 46:1823–1826
34. Lei A, He M, Zhang X (2002) Highly enantioselective syntheses of functionalized α-methylene-γ-butyrolactones via Rh(I)-catalyzed intramolecular Alder Ene reaction: application to formal synthesis of (+)-pilocarpine. J Am Chem Soc 124:8198–8199
35. Liu F, Liu Q, He M, Zhang X, Lei A (2007) Rh-catalyzed highly enantioselective formation of functionalized cyclopentanes and cyclopentanones. Org Biomol Chem 5:3531–3534
36. Nicolaou KC, Edmonds DJ, Li A, Tria GS (2007) Asymmetric total syntheses of platensimycin. Angew Chem Int Ed 46:3942–3945
37. Nicolaou KC, Li A, Edmonds DJ, Tria GS, Ellery SP (2009) Total synthesis of platensimycin and related natural products. J Am Chem Soc 131:16905–16918
38. Wender PA, Haustedt LO, Lim J, Love JA, Williams TJ, Yoon J-Y (2006) Asymmetric catalysis of the [5 + 2] cycloaddition reaction of vinylcyclopropanes and π-systems. J Am Chem Soc 128:6302–6303
39. Mikami K, Yusa Y, Hatano M, Wakabayashi K, Aikawa K (2004) Enantioselective spiro ene-carbocyclization of 1,6-enynes catalyzed by tropos rhodium(I) complex with skewphos ligand. Tetrahedron 60:4475–4480
40. Mikami K, Yusa Y, Hatano M, Wakabayashi K, Aikawa K (2004) Highly enantioselective spiro cyclization of 1,6-enynes catalyzed by cationic skewphos rhodium(I) complex. Chem Commun 98–99
41. Mikami K, Aikawa K, Yusa Y, Jodry JJ, Yamanaka M (2002) Tropos or Atropos? That is the Question! Synlett 1561–1578
42. Mikami K, Kataoka S, Yusa Y, Aikawa K (2004) Racemic but tropos (chirally flexible) BIPHEP ligands for Rh(I)-complexes: highly enantioselective ene-type cyclization of 1,6-enynes. Org Lett 6:3699–3701
43. Mikami K, Kataoka S, Aikawa K (2005) Tropos or atropos nature of rhodium complexes bearing a tetrakis(phosphanyl)terphenyl ligand: highly enantioselective catalysis of ene-type cyclization. Org Lett 7:5777–5780
44. McKinstry L, Livinghouse T (1994) On the asymmetric Rh(I) catalyzed [4 + 2] cycloisomerization reaction. Electronic and torsional ligand control of absolute stereoselection. Tetrahedron 50:6145–6154
45. Gilbertson SR, Hoge GS, Genov DG (1998) Rhodium-catalyzed asymmetric [4 + 2] cycloisomerization reactions. J Org Chem 63:10077–10080
46. Aikawa K, Akutagawa S, Mikami K (2006) Asymmetric synergy between chiral dienes and diphosphines in cationic Rh(I)-catalyzed intramolecular [4 + 2] cycloaddition. J Am Chem Soc 128:12648–12649
47. Shibata T, Tahara Y (2006) Enantioselective intramolecular [2 + 2 + 2] cycloaddition of 1,4-diene-ynes: a new approach to the construction of quaternary carbon stereocenters. J Am Chem Soc 128:11766–11767
48. Shibata T, Tahara Y, Tamura K, Endo K (2008) Enantioselective syntheses of various chiral multicyclic compounds with quaternary carbon stereocenters by catalytic intramolecular cycloaddition. J Am Chem Soc 130:3451–3457
49. Tanaka K, Nishida G, Sagae H, Hirano M (2007) Enantioselective synthesis of C2-symmetric dimethyl cyclohexadienedicarboxylates through cationic rhodium(I)/modified-BINAP-catalyzed [2 + 2 + 2] cycloadditions. Synlett 1426–1430
50. Shibata T, Kurokawa H, Kanda K (2007) Enantioselective intramolecular [2 + 2 + 2] cycloaddition of enediynes for the synthesis of chiral cyclohexa-1,3-dienes. J Org Chem 72:6521–6525
51. Wender PA, Takahashi H, Witulski B (1995) Transition metal catalyzed [5 + 2] cycloadditions of vinylcyclopropanes and alkynes: a homolog of the Diels–Alder reaction for the synthesis of seven-membered rings. J Am Chem Soc 117:4720–4721

52. Shintani R, Nakatsu H, Takatsu K, Hayashi T (2009) Rhodium-catalyzed asymmetric [5 + 2] cycloaddition of alkyne-vinylcyclopropanes. Chem Eur J 15:8692–8694
53. Méndez M, Muñoz MP, Nevado C, Cárdenas DJ, Echavarren AM (2001) Cyclizations of enynes catalyzed by $PtCl_2$ or other transition metal chlorides: divergent reaction pathways. J Am Chem Soc 123:10511–10520
54. Soriano E, Ballesteros P, Marco-Contelles J (2004) A theoretical investigation on the mechanism of the $PtCl_2$-mediated cycloisomerization of heteroatom-tethered 1,6-enynes. J Org Chem 69:8018–8023
55. Blum J, Beer-Kraft H, Badrieh Y (1995) A novel platinum tetrachloride-catalyzed cyclorearrangement of allyl propynyl ethers to 3-oxabicyclo[4.1.0]heptenes. J Org Chem 60:5567–5569
56. Fürstner A, Szillat H, Stelzer F (2000) Novel rearrangements of enynes catalyzed by $PtCl_2$. J Am Chem Soc 122:6785–6786
57. Ferrer C, Raducan M, Nevado C, Claverie CK, Echavarren AM (2007) Missing cyclization pathways and new rearrangements unveiled in the gold(I) and platinum(II)-catalyzed cyclization of 1,6-enynes. Tetrahedron 63:6306–6316
58. Lee SI, Kim SM, Kim SY, Chung YK (2006) The gold(I)-catalyzed cycloisomerization of 1,6-enynes to 1,4-dienes. Synlett 2256–2260
59. Shibata T, Kobayashi Y, Maekawa S, Toshida N, Takagi K (2005) Iridium-catalyzed enantioselective cycloisomerization of nitrogen-bridged 1,6-enynes to 3-azabicylo[4.1.0] heptenes. Tetrahedron 61:9018–9024
60. Kerber WD, Koh JH, Gagné MR (2004) Platinum(II)-catalyzed 1,6-diene cycloisomerizations: turnover in the absence of β-hydride elimination. Org Lett 6:3013–3015
61. Feducia JA, Campbell AN, Doherty MQ, Gagné MR (2006) Modular catalysts for diene cycloisomerization: rapid and enantioselective variants for bicyclopropane synthesis. J Am Chem Soc 128:13290–13297
62. Brissy D, Skander M, Retailleau P, Marinetti A (2007) N-heterocyclic carbenes in the synthesis of axially chiral square-planar platinum complexes. Organometallics 26:5782–5785
63. Brissy D, Skander M, Retailleau P, Frison G, Marinetti A (2009) Platinum(II) complexes featuring chiral diphosphines and N-heterocyclic carbene ligands: synthesis and evaluation as cycloisomerization catalysts. Organometallics 28:140–151
64. Brissy D, Skander M, Jullien H, Retailleau P, Marinetti A (2009) Platinum(II) catalysts for highly enantioselective 1,6-enyne cycloisomerizations. Synthetic, structural and catalytic studies. Org Lett 11:2137–2139
65. Lee SI, Kim SM, Choi MR, Kim SY, Chung YK, Han W-S, Kang SO (2006) Au(I)-catalyzed cyclization of enynes bearing an olefinic cycle. J Org Chem 71:9366–9372
66. Nishimura T, Kawamoto T, Nagaosa M, Kumamoto H, Hayashi T (2010) Chiral tetrafluorobenzobarrelene ligands for the rhodium-catalyzed asymmetric cycloisomerization of oxygen- and nitrogen-bridged 1,6-enynes. Angew Chem Int Ed 49:1638–1641
67. Shibata T, Takasaku K, Takesue Y, Hirata N, Takagi K (2002) Iridium complex-catalyzed enantioselective intramolecular [4 + 2] cycloaddition of dieneynes. Synlett 1681–1682
68. Sethofer SG, Staben ST, Hung OY, Toste FD (2008) Au(I)-catalyzed ring expanding cycloisomerizations: total synthesis of ventricosene. Org Lett 10:4315–4318
69. Chao C-M, Beltrami D, Toullec PY, Michelet V (2009) Asymmetric Au(I)-catalyzed synthesis of bicyclo[4.1.0]heptene derivatives via a cycloisomerization process of 1,6-enynes. Chem Commun 6988–6990
70. Watson IDG, Ritter S, Toste FD (2009) Asymmetric synthesis of medium-sized rings by intramolecular Au(I)-catalyzed cyclopropanation. J Am Chem Soc 131:2056–2057
71. Hashmi ASK, Hamzic M, Rominger F, Bats JW (2009) Gold catalysis: enantiotopos selection. Chem Eur J 15:13318–13322

Chapter 11
Coordination-Driven Supramolecular Assembly of Phosphole-Based π-Conjugated Ligands

J. Crassous, C. Lescop and R. Réau

Abstract π-chromophores having a (2-pyridyl)phosphole moiety act as heteroditopic P,N-chelates towards a large range of transition metals. Due to the different nature of the donor atoms in these ligands, stereoselective coordination chemistry processes allow organizing of these derivatives into sophisticated architectures. Coordination-driven synthesis of C_2-symmetrical metallic complexes active in non-linear optics (NLO) and chiral metal-bis(azahelicene phosphole) assemblies are described. Furthermore, 1-phenyl-bis(2-pyridyl)phosphole can act as a N,P,N-chelate with bridging P-atoms in a very original coordination mode to stabilize a variety of metal dimers. Use of such Cu(I) dimers as molecular clips allows the characterization of π-stacked [2,2]metallacyclophanes that self-assemble in a very general way in the solid state along π-stacked columns.

11.1 Introduction

Phospholes are the most studied P-heterocycles due to their ready accessibility, good stability and versatile chemical behavior [1–5]. These group 15 heteroles exhibit limited aromatic character, due to the inherent property of the P-atom

J. Crassous · C. Lescop · R. Réau (✉)
Sciences Chimiques de Rennes, UMR 6226 CNRS, Université de Rennes 1,
Campus de Beaulieu, 35042 Rennes Cedex, France
e-mail: regis.reau@univ-rennes1.fr

J. Crassous
e-mail: jeanne.crassous@univ-rennes1.fr

C. Lescop
e-mail: christophe.lescop@univ-rennes1.fr

M. Peruzzini and L. Gonsalvi (eds.), *Phosphorus Compounds*,
Catalysis by Metal Complexes, 37, DOI: 10.1007/978-90-481-3817-3_11,
© Springer Science+Business Media B.V. 2011

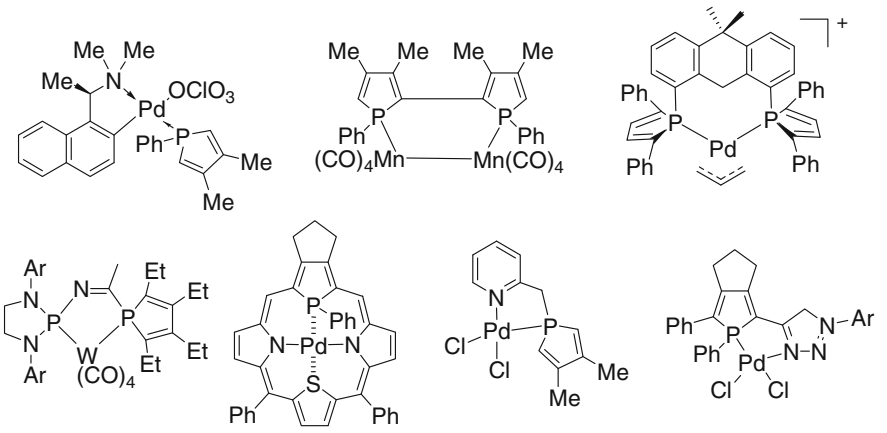


Fig. 11.1 Selected examples of complexes bearing phosphole-based ligands

(pyramidal geometry, inert s-pair effect) [6], resulting in a high reactivity of both their dienic and heteroatom moieties. This behavior, which is very different from that of their N-analogues, makes phospholes appealing derivatives for many purposes. For example, they are versatile synthons for the preparation of various P-heterocycles such as phosphanorbornadienes, via Diels–Alder reactions involving their dienic moiety [7] or according to a 1,5-shift [8] of the P-substituent, or phosphaferrocenes and phosphinines, via transformation into nucleophilic phospholide anions [9]. Furthermore, they have been extensively used as building blocks for the preparation of tailored ligands since their P-atom behaves as a classical two-electron-donor toward transition metals [9–12]. Therefore, a wide variety of both mono- and multi-dentate phosphole-containing ligands, including heteroditopic P,N-donors, have been reported; selected examples developed in the recent years are depicted in Fig. 11.1. This set of complexes illustrates the diversity of phosphole-based ligands that has been investigated, including sophisticated isophlorin derivatives [7–21]. Up to now, the most important application of phosphole complexes is homogeneous catalysis. For examples, phospholes have been used in a diverse range of catalytic processes such as olefin/CO copolymerization [22, 23]. hydroformylation of olefins [24], Suzuki-Myaura and Heck couplings [15, 25]. telomerisation of 1,3-diynes [26, 27], allylic alkylation [28–30], hydrogenation of ketones [31]. For example, in most cases, they are superior to more classic phosphine donors such as triphenylphosphine due to their specific electronic (high s-character of the lone P-pair) and steric (acute endocyclic CPC angle) properties.

More recently, the two main characteristics of the phosphole ring (i.e. low aromaticity and reactivity of the P-atom) have been extensively exploited for the molecular engineering of new π-conjugated molecular materials for opto-electronic purposes [32–40]. Many so-called "small molecules" and polymers incorporating phosphole moieties have been prepared (Fig. 11.2), and the study of their

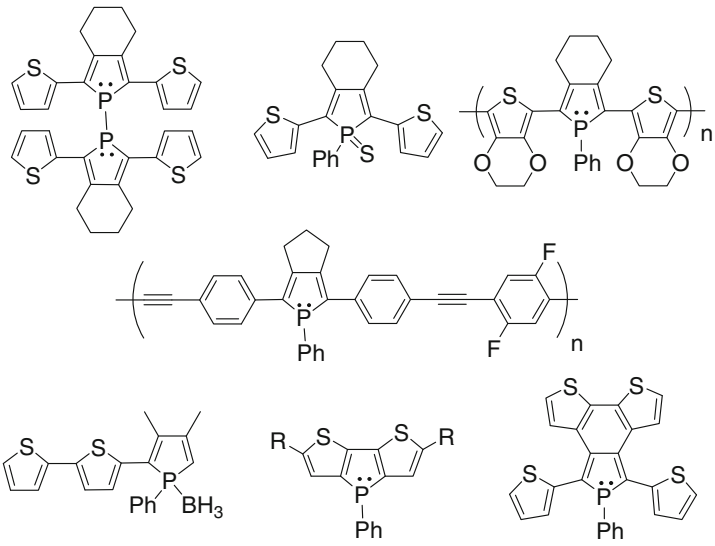


Fig. 11.2 Representative examples of phosphole-based π-conjugated systems

physical behavior has shown that the presence of the P-unit provides these conjugated systems with appealing properties. The possibility to coordinate the P-atom of phosphole-containing extended π-conjugated systems to transition metals considerably extends their potential towards the synthesis of functional materials. For example, the gold complex **A** (Fig. 11.3) exhibits a much higher fluorescence quantum yield than the free ligand (13 vs. 5%) and therefore can be used as an emissive material for OLEDs [32–34].

This chapter is devoted to π-chromophores having a (2-pyridyl)phosphole moiety and the use of coordination chemistry to selectively organize these derivatives into sophisticated architectures. It will be shown that 2-(2-pyridyl)phosphole chromophores are unique π-systems since they can act as heteroditopic P,N-chelates towards a large range of transition metals. Due to the different nature of the donor atoms (a soft P- and a hard N-center according to Pearson's classification) [41, 42], they undergo highly stereoselective coordination processes to d^8 square-planar metal ions by virtue of the anti-symbiotic rule [41, 42]. Furthermore, heteroditopic P,N-ligands usually exhibit hemilabile behavior, a dynamic property that is very important in order to obtain the thermodynamically more stable transition metal complex. In this chapter, the use of these appealing properties for the coordination-driven synthesis of C_2-symmetrical metallic complexes active in non linear optics (NLO) [43] and chiral metal-bis(azahelicene phosphole) assemblies [44–46] **B** will be described (Fig. 11.3). Another remarkable property of mixed pyridine–phosphole ligands is the coordination mode of bis(2-pyridyl)phosphole that acts as a N,P,N-chelate with a bridging P-atom that can stabilize a variety of metal dimers such as complex **C** (Fig. 11.3). The supramolecular synthesis of

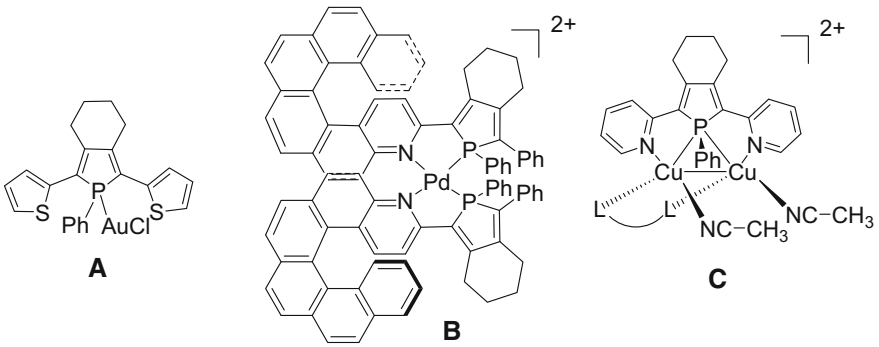


Fig. 11.3 Complexes of phosphole-based π-conjugated systems

π-stacked [2,2]metallacyclophanes based on Cu(I)-dimers of type **C** as molecular clips will be presented [47–50]. Special focus will be devoted to the supramolecular organization of these [2,2]metallacyclophanes within π-stacked columns in the solid state.

11.2 π-Conjugated (2-pyridyl)phospholes

11.2.1 Phosphole: A Weakly Aromatic Heterole With a Reactive Heteroatom

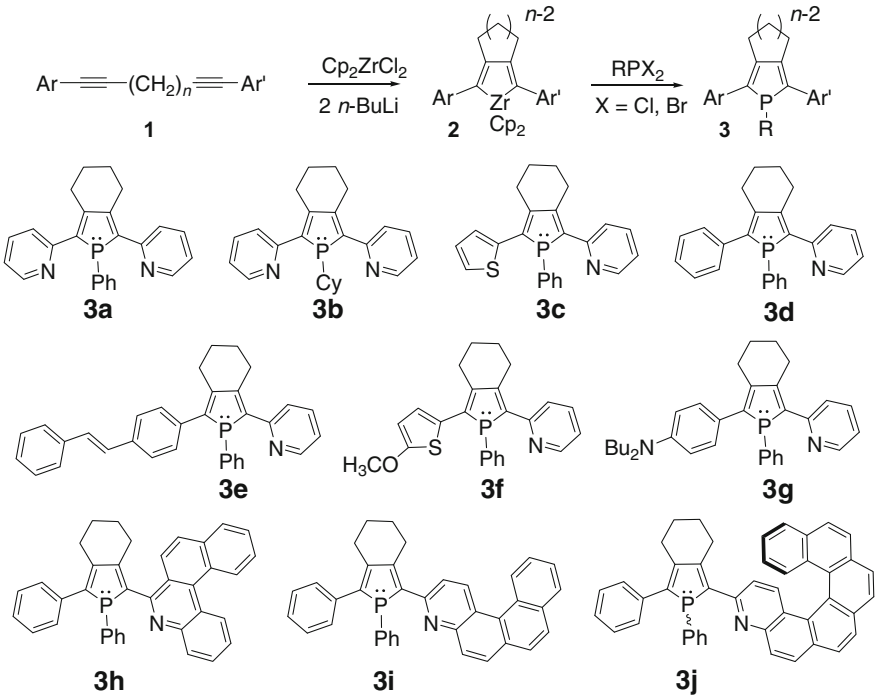
The chemistry surrounding phospholes has been developed over more than 50 years [1–5, 9, 51–53]. While the first phospholes were described in the 1950s, the synthetic routes combining high yields and diversity of substitution patterns were only established in the late 1960s. The feature that dictates the phosphole property (stability, reactivity, electronic character…) is its very low aromaticity [54–59]. A detailed discussion on phosphole aromaticity based on theoretical and experimental data is given in reference [3]. This weak aromatic character is a consequence of two intrinsic properties of phospholes: (1) the tricoordinate P-atom adopts a pyramidal geometry and (2) its lone pair exhibits a high degree of s-character. These two features prevent efficient interaction of the P-lone pair with the endocyclic π-system. Remarkably, the aromatic character of the phosphole ring results from hyperconjugation involving the exocyclic P–R σ-bond and the π-system of the dienic moiety [60–65]. One of the most striking consequence of such weak aromaticity is that the parent phosphole is stable only below −100 °C [66]. However, introducing a phenyl, a cyano, a bulky alkyl or an alkoxy group at the P-atom allows derivatives to be obtained that are stable at room temperature. It is also noteworthy that the aromaticity of phospholes can be strongly influenced by the nature (steric hindrance, electronegativity) of the substituent on the P-atom

[51–53, 61]. In fact, calculations have shown that phospholes with a planar P-atom would be more aromatic than pyrrole, due to the good π-donor ability of planar-P centers. However, this stabilization is not sufficient to overcome the high planarization barrier of the P-atom (35 kcal mol^{-1}), but is responsible for the reduced P-inversion barrier in phosphole (ca. 16 vs. 36 kcal mol^{-1} for phospholanes) [67–69]. Low barrier inversion is another key property of phospholes since inversion at phosphorus can occur at room temperature. Together, these electronic properties (low aromatic character, σ–π hyperconjugation) set phosphole apart from pyrrole and thiophene. In other words, this P-heterole has its own chemistry (synthetic routes, methods of functionalization, etc.) that cannot be predicted by simply extrapolating that of its aromatic S- and N-analogues [1–5, 32–40, 51–53, 70–72].

11.2.2 Synthesis, Structure and Optical Properties of π-Conjugated (2-pyridyl)phosphole Derivatives

Derivatives having a (2-pyridyl)phosphole motif are accessible via the widely applicable 'Fagan–Nugent method' [73, 74] using readily available diynes **1** possessing either a $(CH_2)_3$ or a $(CH_2)_4$ spacer (Scheme 11.1) [75–79]. The zirconacyclopentadiene intermediates **2** are extremely air- and moisture-sensitive derivatives that react in situ with dihalogenophosphanes to give the corresponding phospholes **3a–j** in medium to good yields (Scheme 11.1). This route is highly flexible allowing a variety of electron-deficient (2-pyridyl) and electron-rich (4-methoxythiophene, 4-dimethylaminophenyl) rings to be introduced in the 2,5-positions, and also allowing variation in the nature of the P-substituent (Ph, Cy) (Scheme 11.1). Note that the pyridyl moiety can also be included in sophisticated frameworks such as helicene fragments (**3h–j**, Scheme 11.1). All these derivatives having phenyl or cyclohexyl P-substituents are air-stable and can be purified by standard methods including column chromatography or crystallization. They exhibit classic multinuclear NMR chemical data, including ^{31}P NMR chemical shifts varying between 7.3 and 20.7 ppm [32–40, 44–46, 75–79].

X-ray diffraction studies of (2-pyridyl)phosphole derivatives **3a**,**i**,**j** (Fig. 11.4) show that the twist angles between two adjacent rings are rather small (<40°) and that the phosphorus atoms are strongly pyramidalized, as indicated by the sum of the CPC angles (>295°). The lengths of the C–C linkages between the rings (∼1.46 Å) are in the range expected for Csp^2–Csp^2 single bonds. Together, these metric data suggest a delocalization of the π-system involving the dienic part of the P-ring and the two substituents at its 2,5-positions. In the solid state, the three heteroatom present in **3a** (Fig. 11.4) are in a mutual *syn–syn* arrangement. Theoretical calculations show that this conformation is slightly more stable than the two other N,P,N-arrangements (*syn–anti*, *anti–anti*). However, this isomer is only 1.0 and 4.8 kJ.mol^{-1} more stable than the *syn–anti* and the *anti–anti* isomers, respectively. Furthermore, the energies of the transition structures for the rotation



Scheme 11.1 Synthesis of 2-(2-pyridyl)phosphole derivatives by the Fagan–Nugent method

about the C–C inter-ring bonds revealed low barriers to rotation (12–16 kJ mol^{-1}). These theoretical data, as well as variable temperature NMR studies, suggest of a free rotation about the inter-ring C–C bonds. This is supported by the fact that in the solid state, the P,N-moiety of derivatives **3i**,**j** have an *anti*-arrangement [44–46].

The synthesis and characterization of derivatives **3h–j** deserve a special comment since the azahelicene moieties are chiral fragments. As expected, the naphtho[1,2-f]-quinoline part of **3i** displays a helical geometry with a dihedral angle of 30.1° between the two terminal aromatic rings, according to an X-ray diffraction study (Fig. 11.4). However, the two stereogenic elements (P-centre, azahelicene) of **3h**,**i** undergo rapid inversion in solution and only one set of NMR signals is observed at room temperature. In contrast, phosphole **3j** (Scheme 11.1) features a configurationally stable aza[6]helicene moiety. Its $^{31}P\{^{1}H\}$ NMR spectrum displays two sharp singlets of comparable intensity at 14.0 and 14.5 ppm. In fact, starting with a diyne bearing an enantiomerically pure helix that can be obtained following resolution by chiral HPLC (for example *P*-configuration, Scheme 11.2), two diastereomeric phospholes (i.e. (P,S_P)-**3j**^{1} and (P,R_P)-**3j**^{2}) are obtained due to the presence of the stereogenic P-atom. Their mirror images (i.e. (M,R_P)-**3j**^{1} and (M,S_P)-**3j**^{2}) are synthesized using the *M*-azahelicene. Indeed, a variable temperature $^{31}P\{^{1}H\}$ NMR spectroscopic study revealed an inversion barrier between **3j**^{1} and **3j**^{2} of 16 kcal mol^{-1} at 330 K in $CDCl_3$ [44–46]. Slow crystallization at

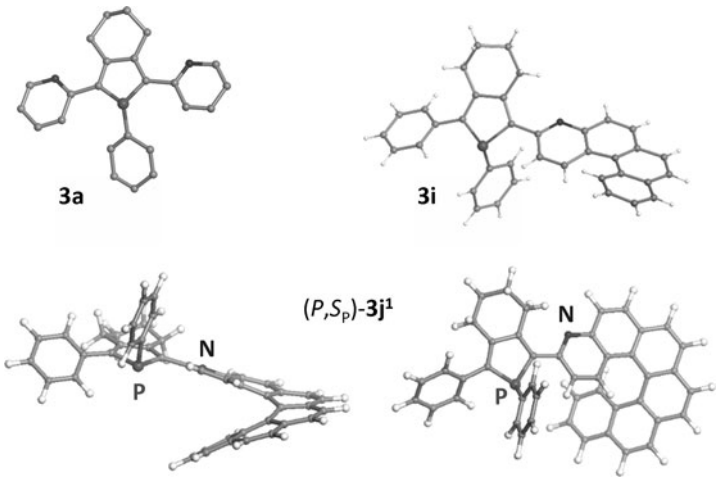


Fig. 11.4 X-ray structures of phospholes **3a**,**i**,**j**

room temperature of the diastereomeric mixture of phospholes **3j**^{1,2} afforded single crystals of **3j**^{1} only (Fig. 11.4). The metric and geometrical data of the 2-(2-pyridyl)phosphole moiety of (*P**,S_P*)-**3j**^{1} are fully consistent with those of the related derivative **3i**. Note that this X-ray structure fits with BP/SV(P) and BP/TZVP optimized calculated structures. For example, the helical curvature of the aza[6]helicene fragment is classic with an angle of 45.8° between the pyridine ring and the terminal phenyl ring. It is noteworthy that the twist angle between the phosphole ring and the aza[6]helicene substituent is relatively small (26.3°), and allows an electronic interaction between the two π-systems [44–46].

The presence of an extended π-conjugated system in phospholes **3a**–**j** is confirmed by the observation of a broad absorption maximum in the visible region. The absorption maxima of phospholes **3f** and **3g** (Scheme 11.1 and Table 11.1) are comparable for both derivatives and are shifted to longer wavelengths

Scheme 11.2 Synthesis of (P,S_P)-**3j**^{1} and (P,R_P)-**3j**^{2} diastereomers from one diyne *P*-**1j** enantiomer

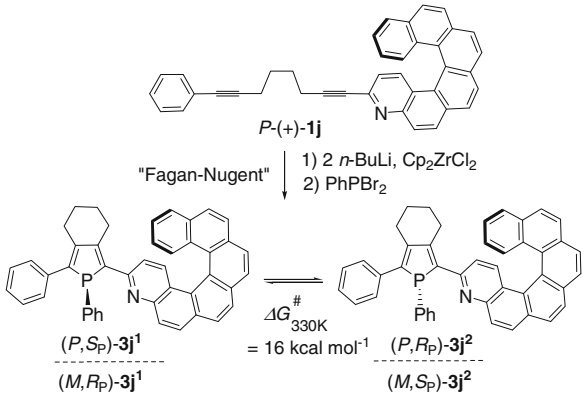


Table 11.1 Physical properties of representative 2-(2-pyridyl)phosphole derivatives

	λ_{max}[a] (nm)	log ε	λ_{em}[a] (nm)	ϕ_f[b] (%)
3a	390	4.02	463	1.1
3c	396	3.64	500	n.d.[d]
3d	364	3.88	475	3
3e	395	4.36	497	15.2
3f	415	4.25	n.d.	n.d.[d]
3g	417	4.25	n.d.	n.d.[d]
3h	375	3.69	389–456[c]	n.d.[d]
3i	406	4.46	499[c]	8
3j	430	4.10	502[c]	n.d.[d]

[a] In THF
[b] Relative to quinine sulfate or fluorescein ±15%
[c] Multi-components emission
[d] Not determined

($\Delta\lambda_{max}$: 20–35 nm) than those recorded for the corresponding derivatives **3c** and **3d** featuring no methoxy or dibutylamino electron-donor end groups, respectively. The absorption spectrum of phosphole **3i** (bearing terminal azahelicenes) is considerably red-shifted compared to that of **3h** which has an inner pyridine moiety in the azahelicene part (Scheme 11.1, Table 11.1). This behavior can be attributed to the fact that **3i** possesses longer, more extended π-conjugated systems than the branched compound **3h** (Scheme 11.1). It is noteworthy that there is a regular bathochromic shift upon increasing the size of the pyridine-based π-system (see the series 2-(2-pyridyl)phosphole **3d**/aza[4]helicene-derivative **3i**/aza[6]helicene-derivative **3j**; Scheme 11.1, Table 11.1). These data clearly show the impact of the helicene composition on the optical properties of mixed phosphole–azahelicene derivatives and indicate that these two π-subunits are electronically coupled. Note that the presence of the helicene moiety also impacts the emission behaviour of phosphole derivatives. For example, at 77 K, compounds **3h–j** (Scheme 11.1) display broad fluorescence emissions (389–499 nm), accompanied by red-shifted phosphorescent emissions ($\tau > 1.3$ s), which are typical for azahelicene moiety. For comparison, at 77 K, no phosphorescence could be detected for the 1,2-diphenyl-5-(2-pyridyl)phosphole **3d** (Scheme 11.1) [45]. Note that 2-(2-pyridyl)phosphole **3e** is the only σ^3,λ^3-phosphole derivative that can be used as electroluminescent material in OLEDs [33].

11.3 Coordination Chemistry of π-Conjugated Systems Incorporating A 2-(2-pyridyl)phosphole Moiety

11.3.1 General Aspects

In the field of π-conjugated materials, two main challenges posed by the fabrication of efficient devices are (1) to devise synthetic strategies allowing ready generation of compounds with diverse structures and electronic properties, and (2)

to control the supramolecular organization of π-systems, since intermolecular interactions alter physical properties of the bulk material. Coordination chemistry is a powerful tool to tackle both these challenges since metals are versatile templates for assembling π-conjugated ligands into well defined molecular structures such as octupolar complexes [80–82], metallocyclophanes [83–86], and molecular knots [87, 88] to name but a few. Considering a given target architecture, this approach simply involves a careful design of the π-conjugated ligands guided by the basic concepts of coordination chemistry (*trans*-effect, hemilability…). Furthermore, coordination chemistry offers a simple way to tune the optical and electronic properties of the π-ligands since both the coordination sphere geometry and the nature of the metal–ligand interaction can be readily modified by varying the metal center.

Derivatives having a 2-(2-pyridyl)phosphole moiety depicted in Scheme 11.1 possess many appealing prerequisites (1,4-P,N fragment, extended π-conjugated systems…) to be used as building blocks for this general approach. Two targets were defined to test and exploite the potential of these P,N-derivatives. First was the in-plane parallel assembly of 1D-dipolar chromophores to give non-centrosymmetric molecules, an important prerequisite for 2nd order NLO activity. Second involves the controlled gathering of helicenes into bis(helicene)complexes in order to form assemblies exhibiting high and tunable chiroptical properties. This chapter will describe these two approaches after a brief description of the coordination chemistry of simple 2-(2-pyridyl)phosphole derivatives to illustrate their main ligand properties.

11.3.2 Coordination Behavior of 2-(2pyridyl)phopshole Derivatives

Simple 2-(2-pyridyl)phosphole derivatives **3a–d** act as 1,4-P,N chelates towards transition metal ions having different coordination spheres, oxidation numbers and charges. Selected examples including neutral and dicationic square-planar Pd(II) [77, 79], and monocationic tetrahedral Ru(II) [78] and Cu(I) [49] complexes are presented in Fig. 11.5. Note that phosphole triazole hybrids (Fig. 11.5) recently synthesized by Matano et al. [19] display similar 1,4-P,N chelate behavior. All these complexes are obtained in high yields (>85%) as air stable derivatives. It is remarkable that these P,N-donors are able to afford air-stable Cu(I)-complexes. Upon coordination, the H^6 of the pyridyl group generally experience a high frequency chemical shift (∼0.6 ppm) since the ring becomes electron-deficient. The formation of the five-membered metallacycle is indicated by a large frequency chemical shift in its ^{31}P NMR spectrum and has been confirmed by X-ray diffraction studies. The angles and the bond lengths within these metallacycles are consistent with known literature values for both P-phenyl and P-cyclohexyl phosphole ligands. For example, the chelate bite angles P–M–N [ca. 80–85°] are

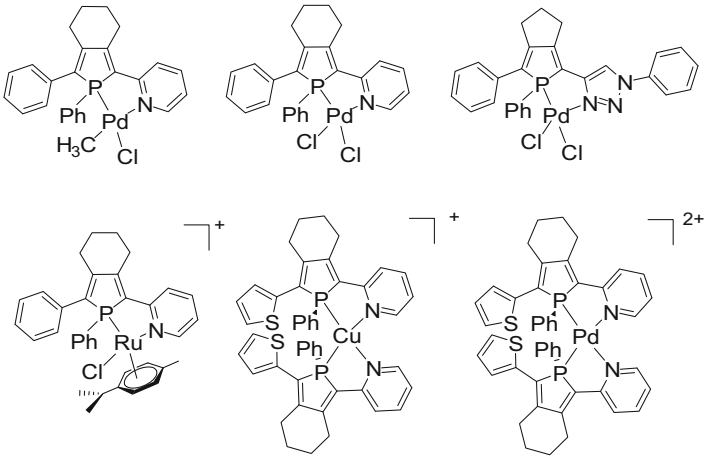
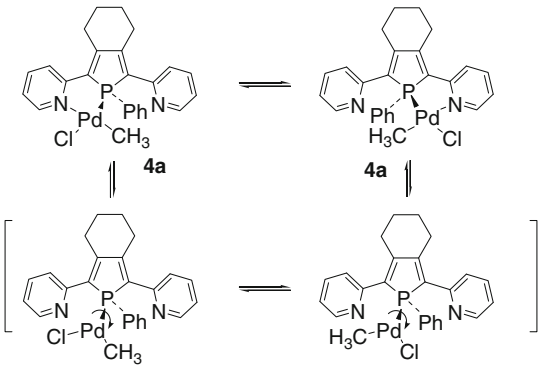


Fig. 11.5 P,N-chelate behavior of 2-(2-pyridyl)phosphole derivatives towards metal ions

similar to values reported for other 1,4-P,N donors such as (phosphinomethyl)oxazolines and phosphine-imines [89–93]. Two peculiar features are that the tetracoordinate P-atom exhibits a severely distorted tetrahedral geometry and that the phosphole C-atom linked to the pyridyl substituent does not possess the expected trigonal planar geometry. These reveal an important ring strain imposed by the rigidity of the 1,4-P,N chelate backbones which contain sp^2-C atoms. The coordinated pyridyl and phosphole rings are not coplanar, however, the twist angles are rather small (ca. 10–15°) allowing an electronic interaction between these two heterocycles to take place. It is noteworthy that single diastereoisomers were formed in the case of the unsymmetrical PdCl(Me)-complexes (Fig. 11.5) with a *cis* arrangement of the methyl group and the phosphorus atom. This stereoselective coordination is clearly due to the heteroditopic nature of the 2-(2-pyridyl)phosphole chelates (*trans* effect).

Two important processes taking place in Pd(II)-coordination sphere have to be underlined. Firstly, complex **4a** possessing pendant pyridyl arm is fluxional at room temperature due to an intramolecular exchange between the pendant and coordinated pyridyl groups (Scheme 11.3). This equilibrium nicely illustrates the hemilabile behavior of (2-pyridyl)phosphole ligands, a property that is of great importance in achieving thermodynamic control in supramolecular synthesis (vide infra). Secondly, a slow isomerisation of complex **5a** to 2-phospholene complex **6a** takes place at room temperature via an allylic rearrangement [94, 95]. This transformation is quantitative and highly stereoselective with only one diastereoisomer being formed (with the H and 1-phenyl group in a *cis* position, see Scheme 11.3). This transformation is also observed for the $PdCl_2$ complex of **1d** in the presence of pyridine at reflux in CH_2Cl_2 [94]. This process provides a unique and powerful method to access to 2-pyridyl-2-phospholene derivatives that can be obtained in an optically pure form due the high inversion barrier of their P-atom

Scheme 11.3 Hemilability of 2-(2-pyridyl)phosphole ligands

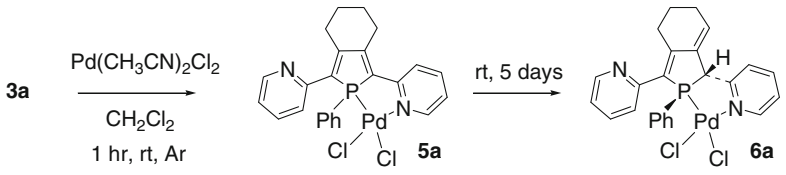


[30]. However, it is a potential drawback in our approach since the pathway of the π-system, and therefore the electronic property of the ligand, is altered on going from phosphole to phospholene subunits (Scheme 11.4).

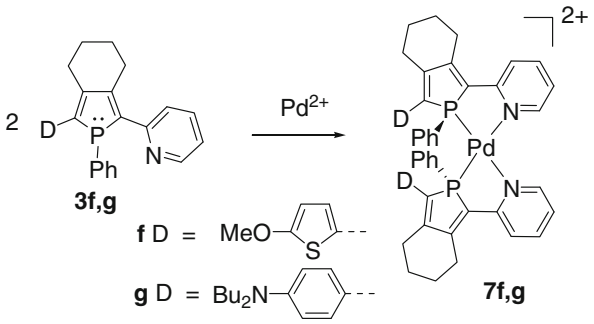
These results show that 2-(2-pyridyl)phospholes behave as classic 1,4-P,N ligands in spite of their rather rigid structure. They possess all the appealing attributes of heteroditopic donors such as stabilization of metal ions with different oxidation states, stereoselective coordination and hemilabile behavior.

11.3.3 NLO-Active C_2-Symmetrical Complexes

A fruitful strategy to optimize nonlinear optical activity of dipoles involves gathering together identical one dimensional (1D) donor(D)–acceptor(A) substituted chromophores leading to molecular non-centrosymmetrical multi(dipolar) systems. This general approach, that is mainly based on organic synthetic approaches [96], was extended to coordination chemistry [97] using the fact that 2-pyridylphosphole derivatives are heteroditopic 1,4-chelates which can control the orientation of a second chelating ligand in the coordination sphere of a square planar d^8-metal centre (Pd^{2+}, Pt^{2+}) [43]. Phospholes **3f**,**g** (Scheme 11.1) have a typical '*D*-(π-bridge)-A' dipolar NLO-phore topology and they exhibit moderate NLO activities ($\beta_{1.9\ \mu m,} \approx 30 \times 10^{-30}$ esu) due to the weak acceptor character of the



Scheme 11.4 Isomerization of phosphole complex **5a** to 2-pyridyl-2-phospholene-Pd complex **6a**

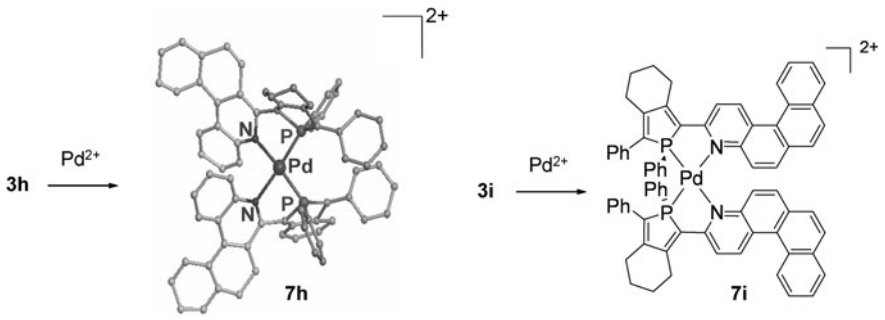


Scheme 11.5 Stereoselective synthesis of NLO-active complexes **7f**,**g**

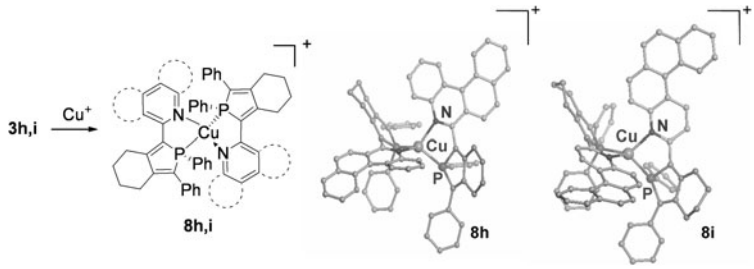
pyridine group [43]. These 1,4-P,N chelates undergo stereoselective coordination leading to a close parallel alignment of the 1-dimensional dipoles on the square-planar d^8-Pd(II) template (Scheme 11.5). Thus, the *trans*-effect can overcome the natural anti-parallel alignment tendency of 1D-dipolar chromophores at the molecular level. The non-centrosymmetric complexes **7f**,**g** (Scheme 11.5) exhibit fairly high NLO activities ($\beta_{1.9\mu m}$ ca. 170–180 $\times$ 10^{-30} esu), that are much higher than those of the free ligands. This NLO activity enhancement is probably due to the onset of ligand-to-metal-to-ligand charge transfer (LMLCT), which contributes coherently to the second harmonic generation [43]. Indeed, construction of 1-dimensional dipolar ligand using a 2-(2-pyridyl)phosphole skeleton allows a predictable and very simple molecular engineering using the basic concepts of coordination chemistry to be performed.

11.3.4 Metal Bis(aza[n]helicenephosphole) Complexes

Helicenes are fascinating molecules endowed with helical chirality and π-conjugated backbones [98–101]. The most appealing attribute of helicene derivatives is their huge chiroptical properties (optical rotation, circular dichroism) [102–104] that make them promising building blocks for the synthesis of functional molecular materials (e.g., non linear optical materials, chiral wave-guides…) [105–112]. The potential use of helicene derivatives towards devices depends greatly on the facility of generating different frameworks in order to modulate and to optimize their electronic and optical properties. Therefore, we have investigated the synthesis of helicene derivatives bearing a 2-(2-pyridyl)phosphole moiety that could form stable metal-bis(helicene) complexes. It was expected that using one P,N-helicene, structural diversity could be easily generated simply by changing the metal ion (variation of coordination geometry, of electronic property, charge number…). Furthermore, it was anticipated that the nature of the metal would impact the chiroptical properties of the metal-bis(helicene) complexes.



Scheme 11.6 Synthesis of Pd^{II}-complexes **7h** and **7i** from phospholyl-aza[4]helicenes. View of the X-ray crystal structure of dicationic complex **7h** (H atoms, counteranions and solvent molecules have been omitted)



Scheme 11.7 Synthesis of Cu^{I}-complexes **8h** and **8i** from phospholyl-aza[4]helicenes. Views of the X-ray crystal structure of monocationic complexes **8h** and **8i** (one stereoisomer, H atoms, counteranions and solvent molecules have been omitted for clarity)

In order to gain more insight into the coordination behavior of mixed helicene-phosphole based P,N chelates, the two molecules **3h**,**i** which differ only by the position of the N-atom within the helix (Scheme 11.1), were investigated. Pd(II) and Cu(I), a square-planar d^8 and a tetrahedral d^{10} metal center, respectively, were selected. Derivatives **3h**,**i** reacted with 0.5 eq. of $[Pd(CH_3CN)_4](SbF_6)_2)$ yielding the C_2-symmetrical chiral Pd-bis(phosphole-azahelicene) **7h**,**i** as pairs of enantiomers (Scheme 11.6). Likewise, the reaction of derivatives **3h**,**i** with a Cu^{I} source (CuCl or $[Cu(CH_3CN)_4](PF_6)_2$, 2:1 molar ratio) in CH_2Cl_2 solution at room temperature, gave rise to the new complexes **8h**,**i** (Scheme 11.7).

Interestingly, the X-ray diffraction study of complex **7h** (Scheme 11.6) and **8h**,**i** (Scheme 11.7) revealed that the twist angle between the phosphole ring and the azahelicene (<50°) allows an electronic interaction between these two π-units to take place.[46, 45] The helical shape of the aza[4]helicene part is not perturbed upon complexation since the twist angle between the two terminal aromatic rings of the aza[4]helicene (33.1°) is comparable to that of the free ligand (30.1°) [45, 46]. This result shows that mixed phosphole-azahelicene derivatives can act as

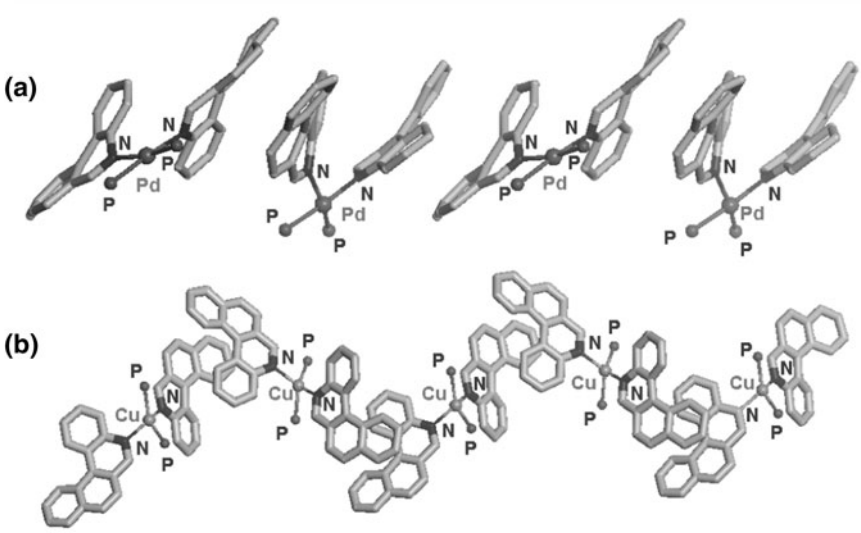
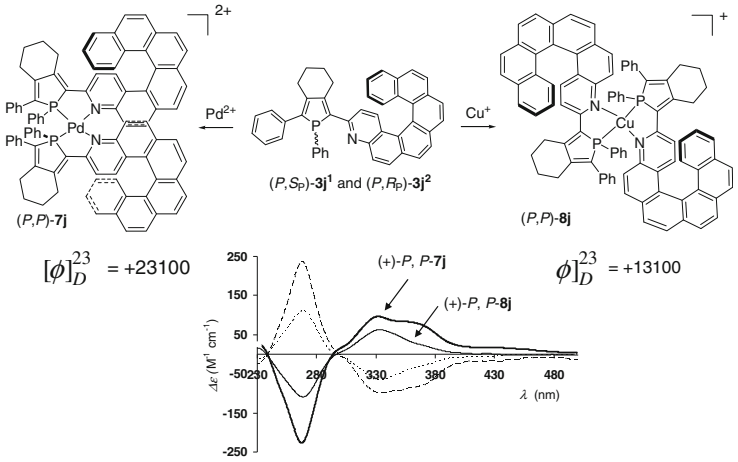


Fig. 11.6 Simplified views of the supramolecular arrangement of complexes **7h** (**a**) and **8h** (**b**)

1,4-chelates to form metal-bis(phosphole–azahelicene) assemblies with different topologies.

It is worth noting that the angle between the two N-Pd-D planes of Pd(II) complex **7h** is 17.3° (Scheme 11.6). This distortion, which is due to the overlapping of the two coordinated azahelicene moieties, results in a chiral coordination sphere around the Pd^{II} centre with either a Λ or a Δ configuration. It is likely that the configuration at the metal is maintained in solution due to the overlapping of the helices (Scheme 11.6). It is remarkable that amongst the numerous possible stereoisomers (26), only one pair of enantiomers is obtained in the solid state (M_{helix1}, M_{helix2}, S_{P1}, S_{P2}, Λ_{Pd}) and (P_{helix1}, P_{helix2}, R_{P1}, R_{P2}, Δ_{Pd}) [45, 46]. This high stereoselectivity is due to a set of specific properties of the mixed azahelicene–phosphole ligands due the P,N-donor moiety, the ease of inversion of the phosphole P-atom and the presence of the bulky helicene fragment. For example, for obvious steric reasons, the phenyl substituents of the phosphole ligands are in *trans* positions with respect to the PdN_2P_2 coordination plane and the two azahelicenes moieties are homochiral (Scheme 11.6). It is furthermore very likely that the hemilabile nature of the P,N-chelates **3h**,**i** is a clue to obtaining the more thermodynamically stable complex via the establishment of coordination–decoordination equilibria.

An additional interesting point to be noticed is the solid-state organization of Pd(II) and Cu(I) complexes **7h** and **8h** into columns in which each molecule stacked with its enantiomeric neighbor (Fig. 11.6, intermolecular distance 3.5–3.6 Å). This type of supramolecular organisation, which is due to π-stacking of the



Scheme 11.8 Synthesis of Pd- and Cu-bis(aza[6]helicenephosphole) **7j** and **8j** from $\mathbf{3j^{1,2}}$. CD spectra in CH_2Cl_2 at 293 K of (+)-(*P*,*P*)-**7j** (plain line) and (+)-(*P*,*P*)-**8j** complexes (*dashed lines*), and of their respective enantiomers

azahelicene moieties, is well-known in helical molecule chemistry [98–101]. This result shows that the presence of the metal center does not prevent metal(phosphole-aza[n]helicene) complexes from behaving as regular helicene derivatives.

Following this preliminary study with model compounds, the diastereomeric mixture of interconverting aza[6]helicene-phospholes (*P*,S_P)-$\mathbf{3j^1}$ and (*P*,R_P)-$\mathbf{3j^2}$ (Scheme 11.2) was reacted with $[Pd(CH_3CN)_4](SbF_6)_2$ (2:1 molar ratio) affording complex **7j** (78% yield) (Scheme 11.8). The simplicity of its NMR spectra clearly shows that the coordination of aza[6]helicene-phospholes $\mathbf{3j^{1,2}}$ onto Pd^{II} is highly stereoselective [44]. This suggests that complex **7j** is obtained as a single enantiomer, whereas its mirror image is prepared using the mixture of (*M*,R_P)-$\mathbf{3j^1}$ and (*M*,S_P)-$\mathbf{3j^2}$ ligands. The fact that complex **7j** is obtained as a single enantiomer starting from (*P*,S_P)-$\mathbf{3j^1}$ and (*P*,R_P)-$\mathbf{3j^2}$ confirms the results obtained with the model ligands: the configuration of the helix controls the configuration of the other stereogenic centers, i.e. the phosphole P- and the Pd-atoms. This is also supported by calculations at the BP/SV(P) level of theory performed for the ligand having a *P*-helix revealing that the $[Pd(\mathbf{3j^1})_2]^{2+}$ assembly, in which the P-atom has an *R* configuration and a Δ configuration around the Pd center, is 19.4 kcal/mol more stable than its S_P,Δ_{Pd} diastereomer $[Pd(\mathbf{3j^2})_2]^{2+}$ (Fig. 11.7). Furthermore, the complex having a Λ_{Pd} configuration (*P*-helix, R_P) is not a minimum on the potential energy surface [44].

The same synthetic approach using $[Cu(CH_3CN)_4](PF_6)$ (2:1 ratio) afforded complex **8j** (86% yield, Scheme 11.8). The synthesis of complexes **7j** and **8j** enabled to investigate the impact of the metal's nature on the chiroptical properties

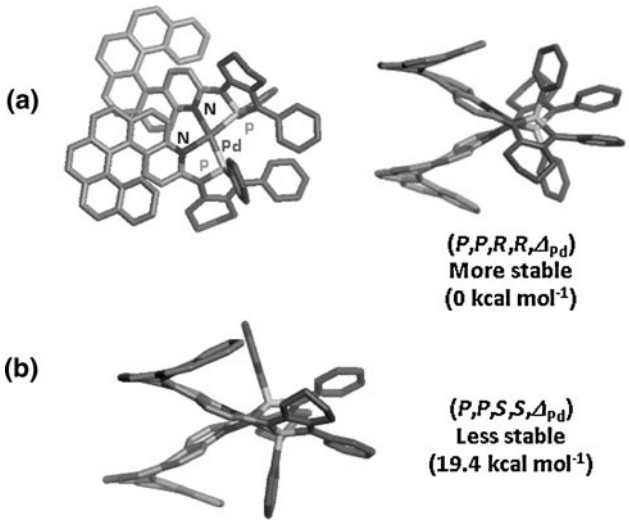


Fig. 11.7 Optimized structures and relative energies for **7j** ($[Pd(\mathbf{3j^1})_2]^{2+}$ (**a**) and $[Pd(\mathbf{3j^2})_2]^{2+}$ (**b**)) by DFT calculations

of these chiral metal-bis(helicene) assemblies. The specific molar rotation measured in CH_2Cl_2 of the Pd(II)-complex **7j** ($[\phi]_D^{23} = 23{,}100 \pm 2\%$) is much larger than that of its Cu(I)-analogue **8j** ($[\phi]_D^{23} = 13{,}100 \pm 2\%$). Moreover, their CD spectra are very different. For example, *P*-helicene-containing complexes **7j** and **8j**, namely (+)-(*P*,*P*)-**7j** and (+)-(*P*,*P*)-**8j** (Scheme 11.8), both display two intense CD bands at 270 nm (negative) and around 330 nm (positive). However, the magnitude of CD spectrum of Pd(II)-complex **7j** is much larger than that of the Cu(I)-complex **8j** (Scheme 11.8). Furthermore, the CD of Pd(II)-assembly **7j** displays intense bands at ~370 nm as well as weak bands at low energy wavelengths (410–450 nm) that are not observed for Cu(I)-complex **8j** (Scheme 11.8). These results clearly show that (1) it is possible to perform a coordination-driven tuning of chiroptical properties of phosphole-modified azahelicenes, and that (2) it is more efficient to organize these heteroditopic ligands around a square-planar Pd(II)- than around a tetrahedral Cu(I)- metal centre [44–46].

In conclusion, phosphole-modified azahelicenes appear to be well designed to self-assemble onto metal ions in a highly stereoselective way, affording original chiral elaborated architectures. Their coordination onto d^8 Pd^{II} center is highly stereoselective due to a unique combination of specific electronic (*trans effect*), steric (presence of the bulky helicene and P-substituent) and dynamic (fast inversion at P) properties. Indeed, in spite of their peculiar structures and the presence of sterically demanding azahelicene substituents, the heteroditopic P,N-moieties of derivatives **3h**,**i** dictate their coordination behaviour allowing a predictable coordination driven molecular engineering to be performed.

11.4 2,5-Bis(2-pyridyl)phospholes: N,P,N-Pincers for $Cu(I)_2$-clips Controlling the Supramolecular Organization of Extended π-Systems

11.4.1 Bimetallic Complexes Bearing a Bridging Phosphane Donor

2,5-Bis(2-pyridyl)phosphole **3a** (Scheme 11.1) is a very efficient N,P,N-pincer for the stabilisation of bimetallic complexes including metal ions such as Pd(I), Pt(I), Ag(I) and Cu(I). In these structures [47–50, 79, 113–115], the P-atom of **3a** exhibits a bridging phosphane coordination mode, which is a very rare coordination mode for phosphines [116–120]. For example, the X-ray crystal structure of Pd^{I}-dimer **9a** (Fig. 11.8) clearly shows that the Pd(I) dication contains two square–planar metal centres capped by two 2,5-bis(2-pyridyl)phospholes **3a** acting as 6-electron μ-1kN:1,2kP:2kN donors with equivalent P–Pd distances [Δ(Pd–P) = 0.01 Å] [79, 113]. Among the bimetallic complexes based on ligand **3a**, the Cu(I)-dimer **10a[1]** (Scheme 11.9), that is obtained by reacting **3a** with $[Cu(CH_3CN)_4](PF_6)$ in a 1:1 molar ratio, has a remarkable structure. Its X-ray diffraction study [47, 49] revealed that the Cu^{I}-atoms are bound to two bis(2-pyridyl)phosphole ligands **3a**, one acting as a μ-1κN:1,2κP:2κN donor and one acting as a 1κN:2κP-chelate. The coordination spheres of the tetrahedral Cu(I)-ions are completed by acetonitrile ligands. The metal–metal distance in **10a[1]** (2.555(1) Å) is fairly short suggesting metallophillic interactions between the two d^{10} metal centres. The two Cu(I)-atoms are not equivalent and therefore the μP-Cu distances are different ($\Delta(\mu$P–Cu) = 0.087 Å). Note that dimer **10a[2]**, in which the 1κN:2κP**3a** is replaced by a 1κP:2κP-dppm (bis(diphenylphosphino)methane), can be obtained by reacting **3a**, $[Cu(CH_3CN)_4](PF_6)$ and dppm in a 1:2:1 molar ratio. These two Cu^{I}-complexes [47, 49] possess a unique *U*-topology, i.e. two *cis* coordinatively labile sites are closely aligned. In fact, the bridging coordination mode of the phosphole ligand **3a** imposes a short intermetallic distance [**10a[1]**, 2.555(1) Å **10a[2]**, 2.667(1) Å] resulting in a close proximity of the two kinetically labile acetonitrile ligands (N–N distances, ca. 3.2 Å). Bis(2-pyridyl)phosphole **3a**

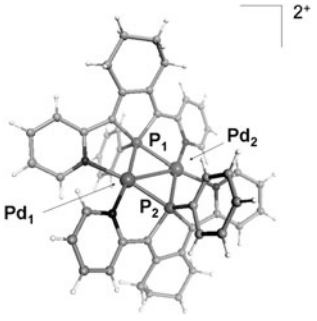
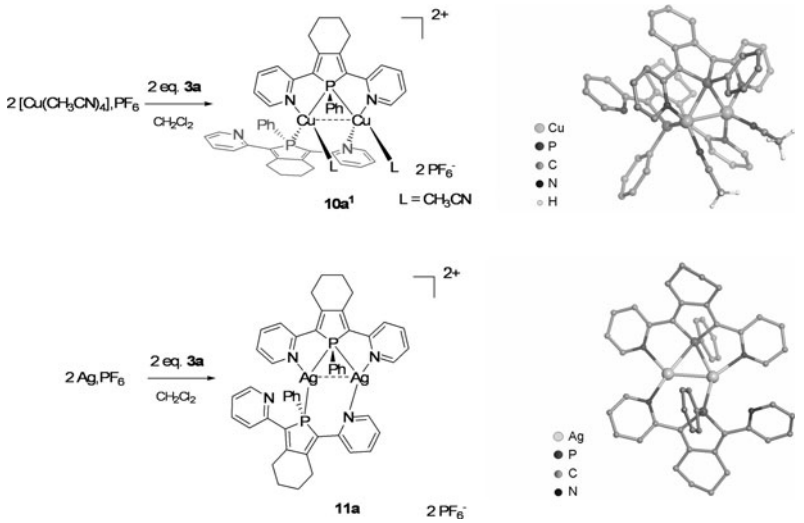


Fig. 11.8 View of the solid-state structure of the dicationic Pd(I)-dimer **9a**

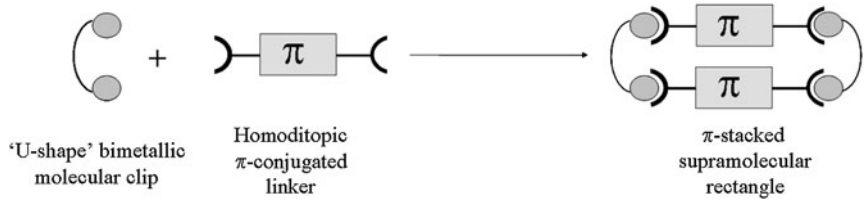


Scheme 11.9 Synthesis and view of the solid-state structure of dicationic complexes **10a**[1] and **11a**

can also stabilize Ag^{I}-dimers such as complex **11a** (Scheme 11.9) [114, 115]. This complex features two distorted trigonal planar Ag^{I} ions tethered by one bis(2-pyridyl)phosphole ligand **3a** acting as a 6-electron μ-1κN:1,2κP:2κN donor and one acting as a 4-electron 1κN:2κP-chelate. The metric data associated with the μ-1κN:1,2κP:2κN-**3a** donor in dimer **11a** are very similar to those of Cu^{I}-complex **10a**[1]. The μ-P centre displays a semi-bridging coordination mode ($\Delta(\mu P–Ag) = 0.148$ Å) and the metal–metal distance is about 2.7040(6) Å. In contrast to Pd(I)-complex **9a**, these Cu(I)- and Ag(I)-dimers are of interest since they are potentially reactive either through ligand exchange of the labile acetonitrile ligands (**10a**[1,2]) or through extension of the coordination metal sphere **(11a)**.

11.5 Coordination-Driven Synthesis Of π-Stacked [2.2]-Paracyclophane Analogues

The unique *U*-topology of Cu^{I}-complexes **10a**[1,2] (Scheme 11.9) is expected to be retained in supramolecular assemblies due to the rigidity of the N,P,N-pincer **3a** and the presence of the additional P,N- or P,P-chelate. This property has been exploited for the synthesis of [2,2]paracyclophane analogues using supramolecular coordination-driven chemistry. Indeed, the synthesis of these π-stacked molecular assemblies is of great importance in understanding the electronic interactions between individual chromophores [121–123]. However, straightforward routes to



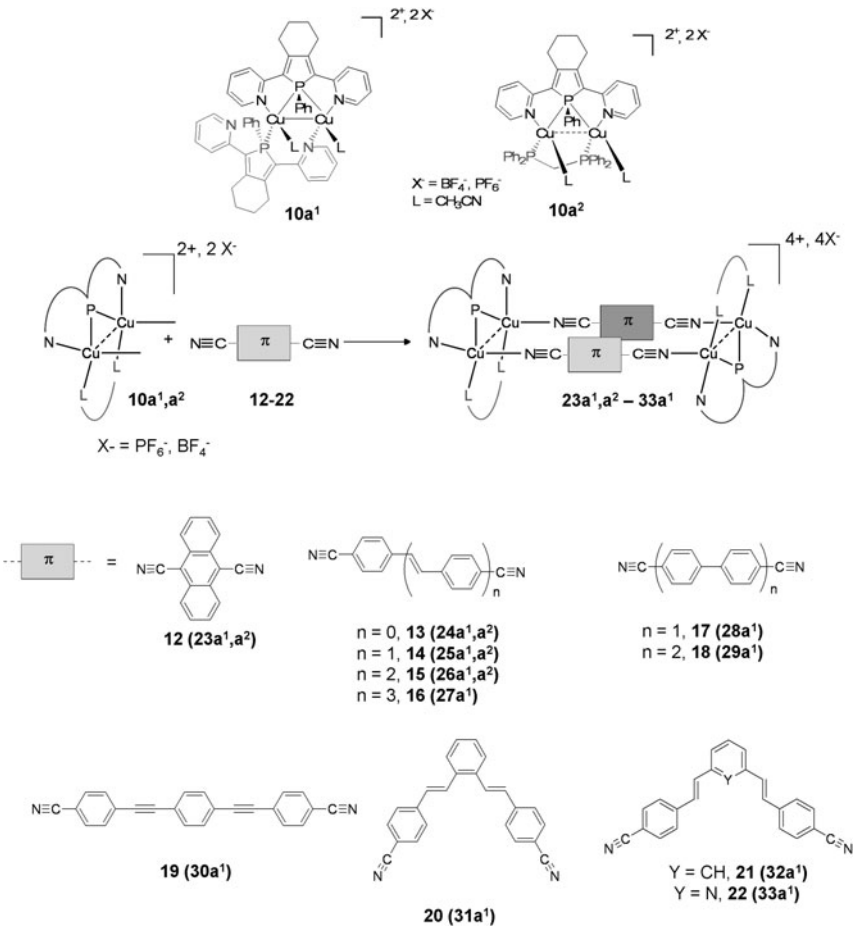
Scheme 11.10 Coordination-driven supramolecular synthesis of [2,2]-paracyclophanes analogues according to the directional bonding approach

these assemblies as well as for tailoring their structure remain a challenge to chemical synthesis.

Following the concepts of the "Directional-Bonding Approach" (Scheme 11.10) [124–128], the construction of metalloparacyclophanes **23a**^{1,2}–**33a**^{1,2} was conducted upon reacting the bimetallic clips **10a**^{1,2} having a *U*-topology with the linear homoditopic π-conjugated linkers **12**–**22** (Scheme 11.11) [48, 50]. X-ray diffraction studies of the supramolecular assemblies based on the shorter linkers (Fig. 11.9) showed that the metric data of the dimetallic clips **10a**^{1,2} do not change significantly upon their incorporation into the self-assembled structures demonstrating the conformational rigidity of the Cu^{I}-based subunits. In all cases, the four Cu-atoms lie in the same plane defining a rectangle and the aromatic moieties of the chromophores are parallel as a result of hindered rotation. Moreover, due to the short Cu^{I}–Cu^{I} intermetallic distances imposed by the bridging phosphane coordination mode, these aromatic moieties participate in face-to-face π-interactions (phenyl centroid–centroid distances: 3.4–3.5 Å) with small lateral offsets (Fig. 11.10).

The ditopic linker limit in this coordination-driven self-assembly process was investigated with the use of oligo(phenylene vinylene) (OPV) linkers **14**–**16** of increasing lengths (Scheme 11.11). In all cases, compounds having a gross structure that mimics the [2,2]-paracyclophane skeleton were obtained. The dimensions of these nano-sized rectangles are fixed by the size of the ditopic ligands and vary from 18.1 Å for **25a**^{1,2}, to 31.5 Å for **27a**^{1} (Cu–Cu distances) with an overall dimension of **27a**^{1} of about 46.5 Å in length (Fig. 4.3) [50].

The versatility of this coordination-driven synthetic approach towards π-stacked metallocylophanes was further demonstrated by the introduction of π-conjugated linkers having various chemical compositions or geometries. For examples, oligo(phenyl)- and oligo(phenylene ethynylene)-based linker **17**–**19**, that are widely investigated and useful building blocks for the tailoring of semiconducting organic materials, as well as 'angular' π-ditopic linkers **20**–**22** were successfully reacted with the molecular clip **10a**^{1} affording the corresponding π-stacked 2,2-paracyclophanes analogues **28a**^{1}–**33a**^{1} (Fig. 4.4). In assemblies **29a**–**30a**, the oligo(phenyl)- and oligo(phenylene ethylene)-based π-conjugated walls have an almost face-to-face arrangement (lateral offset <1.2 Å) with short intramolecular contacts (<3.7 Å,) revealing π–π interactions. These compounds



Scheme 11.11 Supramolecular synthesis of π-stacked metallocyclophanes **23a^{1,2}**–**33a**

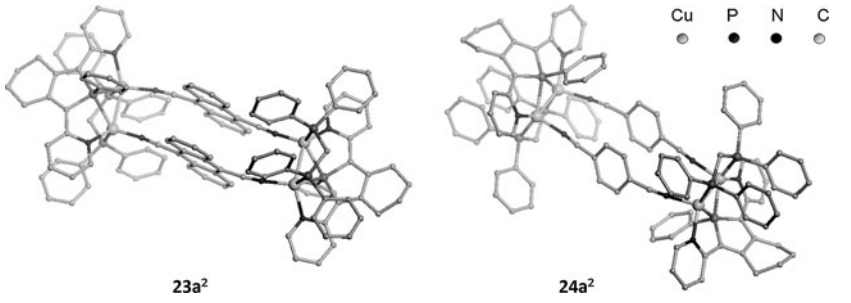


Fig. 11.9 X-ray crystal structures of the tetracationic assemblies **23a^2** and **24a^2** (H atoms, counteranions and solvents have been omitted for clarity)

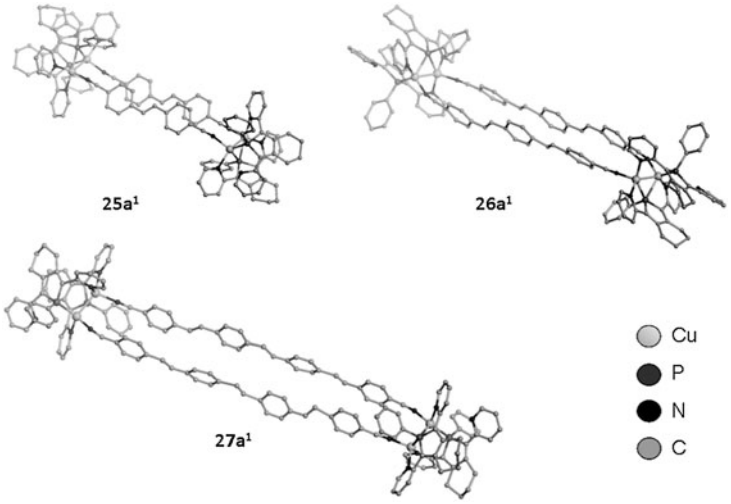


Fig. 11.10 Views of the solid state structures of the tetracationic supramolecular rectangles **25a**^{1}–**27a**^{1} (H atoms, counteranions and solvent molecules have been omitted for clarity)

are the first examples of π-stacked [2,2]paracyclophane derivatives incorporating tetraphenyl and 1,4-(bisphenylethynyl) π-moieties. The 'angular' π-linkers are located on the same side of the $(Cu)_4$ surface (Fig. 11.11, **31a**^{1} and **33a**^{1}), and participate in π–π interactions as indicated by the short inter-plane distances (<3.6 Å) with a 'parallel displaced' arrangement (2.3–2.5 Å). The coordination directional angles of the ditopic linkers are very acute (**31a**^{1}, 75.7–79.4°; **33a**^{1}, 104.0°) affording these π-stacked supramolecular [2.2]paracyclophanes **31a**^{1} and **33a**^{1} with an unprecedented topology [50].

These results show that, in spite of the repulsive interactions between the closed-shell π-clouds of the homoditopic ligands, the molecular clips **10a**^{1,2} can force face-to-face π-stacking of aromatic derivatives upon coordination into well-defined supramolecular metalloparacyclophanes. Indeed, due to their rigidity and unique topology, complexes **10a**^{1,2} are unique building blocks for the synthesis of π-stacked molecular assemblies having a [2.2]paracyclophane-like topology. This result opens appealing perspectives for the design of multifunctional molecular materials via this supramolecular assembling approach.

Moreover, the stacking pattern of the metalloparacyclophanes **25a**^{1}–**27a**^{1} and **29a**^{1}–**30a**^{1} is remarkable. These supramolecular rectangles self-organise into columns with short intermolecular distances (ca. 3.6 Å). In these columns, the cationic rectangles have a parallel-displaced arrangement along the *a*-axis. Unique infinite columnar stacks resulting from *intra*- and *inter*-molecular π–π interactions of the linear π-conjugated chromophores **14**–**16** and **18**,**19** are thus formed at the macroscopic scale (Fig. 11.12) [48, 50]. It is noteworthy that this type of supramolecular organization is not observed for the free ditopic linkers. In all cases, the infinite π-stacked columns are parallel (Fig. 11.13 for derivative **29a**^{1}).

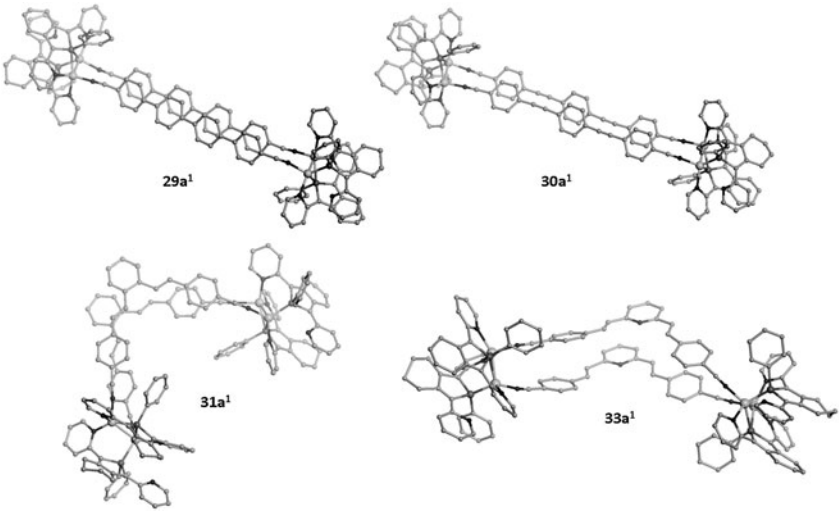


Fig. 11.11 X-ray molecular structures of the tetracationic assemblies **29a¹**–**31a¹** and **33a¹** (H atoms, counteranions and solvents have been omitted for clarity)

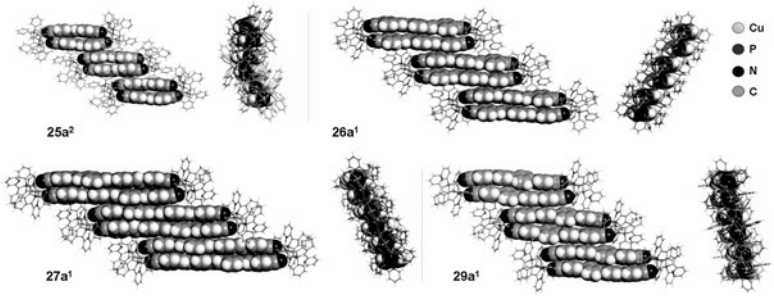


Fig. 11.12 'Side' and 'lateral' views of the stacking patterns of π-stacked metallocyclophanes **25a²**–**27a¹** and **29a¹** observed in single crystals

This arrangement generates channels that are filled by disordered CH_2Cl_2 solvent molecules, located in the vicinity of the π-conjugated linkers, and the PF_6^- or BF_4^- counter-anions that stand close to the dicationic $(Cu^I)_2$-clips. It is particularly striking that despite using π-conjugated linkers with quite different chemical composition (OPV, oligo(phenyl), oligo(phenylene ethynylene)), the same general hierarchical organization is observed upon reaction with the $(Cu^I)_2$-clips **10a¹⁻²**: first a local face-to-face organisation of two π-systems within a metallacyclophane, then an infinite 'parallel-displaced supramolecular arrangement' of these self-assembled structures in one direction. This supramolecular self-organization of linear π-conjugated oligomers in the solid state, although discovered by serendipity, seems to have a general and predictable character.

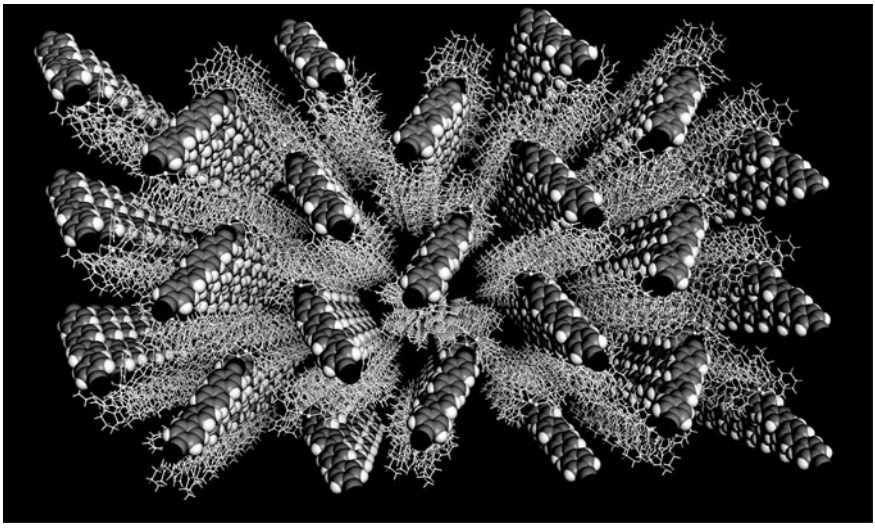


Fig. 11.13 View of the columnar stacks of derivative **29a**[1], counter-ions and disordered solvent molecules have been omitted

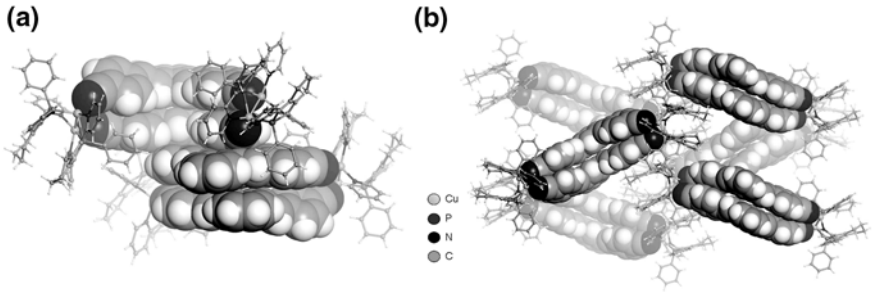
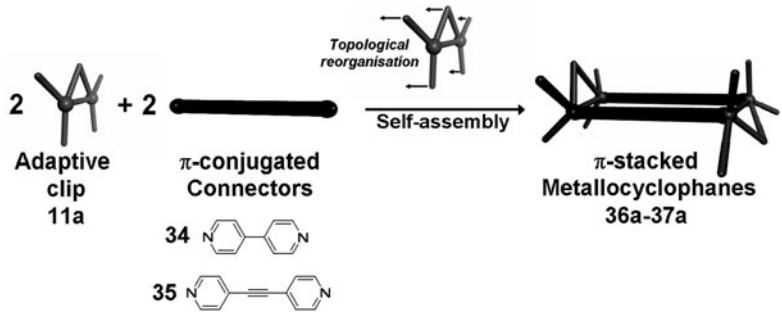


Fig. 11.14 **a** Supramolecular dimer observed in single crystals of metallacycle **31a**[1]; **b** organisation of the neighboring metallacycles in the single crystals of supramolecular assembly **32a**[1]

In contrast, in the case of the π-stacked supramolecular rectangles based on the angular linkers **20**–**22**, the formation of infinite networks driven by intermolecular π–π interacting molecules is not observed in the solid state. Derivative **31a**[1] aggregates into dimers (Fig. 11.14a) that exhibit parallel displaced π–π interactions (intermolecular distances, ca. 3.0 Å) while the isostructural derivatives **32a**[1] and **33a**[1] are isolated supramolecules in the solid state with no intermolecular π-contacts (Fig. 11.14b).

Therefore, the geometry of the π-connectors has a dramatic influence on the dimensionality of the supramolecular π-stacked arrays with the formation of infinite stacks with linear linkers (Fig. 11.13) and 2- or 4-fold stacks with angular linkers (Fig. 11.14). These structure-supramolecular organization relationships



Scheme 11.12 Synthesis of π-stacked metallocyclophanes **36a**, **37a** using the adaptative Ag^{I}-dimer molecular clip **11a**

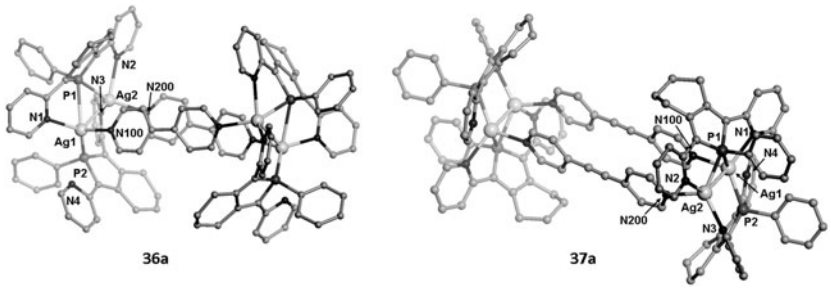


Fig. 11.15 X-ray crystal structures of the tetracationic assemblies **36a** and **37a** (H atoms, counteranions and solvents have been omitted for clarity)

open interesting perspectives for the development of a rational approach towards well-defined discrete or infinite π-stacked organic materials.

In contrast to Cu^{I} molecular clip **10a**[1,2], which bears two *cis*-coordinatively labile acetonitrile ligands (Scheme 4.1), the Ag^{I} bimetallic complex **11a** clearly does not possess a programmed *U*-shape with strongly directional available coordination sites. However, considering the ability of the Ag^{I} ions to access coordination modes higher than trigonal planar, we have investigated the use of **11a** as an 'adaptative' molecular clip for the coordination-driven supramolecular synthesis of π-stacked metallocyclophanes.

The reaction of Ag(I)-dimer **11a** with the 4-pyridine capped π-conjugated homodipotic linkers **34** and **35** (Scheme 11.12) afforded the supramolecular assemblies **36a** and **37a**, respectively, that were characterized by single-crystal X-ray diffraction study (Fig. 11.15) [114, 115]. In these new π-stacked supramolecular rectangles two Ag^{I}_{2}(**3a**)$_2$ dimers are connected by two π-linkers via coordination of their pyridyl termini. The tetracoordinated Ag^{I} metal centres in these assemblies exhibit a distorted tetrahedral coordination sphere that has clearly necessitated *a profound reorganisation of the metal coordination sphere* during the self-assembly process [114]. Therefore, π-stacked supramolecular rectangles can be obtained

either using rigid Cu^I-based molecular clips **10a**^{1,2} having a *U*-shape or from adaptive bimetallic Ag^I complex **11a**. It is noteworthy that the general mechanism leading to supramolecular π-stacked metallocyclophanes is quite different using the rigid clip **10a**^{1,2} or the adaptive clip **11a**. With **10a**^{1,2}, the formation of the assemblies implies a ligand exchange process, which is the classic building process used in the "*Directional-Bonding Approach*" (Scheme 11.11). In contrast, with the adaptive clip **11a** a simple coordination of the incoming linker is required. Note that using the Ag^I-dimer clip **11a** and the linkers **34**–**35**, no supramolecular organization of the supramolecular rectangles **36a**–**37a** within π-stacked columns is observed.

11.6 Conclusions

The results presented in the field of NLOphores and chiral helicoidal derivatives illustrate that, using the basic concepts of coordination chemistry, π-conjugated systems bearing 2-(2pyridyl)phosphole moiety can be selectively organized within sophisticated molecules. This approach is an appealing alternative to classic organic strategies for the generation of structural diversity to be generated. The investigation of the coordination behavior of mixed phosphole-pyridine ligands led to the discovery that 2,5-bis(2-pyridyl)phosphole is a very efficient N,P,N-pincer for the stabilization of bimetallic complexes. The fact that the P-center of this ligand acts as a μ-donor has been exploited to design molecular clips allowing the synthesis of π-stacked metallocyclophanes. This last approach is very promising for the design of advanced materials since it allows π-conjugated oligomers to be stacked within infinite columns.

References

1. Mathey F (2001) Phosphorus-carbon heterocyclic chemistry: the rise of a new domain. Elsevier Science Ltd, Oxford
2. Dillon K, Mathey F, Nixon JF (1998) Phosphorus: the carbon copy. Wiley, Chichester
3. Nyulaszi L (2001) Aromaticity of phosphorus heterocycles. Chem Rev 101:1229
4. Mathey F (2003) Phospha-organic chemistry: Panorama and perspectives. Angew Chem Int Ed 42:1578
5. Baumgartner T, Réau R (2006) Organophosphorus pi-conjugated materials. Chem Rev 106:4681
6. Regitz M, Scherer OJ (1990) Multiple bonds and low coordination in phosphorus chemistry. Georg Thieme Verlag, Stuttgart
7. Leung PH (2004) Asymmetric synthesis and organometallic chemistry of functionalized phosphines containing stereogenic phosphorus centers. Acc Chem Res 37:169
8. Mathey F (2004) Transient 2H-phospholes as powerful synthetic intermediates in organophosphorus chemistry. Acc Chem Res 37:954
9. Réau R, Dyer P (2008) In: Katritzky AR, Ramsden CA, Scriven EFV, Taylor RJK (eds) Comprehensive heterocyclic chemistry III. Elsevier, Oxford, vol 3, p 1029 (references therein)

10. Hissler M, Lescop C, Réau R (2008) Coordination chemistry of phosphole ligands: from supramolecular assemblies to OLEDs. C R Chimie 11:628
11. Crassous J, Réau R (2008) pi-Conjugated phosphole derivatives: synthesis, optoelectronic functions and coordination chemistry. Dalton Trans 6865
12. Hissler M, Lescop C, Réau R (2007) Functional phosphorus-based pi-conjugated systems: structural diversity without multistep synthesis. Pure Appl Chem 79:201
13. Ogasawara M, Ito A, Yoshida K, Hayashi T (2006) Synthesis of 2,5-bis(binaphthyl)-phospholes and phosphametallocene derivatives and their application in palladium-catalyzed asymmetric hydrosilylation. Organometallics 25:2715
14. Tissot O, Hydrio J, Gouygou M, Dallemer F, Daran JC, Balavoine GGA (2000) Some aspects of the structural and coordination chemistry of the 2,2′-biphosphole. Tetrahedron 56:85
15. Escalle A, Mora G, Gagosz F, Mezailles N, Le Goff XF, Jean Y, Le Floch P (2009) Cationic dimetallic gold hydride complex stabilized by a xantphos–phosphole ligand: synthesis, X-ray crystal structure, and density functional theory study. Inorg Chem 48:8415
16. Thoumazet C, Melaimi M, Ricard L, Le Floch P (2004) (2,5-diphenylphospholyl)-2-methylpyridine and 2-methyl-5R-phenyloxazoline $PdCl_2$ complexes: syntheses, X-ray crystal structures and use in the Miyaura and Heck coupling reactions. C R Chimie 7:823
17. Matano Y, Nakabuchi T, Fujishige S, Nakano H, Imahori H (2008) Syntheses, structures, and coordination chemistry of phosphole-containing hybrid calixphyrins: promising macrocyclic P,N-2,X-mixed donor ligands for designing reactive transition-metal complexes. J Am Chem Soc 130:990
18. Matano Y, Miyajima T, Ochi N, Nakabuchi T, Shiro M, Nakao Y, Sakaki S, Imahori H (2008) Redox-coupled complexation of 23-phospha-21-thiaporphyrin with group 10 metals: a convenient access to stable core-modified isophlorin–metal complexes. J Am Chem Soc 130:16446
19. Matano Y, Nakashima M, Saito A, Imahori H (2009) Phosphole-triazole hybrids: a facile synthesis and complexation with Pd(II) and Pt(II) Salts. Org Lett 11:3338
20. Burck S, Gudat D, Nieger M (2007) Metal-assisted, reversible phosphinyl phosphination of the carbon-nitrogen triple bond in a nitrile. Angew Chem Int Ed 46:2919
21. Burck S, Gudat D, Nieger M (2009) Cleavage of polarized P–P bonds in n-heterocyclic diphosphines in reactions with metal olefin complexes. Organometallics 28:1447
22. Sauthier M, Leca F, Toupet L, Réau R (2002) Palladium complexes of a novel family of P,N-chelates, the 2-(2-pyridyl)phospholes: synthesis, structural characterization, and catalytic activity for olefin/CO copolymerization. Organometallics 21:1591
23. Doherty S, Robins EG, Knight JG, Newman CR, Rhodes B, Champkin PA, Clegg W (2001) Selectivity for the methoxycarbonylation of ethylene versus CO-ethylene copolymerization with catalysts based on C-4-bridged bidentate phosphines and phospholes. J Organomet Chem 640:182
24. Tissot O, Gouygou M, Dallemer F, Daran JC, Balavoine GGA (2001) New rhodium(I) and iridium(I) complexes of the chiral 1,1′-diphenyl-3,3′,4,4′-tetramethyl-2,2′-biphosphole ligand—synthesis and applications to catalytic hydrogenation and hydroformylation reactions. Eur J Inorg Chem 2385
25. Thoumazet C, Ricard L, Grutzmacher H, Le Floch P (2005) Dibenzo[a,d]cycloheptenyl dibenzophosphole palladium dichloride: synthesis, X-ray-crystal structure and application in the Suzuki-Miyaura coupling. Chem Comm 1592
26. Leca F, Réau R (2006) 2-Pyridyl-2-phospholenes: new P,N ligands for the palladium-catalyzed isoprene telomerization. J Catal 238:425
27. de Souza RF, Bernardo-Gusmão K, Cunha GA, Loup C, Leca F, Réau R (2004) Ethylene dimerization into 1-butene using 2-pyridylphosphole nickel catalysts. J Catal 226:235
28. Cortes JGL, Ramon O, Vincendeau S, Serra D, Lamy F, Daran JC, Manoury E, Gouygou M (2006) New chiral ferrocene-bridged phosphole–phosphane ligands. Eur J Inorg Chem 5148

29. Mourgues S, Serra D, Lamy F, Vincendeau S, Daran JC, Manoury E, Gouygou M (2003) Chiral [(dialkylamino)methyl](phospholyl)ferrocene ligands as a new class of 1,2-disubstituted ferrocene ligands. Eur J Inorg Chem 2820
30. Leca F, Fernandez F, Muller G, Lescop C, Réau R, Gomez M (2009) Enantiomerically pure P,N chelates based on phospholene rings: palladium complexes and catalytic applications in allylic substitution. Eur J Inorg Chem 5583
31. Thoumazet C, Melaimi M, Ricard L, Mathey F, Le Floch P (2003) A cationic 1-(2-methylpyridine)phosphole cymene ruthenium chloride complex as an efficient catalyst in the transfer hydrogenation of ketones. Organometallics 22:1580
32. Fave C, Cho TY, Hissler M, Chen CW, Luh TY, Wu CC, Réau R (2003) First examples of organophosphorus-containing materials for light-emitting diodes. J Am Chem Soc 125:9254
33. Su HC, Fadhel O, Yang CJ, Cho TY, Fave C, Hissler M, Wu CC, Réau R (2006) Toward functional pi-conjugated organophosphorus materials: design of phosphole-based oligomers for electroluminescent devices. J Am Chem Soc 128:983
34. Fadhel O, Gras M, Lemaitre N, Deborde V, Hissler M, Geffroy B, Réau R (2009) Tunable organophosphorus dopants for bright white organic light-emitting diodes with simple structures. Adv Mater 21:1261
35. Fave C, Hissler M, Kárpáti T, Rault-Berthelot J, Deborde V, Toupet L, Nyulászi L, Réau R (2004) Connecting pi-chromophores by sigma-P–P bonds: new type of assemblies exhibiting sigma-pi-conjugation. J Am Chem Soc 126:6058
36. Matano Y, Miyajima T, Imahori H, Kimura Y (2007) Synthesis of 2-aryl-5-styrylphospholes: promising candidates for the phosphole-based NLO chromophores. J Org Chem 72:6200
37. Dienes Y, Durben S, Karpati T, Neumann T, Englert U, Nyulaszi L, Baumgartner T (2007) Selective tuning of the band gap of pi-conjugated dithieno[3,2-b : 2′,3′-d]phospholes toward different emission colors. Chem Eur J 13:7487
38. Fukazawa A, Hara M, Okamoto T, Son EC, Xu C, Tamao K, Yamaguchi S (2008) Bis-phosphoryl-bridged stilbenes synthesized by an intramolecular cascade cyclization. Org Lett 10:913
39. Fukazawa A, Yamada H, Yamaguchi S (2008) Phosphonium- and borate-bridged zwitterionic ladder stilbene and its extended analogues. Angew Chem Int Ed 47:5582
40. Ngoc Huy HT, Donnadieu B, Mathey F, Muller A, Colby K, Bardeen CJ (2008) A novel family of phosphole-thiophene oligomers for optoelectronic applications. Organometallics 27:5521
41. Pearson RG (1973) Antisymbiosis and trans effect. Inorg Chem 12:712
42. Harvey JN, Heslop KM, Orpen AG, Pringle PG (2003) Factors controlling the relative stabilities of cis- and trans-[PtX2L2] isomers: Chatt and Wilkins—50 years on. Chem Commun 278
43. Fave C, Hissler M, Sénéchal K, Ledoux I, Zyss J, Réau R (2002) Ligand trans-effect: using an old concept as a novel approach to bis(dipolar) NLO-phores. Chem Commun 1674
44. Graule S, Rudolph M, Vanthuyne N, Autschbach J, Roussel C, Crassous J, Réau R (2009) Metal-Bis(helicene) assemblies incorporating pi-conjugated phosphole–azahelicene ligands: impacting chiroptical properties by metal variation. J Am Chem Soc 131:3183
45. Graule S, Rudolph M, Shen W, Lescop C, Williams JAG, Autschbach J, Crassous J, Réau R (2010) Assembly of pi-Conjugated phosphole azahelicene derivatives into chiral coordination complexes: an experimental and theoretical study. Chem Eur J 16:5976
46. Shen W, Graule S, Crassous J, Lescop C, Gornitzka H, Réau R (2008) Stereoselective coordination of ditopic phospholyl-azahelicenes: a novel approach towards structural diversity in chiral pi-conjugated assemblies. Chem Comm 850
47. Leca F, Lescop C, Rodriguez E, Costuas K, Halet JF, Réau R (2005) Bridging phosphanes: exotic or versatile binucleating ligands? Angew Chem Int Ed 44:4362
48. Nohra B, Graule S, Lescop C, Réau R (2006) Mimicking [2,2]paracyclophane topology: molecular clips for the coordination-driven cofacial assembly of pi-conjugated systems. J Am Chem Soc 128:3520

49. Nohra B, Rodriguez-Sanz E, Lescop C, Réau R (2008) Chemistry of bridging phosphanes: Cu-I dimers bearing 2,5-bis(2-pyridyl)phosphole ligands. Chem Eur J 14:3391
50. Yao Y, Shen W, Nohra B, Lescop C, Réau R (2010) Coordination-driven hierarchical organization of pi-conjugated systems: from molecular to supramolecular pi-stacked assemblies. Chem Eur J 16:7143
51. Quin LD, Quin GS (2001) In: Mathey F (ed) Phosphorus-carbon heterocyclic chemistry: the rise of a new domain. Elsevier Science Ltd, Oxford
52. Mathey F (1988) The organic chemistry of phospholes. Chem Rev 88:429
53. Quin LD (1996) In: Katritzky AR (ed) Comprehensive heterocyclic chemistry. Pergamon, Oxford, p 757
54. Schleyer PvR, Freeman PK, Jiao H, Goldfuss B (1995) Aromaticity and antiaromaticity in concepts 5-membered C(4)H(4)X ring-systems—classical and magnetic may not be orthogonal. Angew Chem Int Ed 34:337
55. Chesnut DB, Quin LD (1994) Characterization of NMR deshielding in phosphole and the phospholide ion. J Am Chem Soc 116:9638
56. Dransfeld A, Nuylaszi L, Schleyer PvR (1998) The aromaticity of polyphosphaphospholes decreases with the pyramidality of the tricoordinate phosphorus. Inorg Chem 37:4413
57. Nyulaszi L (1996) J Phys Chem 100:6194
58. Nyulaszi L (1995) Effects of substituents on the aromatization of phosphole. J Phys Chem 99:586
59. Quinonero D, Garau C, Frontera A, Ballester P, Costa A, Deya PM (2002) Quantification of aromaticity in oxocarbons: the problem of the fictitious "nonaromatic" reference system. Chem Eur J 8:433
60. Schäfer W, Schweig A, Mathey F (1976) Theory and application of photoelectron-spectroscopy 60. Phospholes—electronic-structure. J Am Chem Soc 98:407
61. Mattmann E, Mathey F, Sevin A, Frison G (2002) De-aromatizing phosphole. J Org Chem 67:1208
62. Mattmann E, Mercier F, Ricard L, Mathey F (2002) Synthesis of new tricyclic phosphines and phosphinites by intramolecular Diels–Alder reactions of trivalent phospholes. J Org Chem 67:5422
63. Nyulaszi L, Holloczki O, Lescop C, Hissler M, Réau R (2006) An aromatic-antiaromatic switch in P-heteroles. A small change in delocalisation makes a big reactivity difference. Org Biomol Chem 4:996
64. Delaere D, Nguyen-Nguyen PT, Nguyen MT (2004) Remarkable influence of fluorine substitution on electronic and thermochemical properties of phospholes. Chem Phys Lett 383:138
65. Mattmann E, Simonutti D, Ricard L, Mercier F, Mathey F (2001) Enhancing the dienic reactivity of phospholes: an improved access to trivalent 7-phosphanorbornenes. J Org Chem 66:755
66. Charrier C, Bonnard H, de Lauzon G, Mathey F (1983) Proton [1,5] shifts in P-unsubstituted 1H-phospholes—synthesis and chemistry of 2H-phosphole dimers. J Am Chem Soc 105:6871
67. Egan W, Tang R, Zon G, Mislow K (1971) Barriers to pyramidal inversion at phosphorus in phospholes, phosphindoles, and dibenzophospholes. J Am Chem Soc 93:6205
68. Delaere D, Dransfeld A, Nguyen MT, Vanquickenborne LG (2000) Theoretical study of the structure-property relationship in phosphole monomers. J Org Chem 65:2631
69. Pelzer S, Wichmann K, Wesendrup R, Schwerdtfeger P (2002) Trends in inversion barriers IV. The group 15 analogous of pyrrole. J Phys Chem A 106:6387
70. Sebastian M, Hissler M, Fave C, Rault-Berthelot J, Odin C, Réau R (2006) Phosphole-modified poly(thiophene)s: unique postfunctionalizable conjugated polymers that sense elemental chalcogenides. Angew Chem Int Ed 45:6152
71. Lemau de Talancé V, Hissler M, Zhang LZ, Kárpáti T, Nyulászi L, Caras-Quintero D, Bäuerle P, Réau R (2008) Synthesis, electronic properties and electropolymerisation of EDOT-capped sigma(3)-phospholes. Chem Commun 2200

72. Matano Y, Miyajima T, Fukushima T, Kaji H, Kimura Y, Imahori H (2008) Comparative study on the structural, optical, and electrochemical properties of bithiophene-fused benzo[c]phospholes. Chem Eur J 14:8102
73. Fagan PJ, Nugent WA (1988) Synthesis of main group heterocycles by metallacycle transfer from zirconium. J Am Chem Soc 110:2310
74. Fagan PJ, Nugent WA, Calabrese JC (1994) Metallacycle transfer from zirconium to main-group elements—a versatile synthesis of heterocycles. J Am Chem Soc 116:1880
75. Le Vilain D, Hay C, Deborde V, Toupet L, Réau R (1999) 2,5-Di(2-pyridyl)phospholes: model compounds for the engineering of pi-conjugated donor-acceptor co-oligomers with a chemically tunable HOMO-LUMO gap. Chem Commun 345
76. Hay C, Fischmeister C, Hissler M, Toupet L, Réau R (2000) Electropolymerization of pi-conjugated oligomers containing phosphole cores and terminal thienyl moieties: optical and electronic properties. Angew Chem Int Ed 39:1812
77. Hay C, Sauthier M, Deborde V, Hissler M, Toupet L, Réau R (2002) A bridging ligand featuring terminal 2-pyridylphosphole moieties: synthesis, optical properties and Ru(II)-complex. J Organomet Chem 643–644:494
78. Sauthier M, Le Guennic B, Deborde V, Toupet L, Halet JF, Réau R (2001) A rare phosphane coordination mode: a symmetrically mu(2)-bridging phosphole in a dinuclear palladium(I) complex. Angew Chem Int Ed 40:228
79. Hay C, Hissler M, Fischmeister C, Rault-Berthelot J, Toupet L, Nyulaszi L, Réau R (2001) Phosphole-containing pi-conjugated systems: from model molecules to polymer films on electrodes. Chem Eur J 7:4222
80. Senechal-David K, Hemeryck A, Tancrez N, Toupet L, Williams JAG, Ledoux I, Zyss J, Boucekkine A, Guegan JP, Le Bozec H, Maury O (2006) Synthesis, structural studies, theoretical calculations, and linear and nonlinear optical properties of terpyridyl lanthanide complexes: new evidence for the contribution of f electrons to the NLO activity. J Am Chem Soc 128:12243
81. Le Bouder T, Maury O, Bondon A, Costuas K, Amouyal E, Ledoux I, Zyss J, Le Bozec H (2003) Synthesis, photophysical and nonlinear optical properties of macromolecular architectures featuring octupolar tris(bipyridine) ruthenium(II) moieties: evidence for a supramolecular self-ordering in a dentritic structure. J Am Chem Soc 125:12284
82. Maury O, Le Bozec H (2005) Molecular engineering of octupolar NLO molecules and materials based on bipyridyl metal complexes. Acc Chem Res 38:691
83. Hartshorn CM, Steel PJ (1996) Self-assembly and X-ray structure of a dimetallopara-cyclophane incorporating a pi-pi stacked subunit. Inorg Chem 35:6902
84. Munakata M, Ning GL, Suenaga Y, Kurodo-Sowa T, Maekawa M, Ohta T (2000) A one-dimensional metallocyclophane with columnar aromatic stacking: the silver(I) eta(2)-coordination complex of 1,2-benztriphenylene. Angew Chem Int Ed 39:4555
85. Yoshizawa M, Nakagawa J, Kumazawa K, Nagao M, Kawano M, Ozeki T, Fujita M (2005) Discrete stacking of large aromatic molecules within organic-pillared coordination cages. Angew Chem Int Ed 44:1810
86. Chu Q, Swenson DC, MacGillivray LR (2005) A single-crystal-to-single-crystal transformation mediated by argentophilic forces converts a finite metal complex into an infinite coordination network. Angew Chem Int Ed 44:3569
87. Rapenne G, Dietrich-Buchecker C, Sauvage JP (1996) Resolution of a molecular trefoil knot. J Am Chem Soc 118:10932
88. Meskers CJ, Dekkers HPJM, Rapenne G, Sauvage JP (2000) Chiroptical properties of an optically pure dicopper(I) trefoil knot and its enantioselectivity in luminescence quenching reactions. Chem Eur J 6:2129
89. Braunstein P, Naud F (2001) Hemilability of hybrid ligands and the coordination chemistry of oxazoline-based systems. Angew Chem Int Ed 40:680
90. Helmchem G, Pfaltz A (2000) Phosphinooxazolines—a new class of versatile, modular P,N-ligands for asymmetric catalysis. Acc Chem Res 33:336

91. Chen YC, Chen CL, Chen JT, Liu ST (2001) Well-controlled block polymerization/copolymerization of alkenes and/or carbon monoxide by cationic palladium methyl complexes. Organometallics 20:1285
92. Reddy KR, Surekha K, Lee GH, Peng SM, Liu ST (2000) Palladium(II) complexes with phosphorus-nitrogen mixed donors. Efficient catalysts for the Heck reaction. Organometallics 19:2637
93. Reddy KR, Surekha K, Lee GH, Peng SM, Liu ST (2001) Study of insertion of olefins and/or carbon monoxide into phosphine-imine palladium methyl complexes. Organometallics 20:1292
94. Leca F, Lescop C, Toupet L, Réau R (2004) A new family of P,N chelates: stereoselective synthesis of 2-pyridyl-2-phospholenes in the coordination sphere of palladium(II) complexes. Organometallics 23:6191
95. Leca F, Sauthier M, le Guennic B, Lescop C, Toupet L, Halet JF, Réau R (2003) Stereospecific isomerisation of P-heterocycles triggered by coordination: synthesis of the first P,N-chelates featuring a 2-phospholene moiety. Chem Commun 1774
96. Terenziani F, D′Avino G, Painelli A (2007) Multichromophores for nonlinear optics: designing the material properties by electrostatic interactions. Chem Phys Chem 8:2433
97. Coe BJ, Curati NRM (2004) Metal complexes for molecular electronics and photonics. Comments Inorg Chem 25:147
98. Katz TJ (2000) Syntheses of functionalized and aggregating helical conjugated molecules. Angew Chem Int Ed 39:1921
99. Urbano A (2003) Recent developments in the synthesis of helicene-like molecules. Angew Chem Int Ed 42:3986
100. Martin RH (1974) Helicenes. Angew Chem Int Ed 13:649
101. Rajca A, Miyasaka M (2007) In: Müller TJJ, Bunz UHF (eds) Functional organic materials. Wiley-VCH, Weinheim, p 543
102. Furche F, Ahlrichs R, Wachsmann C, Weber E, Sobanski A, Vogtle F, Grimme S (2000) Circular dichroism of helicenes investigated by time-dependent density functional theory. J Am Chem Soc 122:1717
103. Grimme S, Harren J, Sobanski A, Vogtle F (1998) Structure/Chiroptics relationships of planar chiral and helical molecules. Eur J Org Chem 8:1491
104. Autschbach J, Ziegler T, van Gisbergen SJA, Baerends EJ (2002) Chiroptical properties from time-dependent density functional theory. I. Circular dichroism spectra of organic molecules. J Chem Phys 116:6930
105. Botek E, André JM, Champagne B, Verbiest T, Persoons A (2005) Mixed electric-magnetic second-order nonlinear optical response of helicenes. J Chem Phys 122:234713
106. Herman WN, Kim Y, Cao WL, Goldhar J, Lee CH, Green MM, Jain V, Lee MJ (2003) Amorphous thin films of chiral binaphthyls for photonic waveguides. J Macromol Sci Part A A40:1369
107. Takenaka N, Sarangthem RS, Captain B (2008) Helical chiral pyridine N-oxides: a new family of asymmetric catalysts. Angew Chem Int Ed 47:9708
108. Weix DJ, Dreher SD, Katz TJ (2000) [5]HELOL phosphite: a helically grooved sensor of remote chirality. J Am Chem Soc 122:10027
109. Reetz MT, Beuttenmüller EW, Goddard R (1997) First enantioselective catalysis using a helical diphosphane. Tetrahedron Lett 38:3211
110. Reetz MT, Sostmann S (2000) Kinetic resolution in Pd-catalyzed allylic substitution using the helical PHelix ligand. J Organomet Chem 603:105
111. Samal M, Misek J, Stara IG, Stary I (2009) Organocatalysis with azahelicenes: the first use of helically chiral pyridine-based catalysts in the asymmetric acyl transfer reaction. Collect Czech Chem Commun 74:1151
112. Bossi A, Licandro E, Maiorana S, Rigamonti C, Righetto S, Stephenson GR, Spassova M, Botek E, Champagne B (2008) Theoretical and experimental investigation of electric field induced second harmonic generation in tetrathia[7]helicenes. J Phys Chem C 112:7900

113. Leca F, Sauthier M, Deborde V, Toupet L, Réau R (2003) Chemistry of bridging phosphanes: Pd-I dimers bearing 2,5-dipyridylphosphole ligands. Chem Eur J 9:3785
114. Welsch S, Lescop C, Scheer M, Réau R (2008) Ag-I bimetallic molecular clips with adaptive coordination behavior for supramolecular chemistry. Inorg Chem 47:8592
115. Welsch S, Nohra B, Peresypkina EV, Lescop C, Scheer M, Réau R (2009) Chemistry of bridging phosphanes: a comparative study within Cu–I–Ag–I–Au–I triad-based homonuclear dimers. Chem Eur J 15:4685
116. Pechmann T, Brandt CD, Werner H (2000) Angew Chem Int Ed 39:3909
117. Braunstein P, Boag NM (2001) Breaking the rule: synthesis and molecular structure of dinuclear rhodium complexes with bridging and semibridging trialkylphosphane ligands. Angew Chem Int Ed 40:2427
118. Pechmann T, Brandt CD, Röger C, Werner H (2002) A new type of chainlike tetranuclear rhodium complexes with PR_3 and $AsMe_3$ as bridging ligands. Angew Chem Int Ed 41:2301
119. Pechmann T, Brandt CD, Werner H (2003) The truly symmetrical doubly-bridging mode of Pechmann trimethylphosphine in a dinuclear rhodium complex. Chem Commun 1136
120. Brandt TCD, Werner H (2004) A new family of dinuclear rhodium complexes containing tertiary phosphanes in a semibridging or doubly bridging bonding mode. Chem Eur J 10:728
121. Meyer EA, Castellano RK, Diederich F (2003) Interactions with aromatic rings in chemical and biological recognition. Angew Chem Int Ed 42:1210
122. Bartholomew GP, Bazan GC (2001) Bichromophoric paracyclophanes: models for interchromophore delocalization. Acc Chem Res 34:30
123. Hoeben FJM, Jonkheijm P, Meijer PW, Schenning APJ (2005) About supramolecular assemblies of pi-conjugated systems. Chem Rev 105:1491
124. Leininger S, Olenyuk B, Stang PJ (2000) Self-assembly of discrete cyclic nanostructures mediated by transition metals. Chem Rev 100:853
125. Seidel RS, Stang PJ (2002) High-symmetry coordination cages via self-assembly. Acc Chem Res 35:972
126. Holliday GJ, Mirkin CA (2001) Strategies for the construction of supramolecular compounds through coordination chemistry. Angew Chem Int Ed 40:2022
127. Fujita M, Tominaga M, Hori A, Therrien B (2005) Coordination assemblies from a Pd(II)-cornered square complex. Acc Chem Res 38:369
128. Gianneschi NC, Masar MS, Mirkin CA (2005) Development of a coordination chemistry-based approach for functional supramolecular structures. Acc Chem Res 38:825

Chapter 12
Phosphorus Based Macrocyclic Ligands: Synthesis and Applications

Andrey A. Karasik and Oleg G. Sinyashin

Abstract Phosphorus based macrocyclic ligand chemistry in respect of the effectiveness of synthetic approaches, 3D structures, coordination and supramolecular system design, as well as application in catalysis has been discussed.

12.1 Introduction

Since the pioneering work of Charles J. Pedersen, Donald J. Cram and Jean-Marie Lehn, macrocyclic chemistry attracted a considerable attention from chemists all over the world [1–4]. An ability of macrocycles to be highly selective receptors (host molecules) for a number of metal and organic cations or anions, as well as for the small or even huge (e.g. fullerenes) neutral organic substances is the reason of that interest [5–8]. The design of molecular devices such as molecular containers and reactors on one hand, and molecular switches (based on catenanes and molecular knots) on the other hand is another area of the macrocyclic chemistry application. So, the macrocyclic chemistry plays an important role in the material science, especially in the construction of nano-sized materials on the "bottom-up" principles [5, 6, 9–11].

It has been shown that the incorporation of heteroatoms (O,N,S…) into the macromolecular framework restrains their conformational freedom of the donor atom and preorganizes them in the mode necessary for a specific binding of target particles leading to the novel binding properties of these atoms. It is obvious that

A. A. Karasik (✉) · O. G. Sinyashin
A.E.Arbuzov Institute of Organic and Physical Chemistry,
Kazan Scientific Center of Russian Academy of Sciences,
Arbuzov str. 8, 420088, Kazan, Russia
e-mail: karasik@iopc.ru

M. Peruzzini and L. Gonsalvi (eds.), *Phosphorus Compounds*,
Catalysis by Metal Complexes, 37, DOI: 10.1007/978-90-481-3817-3_12,
© Springer Science+Business Media B.V. 2011

incorporation of phosphorus atom into the macrocyclic skeleton should lead to the specific properties of the discussed molecules. First of all P(III) donor centers are soft in contrast with the hard O and N counterparts that is why the specific coordination ability to the soft metal ions should appear. Secondly the well-known ability of P(III) species to form transition metal based catalysts of various organic reactions should be modified by additional bonding of metal centers or organic substrates with macrocycle fragments via dative or weak interactions. Thirdly the specific reactivity and the structural variability of phosphorus could be utilized for the additional functionalization of the macrocyclic objects or for the rational design of macrocyclic molecular devices [12, 13].

However, there are some noticeable problems concerning the availability of P-based macrocycles. In contrast with the "common" heteroatoms such as O and N the inversion barrier of P(III) is higher. So compounds containing two or more phosphorus atoms are usually obtained as a mixture of stereomers, which require separation in order to obtain the individual macrocycles. Another problem is the known instability of phosphines (the most intriguing class of ligands) to oxidation.

So, the availability of the P-containing macrocyclic compounds is one of the key points for their use in the fields of catalysis, supramolecular chemistry and nanomaterials.

At the present time three main strategies for macrocyclic synthesis may be identified:

1. Macrocyclization under high-dilution conditions.
2. Template synthesis of macrocycles.
3. Covalent self-assembly of macrocycles.

The first two approaches have been used for a long time and have a number of well-known advantages and disadvantages. The high-dilution macrocyclization as a rule requires the fast irreversible reactions, and the participation of more than two molecules is undesirable. Another disadvantage is the large amounts of solvents and/or using special dosing devices for the slow simultaneous addition of both reagents. It increases the reaction time and complicates the technique. In addition the regio- and stero-selectivity of the irreversible macrocyclization reactions are usually low. The main problem of the template macrocyclisations is the final demetallation step for the release of the obtained macrocyclic phosphorus ligand, because the metal complexes are usually very stable due to the P–M coordination and the macrocyclic effect. The last approach, namely the covalent self-assembly of macrocycles, has been formed recently. The distinctive feature of the covalent self-assembly processes is their ability of the self-correction, then the "incorrect" intermediate or product is able to decompose into starting compounds due to the reversibility of the reaction. These compounds react further to give more thermodynamically stable "correct" combination. The self-correction is a reason of the high selectivity of the covalent self-assembly processes [14–17].

If some types of macrocycles with a unique shape, distinct architecture, and set of functional groups become easily available from natural or synthetic sources,

they would start to inspire the imagination of the chemists to the wide and effective search for novel molecular materials and devices.

The sizes and forms of the intramolecular cavities formed by macrocycles, as well as the kind and number of heteroatoms are important factors to influence their complexation and recognition properties.

That is why the material in the chapter is divided according to the structural motif starting from flexible P-based corands, analogues of crown-ethers, proceeding with P-containing cyclophanes and finishing with phosphorus cryptands. The main synthetic methods; structural features, reactivity, known molecular devices, co-ordination compounds and catalytic properties will be described for each structure type. We hope that the represented information will help to the chemists working not only in the field of organophosphorus chemistry, but also in the fields of co-ordination chemistry and catalysis, as well as in the fields of molecular recognition, constructing of molecular devices and novel materials on "bottom-up" principles to imagine future applications which, perhaps, have not been established yet.

There are few reviews dealing with P-containing macrocycles [18–20] including recent ones [21, 22] appeared within the last decade. So, in present work we will concentrate on the recent results giving them in more details in comparison with the earlier data.

12.2 Phosphorus-Based Corands

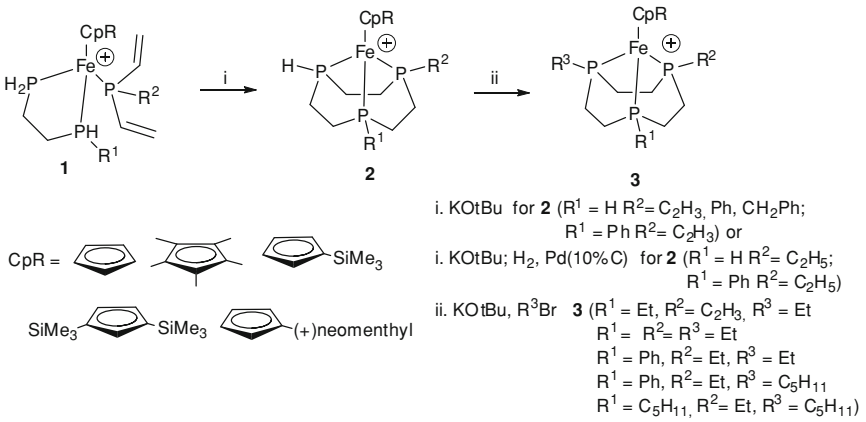
In this part we will discuss compounds without small cycles incorporated into the macrocyclic backbone and will include only few examples of *ortho*-phenylene or similar rings incorporation because it does not play an important and specific role in the macrocycle synthesis, structure and properties.

12.2.1 Homoleptic P-Containing Corands

Unlike their nitrogen analogues, homoleptic macrocyclic phosphines represent a rare class of ligands. Some of the apparent lack of interest relates to the difficulty of their preparation and, for most derivatives, their inherent instability to air.

Homoleptic P-containing macrocyclic chemistry is mainly focused on the coordination chemistry applications, namely the design of unusual complexes of the late transition metals and the homogenous catalysis of organic reactions. The majority of metal-promoted catalyses requires mutually *cis* coordination sites in order to facilitate the desired transformations.

Iron(II) templates **1** based on a $[(\eta^5\text{-}Cp^R)Fe]^+$ core have been employed for the successful synthesis of 1,4,7-triphosphacyclononane derivatives **2** from a range of appropriately functionalized coordinated diphosphines and monophosphines (Scheme 12.1). 1,2-Diphosphinoethane or (2-phosphinoethyl)phenylphosphine undergo a base-catalyzed Michael-type addition to trivinylphosphine,

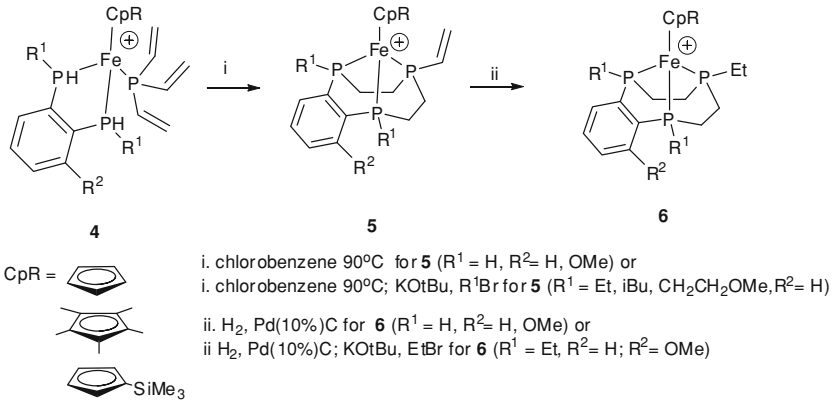


Scheme 12.1 Template synthesis of 1,4,7-triphosphacyclononanes **2** and **3**

divinyl(benzyl)phosphine, or divinyl(phenyl)phosphine to give derivatives **2** containing coordinated triphosphacyclononanes bearing one or two secondary phosphine donors. For coupling reactions with trivinylphosphine, a pendant vinyl function remains in the macrocyclic product **2** (R^2 = Vinyl) which is readily hydrogenated to the corresponding ethyl derivatives **2** (R^2 = Et). Further functionalization of coordinated secondary phosphine centers of the initially formed macrocycles **2** is achieved by proton abstraction followed by addition of the appropriate alkyl halide electrophile and gives rise to tritertiary-triphospha-cyclononanes **3** (Scheme 12.1). It should be mentioned that various substituents on the cyclopentadienyl ligand were exploited including chiral (+)neomenthyl group giving rise to the additionally functionalized organometallic complexes. The rates of macrocyclization show a dependence on the nature of the substituents on the cyclopentadienyl ligand [23].

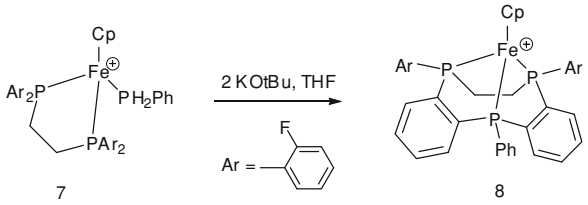
Nine-membered macrocycles **5**–**6** with three phosphorus atoms and fused o-benzo fragment have been prepared in high yield by the analogous coupling of 1,2-diphosphinobenzenes with trivinylphosphine on a cationic templates **4** (Scheme 12.2). This sequence constitutes a versatile high yield and stereoselective synthetic route to a new class of co-ordinated triphosphacyclononanes bearing a rigid *o*-phenylene backbone link. The efficiency of the synthesis depends markedly upon the nature of the CpR ligand. The new secondary phosphine macrocycles **5**, **6** (R^1 = H) prepared by this route are readily alkylated to tritertiary triphosphine macrocycles **5**, **6** (R^1 = Et, i-Bu) bearing alkyl substituents and pendant functions ($R^1 = CH_2CH_2OMe$) (Scheme 12.2) [24, 25]. The procedure of the release of 9-membered triphosphorus macrocycles has not been described yet [23–25].

Nine-membered triphosphorus macrocycle **8** with two o-phenylene backbone functions has been stereoselectively prepared on a $CpFe^+$ template **7** by two successive nucleophilic attacks of coordinated phosphide on a coordinated 1,2-bis(di(o-fluorophenyl)phosphino)ethane (Scheme 12.3) [26].



Scheme 12.2 Template synthesis of 1,4,7-triphosphacyclononanes **5** and **6**

Scheme 12.3 Template synthesis of 1,4,7-triphosphacyclononane **8**



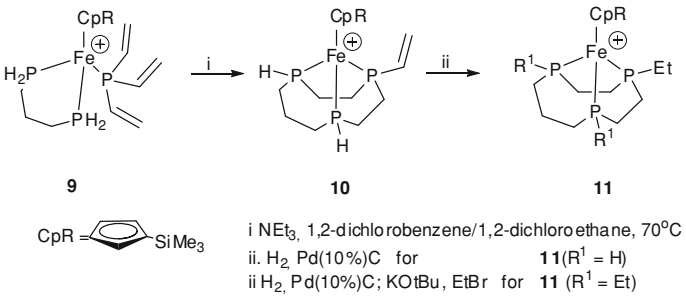
The complex of 10-membered cyclic triphosphine **10** has been prepared by the base catalyzed template cyclization of 1,3-bis(phosphino)propane and trivinylphosphine at the metal center ([(η^5-$Me_3SiC_5H_4$)Fe]) **9** (Scheme 12.4). Hydrogenation of vinyl substituent followed by alkylation of secondary phosphino group lead to complexes **11** with three endocyclic tertiary phosphino moieties.

A related radical-initiated iron-template reaction between 1,2-bis(phosphino)ethane and diallylphosphines gave complex **12** with nonsymmetric 3-methyl-1,4,7-triphosphacyclodecane ligand (Scheme 12.5). This macrocycle is the result of two intramolecular hydrophosphination reactions: the first one generates a five-membered (chelate) ring with an exo-methyl group and the second gives a six-membered chelate.

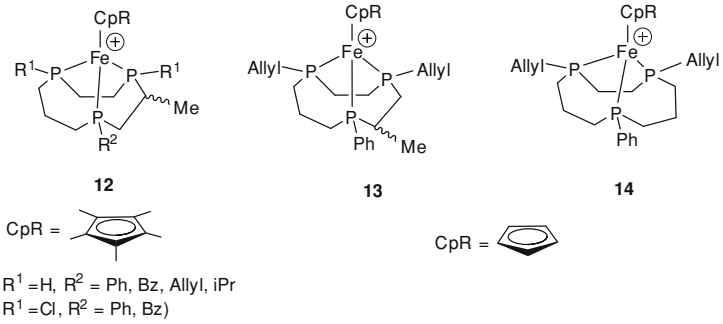
The [(η^5-CpR)Fe]$^+$ fragment also controls the cyclization of 1,2-bis(diallylphosphino)-ethane with phenylphosphine to give a ternary complex **14** containing the symmetrical 11-membered macrocycle 1-phenyl-4,8-diallyl-1,4,8-triphosphacycloundecane, in addition to the unsymmetrical **13** (Scheme 12.5).

To date the above described ligands remain unknown in the free uncoordinated state. The iron center does undergo reversible one-electron oxidation in most cases, although attempts to scavenge the iron from the oxidized Fe(III) complexes with various agents (CN^-, EDTA, OH^-) had not been successful [27].

A high dilution way to the 11-membered macrocycle **15** was suggested. It has been shown that two phenyl substituents of bis(phenylphosphino)benzo unit are



Scheme 12.4 Template synthesis 10-membered cyclic triphosphines **10** and **11**

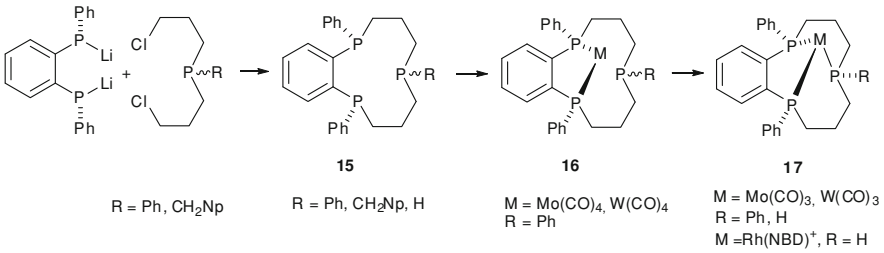


Scheme 12.5 10-Membered cyclic triphosphines **12**–**14**

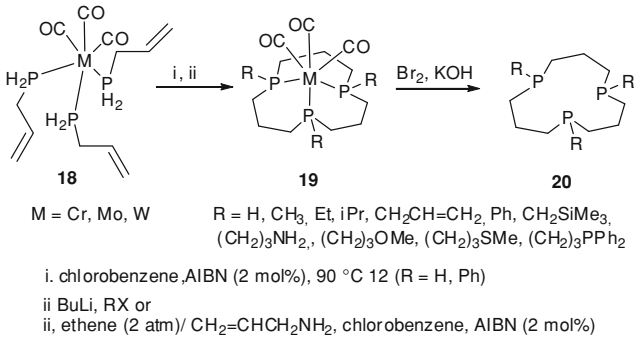
situated in *cis*-positions whereas phenyl of incoming phosphine unit is situated in *trans*-position. So ligand **15** easily displaced only two carbonyl groups of metal carbonyls to give complexes *cis*-**16** which slowly (>24 h) and inefficiently converts to *fac*-**17** [28, 29]. However, a mixture of *meso-cis* and *meso-trans* isomers of **15** upon heating with $W(CO)_6$ in boiling mesitylene for 16 h (that allowed pyramidal inversion of phosphorus) gave desired *fac*-**17** (M = W) in 41% yield [30].

An interesting and efficient strategy was used for the preparation of 11-membered cyclic triphosphine **15**. High dilution condensation of bis(3-chloropropyl)(α-naphthylmethyl)phosphinesulfide with bisphosphides and further removal of the α-naphthylmethyl group with potassium naphthalenide followed by the removal of sulfur with LAH afforded P–H functionalized macrocycle **15** (R=H) as a mixture of two diastereomers (Scheme 12.6). It has been shown that both isomers readily form *fac*-complexes with tridentate macrocyclic ligands. Taking into account the mutual *cis*-orientation of Ph groups this result indicates the relatively fast inversion of the secondary phosphine unit [31].

Synthesis of 12-membered macrocycles **19** (M = Mo, R = H) with three phosphorus atoms in 1,5,9-positions was the first example of the use of a template method for the stereoselective preparation of a P3 macrocycles (Scheme 12.7).



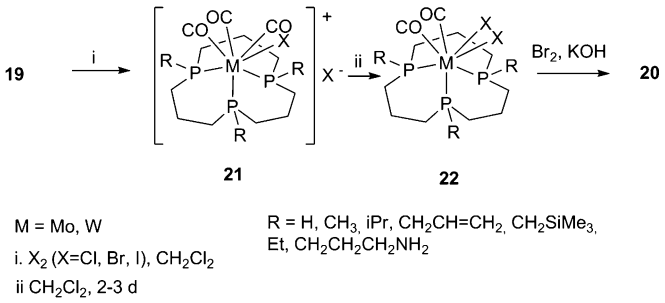
Scheme 12.6 Macrocyclization under high-dilution conditions and transition metal complexes of 11-membered cyclic triphosphines **15**



Scheme 12.7 Template synthesis of 12-membered macrocycles **20**

The synthesis of **19** (M = Mo, M = Cr, R = H) was achieved by the radical-induced coupling of three allylphosphine ligands in **18** [32, 33].

The tritertiary 1,5,9-triphosphacyclododecane ligand complexes **19** (M = Mo, R = Me, $CH_2CH{=}CH_2$, iPr, CH_2SiMe_3, $CH_2CH_2CH_2NH_2$; M = Cr, R = Me, Et, Bz, CH_2CH_2OEt, $(CH_2)_3OMe$, $(CH_2)_3SMe$, $(CH_2)_3NH_2$, $(CH_2)_3PPh_2$) were prepared from the trisecondary 1,5,9-triphosphacyclododecane precursor **19** (M = Mo, Cr; R = H) via deprotonation and further alkylation procedures (Scheme 12.7). The tungsten trisecondary 1,5,9-triphosphacyclododecane analogue **19** (M = W; R = H) has been synthesized and also serves as an intermediate to the tungsten complexes of the tertiary phosphine macrocyclic ligands **19** (M = W; R = CH_2SiMe_3, $CH_2CH_2CH_2NH_2$). The synthetic routes are general and allow access to a range of macrocyclic triphosphines with alkyl, o-aminoalkyl and alkenyl functions on phosphorus [34, 35]. The selective functionalisation of a single phosphorus atom in the macrocycle **19** has been achieved by deprotonation and subsequent reaction with an ether containing an alkyl halide group. Yields of the monosubstituted products are very sensitive to the reaction conditions. A series of the P3 macrocycles **20** (R = CH_2CH_2OMe, $CH_2CH_2CH_2OMe$, Ph, iPr) were released from their templates by the oxidation and the subsequent base digestion.



Scheme 12.8 Oxidative addition of halogens (Cl_2, Br_2, I_2) to molybdenum and tungsten tricarbonyl complexes **19**

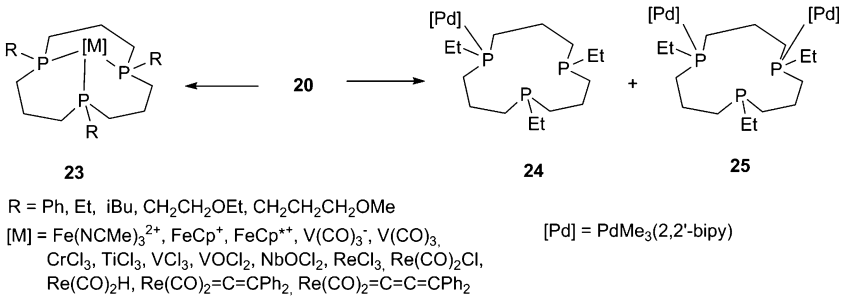
The liberation proceeds stereoselectively to give the *syn–syn* isomer exclusively with reasonably good yields (40–70%) [12, 36].

Interaction of **19** (M = Mo, R = H) with CX_4 (X = Cl, Br) lead to the **19** (R = Cl, Br). Free triphenyl substituted 1,5,9-triphosphacyclododecane **20** (R = Ph) has been prepared via the templated reaction of 1,5,9-trichloro-1,5,9-triphosphacyclododecane-molybdenum complex with phenylcopper or diphenylcuprate and further liberation by Mo oxidation by I_2 [37].

Triphosphamacrocycle complexes of molybdenum(II) and tungsten(II) **22** have been prepared by oxidative addition of halogens (Cl_2, Br_2, I_2) to molybdenum and tungsten tricarbonyl complexes **19** (Scheme 12.8). The metal(0) precursors give rise initially to seven-coordinate salts **21** with a halide anion which may be exchanged for other counter ions. The seven-coordinate complexes **21** are all fluxional in solution. The salts all convert slowly into the neutral seven-coordinate dicarbonyldihalogeno complexes **22** in solution [38].

A template synthesis of twelve-membered triphosphorus macrocycles **20** (R = Ph, Et) has been developed based upon the intramolecular hydrophosphination of allylphosphine coordinated to the (η^5-cyclopentadienyl)iron(II) cation; the resulting iron complex of tri-secondary macrocycle 1,5,9-triphosphacyclododecane is readily alkylated with ethene to give **20** (R = Et) which is in turn liberated stereospecifically as the *syn–syn* isomer of the free ligand. Related reactions with phenyl(allyl)phosphine lead directly to the triphenyl macrocycle **20** (R = Ph) which is also demetallated stereospecifically [39].

The macrocycles **20** (R = Ph and Et) have been used for the design of a series of the piano–stool iron complexes with facially capping triphosphorus macrocyclic ligands **23** (Scheme 12.9) [40]. At the same time ligand **20** (R = Et) does not displace 2,2′-bipyridine from [$PdMe_3(O_3SCF_3)$(2,2′-bipy)]. Instead it acts as monodentate or bridging bidentate ligand giving corresponding mono- and bi-nuclear palladium complexes **24** and **25**, which appear to be unstable at room temperature reductively eliminating ethane [41]. The macrocycle **20** (R = Et) forms stable complexes under photolytic conditions starting from vanadium carbonyl precursors in which the macrocycle acts as a facially capping tridentate ligand for the simple carbonyls **23** (R = Et, [M] = $V(CO)_3^-$) and as a bidentate

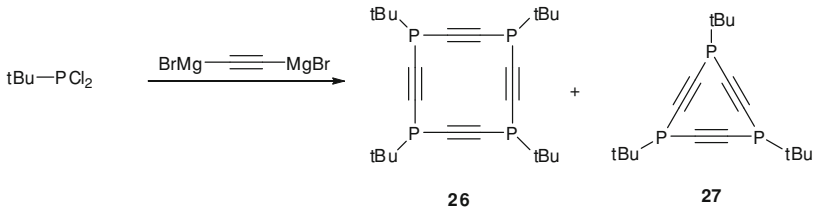


Scheme 12.9 Synthesis of transition metal complexes **23**–**25** of 12-membered triphosphorus macrocycles **20**

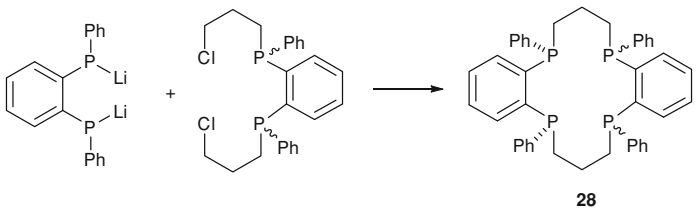
chelating ligand for the cyclopentadienylcarbonyl (M = $V(CO)_2Cp$). The compound **23** can be oxidized to the neutral 17 electron complex *fac*-**23** (R = Et, [M] = $V(CO)_3$), which is a rare example of a V(0) carbonyl complex [42]. It has been demonstrated that the macrocycles **20** (R = Et, CH_2CH_2OEt, $CH_2CH_2CH_2OMe$) act as facially capping triphosphorus macrocyclic ligands and form relatively robust six-coordinate complexes with early transition metals **23** (R = Et, CH_2CH_2OEt, $CH_2CH_2CH_2OMe$, M = $CrCl_3$, $TiCl_3$, VCl_3, $VOCl_2$ and $NbOCl_2$) (Scheme 12.9) [43]. Some early transition metal complexes **23** (M = $CrCl_3$, $TiCl_3$, VCl_3, R = Et, Ph, $CH_2CH_2CH_2OMe$) have been examined for their activity towards ethene and propene polymerisation. All complexes of the type **23** display moderate catalytic activity in the homogeneous polymerisation of ethene when combined with an alkyl aluminium co-catalyst to give very high molecular weight polymers. Substitution of the P-bonded alkyl group with a pendant ether function was found to switch the catalytic activity of chromium(III) complexes from the polymerisation to oligomerisation. A nickel halide complex of **20** (R = Et), which constitutes a new class of homogeneous alkene polymerisation catalysts, was found to be active in alkene polymerisation. The stability and activity of these systems is substantially greater than for related acyclic phosphine ligand complexes and is presumably due to the macrocyclic coordination effect [44].

The synthesis of Re(III), Re(I) and Mn(I) complexes of the macrocyclic phosphine ligand **20** (R = Et, iBu) was described. The reaction of **20** with $ReCl_3(PPh_3)_2(CH_3CN)$ or $ReCl_3(PPhMe_2)_3$ gives rise to the octahedral d^4 complexes **23** (R = Et, iBu, M = $ReCl_3$). The reduction of **23** (R = iBu, M = $ReCl_3$) with Na/Hg under a CO atmosphere gives the rhenium(I) compound **23** (R = iBu, M = $Re(CO)_2Cl$), which undergoes further reactivity to give hydride (M = $Re(CO)_2H$), vinylidene (M = $Re(CO)_2$=C=CPh_2) and allenylidene (M = $Re(CO)_2$=C=C=CPh_2) compounds. With $Mn(CO)_5Br$ 12-membered macrocycle **20** (R = Et) gives the octahedral d^6 complex **23** (R = Et, M = $Mn(CO)_2Br$).

The catalytic activity of the phosphorus macrocycle complexes **23** (R = iBu, M = $Re(CO)_2Cl$ and $Re(CO)_2H$) in cyclic alkenes polymerisation was studied. Addition of norbornene to the solution of activated catalyst results in the strongly exothermic reaction proceeding at a reasonable rate at 0 °C. The behaviour of the



Scheme 12.10 Synthesis of 12-membered macrocycle **26**



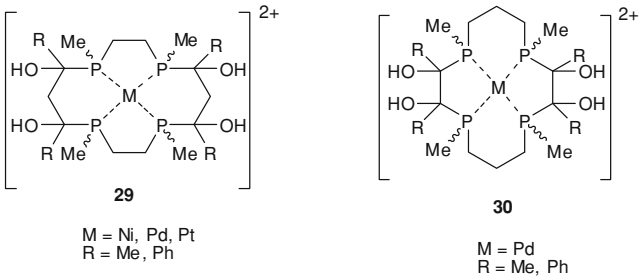
Scheme 12.11 Synthesis under high-dilution conditions of 14-membered cyclic tetraphosphine **28**

catalyst is dramatically influenced by the nature of the P-alkyl substituents. Thus, with R = iBu, a low molecular weight polymer is obtained (also with a relatively narrow polydispersity). In the case of the ethyl derivative, the catalytic system is more active than in the case of its bulkier analogue and a polymer product with a much higher molecular weight (and also a higher polydispersity) is obtained. The manganese complexes **23** (R = Et, M = $Mn(CO)_2Br$) is also active in ROMP under similar conditions although the molecular weight of the polymer is substantially lower [45].

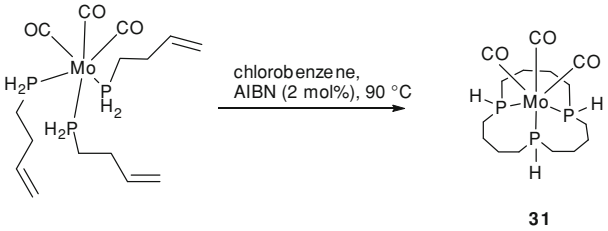
12-Membered macrocycle **26** containing four phosphorus atoms was synthesized from tert-butylphosphinous dichloride and ethenylmagnesium bromide in 11% isolated yield (Scheme 12.10). The *cis–trans* isomer was the only one observed for 9-membered cyclic compound **27** and *all-trans* for 12-membered **26**. The *all-trans* isomer was isolated in a pure state [46].

14-Membered tetraphosphine macrocycle **28** was obtained utilizing high dilution procedure as a mixture of two mutually intercoverted isomers (Scheme 12.11). As in the case of the analogous 11-membered compounds **15** only the *cis* configuration of phenyl groups of the o-bis-(tert-phosphino)benzo unit is observed in the macrocycle and the substituents of the phosphorus atoms occupy pseudoequatorial positions. In one isomer all lone pairs of P-atoms pointed into the molecular cavity [47].

Few 14-membered tetraphosphorus macrocycles **29** and **30** (Scheme 12.12) were obtained via addition reactions of bis(secondaryphosphino)ethanes and –propanes coordinated on the square templates (Ni(II), Pd(II) and Pt(II)) with 1,3-dicarbonyl (acetylacetone, malonodialdehyde) and 1,2-dicarbonyl (diacetyl, dibenzoyl) compounds correspondingly. The complexes of macrocycles were



Scheme 12.12 Transition metal complexes of 14-membered cyclic tetraphosphines **29–30**



Scheme 12.13 Template synthesis of 15-membered macrocycle **31**

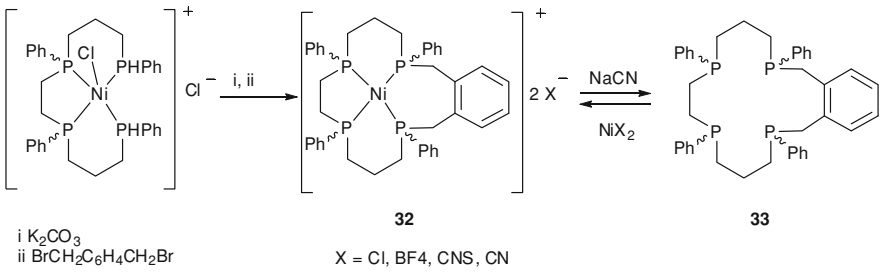
obtained as a mixture of stereoisomers and macrocycles could not be liberated from the transition metal ion. Reaction with acetylacetone demonstrates higher diastereoselectivity and gives only two isomers. First isomer is derived from the *meso*-form of initial diphosphinoethane and second from the racemic one [48, 49].

The 15-membered macrocycle **31** was obtained in high yields from *cis*-$[Mo(CO)_3(H_2PCH_2CH_2CH{=}CH_2)_3]$ utilizing the same template synthetic approach as that for 12-membered macrocycles **20** (Scheme 12.13) [50].

Stereoisomeric mixture of nickel complexes of 16-membered macrocycle **32** was obtained using both templating and high-dilution procedures. The isomers of macrocycle **33** were liberated from nickel by cyanide (Scheme 12.14) [51]. Macrocyclic tetraphosphine demonstrated an ability to form square–planar complexes with various nickel salts [52].

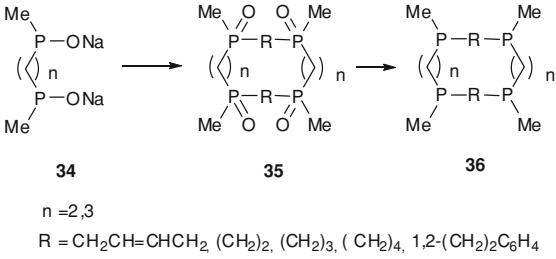
The analogous alkylation of the phosphinate salts **34** under high dilution conditions with α,ω-dibromoalkanes gave rise to the various macrocycles **35**. In some cases diastereomers were separated by the chromatography and were reduced by $LiAlH_4/CeCl_3$ to the macrocyclic tertiary tetraphosphines **36** ($n = 2$, R = 1,2-$(CH_2)_2C_6H_4$) (Scheme 12.15) [53, 54].

Only one isomer of the 16-membered heterocycle **37** was synthesized in four steps from tribenzylphosphine by successive quaternization with the appropriate alkylating agents and debenzylations with $LiAlH_4$. The isolated diastereomer of **37** formed moderately air-stable complexes $[MnX_2L]$ (X = Cl, Br, I, NCS)

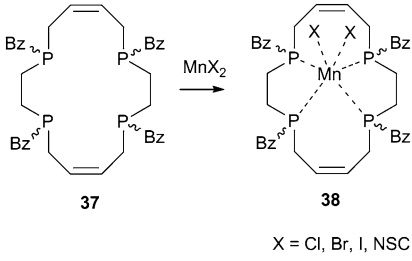


Scheme 12.14 Synthesis of 16-membered macrocycle **33**

Scheme 12.15 Synthesis of macrocycles **36** via alkylation under high dilution conditions and reduction procedures



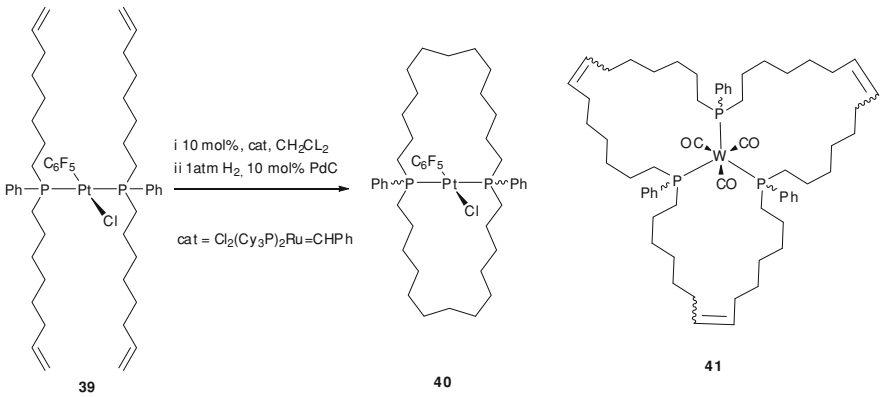
Scheme 12.16 Synthesis of manganese complexes **38** of 16-membered macrocycle **37**



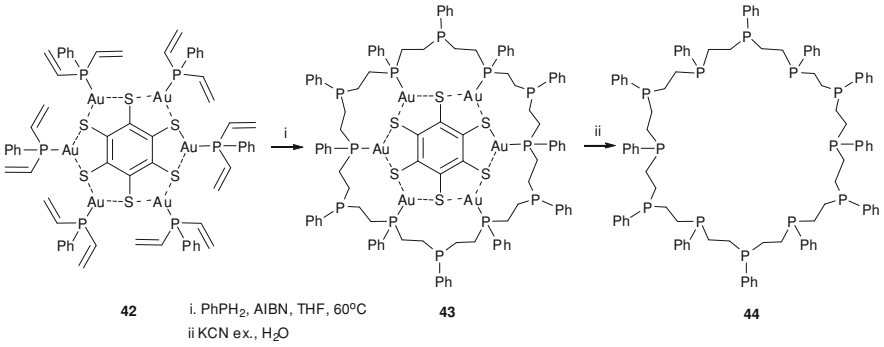
(Scheme 12.16). This finding had been ascribed to the steric protection and chelate effect of the tetraphosphine macrocyclic ligand [55].

Unique 30-membered diphosphine **40** and 45-membered triphosphine **41** macrocycles were obtained via a Grubbs'type methathesis coupling of the terminal unsaturated groups at the ends of lengthy alkenyl substituents of coordinated phosphines in *trans* square-planar platinum and facial octahedral tungsten complexes (Scheme 12.17) [56].

Generally, methods for the preparations of large ring compounds (containing more than six heteroatoms) are highly inefficient with the success depending strongly on the preorganization of reactants prior to macrocycle assembly. The use of a single metal ion template limits the size of the phosphine macrocycle that can be synthesized. The formation of the gold complex of 36-membered polyphosphorus macrocycle **43** was performed by the heating of hexagold template **42** with an excess of $PhPH_2$ and AIBN. The macrocyclic complex **43** was isolated as a red solid.



Scheme 12.17 Synthesis of **30–40** and 45-membered macrocycle **41** via a Grubbs'type methathesis coupling

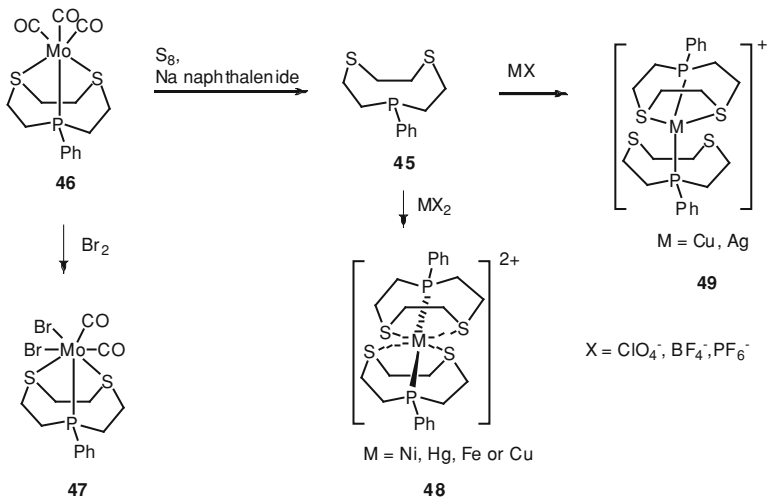


Scheme 12.18 Template synthesis of 36-membered macrocycle **44**

The possibility of multiple isomers formation exists resulting from different configurations of each of 12 phosphorus atoms. In a preliminary attempt to isolate the free macrocycle **44**, by heating of **43** in an aqueous solution of KCN only ^{31}P NMR evidence of the preparation of the desired **44** was obtained (Scheme 12.18) [57].

12.2.2 Hybrid P and O/N/S-Containing Corands

As a general trend, the interest in the chemistry of hybrid phosphorus–oxygen, nitrogen or/and sulfur donor ligands is mainly focused on the phenomenon of their hemilability and their potential use in catalytic processes. Other possibilities are found when these P,X (O, N, S) donors are integrated in macrocyclic systems, such as the documented ability of their derivatives to interact selectively with ionic species

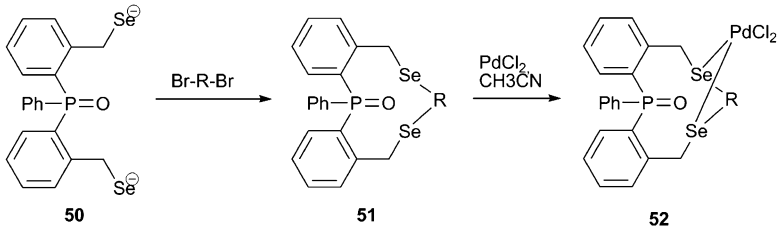


Scheme 12.19 Transition metal complexes **46**–**49** of 9-membered hybrid P,S,S-macrocycle **45**

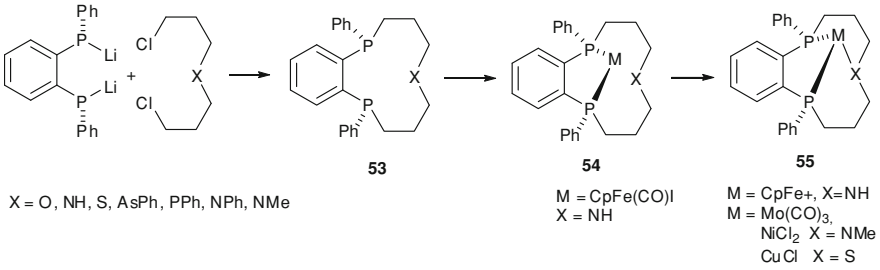
so that macrocycles act as chemical sensors for cations and anions. Phosphorus-containing mixed donor macrocycles show a promise for the modern supramolecular chemistry due to their complexation ability and molecular recognition ability. The sizes of the macrocyclic cavities and the kind and number of heteroatoms are important factors to influence their complexation and recognition properties.

The 9-membered hybrid P,S,S-macrocycle **45** was obtained under high dilution conditions from bis(2-thiolatoethyl)phenylphoshine and 1,2-dichloroethane in 54% yield [58, 59]. The same ligand was synthesized on the *fac*-$Mo(CO)_3$ template **46**. Treatment of the *fac*-**46** with S results in the loss of the $Mo(CO)_3$ fragment and the isolation of the sulphide of **45**. Its reduction with Na naphthalenide affords the parent ligand **45** (Scheme 12.19). Complex **46** with Br_2 affords seven-coordinate complex **47** [60]. Complexes **48** and **49** prepared by the interaction of **45** with anhydrous perchlorate, hexafluorophosphate, or tetrafluoroborate salts of corresponding metals in acetonitrile or nitromethane (Scheme 12.19) demonstrated further evidence of enhanced stability in comparison with complexes of homoleptic thioanalogues. The copper(I) complex **49** was shown to be tetrahedral, with one ligand facially tridentate and the other monodentate and coordinated via the phosphorus. Ligand **45** exhibits both endodentate and exodentate conformations in the complex **49**. The Hg ion of **48** (M = Hg) is in a very distorted octahedral environment with two short Hg–P bonds (av. 2.404 Å) and four long Hg–S bonds (av. 3.092 Å) [58, 59].

Electrospray mass spectrometry and TGA reveals that bis(1-phenyl-1-phospha-4,7-dithiacyclononane)iron(II) **48** (M = Fe) is more susceptible to ethene loss than bis(1,4,7-trithiacyclononane)iron(II). This is in accordance with X-ray crystallographic studies, which show that the C–S bonds are longer in the former complex suggesting an increased population of the C–S acceptor orbitals [61].



Scheme 12.20 Synthesis and formation of palladium (II) Se, Se-complexes of macrocycles **51**

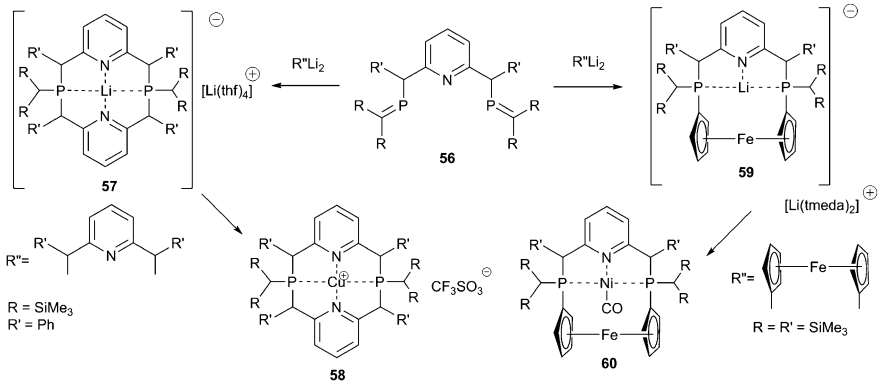


Scheme 12.21 Macrocyclization under high-dilution conditions and formation of transition metal complexes of 11-member macrocycles **53**

A wide range of P,Se,O-containing macrocycles has been obtained from diselenide **50** starting from a 10-membered macrocycle **51** (R = CH_2). A one-pot reaction was developed. Thus, 10- to 17-membered macrocycles **51** with one phosphorus and two selenium atoms were synthesized in yields from 12 to 30% (Scheme 12.20). Neither a template nor high dilution conditions had been applied in these reactions. Preliminary results showed that **51** formed chelate Pd(II) complexes **52** through two Se atoms [62].

Incorporation of an *o*-phenylenebisphosphino moiety into the rings, developed by Kyba et al. in a series of 11-membered macrocycles **53** [63], allows the corresponding metal complexes **54**–**55** to exhibit unusual electrochemical properties [64]. The presence of rigid phenylene fragment leads to the existence of **53** in *meso*-form. Complexes **55** were prepared on the basis of this ligand [30]. **55** (M = $Mo(CO)_3$) is *fac* octahedral, *cis*-**55** (M = $NiCl_2$) is square pyramidal with the NH moiety at the apical position, and **55** (M = CuCl) is tetrahedral with three coordinated P,P,X-macrocyclic ligand **53** (Scheme12.21) [65].

The coordination chemistry of a 11-membered phosphamacrocycle **53** (X = NH) with (η^5-cyclopentadienyl)dicarbonyliodoiron and (η^5-pentamethylcyclopentadienyl)dicarbonyliodoiron was investigated. Thus **53** reacts with $CpFe(CO)_2I$ in benzene under photochemical conditions to yield a mixture of **54** (M = $Cp(CO)Fe^+$) and **55** (M = $CpFe^+$). The conversion of **54** (M = $Cp(CO)Fe^+$)



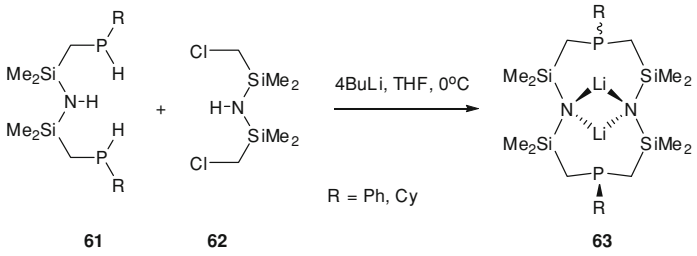
Scheme 12.22 Template synthesis of macrocyclic complexes **58** and **60**

into **55** (M = $CpFe^+$) was achieved by photochemical treatment of **54** (M = $Cp(CO)Fe^+$) in acetonitrile [66].

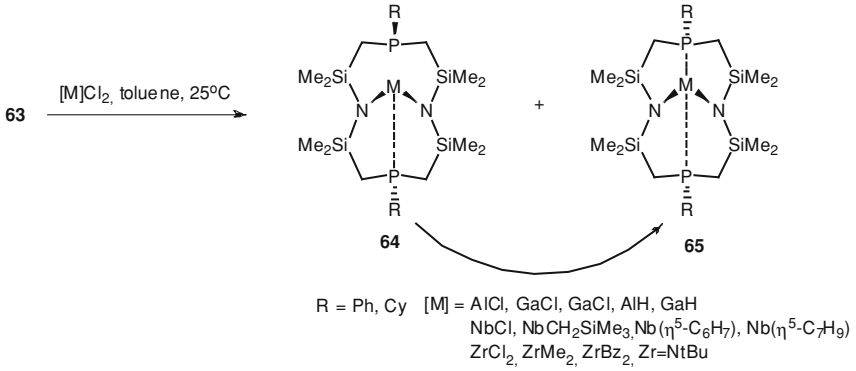
A novel synthetic approach to 12-membered macrocyclic hybrid ligands **57** and **59** containing a PC_2EC_2P (E = N, O, S) backbone based on a coupling reaction between two alkalimetal-fixed carbanionic centers (template) and two specifically connected, electrophilic phosphorus centers of **56** has been developed (Scheme 12.22). The macrocyclic ring of the CuI complex **58** features the same conformation as initial lithium salt **57**. The copper ion, however, forms a "seesaw" arrangement with the two phosphorus and nitrogen atoms. Such a coordination geometry with a quasilinear P–Cu–P (169°) and right-angle N–Cu–N alignment is without precedent in the chemistry of the copper(I) ion and possibly explains the observed fluorescence of the complex. The virtually trigonal-monopyramidal coordination geometry of the nickel center in the complex of 1,10-diphospha(2)-2,6-pyridino(2)-1,1′-ferrocenophane **60** is also without precedent: two phosphorus centers and the CO ligand occupy the equatorial positions [67, 68].

Reaction of a mixture of secondary diphosphinosilazane **61** obtained from LiPHR and dichlorosilazane **62** in almost quantitative yield, and **62** itself at low temperature in THF in the presence of four equivalents of either butyllithium (BuLi) or lithium diisopropylamide (LDA) leads to the formation of *syn*- and *anti*-isomers of 12-membered ring macrocycle **63** in very high yields (Scheme 12.23). Lithium ions serve to template the phosphorus–carbon bond formation resulting in extremely high yields and with the excellent control of stereochemistry. These large heterocyclic rings include two disilylamido donors and two phenylphosphine units mutually *trans* disposed. The relative stereochemistry at the phosphorus centres is controllable by the use of the temperature and the solvent [69].

The reaction of the macrocyclic ligand *anti*-**63** (R = Ph) with $AlCl_3$ or $GaCl_3$ leads to the formation of the four-coordinated species **64** with a distorted tetrahedral geometry, and only one of the phosphine donors of the ligand **63** binds with the metal (Scheme 12.24). The addition of $AlCl_3$ or $GaCl_3$ to the *syn*-**63** yields



Scheme 12.23 Template synthesis of of 12-membered ring macrocycle **63**

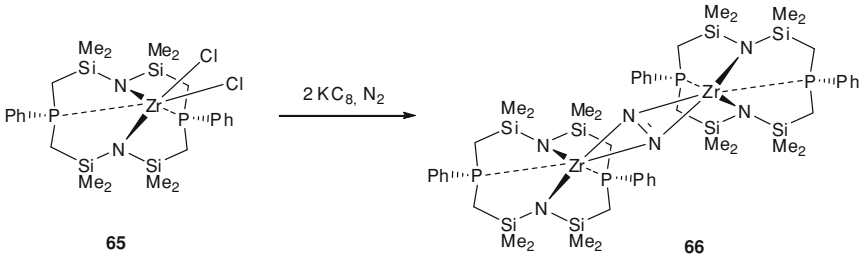


Scheme 12.24 Synthesis of complexes of the macrocycle **63**

the five-coordinate complexes **65** with a trigonal bipyramidal geometry about the metal atom, necessitating the coordination of both phosphorus atoms. Heating the complexes **64** results in the clean conversion to the *syn*-complexes **65**, with pyramidal inversion observed at phosphorus [70]. Addition of $LiAlH_4$ or $LiGaCl_4$ to the monomeric chlorides syn-**65** (R = Ph, M = AlCl, GaCl, InCl) results in the formation of the aluminum hydride syn-**65** (R = Ph, M = AlH or GaH) [71].

Similar niobium complex **65** (R = Ph, Cy) was obtained and subsequent replacement of the chlorides was achieved to give the paramagnetic alkyl complexes **65** (R = Ph, Cy, M = $NbCH_2SiMe_3$, $NdCH(SiMe_3)_2$) [72]. Hydrogenolysis of the latter in benzene or toluene causes hydride addition to the aromatic solvent resulting in the formation of the π-bonded complexes **65** (R = Ph, Cy, M = Nb(η^5-C_6H_7), Nb(η^5-C_7H_9)) in benzene and toluene, respectively. Performing of the hydrogenation at a higher pressure of 29 atm at room temperature causes the catalytic hydrogenation of benzene to cyclohexane [73].

A series of zirconium(IV) complexes that incorporate the macrocyclic bis (amido-phosphine) ligand **63** (R = Ph) were described. The starting material, complex **65** (R = Ph, M = $ZrCl_2$) was prepared by reaction of *syn*-**63** with $ZrCl_2(THF)_2$. The subsequent replacement of the chloride ligands has been



Scheme 12.25 Synthesis of the side-on bound dinitrogen complex **66**

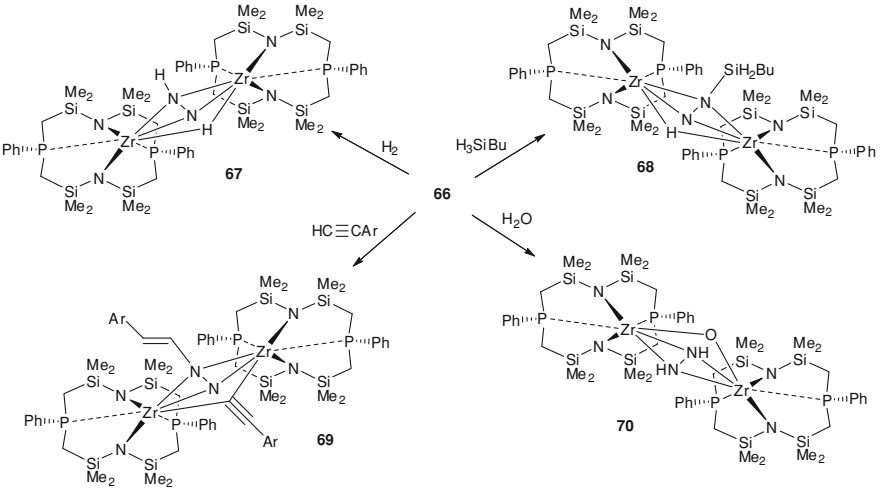
achieved to generate the dialkyl complexes **65** (R = Ph, M = $ZrMe_2$, $ZrBz_2$). In addition, the *tert*-butylimido complex **65** (R = Ph, M = Zr(NBut)) was prepared by addition of LiNHtBu to **65** (R = Ph, M = $ZrCl_2$). Zr center sits above the plane defined by the donor atoms of the macrocyclic ligand (Scheme 12.24) [74].

Upon the reduction of **65** (M = $ZrCl_2$) with 2 equivalents of potassium graphite (KC_8) under N_2, the corresponding dark-blue N_2 complex (**66**) was obtained in a high yield (Scheme 12.25). An improvement of the synthesis of **66** was (up to 95% yield) achieved by changing the solvent to very dry THF and initiating the reduction reaction at a low temperature. N_2 unit is bound side-on with a N–N bond length of 1.43(1) Å. Formally, the oxidation state of each Zr is 4^+ and the bridging N_2 is a N_2^{4-}unit [75, 76]. Analogous dinitrogen niobium complex was obtained by the reduction of **65** (M = NbCl) [77].

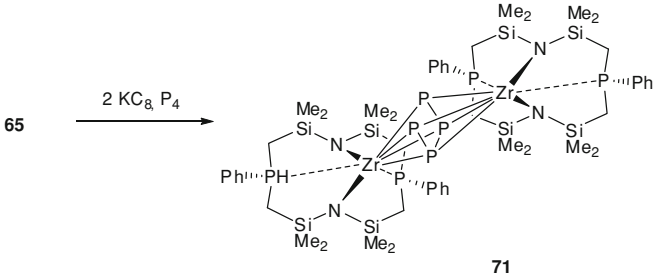
In the reaction of dihydrogen with a side-on bound dinitrogen complex of zirconium **66** instead of the displacement of the dinitrogen moiety, a complex containing both a bridging hydride and a bridging hydrazido unit with a nitrogen–hydrogen bond was observed (Scheme 12.26). This reaction was extended to primary silanes to produce species that contained a nitrogen–silicon bond [75, 76, 78]. The reaction of **66** with a slight excess of phenylacetylene results in the formation of the substituted styryl–hydrazido complexes **69** [79]. Oxodiazenide **70** was isolated in moderate yield after the slow addition of slightly <1 equivalents of H_2O to **66** at low temperature [75, 76]. So, the rare dinitrogen activation occurred in the coordination sphere of Zr complexes with hybrid 12-membered macrocyclic ligand **63** [80, 81].

Recently an example of white phosphorus activation by complexes containing diamidodiphosphine macrocycle **63** was found. A new dinuclear zirconium complex **71** that has a bridging intact planar square P_4 unit was obtained in the reduction of **65** using white phosphorus as an additional ligand (Scheme 12.27) [82].

The condensation of diselenide compound **72** with selenium-containing diols in the presence of sodium *tert*-butoxide gave 14-membered and 18-membered P,O,Se-containing macrocyclic ligands **73** and **74,** respectively (Scheme 12.28). **73** and **74** contain soft donor Se-atoms and hard donor phosphineoxide group. Reaction of **73** with palladium(II) chloride gave a 2:1 complex **75** through Se-atoms, whereas **74** gave a 1:1 complex **76** [62].



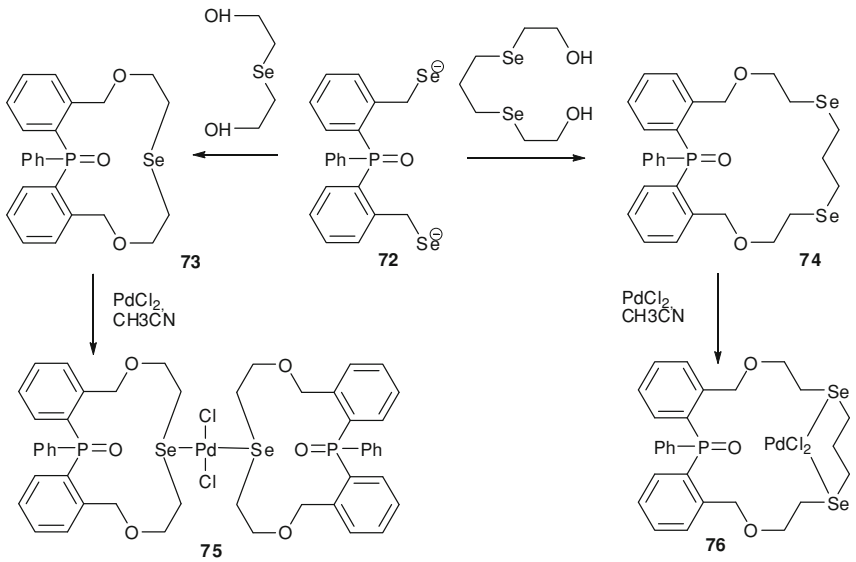
Scheme 12.26 Dinitrogen activation occurred in the coordination sphere of Zr complexes **66** with hybrid 12-membered macrocyclic ligand **63**



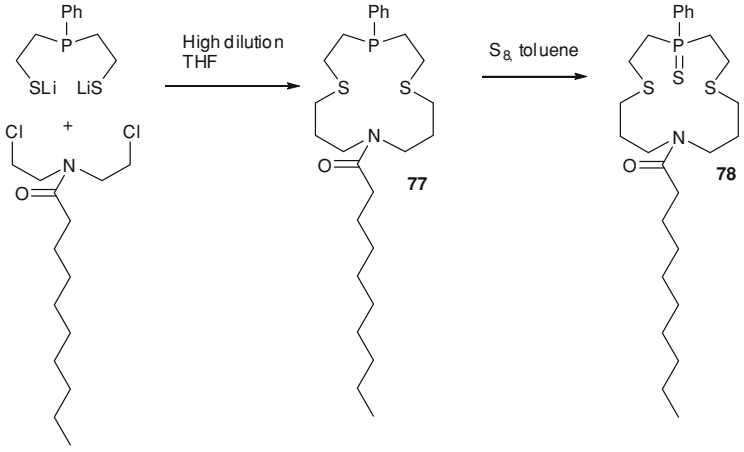
Scheme 12.27 White phosphorus activation by complex **65** containing diamidodiphosphine macrocycle **63**

The 14-membered macrocyclic phosphine **77** and corresponding sulfide **78** were prepared by the macrocyclization under high dilution conditions and further oxidation with sulfur (Scheme 12.29). Both ligands were used as ionophores in an all-solid state poly(vinylchloride) matrix membrane electrode. The sulfide **78** based electrode exhibited a Nernstian response towards copper (II) ions with a cationic slope of 30.7 mV/pCu and a detection limit of 5.97×10^{-7} M. The potential response remains almost unchanged over the pH range 3.9–6.4 at least 7 months. Sensors based on the macrocycles **77** and **78** demonstrate the copper (II) ion sensitivity over other metal ions [83].

Dithiamacrocycle incorporating a phosphine donor group **79** was synthesized (Scheme 12.30) and tested as neutral carrier in poly(vinylchloride) membranes. ClO_4^-—selective chemical field-effect transistor and ion-selective electrode



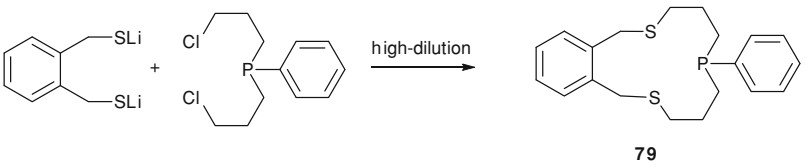
Scheme 12.28 Synthesis of 14-membered and 18-membered P,O,Se-containing macrocyclic ligands **73** and **74** and their palladium(II) complexes **75** and **76**



Scheme 12.29 Synthesis under high-dilution conditions of 14-membered P,S,N-containing macrocyclic ligand **77**

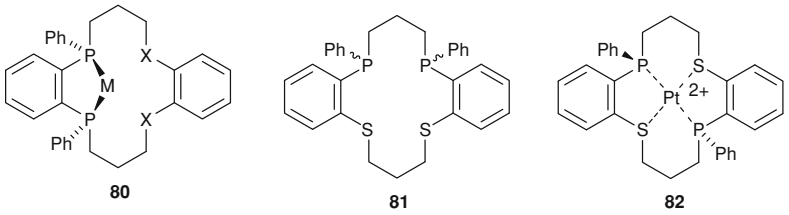
devices based on these plasticized membranes were developed. Both devices showed Nernstian response and a wide working pH range [84, 85].

Various 14-member P_2X_2ring systems were prepared from 1,2-bis(phenylphosphino)benzene. A high-dilution macrocyclization technique gave these species as colorless crystal materials in yields ranging from 18 to 45% [47, 86].



79

Scheme 12.30 Synthesis under high-dilution conditions of 13-membered P,S-containing macrocyclic ligand **79**



80 81 82

X = S, O, NMe
M = $FeCl_2L$, $CoCl_2L$ L-corresponing macrocycle

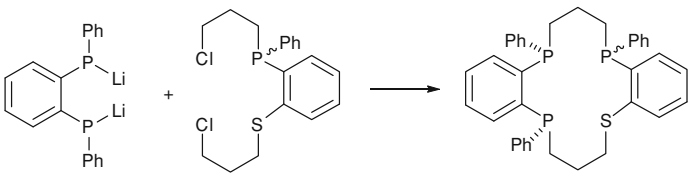
Scheme 12.31 Transition metal coplexes **80–82** of 14-membered P,S-containing macrocyclic ligands

It was shown that the modifying heteroatoms X were not ligating the transition metals. Instead, complexes of the type $(L)_2M$ **80** were formed where four phosphino sites were coordinated to the octahedral metal center, as exemplified with **80** (X = S) and **80** (X = O) (Scheme 12.31) [87].

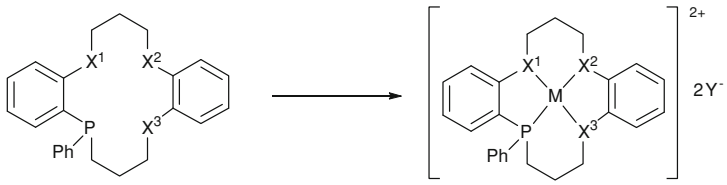
The 14-membered macrocycle **81** where P and S were separated by *ortho*-phenylene fragment was synthesized as a mixture of diastereomers from 1-(mercapto)-2(phenylphosphino)benzene by the deprotonation and the treatment with 1,3-dihalopropanes. The diastereomers were isolated in the pure state. A similar macrocycle with trans-disposition of phosphine groups was obtained via stepwise condensation of S-protected 1-(methoxymethylthio)-2-(phenylphosphino)benzene. The square–planar Pt(II) complex **82** (Scheme 12.31) of the *rac*-diastereomer of this ligand was characterized by X-ray analysis [88].

14-Membered macrocyclic triphosphine **83** was prepared by the high-dilution condensation of dilithium 1,2-di(phosphido)benzene with 1-[(3′-chloropropyl)-phenylphosphino]-2-[(3′-chloropropyl)thio]benzene (Scheme 12.32). The diastereomers of **83** were separated [88].

A number of transition metal complexes **85** of 14-membered ligands **84** were synthesized (Scheme 12.33). In spite of the mutual *cis*- or *trans*-disposition of substituents at phosphorus atoms macrocyclic molecules act as tetradentate ligands forming square–planar surroundings around the transition metal ion situated in the middle of the macrocyclic cavity [89].



Scheme 12.32 Synthesis under high-dilution conditions of 14-membered P,S-containing macrocyclic ligand **83**



$X^1 = X^3 = S$, $X^2 = PPh$ (*cis* and *trans*)
$X^1 = X^2 = S$, $X^3 = PPh$ (*cis* and *trans*)
$X^2 = X^3 = S$, $X^1 = PPh$ (*cis*)
$X^2 = S$, $X^1 = X^3 = PPh$ (*cis*)
$X^2 = S$, $X^1 = PPh$ (cis) $X^3 = PPh$ (*trans*)

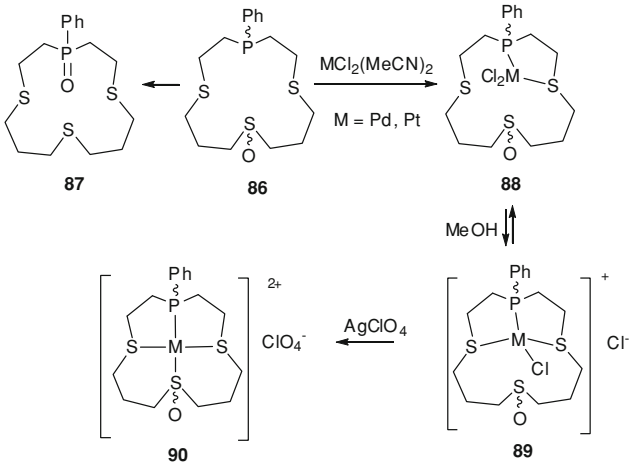
M = Ni, Pd, Pt
Y = Cl, ClO_4, BF_4, PF_6

Scheme 12.33 Transition metal complexes **85** of 14-membered P,S-containing macrocyclic ligands **84**

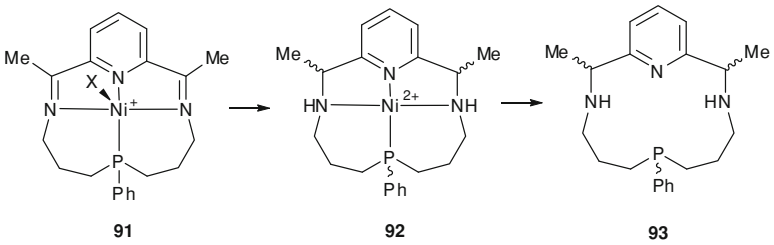
14-membered macrocycle **86** was isolated in 26% yield as a 1:1 mixture of two isomers as a result of the Cs_2CO_3-mediated coupling of bis(3-chloropropyl)sulfoxide with bis(mercaptoethyl)phenylphosphine. **86** slowly transformed into **87** (Scheme 12.34), but in the presence of the iodine traces, the rearrangement occurred spontaneously and took 30 min.

When treated with $[MCl_2(MeCN)_2]$ (M = Pd, Pt), the sulfinyl-substituted macrocycle **86** functions as a bidentate ligand via its P and one of the thioether S donor atoms giving the corresponding neutral square–planar complexes *cis*-**88**. In both complexes, the sulfoxide group is not involved in metal complexation. However, when the dichloro complexes were treated with silver perchlorate, the corresponding complexes **90** were formed where the macrocycle acted as a tetradentate ligand (Scheme 12.34). In both perchlorate salts, the ambidentate sulfoxide functions are coordinated to the metal center via their S donor. In contrast to the reported acyclic analogues, the sulfoxide–metal bonds are kinetically stable [90].

Five-coordinated nickel complexes of 14-membered P,N-macrocycle **91** were obtained by heating under reflux an ethanolic solution containing bis(3-aminopropyl)phenylphosphine, 2,6-diacetylpyridine, and $NiX_2 \cdot 6H_2O$ (X = Br, I), followed by the addition of NH_4PF_6. The reduction of imine groups in the complexes with sodium borohydride or PtO-H_2 gave **92**. The free ligand **93** was released by heating **92** with cyanide (Scheme 12.35) [91].



Scheme 12.34 Transition metal coplexes **88–90** of 14-membered P,S,O-containing macrocyclic ligands **86**



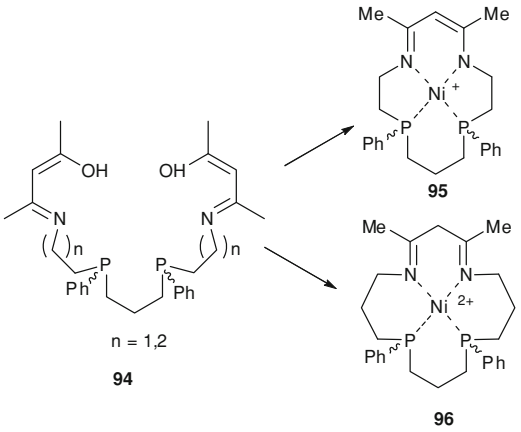
Scheme 12.35 Synthesis of 14-membered P,N-macrocycle **93**

The other example of the 14-membered macrocyclic Schiff-base phosphine ligand **95** was obtained by the ring closure of the linear precursor **94** with the elimination of acetylacetone on $Ni(OAc)_2$ template (Scheme 12.36). The 16-membered homologue **96** was obtained using the same reaction [92].

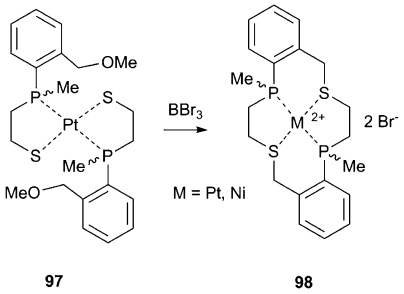
Treatment of a mixture of stereoisomers of *trans*-platinum(II) complex **97** with boron tribromide resulted in the cyclisation at sulfur to give the complex **98** (Scheme 12.37). Its treatment with aqueous hydroxide and potassium cyanide yielded corresponding free *rac*- and *meso*-14-membered macrocyclic diphosphines in 6 and 0.5% yields only. Both isomers readily formed square–planar complexes of Ni(II) [93].

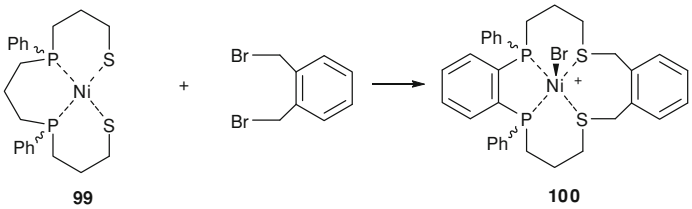
The metal template reaction of **99** with 1,2-xylylene dibromide resulted in the formation of five-coordinated nickel complex of 16-membered ligand **100** (Scheme 12.38) [94].

Scheme 12.36 Synthesis of 14- and 16-membered P,N-macrocycles **95** and **96** by the ring closure on $Ni(OAc)_2$ template



Scheme 12.37 Template synthesis of 14-membered P,S-macrocycle **98**

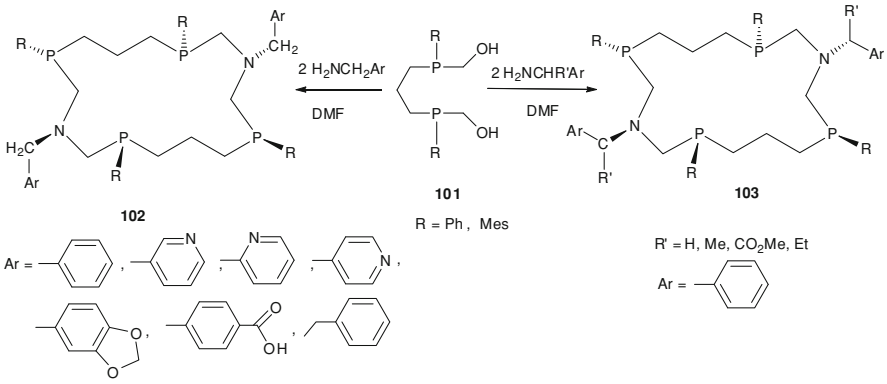




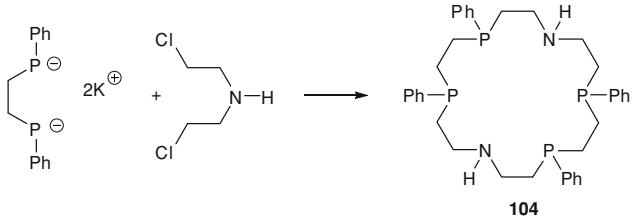
Scheme 12.38 Template synthesis of 16-membered P,S-macrocycle **100**

The unexpected example of the covalent self-assembly of flexible 16-membered macrocyclic tetraphosphines **102** and **103** was found in the course of condensations of secondary diphosphines with formaldehyde and aralkylamines, including those with various heteroaryl fragments (Scheme 12.39).

The reactions of 1,3-bis(arylphosphino)propanes **101** with formaldehyde and benzylamines or their heteroanalogues and even phenethylamine in the usual concentration range (0.1–0.5 M) at elevated temperatures (80–110 °C) and in the absence of templating reagents led to the formation of *RSSR*-isomers of macrocyclic aminomethylphosphines (corands) **102** in good yields and with



Scheme 12.39 Covalent self-assembly of 16-membered P,N-containing macrocycles **102** and **103**



Scheme 12.40 Synthesis of 18-membered P,N-containing macrocycle **104**

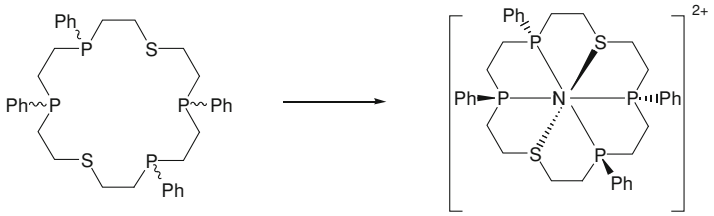
excellent stereoselectivity in spite of the fact that the starting diphosphines exist as the mixtures of rac- and meso-stereoisomers [95, 96]. It should be mentioned that analogous reactions with less basic and active in the condensation arylamines gave only corresponding 1-aza-3,7-diphosphacyclooctanes [97].

The found covalent self-assembly process allowed also to obtain a series of optically active tetraphosphine ligands **103** as single *RSSR*-stereoisomers on the basis of various chiral amines [98].

In the solid state one half of the 16-membered cycle, $–CH_2P(CH_2)_3PCH_2N–$, has a distorted crown conformation with a nearly axial orientation of the lone pairs of the heteroatoms, and the other half is its inverted (or pseudoinverted for the chiral corands **103**) with the lone pairs pointing to the opposite sides of the macrocycle. Two phosphorus atoms of each half have different configurations [95, 96, 98].

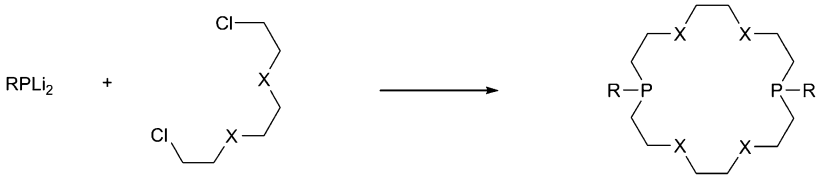
The series of 18-membered cycles containing different heteroatoms separated by ethylene fragments and in common resembling 18-crown-6 were obtained by different methods.

The reaction of dipotassium 1,2-ethylenebis(phosphenide) with bis(2-chloroethyl)amine in THF at room temperature led to the 18-membered P,N-macrocycle **104** for which four possible stereoisomers were isolated (Scheme 12.40).



105 106

Scheme 12.41 Synthesis of nikel(II) complex **106** of 18-membered P,S-containing macrocycle **105**



107

X = O, S
R = Bn, c-C_6H_{11}, Ph

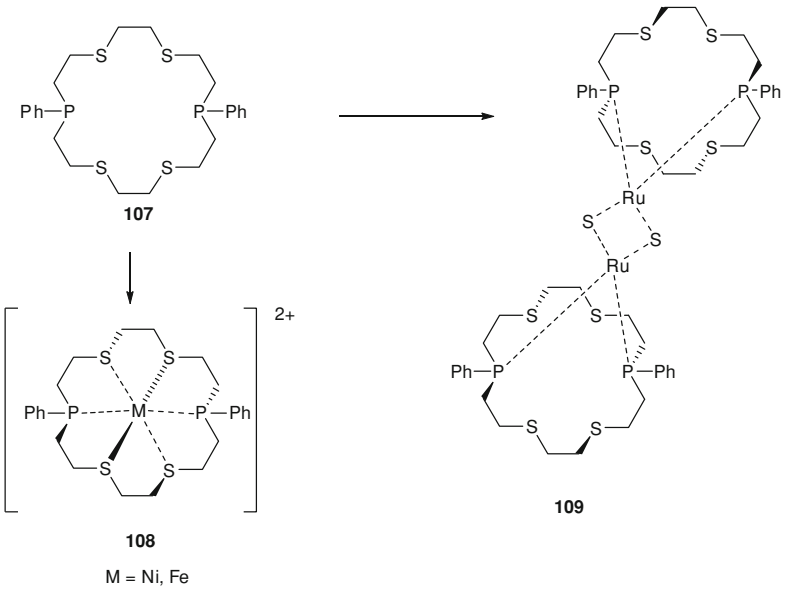
Scheme 12.42 Synthesis under high-dilution conditions of 18-membered P,S- and P,O-containing macrocycles **107**

The crystallographic study of one stereoisomer of Ni(**104**)$(BF_4)_2$ .2Me_2CO showed that the N-atoms are not coordinated to the metal [99].

The synthesis and characterization of several diastereomers of **105**, as well as their Ni(II) complexes **106** have been described. In the complex of (RSSR)-isomer of **105** the nickel atom lies in a centre of symmetry and is surrounded by the six donor atoms of the ligand (Scheme 12.41). The four phosphorus atoms of the macrocycle lie in a plane. The two sulfur atoms are located approximately at the apical positions of a strongly elongated octahedron, the $P(CH_2)_2S(CH_2)_2P$ moieties adopting a facial arrangement [100–102].

The phosphino-crown ethers and thioethers **107** were prepared under high-dilution conditions in one step from appropriate dilithiumorganophosphides and 1,2-bis(chloroethoxy)ethane or 1,2-bis(chloroethylthio)ethane, respectively (Scheme 12.42). Yields of diastereomeric mixtures of ligands **107** were from 4 to 15%. **107** formed stable complexes with common brutto formula $LFeCL_2$, $LCoCl_2$ and $LNiCl_2$, $LMo(CO)_5$ and $LMo(CO)_3$ (L = **107,** R = Ph, X = O) [103].

18-Membered macrocycle **107** was detected in reaction mixtures during the synthesis of 9-membered ring **45** (see above). Once the presence of **107** in the reaction mixture had been established, the method was modified to optimize its yield to ca. 90% by slow addition of 1,2-dichloroethane to a relatively high concentration (C $\sim$ 0.1 M) mixture of $PhP(CH_2CH_2SH)_2$ and caesium carbonate. Reaction of **107**

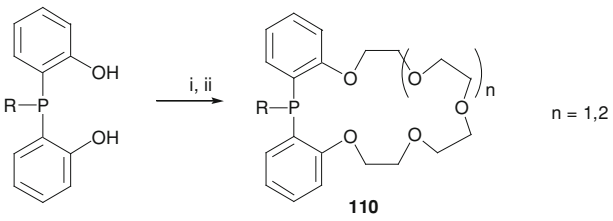


Scheme 12.43 Transition metal coplexes **108–109** of 18-membered P,S-containing macrocyclic ligand **107**

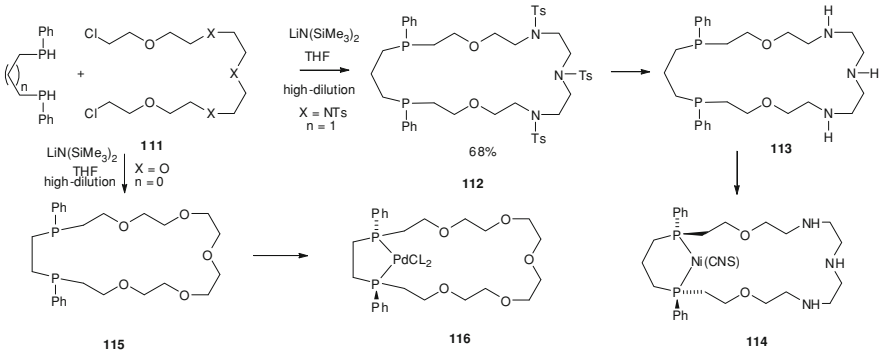
with $[Ni(H_2O)_6](BF_4)_2$ or $Fe(BF_4)_2$ affords **108** (M = Ni or Fe) (Scheme 12.43). The structure of **108** (M = Ni) is a tetragonally distorted octahedron in which there are two short Ni–S bonds [2.2152(6) Å] and two long Ni–S bonds [2.9268(6) Å]. Unlike that the structure of **108** (M = Fe) is octahedral with approximately equal Fe–S bonds. The results of P–C and C–S bond rupture were observed in the reaction of ruthenium(III) triflate with **45** which unexpectedly afforded crystals containing **109**, in which the two ruthenium centres are bridged by two sulfides and two ligands **107** are coordinated only through the phosphine centres [104].

Treatment of bis(2-hydroxyphenyl)phenylphosphine with sodium hydride followed by the appropriate alkylene ditosylate afforded 18- and 21-membered phosphacrown ethers **110** correspondingly (Scheme 12.44) [105].

21-Membered phosphacrown **115** and 22-membered azaphosphacrown **112** ethers were obtained by the reaction of dilithium 1,3-propylene- or 1,2-ethylene(bisphosphide) with appropriate dichloroalkanes under high-dilution (Scheme 12.45). *Rac*- and *meso*-isomers of 22-membered N-tosylated azaphosphacrown ether **112** were separated using the different solubility of their $NiCl_2L$ complexes. The air-sensitive free ligand **112** was obtained by cyanolysis under nitrogen in methylene chloride. The two diastereoisomers of **112** could be equilibrated to an equimolar mixture upon fusion of either *syn* or *anti* form, and after several cycles of thermal isomerization followed by diastereomeric separation the original mixture could be converted largely into either the *rac* or *meso* diastereoisomer. Detosylation of *syn*- or *anti*- **112** was achieved without isomerization



Scheme 12.44 Synthesis of 18- and 21-membered phosphacrown ethers **110**

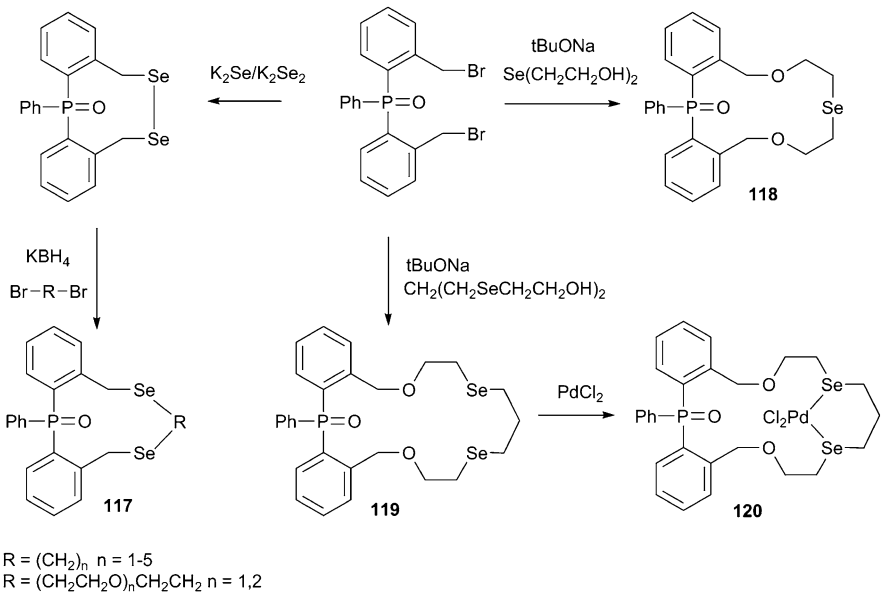


Scheme 12.45 Synthesis under high-dilution conditions and transition metal complexes of 21- and 22-membered macrocycles **115** and **112**

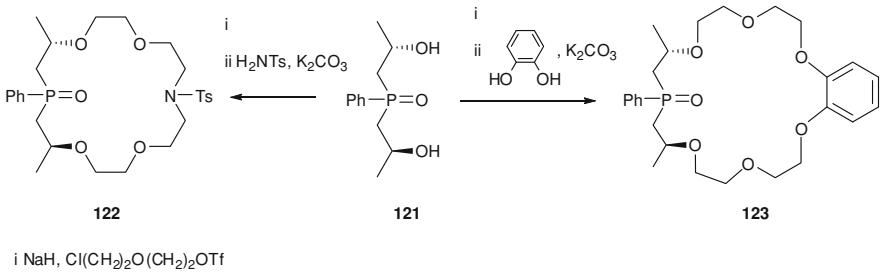
by the addition of 6 equivalents of sodium naphthalenide in 1,2-dimethoxyethane (DME) in the presence of 3 equivalents of tert-butyl alcohol at –45 °C.

Reaction between $NiC1_26H_20$ and *anti*-**113** followed by the addition of HBF_4-etherate, gave [*anti*-(**113**)Ni]$(BF_4)_2$. A metathesis of this latter complex with an excess of NaSCN resulted in the formation of the racemic diastereoisomer, *anti*-**114** [106].

A one-pot reaction was developed for the simultaneous introduction of phosphorus and selenium atoms into the ring system of macrocycles **117** starting from selenium via reduction with KBH_4, treatment with bis[o-(bromomethyl)-phenyl]phenylphosphine oxide and reduction with KBH_4 followed by the addition of an appropriate dibromide. Thus, 10–17-membered macrocycles **117** containing one phosphorus and two selenium atoms were synthesized. The condensation of bis[o-(bromomethyl)phenyl]phenylphosphine oxide with selenium-containing diols in the presence of sodium tert-butoxide gave macrocyclic ligands **118** and **119**, respectively (Scheme 12.46). Reaction of **119** with palladium(II) chloride gave the 1:1 chelate complex **120** bonded to the selenium atoms [62].



Scheme 12.46 Synthesis and transition metal complexes of P,Se- and P,O,Se-containing macrocycles **117–119**



Scheme 12.47 Synthesis of chiral P,O,N- and P,O-containing macrocycles **122** and **123**

(*S*,*S*)-Bis(2-hydroxypropyl)(phenyl)phosphine oxide **121** is a suitable chiral precursor for the synthesis of 1-phospha-11,12-benzo-21-crown-7 **123** and 1-phospha-10-aza-18-crown-6 **122** derivatives, the first examples of optically pure, crown-ether-like, phosphorus-containing macrocycles (Scheme 12.47). The complexation of Na^+ by the crown ether moiety of the macrocyclic ring has been observed [107].

The properties of the macrocycles are dependant upon ring size. The properties of small (9–11-membered macrocycles) are similar to common heterocycles. The lone pairs (LP's) of the phosphorus atoms are predisposed by the cycle conformation and the configuration of corresponding P-atoms. The larger macrocyclic ligands could wrap around the cental ion giving the stable coordination chelates

even with the opposite orientation of P donor centres LP's, and the much larger macrocycles could be regarded as molecular reactors, because not only the metal atom but, in addition to the metal ion, entire organic molecules could be incorporated into the molecular cavity.

Taking into account the hard donor character of oxygen or nitrogen atoms and the ability of phosphorus to have a variable environment, few different strategies in the design of the corresponding macrocyclic species (catalysts, molecular devices—chemical sensors) have been developed. First is the constructing of macrocyclic polyphosphines and phosphites with soft P donor sites utilizing the ability of phosphines to form stable transition metal complexes in contrast to oxygen or nitrogen. That is an example of well-known hybrid ligand strategy of preparing hemilabile transition metal precursors for homogeneous catalysts. The incorporation of donor atoms into the macrocyclic framework usually increases the stability of the labile M–X bonds. On the other hand, the presence of soft phosphino groups should modify the well known receptor properties of crown- and azacrownethers.

The second approach is the incorporation of four-coordinated phosphorus species bearing P=O/P=S and even harder $P–O^-$ donor groups which could increase sensitivity of desired sensors.

The third approach is the specific reactivity of phosphorus which opens new avenues for the further chemical modification of macrocyclic framework.

12.3 P-Containing Cyclophanes

Macrocycles containing aromatic or heterocyclic units within the macrocyclic core have been actively investigated for the last few decades [108–111]. The cyclic units, being rigid building blocks, allow the design and synthesis of molecular cavities having defined spatial characteristics, and also serve as binding sites for hosts capable of interacting with their π-electron systems. On the other side heterocyclic rings are also of special interest for the construction of cyclophane-type molecules [112–115] because the presence of donor heteroatoms provides the means for the incorporation of a binding site for transition metals within the macrocyclic structure.

However, the chemistry of P-based cyclophane ligands is less developed than that of their oxygen or nitrogen analogues [18–22]. This fact has been mainly attributed to the air sensitivity of these compounds and the poor yields obtained in their preparations by high-dilution [18–22] or template methods [18–22], although the high-yield synthesis of a few types of phosphamacrocycles has been reported [23, 116, 117]. This is a severe drawback for their large-scale application, but if P-containing cyclophanes with a unique shape, distinct architecture, and set of functional groups become easily available from natural or synthetic sources, they would start to inspire the imagination of chemists to devise novel sophisticated receptors, machines, and devices [1–11], as well as new types of molecular reactors [118].

Macrocycles formed from aromatic and/or the heterocyclic units with three-coordinated phosphorus atoms as donors [18, 21] are able to provide a variety of donor–acceptor and intermolecular interactions and are of interest both for supramolecular chemistry (in particular as selective sensors [83]) and as unusual ligands for transition metal catalyzed reactions in organic synthesis [119, 120], as the geometry and well-defined position of the coordinated donor centers could lead to specific catalytically active complexes [44, 121].

12.3.1 Compounds with Small Organic Cycles Incorporated into the Macrocyclic Backbone

The subjects of this part are compounds with small organic cycles which are incorporated into the P-based macrocyclic backbone and determine the structure and specific properties of the macrocycles to an essential extent.

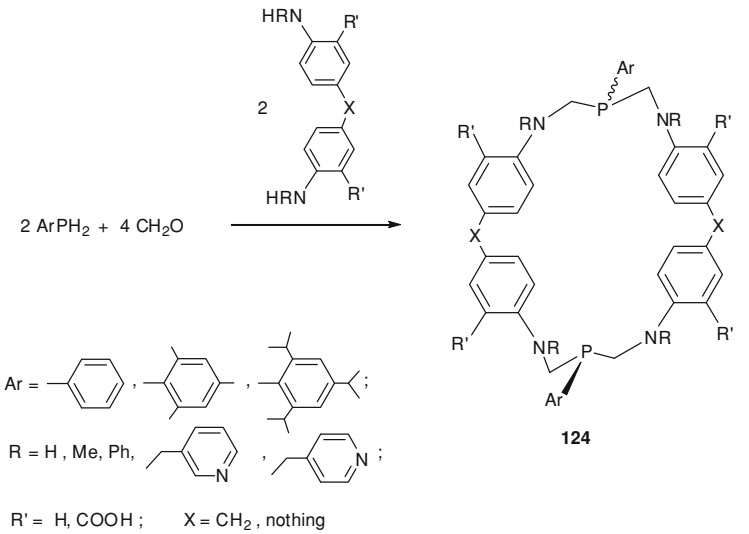
In order to systematize P-containing cyclophanes we will take into account the nature of the P-containing fragment coupling phane units.

The covalent self-assembly approach in the course of a Mannich-type condensation was used for the synthesis of P,N-containing cyclophanes with an aminomethylphosphine backbone. The condensations in the three-component systems: primary phosphine/formaldehyde/secondary diamine with angular di(p-phenylene)methane spacer (or bis(4-amino-3-carboxyphenyl)methane) or with linear biphenylene spacers led to the formation of N-containing macrocyclic diphosphines **124** as a result of [2 + 2]-condensation (Scheme 12.48). The condensations were performed in DMF at the reagents concentrations of 0.1–0.3 M at 100–110 °C or at ambient temperature in the case of N-pyridylmethyl substituted diamines [122].

All macrocycles **124** were formed as the mixtures of *cis*- and *trans*-stereoisomers. The *trans*-isomers prevailed in the reaction mixtures only slightly, but the fraction crystallization of **124** (Ar = Mes, R = Me, R′ = H, X = CH_2) from DMF led to the individual *trans*-stereoisomer. According to X-ray analysis data all nitrogen atoms of the centrosymmetric molecule of *trans*-**124** (Ar = Mes, R = Me, R′ = H, X = CH_2) are located in the same plane, but only two of them are coordinated in trigonal-planar fashion and their lone electron pairs are conjugated with the π-systems of the phenylene rings. Two other ones are coordinated in near trigonal–pyramidal fashion which indicates the low extent of the conjugation. The neighbouring phenylene rings are strongly twisted and the opposite rings are coplanar, so the macrocyclic cavity is practically collapsed and elongated: the P–P-distance is 11.80 Å, whereas the distance between the opposite aromatic rings is only 5.85 Å [122].

So it has been shown that the covalent self-assembly methodology is also effective for the synthesis of flexible cyclophane macrocyclic systems, the requirements to the building blocks geometry being not very rigid in these cases.

Phosphorus dialdehydes **125** (X = lone pair, R = Ph) react with phosphodihydrazides $Ph(Y)P(N(CH_3)NH_2)_2$ (Y = S, O) to give macrocycles **126**

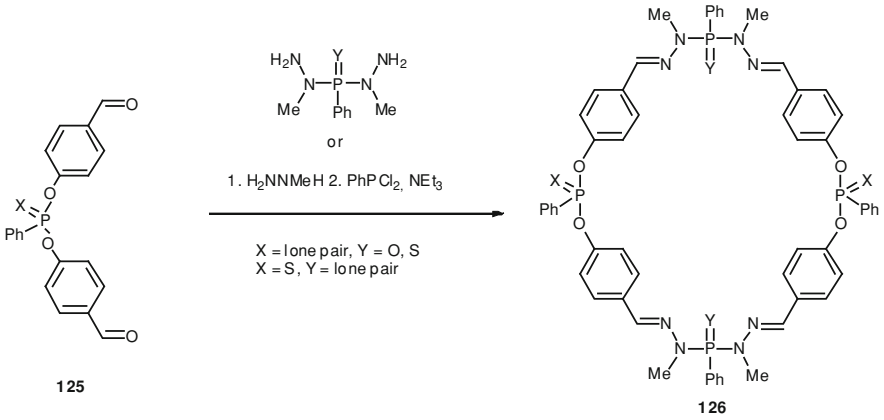


Scheme 12.48 Covalent self-assembly of P,N-containing cyclophanes with aminomethylphosphine backbone **124**

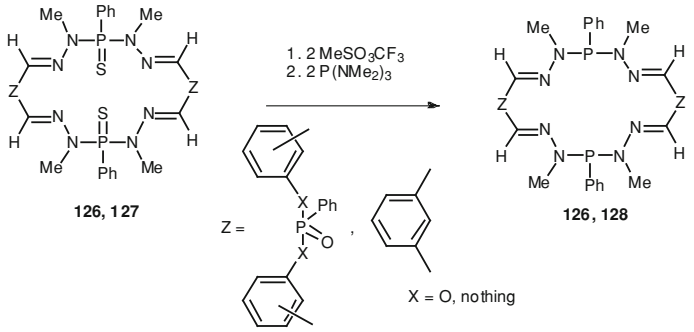
(X = lone pair, Y = S, O) arising from [2 + 2] cyclocondensations. The treatment of phosphodihydrazone $Ph(S)P(OC_6H_4CH{=}N{-}N(Me)H]_2$ obtained in situ with phenyldichlorophosphine affords macrocycle **126** (X = S, Y = lone pair) as well (Scheme 12.49). All macrocycles **126** were obtained in high yields (59–75%) due to the self-assembly processes. Obtained cyclophanes possess tri- and tetracoordinated phosphorus atoms [123].

Clean desulfurization of thiophosphonic macrocycles **126**(X = O, Y = S) and **127** gives rise selectively to new tricoordinated phosphorus containing macrocycles **126**(X = O, Y = lone pair) and **128** (Scheme 12.50). That result is of special importance taking into the account numerous types of macrocycles containing tetracoordinated thiophosphonic fragments obtained by effective cyclocondensation strategy [18, 19].

Symmetric macrocycles **129** with four phenylene fragments (CR_2 = cyclohexylidene [124], R = 1,2,2,6,6-tetramethylpiperidin-4-yl [125], NEt_2 [126], $O\text{-}C_6H_2(Bu\text{-}t)_2\text{-}3,5\text{-}Me\text{-}4$ [124]) were obtained from corresponding dichlorophosphites along with the products of [3 + 3] condensation **130** [126] or in the course of symmetrisation reaction [125, 126]. The similar macrocyclic dimer **131** (R = $O\text{-}C_6H_2(Bu\text{-}t)_2\text{-}3,5\text{-}Me\text{-}4$) with six p-phenylene fragments was synthesized on the basis of the bisphenol $1,4\text{-}C_6H_4(CMe_2C_6H_4OH\text{-}4)_2$ [126]. The symmetrization leading to the cyclophanes **129** ($CR_2 = CMe_2$, $R = NEt_2$) was observed in the reaction of phosphorus ester diamide $1,4\text{-}C_6H_4[CMe_2C_6H_4\text{-}OP(NEt_2)_2\text{-}4]_2$ with bisphenol $Me_2C(C_6H_4OH\text{-}4)_2$, whereas its condensation with $1,4\text{-}C_6H_4(CMe_2\text{-}C_6H_4OH\text{-}4)_2$ afforded the corresponding symmetric macrocyclic phosphoramidite



Scheme 12.49 Covalent self-assembly of P,N-containing cyclophanes **126**

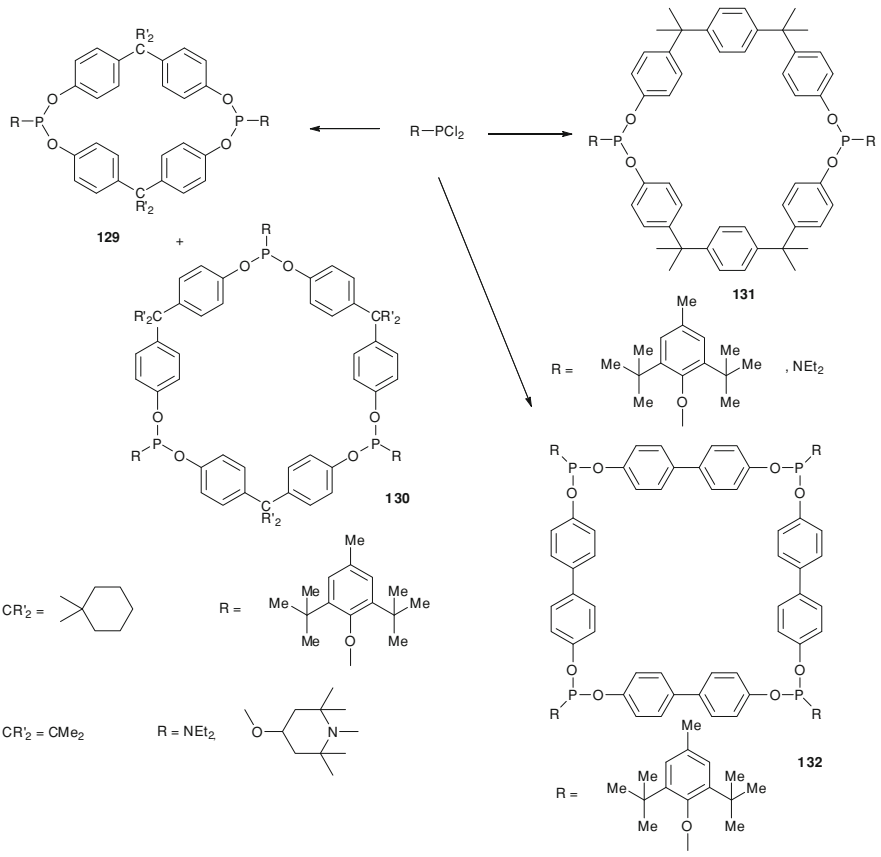


Scheme 12.50 Desulfurization of thiophosphonic macrocycles **126–127**

131 as a mixture of *cis*-and *trans*-isomers (Scheme 12.51) [126]. These results were explained by transesterification reactions which occur prior to the esterification of the phosphorus amide function [125, 126]. The product of [4 + 4]-condensation **132** was also obtained on the basis of the bisphenol with biphenylene spacer [124].

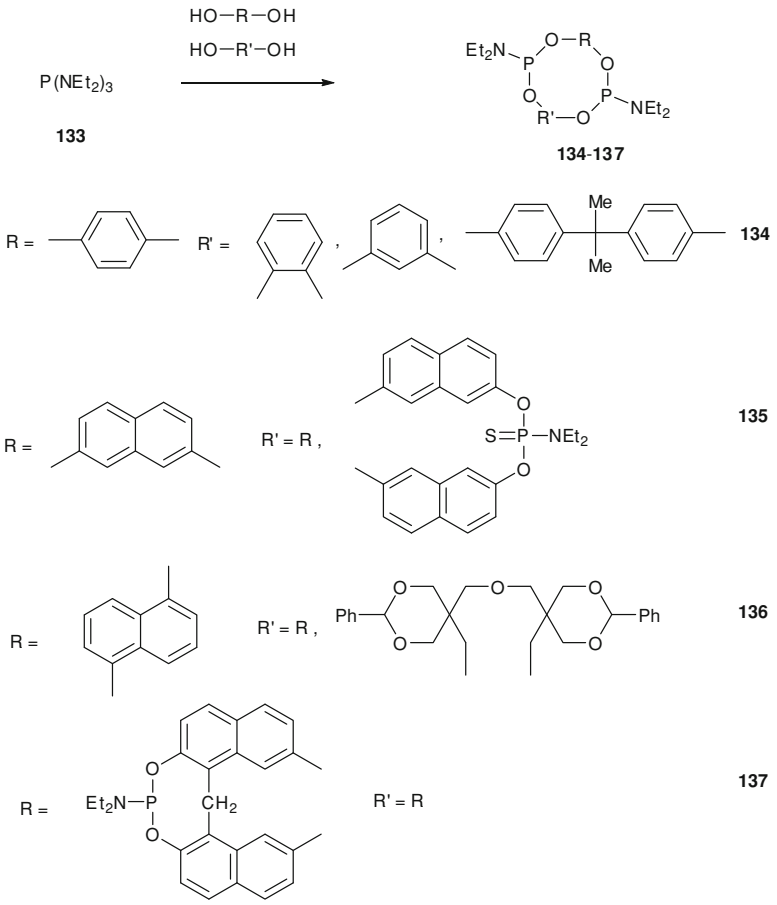
The achievements in the macrocyclic chemistry of phosphite ligands were summarized in a review [22].

A series of various macrocyclic phosphites **134**−**137** obtained in the course of reaction of tris(diethylamino)phosphite **133** with different diols (hydroquinone [127, 128], pyrocatechol [127], resorcinol [129], 4,4′-(propane-2,2-diyl)diphenol [128], 2,7-dihydroxynaphthalene [130], 1,5-dihydroxynaphthalene [131], dipentaerythritol [129, 132], 2,2′,7,7′-tetrahydroxydinaphthylmethane [133]) was reported (Scheme 12.52). Relatively high yields (up to 60%) and stereoselectivity of the reactions, especially in the case of unsymmetrical diphosphites **134**, provide an evidence of self-assembly of the cyclophanes. These results had been reviewed recently [134].



Scheme 12.51 Covalent self-assembly of macrocyclic phosphites **130–132**

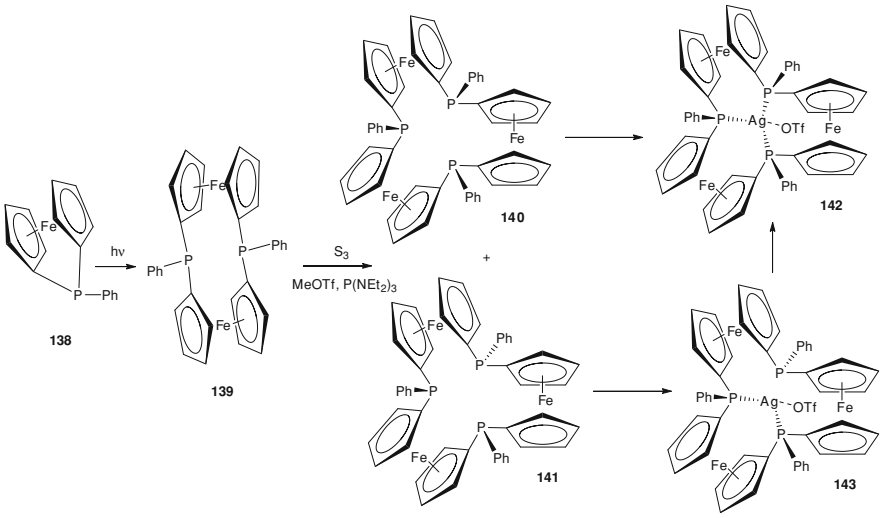
Recently novel tridentate ferrocenylphosphine macrocycles **140–141** have been obtained, isolated and characterized. A photolytic ring-opening reaction of PPh-bridged 1,1′-ferrocenophane **138** gave a mixture of its oligomers **139**. After their sulfurization, GPC separation of low-molecular weight species afforded two isomers of a macrocyclic trimer, in which three 1,1′-ferrocenediyl units and three P(S)Ph groups were alternately linked to form a macrocyclic ring (Scheme 12.53). Although yields of both isomers were low (17% in total), they were successfully desulfurized in good yields without configurational inversion at their phosphorus centers by treatment with $MeOTf/P(NMe_2)_3$ ($OTf = CF_3SO_3$), to give the respective tridentate macrocyclic phosphine ligands **140–141**. When the isomer **140** was heated in toluene at around 80 °C, it isomerized gradually but almost completely to the **141**. The reaction of AgOTf with **140** gave a mononuclear silver complex **142** in which **140** encircled the Ag^+ ion as a tridentate ligand (Scheme 12.53). A similar reaction of **141** gave the same silver complex **142**,



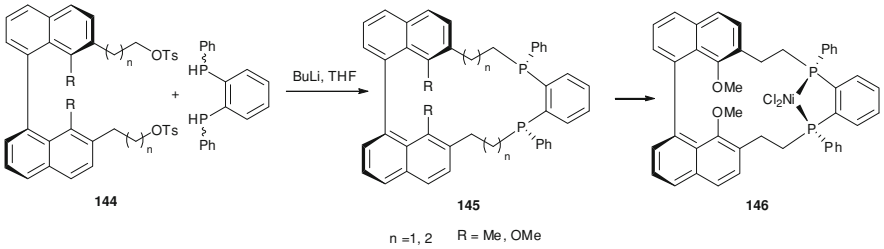
Scheme 12.52 Covalent self-assembly of macrocyclic phosphites **134–137**

indicating that a facile conversion of **140–141** took place upon coordination to the Ag^+ ion of **143** at room temperature [135].

Binaphthyl-based macrocyclic diphosphines **145** (R = Me, MeO, $n = 1$; R = MeO, $n = 2$) were prepared from binaphthalenes **144** and o-phenylene-bis[phenylphosphine] under high-dilution conditions in 55, 49, and 87% yields, respectively (Scheme 12.54). **145** demonstrated a remarkable stability against oxidation due to their rigid conformation, directing the lone pairs of the P atoms toward the center of the ring. Contrary to the expectation, the crystal structure of the $NiC1_2$ complex **146** shows the NiP_2C1_2 plane completely twisted out of the macrocycle, which demonstrates the flexibility of this compound and makes it less suitable candidate for efficient chiral catalysis [136, 137].

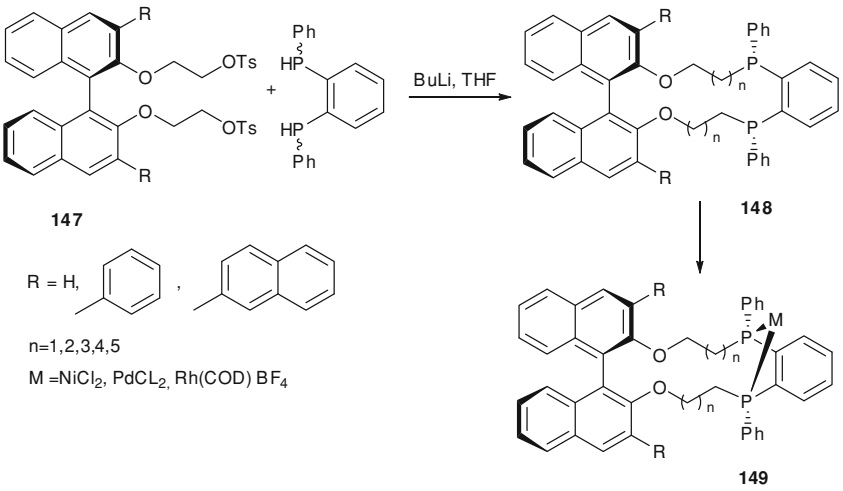


Scheme 12.53 Synthesis of tridentate ferrocenylphosphine macrocycles **140**–**141** and their silver(I) complexes **142**–**143**



Scheme 12.54 Synthesis under high-dilution conditions of binaphthyl-based macrocyclic diphosphines **145**

The synthesis of the 1,1′-binaphthyl-based macrocyclic bisphosphine ligands (racemic and optically active) **148** (R = H; n = 1–5) under high dilution conditions was reported. In all cases the nonsymmetrical diastereomer was formed predominantly (n = 3–5) or even exclusively (n = 1,2) (Scheme 12.55). In a few cases isomers were isolated and identified. Macrocycles **148** formed air-stable square–planar *cis* complexes **149** (M = $NiCl_2$ or $PdCl_2$; n = 1–5). Complexes with C1-symmetrical ligands show less steric strain than compounds with C2 symmetry. Enhanced strain causes an opening of the biaryl angle from the cisoid (60–75°) to the transoid form (100–115°) and an out-of-center twist of the phosphorus lone pairs or the Cl_2NiP_2 fragment of the molecule. This conformation is especially easily adopted, as a flattening of the binaphthyl fragment causes an expansion of the macrocycle. This gives enough space for one phenyl ring and the P–C_6H_4–P fragment to be tolerated "inside" the cycle [138, 139].

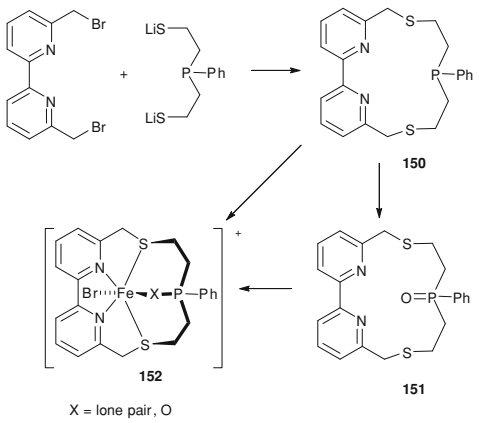


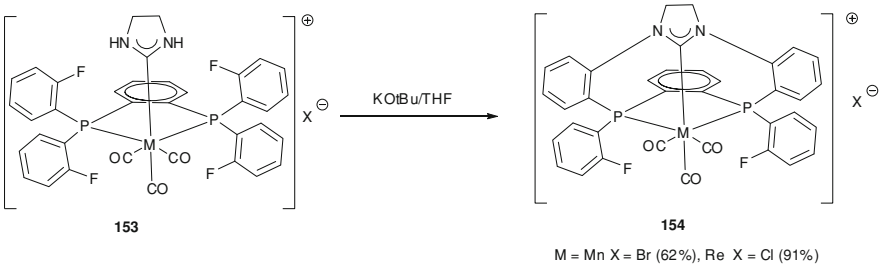
Scheme 12.55 Synthesis under high-dilution conditions of binaphthyl-based macrocyclic diphosphines **145** and chelate complexes **149**

The application of macrocyclic binaphthyl ligands **148** (R = H, n = 1) in allylic alkylation reactions was reported [140]. **148** (R = H, n = 1) was found to be most effective in allylic alkylation reactions with asymmetric inductions up to 86% e.e. To further improve the asymmetric induction the area of chiral interaction was extended by introducing aromatic substituents R of different size [141]. The new ligands **148** (R = Ph, Np) showed asymmetric induction values of up to 98% e.e. if used in palladium catalyzed allylic alkylation reactions. Thus, allylic alkylation of PhCH:CHCH(Ph)OAc with dimethyl malonate in the presence of catalyst $[Pd(C_3H_5)Cl]_2$/**148** (R = Ph) gave 94% (S)-PhCH:CHPhCH$(CO_2Me)_2$ in 96% e.e. [141]. The mononuclear complexes **149** (R = H, n = 3–5, M = [Rh(COD)]BF_4) were prepared by adding 1,1′-binaphthyl-based diphosphine macrocyclic ligands **148** (R = H, n = 3–5) to a dichloromethane solution of $[Rh(COD)_2]BF_4$ (COD = 1,5-cyclooctadiene). Hydroformylation of styrene was carried out using solutions of rhodium-diphosphine catalyst prepared from [Rh(acac)$(CO)_2$] and chiral macrocyclic diphosphines **148** (R = H, n = 3–5). At 30 bar of CO/H_2 (1:1) and 65 °C regioselectivities of 2-phenylpropanal formation were >92% when all chiral diphosphines were added in a P–P/Rh ratio of 2 [121].

A new 2,2′-bipyridine-based 15-membered phosphadithiamacrocycle **150** has been synthesized by the reaction of 6,6′-bis(bromomethyl)-2,20-bipyridine and dilithium 3-phenyl-3-phosphapenta-1,5-dithiolate under high-dilution (Scheme 12.56). The phosphoryl derivative **151** was synthesized by direct oxidation of **150** at open atmosphere. The reaction of **150** and **151** with Fe(II) perchlorate gave the complexes **152** (X = lone pair, O). In both cases, a distorted octahedral environment is achieved at the Fe(II), with five sites occupied by the macrocycles **150** and **151** and the sixth by a monodentate bromine ligand. The bond distances found in the complex cation **152** (X = O) are compatible with a high-spin

Scheme 12.56 Synthesis under high-dilution conditions of 2,2′-bipyridine-based 15-membered phosphadithiamacrocycle **150** and its iron(II)complexes **152**





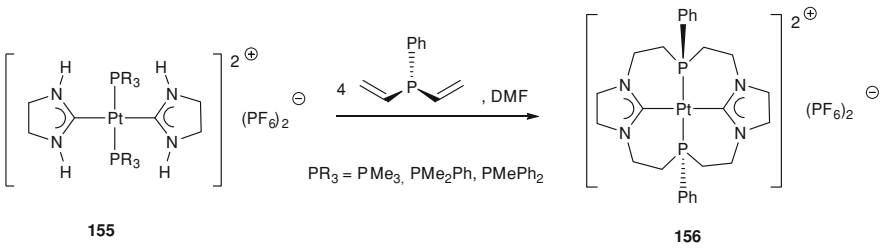
Scheme 12.57 Template synthesis of cyclophane **154**

configuration. However, the same parameters for **152** (X = lone pair) and their magnetic character are only compatible with a low-spin configuration [112].

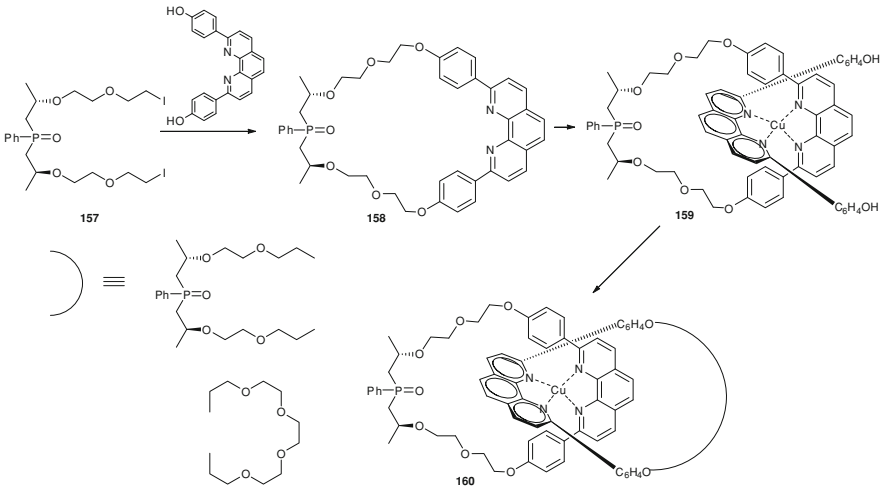
Unusual type of P-based cyclophane **154** containing NH,NH-functionalized carbene heterocyclic fragment coordinated to the transition metal was obtained by metal template assisted cyclization reactions of the diphosphine ligand bearing reactive 2-fluoro substituents at phenyl groups on phosphorus atoms and carbene heterocycle in coordination sphere of **153** (Scheme 12.57). Aerial oxidation of the complexes of the cyclophane ligand resulted in the isolation of the free macrocycle as di(phosphine oxide)/imidazolidinium salt [142, 143].

The macrocyclic diphosphacyclophane **156** containing two heterocyclic carbene fragments similar to that of **154** was obtained by the template-controlled addition of the N–H bonds of the NH,NH-stabilized carbene ligands of complex **155** to the vinylic double bonds of divinyl(phenyl)phosphine (Scheme 12.58) [144].

The first [2]catenane **160** functionalized with phosphorus-containing groups has been prepared recently. The synthetic approach is based on the advantage of the



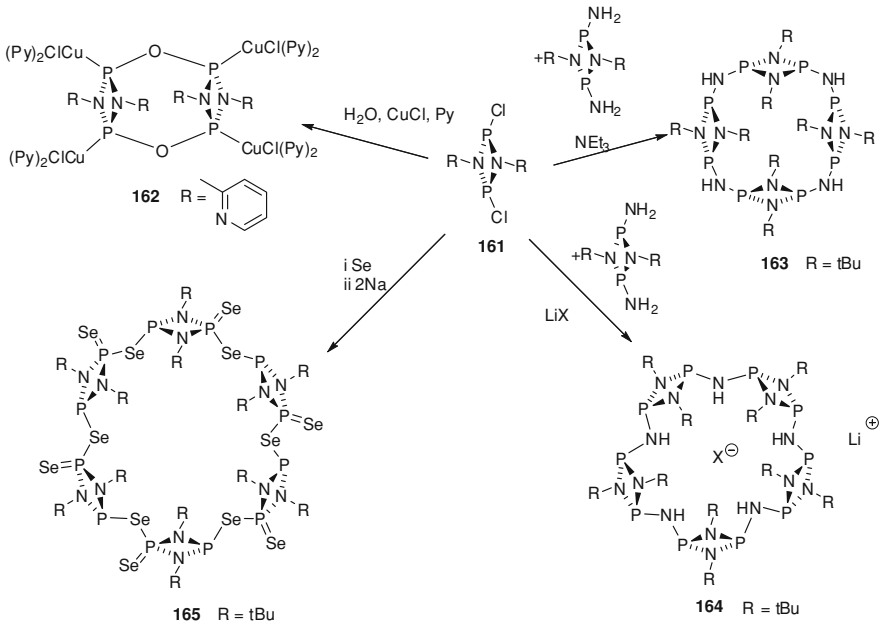
Scheme 12.58 Template synthesis of cyclophane **156**



Scheme 12.59 Template synthesis of [2]catenane **160**

temporary, three-dimensional template effect of copper(I)/phenanthroline complexes to create the core of the interlocking rings. The diiodide (*S,S*)-**157** reacts with the phenanthroline diphenol in DMF in the presence of cesium carbonate under high-dilution conditions giving the expected 33-membered macrocycle (*S,S*)-**158** in 30% yield. The interlocking rings were obtained by addition of the phosphorus-containing diiodide (*S,S*)-**157** to the precatenane **159** generated in situ from (*S,S*)-**158**, copper(I) hexafluorophosphate, and the phenanthroline diphenol in the presence of cesium carbonate (Scheme 12.59).

After the purification of the reaction mixture the cationic catenane **160** was obtained. After removal of the copper, the two diastereoisomers of the free catenane **160** were separated by preparative HPLC and fully characterized. **160** represents an unprecedented class of chiral phosphorus derivatives, that is, phosphorus-containing chiral [2]catenanes, whose properties in coordination chemistry and catalysis should be investigated [145].



Scheme 12.60 Synthesis of cyclophanes formed by few four-membered P-containing rings linked by one-atom spacers **162–165**

12.3.2 Compounds with P-Containing Small Rings Incorporated into the Macrocyclic Backbone

The methods of synthesis and applications in the coordination, supramolecular chemistry and catalysis of the cyclophanes bearing small P-containing ring in the core macrocyclic structures are the subject of this chapter. Material in the chapter is presented in the sequence according to the size and nature of P-containing rings.

Macrocyclophanes formed by few four-membered P-containing rings linked by one-atom spacers **162–165** were obtained in good yields (27, 67, 44 and 45%, respectively) using *cis*-isomer of 2,4-dichloro-1,3-diaza-2,4-diphosphacyclobutane **161** as pre-organized building block (Scheme 12.60). The number of heterocyclic units in the macrocycles was determined by the nature of the spacer and the presence of templating agents. Hydrolysis of 2,4-dichloro-1,3-diaza-2,4-diphosphacyclobutane in the presence of CuCl gave complex **162** containing a tricyclic ligand [146]. The *exo*-coordination of transition metal on P-atoms is the first example which demonstrates the potential of ligands of this class. Changing the oxygen spacer to the selenium one leads to the formation of macrocycle **165** with six four-membered rings incorporated into the cyclophane framework [147]. It has been shown that tetrameric nitrogen-bridged macrocycle **163** was obtained by the

condensation of **161** and $[(NH_2)P\text{-}(m\text{-}NtBu)]_2$ in the presence of Et_3N [148]. However, the pentameric homologue **164** is produced exclusively if this reaction is undertaken in the presence of I^- ions, acting as kinetic templates [149, 150].

The planes of the P-containing rings are aligned almost exactly perpendicular to the macrocyclic plane formed by phosphorus and bridging heteroatoms. The cylindrical intramolecular cavities were formed with lone pairs of phosphorus atoms pointing out of the cavity and N–H bonds for **163–164** or lone pairs of O and Se for **162** and **165** looking into the cavity. **164** was obtained like host–guest complex with halide anion demonstrating an ability to serve for anion recognition [151]. The anion could be removed by interaction with alkali metal alcoholate and changed by neutral molecular guest (CH_2Cl_2) [152]. The cavity of **165** is large enough to include THF as a guest molecule [147].

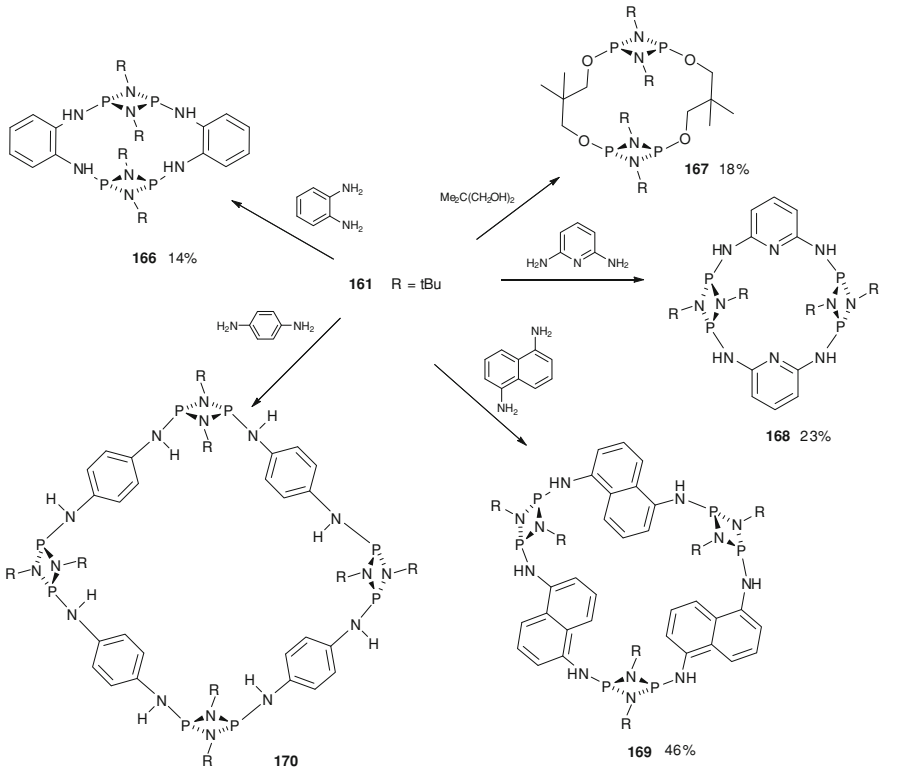
Cyclophanes **166–168** containing two 1,3-diaza-2,4-diphosphacyclobutane units were obtained by the reactions of the appropriate diols and diamines with the 1,3-di-t-butyl-2,4-dichloro-1,3-diaza-2,4-diphosphacyclobutane **161** (Scheme 12.61). P,N-heterocyclic fragments are nearly co-planar and perpendicular to the macrocyclic plane whereas arylene groups lie almost within that plane [153]. Dropwise addition of a dilute solution of **161** to a dilute solution of the 1,5-diaminonaphthalene gave **169** with three P-based units in the core cycle in 46% yield after workup. The planes of the naphthyl groups are inclined by a mean dihedral angle of ca. 35.5° with respect to the N_6 mean plane of **169**, resulting in a cone-shaped cavity that is reminiscent of coordinated and uncoordinated calixarenes. Interestingly, two toluene molecules are located within the cavities of each molecule of **169**, so that each void has two pairs of symmetry-related guests. The Me group of one of these molecules is orientated towards the centroids of each of the macrocycles, forming long-range C–H…arene contacts with the naphthylene rings [154].

The tetrameric macrocycle **170**, obtained from the reaction of **161** with p-phenylenediamine, has an unusual folded conformation in the solid state and contains a roughly tetrahedral arrangement of endo N–H groups providing the potential for tetrahedral capsulation of anionic guests [155].

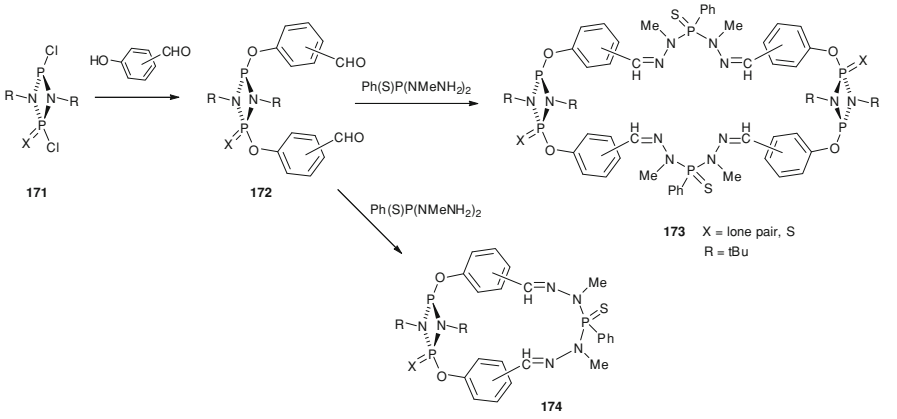
The results illustrate that the formation of discrete macrocycles depends among other factors on the steric demands and length of the organic spacer as well as the reaction conditions.

Cyclocondensation of phosphonodihydrazide $PhP(S)(NMeNH_2)_2$ with diphosphorus m,m′ or p,p′ dialdehydes **172** prepared by treatment of 1,3-di-tert-butyldiaza-2,4-dichlorodiphosphetidine **171** with 3- or 4-hydroxybenzaldehyde led to the cyclophanes **174** and **173** containing one or two heterocyclic units (Scheme 12.62) [156, 157]. It should be noticed that **174** compound is a minor product [156, 157].

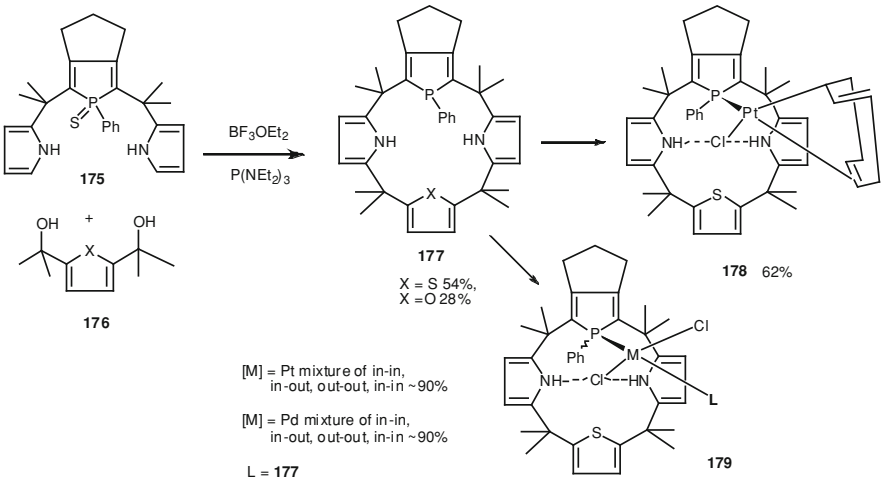
Phosphole-containing hybrid calixpyrroles were prepared by $BF_3{\cdot}OEt_2$-promoted condensation reactions of phosphatripyrranes **175** with corresponding 2,5-bis(1-hydroxy-1-methylethyl)heteroles **176** under high dilution (Scheme 12.63) [158, 159]. Both **177** were obtained in rather high yields. To prepare a phosphole-containing calixpyrrole **177**, reductive desulfurization of the intermediate was examined [158, 159]. Each of the cyclophanes provided a



Scheme 12.61 Synthesis of cyclophanes formed by 1,3-diaza-2,4-diphosphacyclobutane units **166–170**



Scheme 12.62 Synthesis of cyclophanes containing 1,3-diaza-2,4-diphosphacyclobutane units **173–174**

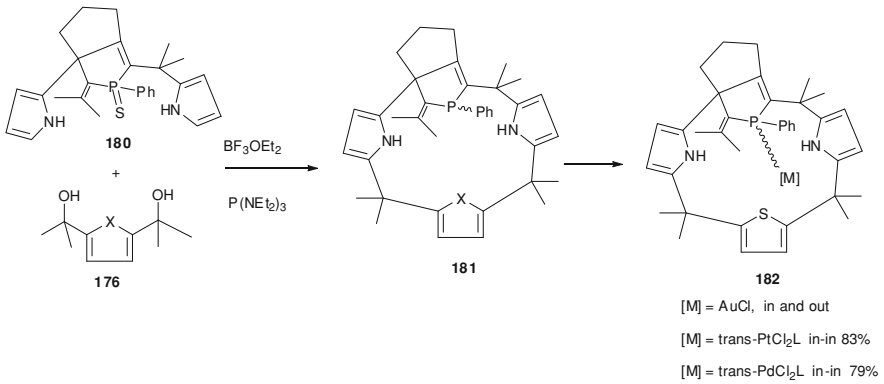


Scheme 12.63 Synthesis of phosphole-containing hybrid calixpyrroles **177** and their transition metal complexes-**178–179**

trapezoid cavity with a cone conformation and was obtained as a mixture of two conformers, with the lone pair of the phosphorus atom located inside (*in*) and outside (*out*) the cavity [159]. The complexation reactions of the two equivalents of **177** with Pt(II), and Pd(II) ions afforded both of the *in* and *out* type complexes **179**, where the *in* type complexes were the thermodynamically favored products (Scheme 12.63). In the *in-in* type complexes **179** the M–Cl fragment is bound above the cavities of the two macrocyclic ligands as though it is wrapped around. Heating of **177** with the equimolar amount of $PtCl_2$(COD) gave the Pt(II)-mono(phosphine) complex **178** in 62% yield. The COD-like group coordinates as an anionic, 1,2-η^2-6-σ-cycloocta-1,4-dienyl ligand. The direct conversion of the neutral COD ligand to the anionic, nonsubstituted cycloocta-1,4-dienyl ligand is rare for group 10 chemistry, representing the unique binding ability of the cyclophane ligand **177** [158]. In the all *in* type complexes two pyrrole rings are tilted to direct the NH protons towards the chlorine atom bound to transition metal. Thus, there is a cooperative hydrogen-bonding interaction between the M–Cl moiety and the two NH protons, which contributes to defining the coordination geometry at the metal centers in **178–179**.

Compound **180** obtained unexpectedly along with phosphatripyrranes **175** gave corresponding cyclophanes **181** with 2,3-dihydrophosphole unit (Scheme 12.64). The interconversion between the *in* and *out* type conformers of **181** was sufficiently slow to isolate each of them. In the *in-in* type Pd(II) complex **182**, two asymmetric cyclophane ligands coordinated to one palladium center have the same geometry and adopt partial cone conformations. The coordination mode of **181** is similar to those of **177** [158].

The calixphyrins **184** and **185** were prepared from phosphatripyrrane **175** and the corresponding 2,5-bis[hydroxy(aryl)methyl]heteroles **183** by addition of BF_3

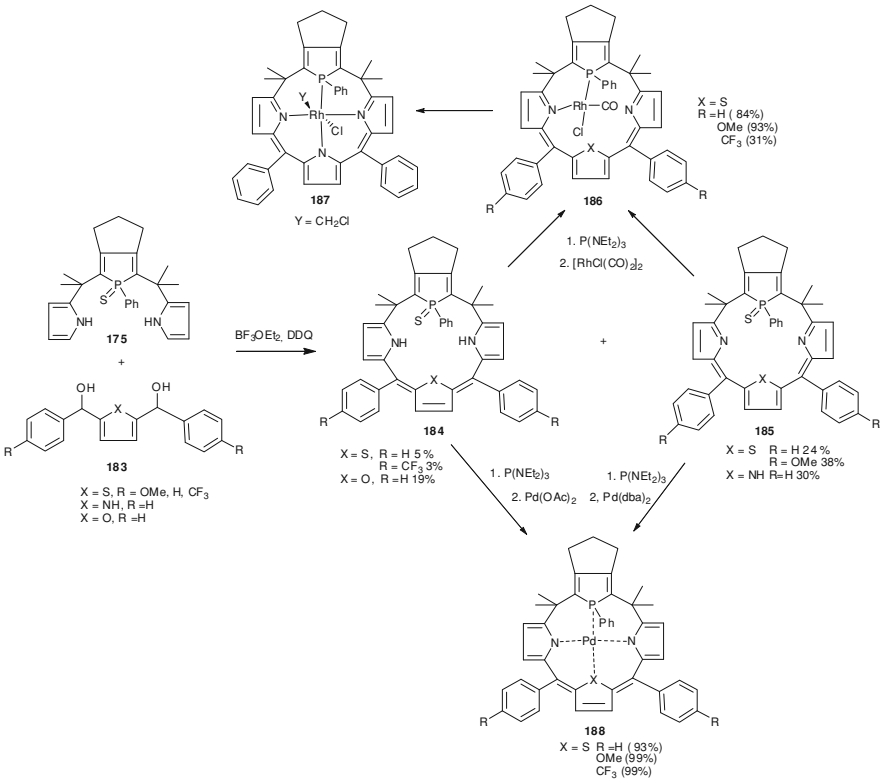


Scheme 12.64 Synthesis of cyclophanes **181** with 2,3-dihydrophosphole unit and its transition metal complexes **182**

OEt_2 to their diluted CH_2Cl_2 solution, followed by treatment with 2.2 equivalents of 2,3-dichloro-5,6-dicyanobenzoquinone (DDQ) (Scheme 12.65) [160, 161]. When treated with excess of $P(NMe_2)_3$, the cyclophanes with four-coordinated phosphorus **184**–**185** were converted to the P(III) species in high yields.

For all calixphyrins characterized by X-ray analysis, the 2e-oxidized macrocyclophane **184** (X = O, R = H) is largely twisted at the N–O–N unit with dihedral angles between the pyrrole and furan ring planes equal to 26.9–29.4°. By contrast, the 4e-oxidized cyclophanes **185** (X = S and NH, R = H) are composed of almost flat N–X–N planes (X = S, N) with small dihedral angles of 1.9–10.1° [162]. The observed conformation differs considerably from those of the 5,10-porphodimethene-type calix[4]phyrins **177**,which exhibit a nonplanar, twisted conformation. The phosphole cycle is almost orthohonal to the macrocyclic plane and the *P*-phenyl group is located outside the macrocycle, probably due to steric reasons. As a consequence, the lone pair of the phosphorus atom is oriented inside the core.

The obtained calixphyrines **184** and **185** behave as redox-active ligands giving complex **188** starting from Pd(II) and Pd(0) derivatives correspondingly in spite of the oxidation state of the initial cyclophanes [160]. On the other hand 2e-oxidized ligand **184** (X = S, R = CF_3) undergo further oxidation to the complex **186** of the corresponding 4e-ox cyclophane ligand in course of complexation with half equivalent of $[Rh(CO)_2Cl]_2$ [161]. Unlike the complexation with $Pd(DBA)_2$, the reduction of the 4e-oxidized N–S–N unit of **185** does not occur in case of Rh(I) complex formation, and the calixphyrin platform in **186** seems to behave as a neutral, bidentate P,N-ligand [162]. In sharp contrast to the previous result **185** (X = NH) showed unexpected reactivity. Upon adding CH_2Cl_2 solution of Et_3N to a mixture of **185** (X = NH) and $[RhCl(CO)_2]_2$, the oxidative addition of the solvent took place, affording the rhodium(III) complex **187** as a deep blue solid in 79% yield [162].

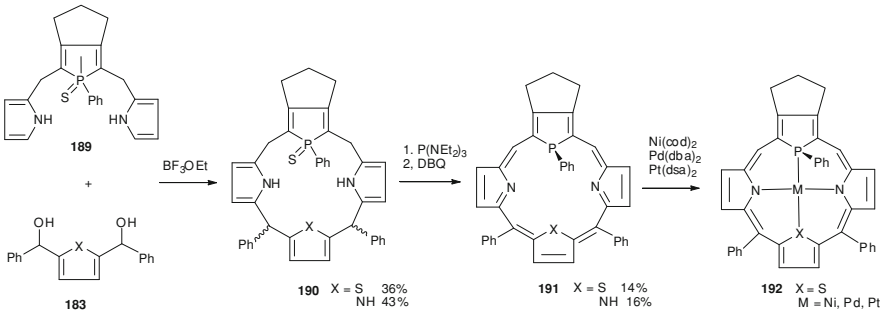


Scheme 12.65 Synthesis of calixphyrins **184** and **185** and their transition metal complexes **186–188**

It is also important to note that the hybrid calixphyrin-palladium and -rhodium complexes catalyze the Heck reaction (*p*-bromobenzaldehyde with *n*-butyl acrylate in *N*,*N*-dimethylacetamide at 100 °C) and hydrosilylations (acetophenone with Ph_2SiH_2 and of phenylacetylene with $PhMe_2SiH$), respectively, with high efficiency. The present results demonstrate the potential utility of the phosphole-containing hybrid calixphyrins as highly promising hemilabile macrocyclic ligands for the construction of efficient transition-metal catalysts [160, 162].

Phosphole-containing hybrid calixpyrroles **190** prepared by $BF_3{\cdot}OEt_2$-promoted condensation reactions of phosphatripyrranes **189** with corresponding 2,5-bis(1-hydroxy-1-methylethyl)heteroles **183** as a mixture of three diastereomers were successfully reduced to the corresponding phosphine and then oxidized by DDQ to afford the phosphorus containing core-modified porphyrins **191** (Scheme 12.66) [163, 164]. The obtained hybrid porphyrins **191** are composed of a bridged [18]annulene π-system and display high aromaticity in terms of both geometric and magnetic criteria [163, 164].

When treated with Ni(COD) (COD = 1,4-cyclooctadiene), $Pd(DBA)_2$ or $Pt(DBA)_2$ (DBA = dibenzylideneacetone) under suitable reaction conditions



Scheme 12.66 Synthesis of calixpyrroles **190** and core-modified porphyrins **191**

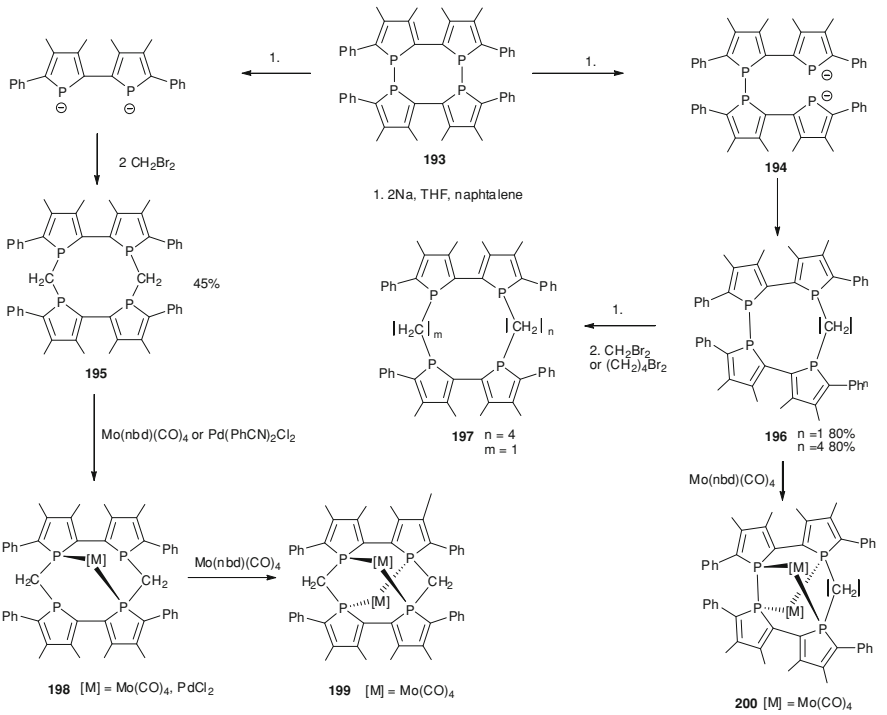
P-containing porphyrine **191** (X = S) produced isophlorin–metal complexes **192** by redox-coupled complexation. The experimental and theoretical results witness that the isophlorin complexes **192** possess nonaromaticity [165].

Phosphole tetramer **193**, obtained by the pyrolysis of 1-phenyl-3,4-dimethylphosphole, incorporates two 2,2′-biphospholyl units linked by two P–P bonds. The P–P bonds could be reductively cleaved to form dianions containing one or two (**194**) 2,2′-biphospholyl units. Alkylation of those dianions with dihaloalkanes lead to the cyclophanes **195–197** (Scheme 12.67) [166].

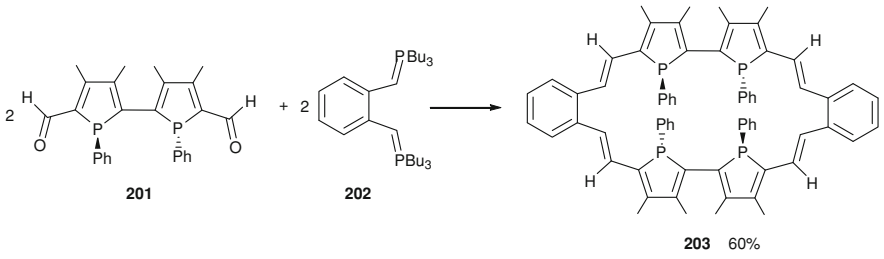
Since the phosphorus atoms of these macrocycles are all included in phosphole rings, they readily invert close to room temperature. The macrocycles **195–197** can therefore adopt their conformations to the stereochemical requirements of the complexed metals. Macrocycles **195** and **196** can chelate either one (**198**) (M = $Mo(CO)_4$ [166], $PdCl_2$ [167]) or two (**199–200**) (M = $Mo(CO)_4$ [166]) metal-containing units via their diagonal phosphorus atoms. The structure of the cage complex **200** shows a Mo–Mo distance of 5.883 Å [166]. Life-times of the palladium catalyst based on the cyclophane ligand **195** in Stille cross-coupling and Heck reactions demonstrate extraordinary resistance of the catalyst towards degradation [167].

Macrocyclic tetraphosphole **203** was obtained upon reaction of bis-aldehyde **201** with bis-ylide **202** in high yield and with high stereoselectivity perhaps due to the self-assembly processes (Scheme 12.68). The X-ray crystal structure analysis of **203** shows a distorted 24-membered macrocycle with an all-trans-disposition of the four phosphorus-phenyl substituents which provide some steric protection to the central cavity [168].

The original route to the cyclophanes **206–207** with phosphinine units incorporated into the macrocyclic framework was suggested recently and consisted of step by step substitutions of pivalonitrile from available 1,3,2-diazaphosphinine **204** by silylated diynes (Scheme 12.69). In a first step, 1 equivalent of the selected diyne is reacted with 2 equivalents of 1,3,2-diazaphosphinine **204** to afford a bis(1,2-azaphosphinine) intermediate **205** which did not need to be isolated. In the second step, which was performed under dilute conditions to minimize the



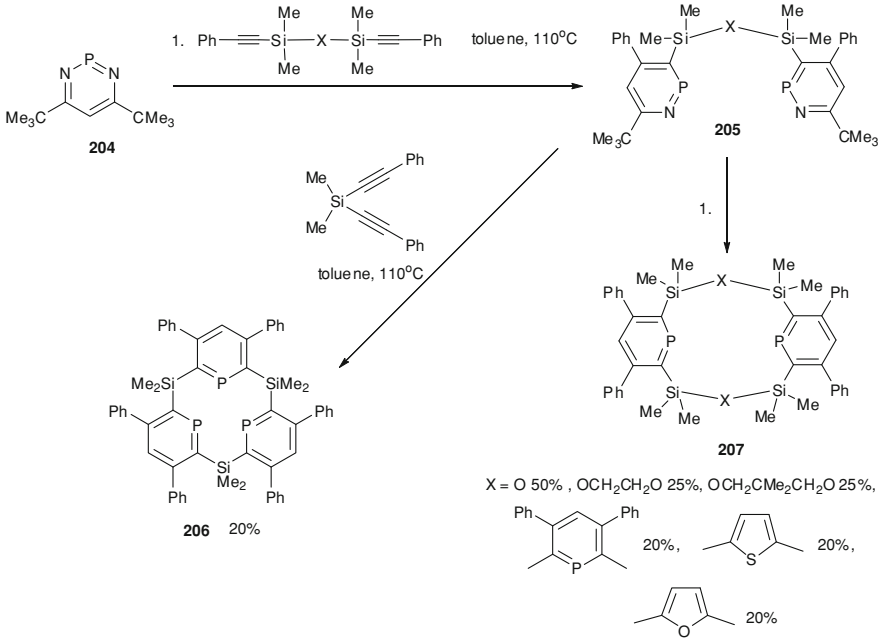
Scheme 12.67 Synthesis of phosphole based cyclophanes **193–197** and their transition metal complexes **198–200**



Scheme 12.68 Synthesis of macrocyclic tetraphosphole **203**

formation of linear oligomers, the cavity is closed by the reaction with a second equivalent of diyne [169, 170].

In the solid state, cyclophane **206** containing three phosphinine fragments adopts a partial cone-type structure. Two phosphorus-atom lone pairs point towards the top of the cavity and are located above the plane defined by three silicon atoms, the third one points below this plane [169]. Calix[4]phosphinines **207** adopt an opened-out partial cone conformation with the two opposing

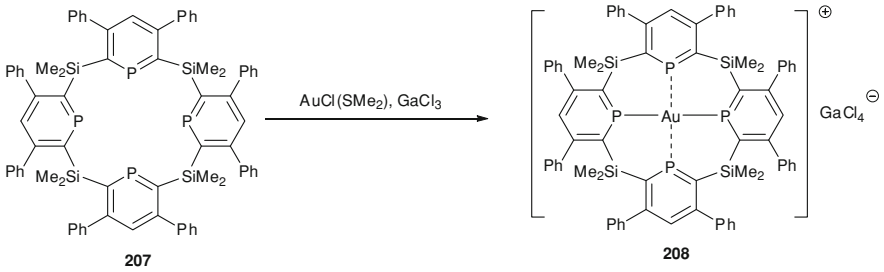


Scheme 12.69 Synthesis of cyclophanes **206–207** with phosphinine units incorporated into the macrocyclic framework

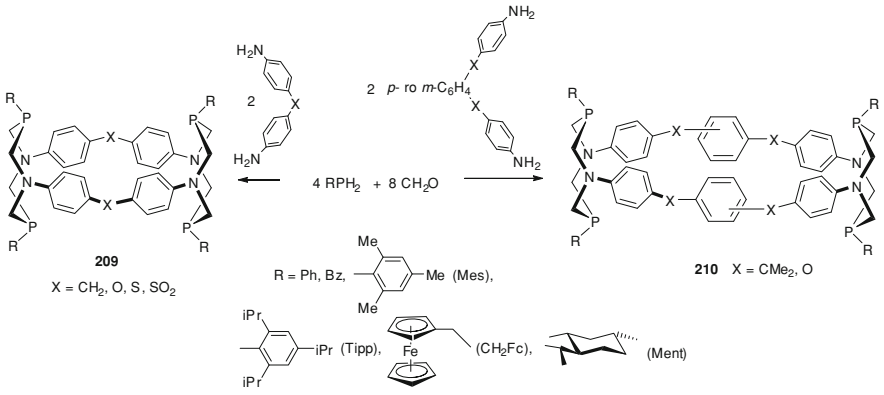
phosphinine subunits lying in two perfectly parallel planes; these planes are nearly perpendicular to the plane that bears two other heterocycles and is defined by the four silicon atoms. Interestingly, these two phosphorus atoms point in opposite directions, probably to minimize interactions with the other two lone pairs [169].

Calix[4]phosphinine **207** represent a new class of macrocycles incorporating sp^2-hybridized phosphorus atoms with unique electronic balance between *s*-donating and *p*-accepting properties. Complex **208** was prepared by allowing one equivalent of the macrocycle **207** (X = 2,4-Ph_2C_5PH-1,5) to react with [AuCl(SMe_2)], followed by treatment with $GaCl_3$ as chloride abstractor (Scheme 12.70) [171]. The four phosphorus atoms lie in the same plane, but only two subunits are bound to the Au(I) center, the two other showing only very weak interactions. The electrochemical reduction of complex **208** proceeds as a quasi-reversible process indicating the formation of the rare Au(0) complex [171]. The lower reduction potential recorded for complex **208** is in full agreement with the strong *p*-acceptor character of the macrocyclic phosphinines [172].

The Mannich-type condensation of various primary phosphines with formaldehyde and primary aromatic diamines with spatially divided amine groups allowed to obtain several types of cage P,N-containing cyclophanes **209–210** with two 1,5-diaza-3,7-diphosphacyclooctane fragments in the basic framework (Scheme 12.71) [173–179]. The spacers of the starting diamines were formed by



Scheme 12.70 Gold complex **208** of calix[4]phosphinines **207**

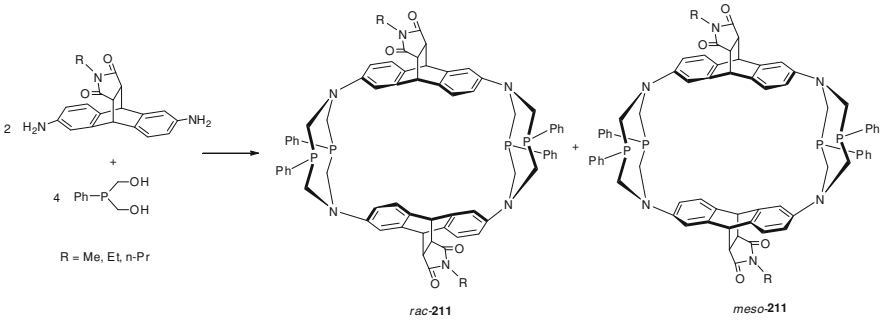


Scheme 12.71 Covalent self-assembly of cyclophanes **209**–**210** with two 1,5-diaza-3,7-diphosphacyclooctane fragments in the basic framework

two or three phenylene fragments linked by one-atom bridges. These structures of diamines appeared to be favorable for the covalent self-assembly of cage macrocyclic tetraphosphines due to the spatial complementarity of the building blocks forming macrocycles and the possibility of the formation of planar conjugated systems with the participation of nitrogen atoms included into the eight-membered heterocyclic fragment of the target cyclophane [175, 176].

The condensations were performed in hot DMF (110 °C) or toluene (100 °C) at the phosphine concentrations of 0.1–0.3 M and led to the cage P,N-containing cyclophanes **1**–**15** in good or satisfactory yields [173–179]. It indicated that the covalent self-assembly took place and this conclusion was confirmed by the NMR monitoring of the reactions which showed that they proceeded through the formation of series of intermediates and the reaction mixtures were enriched by the macrocycles only at the final steps [175].

2,6-Diamino-9,10-dihydro-9,10-ethanoanthracenes also satisfied the complementarity principle. These diamines had the total chirality so their racemates reacted with bis(hydroxymethyl)phenylphosphine under the analogous conditions

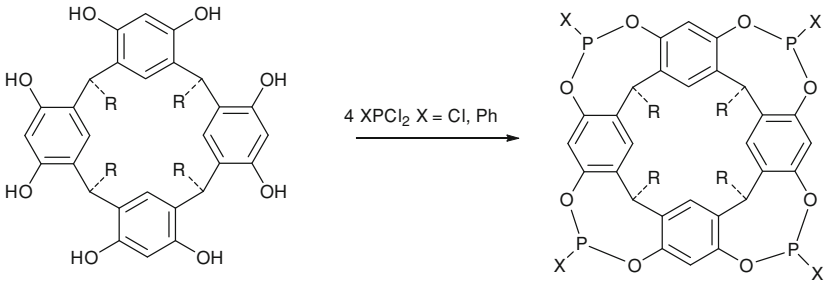


Scheme 12.72 Covalent self-assembly of cyclophanes **211** with chiral intramolecular cavity

to give the corresponding cyclophanes **211** as the mixtures of two regioisomers [180].

The less soluble isomers *rac*-**211** of all cyclophanes **211** were isolated as individual compounds. The macrocycle *rac*-**211** (R = Me) appeared to be a racemic isomer formed by the same enantiomers of the starting diamine according to X-ray analysis data. More soluble isomers of **211** are *meso*-isomers formed by the opposite enantiomers of the diamines [180].

The structures of cyclophanes **209**–**211** are mainly determined by the nature of the diamine spacers. Their 1,5-diaza-3,7-diphosphacyclooctane fragments have chair–chair conformations with phosphorus LP's directed inward the macrocyclic cavities both in the solid state and in solutions [173–181]. The total conformations of the cyclophanes may be described as near cylindrical for 28-membered macrocycles **209** [173–175, 180], elongated cylindrical for 36-membered ones **210** (*meta*-, X = O) [176] and helically twisted for 38-membered macrocycle **210** (*para*-, X = CMe_2) [179, 182]. All cyclophanes have large hydrophobic intramolecular cavities with free volumes from 100–120 to about 200 $Å^3$. In the solid state the intramolecular cavities of 28- and 36- membered macrocycles enclose the methyl groups of the solvent (DMF, DMA or DMSO). The location of these groups indicates the existence of the binding H-π-interactions between their protons and phenylene fragments of the macrocycles [173–176, 180, 181]. The ability of this class of macrocycles to increase noticeably the square bounded by the upper rim if it is necessary for the penetration of the relatively large molecules had been demonstrated [181]. 38-membered macrocycle **210** (*para*-, X = CMe_2, R = C_6H_2-(Pr-i)$_3$-2,4,6) encapsulates one of the solvate benzene molecules inside the macrocyclic cavity demonstrating the ability of new P,N-containing cyclophanes to bind aromatic hydrocarbon guests [179]. The benzene molecule is isolated from the environment due to the helical conformation of the macromolecule and the presence of bulky substituents on the phosphorus atoms and conformational changes of the macrocycle are necessary for the guest to leave the cavity. NMR investigations of **210** (*para*-, X = CMe_2) indicate that the supramolecular host–guest organization with the aromatic compound located in the macrocyclic cavity is retained in aromatic solvents [179, 182].



212 R=Me, CH_2CH_2Ph **213** (X=Cl, Ph)

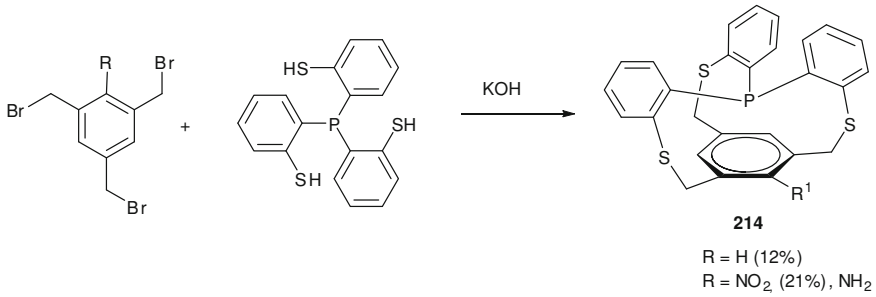
Scheme 12.73 Synthesis of cyclophanes **213** with with eight-membered P-containing rings incorporated into the cyclophane framework

Calixresorcinarene **212** (R = CH_2CH_2Ph) reacts with dichlorophenylphosphine in presence of pyridine to give **213** (R = CH_2CH_2Ph, X = Ph) [183] with eight-membered P-containing rings incorporated into the cyclophane framework (Scheme 12.73). The diastereomer with all phenyl groups on phosphorus atoms directed outwards and lone pairs directed inwards was preferred [183, 184]. The compounds **213** (R = Me, X = Cl) had been also isolated [185] as well as the products of their interaction with MeMgBr, Me_3SiNMe_2 and $HNMe_2$).

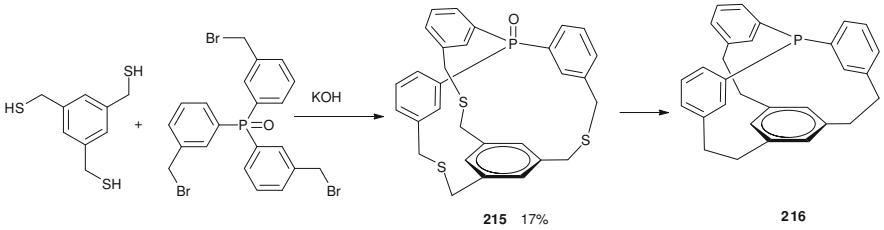
12.4 P-Containing Cryptands

Macrobicyclic and other cage compounds play an important role in supramolecular chemistry [1–11]. They are used for the complexation of cations and anions and also for the molecular recognition of neutral substrates. The synthesis, structure, and properties of numerous macrobicyclic cages have been intensively studied during the past few decades. In fact, several synthetic strategies may be devised for the construction of such molecular architectures. The more direct one is the tripod–tripod coupling, a molecular self-assembly process that implies the formation of three bonds in a single step [186]. A reaction of this type requires complementary components containing two or more interaction sites capable of establishing multiple connections, and the reversibility of the connecting events in order to allow the full exploration of the energy hypersurface of the system [187–189]. A major drawback of tripod–tripod coupling is the occurrence of extensive side reactions, which minimize the yield of the expected bicyclic product. Only in limited cases [190–200], such processes have been carried out in synthetically useful yields, provided that fine tuning of reagents, reactions, and conditions could be achieved.

Phosphorus-containing macrobicyclic compounds, however, have been investigated much less. The P-containing bimacrocycle and cryptand ligands are very



Scheme 12.74 Synthesis under high-dilution conditions of cryptand **214**



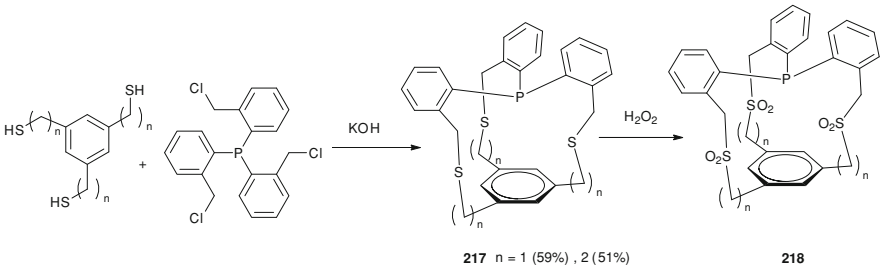
Scheme 12.75 Synthesis under high-dilution conditions of P,S-containing cryptand **215**

narrow and specific area of phosphorus chemistry exemplified by just few structural types.

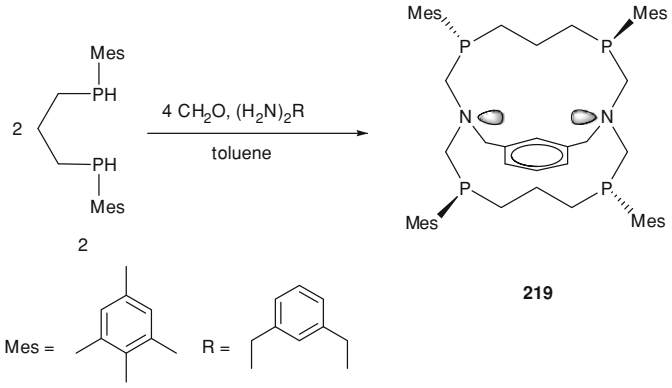
Cryptands **214** (R = H) were prepared from tris(2-mercaptophenyl)phosphine by the base-promoted condensation with 1,3,5-tris(bromomethyl)benzenes under conditions of high dilution (2.8 mM) in refluxing 2:1 benzene-ethanol with 12% yield (Scheme 12.74). Due to a strong preference for an *in*-geometry (pyramidalization of the phosphine toward the basal ring) and the consequent steric shielding, the phosphine of **214** (R = H) was quite unreactive: it was not protonated by anhydrous HBr, and even when **214** (R = H) was heated in refluxing hydrogen peroxide and acetic acid, the corresponding trisulfone was obtained without formation of the phosphine oxide [201, 202]. The presence of acceptor (NO_2) or donor (NH_2) groups in the basal ring does not change the properties of the cryptands significantly [203].

High-dilution coupling of 1,3,5-tris(mercaptomethyl)benzene with tris((3-bromomethyl)phenyl)phosphine oxide afforded the phosphathiacyclane **215** in 17% yield (Scheme 12.75). **215** was converted into the C_3-symmetric monophosphine 17-phospha[2.2.2](1,3,5)-benzeno(3,3′,3″)triphenylmethanophane **216** in three steps. In contrast with phosphathiacyclanes **214**, the isomer with an "out" orientation of the phosphorus LP was the predominant one [204].

Tris[2-(chloromethyl)phenyl]phosphine and 1,3,5-tris(mercaptomethyl or ethyl)benzenes were condensed, under conditions of high dilution (1.1 mM for each component) in 2:1 benzene–ethanol with KOH as the base, to give the



Scheme 12.76 High dilution synthesis of P,S-containing cyclophanes **217**

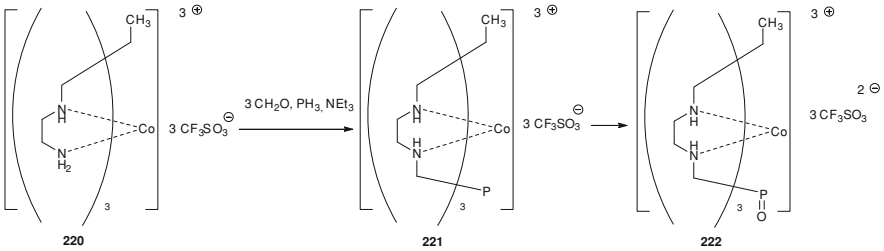


Scheme 12.77 Covalent self-assembly of P,N-containing cryptand **219**

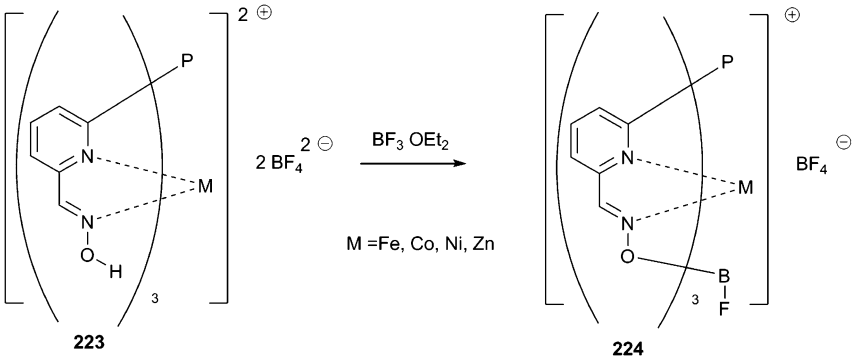
in-phosphines **217** in 59 and 51% yields, respectively (Scheme 12.76). The phosphines were very resistant to the oxidation, and even prolonged treatment with hydrogen peroxide in acetic acid at reflux returned only the trisulfones **218** in excellent yields [205, 206].

The *in*-geometry of the highly crystalline **217** was unambiguously established by X-ray analysis [205]. When the *in*-isomer **217** ($n = 1$) was heated at temperatures great enough to invert the triarylphosphine, the corresponding *out*-isomer was not observed, but this isomer was trapped by heating with sulfur to give an *out*-phosphine sulfide. The sulfurization of **217** ($n = 1$) is 10,000 times slower than the corresponding sulfuration of triphenylphosphine, and the rate-determining step for the former reaction appears to be the phosphine inversion. The desulfurization with hexachlorodisilane at room temperature smoothly returned the *in*-cyclophane **217** ($n = 1$), with no *out*-intermediate detected [206].

The Mannich-type condensation with the participation of two bifunctional reagents, namely1,3-bis(mesitylphosphino)propane and m-xylylenediamine, led to the first representative of unique P,N-containing cryptand **219** (Scheme 12.77) [207]. The cryptand **219** was formed stereoselectively as a single *RRRR/SSSS* diastereomer. The lone electron pairs of the phosphorus atoms have axial



Scheme 12.78 Template synthesis of P,N-containing cryptand **221**



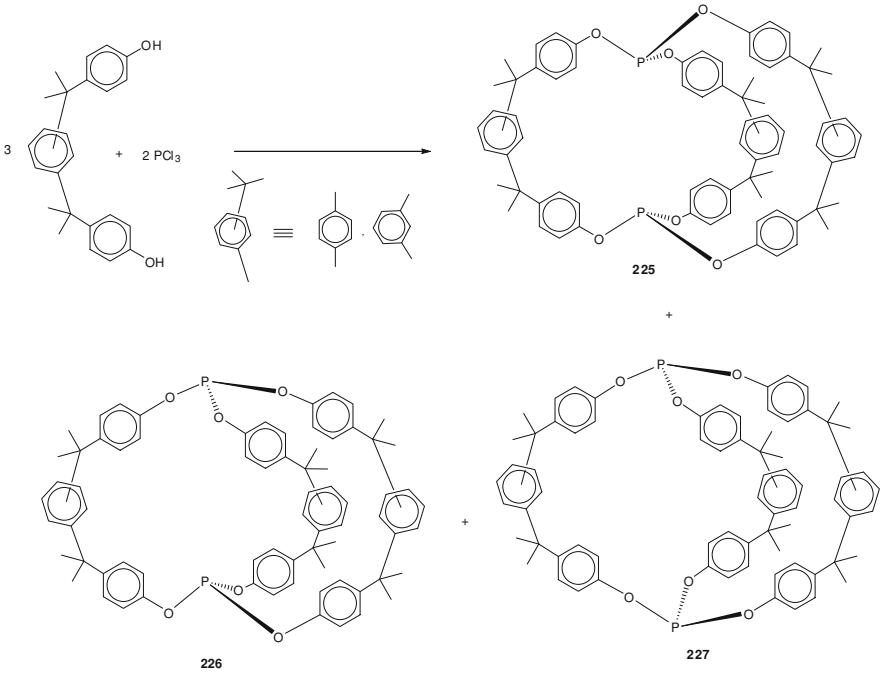
Scheme 12.79 Template synthesis of P,N,O,B-containing cryptand **224**

orientation relative to 16-membered ring and their directions alternate, whereas the lone electron pairs of nitrogen atoms are directed into the cavity [207]. These results show the efficiency of the covalent self-assembly approach for the synthesis of P,N-containing corands and cryptands.

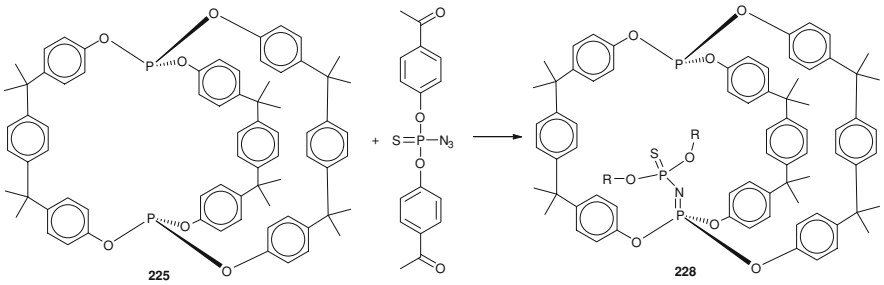
Mannich-type condensation of 4,4′,4″-ethylidyne-tris(3-azabutane-l-amine) complex **220** with excess of paraformaldehyde, phosphine, and triethylamine gave cryptand **221** with an encapsulated cobalt ion (Scheme 12.78). The phosphine was partly oxidized in the course of reaction and structure of corresponding oxide **222** was established by X-ray analysis [208].

The boron-containing clathrochelate **224** was obtained by the interaction of metal-containing phosphines **223** with boron trifluoride etherate (Scheme 12.79) [209].

A multi-step one-pot reaction of spatially divided bisphenols with PCl_3 lead to the phosphorus containing *in,in*-**225**, *in,out*-**226** and *out,out*-cryptand **227** (Scheme 12.80) [210, 211]. In spite of relatively low yields (not exceeding 7%) cryptands **225–227** (*in,in- meta* and *para, in,out –meta* and *para, out,out –meta* and *para*) were isolated in pure state and their structures were established in solid state and solutions [210, 211]. Increasing the bisphenol curvature from the *para*- to the *meta*-central phenylene unit leads to a dramatic change in the P–P distances



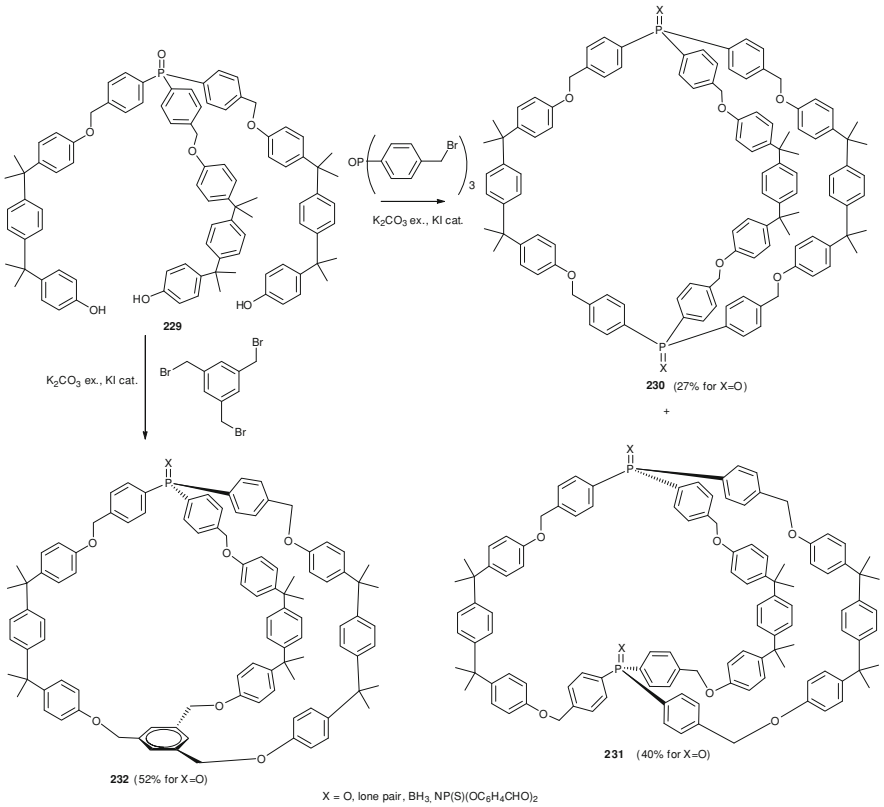
Scheme 12.80 Covalent self-assembly of P,O-cryptands **225**–**227**



Scheme 12.81 Staudinger reaction of *in,in*-cryptand **225** with thiophosphorylazide

(from 8.3–10.5 to 4.5–5.3 Å) and in cavity volumes. Phosporus atoms in the *in*-position have a decreased reactivity, e.g. they are more slowly oxidized by cumene hydroperoxide than *out*-P atoms [210].

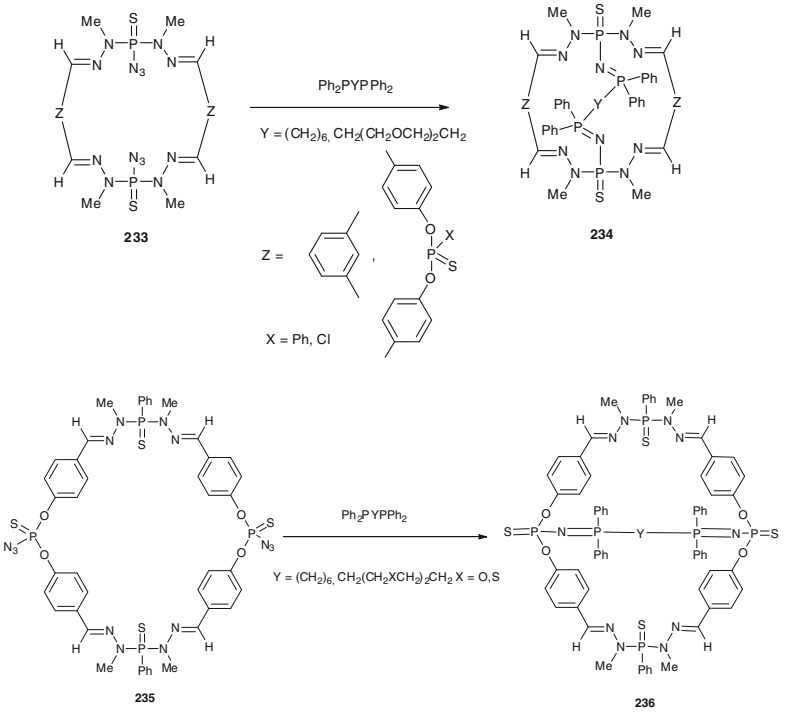
Reaction of *in,in*-**225** with thiophosphoryl azide affords *in,in*-phosphite-imidophosphate **228** as a main product (52%) (Scheme 12.81). Compound **228** is the first example of the modification of in-bridgehead positions in macrobicyclic compounds with groups larger than methyl. The benzaldehyde arms of the in-substituent in **228** jut out of the cage bars. The benzaldehyde arms can move



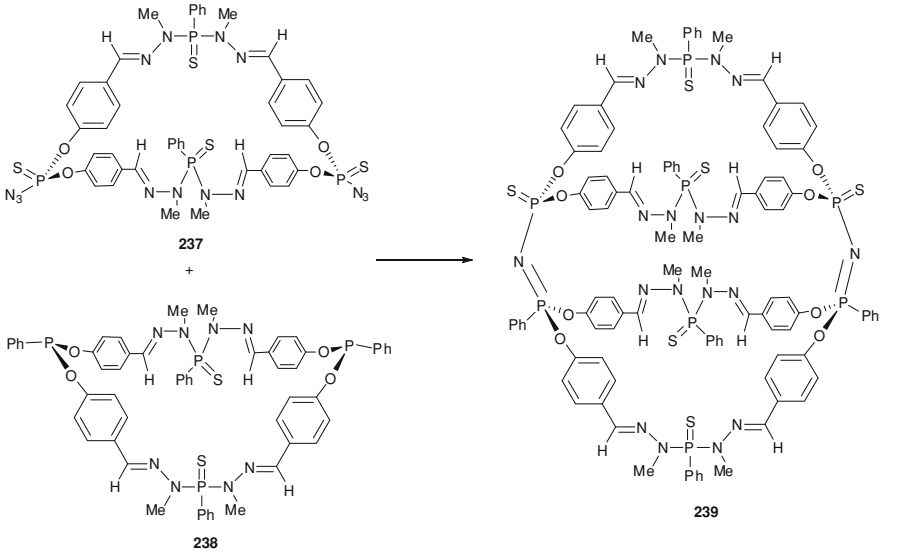
Scheme 12.82 Synthesis under high-dilution conditions of the macrobicyclic products **230–232** by a tripod-coupling reaction of preorganized trisphenol **229**

between the gaps of the cage. This provides access to specific modification of the cavity of macrobicyclic compounds in order to adopt macrobicyclic hosts to special substrates for molecular recognition or to design novel ligands for metalcatalyzed reactions with a defined microenvironment [13, 212].

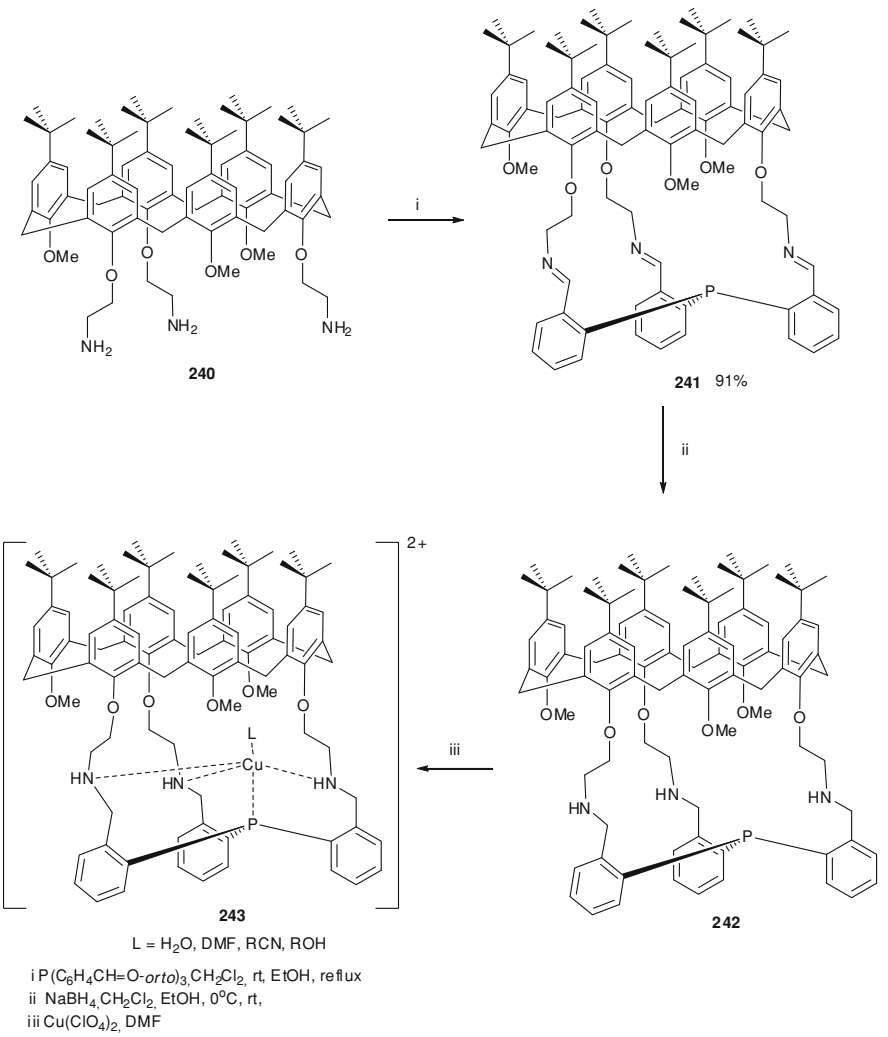
The synthesis of the macrobicyclic products **230–232** (X = O) were accomplished by a tripod-coupling reaction of preorganized trisphenol **229** and corresponding tribromides under dilute conditions (Scheme 12.82). The phosphine oxides **230–232** (X = O) were formed in a comparatively high yields of 27–52% [212, 213]. The crystal structure of **232** showed a huge hole and a distance between the bridgehead fragments of about 11 Å. Obtained cryptand phosphine oxides were effectively reduced with the retention of configuration using trichlorosilane and triethylamine. Corresponding phosphines **230–232** (X = lone pair) were stabilized by formation of borane complexes **230–232** (X = BH_3) [213] and underwent a Staudinger reaction [13] to give *in,in*- and *in,out*-isomers of bisiminophosphoranes.



Scheme 12.83 Staudinger reactions of phosphorhydrazide-based macrocycles **233** and **235**



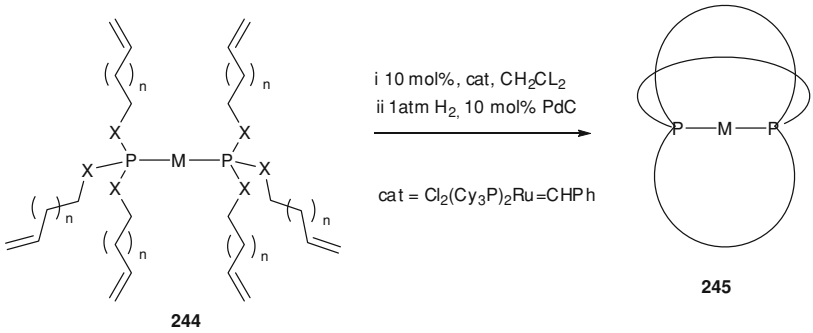
Scheme 12.84 Synthesis of **239**



Scheme 12.85 Synthesis of PN_3-calix[6]cryptands **241**–**242** and copper complexes **243**

Staudinger reactions of phosphorhydrazide-based macrocycles **233** and **235** with azido functions on phosphorus atoms available via well-known Schiff reactions applied to the corresponding phosphohydrazides, with α,ω-diphosphinoalkanes ($Ph_2P(CH_2)_2T(CH_2)_2T(CH_2)_2PPh_2$ (T = O, S) or $Ph_2P(CH_2)_6PPh_2$) give rise to the tetraphosphorus cryptand **234** (Z = *meta*-C_6H_4) or hexaphosphorus cryptands **234** (Z = P(S)PX-(OC_6H_4-)$_2$, X = Ph, Cl) and **236** (Scheme 12.83) [214].

The tetraphosphorus macrocycle **238** possessing two tricoordinated phosphorus atoms reacts with **237** in similar way producing very original tris-macrocyclic cryptand **239** (Scheme 12.84) [214].



Scheme 12.86 Synthesis of "gyroscope-like" cryptands **245** via alkene metathesis/hydrogenation reaction sequences

A C3v-symmetrical PN_3-calix[6]cryptand **241** was prepared from **240** with triphenylphosphine bearing aldehyde substituents in the ortho position of the phenyl rings and was isolated in high yield (91%). Among the many different tested tripodal aldehydes, only the triphenylphosphine derivative perfectly fits from a geometrical point of view with the calixarene structure and displayed such a remarkable reactivity with calix[6]triamine **240**. Cryptand **242** was obtained by adding, dropwise at low temperature, trisimine **241** to a large excess of $NaBH_4$ in ethanol (Scheme 12.85). The P,N-cap rigidifies the calixarene core in a cone conformation, thereby offering a well-defined hydrophobic cavity open at the large rim. Host **242** was shown to strongly bind ammonium guests with a 16-fold selectivity in favor of ethylammonium over propylammonium [215]. Cu(II) complexes **243** were readily obtained upon stoichiometric reaction of copper(II) perchlorate with the ligand **242**. The aqua complex **243** (L = H_2O) was isolated as an air stable blue-green complex. In strong contrast to known Cu(II) phosphine complexes, **243** was very stable in solution and no phosphine oxidation has been observed. The water ligand was easily substituted for a variety of guests such as nitriles, amides, and alcohols. X-ray analysis of **243** (L = DMF), showed a 5-coordinate Cu(II) center with all donors of the PN_3 cap strongly bound and the DMF ligand situated in the heart of the calixarene cavity [216, 217].

Unique "gyroscope-like" [218] cryptands **245** were obtained via alkene metathesis/hydrogenation reaction sequences applied to the trans tris(ω-alkylene) phosphine [219–221] or –phosphite [222] ligands coordinated to the trigonal bipyramidal (M = $Fe(CO)_3$ [219, 222]), square planar (RhCl(CO), $PtHal_2$, $PtPh_2$, $PdHal_2$ [220]), and octahedral ($Re(CO)_3Hal$ [221]) metal matrix (Scheme 12.86). The approach appeared to be very effective especially in the case of trigonal

bipyramidal central ions (total yields ~60%) due to the right preorganization of reacting groups in the predominant conformation [219, 222].

12.5 Concluding Remarks

The development of the synthetic chemistry of macrocyclic P(III)-based ligands is directly connected with the development of coordination and supramolecular chemistry and catalysis.

During last decade the methods for the preparation of macrocyclic compounds have developed in the direction of more mild and sophisticated approaches combining the best ideas from soft templating and self-assembly. As a result, a number of unique P-containing macrocycles, especially phosphacyclophanes and cryptands have been obtained in reasonable to high yields and in unpredicted stereoselectivities. The progress in the synthetic access has helped to stimulate further development of applications. To our mind the most interesting and promising application of P-based macrocycles will be creation of new generation of catalysts for non-traditional organic or even inorganic processes (e.g. activation of small stable molecules—N_2, H_2, P_4) and molecular devices based on specific reactivity of phosphorus incorporated into macrocycles.

The chemistry of phosphorus-containing macrocycles is one of the fastest developing areas of P-chemistry. The most promising compounds have been synthesized within the last two decades and applications of these classes of compounds are presently under intensive investigation.

References

1. Pedersen CJ (1987) The discovery of crown ethers. Noble Lecture 497–511
2. Cram DJ (1987) The design of molecular hosts, guests, and their complexes. Noble Lecture 419–437
3. Lehn J-M (1987) Supramolecular chemistry—scope and perspectives molecules, supermolecules, molecular devices. Noble Lecture 444–491
4. Lehn J-M (1988) Supramolecular chemistry–scope and perspectives molecules, supermolecules molecular devices. (Noble lecture) Angew Chem Int Ed 27:89–112
5. Steed JW, Atwood JL (2000) Supramolecular chemistry. Wiley, Chichester
6. Gloe K (2005) Macrocyclic chemistry. Springer, Dordrecht
7. Chapman RG, Sherman JC (1997) Templation and encapsulation in supramolecular chemistry. Tetrahedron 53:15911–15945
8. Haino T, Yanase M, Fukunaga C, Fukazawa Y (2006) Fullerene encapsulation with calix[5]arenes. Tetrahedron 62:2025–2035
9. Rao CNR, Muller A, Cheetham AK (2007) Nanomaterials chemistry: recent developments and new directions. Wiley-VCH, Weinheim
10. Steed JW, Turner DR, Wallace KJ (2007) Core concepts in supramolecular chemistry and nanochemistry. Wiley-VCH, Weinhein
11. Stoddart JF, Colquhoun HM (2008) Big and little Meccano. Tetrahedron 64:8231–8263

12. Edwards PG, Ingold F, Liyanage SS, Newman PD, Wong W-K, ChenPendant Y (2001) Functionalised triphosphamacrocycles. Eur J Inorg Chem 2865
13. Bauer I, Gruner M, Goutal S, Habicher WD (2004) Staudinger reaction at in-bridgehead positions of phosphorus macrobicyclic compounds. Chem Eur J 10:4011
14. Philp D, Stoddart JF (1996) Self-assembly in natural and unnatural systems. Angew Chem Int Ed Engl 35:1154–1196
15. Greig LM, Philp D (2001) Chem Soc Rev 30:287
16. Leininger S, Olenyuk B, Stang PG (2000) Self-assembly of discrete cyclic nanostructures mediated by transition metals. Chem Rev 100:853–908
17. Swiegers G, Malefetse T (2002) Self-assembled nanoreactors. Coord Chem Rev 225:91–121
18. Caminade A-M, Majoral JP (1994) Synthesis of phosphorus-containing macrocycles and cryptands. Chem Rev 94:1183–1213
19. Caminade A-M, Majoral JP (1996) Phosphorhydrazide macrocycles and cryptands. Synlett 1019–1028
20. Pabel M, Wild B (1996) Rings containing phosphorus. In: Comp Hetecycl Chem II: 947–969
21. Pabel M, Wild SB (2001) Macro- and spiro-heterocycles. In: Mathey F (ed) Phosphorus-carbon heterocyclic chem: the rise of a new domain. Pergamon, Amsterdam
22. Bauer I, Habicher WD, Antipin IS et al (2004) Phosphorus macrocycles and cryptands. Russ Chem Bull 53:1402–1416
23. Edwards PG, Haigh R, Li D, Newman PD (2006) Template synthesis of 1,4,7-triphosphacyclononanes. J Am Chem Soc 128:3818–3830
24. Edwards PG, Whatton ML, Haigh R (2000) A new nine-membered triphosphorus macrocycle. Organometallics 19:2652–2654
25. Edwards PG, Whatton ML (2006) Template synthesis of 9-membered triphospha-macrocycles with rigid o-phenylene backbone functions. Dalton Trans 442–450
26. Albers T, Edwards PG (2007) Template synthesis of benzannulated triphosphacyclononanes—a new class of phosphacrowns via template assisted nucleophilic P–C bond formation. Chem Commun 858–860
27. Battle AR, Edwards PG, Haigh R et al (2007) Synthesis and characterization of Iron(II) complexes of 10- and 11-membered triphosphamacrocycles. Organometallics 26:377–386
28. Kyba EP, Hudson CW, McPhaul MJ et al (1977) Polyphosphino macrocyclic ligand systems. J Am Chem Soc 99:8053–8054
29. Kyba EP, John AM, Brown SB et al (1980) Triligating 11-membered rings containing tert-phosphino sites. Synthesis and structure. J Am Chem Soc 102:139
30. Kyba EP, Davis RE, Liu ST et al (1985) Structural characterization of tridentate 11-membered phosphino macrocyclic complexes of transition metals. Examples of octahedral, square-pyramidal and tetrahedral geometries. Inorg Chem 24:4629–4634
31. Kyba EP, Liu ST (1985) Phosphino macrocycles. 140. Synthesis of unusual phosphine ligands. Use of the 1-naphthylmethyl moiety as a P–H protecting group in the synthesis of a phosphino macrocycle that contains a secondary-phosphino ligating site. Inorg Chem 24:1613–1616
32. Diel BN, Brandt PF, Haltiwanger RC et al (1982) Metal-templated synthesis of a macrocyclic triphosphine-molybdenum complex, *fac*-$(CO)_3Mo(PHC_3H_6)_3$. J Am Chem Soc 104:4700–4701
33. Edwards PG, Fleming JS, Liyanage SS et al (1996) Primary alkenyl phosphine complexes of chromium and molybdenum; synthesis and characterisation of tricarbonyl(1,5,9-triphosphacyclododecane)chromium(0). J Chem Soc Dalton Trans 1801–1807
34. Coles SJ, Edwards PG, Fleming JS et al (1995) 1,5,9-Triphosphacyclododecane complexes of molybdenum and tungsten. Crystal structure of tricarbonyl[1,5,9-tris(isopropyl)-1,5,9-triphosphacyclododecane]-molybdenum(0). J Chem Soc Dalton Trans 1139–1145

35. Edwards PG, Fleming JS, Liyanage SS (1997) Chromium and molybdenum complexes of tertiary alkyl and pendant donor triphosphamacrocycles. J Chem Soc Dalton Trans 193–197
36. Coles SJ, Edwards PG, Fleming JS et al (1996) The liberation, characterisation and X-ray crystal structure of 1,5,9-triphospha-1,5,9-tris(2-propyl)cyclododecane. Chem Commun 293–294
37. Jones DJ, Edwards PG, Tooze RP et al (1999) The template synthesis of triaryl functionalised 1,5,9-triphosphacyclododecane on molybdenum using organocopper reagents. J Chem Soc Dalton Trans 1045–1046
38. Coles SJ, Edwards PG, Fleming JS et al (1995) Triphosphorus macrocycle complexes of divalent group 6 transition metals. Crystal structure of bromotricarbonyl-[1,5,9-tris(isopropyl)-1,5,9-triphosphacyclododecane]-molybdenum(II) tetraphenylborate. J Chem Soc Dalton Trans 4091–4097
39. Price AJ, Edwards PG (2000) A new template for the synthesis of triphosphorus macrocycles. Chem Commun 899–900
40. Edwards PG, Abdul Malik KM, Ooi L et al (2006) Iron complexes of facially capping triphosphorus macrocycles. Dalton Trans 433–441
41. Bayler A, Canty AJ, Edwards PG et al (2000) Trimethyl-palladium(IV) and -platinum(IV) complexes containing phosphine donor ligands, including studies of 1,5,9-triethyl-1,5,9-triphosphacyclodecane and X-ray structural studies of palladium(II) and palladium(IV) complexes. J Chem Soc Dalton Trans 3325–3330
42. Baker RJ, Edwards PG, Farley RD et al (2003) Low valent carbonylvanadium complexes of the triphosphorus macrocycle 12[ane]P_3Et_3. DaltonTrans 944–948
43. Baker RJ, Davies PC, Edwards PG et al (2002) Early transition metal complexes of triphosphorus macrocycles. Eur J Inorg Chem 1975–1984
44. Baker RJ, Edwards PG (2002) Transition metal complexes of triphosphorus macrocycles: a new class of homogeneous olefin polymerisation catalysts. J Chem Soc Dalton Trans: 2960–2965
45. Baker RJ, Edwards PG, Gracia-Mora J et al (2002) Manganese and rhenium triphosphorus macrocycle complexes and reactions with alkenes. J Chem Soc Dalton Trans 3985–3992
46. Scott LT, Unno M (1990) Novel heterocycles comprising alternating phosphorus atoms and alkyne units. J Am Chem Soc 112:7823–7825
47. Kyba EP, Davis RE, Hudson CW et al (1981) Tetradentate 14-membered tert-phosphino-containing macrocycles. J Am Chem Soc 103:3868–3875
48. Bartsch R, Hietkamp S, Morton S et al (1983) Reactions of coordinated ligands. 12. Single-stage template syntheses of tetradentate macrocyclic phosphine complexes. Inorg Chem 22:3624–3632
49. Bartsch R, Hietkamp S, Peters H et al (1984) Reactions of coordinated ligands. 13. Template syntheses of 14- to 16-membered tetraphosphacycloalkanes using bis(tertiary phosphines) with protected carbonyl groups in the alkyl side chains. Inorg Chem 23:3304–3309
50. Diel BN, Brandt PF, Haltiwanger RC et al (1989) Metal-templated synthesis of macrocyclic (triphosphine)molybdenum complexes. Inorg Chem 28:2811–2816
51. DelDonno TA, Rosen W (1977) Preparation of a tetraphosphine macrocyclic ligand. J Am Chem Soc 99:8051–8052
52. DelDonno TA, Rosen W (1978) Studies of a 15-membered tetraphosphorus macrocyclic ligand. Inorg Chem 17:3714–3716
53. Toulhoat C, Vidal M, Vincens M (1993) Polyoxydes de polyphosphines bicycliques alkyles sur le phosphore. Phosphorus Sulfur Silicon 78:119–132
54. Vincens M, Gong-Cheng F, Toulhoat C et al (1988) Synthese de nouveaux oxydes de tetraphosphines macrocycliques. Tetrahedron Lett 29:6247–6248
55. Li GQ, Govind R (1995) Synthesis and characterization of a tetraphosphine macrocyclic ligand and its manganese(II) complexes. Inorg Chim Acta 231:225–228

56. Bauer EB, Ruwwe J, Martín-Alvarez JM et al (2000) Olefin metatheses in metal coordination spheres: novel trans-spanning bidentate and facially-spanning tridentate macrocyclic phosphine complexes. Chem Commun 2261–2262
57. Harnisch JA, Angelici RJ (2000) Gold and platinum benzenehexathiolate complexes as large templates for the synthesis of 12-coordinate polyphosphine macrocycles. Inorg Chim Acta 300–302:273–279
58. Smith RJ, Powell AK, Barnard N et al (1993) Copper and nickel complexes of the new phosphadithiamacrocycle 1-phenyl-1-phospha-4,7-dithiacyclononane. J Chem Soc Chem Commun 54–56
59. Blower PJ, Chadwick AV, Jeffery JC et al (1999) Synthesis and coordination chemistry of 1-phenyl-1-phospha-4,7-dithiacyclononane. Inorg Chim Acta 294:170–178
60. Blower PJ, Jeffery JC, Miller JR et al (1997) Template synthesis and reactions of tricarbonylmolybdenum phosphadithiamacrocyle complexes. Inorg Chem 36:1578–1582
61. Sowrey FE, Blower PJ, Jeffery JC et al (2002) The effect of substitution of a thioether donor by a phosphine donor in thiacrown complexes of iron. Inorg Chem Commun 5:832–836
62. Li JL, Meng JB, Wang YM et al (2001) Synthesis of phosphorus- and selenium-containing macrocycles and their complexation with $Pd(II)Cl_2$. J Chem Soc Perkin Trans 1:1140–1146
63. Kyba EP, Chou SS (1980) 11-Membered macrocycles containing the diars moiety. J Am Chem Soc 102:7012–7014
64. Fox MA, Campbell KA, Kyba EP (1981) Electrochemical behavior of metal tricarbonyl complexes of several tridentate macrocycles containing soft (P,S) ligating sites. Inorg Chem 20:4163–4165
65. Kyba EP, Brown SB (1980) Group 6 transition-metal complexes of two macrocycles containing tertiary-phosphino and -amino ligating sites. Inorg Chem 19:2159–2162
66. Liu C-Y, Cheng M-C, Peng S-M et al (1994) Coordination of an amino-phosphino macrocycle with (η^5-cyclopentadienyl)- and (η^5-pentamethylcyclopentadienyl)-iron complexes. J Organomet Chem 468:199–203
67. Ekici S, Nieger M, Glaum R et al (2003) A strategy for the synthesis of phosphorus-containing macrocycles–ligands for exceptional coordination geometries. Angew Chem Int Ed 42:435–438
68. Ekici S, Gudat D, Nieger M et al (2002) Kinetically controlled protonation of a cyclic phosphamethanide complex to a ph-phosphonium ylide. Angew Chem Int Ed 41:3367–3371
69. Fryzuk MD, Love JB, Rettig S (1996) Facile P_2N_2 macrocycle formation promoted by lithium templating. The X-ray crystal structures of syn-$Li_2(thf)(P_2N_2)$ and anti-$Li_2(thf)_2(P_2N_2)$ [P_2N_2=$PhP(CH_2SiMe_2NSiMe_2CH_2)_2PPh$. J Chem Soc Chem Commun 2783–2784
70. Fryzuk MD, Giesbrecht GR, Rettig S (1998) Pyramidal inversion at phosphorus facilitated by the presence of proximate lewis acids. Coordination chemistry of group 13 elements with the macrocyclic bis(amidophosphine) ligand [P_2N_2] ([P_2N_2]) [$PhP(CH_2SiMe_2NSiMe_2CH_2)_2PPh$]). Inorg Chem 37:6928–6934
71. Fryzuk MD, Giesbrecht GR, Rettig S et al (1999) Synthesis and characterization of Group 13 hydrides and metal-metal bonded dimers stabilized by the macrocyclicbis(amido-phosphine) ligand [P_2N_2] ([P_2N_2]-[$PhP(CH_2SiMe_2NSiMe_2CH_2)_2PPh$]). J Organomet Chem 591:63–70
72. Fryzuk MD, Kozak CM, Bowdridge MR et al (2001) Macrocyclic complexes of niobium(III): synthesis, structure, and magnetic behavior of mononuclear and dinuclear species that incorporate the [P_2N_2] system. Organometallics 20:3752–3761
73. Fryzuk MD, Kozak CM, Bowdridge MR et al (2002) Cyclohexadienyl niobium complexes and arene hydrogenation catalysis. Organometallics 21:5047–5054
74. Fryzuk MD, Love JB, Rettig S (1998) Synthesis and structure of zirconium(IV) complexes stabilized by the bis(amido-phosphine) macrocycle [P_2N_2]{[P_2N_2])PhP-$(CH_2SiMe_2NSiMe_2CH_2)_2PPh$}. Organometallics 17:846–853
75. Fryzuk MD, Love JB, Rettig S et al (1997) Transformation of coordinated dinitrogen by reaction with dihydrogen and primary silanes. Science 275:1445–1447

76. Morello L, Ferreira MJ, Patrick BO et al (2008) Side-on bound dinitrogen complex of zirconium supported by a P_2N_2 macrocyclic ligand. Inorg Chem 47:1319–1323
77. Fryzuk MD, Kozak CM, Bowdridge MR et al (2002) Nitride formation by thermolysis of a kinetically stable niobium dinitrogen complex. J Am Chem Soc 124:8389–8397
78. Basch H, Musaev DG, Morokuma K et al (1999) Theoretical predictions and single-crystal neutron diffraction and inelastic neutron scattering studies on the reaction of dihydrogen with the dinuclear dinitrogen complex of zirconium $[P_2N_2]Zr(P_2N_2)Zr[P_2N_2](P_2N_2)PhP(CH_2SiMe_2NSiMe_2CH_2)_2PPh$. J Am Chem Soc 121:523–528
79. Morello L, Love JB, Patrick BO et al (2004) Carbon-nitrogen bond formation via the reaction of terminal alkynes with a dinuclear side-on dinitrogen complex. J Am Chem Soc 126:9480–9481
80. Ohki Y, Fryzuk MD (2007) Dinitrogen activation by group 4 metal complexes. Angew Chem Int Ed 46:3180–3183
81. Fryzuk MD (2003) Activation and functionalization of molecular nitrogen by metal complexes. Chem Rec 3:2–11
82. Seidel WW, Summerscales OT, Patrick BO et al (2009) Activation of white phosphorus by reduction in the presence of a zirconium diamidodiphosphine macrocycle: formation of a bridging square-planar cyclo-P_4 unit. Angew Chem Int Ed 48:115–117
83. Marques de Oliveira IA, Pla-Roca M, Escriche L et al (2006) New membrane for copper-selective electrode incorporating a new thiophosphoril-containing macrocycle as neutral carrier. Mater Sci Eng C 26:394–398
84. Casabo J, Escriche L, Perez-Jimenez C et al (1996) Application of a new phosphadithiamacrocycle to ClO_4–selective CHEMFET and ion-selective electrode devices. Anal Chim Acta 320:63–68
85. Errachid A, Perez-Jimenez C, Casabo J et al (1997) Perchlorate-selective MEMFETs and ISEs based on a new phosphadithiamacrocycle. Sens Actuators B: Chem B43:206–210
86. Kyba EP, Chou S-SP (1981) Phosphino-macrocycles. 8. High-dilution syntheses of 14-membered tetradentate macrocycles incorporating the diars moiety. J Organomet Chem 46:860–863
87. Kyba EP, Alexander DC, Hoehn A (1982) Phosphinomacrocycles. Part 12. (Tertiary phosphinomacrocycle)cobalt(II) halide coordination chemistry. Identification and interconversion of four types of complexes. Organometallics 1:1619–1623
88. Kyba EP, Clubb CN, Larson SB et al (1985) Synthesis of 14-membered phosphorus-sulfur P_2S_2 and P_3S macrocycles which contain the 1-thio-2-(phenylphosphino)benzene moiety. Determination of stereochemistries of the free ligands and of a platinum(II) complex. J Am Chem Soc 107:2141–2148
89. Kyba EP, Davis RE, Fox MA et al (1987) Phosphinomacrocycles. 16. Complexation of the nickel(II) triad with 14-membered macrocyclic P_4-nSn (n = 2, 1, 0) ligands. Study of the effects on coordination of the relative configuration at the phosphines and the number and placement of thioether sites. Inorg Chem 26:1647–1658
90. Leung P-H, Liu A, Mok KF et al (1999) Synthesis and coordination chemistry of a 14-membered macrocyclic ligand containing one phosphorus, two sulfur and one ambidentate sulfoxide donor sets. J Chem Soc Dalton Trans Inorg Chem 8:1277–1282
91. Riker-Nappier J, Meek DW (1974) Nickel(II) complexes of two new phosphorus-nitrogen macrocyclic ligands. J Chem Soc Chem Commun 442–443
92. Scanlon LG, Tsao YY, Toman K et al (1982) Synthesis and characterization of the macrocyclic complexes $[Ni(Me)_2[14]dienatoN_2P_2)]PF_6$ and $[Ni(Me_2[16]dieneN_2P_2)](PF_6)_2$. Crystal structure of $[Ni(Me_2[16]dieneN_2P_2)](PF_6)_20.5H_20$. Inorg Chem 21:1215–1221
93. Jones TL, Willis AC, Wild SB (1992) Metal template synthesis of a 14-membered trans–P2S2 chelating macrocycle. Inorg Chem 31:1411–1416
94. Marty W, Schwartzenbach G (1970) Synthesis of heterocycles in the ligand sphere of metal ions. Chimia 24:431–433

95. Naumov RN, Karasik AA, Sinyashin OG et al (2004) Unexpected formation of a novel macrocyclic tetraphosphine: (RSSR)-1,9-dibenzyl-3,7,11,15-tetramesityl-1,9-diaza-3,7,11,15-tetraphosphacyclohexadecane. Dalton Trans 357–358
96. Naumov RN, Karasik AA, Kozlov AV et al (2008) Stereoselective synthesis and interconversions of 1,9-diaza-3,7,11,15-tetraphosphacyclohexadecanes. Phosphorus Sulfur Silicon Relat Elements 183:456–459
97. Karasik AA, Naumov RN, Spiridonova YS et al (2007) Synthesis, molecular structure and coordination chemistry of the first 1-aza-3,7-diphosphacyclooctanes. Z Anorg Allg Chem 633:205–210
98. Naumov RN, Karasik AA, Kanunnikov KB et al (2008) Synthesis of novel chiral macrocyclic tetraphosphine–1,9-di-R,R(and S,S)-α-methylbenzyl-3,7,11,15-tetramesityl-1,9-diaza–3,7,11,15–(RSSR)-tetraphosphacyclohexadecane. Mendeleev Commun 18:80–81
99. Ciampolini M, Nardi N, Zanobini F et al (1983) Sexidentate phosphorus containing macrocyclic ligands. Synthesis of 1,10-dipropyl-4,7,13,16-tetraphenyl-1,10-diaza-4,7,13,16-tetraphospha-cyclooctadecane. Inorg Chim Acta 76:L17–L19
100. Ciampolini M, Nardi N, Dapporto P et al (1984) Synthesis and characterisation of the five diastereoisomers of 4,7,13,16-tetraphenyl-1,10-dithia-4,7,13,16-tetraphosphacyclooctadecane: Crystal structure of the nickel bromide complex of the β-isomer. J Chem Soc Dalton Trans 575–579
101. Ciampolini M, Nardi N, Dapporto P et al (1984) Macrocyclic polyphosphane ligands. Cobalt(II) and nickel(II) complexes of (4RS, 7RS, 13RS, 16RS)-Tetraphenyl-1,10-dithia-4,7,13,16-tetraphosphacyclo-octadecane and crystal structure of the nickel dibromide complex. J Chem Soc Dalton Trans 995–998
102. Mealli C, Sabat M, Zanobini F et al (1985) Macrocyclic polyphosphane ligands. Iron(II), cobalt(II) and nickel(II) complexes of (4RS,7RS,13SR,16SR)-tetraphenyl-1,10-dipropyl-1,10-diaza-4,7,13,16-tetraphosphacyclo-octadecane: crystal structures of their tetraphenylborate derivatives. J Chem Soc Dalton Trans 479–485
103. Maerkl G, Hoferer M (1992) [18]-1,4,10,13-Tetraoxa-7,16-diphosphino-kronenether. [18]-1,4,10,13-Tetrathia-7,16-diphosphino-kronenether. Tetrahedron Lett 33:3621–3624
104. Blower PJ, Jeffery JC, MacLean E et al (2004) Synthesis and coordination chemistry of a diphospha-tetrathia macrocycle, 1,10-diphenyl-1,10-diphospha-4,7,13,16-tetrathiacyclo-octadecane. Inorg Chim Acta 357:4129–4138
105. van Zon A, Torny GL, Frijins JHG (1983) Chemistry of crown ethers. Part XXII. Synthesis and complexing properties of monophospha-crown ethers. Recl Trav Chim Pays-Bas 102:326–330
106. Wei L, Bell A, Warner S, Williams ID et al (1986) Aza- and oxaphosphands.A new class of hard/soft binucleating phosphine macrocycles. J Am Chem Soc 108:8302–8303
107. Theil A, Hitce J, Retailleau P et al (2006) A synthetic approach to macrocyclic, chiral phosphane derivatives with crown-ether-like structures. Eur J Org Chem 154–161
108. Meyer EA, Castellano RK, Diederich F (2003) Interactions with aromatic rings in chemical and biological recognition. Angew Chem Int Ed 42:1210–1250
109. Dalley NK, Kou X, Bartsch RA et al (2003) Synthesis of new cyclophane host molecules and crystal structures of their compounds with hydrocarbon guests. J Incl Phen Macrocycl Chem 45:139–148
110. Dalley NK, Kou X, Bartsch RA et al (1997) Synthesis of a new cyclophane host and crystal structures of its compounds with neutral guests. J Incl Phen Mol Recogn Chem 29:323–334
111. Bartsch RA, Kus P, Dalley NK et al (2002) A novel cyclophane–anthracene complex. Tetrahedron Lett 43:5017–5019
112. Escriche L, Casabo J, Muns V et al (2006) New phosphathiamacrocycles containing polypypiridine units. Polyhedron 25:801–808
113. Cafeo G, Garozzo D, Kohnke FH et al (2004) From calixfurans to heterocyclophanes containing isopyrazole units. Tetrahedron 60:1895–1902

114. Simons RS, Garrison JC, Kofron WG et al (2002) Synthesis and structural characterization of two bis-imidazolium-linked cyclophanes: precursors toward 'carbeneporphyrinoid' ligands. Tetrahedron Lett 43:3423–3425
115. Rajakumar P, Dhanasekaran M (2002) Synthesis of intra-annularly functionalized cationic pyridinophanes. Tetrahedron 58:1355–1359
116. Mathey F, Mercier F, Le Floch P (1999) New carbon-phosphorus macrocycles. Phosphorus Sulfur Silicon Relat Elem 144–146:251–256
117. Edwards PG, Fleming JS, Liyanage SS (1996) Stereoselective synthesis of 1,5,9-triphosphacyclododecane and tertiary derivatives. Inorg Chem 35:4563–4568
118. Vriezema DM, Aragones MC, Elemans JAAW et al (2005) Self-assembled nanoreactors. Chem Rev 105:1445–1490
119. Ohkuma T, Noyori R (2004) In: Beller M, Bolm C (eds) Transition metals for organic synthesis. Wiley-VCH, Weinheim
120. Goedheijt MS, Kamer PC, Reek NH et al (2004) In: Cornils B, Herrmann WA (eds) Aqueous-phase organometallic catalysis. Wiley-VCH, Weinheim
121. Pamies O, Net G, Widhalm M et al (1999) Rhodium cationic complexes using macrocyclic diphosphines as chiral ligands: application in asymmetric hydroformylation. J Organomet Chem 587:136–143
122. Ignat'eva SN, Balueva AS, Karasik AA et al (2007) Synthesis of novel paracyclophanes with linear P,N-containing spacers. Russ Chem Bull 56:1828–1837 (Izv RAN, ser Chim (2007) 56:1760–1770)
123. Prevote D, Galliot C, Caminade A-M et al (1995) Tricoordinated phosphorus-containing macrocycles: new synthetic strategies. Heteroat Chem 6:313–318
124. Bauer I, Habicher WD (2002) Phosphite macrocycles of varying size. Tetrahedron Lett 43:5245–5248
125. Bauer I, Habicher WD (1997) Synthesis of new phosphorus-containing macrocycles. Phosphorus Sulfur Silicon Relat Elem 130:89–105
126. Bauer I, Habicher WD, Jones PG et al (1998) Synthesis of symmetric macrocyclic phosphoramidites. Phosphorus Sulfur Silicon Relat Elem 143:19–31
127. Blokhin YI, Kornilov KN, Volchenkova YV (2009) Synthesis of the first unsymmetrical macroheterocycle containing endocyclic phosphorus atoms from pyrocatechol and hydroquinone. Russ J Gen Chem 79:200–202 (Zhurnal Obshchei Khimii (2009) 79:212–214)
128. Blokhin YI, Kornilov KN, Volchenkova YV (2009) Synthesis of unsymmetrical phosphorus-containing macrocycles on the basis of hydroquinone, 4,4′-(propane-2,2-diyl)diphenol, and resorcinol. Russ J Org Chem 45:900–903 (Zhurnal Organicheskoi Khimii (2009) 45:912–915)
129. Predvoditelev DA, Strebkova EV, Malenkovskaya MA et al (2007) Design of phosphorus-containing macrocycles on the basis of dipentaerythritol. Zhurnal Organicheskoi Khimii 43:638–639
130. Rasadkina EN, Slitikov PV, Evdokimenkova YB et al (2003) Macrocyclic systems on the basis of phosphorus acids and 2,7-dihydroxynaphthalene. Russ J Gen Chem 73:1208–1212 (Zhurnal Obshchei Khimii (2003) 73:1279–1283)
131. Nifant'ev EE, Rassadkina EN et al (2001) Dioxaphosphacyclanes. synthesis and chemical properties. Russ J Gen Chem 71:179–187 (Zh Obsch Chim (2001) 71:203-212)
132. Predvoditelev DA, Malenkovskaya MA, Nifant'ev EE (2006) New phosphorus-containing macroheterocyclic cavitands. Russ J Gen Chem 76:1205–1209 (Zhurnal Obshchei Khimii (2006) 76:1254–1259)
133. Maslennikova VI, Sotova TY, Vasyanina LK et al (2007) Regiodirected phosphorylation of 2,20,7,70-tetrahydroxydinaphthylmethane. Tetrahedron 63:4162–4171
134. Nifantyev EE, Slitikov PV, Rasadkina EN (2007) Synthesis of arylenephosphamacrocycles using tri- and pentavalent phosphorus compounds. Uspehi Khimii 76:362
135. Mizuta T, Aotani T, Imamura Y et al (2008) Structure and properties of the macrocyclic tridentate ferrocenylphosphine ligand (-$PhPC_5H_4FeC_5H_4$-)$_3$. Organometallics 27:2457–2463

136. Widhalm M (1990) Axial-chiral macrocyclic diphosphines. Monatshefte Chem 121:1053–1057
137. Widhalm M, Kratky C (1992) Synthesis and x-ray structure of binaphthyl-based macrocyclic diphosphines and their nickel(II) and palladium(II) complexes. Chem Ber 125:679–689
138. Widhalm M, Klintschar G (1994) Synthesis and stereochemistry of chiral macrocycles including a 1,2-bis(phenylphosphanyl)benzene unit. Chem Ber 127:1411–1426
139. Widhalm M, Klintschar G (1994) Relative and absolute configurations of diastereomeric macrocyclic diphosphine ligands and their Ni(II) complexes. Tetrahedron Asym 5:189–192
140. Widhalm M, Wimmer P, Klintschar G (1996) Macrocyclic diphosphine ligands in asymmetric carbon-carbon bond-forming reactions. J Organomet Chem 523:167–178
141. Yan Y-Y, Widhalm M (1998) Synthesis and application of macrocyclic binaphthyl ligands with extended chiral bias. Tetrahedron Asym 9:3607–3610
142. Kaufhold O, Stasch A, Pape T et al (2009) Metal template controlled formation of [11]ane-P_2CNHC macrocycles. J Am Chem Soc 131:306–317
143. Kaufhold O, Stasch A, Edwards PG (2007) Template controlled synthesis of a coordinated [11]ane-P_2CNHC macrocycle. Chem Commun 1822–1824
144. Flores-Figueroa A, Pape T, Feldmann K-O et al (2010) Template-controlled synthesis of a planar [16]ane-P_2CNHC_2 macrocycle. Chem Commun 46:324–326
145. Theil A, Mauve C, Adeline M-T, Marinetti A et al (2006) Phosphorus-containing [2]catenanes as an example of interlocking chiral structures. Angew Chem Int Ed 45:2104–2107
146. Bond AD, Doyle EL, García F et al (2003) Exo-metal coordination by a tricyclic $[\{P(\mu\text{-N-2-NC}_5H_4)\}_2(\mu\text{-O})]_2$ dimer in $[\{P(\mu\text{-N-2-NC}_5H_4)\}_2(\mu\text{-O})]_2\{CuCl\cdot(C_5H_5N)_2\}_4$ {2-NC_5H_4 = 2-pyridyl, C_5H_5N = pyridine). Chem Commun 2990–2991
147. Gonzlez-Calera S, Eisler DJ, Morey JV et al (2008) The selenium-based hexameric macrocycle $[(Se=)P(\mu\text{-N}^t\text{Bu})_2P(\mu\text{-Se})]_6$. Angew Chem Int Ed 47:1111–1114
148. Bashall A, Doyle EL, Tubb C et al (2001) The tetrameric macrocycle $[\{P(\mu\text{-N}^t\text{Bu})\}_2NH]_4$. Chem Commun 2542–2543
149. Garcia F, Goodman JM, Kowenicki RA et al (2004) Selection of a pentameric host in the host–guest complexes $\{[\{[P(\mu\text{-N}^t\text{Bu})]_2(\mu\text{-NH})\}_5]\cdot I\}^-[Li(thf)_4]^+$ and $[\{[P(\mu\text{-N}^t\text{Bu})]_2(\mu\text{-NH})\}_5]\cdot HBr\cdot THF$. Chem Eur J 10:6066–6072
150. Bashall A, Bond AD, Doyle EL et al (2002) Templating and selection in the formation of macrocycles containing $[\{P(\text{-N}^t\text{Bu})_2\}(\text{-NH})]_n$ frameworks: observation of halide ion coordination. Chem Eur J 8:3377–3385
151. Doyle EL, Riera L, Wright DS (2003) Toroidal main group macrocycles: new opportunities for cation and anion coordination. Eur J Inorg Chem 3279–3289
152. Garcıa F, Kowenicki RA, Kuzu I et al (2005) The first complex of the pentameric phosphazane macrocycle $[\{P(l\text{-N}^t\text{Bu})\}_2(l\text{-NH})]_5$ with a neutral molecular guest: Synthesis and structure of $[\{P(l\text{-N}^t\text{Bu})\}_2(l\text{-NH})]_5(CH_2Cl_2)_2$. Inorg Chem Commun 8:1060–1062
153. Garcıa F, Kowenicki RA, Kuzu I et al (2004) The formation of dimeric phosph(III)azane macrocycles $[\{P(\mu\text{-N}^t\text{Bu})\}_2\cdot LL]_2$ [LL = organic spacer]. Dalton Trans 2904–2909
154. Dodds F, Garcia F, Kowenicki RA et al (2005) Synthesis and structure of the calixarene-like phosph(III)azane macrocycle $[\{P(\mu\text{-N}^t\text{Bu})\}_2\{1,5\text{-}(NH)_2C_{10}H_6\}]_3$. Chem Commun 3733–3735
155. Dodds F, García F, Kowenicki RA et al (2005) The folded, tetrameric phosph(III)azane macrocycle $[\{P(\mu\text{-N}^t\text{Bu})\}_2\{1,4\text{-}(NH)_2C_6H_4\}]_4$. Chem Commun 5041–5043
156. Gonce F, Caminade AM, Majoral JP et al (1992) Synthesis and x-ray structure of the first unsymmetric macrocycle containing three inequivalent phosphorus atoms. Bull Soc Chim Fr 129:237–241
157. Gonce F, Caminade AM, Boutonnet F et al (1992) Design of new tools for macrocyclic synthesis. Applications to the preparation of polyphosphorus macrocycles. J Org Chem 57:970–975
158. Matano Y, Nakabuchi T, Miyajima T et al (2006) Phosphole-containing hybrid calixpyrroles: new multifunctional macrocyclic ligands for platinum(II) ions. Organometallics 25:3105–3107

159. Nakabuchi T, Matano Y, Imahori H (2008) Synthesis, structures, and coordinating properties of phosphole-containing hybrid calixpyrroles. Organometallics 27:3142–3152
160. Matano Y, Miyajima T, Nakabuchi T et al (2006) Phosphorus-containing hybrid calixphyrins: promising mixed-donor ligands for visible and efficient palladium catalysts. J Am Chem Soc 128:11760–11761
161. Matano Y, Fujita M, Miyajima T et al (2009) Meso-substituent effects on redox properties of the 5,10-porphodimethene- type P,S,N_2-hybrid calixphyrins and their metal complexes. Organometallics 28:6213–6217
162. Matano Y, Miyajima T, Ochi N et al (2008) Syntheses, structures, and coordination chemistry of phosphole-containing hybrid calixphyrins: promising macrocyclic P,N2,X-mixed donor ligands for designing reactive transition-metal complexes. J Am Chem Soc 130:990–1002
163. Matano Y, Nakabuchi T, Miyajima T et al (2006) Synthesis of a phosphorus-containing hybrid porphyrin. Org Lett 8:5713–5716
164. Matano Y, Nakashima M, Nakabuchi T et al (2008) Monophosphaporphyrins: oxidative π-extension at the peripherally fused carbocycle of the phosphaporphyrin ring. Org Lett 10:553–556
165. Matano Y, Nakabuchi T, Fujishige S et al (2008) Redox-coupled complexation of 23-phospha-21-thiaporphyrin with group 10 metals: a convenient access to stable core-modified isophlorin-metal complexes. J Am Chem Soc 130:16446–16447
166. Laporte F, Mercier F, Ricard L et al (1994) Tetraphosphorus macrocycles from phosphole tetramers. J Am Chem Soc 116:3306–3311
167. Mercier F, Laporte F, Ricard L et al (1997) The use of a ten-membered tetraphosphole macrocycle to increase the lifetime of a palladium catalyst. Angew Chem Int Ed Engl 36:2364–2366
168. Deschamps E, Ricard L, Mathey F (1995) Synthesis and X-ray crystal structural analysis of a tetraphosphole macrocycle. J Chem Soc Chem Commun 1561
169. Avarvari N, Maigrot N, Ricard L et al (1999) Synthesis and X-ray crystal structures of silacalix[n]phosphinines: the first sp2-based phosphorus macrocycles. Chem Eur J 5:2109–2118
170. Mézailles N, Maigrot N, Hamon S et al (2001) Mixed phosphinine-ether macrocycles. J Org Chem 66:1054–1056
171. Mézailles N, Avarvari N, Maigrot N et al (1999) Gold(I) and gold(0) complexes of phosphinine-based macrocycles. Angew Chem Int Ed 38:3194–3197
172. Ferro VR, Omar S, González-Jonte RH et al (2003) The donating and accepting properties of ortho-Si$(CH_3)_3$ phosphinine macrocycles. Heteroat Chem 14:160–169
173. Balueva AS, Kuznetsov RM, Litvinov IA et al (2000) Cyclo-bis{1-[p-(p-phenylenomethyl)-phenyl]-3,7-diphenyl-1,5,3,7-diazadiphosphacyclooctane} as the first representative of a new type of nitrogen-containing macroheterocyclic phosphines. Mendeleev Commun 10:120–121
174. Kuznetsov RM, Balueva AS, Litvinov IA et al (2002) Synthesis of new macrocyclic aminomethylphosphines based on 4, 4'-diaminodiphenylmethane and its derivatives. Russ Chem Bull 51:151–156
175. Balueva AS, Kuznetsov RM, Ignat'eva SN et al (2004) Self-assembly of novel macrocyclic aminomethylphosphines with hydrophobic intramolecular cavities. Dalton Trans 442–447
176. Kulikov DV, Karasik AA, Balueva AS et al (2007) The first representative of a 36-membered P,N,O-containing cyclophane. Mendeleev Commun 17:195–196
177. Karasik AA, Balueva AS, Naumov RN et al (2008) An effective methodology of P,N-macrocycles design. Phosphorus Sulfur Silicon Relat Elem 183:583–585
178. Kulikov DV, Balueva AS, Karasik AA et al (2008) Novel 36- and 38-membered P,N-containing cyclophanes with large hydrophobic cavities. Phosphorus Sulfur Silicon Relat Elem 183:667–668
179. Karasik AA, Kulikov DV, Balueva AS et al (2009) A P,N-containing cyclophane with a large helical hydrophobic cavity: a prospective precursor for the design of a molecular reactor. Dalton Trans 3:490–494

180. Sinyashin OG, Karasik AA, Hey-Hawkins E (2008) New synthetic approaches to chiral cyclic and macrocyclic phosphine ligands. Phosphorus Sulfur Silicon Relat Elem 183:445–448
181. Balueva AS, Kulikov DV, Kuznetsov RM et (2008) Synthesis of 13,17,53,57-tetraphenyl-13,17,53,57-tetrathio-3,7-dithia-1,5(1,5)-di(1,5-diaza-3,7-diphosphacyclooctana)-2,4,6,8(1,4)-tetrabenzenacyclooctaphane with a conical-like intramolecular cavity. J Incl Phen Macrocyclic Comp 60:321–328
182. Latypov SK, Kozlov AV, Hey-Hawkins E, Balueva AS, Karasik AA, Sinyashin OG (2010) Structure, conformation and dynamics of p, n-containing cyclophanes in solution. J Phys. Chem A 114:2588–2596
183. Xu W, Rourke JP, Vittal JJ et al (1995) Transition metal rimmed-calixresorcinarene complexes. Inorg Chem 34:323–329
184. Xu W, Vittal JJ, Puddephatt RJ (1995) Inorganic inclusion chemistry: a novel anion inclusion system. J Am Chem Soc 117:8362–8371
185. Vollbrecht A, Neda I, Thönnessen H et al (1997) Synthesis, structure, and reactivity of tetrakis(O,O-phosphorus)-bridged calix[4]resorcinols and their derivatives. Chem Ber 130:1715–1720
186. Dietrich B, Hosseini MW, Lehn JM et al (1985) Synthesis of macrobicyclic polyamines by direct macrobicyclisation via tripode-tripode coupling. Helv Chim Acta 68:289–299
187. Whitesides GM, Mathias JP, Seto CT (1991) Molecular self-assembly and nanochemistry: a chemical strategy for the synthesis of nanostructures. Science 254:1312–1319
188. Lokey RS, Iverson RL (1995) Synthetic molecules that fold into a pleated secondary structure in solution. Nature 375:303–305
189. Gillard RE, Raymo FM, Stoddart JF (1997) Controlling self-assembly. Chem Eur J 3:1933–1940
190. Vögtle F, Neumann PJ (1970) The 2,11,20-triaza[3,3,3](1,3,5)cyclophane system. J Chem Soc Chem Commun 1464–1465
191. Vögtle F, Lichtenthaler RG (1972) Cyclophanes possessing cavities. Angew Chem Int Ed Engl 11:535–536
192. Lichtenthaler RG, Vögtle F (1973) Vielfach überbrückte aromatische Verbindungen, 6. Dreifach verbrückte Cyclophane. Chem Ber 106:1319–1327
193. Vögtle F, Hohner G (1975) Triply clamped helical triphenylmethane systems. Angew Chem Int Ed Engl 14:497–498
194. Anelli PL, Montanari F, Quici S (1983) Triply bridged polyoxapolyaza-heterophanes derived from 2,4,6-trichloro *s*-triazine. A new strategy in the synthesis of possible receptors of charged and/or neutral species. J Chem Soc Chem Commun 194–195
195. Dietrich B, Guilhem J, Lehn JM et al (1984) Molecular recognition in anion coordination chemistry. structure, binding constants and receptor-substrate complementarity of a series of anion cryptates of a macrobicyclic receptor molecule. Helv Chim Acta 67:91–104
196. Heyer D, Lehn JM (1986) Anion coordination chemistry—synthesis and anion binding features of cyclophane type macrobicyclic anion receptor molecules. Tetrahedron Lett 27:5869–5872
197. Friedrichsen BP, Whitlock HW (1989) Concave functionality: intracavity phosphine oxide as a locus of complexation. J Am Chem Soc 111:9132–9134
198. Friedrichsen BP, Powell DR, Whitlock HW (1990) Sterically encumbered functional groups: an investigation of endo versus exo phosphoryl complexation using proton and phosphorus-31 NMR. J Am Chem Soc 112:8931–8941
199. Osvath P, Sargeson AM (1993) Synthesis of a large cavity homoleptic thioether cage and its cobalt(III) complex. J Chem Soc Chem Commun 40–42
200. Houalla D, Moureau L, Skouta S et al (1995) New macrocycles containing bicyclophosphorane moieties Iv[1]. macrocycles issued from polyethyleneglycols and triethanolamine. Phosphorus Sulfur Silicon Relat Elem 103:199–204
201. Pascal RA, West AP, van Engen D (1990) Synthesis and structure of an in-phosphaphane: enforced interaction of a phosphine and an aromatic ring. J Am Chem Soc 112:6406–6407

202. L′Esperance RP, West AP, van Engen D et (1991) in-Cyclophanes containing second-row elements poised above aromatic rings. J Am Chem Soc 113:2672–2676
203. West AP, Smyth N, Kraml CM et al (1993) Synthesis, molecular structure, and properties of in-phosphaphanes with substituted basal aromatic rings. J Org Chem 58:3502–3506
204. Bolm C, Barry K (1988) Sharpless synthesis of a C3-symmetric phospha[2.2.2]cyclophane. Tetrahedron Lett 29:5101–5104
205. Dell S, Ho DM, Pascal RA (1999) In- and out-cyclophanes bearing non-hydrogen bridgehead substituents. J Org Chem 64:5626–5633
206. Chen YT, Baldridge KK, Ho DM et al (1999) Interconversion and reactions of in- and out-isomers of a triarylphosphine-containing cyclophane. J Am Chem Soc 121:12082–12087
207. Naumov RN, Kozlov AV, Kanunnikov KB et al (2010) The first example of stereoselective self-assembly of a cryptand containing four asymmetric intracyclic phosphane groups. Tetrahedron Lett 51:1034–1037
208. Hoehn A, Geue RJ, Sargeson AM et al (1989) Phospha-capped cobalt(III) cage molecules: synthesis, properties, and structure Chem Commun 1644–1645
209. Parks JE, Wagner BE, Holm RH (1970) Three-dimensional macrocyclic encapsulation reactions. I. Synthesis of six-coordinate complexes with nonoctahedral stereochemistry. J Am Chem Soc 92:3500–3502
210. Bauer I, Rademacher O, Gruner M et al (2000) Synthesis and isolation of homeomorphous isomers of P-containing cryptands. Chem A Eur J 6:3043–3051
211. Bauer I, Frohlich R, Ziganshina AY et al (2002) Synthesis and structural peculiarities of homeomorphic phosphorus bridgehead macrobicyclic compounds and novel dioxaphospha[3.1.1.]p,m,p-cyclophanes. Chem A Eur J 8:5622–5629
212. Daebritz F, Theumer G, Gruner M et al (2009) New conformational flexible phosphane and phosphane oxide macrobicycles. Tetrahedron 65:2995–3002
213. Daebritz F, Jaeger A, Bauer I (2008) Synthesis, derivatization and structural characterization of a new macrobicyclic phosphane oxide cryptand. Eur J Org Chem 33:5571–5576
214. Mitjaville J, Caminade A-M, Mathieu R et al (1994) New synthetic strategies for phosphorus-containing cryptands and the first phosphorus spherand type compound. J Am Chem Soc 116:5007–5008
215. Zeng X, Hucher N, Reinaud O et al (2004) A novel receptor based on a C_{3v}-symmetrical PN_3-calix[6]cryptand. J Org Chem 69:6886–6889
216. Izzet G, Zeng X, Over D et al (2007) First Insights into the electronic properties of a Cu(II) center embedded in the PN_3 cap of a calix[6]arene-based ligand. Inorg Chem 46:375–377
217. Over D, Lande A, Zeng X (2009) Replacement of a nitrogen by a phosphorus donor in biomimetic copper complexes: a surprising and informative case study with calix[6]arene-based cryptands. Inorg Chem 48:4317–4330
218. Skopek K, Hershberger C, Gladysz A (2007) Self-assembled nanoreactors. Coord Chem Rev 251:1723–1733
219. Shima T, Hampel F, Gladysz JA (2004) Molecular gyroscopes: $Fe(CO)_3$ and $\{Fe(CO)_2(NO)\}^+$ rotators encased in three-spoke stators; facile assembly by alkene metatheses. Angew Chem Int Ed 43:5537–5540
220. Nawara AJ, Shima T, Hampel F et al (2006) Gyroscope-like molecules consisting of PdX_2/PtX_2 rotators encased in three-spoke stators: synthesis via alkene metathesis, and facile substitution and demetalation. J Am Chem Soc 128:4962–4963
221. Hess GD, Hampel F, Gladysz JA (2007) Octahedral gyroscope-like molecules with $m(CO)_3(X)$ rotators encased in three-spoked diphosphine stators: syntheses by alkene metathesis/hydrogenation sequences, structures, dynamic properties, and reactivities. Organometallics 26:5129–5131
222. Skopek K, Gladysz JA (2008) Syntheses of gyroscope-like molecules via three-fold ring closing metatheses of bis(phosphine) complexes trans-$L_yM(P((CH_2)_nCH{=}CH_2)_3)_2$, and extensions to bis(phosphite) complexes trans-$Fe(CO)_3(P(O(CH_2)_nCH{=}CH_2)_3)_2$. J Organomet Chem 693:857–866

Chapter 13
Metal Phosphorus Complexes as Antitumor Agents

Alexey A. Nazarov and Paul J. Dyson

Abstract Phosphorus-based ligands are an extremely important class of ligand and they have found many applications, especially in homogeneous catalysis. In addition, a phosphine ligand is found in a gold drug used to treat rheumatoid arthritis. Since metal compounds are also widely used to treat cancer many studies on the anticancer activity of metal–phosphine complexes have been conducted. In this chapter we describe recent highlights in the field, centered on platinum, ruthenium and gold complexes. From this overview it is clear that phosphorus-based ligands offer a number of important advantages compared to other types of ligands. It also becomes clear that studies are in a comparatively early stage and that more attention should be directed towards the design and synthesis of phosphine and other phosphorus ligands for medicinal applications in metal-based chemotherapeutics. Examples of metal–phosphine compounds that target critical enzymes in cancer indicates that these compounds operate via mechanisms quite distinct from other metal-based drugs which damage DNA, and consequently, facilitates rational drug design.

13.1 Introduction

Organophosphorus compounds constitute a well known class of biologically active molecules that have numerous clinical applications including those against glaucoma, cardiovascular diseases, fungal and viral infections [1]. Anticancer

A. A. Nazarov · P. J. Dyson (✉)
Institut des Sciences et Ingénierie Chimiques, Lausanne, Ecole Polytechnique Fédérale de Lausanne (EPFL), 1015 Lausanne, Switzerland
e-mail: paul.dyson@epfl.ch

M. Peruzzini and L. Gonsalvi (eds.), *Phosphorus Compounds*, Catalysis by Metal Complexes, 37, DOI: 10.1007/978-90-481-3817-3_13,
© Springer Science+Business Media B.V. 2011

organophosphorus compounds were introduced into clinical practice at the end of the 1950s, and currently several drugs, e.g. cyclophosphamide [2, 3], etopophos [4], ifosfamide and thiotepa [5] (Fig. 13.1) are widely used as antineoplastic agents.

The clinical success of cisplatin, carboplatin and oxaliplatin (Fig. 13.1) resulted in the use of metal complexes in a large number of chemotherapeutic schemes for the treatment of malignant tumors [6, 7]. Despite significant achievements of the classical antitumor active platinum-based drugs, side effects leading to general toxicity, and acquired or primary resistant against certain tumor types, has motivated the search for more effective and target-specific compounds [8, 9].

The combination of phosphorus ligands (phosphines, phosphonates and phosphites) with transition metals represent one way to overcome the limitations of the platinum drugs, i.e. by providing a highly tunable platform in terms of chemical modifications as well as targeted approach (see below). For example, platinum(II) complexes with aminomethyl phosphonic ligands have been found to specifically target bone malignancies [10]. The introduction of PTA (1,3,5-triaza-7-phosphatricyclo-[3.3.1.1]decane) into organometallic Ru(II)-arene systems resulted not only to formation of water-soluble complexes but also in selective antimetastatic activity [7]. A number of Pt, Ru and Au complexes with phosphorus ligand are active against cisplatin resistant tumors. It is particularly noteworthy that a Au-phosphine complex, auranofin, which is used in the clinic to treat rheumatic arthritis also shows significant anticancer activity [11].

In this chapter an overview of the recent developments in the synthesis and biological evaluation of anticancer platinum, ruthenium and gold complexes containing phosphorus ligands is described. A review describing the medicinal chemistry of metal complexes with phosphine ligands has been published previously [12] that covers the literature until 1988. In this chapter we only consider work in the field that has been reported after this date, moreover, selected examples are given. This chapter is not intended to be comprehensive but gives an

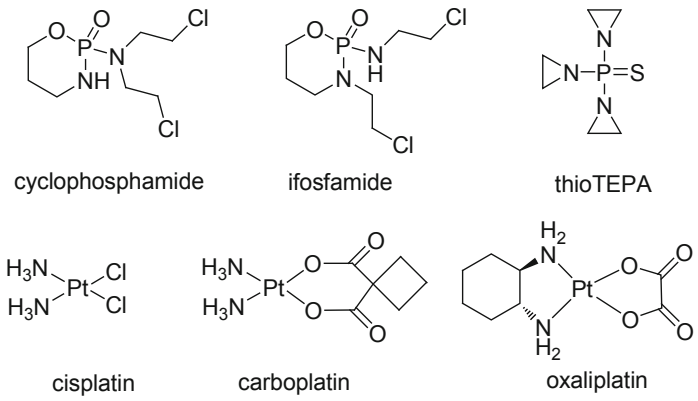


Fig. 13.1 Examples of organophosphorus and Pt anticancer drugs used in the clinic

overview of compounds that should interest chemists working with phosphines and other phosphorus containing ligands.

13.2 Platinum Complexes

The clinical approval of cisplatin as an anticancer drug inspired research for more active and more specific antitumor platinum compounds. In order to investigate the influence of non-nitrogen donor ligands on anticancer activity, several Pt(II) complexes based on phosphines resembling to some extent the cisplatin structure, were tested for their antitumor activity (Fig. 13.2). In general, results were discouraging since none of compounds showed an increase in antitumor activity compared to cisplatin. Indeed, in most of cases the complexes were found to be inactive [12–15]. The strong *trans* effect of the phosphine ligand and high stability of the Pt–P bond were proposed as the reasons for the low activity of these complexes.

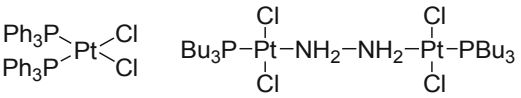


Fig. 13.2 Examples of Pt(II) phosphine complexes evaluated for anticancer activity

Adjusting the lipophilic character, solubility and stability of compounds by coordination of the PTA ligand to the platinum(II) center to afford a series of mono and dinuclear complexes was undertaken (Fig. 13.3). PTA is a cage adamantane-type phosphine, first synthesised in 1974 by Daigle, that provides water solubility to transition metal complexes and has found extensive applications in homogeneous catalysis [16]. The PTA ligand appears to be very useful for fine tuning the solubility and target specificity of metal drugs. Platinum complexes with PTA were found to have higher solubility and cytotoxicity in comparison to complexes with other phosphines [17–19]. Moreover, the complexes were found to be active on both cisplatin sensitive and cisplatin resistance cell lines indicating a different

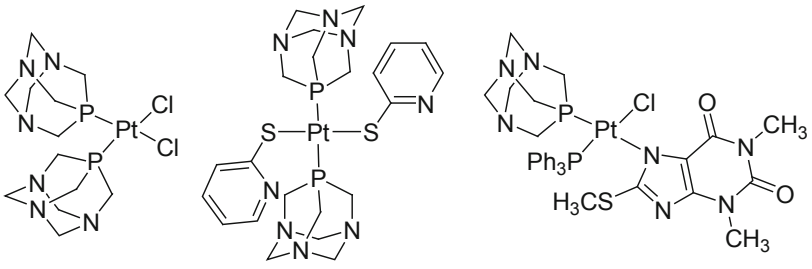


Fig. 13.3 PTA containing Pt(II) complexes

mechanism of action to the established platinum drugs. A complex with PTA and thionate ligands following in vitro screening was found to be one of most cytotoxic Pt(II) compounds containing phosphine ligands [20].

The application of aminophosphine ligands resulted in Pt(II) complexes with pH sensitive properties (Fig. 13.4). As a function of the pH and the chloride concentration, such complexes can exist as a closed ring or an open (or partially open) system. Such a system may be able to exploit the acidic character of a tumor environment for activation inside the tumor cell. That is, at the pH typical of healthy cells, the complex would exist in the closed metallo-ring form, which is unreactive, but at the lower pH of cancer tissue the system should open and become reactive and consequently cytotoxic [21].

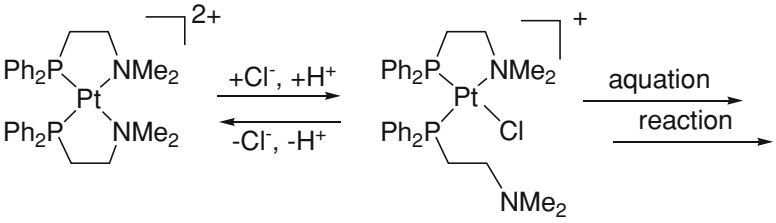


Fig. 13.4 Examples of pH and Cl^- sensitive Pt(II) phosphine complexes in closed form (*left*) and partly open form (*right*)

While transplatin is not an active anticancer drug some *trans* platinum complexes, however, are highly cytotoxic. In the search for active *trans* platinum compounds several complexes with triphenylphosphine or dimethylphenylphosphine ligands have been studied (Fig. 13.5), and found to be active on various cancer cell lines, with no cross resistance to cisplatin observed [22]. Apoptotic cell death with no G1 and G2/M accumulation in the cell cycle, typical for the cisplatin, was observed indicating a non-classical mechanism of action.

Phosphonic acids have been used to substitute the dicarboxylate moiety in carboplatin and oxaliplatin in order to improve solubility and pharmacological properties such as tumor selectivity and general toxicity (Fig. 13.6) [23, 24]. The introduction of the phosphonic functionality led to complexes active in studies on several tumor models with activity found to be similar or better than cisplatin or carboplatin although severe kidney toxicity was observed in vivo [23].

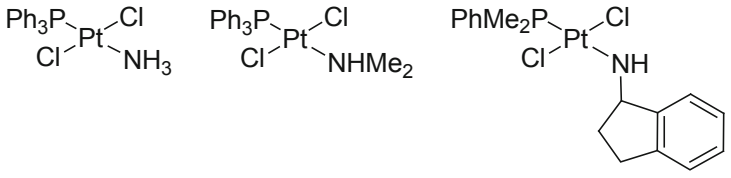


Fig. 13.5 Examples of *trans*-Pt(II) complexes

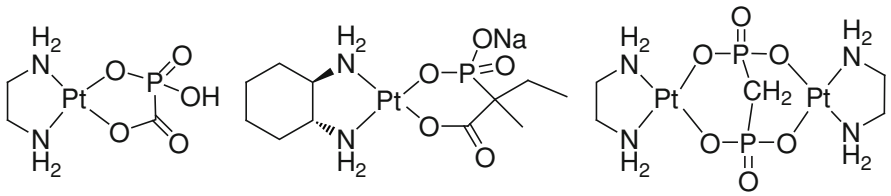


Fig. 13.6 Examples of Pt(II) complexes containing phosphonic acids

Bis-phosphonates may act as bridging ligands giving dinuclear platinum(II) complexes with high stability under physiological conditions. The dinuclear complexes were found to overcome multidrug resistance on several cancer cell lines [24].

The affinity of the phosphonates and bisphosphonates to Ca^{2+} ions led to their application in the treatment of osteoporosis, hypercalcemia, and the inhibition of bone resorption [25]. This property also led to the development of platinum complexes (Fig. 13.7) that have been used to specifically target bone cancer [26, 27]. The bisphosphonate functionality strongly interacts with the bone surface directing the platinum to the tumor. The complexes are active against different cancer cell lines and are more active following addition of Ca^{2+} ions and were found to be particularly active against the transplanted osteosarcoma in in vivo studies [28].

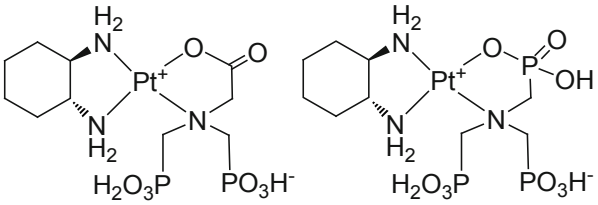


Fig. 13.7 Pt(II) complexes with bone-seeking phosphonate ligands

13.3 Ruthenium Complexes

Two ruthenium containing anticancer complexes NAMI-A and KP1019 (Fig 13.8) are currently undergoing clinical evaluation which has stimulated significant interest in the development of new Ru-based anticancer complexes [8]. In recent years, ruthenium(II)-arene complexes have been extensively evaluated as anticancer agents, with the ruthenium stabilised in the oxidation state (+2) by the η^6coordinated arene [29].

Compared to Pt containing phosphine compounds that have been evaluated for anticancer activity only a few examples of ruthenium complexes with phosphorus ligands, with the exception of the RAPTA family, have been prepared and tested

for anticancer activity. In addition, cycloruthenated compounds (Fig. 13.8) with different phosphine ligands [30] were screened for anticancer activity on the A-172 glioblastoma and HCT-116 adenocarcinoma cell lines and were found to have an activity similar to cisplatin. A tris(*o*-anisyl)phosphane Ru(III) complex [31] was found to be highly cytotoxic on human ovarian cancer cell lines A2780 and A2780cisR (the latter being the cisplatin resistant strain).

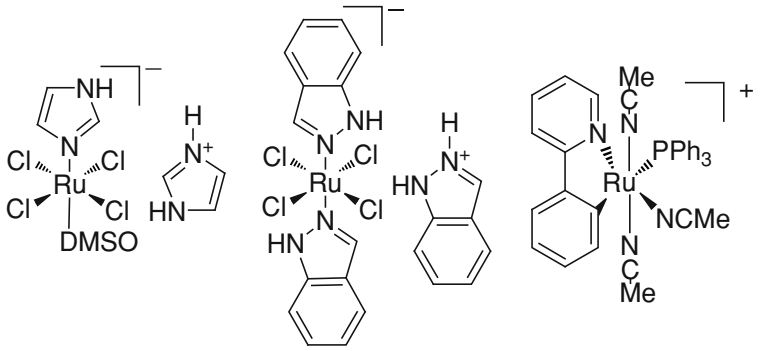


Fig. 13.8 NAMI-A, KP-1019 and a phosphine containing cycloruthenated Ru(II) complex

The water soluble phosphine PTA present in Ru(η^6-p-cymene)Cl_2PTA [32], termed RAPTA-C, is the prototype and most widely evaluated member of the RAPTA type complexes. RAPTA-C (Fig. 13.9) shows pH-dependent damage to the DNA, however, cytotoxicity in in vitro studies is generally low in comparison to cisplatin but with selectivity towards cancer cells. In subsequent studies RAPTA-C was found to be good antimetastatic agent, and in studies on CBA mice bearing the MCa mammary carcinoma, the number and weight of metastasis were reduced, with only mild effects on the primary tumour noted [33].

Structural analogues of RAPTA-C were prepared and relationships in terms of in vitro and in vivo activity and drug uptake have been established [34]. Changing the *p*-cymene ring to toluene led to improved antimetastatic properties compared to RAPTA-C. The introduction of an ester group resulted in increase in cellular uptake. Further fine tuning of the cytotoxicity by attaching functional groups such

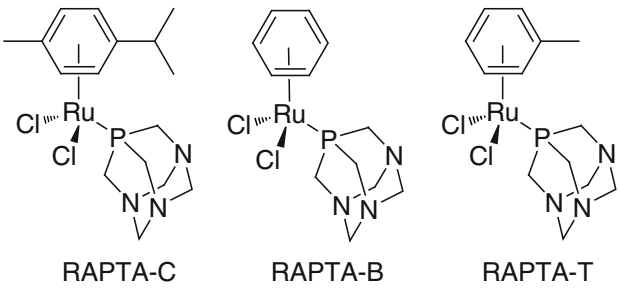


Fig. 13.9 Examples of RAPTA complexes

as fluorous groups [35], imidazolium or crown ethers to the arene have been reported [33], however, while greater cytotoxicities were sometimes observed, in vivo studies have not been reported. Notably, it was found that replacement of PTA by Me-PTA$^+$ reduced selectivity towards malignant cells [33]. Substitution of the arene with [9]aneS_3 resulted in a complex with similar in vitro properties to RAPTA-C and the addition of a second PTA ligand into the structure was shown to increase selectivity towards cancerogenic cells in vitro [36] (Fig. 13.10).

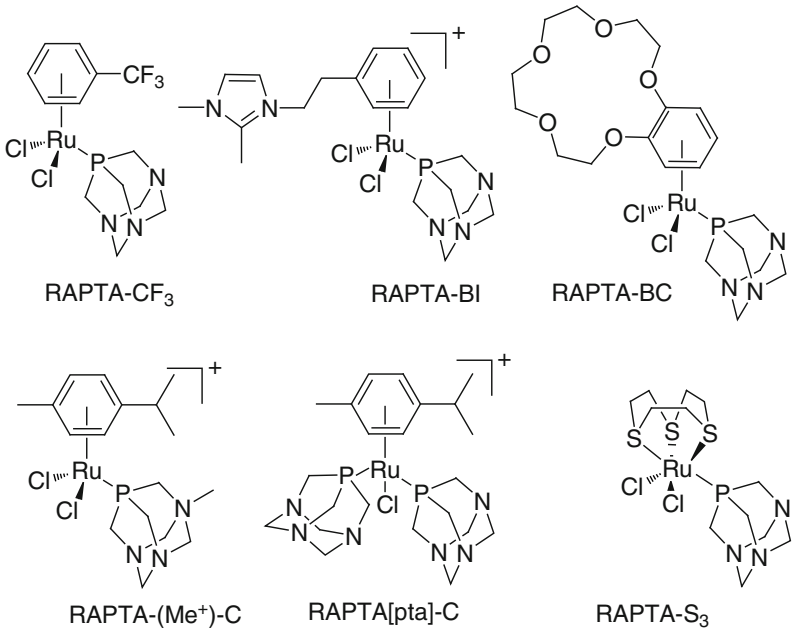


Fig. 13.10 Examples of RAPTA-type complexes explored as antitumor agents

Aquation of one chlorido ligand in RAPTA compounds in aqueous solution is observed and the degree of aquation/hydrolysis depends on the concentration of the complex, the temperature, pH and the chloride concentration. The replacement of the chlorido leaving groups by dicarboxylate ligands results in complexes that resist hydrolysis with in vitro activity similar to RAPTA-C, but remarkably different in vivo activity [37] (Fig. 13.11).

The mechanism of action of RAPTA complexes has been the subject of detailed investigations in the last few years. Compared to Pt complexes the affinity of RAPTA complexes bind to DNA is significantly lower and therefore different cellular components have been considered as targets for these complexes. Inhibition of cathepsin B, a protease implicated in metastasis, has been reported with IC_{50} values typically in the low μM range. Computational studies suggest a good fit of the RAPTA complexes in the active site of cathepsin B, with the phosphine ligand playing an important role in docking [38] (Fig. 13.12).

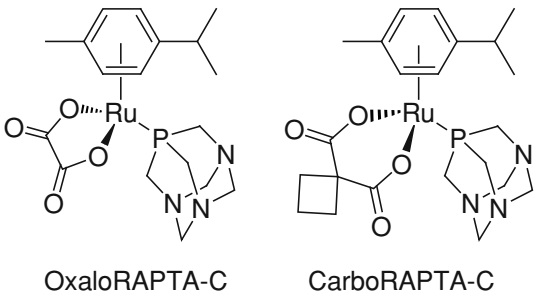


Fig. 13.11 RAPTA-C derivates that modulate hydrolysis

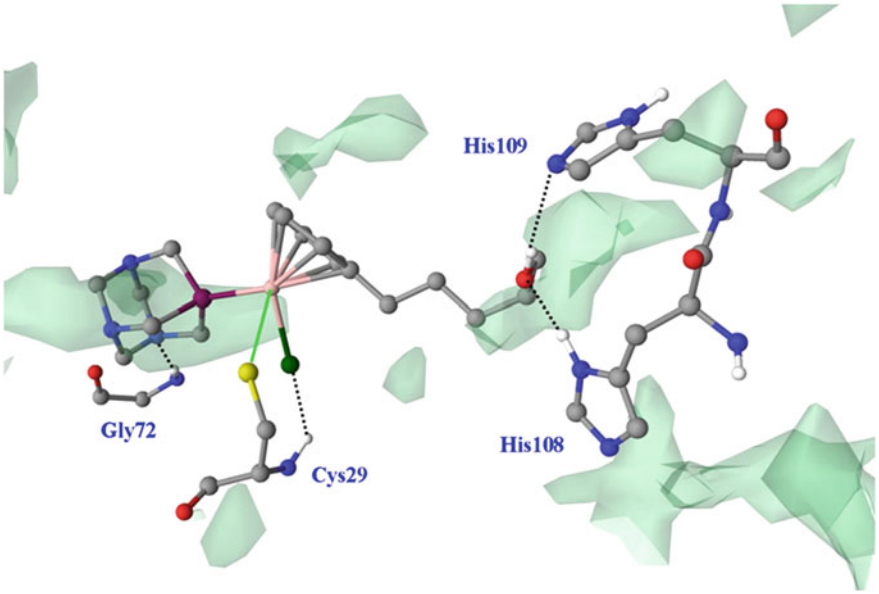


Fig. 13.12 Figure of cathepsin B docking studies showing the main interactions of the ligand with the residues flanking the active site. Adapted from Ref. [38]

The rational design of RAPTA complexes via modification of the arene moiety has been used to overcome specific problems or to exploit unique cancer biology pathways. For example, Glutathione-S-transferases (GSTs) are often over-expressed in primary and metastatic tumors that are resistant to chemotherapy. A well known inhibitor of this enzyme, ethacrynic acid, has been tethered to the arene moiety via both ester and amide linkers. The resulting compounds show inhibition of GST P1-1 activity on wild and mutant enzymes at similar concentration or at a lower concentration than ethacrynic acid itself. The nature of binding to the enzyme was studied by mass spectrometry and X-ray diffraction. In the crystallographic study the 'ethacrynic' part of the molecule fits into the catalytic pocket with additional stabilization by the ruthenium(II) center via interaction with Cys residues [39] (Fig. 13.13).

The RAPTA structure has also been modified with a triphenylphosphine ligand (Fig. 13.14) to give a complex with improved cytotoxicity, cellular uptake and higher affinity towards DNA [40, 41]. Various other phosphines co-ligands have also been evaluated, notably phosphine moieties with perfluorinated alkane chains that were found to endow the compounds with thermosensitive properties (Fig. 13.14) [42]. Thermotherapy is a treatment in which a heat source is applied

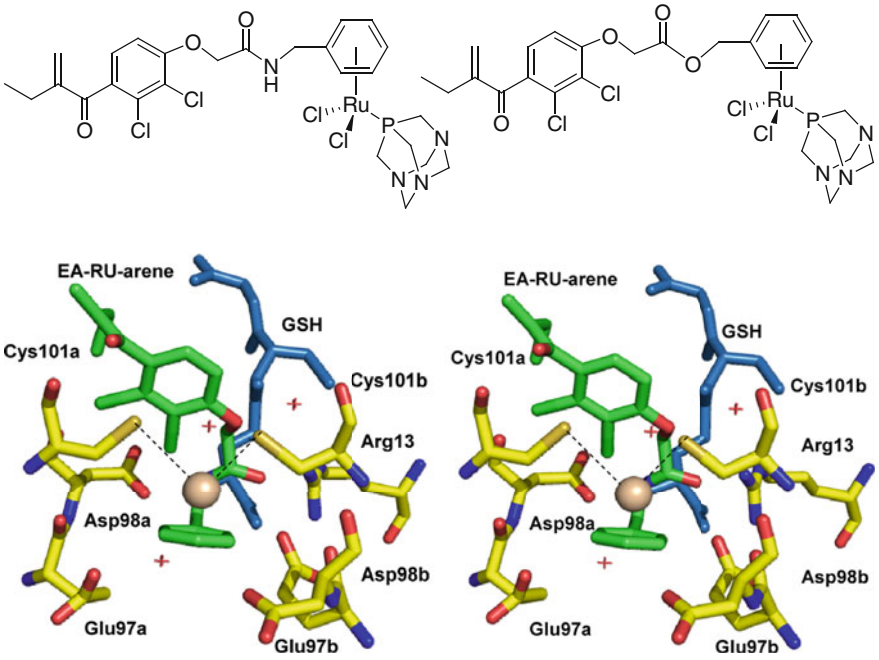


Fig. 13.13 Examples of RAPTA-type complexes containing the ethacrynic acid moiety (*top*) and views of the ruthenium complex at the GST P1-1 dimer interface (*bottom*). The PTA moiety and bonds between the Ru center and the arene ring have been omitted for clarity. Copyright Wiley–VCH Verlag GmbH & Co. KGaA. Reproduced with permission from Ref. [39]

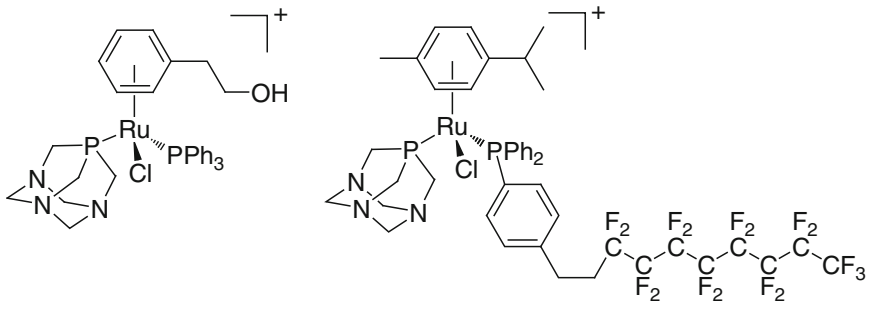


Fig. 13.14 RAPTA derivatives with an additional phosphine co-ligand

to the tumour area causing an increase in temperature. The compact, disordered structure of tumour cells makes them less effective at dissipating heat than healthy cells and as result, the cells become weakened and more sensitive to chemotherapy. A number of specifically designed thermoresponsive macromolecules have been investigated for applications in thermotherapy, and the complexes with phosphine ligands with perfluorinated alkane chains are the first molecular compounds to exhibit thermosensitive properties and are more cytotoxic in cancer cells at elevated temperatures relative to cells at 37 °C.

Overexpression of glucose receptors in the cancer cells lead to an increase in glycolytic activity and glucose uptake. Organometallic ruthenium(II)-arene complexes based on phosphite-carbohydrate ligands (Fig. 13.15) have been prepared in order to increase the delivery of the ruthenium complex into cancer cells. The compounds were found to be moderately active against different human tumor cell lines. In addition, some degree of selectivity for cancer cells was observed [43]. Interestingly, both Ru centers and phosphite ligand are prone to hydrolyse in water, the complexes undergo aquation of the first halido ligand, followed by the hydrolysis of a P–O bond of the phosphite ligand. The P–O bond in the free ligand undergoes hydrolysis at a very slow rate, whereas hydrolysis of the P–O bond occurs rapidly when the phosphite is coordinated to the ruthenium center, and only following aquation at the metal. This transformation is suppressed by free chloride ions in solution or by substitution of chloride ligands with dicarboxylate moieties [44].

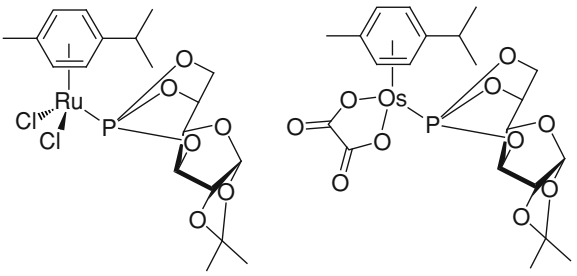


Fig. 13.15 Sugar based Ru(II) and Os(II)-arene complexes

13.4 Gold Complexes

The clinical success of auranofin, a Au(I) complex with a triethylphosphine ligand, as an antiarthritic drug has led to research on gold complexes as antitumor agents. The selective activity of auranofin against P388 leukemia was demonstrated in vitro with targeting of mitochondria shown to be a possible mechanism of action. A large number of monodentate gold(I) phosphine complexes have been evaluated as potential anticancer agents (Figs. 13.16, 13.17 and 13.18). In general, the complexes show promising activity in vitro, however, in the presence of serum proteins as well as in in vivo evaluations, only complexes with strong *trans*-ligands demonstrate good activity [12].

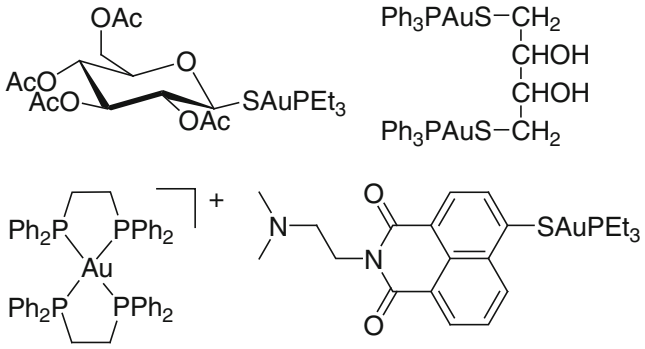


Fig. 13.16 Auranofin (*top left*) and examples of other Au(I) complexes with phosphine ligands

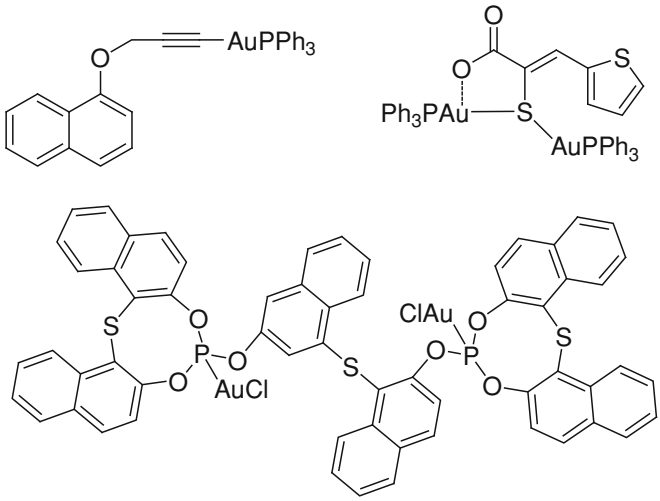


Fig. 13.17 Examples of Au(I) complexes with anticancer activity

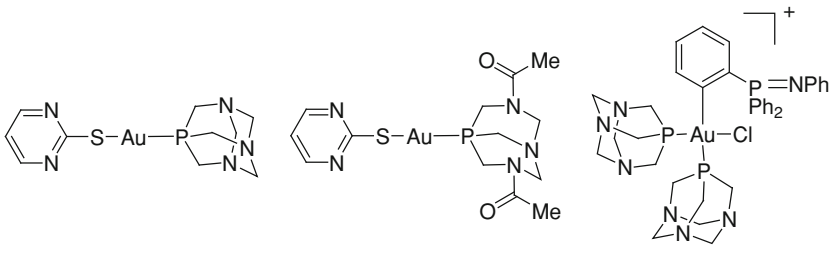


Fig. 13.18 Examples of PTA based Au complexes

A number of gold(I) complexes with bis(diphenylphosphine)ethane (dppe) and related ligands, both monodentate and chelating, were screened for their anticancer properties [45]. Out of the series studied, the complex $[Au(dppe)_2]^+$ showed the most promising results with remarkable in vitro and in vivo activity on different tumor models. The complex progressed into preclinical studies although the studies were subsequently abandoned due severe hepatotoxicity and cardiovascular toxicity [46]. Structural modifications allowed the lipophilicity of the compound to be tuned, which improved the toxicity and selectivity profile, however, none of these subsequent compounds advanced into clinical trials [47].

Recently, several mono and dinuclear gold(I) complexes with phosphine or phosphite ligands have been screened for anticancer activity and good in vitro activity equal or superior to cisplatin was reported [48–51].

The PTA ligand has also been used in combination with Au(I) and Au(III) metal centers (Fig. 13.18). The complexes were found to be remarkably active against the cisplatin resistant A2780cisR cell line and inhibition of cytosolic and mitochondrial thioredoxin reductases was proposed as a possible mechanism of action [20, 52, 53].

Au(I) complexes with phosphole ligands (Fig. 13.19) were found to be highly effective antiproliferative compounds in vitro against glioblastoma cell lines and were also found to be irreversible inhibitors of glutathione reductase at nanomolar concentrations [54]. Detailed information on the interaction of one of the complexes was obtained by X-ray crystallography. In the structure one molecule was found to covalently bind to the Cys284 residue on the surface of enzyme with a

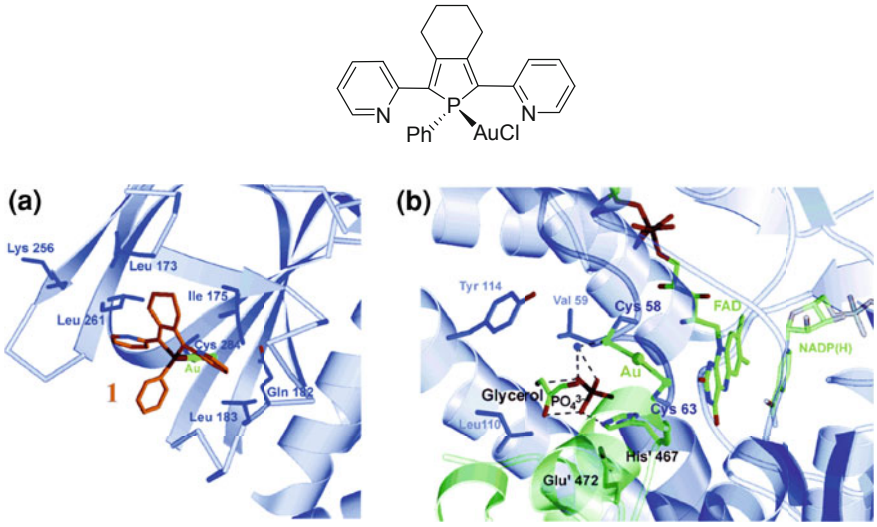


Fig. 13.19 A phosphole based Au(I) complex (*top*) and view of the complex bound to human glutathion reductase (*bottom*). **a** Surface-exposed. **b** At active site: (Cys58-S)-Au-(S-Cys63) Copyright Wiley–VCH Verlag GmbH & Co. KGaA. Reproduced with permission from Ref. [54]

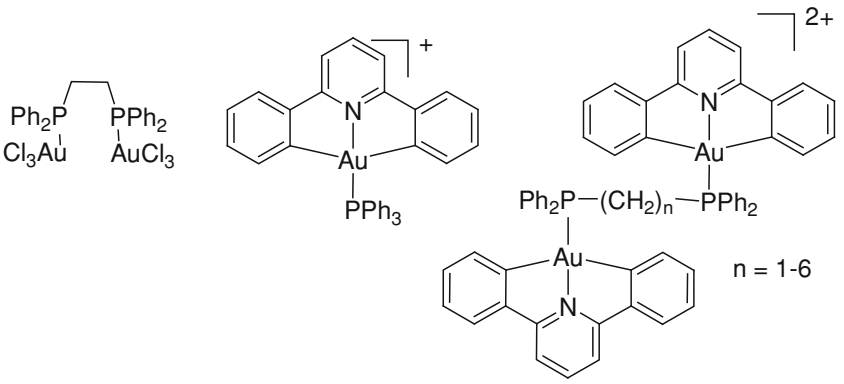


Fig. 13.20 Au(III) complexes with anticancer activity

second Au ion, which has lost the phosphole ligand, coordinating to the active site of enzyme between Cys58 and Cys63.

Square planar Au(III) complexes that are isoelectronic and structurally similar to Pt(II) compounds have also been a focus of interest in recent years. However, their kinetic lability, light sensitivity and reduction to Au(I) under physiological conditions have hampered studies. Consequently, only few examples of gold(III) compounds endowed with anticancer activity have been reported in the literature [12]. For example, Au(III)-ddpe complexes (Fig. 13.20) were evaluated in vivo on mice with P388 leukemia and a >50% increase in lifespan was observed relative to untreated controls [45, 55]. A series of cyclometallated Au(III) complexes that are stable under physiological conditions have also been reported. The complexes were active against a panel of cancer cell lines with IC_{50} values in the low μM range [56].

13.5 Conclusions

In this chapter we have surveyed recent research on the application of phosphine and other phosphorus ligand containing metal-based compounds as chemotherapeutics for the treatment of cancer. Much progress has been made in recent years and a gold-based dppe complex even entered advanced in vivo evaluation, although the studies were finally abandoned due to toxic side-effects. Nevertheless, a gold complex with a triethylphosphine ligand is used in the clinic to treat rheumatoid arthritis. Studies have shown that replacement of the triethylphosphine ligand by PTA, a much more stable and water soluble ligand, leads to a compound that has superior pharmacological properties. This observation paves the way for further fine-tuning of the ligand which has, thus far, hardly been attempted.

There is a growing body of evidence to suggest that metal–phosphine compounds do not exert their cytotoxic effect via the same mechanism as classical

platinum(II) drugs. DNA does not appear to be the main target and interactions with enzymes appear to be deciding. Notably, the crystal structures of enzymes containing metal–phosphine complexes show that the phosphine has an important role to play in molecular recognition. Since the majority of new drugs entering the market are chiral compounds one can envisage that chiral phosphine ligands could become important in medicinal chemistry. Indeed, the extensive studies on chiral phosphines for enantioselective catalysis should be transferred to the development of new drug molecules. While much research is clearly needed in this field it seems likely that before long metal–phosphorus compounds will find new applications in medicine.

Acknowledgments Funding from the Swiss National Science Foundation and the European Commission Marie Curie Action CT-220890-SuRuCo and stimulating discussions with members of PhoSciNet are gratefully acknowledged.

References

1. Yudelevich VI, Komarov EV, Ionin BI (1985) Organophosphorus drugs. Khim Farm Zh 19:668–685
2. Ludeman SM (1999) The chemistry of the metabolites of cyclophosphamide. Curr Pharm Des 5:627–643
3. Wardle NJ, Bligh SWA, Hudson HR (2005) Organophosphorus chemistry: therapeutic intervention in mechanisms of viral and cellular replication. Curr Org Chem 9:1803–1828
4. Hande KR (1998) Etoposide: four decades of development of a topoisomerase II inhibitor. Eur J Cancer 34:1514–1521
5. van Maanen MJ, Smeets CJM, Beijnen JH (2000) Chemistry, pharmacology and pharmacokinetics of N,N′,N″-triethylenethiophosphoramide (thioTEPA). Cancer Treat Rev 26:257–268
6. Lippert B (1999) Cisplatin Chemistry and biochemistry of a leading anticancer drug. VHCA, Zürich
7. Dyson PJ, Sava G (2006) Metal-based antitumour drugs in the post genomic era. Dalton Trans 1929–1933
8. Jakupec MA, Galanski M, Arion VB et al (2008) Antitumor metal compounds: more than theme and variations. Dalton Trans 183–194
9. Galanski M, Jakupec MA, Keppler BK (2005) Update of the preclinical situation of anticancer platinum complexes: novel design strategies and innovative analytical approaches. Curr Med Chem 12:2075–2094
10. Jakupec MA, Galanski M, Slaby S et al (2002) Structure-activity relationships of platinum(II) phosphonate compounds for the treatment of bone malignancies. Eur J Cancer 38:82
11. Shaw CF III (1999) Gold-based therapeutic agents. Chem Rev 99:2589–2600
12. Berners-Price SJ, Sadler PJ (1988) Phosphines and metal phosphine complexes: relationship of chemistry to anticancer and other biological activity In: Structure and Bonding. Springer, Berlin
13. Kozelka J, Segal E, Bois C (1992) Cytotoxic activity of platinum (II) complexes with tri-n-butylphosphine. Crystal structure of the dinuclear hydrazine-bridged complex, cis,cis-$[PtCl(PBu_3^n)_2(\mu\text{-}N_2H_4)PtCl(PBu_3^n)_2]$ $(ClO_4)_2$*2$CHCl_3$. J Inorg Biochem 47:67–80
14. Cleare MJ, Hoeschele JD (1973) Antitumor activity of group VIII transition metal complexes. I. Platinum(II) complexes. Bioinorg Chem 2:187–210

15. Khokhar AR, Xu Q, Siddik ZH (1990) Synthesis, characterization, and antitumor activity of 1,2-bis(diphenylphosphino) ethane platinum(II) and palladium(II) complexes. J Inorg Biochem 39:117–123
16. Phillips AD, Gonsalvi L, Romerosa A et al (2004) Coordination chemistry of 1,3,5-triaza-7-phosphaadamantane (PTA): transition metal complexes and related catalytic, medicinal and photoluminescent applications. Coord Chem Rev 248:955–993
17. Bergamini P, Bertolasi V, Marvelli L et al (2007) Phosphinic platinum complexes with 8-thiotheophylline derivatives: synthesis, characterization, and antiproliferative activity. Inorg Chem 46:4267–4276
18. Dolfen D, Schottler K, Valiahdi S-M et al (2008) Synthesis, structures and in vitro cytotoxicity of some platinum(II) complexes containing thiocarbamate esters. J Inorg Biochem 102:2067–2071
19. Romerosa A, Bergamini P, Bertolasi V et al (2004) Biologically active platinum complexes containing 8-Thiotheophylline and 8-(Methylthio)theophylline. Inorg Chem 43:905–913
20. Miranda S, Vergara E, Mohr F et al (2008) Synthesis, characterization, and in vitro cytotoxicity of some gold(I) and trans platinum(II) thionate complexes containing water-soluble PTA and DAPTA ligands. X-ray crystal structures of $[Au(SC_4H_3N_2)(PTA)]$, trans-$[Pt(SC_4H_3N_2)_2(PTA)_2]$, trans-$[Pt(SC_5H_4\ N)_2(PTA)_2]$, and trans-$[Pt(SC_5H_4\ N)_2(DAPTA)_2]$. Inorg Chem 47:5641–5648
21. Habtemariam A, Watchman B, Potter BS et al (2001) Control of aminophosphine chelate ring-opening in Pt(II) and Pd(II) complexes: potential dual-mode anticancer agents. Dalton Trans 1306–1318
22. Ramos-Lima Francisco J, Quiroga AG, Garcia-Serrelde B et al (2007) New trans-platinum drugs with phosphines and amines as carrier ligands induce apoptosis in tumor cells resistant to cisplatin. J Med Chem 50:2194–2199
23. Hollis LS, Miller AV, Amundsen AR et al (1990) Cis-diamineplatinum (II) complexes containing phosphono carboxylate ligands as antitumor agents. J Med Chem 33:105–111
24. Margiotta N, Ostuni R, Gandin V et al (2009) Synthesis, characterization, and cytotoxicity of dinuclear platinum-bisphosphonate complexes to be used as prodrugs in the local treatment of bone tumours. Dalton Trans 10904–10913
25. Fleisch H (2000) Bisphosphonates in bone disease: from the laboratory to the patient. Academic Press, San Diego
26. Bloemink MJ, Diederen JJH, Dorenbos JP et al (1999) Calcium ions do accelerate the DNA binding of new antitumor-active platinum aminophosphonate complexes. Eur J Inorg Chem 1655–1657
27. Galanski M, Slaby S, Jakupec MA et al (2003) Synthesis, characterization, and in vitro antitumor activity of osteotropic diam(m)ineplatinum(II) complexes bearing a N,N-bis (phosphonomethyl)glycine ligand. J Med Chem 46:4946–4951
28. Klenner T, Valenzuela-Paz P, Keppler BK et al (1990) Cisplatin-linked phosphonates in the treatment of the transplantable osteosarcoma in vitro and in vivo. Cancer Treat Rev 17:253–259
29. Hartinger CG, Dyson PJ (2009) Bioorganometallic chemistry-from teaching paradigms to medicinal applications. Chem Soc Rev 38:391–401
30. Leyva L, Sirlin C, Rubio L et al (2007) Synthesis of cycloruthenated compounds as potential anticancer agents. Eur J Inorg Chem 3055–3066
31. van Rijn Jimmy A, Marques-Gallego P, Reedijk J et al (2009) A novel ruthenium(III) complex with a tridentate dianionic P,O,O-ligand showing high cytotoxic activity. Dalton Trans 10727–10730
32. Allardyce CS, Dyson PJ, Ellis DJ et al (2001) $Ru(\eta^6$-p-cymene$)Cl_2$(pta) (pta = 1,3,5-triaza-7-phosphatricyclo 3.3.1.1 decane): a water soluble compound that exhibits pH dependent DNA binding providing selectivity for diseased cells. Chem Commun 1396–1397
33. Scolaro C, Bergamo A, Brescacin L et al (2005) In vitro and in vivo evaluation of ruthenium(II)-arene PTA complexes. J Med Chem 48:4161–4171

34. Scolaro C, Geldbach TJ, Rochat S et al (2006) Influence of hydrogen-bonding substituents on the cytotoxicity of RAPTA compounds. Organometallics 25:756–765
35. Renfrew AK, Phillips AD, Tapavicza E et al (2009) Tuning the efficacy of ruthenium(II)-arene (RAPTA) antitumor compounds with fluorinated arene ligands. Organometallics 28:5061–5071
36. Serli B, Zangrando E, Gianferrara T et al (2005) Is the aromatic fragment of piano-stool ruthenium compounds an essential feature for anticancer activity? The development of New Ru^{II}-[9]aneS_3 analogues. Eur J Inorg Chem 3423–3434
37. Ang WH, Daldini E, Scolaro C et al (2006) Development of organometallic ruthenium-arene anticancer drugs that resist hydrolysis. Inorg Chem 45:9006–9013
38. Casini A, Gabbiani C, Sorrentino F et al (2008) Emerging protein targets for anticancer metallodrugs: inhibition of thioredoxin reductase and cathepsin B by antitumor ruthenium(II)-arene compounds. J Med Chem 51:6773–6781
39. Ang Wee H, Parker Lorien J, De Luca A et al (2009) Rational design of an organometallic glutathione transferase inhibitor. Angew Chem Int Ed 48:3854–3857
40. Romerosa A, Campos-Malpartida T, Lidrissi C et al (2006) Synthesis, characterization, and DNA binding of new water-soluble cyclopentadienyl Ruthenium(II) complexes incorporating phosphines. Inorg Chem 45:1289–1298
41. Scolaro C, Chaplin AB, Hartinger CG et al (2007) Tuning the hydrophobicity of ruthenium(II)-arene (RAPTA) drugs to modify uptake, biomolecular interactions and efficacy. Dalton Trans 5065–5072
42. Renfrew AK, Scopelliti R, Dyson PJ (2010) Use of perfluorinated phosphines to provide thermomorphic anticancer complexes for heat-based tumor targeting. Inorg Chem 49: 2239–2246
43. Berger I, Hanif M, Nazarov AA et al (2008) In vitro anticancer activity and biologically relevant metabolization of organometallic ruthenium complexes with carbohydrate-based ligands. Chem Eur J 14:9046–9047
44. Hanif M, Nazarov AA, Hartinger CG et al (2010) Osmium(II)– versus ruthenium(II)–arene carbohydratebased anticancer compounds: similarities and differences. Dalton Trans 39: 7345–7352
45. Mirabelli CK, Hill DT, Faucette LF et al (1987) Antitumor activity of bis(diphenyl-phosphino)alkanes, their gold(I) coordination complexes, and related compounds. J Med Chem 30:2181–2190
46. Berners-Price SJ, Bowen RJ, Galettis P et al (1999) Structural and solution chemistry of gold(I) and silver(I) complexes of bidentate pyridyl phosphines: selective antitumour agents. Coord Chem Rev 185–186:823–836
47. Barnard PJ, Berners-Price SJ (2007) Targeting the mitochondrial cell death pathway with gold compounds. Coord Chem Rev 251:1889–1902
48. Schuh E, Valiahdi SM, Jakupec MA et al (2009) Synthesis and biological studies of some gold(I) complexes containing functionalised alkynes. Dalton Trans 10841–10845
49. Suresh D, Balakrishna MS, Rathinasamy K et al (2008) Large-bite bis(phosphite) ligand containing mesocyclic thioether moieties: synthesis, reactivity, group 11 (Cu-I, Au-I) metal complexes and anticancer activity studies on a human cervical cancer (HeLa) cell line. Dalton Trans 2285–2292
50. Barreiro E, Casas JS, Couce MD et al (2010) Dinuclear triphenylphosphinegold(I) sulfanylcarboxylates: synthesis, structure and cytotoxic activity against cancer cell lines. J Inorg Biochem 104:551–559
51. Bagowski CP, You Y, Scheffler H et al (2009) Naphthalimide gold(I) phosphine complexes as anticancer metallodrugs. Dalton Trans 10799–10805
52. Vergara E, Casini A, Sorrentino F et al (2010) Anticancer therapeutics that target selenoenzymes: synthesis, characterization, in vitro cytotoxicity, and thioredoxin reductase inhibition of a series of gold(I) complexes containing hydrophilic phosphine ligands. Chem Med Chem 5:96–102

53. Shaik N, Martínez A, Augustin I et al (2009) Synthesis of apoptosis-inducing iminophosphorane Organogold(III) complexes and study of their interactions with biomolecular targets. Inorg Chem 48:1577–1587
54. Urig S, Fritz-Wolf K, Réau R et al (2006) Undressing of phosphine gold(I) complexes as irreversible inhibitors of human disulfide reductases. Angew Chem Int Ed 45:1881–1886
55. Snyder RM, Mirabelli CK, Johnson RK et al (1986) Modulation of the antitumor and biochemical properties of bis(diphenylphosphine)ethane with metals. Cancer Res 46:5054–5060
56. Li CK-L, Sun RW-Y, Kui SC-F et al (2006) Anticancer cyclometalated $[Au^{III}_m(C\hat{}N\hat{}C)_mL]^{n+}$ compounds: synthesis and cytotoxic properties. Chem Eur J 12:5253–5266

Index

A
Air-sensitive phosphines, 1–3
Alder-Ene type cycloisomerizations
  Mechanisms, 309, 315
  With palladium catalysts, 307–314
  With rhodium catalysts, 320
  Spirocyclic products, 310, 320
  synthesis of γ-lactones and lactames, 317
  Trisubstituted alkenes, 320
Alkene metathesis/hydrogenation, 433
Alkyne hydrations, 184, 205
Allylation of Amines
  Phosphabarrelene-palladium catalysts, 172
Allylic alcohol isomerizations, 184, 207–208
Alzheimer disease, 291
Applications, 2
Associative mechanism, 62
Asymmetric alkylation, 272
Asymmetric catalysis, 12–14, 135–143
  asymmetric allylic substution, 135–137
  asymmetric Methoxycarbonylation, 137–138
  asymmetric Suzuki coupling, 138–139
  asymmetric hydrogenation of ketones, 139–143
  mechanistic studies, 141–143
Atomic Force Microscopy (AFM), 281, 285
Auranofin, 455
Azahelicene-phosphole, 356

B
Base-catalyzed Michael-type addition, 377
Basicity, 5–6
Benzonitrile hydration, 184, 205
Bergmann cyclization, 43–44
Bicarbonate hydrogenation, 184, 196–198
2,5-bis(2-pyridyl)phosphole, 359
Bis(diphenylphosphine)acetylene, 31–43, 45–48
Bis(hydroxymethyl)phosphines, 12–14
  Resonance structures, 31
  $\Delta\nu(C \equiv C)$, 31, 33, 45, 47–48
  Raman spectrum, 31
  Organometallic macrocycles, 31–43
  Organometallic cages, 45–48
Bis(diphenylphosphine)diacetylene, 31
  Organometallic macrocycles of, 33–34, 38–40
  Organometallic cages of, 45–46
Bisphenol, 406, 428
Bisphosphine pathway, 57, 61–62, 64–66, 77–78
Bridging phosphane, 359

C
C-P bond formation, 214
Cages
  Organic phosphine acetylenic, 29–31
  Organometallic phosphine acetylenic, 36, 40, 45–48
Catalysts
  Iridium, 333
  Palladium, 306–316
  Platinum, 329–340
  Rhodium, 314–340
Chemoselective hydrogenations, 184, 187–188
  C=C bond hydrogenations, 188–196
  allylic alcohol hydrogenations, 192–193
Chiral ligands
  BINAP, 308–338

C (*cont.*)
Ph-Binepine, 331
Chiraphos, 331
Conformationally flexible ligands, 322
H8-BINAP, 326
DuPHOS, 314, 323
MeO-BIPHEP, 334–337
Phosphoramidites, 328
Phosphine-oxazoline, 310
SEGPHOS, 308, 312, 335
Skewphos, 320, 333
TolBINAP, 324, 333
TRAP, 308
Xylyl-BIPHEP, 321
Chiral phosphabarrelenes, 170–171, 173, 176
Chiral phosphinines, 157, 167, 169, 176
Cis/trans isomerization, 65–66, 68, 73
Cisplatin, 446
Cluster, 274, 276
Cobalt
Bis(diphenylphosphine)acetylene macrocycles, 42–43
π-conjugated materials, 21–49
π-conjugated system, 344
Conjugation, 4–8
Convergent process, 266
Coordination, 343
Coordination chemistry, 5–6, 13–14, 129–135
rhodium, 129–130
iridium, 130–132
palladium, 132–133
platinum, 133–135
Copper, 270, 272
Bis(diphenylphosphine)acetylene macrocycles, 40, 46
Bis(diphenylphosphine)acetylene cages, 40, 45–46
Ortho-bis(diphenylphosphino-ethynyl) benzene macrocycles, 44
Bis(diphenylphosphine)diacetylene cages, 46
Covalent self-assembly, 376–377, 398–399, 405, 423, 428
Cross-coupling reactions, 57, 59–60, 63–64, 68–69, 77–78, 171, 176
Cyanolysis, 401
Cyclodimerization
Phosphinine-iron catalysts, 162
Cycloisomerization
Phosphinine-nickel catalysts, 166
Cyclophosphamide, 450
Cyclotrimerization
Phosphinine-iron catalysts, 162
Cyclotriphosphazene, 267–268, 272

D
Dendrimer, 265–296
Dendritic catalyst, 268–272
Dendron, 266, 269, 277
Dense packing limit, 267
Density Functional Theory, 7–8
DFT, 57, 60, 64, 68, 70–73, 75–76
Di-phosphinines, 158, 174–175
Dialkylarylphosphines, 11–14
Dichlorophosphines, 9–10
Diphosphene, 89, 98, 101, 103–105
Dissociative mechanism, 61–63, 66, 70–71, 74–76
Divergent process, 276
DNA, 280–283, 286–288, 290

E
Electrochemistry, 5–6
Electrode, 279–280
Electrophilic activations, 313
Enantiomeric excess, 272
Enantiotopos selection, 336
Entropic contributions, 76
Etopophos, 446

F
fac-Mo(CO)3 template, 388
Facially capping triphosphorus macrocyclic ligands, 382
Fagan-Nugent reaction, 347
Ferrocene, 279
Film, 280, 283, 286
Fluorescence, 278, 281, 285–287, 289

G
Gel, 277
Glaucoma, 291
Gold
Bis(diphenylphosphine)acetylene macrocycles, 40–42
Bis(diphenylphosphine)acetylene cages, 46–47
Gold anticancer complexes, 446–454
dppe, 456
glutathion reductase inhibitors, 460

PTA, 459
Gold-catalysis, 176
Grubbs'type methathesis, 386

H
H-phosphinates, 233–234
H-phosphonates, 215–225, 243–252
Heck reaction, 271, 274, 419–420
Helical chirality, 354
Helicenes, 349–350, 354
Heteroditopic ligand, 352–353
High-dilution conditions, 376, 380, 384, 388, 394–395, 402, 410–411, 426–427
HIV, 291
Human immune system, 292, 296
Hybridization, 285–286
Hydroformylation
  Phosphinine-rhodium catalysts, 162, 174
  Phosphabarrelene-rhodium catalysts, 170
  Tandem hydroformylation-cyclization, 173
Hydrogenation
  Phosphinine-rhodium catalysts, 166
  Phosphinine-iridium catalysts, 166
  Phosphabarrelene-rhodium catalysts, 170
Hydrophosphination, 11–12
Hydrophosphinations, 234–243, 252–254
  alkenes, 234–238
  palladium, 234, 239, 241, 252
  platinum, 234–235, 252–253
  nickel, 235–238, 252–253
  lanthanum, 236
  calcium, 237
  alkynes, 238–243
  regioselectivity, 239
  stereoselectivity, 239
  ytterbium, 240
  imine, 240
  diphenylphosphinoalkenols, 241
  ruthenium, 241–242
  copper, 242
  aldehydes, 252–254
  imines, 252–253
  niobium, 252–254
Hydrophosphinylations, 226–231, 252
  alkynes, 225–231
  palladium, 225–228, 230–231
  β-isomers, 226, 230
  α-isomers, 226, 230
  regioselectivity, 227
  diphenylphosphinic acid, 227
  rhodium, 229
  copper, 231
  carbocyclization of diynes, 231
  imines, 252
  PrPB complex, 252
Hydrophosphonylations, 233–234
  alkynes, 233–234
  palladium, 233
  copper, 234
Hydrophosphorylations, 215–225, 243–252
  alkynes, 215–221
  vinylphosphonates, 216–221
  phosphine ligands, 216–225
  palladium, 216–225
  platinum, 217–218
  rhodium, 218–219, 223
  α-isomers, 218
  β-isomers, 218
  nickel, 220
  alkenes, 221–224
  dienes, 224–225
  aldehydes, 243–249
  titanium, 243–246, 250
  ALB catalyst, 243, 246–247
  LLB catalyst, 243, 246–248
  SALEN ligands, 244–245
  zinc, 245
  LSB catalyst, 245–246
  Schiff base, 248–249
  salalen ligands, 248–249
  imines, 250–252
  LPB catalyst, 250–251
  YbPB complex, 250, 252
Hydrosilylation
  Phosphinine-palladium catalysts, 168
  Phosphinine-iridium catalysts, 168
  Phosphabarrelene-platinum catalysts, 172
Hydrosilylation, 12–14

I
Ifosfamide, 450
Imaging, 287
Insertion rections, 107
Intramolecular hydrophosphination, 380–381, 383
Ion-selective electrodes, 393
Ionic liquids, 190
Iridium, 184, 203
  hydroamination, 203
Iron
  Bis(diphenylphosphine)acetylene macrocycles, 38

K
Kinetic resolution, 318
Knoevenagel condensation, 269

L
Layer-by-layer (LbL), 281, 283–284, 287
Ligands synthesis, 122–128
  phosphine-thioethers, 124–126
  phosphine-phospholes, 126
  amine-phospholes, 126
  phosphine-N-heterocyclic carbene precursors, 126–128
  phosphine-acetals, 128

M
Macrocycle, 274–275
Macrocycles
  Organic phosphine acetylenic, 23–30
  organometallic phosphine acetylenic, 31–49
Mannich-type condensation, 405, 423, 427
Mechanisms, 309, 315, 325, 330, 336
Mercury
  Ortho-bis(diphenylphosphino-ethynyl) benzene macrocycles, 43–44
[2,2]metallacyclophane, 360
Metal phosphides, 86, 111–112
  applications, 111–112
  metal-rich, 111
  phosphorus-rich, 86, 111–112
  synthesis, 111–112
Metal-bis-(azahelicene-phosphole), 354
  Stereoselective synthesis, 354
  Molar rotation, 358
  Circular dichroism, 357
Michael addition, 269
Microcapsule, 282–283
Miscellaneous cyclizations
  Synthesis of tetrahydropyranes, 312
  Synthesis of axially chiral compounds, 313
Molecular modelling, 7–8
Molybdenum
  Bis(diphenylphosphine)acetylene macrocycles, 37
  Bis(diphenylphosphine)acetylene cages, 47
Monocyte, 293–295
Monophosphine pathway, 61–62, 65–66
Morita-Baylis-Hillman reaction, 201

N
N,P,N-chelate, 343, 345
Nanoparticles, 274–275, 280, 296
Nanotube, 282, 296
Natural killer (NK), 294–295
Negishi reaction, 59
Nickel
  Bis(diphenylphosphine)acetylene macrocycles, 37
  Bis(diphenylphosphine)acetylene cages, 47
Non linear optics (NLO), 353

O
OLED, 278
OLEDs, 345, 350
Oligonucleotide, 282, 286
Oligophosphanes, 87
Oligophosphanide anions, 86–111
  alkali metal, 90–92
  reactivity, 92–111
  synthesis, 87–92
  transition metal, 92–111
ONIOM, 58, 75
Organic phosphine acetylenes, 21–31
  Scaffolding, 23–31
  Macrocycles, 23–30
  Cages, 29–31
Organometallic phosphine acetylenes, 31–49
  Macrocycles, 31–44, 46–47
    Mixed-metal, 32, 34, 39
    Fluoresence of, 34, 39–40
    Guest inclusion in, 34, 39–40
    In metalclusters, 41–43
  Cages, 36, 40, 45–48
Ortho-bis(diphenylphosphino-ethynyl) benzene, 43
  Organometallic macrocycles of, 43–44
Osmium
  Bis(diphenylphosphine)acetylene macrocycles, 39, 41–42
  Bis(diphenylphosphine)diacetylene macrocycles, 39
Osmium anticancer complexes, 458
Oxidative addition, 57, 59–64, 66, 71, 77

P
P-based corands, 377
  Homoleptic, 378
    Alkylation, 378–379
    Hydrogenation, 379
    9-membered, 379
      1,4,7-triphosphacyclononanes, 378

o-benzo, 379
10-membered, 379
1,4,7-triphosphacyclodecanes, 379
11-membered, 379
Metal carbonyls complexes, 380–381
1,4,8-triphosphacycloundecane, 379
12-membered, 381, 384
1,5,9-triphosphacyclododecanes, 381
catalytic activity, 383
Early transition metal complexes, 383
Functionalisation, 381
iron complexes, 382
liberation, 382
manganese complexes, 384
Molybdenum complexes, 382
palladium complexes, 382
Rhenium complexes, 383
tungsten complexes, 382
14-membered, 384–385
15-membered, 385
16-membered, 386
30-membered, 386
36-membered, 387
hexagold template, 386
45-membered, 386
Hybrid O/N/S-Containing, 387
Chiral, 403
1-phospha-11,12-benzo-21-crown-7, 403
1-phospha-10-aza-18-crown-6, 403
1,10-diphospha(2)-2,6-pyridino(2)-1,10-ferrocenophane, 390
9-membered P,S,S-macrocycle, 388
Complexes, 388
11-membered, 384
Complexes, 390–391
12- membered, 391
Complexes, 393–395
Hydrogenolysis, 391
dinitrogen complex, 392
white phosphorus activation, 392
14-membered, 394
P_2X_2-rings, 394
Complexes, 395–397
Schiff-base phosphines, 397
Reduction, 402
Sulfinyl-substituted macrocycle, 396
Complexes, 400–401
Triphosphine, 395
16-membered, 397–399
covalent self-assembly, 398–399
18-membered, 399–401
Complexes, 400–402
21-membered phosphacrown, 401–402
22-membered azaphosphacrown, 401
Complexes, 401
P,Se,O-containing, 389
P-based macrocycles, 376–377, 379, 404
P-containing cryptands, 425–426
boron-containing, 428
cryptand phosphine oxides, 430
''gyroscope-like'', 433
hexaphosphorus, 432
modification, 429
PN_3-calix[6]cryptand, 432
Complexes, 432
P,N-containing, 427
covalent self-assembly, 427
17-phospha[2.2.2](1,3,5)-benzeno (3,3',3")triphenylmethanophane, 427
Phosphathiacyclane, 426
tetraphosphorus, 432
P-containing cyclophanes, 377, 404–405
Binaphthyl-based, 410–411
allylic alkylation, 411
asymmetric induction, 411
Hydroformylation, 411
2,2'-bipyridine-based, 411
calixphyrins, 417–419
complexation, 417–420
hydrosilylation, 419
Heck reaction, 419
Calixresorcinarene, 425
[2]catenane, 412–413
1,3-diaza-2,4-diphosphacyclobutane units, 415
heterocyclic carbene fragments, 412
macrocyclic phosphoramidites, 406
macrocyclic phosphites, 407
Macrocyclic tetraphosphole, 420
self-assembly, 420
P-containing porphyrine, 420
P,N-containing, 405, 423
covalent self-assembly, 405, 423
1,5-diaza-3,7-diphosphacyclooctane fragments, 423
supramolecular host–guest organization-, 424
thiophosphonic macrocycles, 406
Pph-bridged 1,1'-ferrocenophanes, 408
Silver complex, 408
phosphinine units, 420
Calix[4]phosphinines, 421
phosphole-containing calixpyrrole, 415, 419
complexation, 417
P-H bond addition, 214

P (*cont.*)
regioselectivity, 214
stereoselectivity, 214
P-heterocycle, 343
P–P cleavage, 87–88, 103–104
Para-bis(diphenylphosphino-ethynyl) benzene, 44
Organometallic macrocycles, 44–45
[2,2]paracyclophane, 360
Palladium, 57, 59, 60, 62, 64, 66–72, 184, 202
Bis(diphenylphosphine)acetylene macrocycles, 31–35
Ortho-bis(diphenylphosphino-ethynyl) benzene macrocycles, 43–44
Sonogashira coupling, 184, 202
Pericyclines, 23–29
Phosphapericyclines, 23–27
Phosphasilapericycline, 26
Phosphasulfapericycline, 27
Exploded phosphapericyclines, 28–29
Peripheral blood mononuclear cell, 292–293, 295
Phosphaalkynes, cyclooligomerization, 22–24
Phosphabarrelene-phosphites, 171
Phosphabarrelenes
synthesis, 169
Phosphascorpionates, 22–23
Phosphinates, 232
alkynes, 232
palladium, 232
nickel, 232
Phosphine, 269, 271–272, 274
Phosphine ligands, 57–61, 63–64, 66–69, 71–72, 74–78
bulky ligands, 60, 72–74, 78
chelating ligands, 68, 75, 78
phosphine oxides, 225–231, 252
phosphines, 234–242, 252–254
Phosphinidene, 109–111
Phosphinidene, addition to triple bond, 22–23
Phosphinine-phosphites, 167
Phosphinine-pyridines, 159, 162, 175
Phosphininines
Electronic properties, 152
Frontier orbitals, 152–153
Structural characteristics, 154
Steric properties, 154
Synthesis, 155
Coordination Chemistry, 158
Reactivity, 162
Phospholanes, 9–14
Phospholene, 352
Phospholes, 343
General, 343
Inversion barrier, 347–348
Aromaticity, 346
Synthesis, 347
Photophysical properties, 350
Phosphonites, 9–10
Pincer-type phosphinines, 175
Planar Chiral Ferrocene ligands, 121
Platinum
Bis(diphenylphosphine)acetylene macrocycles, 31–36
Bis(diphenylphosphine)diacetylene macrocycles, 33–34
Ortho-bis(diphenylphosphino-ethynyl) benzene macrocycles, 43–44
Para-bis(diphenylphosphino-ethynyl) benzene macrocycles, 44–45
Platinum, 184
Platinum anticancer complexes, 450–453
$_{31}$P NMR, 86, 90, 92–95, 98, 102–103, 105–106, 108–109, 111
aminophosphine, 448
phosphonic acid, 448–449
PTA, 448, 450
triphenylphosphine, 448, 453
Pore, 276–282
Positive dendritic effect, 270–271, 296
Prion, 290–291
PTA, 183–188
synthesis, 184
basicity, 184
alkylation, 185
upper rim functionalization, 185–186
lower rim functionalization, 186
cage opening, 187
2-(2-pyridyl)phosphole, 346

Q
QM calculations, 58, 66
QM/MM calculations, 58
Quantum dot, 285–286, 290

R
Radical cation, 6–8
Reaction mechanisms, 61, 64–66, 72, 74, 77
Reactivity, 8–12
Receptors, 375
Redox-active ligands, 418
Reductive elimination, 57, 59, 68, 70, 73–78
References, 14–19

Rhenium
Bis(diphenylphosphine)acetylene macrocycles, 38–39
Bis(diphenylphosphine)diacetylene macrocycles, 38–39
Rhodium, 184
Bis(diphenylphosphine)acetylene macrocycles, 37–38, 42
Bis(diphenylphosphine)diacetylene macrocycles, 37–38
olefin hydroformylations, 184, 192, 198–200
cyclodextrins, 200
Ruthenium, 184, 188–198
Bis(diphenylphosphine)acetylene macrocycles, 40–42
Bis(diphenylphosphine)diacetylene macrocycles, 39–40
cyclopentadienyl complexes, 191, 197
hydrido complexes, 191
Kharasch reaction, 204
dendrimer supported catalysts, 206
Ruthenium(II)-arene anticancer complexes, 449–454
cathepsin B inhibitors, 451
Glutathione-S-transferases (GSTs) inhibitors, 452
RAPTA type, 452–453
hydrolysis, 451, 454
thermosensitive, 454
sugar-phosphite, 456
Ruthenium(III) anticancer complexes, 449

S
Silica, 275–276
Silver
Bis(diphenylphosphine)acetylene macrocycles, 36, 47
Bis(diphenylphosphine)acetylene cages, 36, 47
Ortho-bis(diphenylphosphino-ethynyl) benzene macrocycles, 44
Sonogashira reaction, 271
π-π stacking, 356, 361
Staudinger reaction, 430
Stereoselective coordination, 352, 354
Stille coupling, 269
Stille cross-coupling, 420
Stille reaction, 57, 59, 64, 69–72, 77–78
Substrates
Cyclopropyl substituted enynes, 327, 334
Dien-ynes, 322–326, 332–333
En-diynes, 326–327
O-tethered 1,6-enynes, 309–311, 315, 322, 335
N-tethered 1,6- or 1,7-enynes, 308–312, 316, 331
Suzuki reaction, 57, 59, 63–68, 77–78, 274
Suzuki-Miyaura reaction
Phosphinine-nickel catalysts, 176
Phosphinine-palladium catalysts, 176
Phosphabarrelene-palladium catalysts, 171
Synthesis, 3
Synthetic applications, 318–320

T
Tandem Reactions, 173
Template synthesis, 374–379, 382, 384, 387, 389
Iron template, 378–380
template-controlled addition, 412
Thiotepa, 446
Trans-coordinating di-phosphinines, 158, 174
Transfection, 289–290
Transfer hydrogenations, 184, 187–195
Transition-metal-catalysis, 214
Transmetalation, 57, 60, 64–73, 77–78
Tripod coupling, 425, 430
Trisphenol, 430
Tungsten
Bis(diphenylphosphine)acetylene macrocycles, 37
Bis(diphenylphosphine)acetylene cages, 48
Two-photon excited fluorescence, 287

V
Vanadium
Bis(diphenylphosphine)acetylene macrocycles, 38

W
Water-soluble Phosphines, 184

X
X-ray crystallographic analysis, 2–3